Slip-Resistant Connections Made of Carbon and Stainless Steel

Von der Fakultät für Ingenieurwissenschaften, Abteilung Bauwissenschaften,

der Universität Duisburg-Essen zur Erlangung des akademischen Grades

Doktor-Ingenieur

genehmigte Dissertation

von

Nariman Afzali M.Sc.

Referentin: Univ.-Prof. Dr.-Ing. habil. Natalie Stranghöner

Korreferent: Univ.-Prof. Dr.-Ing. habil. Knuth-Michael Henkel

Eingereicht: 2. Dezember 2020

Mündliche Prüfung: 12. Februar 2021

Abteilung Bauwissenschaften der Fakultät für Ingenieurwissenschaften

Institut für Metall- und Leichtbau

Univ.-Prof. Dr.-Ing. habil. Natalie Stranghöner

DuEPublico

Duisburg-Essen Publications online

Abstract

Slip-resistant connections are always used when slip in a connection will endanger the serviceability or the slip resistance is used for ultimate limit reasons. Hence, slip-resistant connections shall be designed to prevent slip in bolted connections. Different guidelines/standards specify slip factors for common surface conditions. For deviating surface conditions, the slip factor shall be determined experimentally. However, practice shows that in many cases the given slip factors are not comparable for the same surface condition.

Furthermore, the available slip factors are valid for slip-resistant connections made of carbon steel. Currently there is no guideline or standard which prescribes a classification for slip-resistant connections made of stainless steel. Stainless steel alloys suffer more from viscoplastic deformations in comparison to carbon steel. For this reason, there have historically been a number of concerns about the use of stainless steel in preloaded bolted connections. Having more viscoplastic deformations might lead to higher losses of preload in stainless steel bolts and consequently may influence the slip-resistant behaviour of the connection. Moreover, a suitable slip factor shall be determined experimentally for each common surface condition. Currently, different test procedures for the determination of slip factors exist. However, in several cases the test procedure is not clear in detail and allows several possible interpretations. This can lead to incomparable results for identical surface preparations. Besides all these parameters, there are still many others which may influence the determination of the slip factor process.

Therefore, a comprehensive investigation was conducted in the European Research Project SIROCO (RF SR-CT-2014-00024) to close the still existing gaps in knowledge in this area. In the frame of this study, the influence of different parameters on the slip-resistant behaviour of bolted connections was investigated. Furthermore, the relaxation behaviour of preloaded bolted connections made of stainless steel was also investigated. A comprehensive experimental investigation was conducted in order to provide a classification for slip-resistant connections made of stainless steel.

In addition, an alternative method for preparing the faying surfaces of slip-resistant connections was developed in order to reduce the preparation time and cost on the one hand, and on the other to significantly improve the slip-resistant behaviour of the connections. A comparative study was then conducted to check the comparability of the results according to EN 1090-2, Annex G; and RCSC, Appendix A. Finally, a simplified test specimen geometry was developed based on the EN 1090-2, Annex G standard test specimen geometry in order to reduce the testing costs for the determination of slip factors.

Kurzfassung

Gleitfeste Verbindungen werden immer dann eingesetzt, wenn Gleiten in einer Verbindung die Gebrauchstauglichkeit gefährdet oder der Gleitwiderstand aus Tragfähigkeitsgründen erforderlich ist. Daher sind gleitfeste Verbindungen so auszulegen, dass ein Gleiten in Schraubverbindungen verhindert wird. Verschiedene Richtlinien/Normen spezifizieren die Haftreibungszahl für gebräuchliche Oberflächenbedingungen. Für davon abweichende Oberflächenbedingungen muss die Haftreibungszahl experimentell bestimmt werden. Die Praxis zeigt jedoch, dass dabei in vielen Fällen die Haftreibungszahlen für die gleiche Oberflächenbeschaffenheit nicht vergleichbar sind.

Darüber hinaus sind die verfügbaren Haftreibungszahlen nur gültig für gleitfeste Verbindungen aus Kohlenstoffstahl. Derzeit gibt es keine Richtlinie oder Norm, die eine Klassifizierung für gleitfeste Verbindungen aus nichtrostendem Stahl angibt. Nichtrostende Stähle leiden im Vergleich zu Kohlenstoffstahl stärker unter viskoplastischen Verformungen. Aus diesem Grund gab es in der Vergangenheit eine Reihe von Bedenken gegenüber der Verwendung von nichtrostendem Stahl in vorgespannten Schraubverbindungen. Größere viskoplastische Verformungen können bei Schrauben aus nichtrostendem Stahl zu höheren Vorspannkraftverlusten führen und somit das Gleitverhalten der Verbindung beeinflussen. Darüber hinaus ist eine geeignete Haftreibungszahl für jede übliche Oberflächenbeschaffenheit experimentell ermittelt werden. Derzeit existieren verschiedene Prüfverfahren zur Bestimmung von Haftreibungszahlen. In einigen Fällen ist das Prüfverfahren jedoch im Detail nicht eindeutig und lässt mehrere Interpretationsmöglichkeiten zu. Dies kann bei identischen Oberflächenvorbereitungen zu nicht vergleichbaren Ergebnissen führen. Neben all diesen Parametern gibt es noch weitere Parameter, welche die Bestimmung der Haftreibungszahl beeinflussen können.

Deshalb wurde im Rahmen des europäischen Forschungsvorhabens SIROCO (RFSR-CT-2014-00024) eine umfassende Untersuchung durchgeführt, um bestehende Fragen zu beantworten und die Wissenslücke in diesem Bereich zu schließen. Im Rahmen dieser Studie wurde der Einfluss verschiedener Parameter auf das Gleitverhalten von Schraubverbindungen untersucht. Darüber hinaus wurde auch das Relaxationsverhalten von vorgespannten Schraubverbindungen aus nichtrostendem Stahl untersucht und eine umfassende experimentelle Untersuchung zur Klassifizierung von gleitfesten Verbindungen aus nichtrostendem Stahl durchgeführt.

Über diese Arbeiten hinaus wurde eine alternative Methode zur Vorbereitung der Kontaktflächen entwickelt, um einerseits die Vorbereitungszeit und -kosten zu reduzieren und andererseits das Gleitverhalten der Verbindungen deutlich zu verbessern. Letztendlich wurde eine Studie durchgeführt, um die Vergleichbarkeit der Ergebnisse gemäß EN 1090-2, Anhang G und RCSC Anhang A zu überprüfen. Abschließend wurde eine vereinfachte Versuchskörpergeometrie in Anlehnung an die Standard- Versuchskörpergeometrie nach EN 1090-2, Anhang G entwickelt, um die Prüfkosten für die Bestimmung der Haftreibungszahl zu reduzieren.

Preface and Acknowledgements

This journey has been a truly life-changing experience for me and would not have been possible without a great deal of support and assistance from many people.

I would like to express my deep and sincere gratitude to my PhD supervisor, Prof. Dr.-Ing. habil. Natalie Stranghöner, for the unconditional support, advice and encouragement she has given me these past years. Without her guidance and constructive feedback, this PhD would not have been achievable.

I would like to thank Prof. Dr.-Ing. habil. Knuth-Michael Henkel for being my second referee, Prof. Dr.-Ing. André Niemann as chairman of the examination board, and Prof. Dr.-Ing. Renatus Widmann and Prof. Dr.- Ing. habil. Jörg Schröder, who accompanied my disputation as examiners.

My thanks also go to Dr. Erik Schedin from Outokumpu Stainless AB, Anders Söderman from BUMAX AB, Markus Federico from International Farbenwerke GmbH and Martin Czysch from SLV Duisburg for their great support.

My special thanks go to all my colleagues in the Institute for Metal and Lightweight Structures. I will never forget the support and friendship you have showed me during these years. I am especially grateful to Christoph Abraham, Lukas Makevičius, Sebastian Stehr and Denis Paluska. Many thanks also to all the student assistants who have worked with me over the years, and to our former and current laboratory staff, especially Christian Schoedon for all the help I received from you.

I gratefully thank my parents-in-law, Mina Madani and Ali Rahemi for their love and constant support.

I will always be in debt to my family in Germany. My thanks to Karin Krupke and Gerhard Krupke, Fereshteh Majidi and Mohammad Zolfaghari, who have always been so kind, helpful and caring in numerous ways at all stages of our life in Germany.

I am extremely grateful to my parents, Zahra Zaheri and Dr. Mohammad Afzali for their love, caring and sacrifices in preparing me for my future. Thank you for always believing in me, encouraging and supporting me to reach my goals. A special thank you to my brother, Nima Afzali for all his helping and caring in any way.

My deepest gratitude goes to my beloved wife, Dr.-Ing. Negar Rahemi, who has been by my side every single minute of this journey. We planned and started this journey together, and without her, it would not be possible for me to be here. I cannot express how grateful I am. Thank you for all your countless sacrifices to help me get to this point. And finally, I want to thank my son, Sam, for being such a good little baby the past two years and making it possible for me to complete what I started.

Essen, in March 2021   Nariman Afzali

Content

List of Figures

List of Tables

Symbols

Latin

a_o	length of the bolt shank
A_o	plain shank area of the bolt
A_s	nominal stress area of the bolt
a_t	length of the threaded part of the bolt
d	bolt diameter
E	Young's modulus of elasticity
k	equal to 0.85 when only three specimens are tested and equal to 0.90 when five or more specimens are tested
k_s	individual slip factor
m	number of interfaces per connection
n	number of bolts per connection
N_{ti}	preload level in the bolt
$\hat{F}_{fr}$	maximum load that the connection could transmit without slip displacement exceeding 0.3 mm
F_g	slip load for a connection
F_g	slip load for a connection
$F_{p,C}$	nominal minimum preload force (0.7 f_{ub} A_s)
$F_{p,C}{}^*$	required preload of 0.7 f_{yb} A_s
F_{Si}	individual slip load for a connection
f_{ub}	nominal tensile strength of bolt
f_{yb}	nominal yield strength of the bolt
P_v	preload level in the bolts
P_z	constant load in long-term test
Q_{const}	constant load
Q_{dyn}	cyclic load
R_s	load level for the creep test
t_n	thickness of the nut
T_t	measured preload in the bolting assemblies

V_{si}	individual slip load

Greek

μ	slip factor
$\mu_{5\%}$	slip factors as 5 % fractile calculated on the basis of the static tests and the passed creep test
μ_{act}	calculated slip factors as mean values considering the actual preload at slip
μ_{ect}	slip factor resulting from the passed extended creep test
μ_i	individual slip factor
μ_{ini}	calculated slip factors as mean values considering the initial preload when the tests start
μ_m	mean slip factor
μ_{nom}	calculated slip factors as mean values considering the nominal preload level
μ_t	considered mean slip factor
μ_{vb}	slip factor
Δ	measured total extension of the bolt
δ	standard deviation of slip factor for all tests
Σt	clamping length
γ_{M3}	partial safety factor

Abbreviations

Al-SM	thermal aluminium spray metallized coating
ASI	alkali-zinc silicate coating
CBG	centre bolts group position
ct	creep test
DFT	dry film thickness (coating thickness)
ect	extended creep test
FhIGP	Fraunhofer Research Institution for Large Structures in Production Engineering IGP, Rostock, Germany
EP	epoxy primer
ESI	ethyl-zinc silicate coating
GB	grit blasted
HDG	hot dip galvanized
IKS	Institut für Korrosionsschutz Dresden GmbH, Dresden, Germany
IML	University of Duisburg-Essen, Institute for Metal and Lightweight Structures, Essen, Germany
LP	loss of preload
LVDT	linear variable differential transformer (displacement transducer)
PE	plate edges position
PUR	zinc-dust paint on polyurethane basis
SB	shot blasted
st	static test
TUD	Delft University of Technology, Delft, Netherlands
Zn-SM	thermal spray metallized with zinc

1 Introduction

1.1 Problem definition

Connections in steel structures are of critical importance. Historically, failure of structural members is rare; however, connection failure has been the major issue which can cause numerous collapses. According to EN 1993-1-8 [1], connections are usually made either with bolts, rivets, pins or welds. Bolted connections are frequently used in steel constructions. Bolting is common in field connections due to their lower installation cost, ease of installation and no need for special equipment [2]. In Germany, the application of high strength bolting assemblies in bolted connections became more common in steel structures around the 1950s, see [3]-[14]. In the design of bolted connections, two kinds of forces must be considered: shear and tension forces. EN 1993-1-8 distinguishes between five bolt categories A to E, see Figure 1-1. Categories A to C are shear connections and categories D and E are tension connections. While the bearing-type connections according to category A and the tensile connections according to category D belong to the non-preloaded connections, the slip-resistant connections of categories B and C (slip-resistant in the serviceability limit state [category B]) and ultimate limit state [category C]) as well as the tensile connections of category E are always designed as preloaded connections.
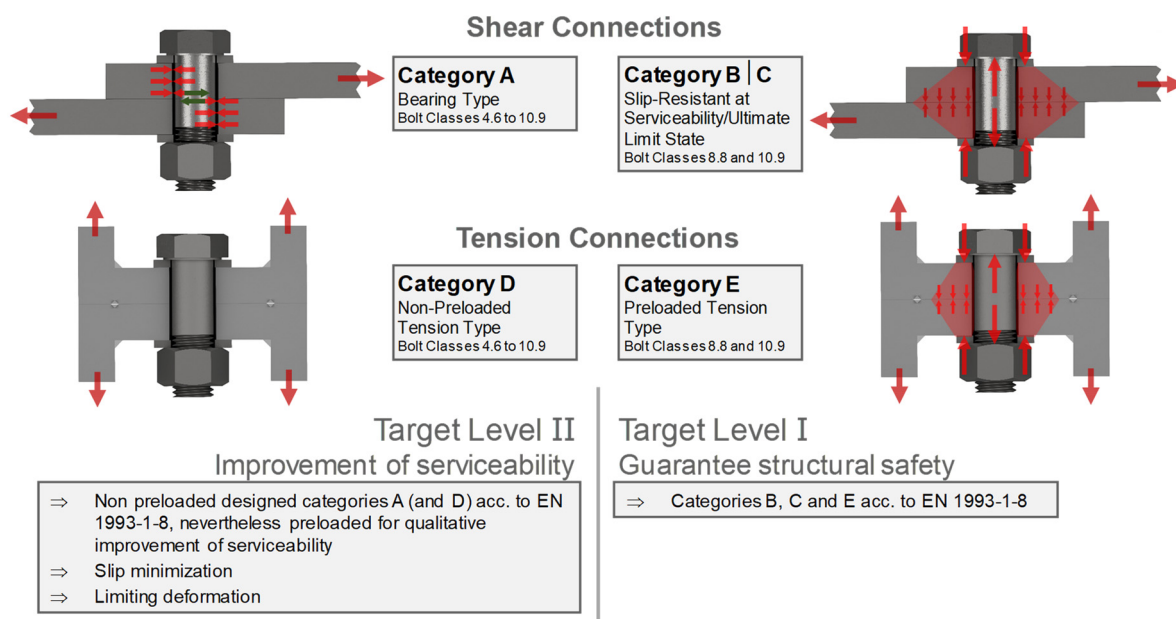
Figure 1-1: Categories of bolted connections according to EN 1993-1-8

Bolting assemblies in connections can be preloaded for different purposes. By considering the type of bolted connection as well as the relevance of safety, two different target levels have been defined by Schmidt [15]. "Target level I" serves to ensure the structural safety in categories B and C and preloaded tension connections in category E which are often used in fatigue loaded applications. In this category the preload level in the bolts shall be guaranteed during the service life of the structure.

For this reason, inspections would be required before, during and after tightening of the bolts. "Target level II" improves the serviceability in the shear connection in category A, as well as the non-preloaded tension connection in category D. For this reason, it is not unusual for pure bearing type connections of category A, where no tightening of the bolt is required, to be preloaded in order to increase the stiffness and load bearing capacity of the connection and to minimise slip and deformation for serviceability reasons. Preloading serves to achieve a significant increase of the fatigue strength under tensile and/or shear stress. For these reasons, preloading of bolted connections is mandatory in structures subjected to cyclic loading. Slip-resistant connections (category B or C) are required when the structure is subjected to heavy impact loads, alternate loading and/or fatigue and slip has to be prevented either at serviceability or ultimate limit state. A slip-resistant connection is typically a suitable choice in lattice towers, bridges, radio masts and wind turbine towers, see Figure 1-2.

Figure 1-2: Garrison Crossing footbridge with slip-resistant connections made of stainless steel (Fort York Bridge, Toronto, Canada) © Juan A. Sobrino, pedelta

Using the slip-resistant connection is also desirable where the bolts are used in slotted holes or in oversize holes and the load is applied parallel or nearly parallel to the slots. In these types of connections, the highest possible slip-resistance is desirable in order to reduce the required number of bolts and therefore also the expenses of the connections to meet the demand of the industry for maintenance-free connections. Essential characteristics of these connections depend on the preload level in the bolts and the condition of the faying surfaces. Not only the initial

bolt preload level is a key factor in this type of connections, the existing bolt preload level over the whole service life also plays an important role in the slip-resistant behaviour of the bolted connections. Many studies determine the slip factors for different surface conditions. However, the presented results seem to be not comparable in many cases, which leads to two essentially important questions: Why does such a variety in slip factors exist for identical surface conditions? And which important factors were not considered in these investigations?

1.2 Objective

The experimental test procedure for determining the slip factor of slip-resistant connections according to the old version of Annex G of EN 1090-2:2011 [16] was not clear in detail and allowed several interpretation possibilities. This could potentially lead to different slip factors for the same surface preparations. Nonetheless, also by reviewing the literature, it can be observed that in some cases the achieved slip factors for identical surface conditions are not comparable despite having the same testing procedure.

The slip-resistant behaviour of connections is influenced by two important factors: the condition of the faying surfaces and the preload level of the bolts. However, other key parameters may also play an important role in the slip-resistant behaviour of the connections. These include:

- test procedures,
- methods for measuring the preload in the bolts (constantly or not),
- coating thickness and measuring method of the coating thickness,
- preparation of the surfaces before coating,
- evaluation of the critical slip load,
- calculation of the slip factor (considering the nominal, initial or actual [at slip] preloads),
- positioning of displacement transducers for the slip measurement,
- clamping length,
- test speed,
- coating material composition, etc.

For this reason, special care has to be taken when comparing slip factors of different investigations due to potential differences in the test specimens and in the way the slip factors were determined. Different guidelines/standards specify slip factors for slip-resistant connections made of carbon steel with some typical faying surfaces by various classes of friction surfaces. Different test procedures are also provided by

different guidelines/standards to determine the slip factor experimentally for deviating surface conditions. However, all regulations are valid for carbon steel only.

Nowadays, in different construction areas, using stainless steel is becoming more and more popular because of its high material strength, ductility and corrosion resistance. Existing design and execution codes/standards do not specify any rules for preloading of stainless-steel bolts and consequently no slip factors are proposed for slip-resistant connections made of stainless steel. Unlike carbon steel, stainless steel alloys are susceptible to viscoplastic deformation at room temperature. Therefore, preloaded bolted connections made of stainless steel may be subject to higher preload losses and consequently to lower slip factors. However, no evidence can be found in the literature to prove this negative influence. For this reason, slip factors for various stainless steel grades with different surface treatments must be determined experimentally if they are intended to be used in steel structures.

Some parts of the present work are based on two national and international projects. In the Euronorm project "Alternative Beschichtungssysteme für gleitfeste Verbindungen" funded by the Federal Ministry of Economics and Technology (Bundesministerium für Wirtschaft und Technologie), Germany, and EuroNorm GmbH via the programme INNO-KOM-Ost (MF130085) between October 2013 to September 2015, various aspects that could influence the slip-resistant behaviour of the connection were investigated, such as the composition of the coating material, the coating thickness and the level of roughness before the coating application. A comparative study was also conducted in order to investigate the determination of slip factors according to EN 1090-2, Annex G; and TL/TP-KOR-Stahlbauten, Annex E, Sheet 85. In this project, the Institute for Metal and Lightweight Structures (IML) (Essen, Germany) cooperated with the Institut für Korrosionsschutz Dresden GmbH (Dresden, Germany), which has expertise in the fields of corrosion protection.

The second project was conducted in the frame of the European research project "Execution and reliability of slip-resistant connections for steel structures using CS and SS" SIROCO (RF SR-CT-2014-00024) funded by the Research Fund for Coal and Steel (RFCS) of the European Commission from July 2014 until June 2017. The research consortium consisted of the following eleven European partners (in alphabetical order): ARUP Group engineering company (London, UK), BUMAX AB (part of Bufab Group, Åshammar, Sweden), European General Galvanizers Association LBG EGGA (Reddicroft, UK), Fraunhofer Research Institution for Large Structures in Production Engineering IGP (Rostock, Germany), Institut für Korrosionsschutz Dresden GmbH (Dresden, Germany), Outokumpu Stainless AB (Avesta, Sweden), Outokumpu Stainless Oy (Tornio, Finland), Teknologian Tutkimuskeskus VTT Oy (Espoo, Finland), The Steel Construction Institute SCI (Ascot, UK), Delft University of Technology, Steel and Timber Department (Delft, The Netherlands) and University of Duisburg-Essen, Institute for Metal and Lightweight

Structures (project coordinator, Essen, Germany). In the frame of this project, it was intended to provide a more clear and improved test procedure to determine the slip factor, to develop innovative surface preparation systems and preloading methods, to close information gaps for slip-resistant connections with hot dip galvanized surfaces, and to solve the lack of knowledge in the design of slip-resistant connections made of stainless steel, etc.

The achievements in both projects associated with this work are presented in different chapters. The rest of this work is independent research conducted at the Institute for Metal and Lightweight Structures in order to cover other aspects of slip-resistant connections made of carbon and stainless steels.

1.3 Outline

A comprehensive investigation is needed in order to close the gap in knowledge for the slip-resistant behaviour of preloaded bolted connections and the execution of slip-resistant connections made of stainless steel.

Chapter 2 contains a brief introductory description of two key parameters that can influence the slip-resistant behaviour of connections. A comprehensive literature review was conducted on available results based on national and international studies.

Various slip factor test procedures are also explained in detail. Different test procedures may affect the determination of the slip factor and lead to completely different slip factors for identical surface preparation.

In many cases, the suggested slip factor values from various standards or studies for the same surface preparations are not comparable. Many different parameters may influence the slip-resistant behaviour of the connections. In *Chapter 3*, a comprehensive investigation was conducted in order to take a closer look at parameters which may influence the determination of the slip factor.

In corrosive environments, the application of slip-resistant connections made of stainless steel is required. However, according to EN 1090-2, preloading of stainless steel bolting assemblies is currently not permitted. The lack of knowledge about the viscoplastic behaviour of stainless steel bolting assemblies is the main obstacle to application of stainless steel for structural purposes. The susceptibility of stainless steel material to viscoplastic deformation may cause additional loss of preload in preloaded bolted connections made of stainless steel. In *Chapter 4*, a comprehensive study was conducted on different grades of stainless steel in order to estimate the loss of preload in the lifetime of the structure. The result was also compared with the results of preloaded bolted connections made of carbon steel.

All presented slip factors in different standards are valid only for slip-resistant connections made of carbon steel. For this reason, an experimental investigation was conducted in *Chapter 5* in order to determine slip factors for different stainless steel

grades with different surface preparations. The slip factor tests were carried out on different treated/untreated faying surfaces. The influence of an additional coating on the slip-resistant behaviour of the connections made of stainless steel was also investigated. Finally, an alternative surface preparation was developed in order to improve the slip-resistant behaviour of untreated faying surfaces, without spending considerable amounts of time and money for the preparation of the faying surfaces.

Different guidelines/standards specify different test procedures for the determination of the slip factor. However, the question arises whether the comparability of the test results is guaranteed. In *Chapter 6*, three different test procedures (EN 1090-2 [17], RCSC [18] and TL/TP-KOR-Stahlbauten [19]) were considered in order to investigate the comparability of the slip factor results.

Furthermore, in *Chapter 7*, a simplified test procedure on the basis of EN 1090-2 and RCSC was developed in order to reduce the size of the test specimens and subsequently the amount of required material, preparation cost, required equipment and hours of labour for performing the tests.

Chapter 8 describes the amendments for different standards, regarding the classifications for slip-resistant connections made of stainless steel and also the simplified test procedure for determination of slip factor tests.

Chapter 9 provides a conclusion based on all numerical and experimental investigations carried out in the frame of this study. This chapter also provides an outlook on future investigations to cover other issues regarding slip-resistant connections made of carbon or stainless steel.

2 State of the art

2.1 General

Slip-resistant connections are a type of preloaded bolted structural steel connection which relies on friction between the faying surfaces that develops with preloading of the high-strength bolts. This type of connection is always used when the connection has to be designed with particularly low slip displacement. When a slip-resistant connection fails, it changes to a bearing-type connection which still can transfer structural forces.

As already mentioned, the performance of slip-resistant connections is mainly influenced by the condition of the faying surfaces and the existing preload level in the bolts. Different guidelines and standards permit some permissible surface treatments for faying surfaces of slip-resistant connections and specify the corresponding slip factors. For other surface conditions not considered in these guidelines/standards or if higher slip factors are required, the slip factor must be determined experimentally according to the specified test procedures.

However, practice has shown that using different test procedures or different interpretations in a testing procedure may lead to incomparable results for identical surface preparations. Many previous studies, standards and guidelines specify different slip factor values for exactly the same surface preparations.

The existing preload level in the bolts influences the slip-resistant behaviour of the connection as well. For this reason, the potential loss of preload must be taken into account during design and execution of steel structures. Therefore, it is necessary to understand this phenomenon more deeply.

2.2 Existing preload level in preloaded bolted connections

In order to guarantee a sufficient preload level in a preloaded bolted connection, various influencing factors must be carefully considered. For this purpose, special attention has to be paid to both tightening methods and the loss of preload over time. A great deal of research has been carried out in order to investigate the loss of preload in preloaded bolted connections. It is generally known that the preload in the bolt is not a constant value but a function of time which decreases when time elapses.

The existing level of preload in the bolts has a direct influence on the slip-resistant behaviour of the connections. The loss of preload in the bolted connections must be realistically estimated and implicitly considered in the design and execution of the structure in such a way that a sufficient preload level remains in the connection during the service life of the structure. Losing preload during the lifetime of slip-resistant connections might lead to unexpected slip and consequently cause failure in the bolted connection.

Many studies [20]-[26] have been conducted in order to better understand the relaxation behaviour of preloaded bolted connections. The preload losses mainly occur due to following reasons:

1. Embedment/plastic deformation of the clamped component surfaces (so-called setting effect): generally, embedment occurs at any surfaces like the threads of the nuts and the bolts, washers and the faying surfaces of the clamped components.

2. Creep/plastic deformation of applied coatings: coated surfaces are susceptible to creep in the coating, and it can lead to a reduction in the shear capacity of the preloaded bolted connection. Previous studies show that an increase in coating thickness would lead to a higher loss of preload in preloaded bolted connections [27], [28], [29].

3. Viscoplastic deformation behaviour (or creep and stress-relaxation) of the structural elements themselves: depending on the type of steel (carbon/stainless steel), this parameter may become more critical for relaxation behaviour of the preloaded bolted connections.

4. Self-loosening in the bolted connection during the operational period; repeated transverse displacements, vibration or thermal cycles may cause micro-movements between the bolt thread and the nut.

Sedlacek and Kammel [30], [31] summarise that the possible loss of preload in slip-resistant connections occurs due to embedment, relaxation, transversal contraction and axial tensile load, while the dynamic load can cause self-loosening in the preloaded bolted connection.

The first drop in the level of preload happens directly after the tightening of the bolt and then gradually decreases as time elapses. The short-term relaxation starts directly after the first drop in the preload level. Different parameters affect short-term relaxation behaviour, such as tightening speed, number of clamped components, clamping length, etc. [21].

Many studies have been conducted in order to investigate the relaxation behaviour of preloaded bolted connections [25], [30], [31], [32], [33]. However, most of these studies consider carbon steel bolted connections. The first investigation regarding loss of preload in bolted connections made of austenitic stainless steel, property classes 70 and 80, was presented by Shemwell and Johns [34]. Unfortunately, these results do not cover other types and property classes of stainless steel bolting assemblies and clamped components.

There are many parameters that contribute to relaxation in preloaded bolted connections, which makes it difficult to predict the actual amount of the loss of preload in the life time of structures. Many attempts have been made in order to finalize an equation to calculate the amount of loss of preload [23], [27], [35].

However, in many cases the results are not accurate enough and the amount of loss of preload has to be determined from experimental investigations.

To close the still existing gaps, a systematic investigation into the loss of preload of stainless steel bolting assemblies has to be carried out.

2.3 Condition of faying surfaces

2.3.1 General

The condition of faying surfaces is one of the main factors that has a great influence on the slip-resistant behaviour of the connection. A high slip factor can be achieved by grit blasted surfaces, but the exposed elements in the connection may be subject to different environmental conditions. Using a protective layer on the surfaces is a common way to prevent corrosion. However, having an additional layer on faying surfaces may influence the slip-resistant behaviour of the connection. The main aim of the following chapters is to compare some of the common surface treatments and their slip factors.

2.3.2 Faying surfaces without any coating

Although no additional layer between the surfaces exists, different slip factor values can be found in the literatures for untreated and blasted surfaces, see Table 2-1.

Blasting of the faying surfaces is a common way to achieve higher slip factor. Selection of the blasting media is a crucial decision in the blasting process. In principle, abrasive blasting processes can be categorized into two main groups according to the shape of the blasting media: grit blasting and shot blasting. The blasting media for the grit blasted process have an angular shape, while the shape of particles for the shot blasting process is spherical. In both processes, the faying surfaces are subjected to successive bombardment by high-velocity abrasive particles.

Using these two different methods may result in different surface roughnesses and topographies for the surfaces and consequently different slip factors. Other important variables in the blasting process are media type, size, particle velocity (blast pressure), distance, and the angle of the blast stream. All these parameters may affect the quality of the blasted surfaces. However, in many literatures, standards and guidelines, the influence of these important factors is neglected and both shot- and grit-blasted surfaces categorised as one group with the same slip factor, see Table 2-1. The Japan Society of Civil Engineers (JSCE:2009) presented the roughness of the faying surfaces as an essential factor on determination of the slip factor. Having different grades of steel may also lead to different slip factors, see Table 2-1. However this influence is not clear in all cases.

The field exposure condition may also have an influence on the slip-resistant behaviour of the connections, see [36], [37].

Table 2-1: Slip factors for uncoated faying surfaces reviewed from literature

Surface condition		Slip factor [-]	Reference
No treatment			
Surfaces as rolled / untreated		0.20	EN 1090-2 [17]
			ECCS No. 37 [38]
			ECCS No. 38 [39]
			BS 5950-1:2000 [40]
			IS 800:2007 [41]
			IS 4000:1992 [42]
Mill scale		0.28	Dusel et al. [43]
		0.36	Young and Hechtman [44]
		0.44 - 0.49	Rumpf [45]
Dry mill scale		0.30-0.46	
Mill scale had been removed		0.20 – 0.34	Hansen and Rumpf [46]
Hand wire brushing only		0.38 – 0.54	
Removed loose mill scale only		0.31 – 0.46	
Ideally rusted surface obtained with chemicals		0.45	JSCE:2009 [47]
Blast cleaned			
Heavily rusted (pitting), without mill scale, blasted		0.30	ECCS-TC 10 [38]
Grit blasted and oiled		0.25	Owens and Cheal [48]
Very high tensile steel, grit blasted		0.33	
Rust-free blast cleaned surface obtained by shot/grit blasting	(indefinite roughness)	0.35	JSCE:2009 [47]
	(10 μm > Ra ≥ 5 μm)	0.40	
	(Ra ≥ 10μm)	0.45	
Grit or shot blasted, Grades 43 or 50		0.48	Owens and Cheal [48]
With shot or grit, degree Sa 2 ½ (S275 and S 690)		0.50	Cruz et al. [49]
Grit blasted (different steel grades)		0.33 - 0.54	Kulak et al. [50]
			Kulak and Fisher [51]
Surfaces blasted with shot or grit with loose rust removed, not pitted		0.50	EN 1090-2 [17]
			ISO 10721-1 [52]
			ECCS No. 38 [39]
			BS 5400-3 [53]
			IS 800:2007 [41]
			IS 4000:1992 [42]
With sand, degree Sa 2 ½ (S 275)		0.48	Cruz et al. [49]
Sand blasted surface, after light rusting		0.52	IS 800:2007 [41]
		0.48	
Sand blasted surface		0.49	Dusel et al. [43]
		0.45 - 0.50	Kim et al. [54]
		0.52	Kulak et al. [50]
			Kulak and Fisher [51]
		0.38 - 0.59	Young and Hechtman [44]
Blast cleaned with Class A coatings		0.33	AASHTO [55]
Blast cleaned or blast cleaned with Class B coatings		0.50	CAN/CSA-S16-09 [59]
With complete mill scale, blasted (removal of all mill scale) Rusted (no pitting), with/without mill scale blasted (removal of all mill scale)		0.50	ECCS No. 37 [38]
Blasted surfaces (Sa 2 ½)		0.50	DIN 18800-7 [56]
Unpainted blast cleaned steel surfaces		0.50	RCSC:2014 [18]
			ANSI/AISC 360-16 [57]
Blast cleaning	(steel grade Q235)	0.45	GB 50017-2003 [58]
	(steel grades Q345, Q390 and Q420)	0.50	
Rusted after blast-cleaning (steel grades Q345, Q390 and Q420)		0.50	

Cont. Table 2-1: Slip factors for uncoated faying surfaces reviewed from literature

Cleaned			
Rough rust-free surface formed with disk grinder		0.25	JSCE:2009 [47]
Unpainted clean mill scale steel surfaces		0.30	RCSC:2014 [18]
			ANSI/AISC 360-16 [57]
Clean mill scale		0.33	IS 800:2007 [41]
			Owens and Cheal [48]
			AASHTO [55]
			CAN/CSA-S16-09 [59]
Clean mill scale (different steel grades)		0.23 - 0.33	Kulak et al. [50]
			Kulak and Fisher [51]
Clean as-rolled surfaces		0.35	AS 4100:1998 [60]
			NZS 3404: 1997 [61]
Tightly adhering clean mill scale, except for quenched and tempered steels		0.33	ISO 10721-1 [52]
For weathered steel clear of all mill scale and with any loose rust removed		0.40	
Flame cleaned, loose rust removed, tight mill scale		0.30	BS 5950-1:2000 [40]
Wire brushed, loose rust removed, tight mill scale		0.30	
Hand-cleaned with wire brush	(steel grade Q235)	0.30	
	(steel grades Q345 and Q390)	0.35	
	(steel grade Q420)	0.40	
Untreated as rolled clean surfaces	(steel grade Q235)	0.30	GB 50017-2003 [58]
	(steel grades Q345 and Q390)	0.35	
	(steel grade Q420)	0.40	
Weathered surfaces clear of all mill scale and loose rust		0.45*	BS 5400-3 [62]
Ideally rusted surface, Unpainted clean mill scale with ideal amount of rust		0.55	JSCE:2009 [47]
* The slip factors should be reduced by 10 % where higher grade bolts in accordance with BS 4395-2 are used.			

2.3.3 Inorganic and organic zinc primer

Inorganic and organic zinc primers are very efficient coatings that provide galvanic protection. SSPC is an American National Standards Institute accredited standards development organization which describes two different types of zinc-rich coatings in the frame of SSPC Paint Specification No. 20 [64]: Inorganic (Type I) and organic (Type II). Inorganic zinc-rich coating is divided into three different groups based on the vehicle type: 1.Type I-A (inorganic post-curing vehicles – water soluble), like alkali-zinc silicate (ASI) coating; 2.Type I-B (inorganic self-curing vehicles – water reducible); and 3.Type I-C (inorganic self-curing vehicles – solvent reducible), like ethyl-zinc silicate (ESI) coating.

All these zinc dust primers may consist of one, two or three components. Both ASI- and ESI-coating systems are common inorganic zinc primers for slip-resistant connections used to achieve a relatively high slip factor and an excellent corrosion protection effect. In Germany, alkali-zinc silicate (ASI-) coating is a common coating system and ethyl-zinc silicate is used around the world for its corrosion protection properties in aggressive environments. However, as a result of the additional layers, some other factors, like coating thickness and composition of the coating material,

may also influence the slip-resistant behaviour of the connection. For this reason, a literature review is conducted to check the variety of the slip factor for coated faying surfaces with inorganic zinc primer, see Table 2-2.

Table 2-2: Slip factors for inorganic zinc primers reviewed from literature

Surface condition		Slip factor [-]	Reference
Coated with alkali-zinc silicate paint with a nominal thickness of 60 µm (dry thickness to be within 40 µm to 80 µm range)		0.40	EN 1090-2 [17]
Surfaces blasted with shot or grit: …b) with alkali-zinc silicate paint with a thickness of 50 µm to 80 µm		0.40	ECCS No. 37 [38]
Blasted and alkali-zinc silicate paint (thickness 20 to 50 µm)		0.30	
Surfaces blasted with shot or grit and painted with alkali-zinc silicate coat (thickness 60 to 80 µm)		0.40	ECCS No. 38 [39]
Surfaces painted with alkali-zinc-silicate (thickness 40 µm)		0.50	DIN 18800-7 [56]/ TL/TP-KOR [19]
Painted with zinc silicate coat, thickness < 60 µmm		0.50	ISO 10721-1 [52]
Painted with zinc dust coat, thickness < 60 µmm		0.35	
Surfaces treated with zinc silicate paint (The slip factor should be reduced by 10 % where higher grade bolts in accordance with BS 4395-2 are used.)		0.35	BS 5400-3 [62]
Inorganic zinc paint coated after blast-cleaning (steel grade Q235)		0.35	GB 50017-2003 [58]
Inorganic zinc paint coated after blast-cleaning (steel grades Q345, Q390 and Q420)		0.40	
Surfaces blasted with shot or grit and painted with alkali-zinc silicate coat (thickness 60-80 µm)		0.30	IS 800:2007 [41] / IS 4000:1992 [42]
Surfaces painted with alkali-zinc silicate (50 µm to 80 µm)		0.46	Owens and Cheal [48]
Grit or shot blasted and coated with zinc silicate primer		0.35 - 0.65	Cheal [63]
Blasted and ethyl-zinc silicate paint (thickness 20 to 50 µm)		0.30	ECCS No. 37 [38]
Blasted and ethyl-zinc silicate paint (thickness 50 to 80 µm)		0.35	
Surfaces blasted with shot or grit and painted with ethyl-zinc silicate coat (thickness 30 to 60 µm)		0.30	ECCS No. 38 [39]
Surfaces blasted with shot or grit and painted with ethyl-zinc silicate coat (thickness 60 to 80 µm)		0.35	
Blast cleaned, inorganic zinc-rich paint		0.50	Kulak et al. [50]
Surfaces treated with zinc silicate paint		0.35	BS 5400-3 [53]
Surfaces blasted with shot or grit and painted with ethyl zinc silicate coat (thickness 30-60) or (thickness 60-80)		0.30	IS 800:2007 [41] / IS 4000:1992 [42]
Blasting with shot or grit, Sa 2 ½, painted with zinc ethyl-silicate (one layer) with 70 µm		0.40	Cruz et al. [49]
Inorganic zinc paint coated after blast cleaning (steel grade Q235)		0.35	GB 50017-2003 [58]
Inorganic zinc paint coated after blast cleaning (steel grades Q345, Q390 and Q420)		0.40	
Inorganic zinc-rich paint	(paint thickness ≤ 65 µm)	0.40	JSCE:2009 [47]
	(paint thickness ≥ 65 µm)	0.50	
Inorganic zinc-rich paint, film thickness of 50 µm ~ 150 µm	Ra ≥ 5 µm	0.40	Tamba et al. [65]
	Ra < 5 µm	0.20	
Inorganic zinc-rich primer, coating thickness about 3 to 4 mils		0.55	Lower [66]
Grit blasted, Zinc silicate primer	Preload level: 160 kN	0.43	Black and Moss [67]
	Preload level: 210 kN	0.40	
	Preload level: 260 kN	0.32	
Shot blasted, Zinc silicate primer	Preload level: 160 kN	0.51	
	Preload level: 210 kN	0.48	
	Preload level: 260 kN	0.42	

This table shows the variety of the slip factor for inorganic zinc primers. The slip factors vary between 0.2 and 0.65. This shows that not only is the type of coating important but the composition of the coating could also be highly critical in determining the slip factor. Beside these parameters, the coating thickness and the preload level could also have a direct influence on slip-resistant behaviour of the connection. Table 2-3 shows the slip factor results for organic zinc primers like epoxy zinc coating systems which also deliver different slip factors. By comparing the results from literature research, it seems that the higher slip factor is more likely to be achieved with inorganic zinc primers. However, this phenomenon cannot be confirmed in all cases.

Table 2-3: Slip factors for organic zinc primers reviewed from literature

Surface condition		Slip factor [-]	Reference
Blast cleaned, organic zinc-rich paint		0.35	Kulak et al. [50]
Organic zinc-rich paint		N/S*	JSCE:2009 [47]
Organic Zn – coating thickness 1.5 mils		0.38	Dusel et al. [43]
Organic Zn – coating thickness 3 mils		0.33	
Organic Zn – coating thickness 6 mils		0.27	
With sand, degree Sa 2 ½, painted with zinc epoxy (one layer) with 70 μm	S 275	0.30	Cruz et al. [49]
	S 690	0.20	
Organic zinc-rich primer, coating thickness about 6 to 7 mils		0.39	Lower [66]
Blast cleaned + phenoxy base organic zinc		0.47	Frank and Yura [68]
* Slip factor test shall be performed			

2.3.4 Spray metallized coatings

Thermal spraying is a process of applying a metallic coating to a surface using a heat source (flame or electric arc) and a coating material (zinc, aluminium, or zinc-aluminium alloy) in a powder or wire form. Compressed air is concentrated around the heat source and sprays the melted coating material onto the surface at high velocity. Metallizing is commonly used as a protective layer to protect metal surfaces against corrosion or as a slip-resistant coating. By considering the type of coating materials, different slip factors are reported in the literature, see Table 2-4.

Table 2-4: Slip factors for thermal spray and metallized faying surfaces reviewed from literature

Surface condition		Slip factor [-]	Reference
Aluminium spray metallized			
Spray metallized with aluminium, thickness > 50 μmm		0.55	ISO 10721-1 [52]
Blasted and sprayed with aluminium (thickness 50-120 μm)		0.50	ECCS No. 37 [38]
Surfaces blasted with shot or grit and spray metallized with aluminium (thickness > 50 μm)		0.50	ECCS No. 38 [39] / IS 800:2007 [41] / IS 4000:1992 [42]
Blast cleaned, aluminium sprayed (t > 2mils)		0.55	Kulak et al. [50]
Surfaces sprayed with aluminium		0.50	BS 5400-3 [62]
Blasted with shot or grit, spray metallized with aluminium		0.50	BS 5950-1:2000 [40]
Metal sprayed with aluminium		0.51	Owens and Cheal [48]
Grit blasted, aluminium metal spray (powder process)	Preload level: 160 kN	0.71	Black and Moss [67]
	Preload level: 210 kN	0.65	
	Preload level: 260 kN	0.60	

Cont. Table 2-4: Slip factors for thermal spray and metallized faying surfaces reviewed from literature

Zinc spray metallized			
Spray metallized with zinc, thickness > 50 μmm		0.40	ISO 10721-1 [52]
Blasted and sprayed with zinc (thickness 20-110 μm)		0.25	ECCS No. 37 [38]
Surfaces blasted with shot or grit and spray metallized with zinc (thickness 50-70 μm)		0.25	ECCS No. 38 [39] / IS 800:2007 [41] / IS 4000:1992 [42]
Blast cleaned zinc sprayed (t > 2 mils)		0.40	Kulak et al. [50]
Surfaces sprayed with zinc		0.40	BS 5400-3 [62]
Blasted with shot or grit, spray metallized with zinc based coating that has been demonstrated to provide a slip factor of at least 0.5		0.50	BS 5950-1:2000 [40]
Blasted with shot or grit, spray metallized with zinc		0.40	
Metal sprayed with zinc		0.46	Owens and Cheal [48]
Shot or grit blasted, degree Sa 3, spray metallized with zinc, coating thickness 75 μm, steel grades S 690 and S 275		0.40	Cruz et al. [49]
Grit blasted, zinc metal spray (powder process)	Preload level: 160 kN	0.59	Black and Moss [67]
	Preload level: 210 kN	0.56	
	Preload level: 260 kN	0.54	
Grit blasted, zinc metal spray (wire process)	Preload level: 160 kN	0.62	
	Preload level: 210 kN	0.55	
	Preload level: 260 kN	0.48	
Metallized surfaces with zinc with different coating thicknesses and preload levels in tension and compression (static tests only)		0.77 – 0.98	Annan and Chiza [69]
Combined zinc metallized–galvanized faying surfaces with different coating thicknesses and preload levels in tension and compression (static tests only)		0.49 – 0.77	Annan and Chiza [70]
Aluminium or zinc spray metalized			
Thermally sprayed with aluminium or zinc or a combination of both to a nominal thickness not exceeding 80 μm		0.40	EN 1090-2 [17]
Metallic spray		N/S*	JSCE:2009 [47]
Metallized		0.48	Kulak and Fisher [51]
Metallized with zinc or aluminium		0.56	Frank and Yura [68]
Aluminium/zinc spray metallized			
Sand blast + Zn/Al metal spraying		0.52 – 0.57	Kim et al. [54]
Grinding + Zn/Al metal spraying		0.43	
Metal sprayed aluminium on zinc		0.49	Owens and Cheal [48]
* Slip factor test shall be performed			

2.3.5 Hot dip galvanized surfaces

Another common protective coating system for carbon steel surfaces is hot dip galvanizing (HDG) according to EN ISO 1461 [71]. Previous studies also show a large variation in slip factors for treated and untreated galvanized faying surfaces, see Table 2-5. The causes of the scattering are the thickness and structure of the coating. These two parameters can be influenced dependent on factors such as the chemical composition of the steel (like silicon content), the thermal mass of the steel component and other galvanizing process variables. Each of these parameters can lead to the creation of a soft layer of pure zinc on the component surfaces which could directly have a negative influence on the slip resistance of the connection. In order to achieve a higher slip factor, the pure zinc layer can be easily removed by

sweep blasting or other techniques or can even be additionally coated with alkali- or ethyl-zinc silicate.

Table 2-5: Slip factors for hot dip galvanized faying surfaces reviewed from literature

Surface condition	Slip factor [-]	Reference
Without any post-treatments		
Hot dip zinc metalized	0.18	ISO 10721-1 [52]
Hot dip galvanized (thickness 80 to140 µm)	0.10	ECCS No. 37 [38]
Surfaces blasted with shot or grit and hot dip galvanized	0.10	ECCS No. 38 [39]
Hot dip galvanized	0.18	Kulak et al. [50]
Surfaces blasted with shot or grit and hot dip galvanized	0.10	IS 800:2007 [41] / IS 4000:1992 [42]
Galvanized	0.20	BS 5950-1:2000 [40]
Hot dip galvanized	N/S*	JSCE:2009 [47]
	0.18	Kulak and Fisher [51]
Galvanized	0.20	Owens and Cheal [48]
Chemical cleaning, hot dip galvanization with a thickness of 160 µm	0.40	Cruz et al. [49] Heistermann et al. [72]
Hot dip galvanized surfaces	0.20-0.34	Valtinat [73]
Hot dip galvanized surfaces – as received	0.21	Birkemoe and Herrschaft [74]
Hot dip galvanized surfaces – weathered	0.20	
Hot dip galvanized + cleaned with acetone	0.32	Black and Moss [67]
With post-treatments		
Hot dipped galvanized and roughened surfaces	0.30	RCSC:2014 [18]/ ANSI/AISC 360-16 [57]
Hot dip galvanized surfaces roughened by wire brushing after galvanizing	0.33	AASHTO:2012 [55]
Galvanized, subsequently wire brushed or grit blasted	0.41	Owens and Cheal [48]
Hot dip galvanized + wire brushed	0.37	Black and Moss [67]
Hot dip galvanized, treated, wire brushed or blasted	0.40	Kulak et al. [50]
Surfaces hot dip galvanized to EN ISO 1461 and flash (sweep) blasted (or equivalent abrasion method)	0.35	EN 1090-2 [17]
Hot dip zinc metallized and lightly blasted, thickness > 50 µmm	0.40	ISO 10721-1 [52]
Galvanized and sand blasted	0.34	Kulak et al. [50]
Hot dip galvanized surfaces, slightly blasted (sweep blasted)	0.20	Valtinat et al. [75]
Hot dip galvanized + sand blasted	0.44	Black and Moss [67]
Surfaces hot dip galvanized to EN ISO 1461 and flash (sweep) blasted and with alkali-zinc silicate paint with a nominal thickness of 60 µm (Dry thickness to be within 40 µm to 80 µm range)	0.40	EN 1090-2 [17]
Hot dip galvanized + alkali-zinc silicate paint finishing coat (thickness 80 to140 µm) and (thickness 50 to 80 µm)	0.20	ECCS No. 37 [38]
Surfaces blasted with shot or grit and hot dip galvanized (thickness 80 to100 µm) and then painted with alkali-zinc silicate coat (thickness 60 to 80 µm)	0.20	ECCS No. 38 [39]
Hot dip galvanized surfaces, degreasing and coated with zinc silicate primer	0.45	Valtinat et al. [75]
Hot dip galvanized + alkali-zinc silicate	0.5	Valtinat [73]
Hot dip galvanized and roughened + epoxy-base organic zinc	0.40	Frank and Yura [68]
Hot dip galvanized + phosphate	0.38	Black and Moss [67]
Hot dip galvanized + chromate	0.26	
* Slip factor test shall be performed		

2.3.6 Further important influencing parameters

It can be seen from the literature that there is potential to have different slip factors for identical surface conditions and the same preload level. Besides these two important parameters (preload level and the condition of faying surfaces), many other factors may influence the determination of the slip factor. The roughness of the surfaces before the coating application, the composition of the coating material, the coating thickness, the positioning of displacement transducers to measure the slip in the connection, the clamping length, the test speed, the evaluation of the slip factor based on static tests only or extended creep tests and many other parameters may all potentially influence the slip-resistant behaviour of the connection.

In addition to all the studies mentioned above, many others have been conducted on this topic, such as [76] – [83], but none has specifically tried to investigate the influence of each parameter individually. In the frame of this thesis, all these parameters were investigated in order to close the gap of knowledge in this area.

2.4 Determination of the slip factor

2.4.1 General

The slip factor can be determined experimentally according to the specified test procedures. However, the test procedures given in different standards/ recommendations vary between countries. In some cases, not only the test procedure but also the geometry of the test specimen, the clamping length, the preload level and even the type of evaluation of the slip factor differs. Generally, the resistance to slip in a slip-resistant connection mainly depends on the condition of the faying surfaces and the existing preload level in the bolts, but the variation of other key parameters may lead to different slip factors for the identical surface treatments as well.

2.4.2 EN 1090-2, Annex G – European standard

2.4.2.1 General

Some results of the current study which were part of the European research project SIROCO have already been implemented in the latest version of Annex G of EN 1090-2 which was published in 2018. The following test procedure is the optimized test procedure compared to EN 1090-2:2011. The differences between these two versions of the test procedures are presented in Chapter 2.4.2.3.

2.4.2.2 Test procedure according to EN 1090-2:2018, Annex G

EN 1090-2:2018 prescribes the minimum slip factor according to the specified class of friction surface, see Table 2-6. To use these values for design purposes no experimental investigation is required. Meanwhile, for the condition of surfaces other than those specified in Table 2-6, the slip factor shall be determined according to the test procedure prescribed in EN 1090-2:2018, Annex G.

According to this test procedure, the slip factor shall be determined by using two specified standard specimen geometries for M16 and M20 bolting assemblies, see Figure 2-1.

Table 2-6: Classifications that may be assumed for friction surfaces according to EN1090-2 [17]

Surface treatment	Class	Slip factor μ
Surfaces blasted with shot or grit with loose rust removed, not pitted	A	0.50
Surfaces hot dip galvanized to EN ISO 1461 and flash (sweep) blasted and with alkali-zinc silicate paint with a nominal thickness of 60 μm	B	0.40
Surfaces blasted with shot or grit: a) coated with alkali-zinc silicate paint with a nominal thickness of 60 μm; b) thermally sprayed with aluminium or zinc or a combination of both to a nominal thickness not exceeding 80 μm	B	0.40
Surfaces hot dip galvanized to EN ISO 1461 and flash (sweep) blasted (or equivalent abrasion method)	C	0.35
Surfaces cleaned by wire-brushing or flame cleaning, with loose rust removed	C	0.30
Surfaces as rolled	D	0.20

(a) For M20 bolting assemblies   (b) For M16 bolting assemblies
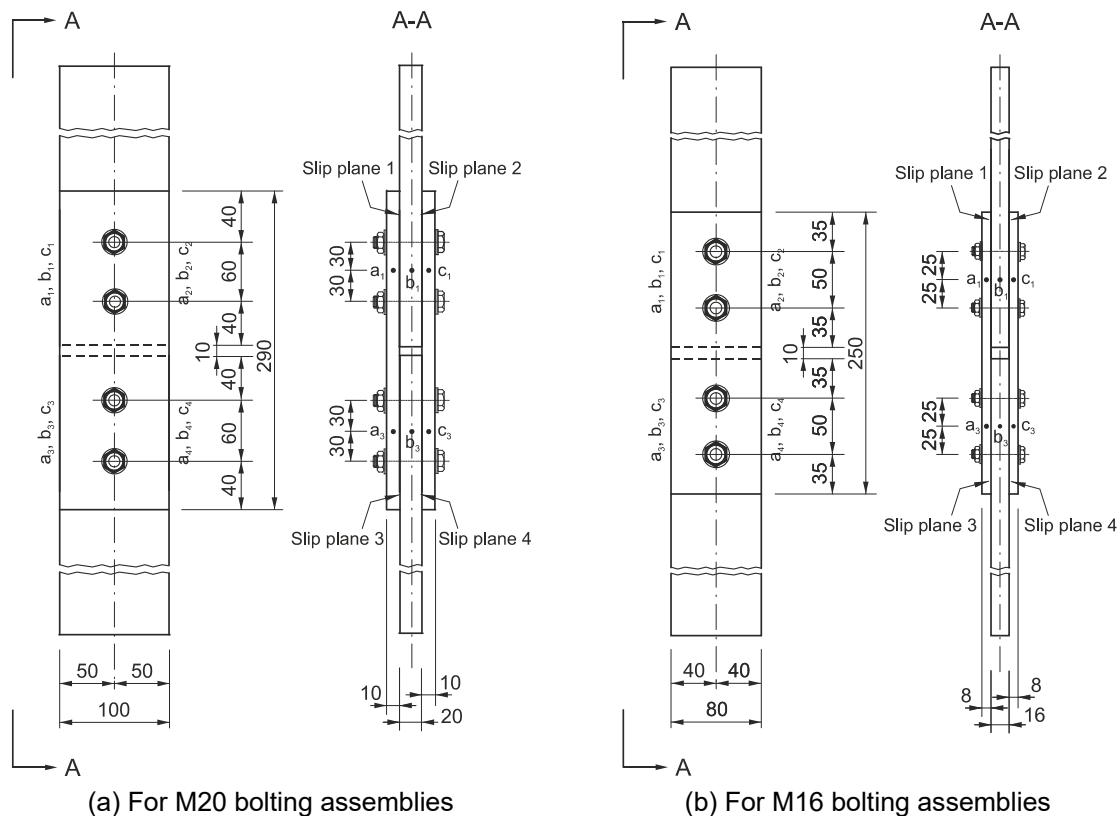
Figure 2-1: Test specimen geometry according to EN 1090-2, Annex G [17]

The slip factor test shall be performed in different steps, see Figure 2-2. In the first step, four static tests (st) must be carried out in tension at normal speed. All tests shall be performed in a tensile testing machine. The duration of each test must be about 10 to 15 min in order to minimize the influence of the test speed on determination of the critical slip load, see Chapter 3.2.5. The slip displacement must be measured as the relative displacement between specific points of the inner (b) and cover plate (a and c), as shown in Figure 2-1. Four slip planes can be defined for each test specimen in a failure mechanism, which can be either a combination of the

slip in slip planes 1 and 2, 3 and 4 or diagonal in slip planes 1 and 4 or 2 and 3. For this reason, the slip has to be evaluated according to the existing failure mechanism, so that two mean slip values shall be determined based on eight measured slip displacements; for more information see Chapter 3.2.8.
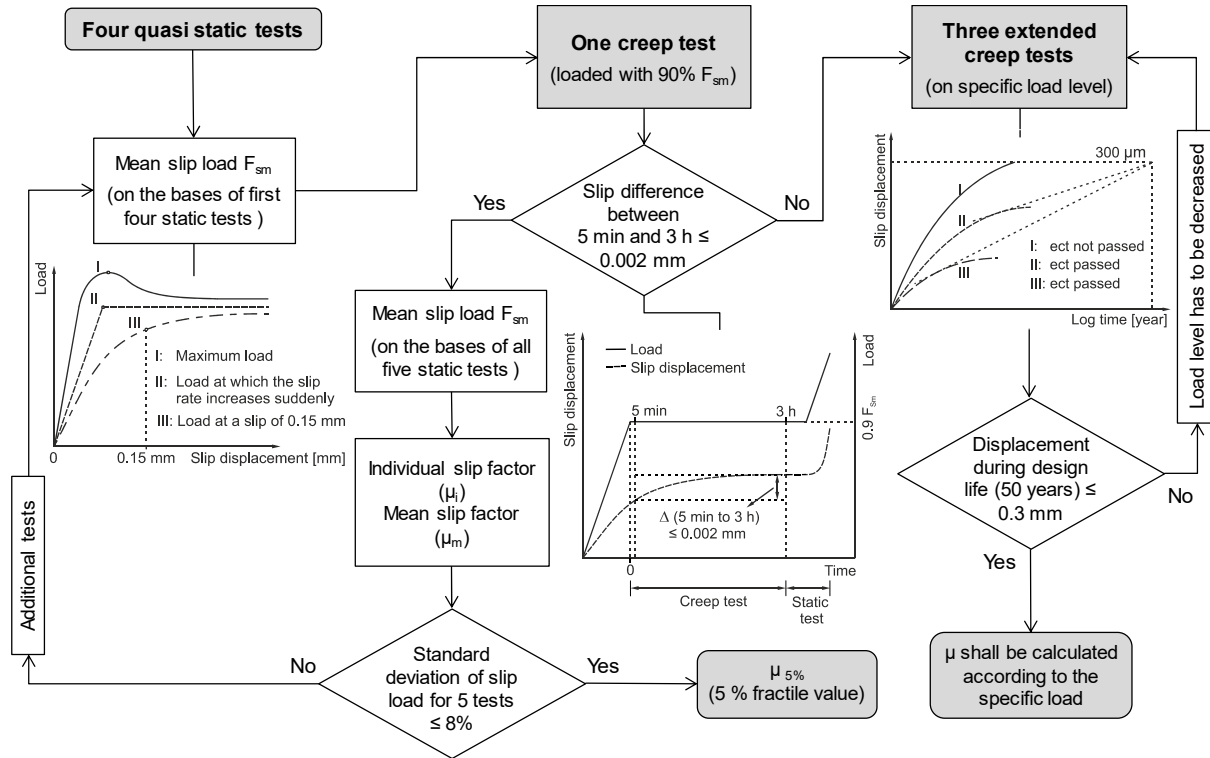
Figure 2-2: Slip factor test procedure acc. to EN 1090-2, Annex G

The individual slip load F_{Si} is defined at 0.15 mm slip displacement or at the peak before 0.15 mm in order to determine the real critical slip load in the connection, see Figure 2-3 (a). More information is presented in Chapter 3.2.4.

The slip factor for an individual specimen μ_i shall be calculated from Equation (2-1), and the mean slip load for one set of four specimens shall be calculated. The preload shall be measured directly with the equipment with an accuracy of $\pm$ 5 %. All the bolts shall be tightened within $\pm$ 5 % of the specified preload, $F_{p,C} = 0.7\ f_{ub}\ A_S$, where f_{ub} is the tensile strength of the bolt and A_S is the tensile stress area of the bolt.

$$\mu_i = \frac{F_{Si}}{4 \cdot F_{p,C}} \tag{2-1}$$

In the second step, the fifth test specimen shall be tested as a creep test (ct). The specimen must be loaded with 90 % of the mean slip load (F_{Sm}) of the four static tests. If the differences between the recorded slip displacement at five minutes and at three hours after reaching the constant load level do not exceed 0.002 mm, a static test must be carried out in order to determine the slip loads, see Figure 2-3 (b). If the standard deviation obtained from five tests exceeds 8 % of the mean value, additional tests have to be carried out. Otherwise, the characteristic value of the slip factor μ shall be calculated as the 5 % fractile value with a confidence level of 75 %.

If the creep test was not passed, at least three extended creep tests (ect) have to be carried out. All three tests have to be evaluated using an extrapolated slip displacement-log time curve. The test will be considered a passed test when the slip does not exceed 0.3 mm after extrapolation to 50 years or the service life of the structure, see Figure 2-3 (c).

According to this test procedure, both short-term and long-term behaviours shall be investigated. The creep and extended creep tests are designed to measure the creep sensitivity of the faying surfaces of the bolted connections under the constant load. The idea behind performing long-term tests is to ensure that the loss of preload in the bolts does not reduce the slip resistance of the connection.

(a) for evaluating the slip load   (b) for evaluating the creep test   (c) for evaluating the extended
        from the static test   creep test
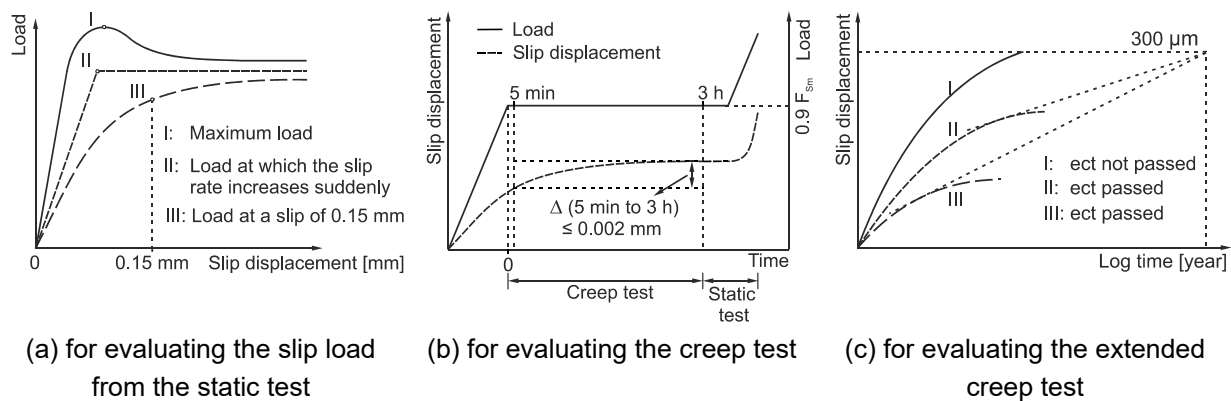
Figure 2-3: Related diagrams for evaluating the static, creep and extended creep tests

2.4.2.3 Differences between EN 1090-2, Annex G 2011 and 2018 versions

As already mentioned, the slip test procedure according to EN 1090-2:2011, Annex G was not clear in some aspects. In the frame of the SIROCO project, many questions regarding slip-resistant connection have been answered. Based on this knowledge, an attempt was made to clarify the slip factor test procedure in the 2018 version.

According to the 2011 version, the slip displacement shall be measured in the direction of the applied load, as the relative displacement between adjacent points on an inner plate and a cover plate. However, the exact position of these points was not clear and allows several possible interpretations. This could potentially lead to a measured slip displacement at a wrong position which consequently could influence the determination of the slip factor. For this reason, in the 2018 version the slip mechanism in the slip-resistant connection was explained in detail and the correct position for measuring the slip displacement stated clearly to prevent any misunderstanding (more information in Chapter 3.2.8).

In the 2011 version, the individual slip load for a connection was defined as the load at which a slip displacement of 0.15 mm occurs. However, as can be seen in Figure 2-3 (a), evaluating the slip factor exactly at 0.15 mm might result in large differences in the slip load. This problem was also addressed clearly in the 2018 version (more

information in Chapter 3.2.4). Other improvements in the 2018 version are aimed at clarification of wording and also the definition of the slip mechanism in slip-resistant connections.

2.4.3 Karlsruhe tests

In 1953, the Karlsruhe University of Applied Sciences started a comprehensive study on the application of pretensioned bolts in steel construction. This study is presented in four different parts, [8]-[11]. The slip-resistant connections were a focus in this study. In the frame of this investigation, a series of tests was carried out on slip-resistant connections in order to acquire the basic knowledge for the application of such connections in steel construction. In this study different test specimens were considered for determination of the slip factor, see Figure 2-4.

(a) Tension-type specimens

(b) Compression-type specimens
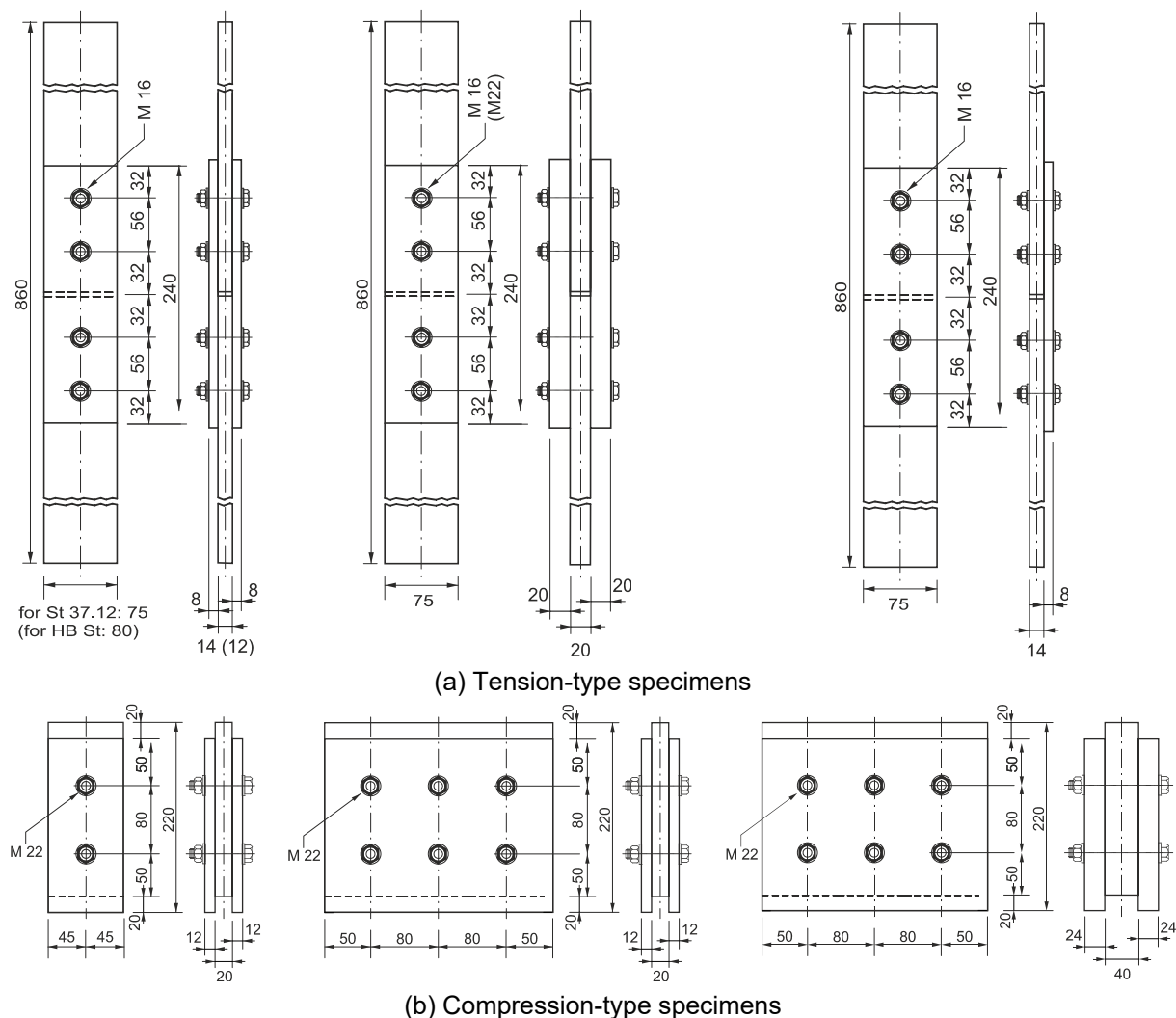
Figure 2-4: Test specimen geometry in Karlsruhe tests [8]

The specimens were made of structural carbon steel St 37 according to DIN 17100 [84] (comparable to S235 according to EN 10025-2 [85]). M16 and M22 bolting assemblies were used in this investigation. The relative slip displacement was measured by dial gauges somewhere in the middle of the test specimens on both sides.

The slip load (P_g) was defined as the corresponding load when a sudden slip displacement occurred. The slip factor (μ) were calculated from Equation (2-2), where n is the number of bolts per connection, m is the number of interfaces per connection and P_v is the preload level in the bolts.

$$\mu = \frac{P_g}{m \cdot n \cdot P_v}$$

(2-2)

The main focus of this study was on slip-resistant connection under static load. In this study different surface conditions were investigated. Different tests were carried out under both tension and compression. However, no comparative investigation was conducted to compare the influence of the type of the test on determination of the slip factor.

2.4.4 ORE - D 90

In the 60s and early 70s, a comprehensive investigation was conducted on the problems of connections with high-strength preloaded bolts in steel structures. The execution of the experimental investigation was carried out at the Official Research and Material Testing Institute for Civil Engineering, Otto-Graf-Institute at the Technical University of Stuttgart, Department for Steel and Reinforced Concrete, Germany [86] - [91].

Various aspects of slip-resistant connections were addressed in this study. In order to determine the slip factor, a slip factor test procedure was used which in some aspects is very similar to the current test procedure according to EN 1090-2, Annex G.

The geometry and the dimensions of the test specimen are shown in Figure 2-5. Besides the thickness of the cover and inner plates, the geometry of the test specimen is very similar to the geometry prescribed in EN 1090-2. Depending on the steel grade (St 37 and St 52 according to DIN 17100 which are comparable with S235 and S355 according to EN 10025-2), some small modification was considered in the test specimen. For each test specimen, four HV M16 bolting assemblies were used (bolts according to DIN 6914 [92] and nuts according to DIN 6915 [93] which are comparable to EN 14399-4 [94] and washers according to DIN 6916 [95] which are comparable to EN 14399-6 [96]). All bolts were tightened to the desired preload of P_v = 10 Mp (≈ 98 kN) which is comparable with the $F_{p,c}$* preload level ($F_{p,c}$* = 0.7·f_{yb}·A_S (= 100 kN for M16 bolting assemblies). In order to achieve this load level, all bolts were calibrated by measuring the elongation of the shank under this load in a tensile testing machine.
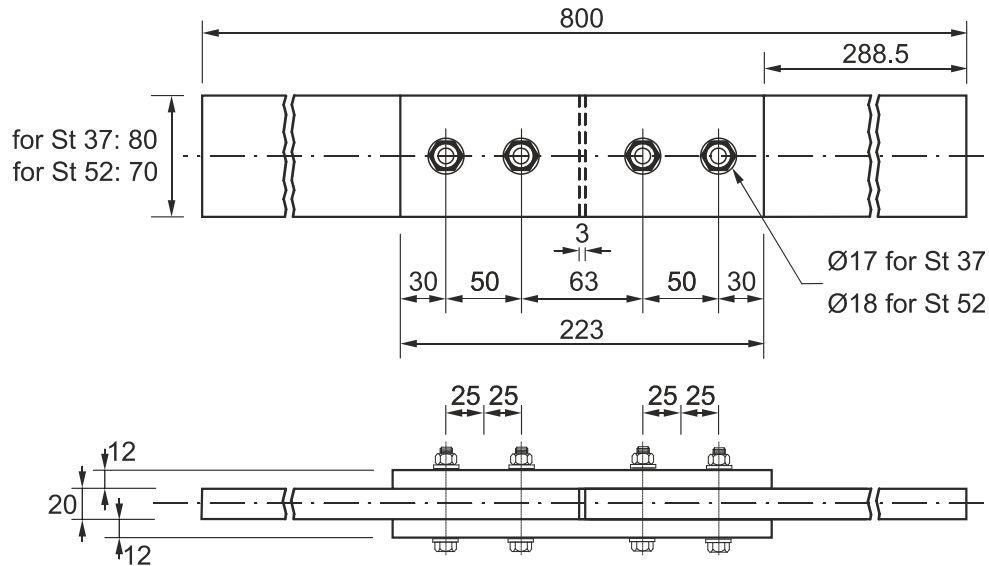
Figure 2-5: Test specimen geometry according to ORE - D 90 [86]

Two dial gauges with an accuracy of 1/1000 mm were mounted on the test specimen. The dial gauge was mounted at the height of the axis of the outer bolt for both upper and lower parts of the specimen. The relative displacement was measured between adjacent points "a" on an inner plate and "b" on the cover plates as shown in Figure 2-5. The slip displacement was only measured at one side of the specimen. All short-term tests were carried out in a tensile testing machine and were loaded stepwise in few minutes with an initial load increase of about 5 Mp ($\approx$ 49 kN) in tension. The relative slip displacements in the individual load stages were read off on both dial gauges. The slip load (P_g) was evaluated as the corresponding load at sudden slip displacement occurrence or at slip displacement of 0.15 mm. EN 1090-2 still prescribes this value as slip criterion for the evaluation of the slip load in static tests. Like Karlsruhe tests, the slip factors (μ) were calculated from Equation (2-2).

Besides the calculation of static slip factor, the long-term behaviour of the connections was also investigated under the constant load over a period of at least 90 hours and a maximum of 200 hours. A connection was considered as a creep-resistant connection when the relative displacement in the connection did not exceed 0.15 mm after extrapolation to 80 years. The μ_r was calculated from Equation (2-3), where P_z is the constant load in a long-term test.

$$\mu^r = \frac{P_z}{m \cdot n \cdot P_v} \tag{2-3}$$

In many different respects, the similarity between this current slip factor test according to EN 1090-2, Annex G; and ORE - D 90 is noticeable. Beside the geometry of the test specimens and the slip criteria, this test procedure was the first to consider the long-term behaviour of the connection in determining the slip factor.

2.4.5 TL/TP-KOR-Stahlbauten, Annex E, Sheet 85

The old TL/TP-KOR-Stahlbauten, Annex E, Sheet 85 prescribes a test procedure to determine the slip factors for alkali-zinc silicate (ASI-) coated surfaces. According to this test procedure, five quasi static tests must be carried out. On the basis of these five tests, ten individual static slip factors shall be determined on the basis of the two-part test specimen geometry. The geometry of the specimen and the dimensions are shown in Figure 2-6.

The test specimens shall be made of structural carbon steel S235. The faying surfaces shall be grit blasted before the coating application. The dry film thickness of the ASI coating on the contact surfaces of the test specimen is fixed at 40 µm. The coated plates must be stored for three days before the start of the test.
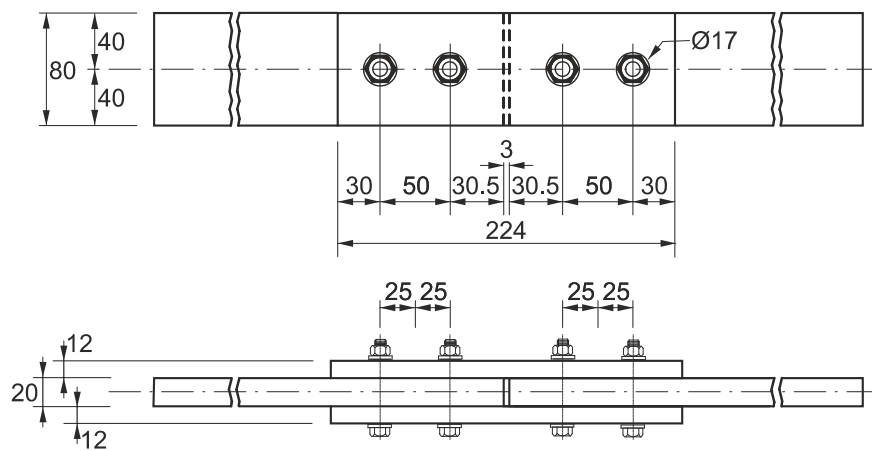
Figure 2-6: Test specimen geometry according to TL-TP-KOR-Stahlbauten [19]

M16 HV bolting assemblies with property class 10.9 shall be used in all the tests. All bolts shall be preloaded to the specified nominal preload level $F_{p,C}$* ($F_{p,C}$* = $0.7 \cdot f_{yb} \cdot A_s$ (= 100 kN for M16 bolting assemblies), where f_{yb}: nominal yield strength of the bolt and A_s: stress area of the bolt). With regard to the execution of the test, it is only prescribed that the tensile load on the test specimen shall be increased up to the sudden sliding of the contact surfaces or up to a displacement of 150 µm. The corresponding tensile load is then referred to as the slip load (Fg). The lowest value of the ten evaluated sliding loads shall be used in order to calculate the final slip factor. No specifications are presented for the measurement of the preload level in the bolts or the slip displacement in the test specimen. The slip factor determined according to Equation (2-4) shall be not less than a value of 0.5 for each test.

$$\mu = \frac{Fg}{4 \times F_{p,C}*} = \frac{Fg}{400} \geq 0.5 \tag{2-4}$$

According to this test procedure, it is not mandatory to measure the preload level before starting the test. For this reason, the preload level at the start of the test could not be guaranteed and that could directly influence the slip-resistant behaviour of the connection. The investigation by Black and Moss [67] has shown the influence of different preload levels on determination of the static slip factors. For this reason it is

important to know the actual preload level in the bolts before any interpretation of the results.

Furthermore, the slip factor shall be determined only based on static tests without considering the long-term behaviour of the connection. For this reason, the long-term relaxation behaviour of the bolt will not be considered in determination of the slip factor. This could lead to an overestimation in determination of the slip factor.

2.4.6 ECCS report no. 37

The European Convention for Constructional Steelwork (ECCS) in 1984 published report no. 37 [38] on determination of slip factor. In this test procedure, slip factors were determined under three different types of loading: 1. Short duration tests, 2. Long duration tests (test under constant load), and 3. Dynamic tests.

All tests were performed in tension on the specified test specimens with M20 or M16, 10.9 bolting assemblies, see Figure 2-7. The preload level used in these tests was comparable with $F_{p,C}$ preload level. In the short duration tests the loads were applied incrementally and the magnitude of the increments chosen in such a way that the relation between load and displacement had sufficient accuracy. The load was kept constant after each increment in order to give the connection time to bed down. Loading was continued until the slip displacement in the connection exceeded 0.3 mm.

(a) for M20 bolting assemblies   (b) for M16 bolting assemblies
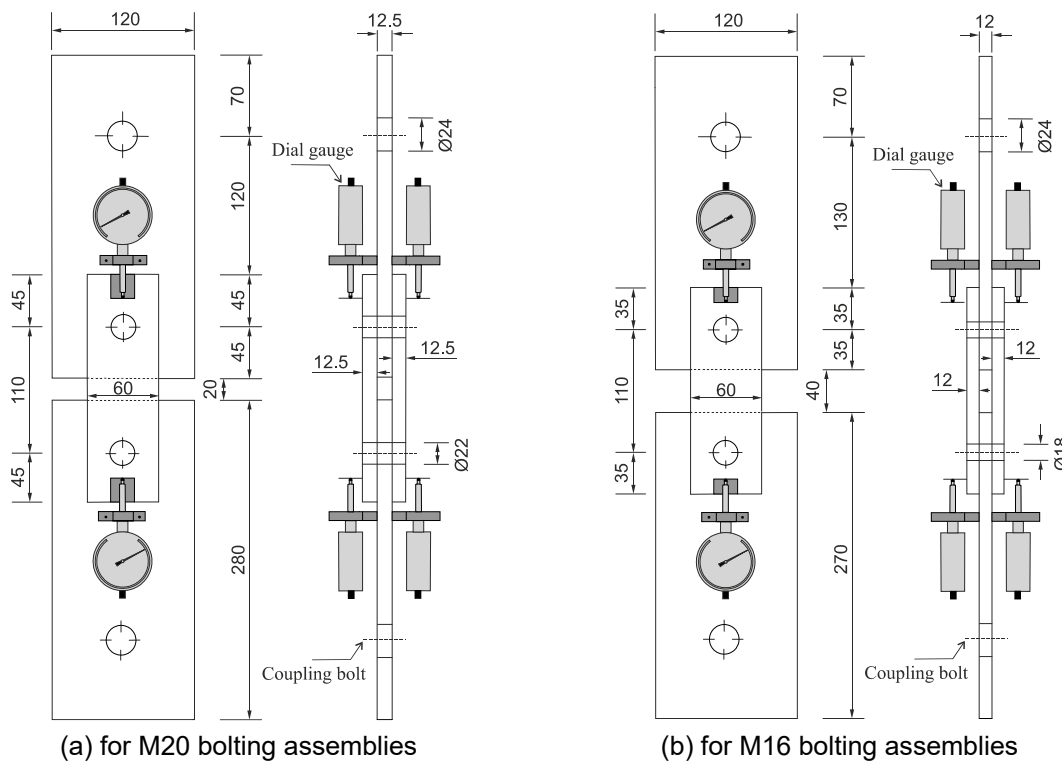
Figure 2-7: Test specimen geometry according to ECCS report no. 37 [38]

The slip load ($\hat{F}_{fr}$) was defined as the maximum load that the connection could transmit without slip displacement exceeding 0.3 mm. The slip factor (μ_{vb}) was

determined from Equation (2-5), where n is the number of bolts per connection and m is the number of interfaces per connection.

$$\mu_{vb} = \frac{\widehat{F}_{fr}}{m \times n \times F_{vn}}$$

(2-5)

If the faying surfaces are coated, the connection will be more susceptible to slipping through under the action of a constant load. For this reason, the long duration tests were performed in order to investigate the creep behaviour of the connection. In a preloaded bolted connection with coated faying surfaces, the slip displacement may occur very slowly under the constant load. For this reason, the maximum load in this step was determined so that the slip displacement in the connection did not exceed 0.3 mm during the service life of the structure.

The slip-resistant connection could be under dynamic loads. As a dynamic load hardly ever occurs alone, during the dynamic tests the specimens shall be loaded under a constant load (Q_{const}) and a cyclic load (Q_{dyn}) additionally applied at various frequencies (0.1 Hz or more) in order to investigate the creep behaviour of the connection under dynamic loading.

In practice, the ratio between Q_{const} and Q_{dyn} could vary greatly for different structures. Even the number of load cycles may also vary in different structures. In the frame of this study, for each test series the ratio between Q_{const} and Q_{dyn} and the number of load cycles were selected in such a way that the slip displacement did not exceed 0.3 mm in the connection during the service life of the structure. As the connection was subjected to both constant and dynamic load, it was decided for this reason to select the constant load level so that the slip displacement in the connection does not exceed 0.15 mm. This means that the maximum value for dynamic load (which was superimposed upon a constant load) was selected so as not to cause a slip displacement of more than 0.15 mm over the service life of the structure. The slip factor for the dynamic test was subsequently calculated as the sum of the slip factor based on both Q_{const} and Q_{dyn}.

ECCS published report no. 38 in 1985 [39], which also prescribes a test procedure for determination of the slip factor. This test procedure is very similar to the test procedure according to EN 1090-2, Annex G, which is presented in Chapter 2.4.2.

2.4.7 British standards (BS 4604-1 and BS 4604-2)

BS 4604 also specifies a test procedure for the determination of the slip factor only based on static tests for preloaded bolted slip-resistant (friction grip) connections. BS 4604-1 [97] covers the use of general grade bolts as specified in BS 4395-1 [98] which is comparable with 8.8 property class according to EN ISO 898-1 [99]. BS 4604-2 [100] covers the use of higher grade bolts with parallel shanks, the bolts being as specified in BS 4395-2 [101], which is comparable with 10.9 bolts property class according to EN ISO 898-1.

Figure 2-8 illustrates the test specimen geometry for determination of slip factor. The test specimens should be tested preferably at least 18 hours after tightening of the bolts. As the loss of preload rate is very high in the first hours and this time could give the test specimen enough time to relax. In the case that the specimens are tested after 2 hours, the slip load shall be taken as 95 % of the test result. The loading application rate should be approximately 50 kN/min and the slip should not occur in less than 3 minutes. The slip displacement shall be measured between adjacent points on an inner and a cover plate. The slip load shall be taken as the load at a slip deformation of at least 0.1 mm.
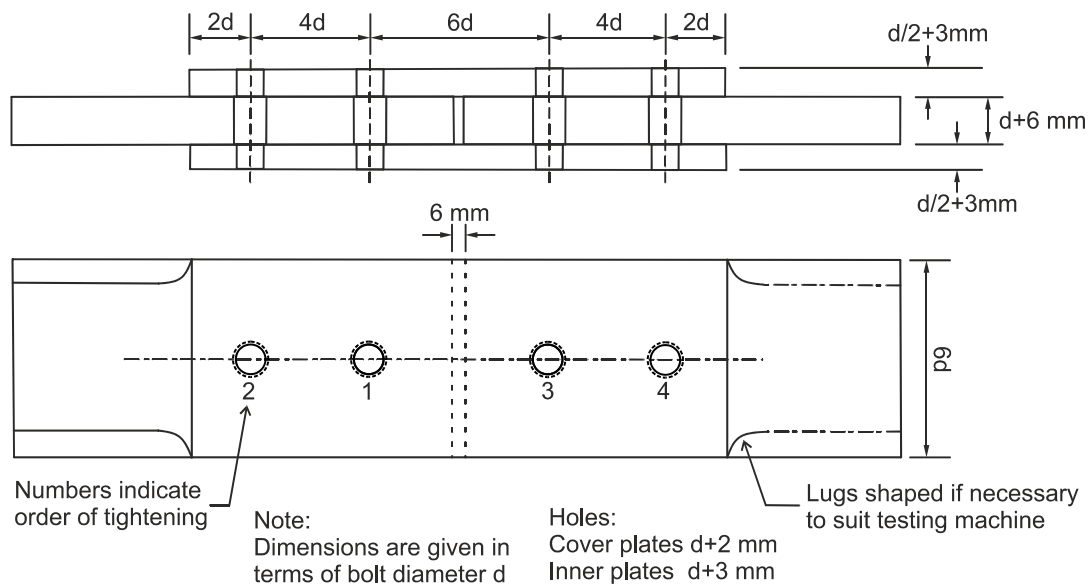
Figure 2-8: Typical test specimen geometry according to BS 4604-1 [97] and -2 [97][100]

The lowest slip load from at least three or more test results should be considered as the slip load for determination of the slip factor. The slip factor for slip-resistant connections with general bolt grades according to BS 4395-1 (comparable with 8.8 bolt property class according to EN ISO 898-1) shall be determined from Equation (2-6).

$$\text{slip factor} = \frac{\text{slip load}}{2 \times \text{minimum proof load of one bolt} \times \text{number of bolts}} \qquad (2\text{-}6)$$

For slip-resistant connections with higher bolt grades according to BS 4395-2 (comparable with 10.9 bolts property class according to EN ISO 898-1), the slip factor shall be calculated from Equation (2-7). In this case the bolts shall be preloaded in order to reach the level between 0.85 and 1.15 times the specified minimum proof load.

$$\text{slip factor} = \frac{\text{slip load}}{2 \times 0.85 \times \text{minimum proof load of one bolt} \times \text{number of bolts}} \qquad (2\text{-}7)$$

In general, this test procedure focuses on short-term behaviour of the slip-resistant connection. According to this test procedure, the relaxation time shall be given to the

specimens before starting the test. However, it is not comparable with the relaxation that could happen in the service life of the structure under the constant load.

2.4.8 Australian/New Zealand standard

According to AS/NZS 5131 [102], the slip factor can be determined experimentally based on the static slip factor test only. The geometry of the test specimen can be chosen as shown in Figure 2-9 (a). However, the use of M20 bolts with 25 mm inner plate and 12 mm cover plate is proven to be the most convenient. At least three tests shall be carried out, but testing five specimens is recommended as a practical minimum number. The bolts shall be preloaded in the same way as to be used in practice to at least the minimum specified preload level. The minimum preload level is approximately equivalent to the minimum proof load derived from a proof load stress of 600 MPa, as specified in AS 4291.1 [103]. The minimum preload level for M20 bolting assemblies is about 145 kN and about 95 kN for M16 bolting assemblies. These values are comparable with preload level $F_{p,C}$ for property class 8.8 for HV-bolting assemblies. The extension of the bolt shall be measured using a dial gauge micrometre or a displacement transducer with a resolution of at least 0.003 mm. In order to determine/calibrate the relation between the preload level and extension in the bolt, a load cell test (calibration test) shall be performed. Alternatively, if there is no load cell to calibrate the tightening procedure, the bolts shall be preloaded to at least 80 % and no more than 100 % of their specified proof load and the preload applied to the bolt can be calculated from Equation (2-8). Where N_{ti} [kN] is the applied preload in the bolt, E is the young's modulus of elasticity with 200000 MPa, Δ [mm] is the measured total extension of the bolt when tightened from finger-tight condition to final tension condition, a_o [mm] is the length of the bolt shank contained within the grip (including the washer thickness) before tensioning, A_o [mm^2] is the plain shank area of the bolt, a_t [mm] is the length of the threaded part of the bolt contained within the grip (including the washer thickness) before tensioning, t_n [mm^2] is the thickness of the nut, in mm, and A_s is the tensile stress area of the bolt.

$$N_{ti} = \frac{E\Delta \times 10^{-3}}{\dfrac{a_o}{A_o} + \left[\dfrac{a_t + \dfrac{t_n}{2}}{A_s} \right]} \tag{2-8}$$

(a) test specimen geometry   (b) position of dial gauges
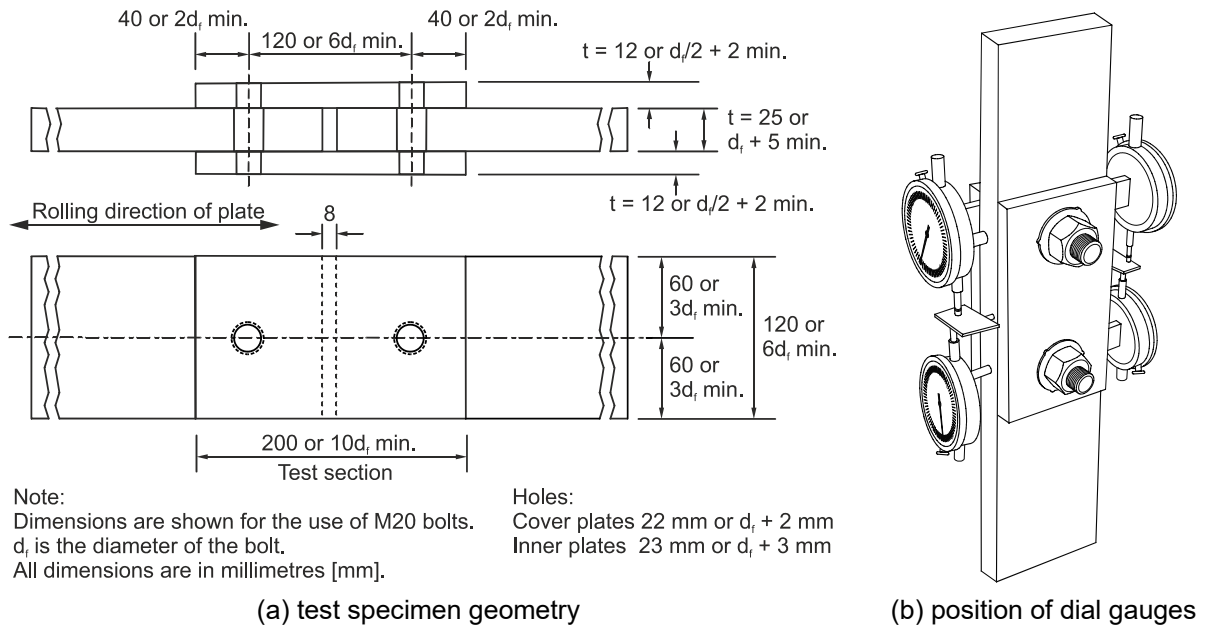
Figure 2-9: Test specimen geometry according to AS/NZS 5131 [102]

The displacement transducers or dial gauge micrometres shall be installed symmetrically on both sides of the specimen in order to measure the relative slip displacement between the inner and the cover plates, as shown in Figure 2-9 (b). All tests shall be performed under tensile loading. The load shall be applied in increments that neither exceed 25 kN nor 0.25 times of the slip load determined from the calculated preload level with a slip factor of 0.35. The loading rate shall not exceed 50 kN/min, and slower loading rates are recommended. Each load increment shall be applied when creep occurred under the constant load of the last increment until the slip load was reached. The slip load shall be defined as the corresponding load when a sudden slip displacement occurs or when slip displacement reaches 0.13 mm. The slip factor to be used in design shall be calculated from Equation (2-9).

$$\mu = k(\mu_m - 164\delta) \qquad \qquad (2\text{-}9)$$

k is equal to 0.85 when only three specimens are tested and equal to 0.90 when five or more specimens are tested. μ_m is the mean slip factor for all individual slip factor tests. δ is the standard deviation of slip factor for all tests. Each test provides two individual slip factors. The individual slip factor shall be calculated from Equation (2-10); here V_{si} is the individual slip load and N_{ti} is the preload level in the bolt as calculated from Equation (2-8).

$$\mu_i = \frac{1}{2}\left(\frac{V_{si}}{N_{ti}}\right) \qquad \qquad (2\text{-}10)$$

If the calculated slip factor from Equation (2-9) is smaller than the lowest individual slip factor μ_i, then the slip factor can be taken as being equal to the lowest individual slip factor.

2.4.9 RCSC (2014) – American standard

According to RCSC, the faying surfaces are categorized in two different classes (Class A or B). The slip factor can either be determined as follows or based on experimental tests.

For Class A surfaces (unpainted clean mill scale steel surfaces or surfaces with Class A coatings on blast cleaned steel or hot dip galvanized and roughened surfaces) the slip factor shall be considered equal to µ = 0.30.

For Class B surfaces (unpainted blast cleaned steel surfaces or surfaces with Class B coatings on blast cleaned steel) the slip factor shall be considered equal to µ = 0.50

RCSC prescribes a test procedure to determine the slip factor (slip coefficient) for coated faying surfaces in slip-resistant (slip-critical) bolted connections. This test procedure was developed by Yura and Frank in 1985 [104] and since then the slip factor tests shall be performed in two steps, see Figure 2-10. In the first step, five static short-term tests shall be carried out with a specified test specimen geometry (7/8 in. diameter ≈ M22), see Figure 2-11. These tests are usually carried out under compression loading. However, the slip load can also be determined under tension loading, as long as the contact surface area per bolt of the test specimen is the same, see Figure 2-11.
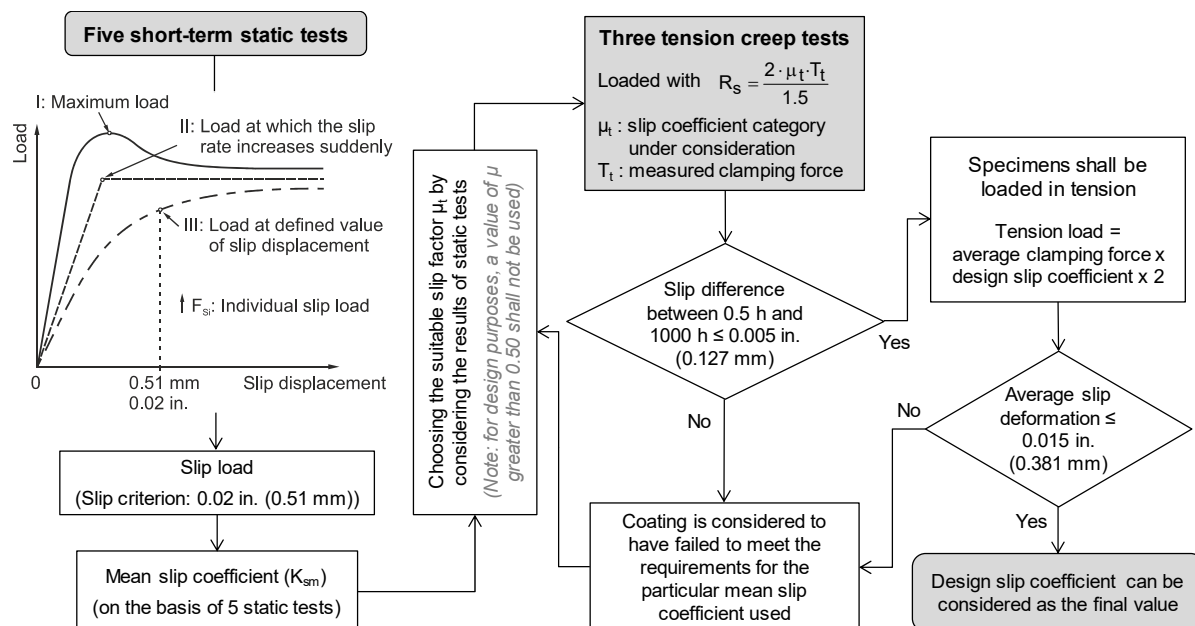
Figure 2-10: Slip factor test procedure according to RCSC (2014)

RCSC prescribes that the loading application rate shall not exceed 25 kips per minute (≈ 111 kN/min) nor 0.003 in. per minute (≈ 0.076 mm/min) slip displacement until the slip load is reached. When a slip of 0.05 in. (1.27 mm) or greater is recorded, the test should be terminated. The preload (clamping force) shall be applied through a 7/8 in. diameter threaded rod as shown in Figure 2-11 and the preload shall be maintained during the short-term static test with an accuracy of 0.5 kips (≈ 2 kN). The

preload of at least 49 kips (218 kN) shall be applied with an accuracy of ± 1 %. The specified minimum bolt preload level can determined as 70 % of the specified minimum tensile strength of the bolts. Based on RCSC, using instrumented bolts with strain gauges can also provide the required measuring accuracy and can be considered as an alternative method of measuring the preload.
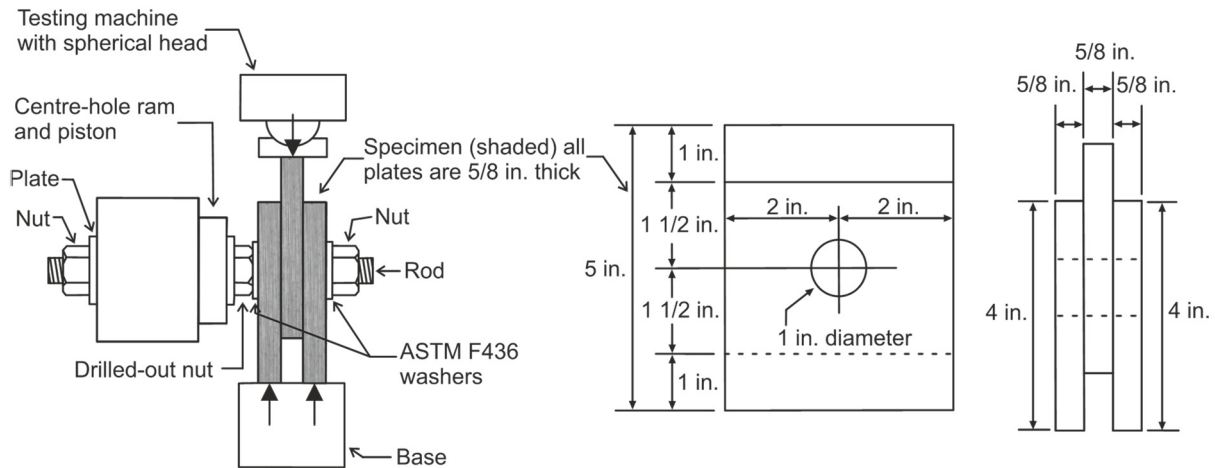
Figure 2-11: Compression-type specimen for short-term static test according to RCSC 2014 [18]

The slip load is defined at 0.02 in. (≈ 0.51 mm) slip displacement or at the peak before 0.02 in., see Figure 2-11. The relative slip displacement between the cover plates and inner plate shall be measured on both sides of each specimen with an accuracy of 0.001 in. (0.025 mm). The individual slip factor μ_i (k_s) shall be calculated from Equation (2-11) and the mean slip factor shall be calculated from all five individual test results.

$$k_s = \frac{slip\ load}{2 \cdot clamping\ force} \tag{2-11}$$

In the second step, the creep test shall be performed with three tension-type specimens, as shown in Figure 2-12, linked together with loose bolts as a single chain, so that all specimens would be loaded with the same load.
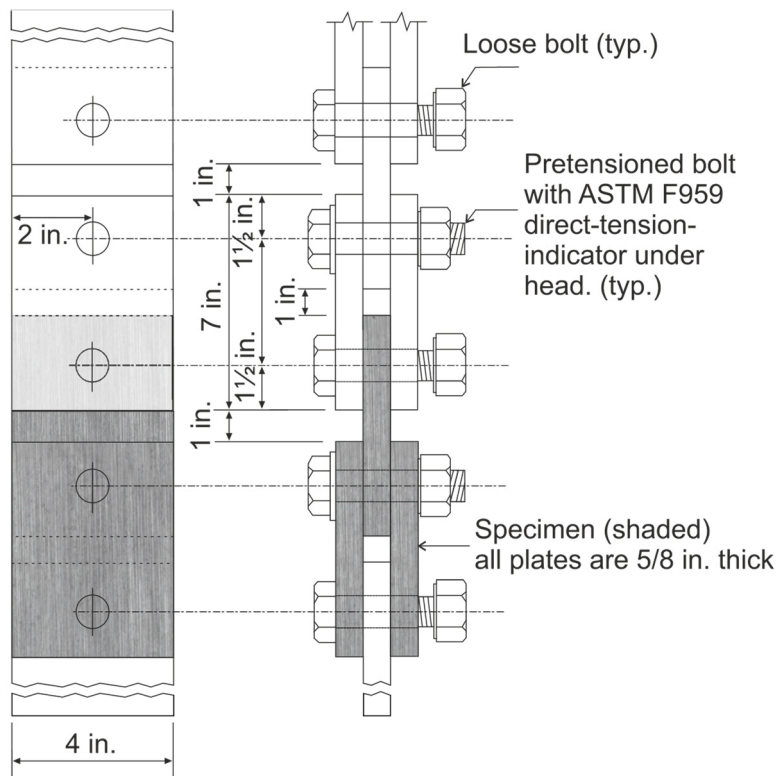
Figure 2-12: Tension-type specimens for creep test according to RCSC 2014 [18]

The load level for the creep test (R_s) has to be determined based on the particular slip factor category under consideration, see Equation (2-12). T_t is the measured preload in the bolting assemblies and μ_t is the considered mean slip factor. For design purposes, the considered mean slip factor should not be greater than 0.5.

$$R_s = \frac{2 \cdot \mu_t \cdot T_t}{1.5} \qquad (2\text{-}12)$$

The specified load level has to be applied and held constant for 1000 hours and the relative slip displacement measured on either side of the specimens.

In case that the difference between the slip displacement at 30 min and 1000 hours after loading the specimens exceeds 0.005 in. (0.127 mm), the specimens shall be loaded again in tension to a load level as follows:

$$\text{load level} = \text{average preload level} \times \text{design slip} \times 2 \qquad (2\text{-}13)$$

If the slip deformation for each specimen does not exceed 0.015 in. (0.381 mm), the design slip factor can be considered as the final value. On the other hand, if the slip deformation is greater than 0.015 in., the coating is considered to have failed and the new creep tests with lower load level shall be performed. RCSC does not specify any specific test procedure for determination of the slip factor for uncoated surfaces.

2.4.10 Guide to design criteria for bolted and riveted joints (Kulak et al.)

Kulak et al. gives some specifications for determination of the slip factor. As can be seen in Figure 2-13, two different test specimen geometry types are recommended, a two-bolt specimen, type A, and a four-bolt specimen, type B. The type A test

specimen is very similar to the test specimen geometries prescribed in EN 1090-2, Annex G, see Figure 2-13 (a) and Figure 2-1. For a short-term static test, the test specimens shall be subjected to gradually or incrementally increasing tensile loads. The relative displacement shall be measured at selected intervals of loadings between points a and c on the inner and the cover plates, see Figure 2-13.

(a) Type A: a two-bolt specimen   (b) Type B: a four-bolt specimen
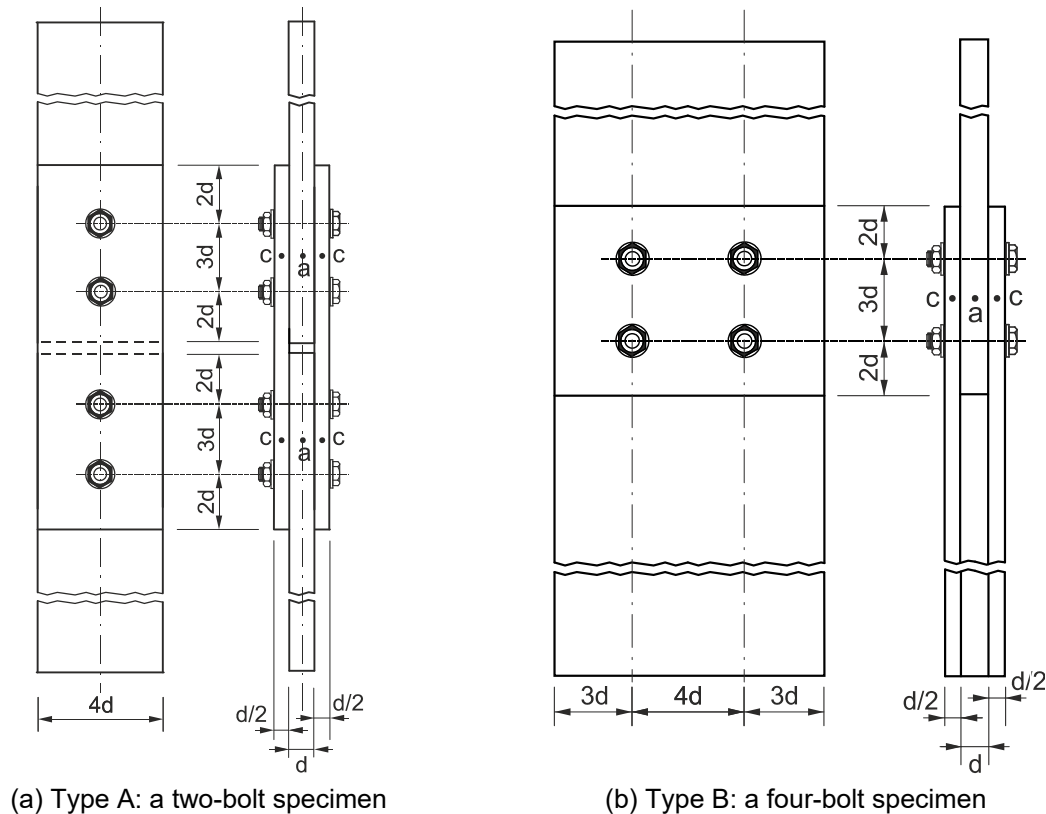
Figure 2-13: Test specimen geometry according to Kulak et al. (2001) [50]

According to this guideline, the slip load shall be defined as the corresponding load when a sudden slip occurs if the slip-resistance of the connection is exceeded. This phenomenon usually happens in slip tests on specimens without coated faying surfaces. For coated specimens, where the slip displacement builds up continuously by cumulative microslips, the slip load can usually be defined as the corresponding load at a slip of 0.02 in ($\approx$ 0.51 mm). A creep test can also be performed in order to evaluate the slip-resistant behaviour of the connection under the sustained loading. According to this guideline, the RCSC specification can be consulted for details of a suitable creep test.

2.4.11 Other standards

The Indian standard IS 4000 specifies the same test procedure/test specimen geometry as Australian/New Zealand standard AS/NZS 5131 for determination of the slip factor.

Canadian standard CAN/CSA-S16-09 refers to RCSC in order to determine the slip factor for coated faying surfaces based on experimental investigations.

According to the experimental investigation presented by Kim et al. [105], there is also some similarity in performing the slip factor test according to South Korean standard and presented test procedures.

2.5 Conclusion

Slip-resistant behaviour of bolted connections strongly depends on the condition of the faying surfaces and the preload level in the bolts. Different standards/guidelines prescribe the slip factors for some common surface preparations. However, as experience shows, these values can be incomparable even for identical surface preparations. Different parameters could be the reason for such scattering in the results. Different standards/guidelines prescribe a test procedure for the determination of the slip factor. Each test procedure includes several parameters that have the potential to change the results.

Different test procedures according to different national and international standards and guidelines were presented in detail. A first look at these test procedures draws our attention to some main differences. Some of these test procedures describe a unique test specimen geometry or preload level for performing the tests. Long-term creep behaviour of the connection is considered in some cases and some test procedures focus only on static behaviour of the connection. Even the type of the tests was different in some test procedures. In addition to all these differences, the evaluation criteria for static, creep or extended creep test also varies from one test procedure to another.

All these parameters can have a direct influence on the determination of the slip factor and cause such variation in slip factor values even for identical surface preparation.

3 Parameters influencing the determination of the slip factor

3.1 General

The determination of the slip factor depends on many factors. Besides the test procedure, there are many other parameters that can directly influence the slip-resistant behaviour of the connections, which may lead to different slip factors for identical surface conditions. In order to clarify the influence of each parameter separately, comprehensive investigations were carried out within the scope of two projects: 1. The European research project SIROCO "Execution and reliability of slip-resistant connections for steel structures using CS and SS" [106], and 2. The Euronorm research project "Alternative coating systems for slip-resistant connections" [107].

3.2 Influence of different evaluation criteria, geometry parameters and preload levels on determination of the slip factor

3.2.1 General

In the frame of the SIROCO project, a comparative experimental study was carried out in order to investigate the influencing parameters on the determination of the slip factor. In the SIROCO project, all slip factor tests were carried out at the Institute for Metal and Lightweight Structures (IML), Essen, Germany, the Fraunhofer Research Institution for Large Structures in Production Engineering IGP (FhIGP) in Rostock, Germany, and Delft University of Technology (TUD), Delft, Netherlands, which are mentioned in related chapters.

3.2.2 Test specifications

For the geometry of the test specimen, M20 bolt geometry according to EN 1090-2 was chosen, see Figure 2-1 (a). The steel grade for the plates was S355J2C+N according to EN 10025-2, and each plate thickness was taken from one batch.

Furthermore, the investigations were carried out for the following six different surface treatments: 1. Grit blasted (GB), 2. Alkali-zinc silicate (ASI) coating, 3. Thermal aluminium spray metallized coating (Al-SM), 4. Thermal spray metallized with zinc (Zn-SM), 5. Hot dip galvanized (HDG), and 6. A combination of alkali-zinc silicate and zinc spray metallized coating (ASI – Zn-SM). In order to constantly measure the actual preload in the bolt during the test, two different methods for measuring the preload in the bolts were selected: 1. Bolts instrumented with strain gauge (SG) and 2. Load cell (LC). For each test specimen, four HV M20 bolting assemblies were selected according to EN 14399-4 and EN 14399-6. The preload level of the bolts was defined as $F_{p,C}$ = 172 kN.

All instrumented bolts with strain gauges were manufactured by drilling a centric hole of 2 mm diameter along the bolt shank, see Figure 3-1. The hole was filled with a two-component adhesive and the BTM-6C (produced by Tokyo Sokki Kenkyujo Co., Ltd.) strain gauges inserted gently into the hole. In order to remove the possible bubbles in the hole, the bolts were placed in a glass vacuum desiccator. In the next step, the bolts were placed in the electric furnace to allow the adhesive to cure.

The load cells used in these test series were prepared by Delft University of Technology (TUD) with a load capacity of 180 kN and a relatively long length (100 mm) compared to the customary load cells that can be purchased on the market. Experience showed that the small customary load cells are very sensitive to irregularities of the clamped parts, see [108]. Therefore, special care has to be taken using these load cells within slip factor tests. This could potentially lead to a wrong estimation of the slip factor.

| (a) Hole drilling | (b) Cleaning the hole | (c) Filling hole with glue | (d) Applying strain gauges |

| (e) Removing bubbles | (f) Curing glue in the oven | (g) Cross section |
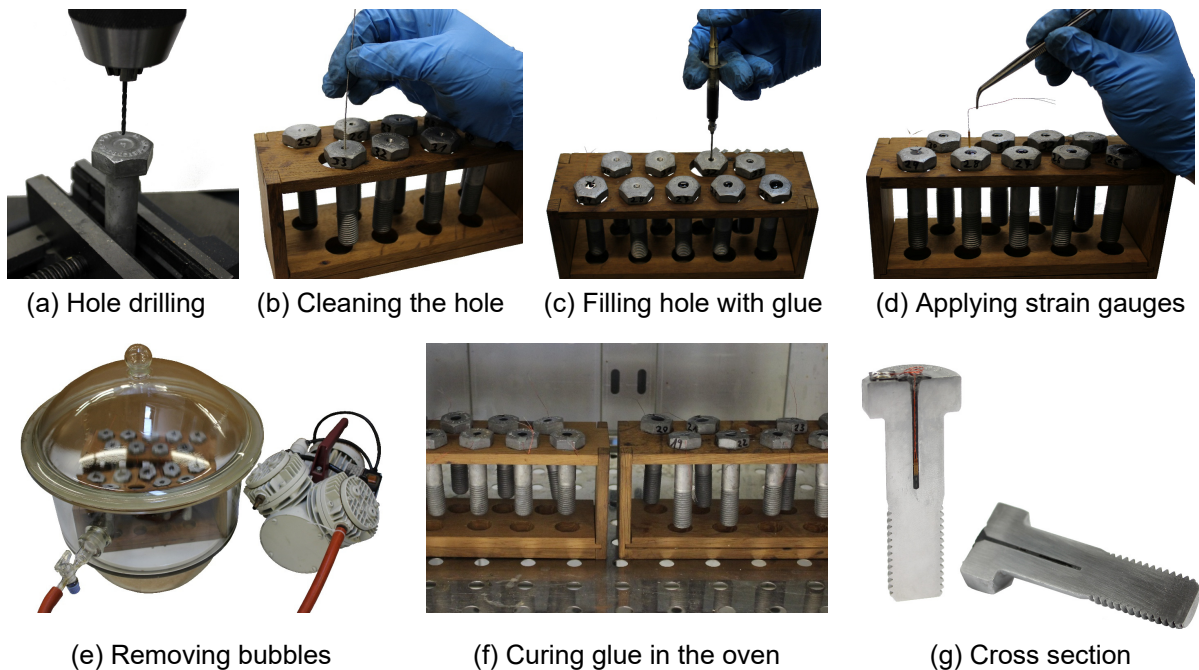
Figure 3-1: Production of the implanted strain gauges at UDE

The internal diameter of the TUD load cells is only 0.1 mm larger than the diameter of the bolts, in order to restrict eccentricities. Four XY11-6/120 strain gauges (produced by HBM) were arranged at a 90° degree offset from each other around the circumference of the load cell body. The strain gauges were combined as a full bridge configuration which is fully compensated for temperature variations, see Figure 3-2.

(a) Strain gauge   (b) Strain gauge mounting   (c) Fixing cables   (d) Insulation
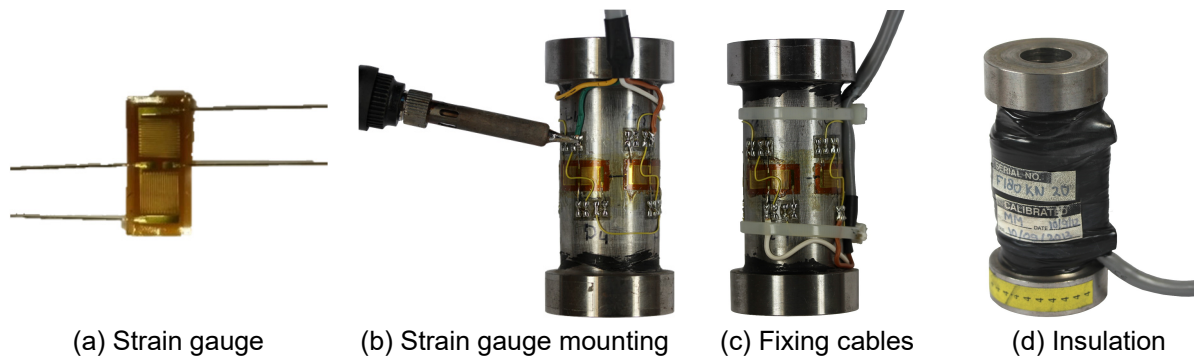
Figure 3-2: Various phases of the production process of the load cells (produced by TUD)

Instrumented bolts and load cells were calibrated separately and also as a combination under stepwise loading, see Figure 3-3. The calibration procedure confirmed the expected robustness and accuracy for both preload measurement methods with an error < 1 % of the full scale.

(a) Strain gauge   (b) Load cell (LC)   (c) Combination of SG and LC
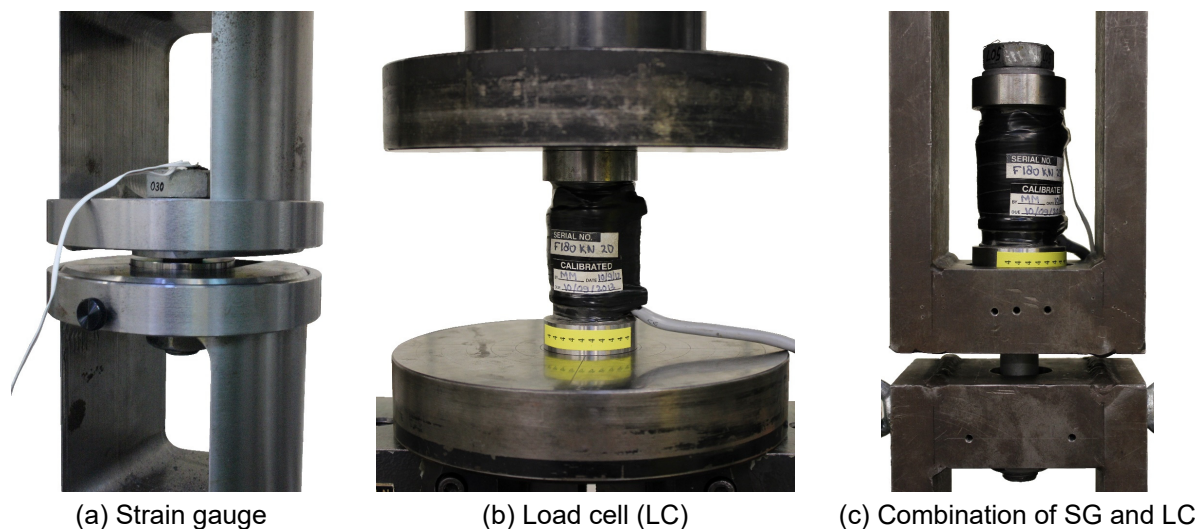
Figure 3-3: Calibration of instrumented bolts and load cells

Different combinations of instrumented bolts with or without small adapters and load cells were considered in order to investigate different methods for measuring the preload and the influence of the clamping length, see Figure 3-4.

The experimental test programme, presented in Table 3-1, includes all information regarding the surface treatment, bolt size, clamping length/ratio and preload level.
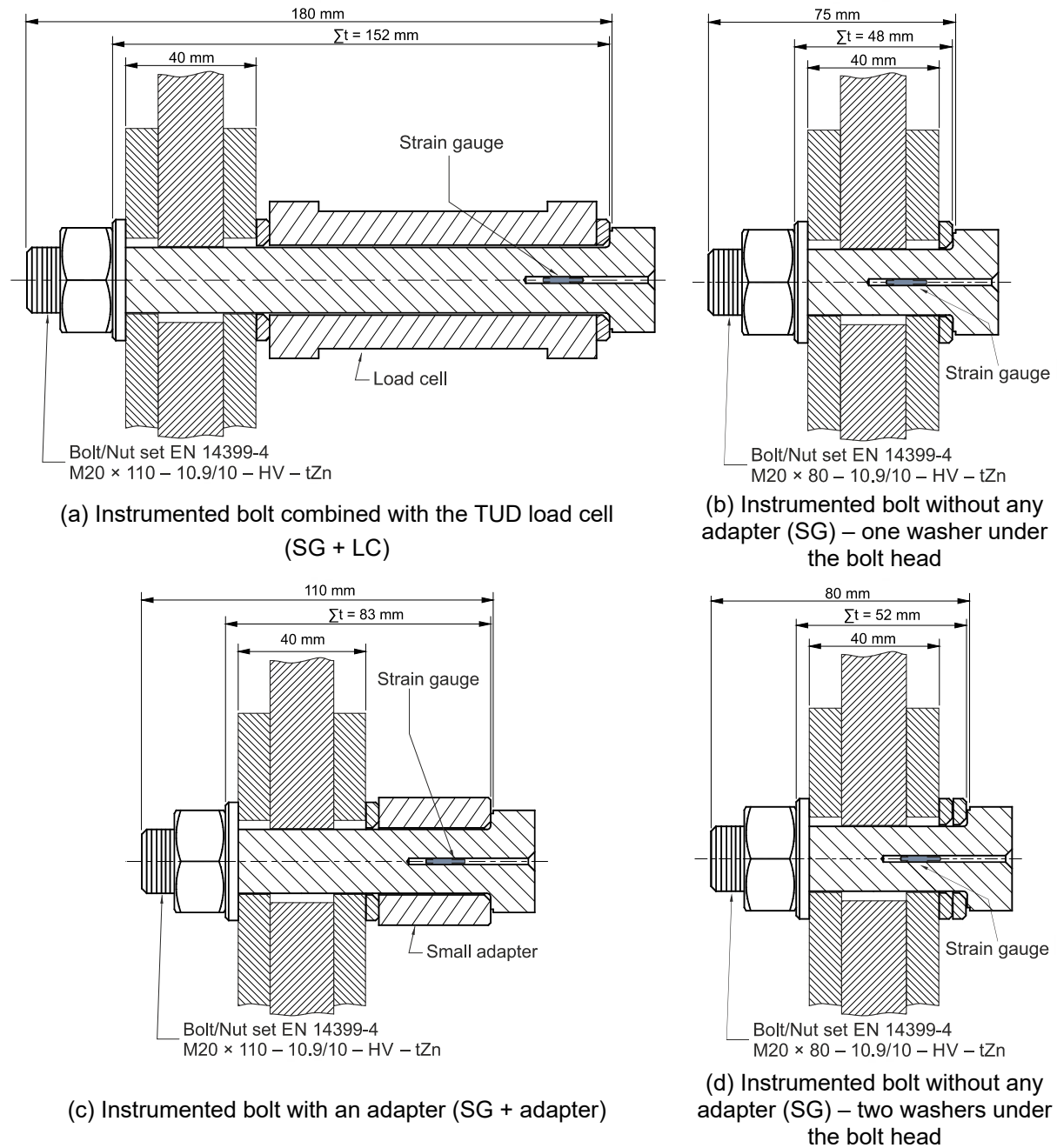
Figure 3-4: Different combinations of instrumented bolt, load cell and small adapter

Within the scope of the SIROCO project, the surface roughness was measured according to EN ISO 4287 [109]. The dry film thickness (DFT) of the coated test specimens was measured according to EN ISO 2808 [110].

The slip displacement was measured as the relative displacement between adjacent points on an inner plate and the cover plates in the direction of the applied load. Two different groups of displacement transducers (LVDTs) were mounted in order to measure the slip displacements in two different positions: using eight LVDTs (no. 1-8) at the centre bolts group (CBG) and four LVDTs (no. 9-12) at the plate edges (PE) positions, see Figure 3-5.

Table 3-1: Test programme for different surface preparations, clamping lengths and preload levels [106]

Series ID	Main surface treatment		Post-treatment			Σt/d [4] [-]	Preload [kN]
	Before main coating	Coating thickness					
	Sa [1] / Rz [2] [μm]	DFT [3] [μm]	Type of treatment	Rz [μm]	DFT [μm]		
Grit blasted surfaces (GB)							
GB-I	Sa 2½ / 80	-	-	-	-	7.6	$F_{p,C}$/172
GB-II						4.2	
GB-III						2.6	
Alkali-zinc silicate (ASI)							
ASI-I	Sa 2½ / 80	60	-	-	-	7.6	$F_{p,C}$/172
ASI-II						4.2	
ASI-III						2.6/2.4	
ASI-IV						2.4	$F_{p,C}$*/160
Thermal aluminium spray metallized (Al-SM)							
Al-SM-I	-	250	-	-	-	4.2	$F_{p,C}$/172
Al-SM-II						2.6/2.4	
Thermal zinc spray metallized (Zn-SM)							
Zn-SM-I	Sa 3 / 100	140	-	-	-	4.2	$F_{p,C}$/172
Zn-SM-II						2.6/2.4	
Zn-SM-III		165				2.4	$F_{p,C}$*/160
Zn-SM-IV							0.9 $F_{p,C}$*/144
Combination of alkali-zinc silicate coating and zinc spray metallized (ASI–Zn-SM)							
ASI–Zn-SM-I	Sa 2½ / 100 – Sa 3 / 100	55 – 170	-	-	-	2.4	$F_{p,C}$/172
ASI–Zn-SM-II							0.9 $F_{p,C}$*/144
Hot dip galvanized (HDG)							
HDG-I	Chemically cleaned	105	-	-	-	7.6	$F_{p,C}$/172
HDG-II							
HDG-III		80				2.4	
HDG–Ref		70					
HDG–NG-I			needle gun (45°)	30	60		
HDG–NG-II			needle gun (90°)	40			
HDG–SB-I			sweep blasted (particle size 0.2 - 0.5 mm)	30	50		
HDG–SB-II			sweep blasted (particle size 0.5 - 1.0 mm)	50	40		
HDG–ASI			sweep blasted (particle size 0.5 - 1.0 mm) + ASI	30	170 [5]		
HDG–ESI			+ ESI		140 [6]		

[1] surface treatment grade [2] surface roughness [3] dry film thickness (coating thickness)
[4] clamping length ratio (Σt: clamping length, d: bolt diameter) [5] 50 μm (HDG) + 120 μm (ASI)
[6] 50 μm (HDG) + 90 μm (ESI)
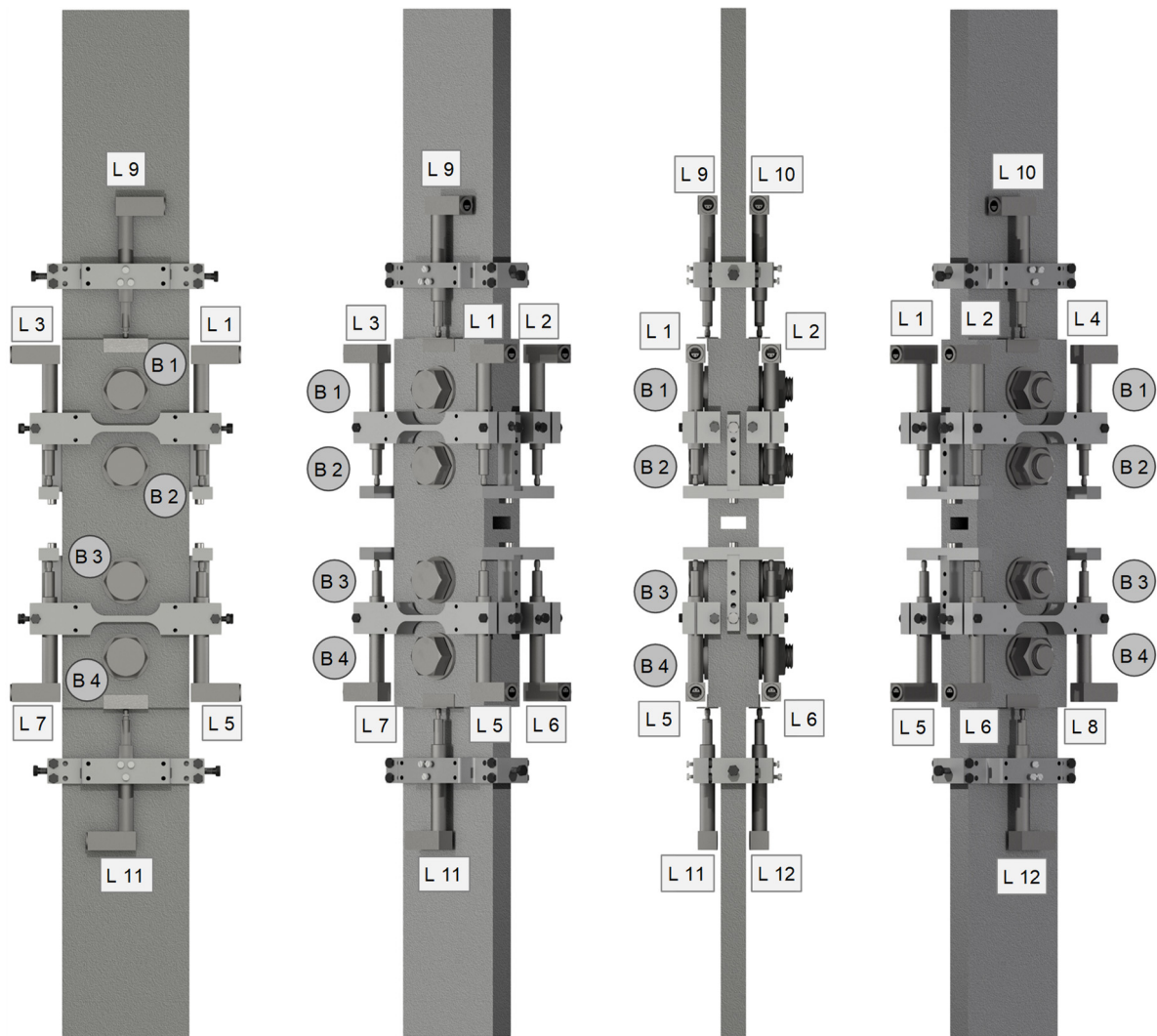
B: bolt   LVDTs 1-8 → CBG (centre bolts group)
L: LVDT (displacement transducer)   LVDTs 9-12 → PE (plate edges)

Figure 3-5: Position of the displacement transducers (LVDTs)

All tests were performed in accordance to EN 1090-2, Annex G, see 2.4.2.2. The determination of the slip factor according to EN 1090-2 is based on the nominal preload level μ_{nom}.

In the frame of this investigation, besides the requirements of EN 1090-2, the slip factors were additionally evaluated by considering the initial preload at the beginning of the test μ_{ini} and the measured actual preload at the onset of slip μ_{act}. The mean values of the static slip factors ($\mu_{nom,mean}$, $\mu_{ini,mean}$ and $\mu_{act,mean}$) and characteristic values ($\mu_{5\%}$ for a passed creep test and μ_{ect} based on a passed extended creep test) are presented in Table 3-2. All results presented in this table are based on the slip measured in the centre bolts group (CBG) position.

Table 3-2: Slip factor test results for different surface preparations, clamping lengths and preload levels [106]

Series ID	DFT[1] [µm]	Σt/d[2] [-]	Preload [kN]	Number of tests st/ct(sp)/ect[3]	$\mu_{nom,mean}$[4] st/st+ct [-]	$\mu_{ini,mean}$[5] st/st+ct [-]	$\mu_{act,mean}$[6] st/st+ct [-]	V (μ_{nom})[7] st/st+ct [%]	Final slip factor [-] $\mu_{5\%}$[8] / μ_{ect}[9]
Grit blasted surfaces (GB)									
GB-I		7.6		4/1/-	0.80/0.79	0.80/0.79	0.87/0.86	1.7/2.8	0.75/-
GB-II	-	4.2	$F_{p,C}$	2/-/-	0.74/-	0.74/-	0.83/-	1.8/-	-/-
GB-III		2.6		2/-/-	0.74/-	0.74/-	0.86/-	3.6/-	-/-
Alkali-zinc silicate coating (ASI)									
ASI-I		7.6		4/1/-	0.72/-	0.73/-	0.76/-	0.8/-	-/-
ASI-II	60	4.2	$F_{p,C}$	2/-/-	0.72/-	0.72/-	0.78/-	3.0/-	-/-
ASI-III		2.6/2.4[10]		2/(3)/2[11]	0.68/-	0.70/-	0.77/-	2.6/-	-/0.56
ASI-IV		2.4	$F_{p,C}$*	4/1/3		0.69/0.68	0.79/0.78	1.1/3.3	-/0.63
Aluminium spray metallized (Al-SM)									
Al-SM-I	250	4.2	$F_{p,C}$	2/-/-	0.75/-	0.74/-	0.89/-	4.1/-	-/-
Al-SM-II		2.6/2.4[10]		4/1(3)/2[11]	0.73/-	0.73/-	0.93/-	2.6/-	-/0.58
Zinc spray metallized (Zn-SM)									
Zn-SM-I	140	4.2	$F_{p,C}$	4/-/1	0.75/-	0.75/-	0.82/-	2.6/-	-/>0.45
Zn-SM-II		2.6/2.4[10]		2/-(2)/4[11]	0.73/-	0.73/-	0.82/-	2.2/-	-/0.44
Zn-SM-III	164	2.4	$F_{p,C}$*	4/-/4	0.73/-	0.74/-	0.83/-	1.8/-	-/0.48
Zn-SM-IV			0.9 $F_{p,C}$*	4/-/3	0.80/-	0.80/-	0.92/-	1.4/-	-/0.48
Combination of alkali-zinc silicate coating and zinc spray metallized (ASI–Zn-SM)									
ASI–Zn-SM-I	55 – 170	2.4	$F_{p,C}$	4/1/4	0.63/-	0.63/-	0.71/-	3.3/-	-/0.44
ASI–Zn-SM-II			0.9 $F_{p,C}$*	4/1/3	0.69/-	0.69/-	0.77/-	3.1/-	-/0.55
Hot dip galvanized (HDG)									
HDG-I	105	7.6		4/1/-	0.47/-	0.47/-	0.48/-	9.0/-	-/-
HDG-II				2/-/2[11]	0.47/-	0.47/-	0.51/-	13.5/-	-/0.35
HDG-III	80			4/-/-	0.12/-	0.12/-	0.12/-	7.0/-	-/-
HDG–Ref	70			4/-/-	0.14/-	0.14/-	0.14/-	11.3/-	-/-
HDG–NG-I	60		$F_{p,C}$	4/1/-	0.23/-	0.23/-	0.24/-	6.6/-	-/-
HDG–NG-II		2.4		4/1/-	0.20/-	0.20/-	0.21/-	3.6/-	-/-
HDG–SB-I	50			4/1/-	0.35/-	0.35/-	0.36/-	11.9/-	-/-
HDG–SB-II	40			4/1/-	0.39/-	0.39/-	0.41/-	10.8/-	-/-
HDG–ASI	70 + 170			4/1/1	0.62/-	0.62/-	0.70/-	4.4/-	-/-
HDG–ESI	70 + 140			4/1/1	0.48/-	0.47/-	0.52/-	3.7/-	-/-

[1] dry film thickness (coating thickness) | [2] clamping length ratio (Σt: clamping length, d: bolt diameter) | [3] st: static test/ct: creep-/ect: extended creep test | [4] $\mu_{nom,mean}$: calculated slip factors as mean values considering the nominal preload level | [5] $\mu_{ini,mean}$: calculated slip factors as mean values considering the initial preload when the tests start | [6] $\mu_{act,mean}$: calculated slip factors as mean values considering the actual preload at slip | [7] V: coefficient of variation for μ_{nom} | [8] $\mu_{5\%}$: slip factors as 5 % fractile calculated on the basis of the static tests and the passed creep test | [9] μ_{ect}: slip factor resulting from the passed extended creep test | [10] clamping length ration for static tests = 2.6 and for stepwise creep and extended creep test = 2.4 | [11] creep and extended creep tests were carried out at FhIGP

All static and creep tests were carried out at the Institute for Metal and Lightweight Structures (IML) of the University of Duisburg-Essen (UDE) using a universal testing machine with a capacity of ± 600 kN. The incremental tensile load was applied at normal speed of 0.01 mm/s (0.6 mm/min). The extended creep tests were carried out in the long-term test rigs that were designed and erected at IML to determine the load level for which the slip does not exceed 0.3 mm over a period of 50 years or the service life of the structure, see Figure 3-6. Some of the creep and extended creep tests are performed at Fraunhofer Research Institution for Large Structures in Production Engineering IGP (FhIGP) in Rostock, Germany; they are mentioned in Table 3-2.
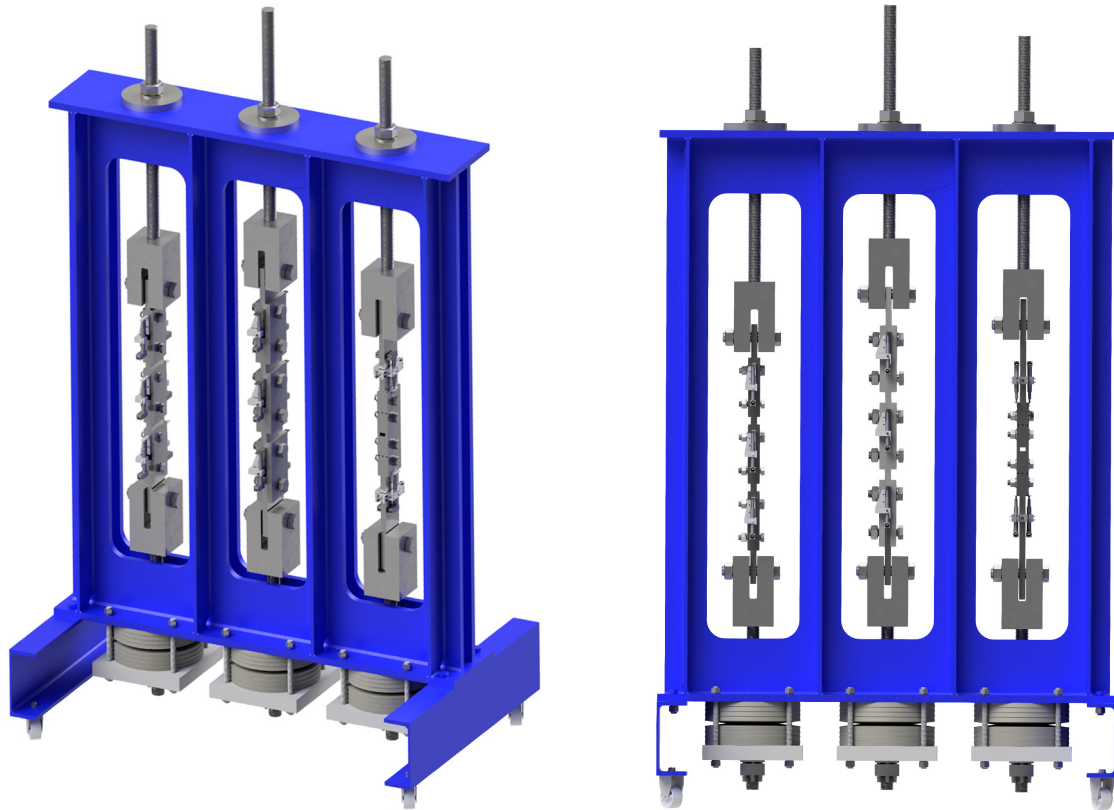
Figure 3-6: Planned 3D model of test rig for performing the extended creep tests according to different standards

Figure 3-7 shows the detail of the long-term test-rigs that were designed and erected at IML. Each test rig was made of a stiff steel frame, in which three extended creep test specimens can be installed. The load was applied with a tensioner with a capacity of 600 kN, see Figure 3-7 (b). Each specimen was connected to the fork connector on both ends and the whole package was mounted in the frame with a M36 threaded rod on both ends. The threaded rod at the upper end of the specimen was instrumented with strain gauges in order to measure the actual load level in the specimen, see Figure 3-7 (c). Under each position a set of spring discs was installed to minimize the drop in the load level caused by slip in the specimen, see Figure 3-7 (d). By removing the tensioner, a drop in the load level can be observed. For this reason, a nut-style tensioner (Superbolt) produced by the NORD-LOCK Inc. company was used in order to keep the load level constant. By turning the jackbolt, it is possible to increase the load level slowly to reach the exact specified constant load level, see Figure 3-7 (e).

(a) IML extended creep test rig

(b) Tensioner with the capacity of 600 kN

(c) Instrumented threaded rod for measuring the load level

(d) Set of spring discs

(e) Increasing the load level using Superbolt

Figure 3-7: IML test rig for extended creep tests

In an extended creep test, the slip deformations of the connections are continuously measured during the whole test while the load level is maintained at a constant level. In the extended creep tests performed in the test rigs, the displacement transducers (LVDTs) were placed at the PE (Plate Edges) position. The elongation of the centre plate between the located LVDTs at the PE and the CBG position may cause some differences regarding the measured slip values as already mentioned. These differences can be more critical in test specimens with higher load-bearing capacity.

In order to calculate the actual slip displacements at CBG position, a correlation was developed between the measured slip at CBG and PE positions based on the results of the corresponding first four static tests. The calculated actual slip displacements at CBG position were then used for evaluation of all extended creep tests. To be able to do this calculation, all static tests were performed including 12 LVDTs at CBG and PE positions, see Figure 3-5.

3.2.3 Different failure mechanisms

As mentioned earlier, in EN 1090-2:2018, Annex G, which was updated based on the results of this investigation, two different failure mechanisms are defined based on four different slip planes in a standard test specimen [111], see Figure 3-8 (a) and (b). The reason for such failure mechanisms is that the preparation of the faying surfaces is a handwork process. Therefore, the contact surfaces in all slip planes do not have the same property, which can lead to a combination of the slip planes as a failure mechanism.

(a) Slip planes 1 and 2 vs. 3 and 4   (b) Slip planes 1 and 4 vs. 2 and 3

(c) Upper/lower section failure mechanism   (d) Diagonal failure mechanism (Zn-SM-II_st1)
(Zn-SM-II_st2)
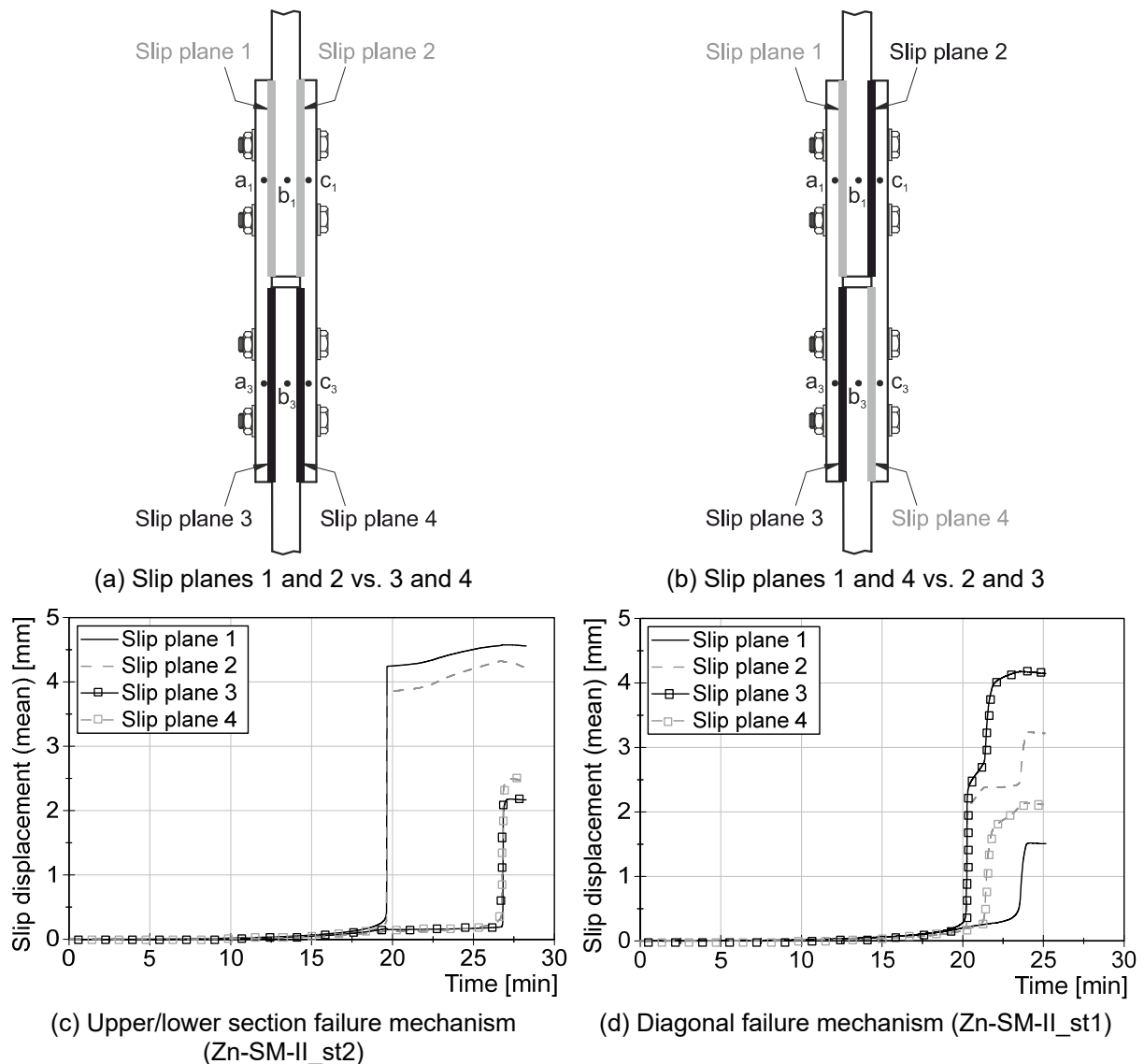
Figure 3-8: Different failure mechanisms for standard test specimens according to EN 1090-2 [106]

Figure 3-8 (c) and (d) show exemplary slip displacement-time diagrams for two different static slip tests for Zn-SM-II test series. As it can be seen in Figure 3-8 (c), the slip occurs in a failure mechanism as a combination of slip in slip planes 1 and 2 vs. 3 and 4 (upper/lower section failure mechanism). However, for the other test specimen from the same test series, the failure mechanism was a combination of slip plane 1 and 4 vs. 2 and 3, see Figure 3-8 (d).

By considering these two possible failure mechanisms, the slip has to be evaluated so that finally two mean slip values are determined on the basis of eight measured displacements at CBG positions.

3.2.4 Evaluation of critical slip load

The slip displacement in a slip-resistant connection must not exceed a certain limit. This value can vary between 0.1 mm to 0.51 mm according to different standards. If the slip resistance of a joint exceeds the limit, the connection shall still remain without any failure in the connection components. The total allowable deformation in a steel structure generally demands a limit on slip displacement in the bolted connection.

In the early sixties, a comprehensive experimental investigation was carried out on slip-resistant connections at the Technical University of Stuttgart. For the first time, the slip load was evaluated as the corresponding load at sudden slip displacement occurrence or at slip displacement of 0.15 mm. This criterion was also used for the evaluation of the long-term tests. A connection was considered a creep-resistant connection when the relative displacement in the connection did not exceed 0.15 mm after extrapolation to 80 years. However, they did not give any explanation of this criterion and why it was considered a slip criterion in slip-resistant connections.

Therefore, an arbitrary approach based on riveted connections was selected in order to explain this limitation [38]. In this type of connection, the rivet does not fill the hole clearance completely so a certain amount of slip displacement occurs before the forces transfer through the shank of the rivet. It was found that this amount of slip could be 0.3 mm. By considering the guidance from the deformation occurring in a riveted connection, it was decided that the limit of 0.3 mm should be considered also for slip-resistant connections. It was observed when slip happened suddenly that it makes no difference to the determination of the slip load whether 0.15 mm or 0.3 mm is chosen as the limit. However, for creep-sensitive coated surfaces, the slip appears gradually. For this reason, a slip displacement of 0.15 mm will occur during the service life of the structure with a smaller level of load in comparison to 0.3 mm.

In 1985, the value of 0.15 mm was selected as a slip criterion for the determination of the slip load in static tests and 0.3 mm as the limitation for extended creep tests [39]. According to Annex G of EN 1090-2:2011, the slip criterion for static tests was specified as a fixed value of 0.15 mm. However, this displacement does not always describe the point of slip. Consequently, considering the 0.15 mm slip criterion might

lead to much lower slip factors. As shown in Figure 2-3 (a), in the latest version of Annex G of EN 1090-2:2018, the load-slip displacement diagrams of the slip tests can be categorized in three different groups where I) the slip load is the maximum (peak) load below a slip of 0.15 mm, II) the slip load is the load at which the slip rate increases suddenly, and III) the slip load is the load corresponding to a deformation of 0.15 mm. Despite this, the new definition of the slip load in the latest version of EN 1090-2:2018 prevents an underestimation for the determination of the slip load, comparing the slip load with different slip criteria must still be done carefully [111]. As can be seen in Figure 3-9 (a) for curve III, having different slip criteria may have a noticeable influence on the determination of the slip factor. Figure 3-9 (b) also shows an exemplary load-slip displacement diagram for static test number four from the AL-SM-II test series for both the upper and lower part of the specimens. As can be seen in this diagram by considering different slip criteria, completely different slip loads can be obtained for the same test.

(a) Schematic diagram

(b) Exemplary diagram from AL-SM-II test series [106]
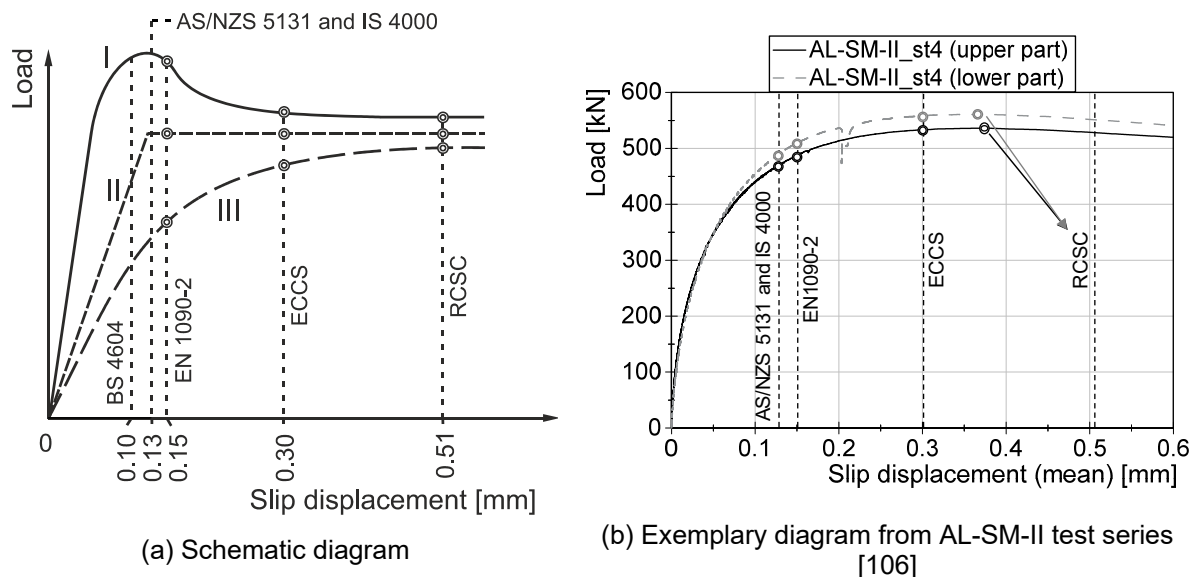
Figure 3-9: Evaluation of slip load from static test considering different standards

3.2.5 Influence of different test speeds

EN 1090-2 specifies that, at first, four static tests shall be carried out at normal speed. Unfortunately, no specific definition is given for normal speed. It is only mentioned that the duration of a static test should be about 10 to 15 min.

The required speed may directly or indirectly depend on the different condition of the faying surfaces, on the preload level or even on the specification of the universal machine. These tests can be performed either as load-controlled or stroke-controlled. For this reason, the specification of the duration of the static slip tests would be no easy task and could lead to confusion.

In the frame of the SIROCO project, a comparative study was performed by the Technical University of Delft (TUD) in order to investigate the influence of the test speed on slip-resistant behaviour of the connection [106], [111]. The investigation

was carried out for three surface treatments: GB, ASI and Zn-SM. Three different test speeds were chosen and all static tests were carried out using the stroke-controlled mode in order to apply the load.

The results show that for the GB test series, there is a tendency towards a slightly higher slip factor with lower loading speed or for longer test durations. However, for the Zn-SM surfaces, the opposite phenomenon was observed, and for the ASI test series no influence was observed under different test durations. Variations in the test durations of ± 5 min compared with the suggested duration according to EN 1090-2 influence the slip factor by only about ± 1.5 %.

The results of this investigation show that the first specimens of a new series of static slip factor tests are necessary to determine the correct loading speed. These test results can be used as a part of the series of four static slip factor tests unless the load duration of these initial tests is outside a time limit ranging from 5 min to 20 min.

3.2.6 Estimating a suitable load level for extended creep test

3.2.6.1 General

In practice, the main difficulty for extended creep tests is to estimate the load level for a successful extended creep test. Since extended creep tests are quite time-consuming and can last for several weeks, it is desirable to estimate the load level for a successful extended creep test as accurately as possible. That will help to reduce the duration of the testing process. With sufficient experience, the load level can already be estimated relatively accurately from the behaviour of the test specimens in the simple creep test. However, if there is insufficient experience or if new coatings are to be applied, it is helpful to use a method where the load level can be estimated experimentally. Such a procedure was developed within the frame of the SIROCO project, but unfortunately it could not be implemented in the new version of EN 1090-2:2018. However, for a future revision of EN 1090-2 it would be desirable to revise the procedure so that it can be incorporated into Annex G.

3.2.6.2 Step test procedure

The new test method for estimating a suitable load level for extended creep tests was developed on the basis of the long-term tests carried out by Gruintjes and Bouwman at the Delft University of Technology in the 1980s [38], which were further developed into a more time-efficient test method called the step test, see [106], [111] and [112].

The step test is performed as an additional test before performing the extended creep tests. The step test makes it possible to estimate the critical load level for a successful execution of the extended creep test. Two different methods (1) and (2) have been developed at the Fraunhofer Research Institution for Large Structures in Production Engineering IGP (FhIGP) in Rostock, Germany, and at Delft University of Technology (TUD), Delft, Netherlands, for the evaluation of this step test, which are

both applicable and can be freely selected. As shown in Figure 3-10 (a), in the step test a regular test specimen is loaded in different steps, e.g. with load steps between approximately 60 % of F_{Sm} and 95 % of F_{Sm} with increments of a 5 % load increase.

D: The duration of the loading steps can vary between 30 min and 90 min.

(a) Step test

D: The duration of the loading steps can vary between 30 min and 90 min.
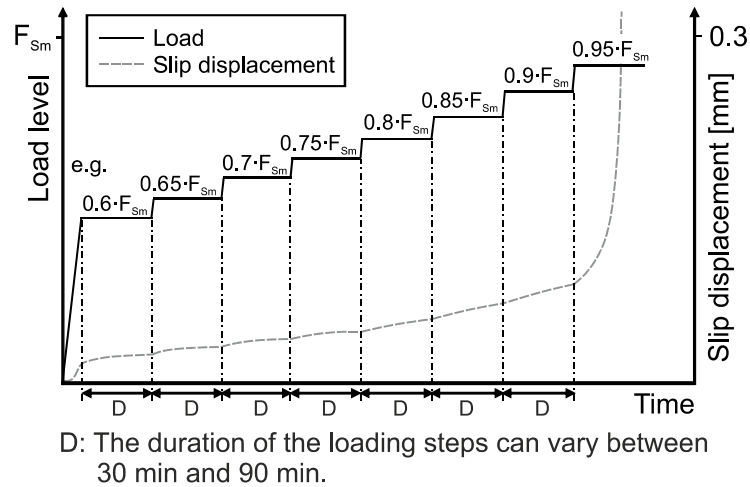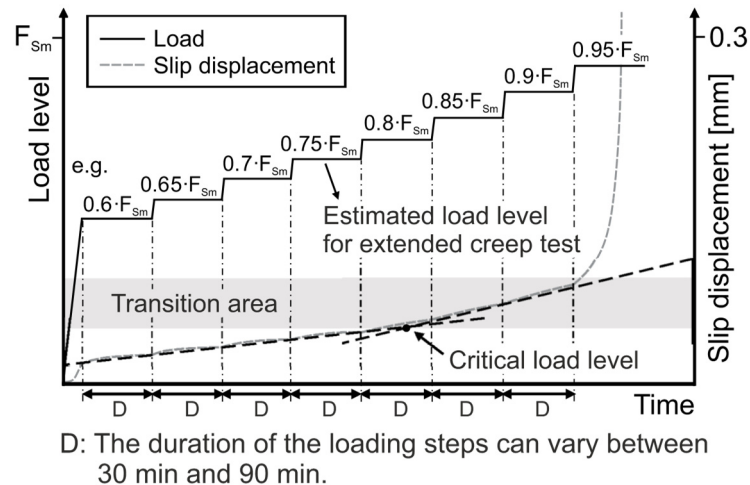
(b) Method (1) for the evaluation of the stepwise test developed by FhIGP

Figure 3-10: Step test developed by FhIGP and TUD in order to estimate the suitable load level for extended creep test [106]

Ideally, the elapsing time for each individual loading step is ideally 90 min, but it can also be reduced to 30 min depending on the selected evaluation method. For the step test, the slip deformation behaviour of the test specimen can be observed, see Figure 3-10. In this figure, an over-proportional increase in the deformations can be observed before the test specimen slips through. As already mentioned, the evaluation of this test can be conducted in two different ways in order to estimate a load level at which the test specimen just does not slip through and it can be expected that the extended creep tests will successfully pass the required criterium.

3.2.6.3 Method (1) for the evaluation of the stepwise test

Method (1) was developed at FhIGP. In order to estimate the suitable load level for the extended creep test, the lower limit of the transition zone in which the slip displacement in the specimen increases exponentially is assumed, see Figure

3-10 (b). Since the sliding behaviour of a test specimen is measured with eight displacement transducers, see Chapter 3.2.3, the averaged deformations from the displacement transducers associated with the respective slip planes must of course be considered.

3.2.6.4 Method (2) for the evaluation of the stepwise test

Method (2), which was developed at TUD, is based on checking the slip rate in the step test. For this purpose, the duration of a load step should be selected with sufficient length, e.g. 90 min. The slip rate in the specimen should be lower at low load levels than at higher load levels. There is only one exception to this, when at the beginning of the first loading step the slip rate is very high for experimental reasons. By considering the rapid increase in the slip rate for higher load levels, it would be possible to estimate a load level which can be assumed so that the extended creep test will be passed at this load level. Figure 3-11 shows the concept for calculating the slip rate for three different time ranges: 1. at the beginning, 2. in the middle, and 3. at the end of the corresponding loading steps, whereby the time ranges are divided into three intervals within the 90-minute elapsing time period. In principle, it is sufficient to determine the slip rate only for a constant time range at the end of the loading step. Experience from SIROCO has shown that the critical load level is reached when the slip rate at the end of the loading step is between 0.1 mm/min and 0.15 mm/min.
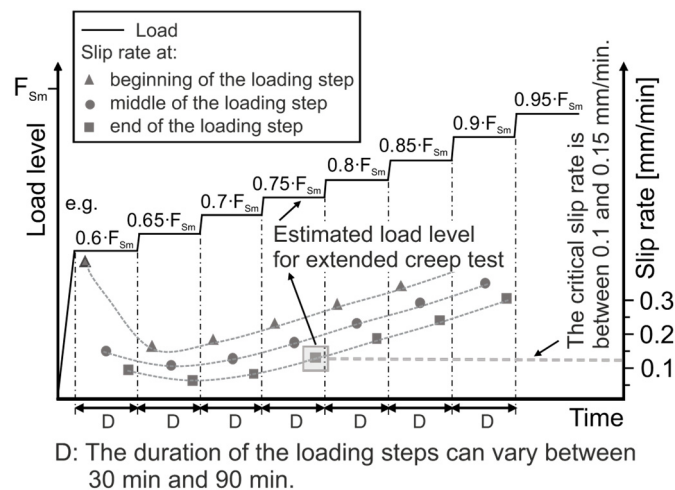
Figure 3-11: Method (2) for the evaluation of the stepwise test developed by TUD in order to estimate the suitable load level for the extended creep test [106]

3.2.7 Methods for measuring the preload in the bolts

In order to guarantee the performance of slip-resistant connections, it is important to be sure about the existing preload level in the bolting assemblies. Over recent years, several methods have been developed in order to control the tightening process through torque, turn, and stretch, to indicate or measure the preload level in the bolts [21], [113], [114] and [115]. The present measurement techniques are strain-gaged bolts, strain-gaged force washers/load cells (LC), load-indicating washers/direct

tension indicators (DTI), alternate design bolts (twist-off bolts), load-indicating bolt, computerized tension-control systems and ultrasonic measurement of stress in a bolt [113]. Not only do none of these available methods really measure stress in the bolt, but most of them are also based on stretch measurement techniques [114].

In the frame of this investigation, two different methods for measuring the preload level in the bolts were selected. Thereafter, a comparative study regarding the accuracy of these methods was conducted. Instrumented bolts were combined with the long load cell for three different surface conditions (GB-I, ASI-I and HDG-I) in order to compare the measured preload levels for the same test specimens, see Figure 3-12 (a).

As mentioned in Chapter 3.2.2, all test specimens were M20 bolt geometry according to EN 1090-2 and all bolts were preloaded to $F_{p,C}$, which is equal to ≈ 172 kN for an M20 bolting assembly. In order to compare these two methods, the initial preloads at the beginning of testing and the actual preloads at the slip in the bolts were measured by SG and LC. The results of preload measurements for all different surface conditions are presented in Figure 3-12 (b), (c) and (d).

The preload losses due to embedment of the clamped component surfaces, creep in the coating material, and transversal contraction can be observed from these diagrams. It can also be seen that the deviations between the measured preload by instrumented bolts with strain gauges and the load cells are negligibly small, with a maximum deviation of 1.3 %.

Furthermore, the mean values of the loss of preloads during the test were detected to be approximately 9 % for grit blasted specimens (GB-I), 7 % for Alkali-zinc silicate coated specimens (ASI-I) and 3 % for hot dip galvanized specimens (HDG-I) [116], [117]. Transversal contraction causes the main part of the loss of preload in slip factor tests. The transversal contraction increases with increasing slip load, which results in preload losses corresponding to the level of the slip load. This phenomenon gives an explanation for the higher loss of preload during the test for grit blasted specimens.
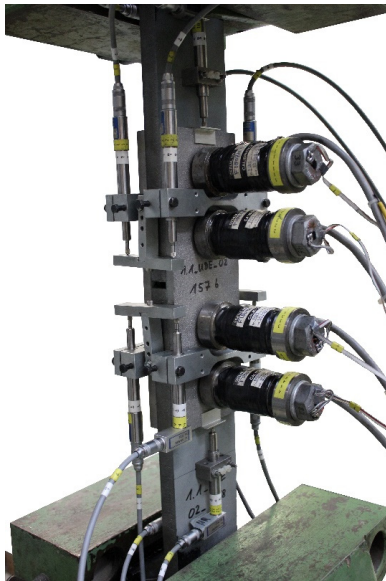
(a) Test setup
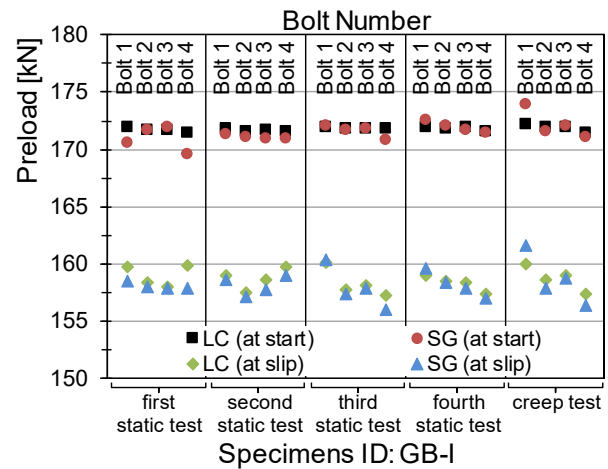
(b) Grit blasted specimens
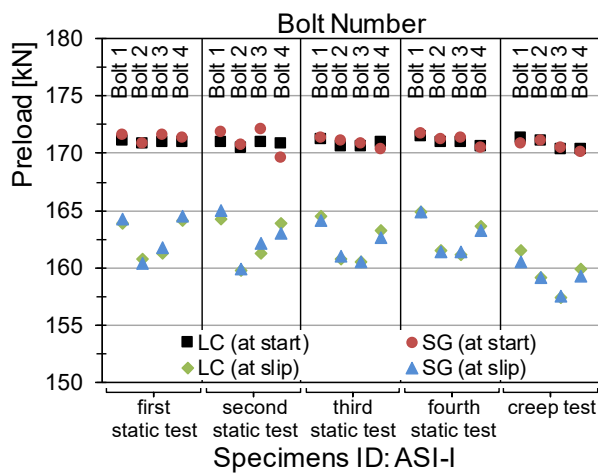
(c) Alkali-zinc silicate coated specimens
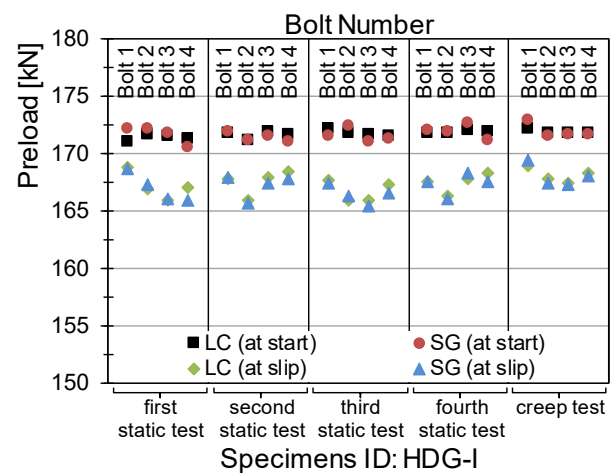
(d) Hot dip galvanized specimens

Figure 3-12: Comparison of preload measurements considering instrumented bolts and load cells for M20 bolting assemblies with $F_{p,C}$ preload level ≈ 172 kN [106]

3.2.8 Position of slip measurement

The position of slip measurement plays an important role in the evaluation of slip factors. As Annex G of EN 1090-2: 2011 (old version) did not exactly prescribe the position of the slip measurement, different positions for measuring the displacement can be found in the literature which may present different slip factors for identical surface conditions. By studying different literature, it can be seen that the most common positions for mounting the LVDTs are CBG (LVDTs 1-8) and PE position (LVDTs 9-12), see Figure 3-5. In order to investigate the influence of the positioning of displacement transducers on the slip measurement and the evaluation of the slip factor, twelve displacement transducers were mounted on the test specimens to measure the slip displacement in both positions [111], [116]. The results of the static and the creep tests based on LVDTs at PE position are summarized in Table 3-3.

Table 3-3: Slip factor test results based on LVDTs at PE position (LVDTs 9-12) [106]

Series ID	Surface preparation		$\Sigma t/d$ [4] [-]	Number of tests st/ct(sp)/ect [5]	$\mu_{nom,mean}$ [6] st/st+ct [-]	$\mu_{ini,mean}$ [7] st/st+ct [-]	$\mu_{act,mean}$ [8] st/st+ct [-]	V (μ_{nom}) [9] st/st+ct [%]
	Sa[1] / Rz[2] [µm]	DFT[3] [µm]						
Grit blasted surfaces (GB)								
GB-I	Sa 2½ / 80	-	7.6	4/1/-	0.61/0.61	0.61/0.61	0.64/0.64	2.0/2.0
GB-II			4.2	2/-/-	0.60/-	0.60/-	0.64/-	1.4/-
GB-III			2.6	2/-/-	0.61/-	0.61/-	0.67/-	1.5/-
Cruz et al. [49]	Sa 2½ / -		2.4	4/1/-	-/0.56	-/-	-/-	-/-
Alkali-zinc silicate coating (ASI)								
ASI-I	Sa 2½ / 80	60	7.6	4/1/-	0.62/-	0.63/-	0.65/-	1.3/-
ASI-II			4.2	2/-/-	0.62/-	0.62/-	0.66/-	2.4/-
ASI-III			2.6/2.4	2/(3)/2	0.60/-	0.61/-	0.66/-	1.7/-
Aluminium spray metallized (Al-SM)								
Al-SM-I	-	250	4.2	2/-/-	0.56/-	0.56/-	0.62/-	2.5/-
Al-SM-II			2.6/2.4	4/1(3)/2	0.56/-	0.56/-	0.64/-	2.3/-
Zinc spray metallized (Zn-SM)								
Zn-SM-I	Sa 3 / 100	140	4.2	4/-/1	0.58/-	0.58/-	0.62/-	4.4/-
Zn-SM-II			2.6/2.4	2/-(2)/4	0.57/-	0.58/-	0.62/-	5.6/-
Combination of alkali-zinc silicate coating and zinc spray metallized (ASI–Zn-SM)								
ASI–Zn-SM-I	Sa 2½/100 – Sa 3/100	55 – 170	2.4	4/1/4	0.58/-	0.59/-	0.65/-	2.7/-
Hot dip galvanized (HDG)								
HDG-I	-	105	7.6	4/1/-	0.46/-	0.46/-	0.47/-	8.5/-
HDG-II			2.4	2/-/2	0.47/-	0.47/-	0.50/-	13.0/-
HDG-III		80		4/-/-	0.12/-	0.12/-	0.12/-	7.1/-

[1] surface preparation grade │ [2] surface roughness │ [3] dry film thickness (coating thickness) │
[4] clamping length ratio (Σt: clamping length, d: bolt diameter) │ [5] st: static test/ct: creep-/ect: extended creep test │ [6] $\mu_{nom,mean}$: calculated slip factors as mean values considering the nominal preload level │
[7] $\mu_{ini,mean}$: calculated slip factors as mean values considering the initial preload when the tests start │
[8] $\mu_{act,mean}$: calculated slip factors as mean values considering the actual preload at slip │ [9] V: coefficient of variation for μ_{nom}

By comparing the results from Table 3-2 and Table 3-3, it can be seen that in some cases the difference between evaluated slip factors based on CBG position (LVDTs 1-8) and PE position (LVDTs 9-12) is noticeable. The greatest differences can be seen in grit blasted surfaces. On the other hand, for HDG-III, both positions represent the same value for the slip factor. The most important question now, therefore, is what is the reason for such a discrepancy between the slip factors for some surface treatments?

In Figure 3-13, for each type of test series one typical test has been chosen (for instance st1: first static test), which is presented by two graphs to represent the behaviour of the upper and lower part of the connection. It can be seen that the stiffness of the slip-deformation behaviour is much higher when measured at CBG position than at PE position. Furthermore, large differences in the slip load result when the 0.15 mm slip criterion is used. Based on LVDTs at PE position, the maximum slip loads are reached far above 0.15 mm for GB-III (for ASI-III, HDG-II, Al-SM-II, Zn-SM-II and ASI-Zn-SM-I the same behaviour was observed). This is explained by the fact that using LVDTs at PE position means the elongation of the plates is implicitly measured as well. The influence of elongation can be more visible when the level of slip load is higher. On the other hand, this phenomenon can be neglected when the slip occurs in the lower load level, for example HDG-III, see Figure 3-13 (b).
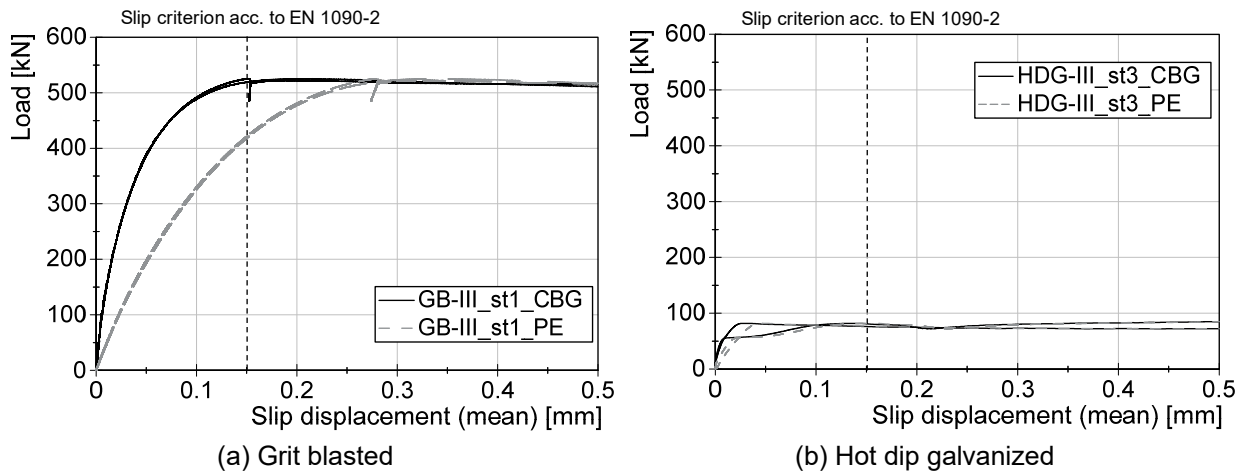
Figure 3-13: Influence of positioning the LVDTs on slip-resistant behaviour of the connection [106]

Consequently, considering the 0.15 mm slip criterion and positioning the LVDTs at PE position might lead to much lower slip factors than positioning them at CBG position. This must be kept in mind when comparing results from the literature. For example, Cruz et al. [49] performed slip factor tests with positions of displacement transducers comparable to those at PE position. The results of grit blasted surfaces fit quite well with the lower slip factors achieved with LVDTs at PE position, see Table 3-3.
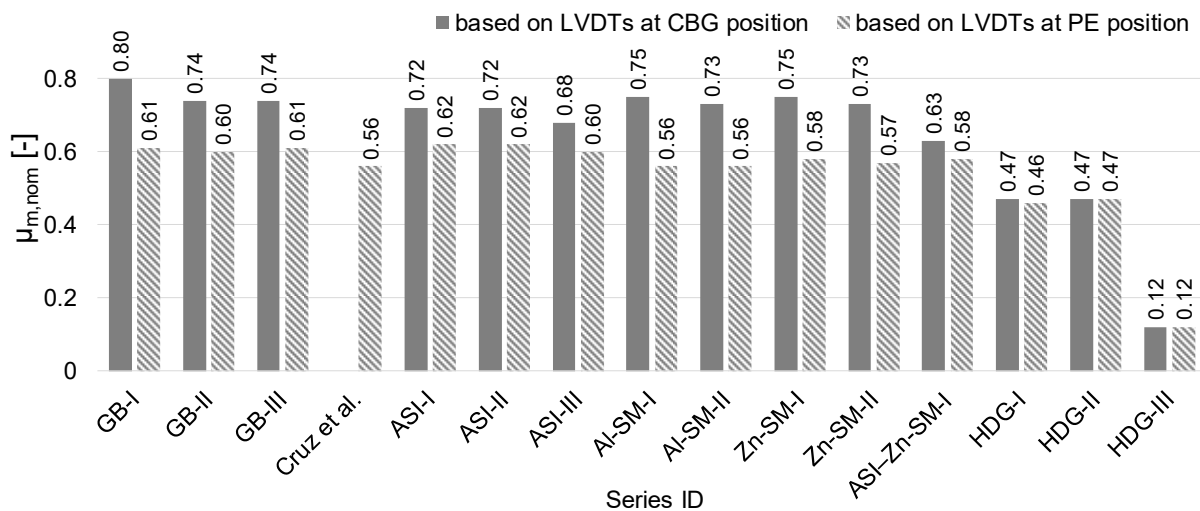
Figure 3-14: Influence of positioning the LVDTs (CBG vs. PE) on determination of the slip factor [106]

3.2.9 Influence of different clamping lengths

3.2.9.1 General

Having longer clamping length ratio would reduce the loss of preload in the connection and consequently may influence the slip-resistant behaviour of the connection. In the frame of this study, the influence of different clamping lengths on the slip-resistant behaviour of bolted connections is investigated based on experimental and numerical observations.

3.2.9.2 Experimental investigations

The relaxation behaviour of bolted connections describes the time-dependent loss of preload due to viscoplastic deformations in bolting assemblies or clamped components. This phenomenon can be influenced by many factors. The resilience of the bolt is one of these parameters which itself is dependent on clamp length, cross section and the Young's modulus of the bolt material [35]. By increasing the clamping length ratio of the connection, the elastic resilience of the bolt increases and it is reasonable to expect a decrease in the loss of preload of the bolts [23], [54].

However, changing the clamping length and consequently the existing preload in the bolt affects the slip-resistant behaviour of the connection. In order to cover this gap of knowledge, an investigation was carried out with four different surface treatments (GB, ASI, Al-SM and Zn-SM) and three different clamping length ratios ($\Sigma t/d$) where Σt is the clamping length and d is the bolt diameter, see Figure 3-4 (a), (c) and (d).

As already mentioned in Chapter 3.2.7, two different methods were selected for measuring the preload (SG and LC). In this case, the use of LCs leads to a relatively large clamping length ratio of the bolts ($\Sigma t/d = 7.6$) which influences the loss of preload and may consequently influence the level of the slip load, see [111], [116], [117] and [118].

Evaluating the mean initial slip factor by considering the initial preload in the bolts without taking into account the large clamping length ratio might lead to an overestimation of the slip factor. This is because a reduction in preload losses due to an increasing clamp length ratio would lead to an increase in the critical slip load level, see Figure 3-15 (a). However, if the mean actual slip factors are evaluated based on the actual preload level, the resulting slip factors of each surface condition do not vary significantly and are nearly on the same level for all three different clamping length ratios, see Figure 3-15 (b).

(a) Initial static slip factor vs. clamping length ratio

(b) Actual static slip factor vs. clamping length ratio
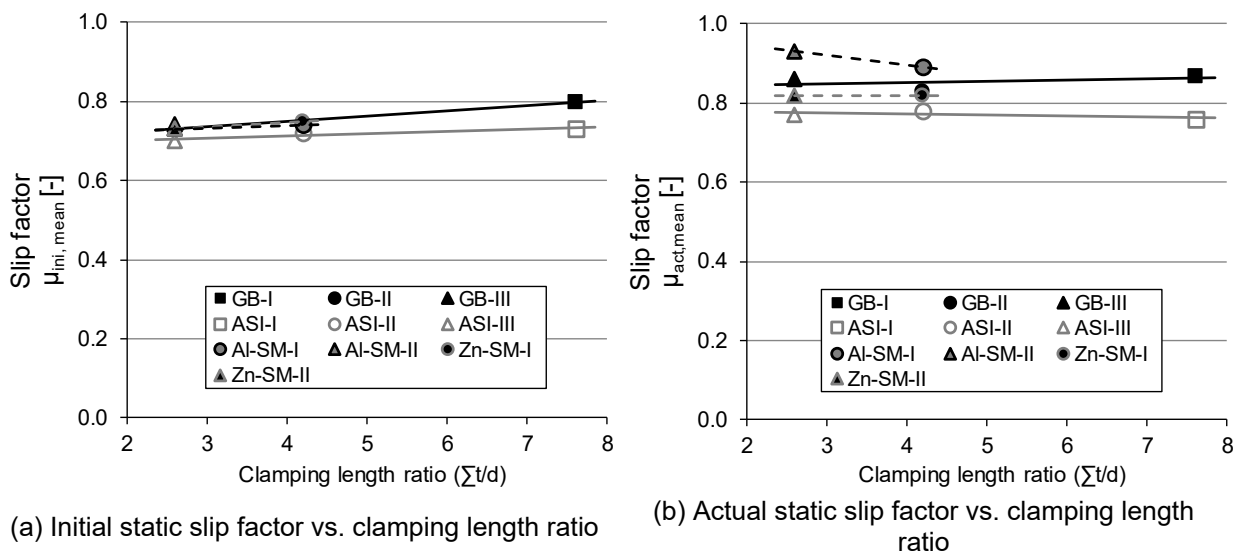
Figure 3-15: Influence of clamping length ratio on initial and actual static slip factor [106]

3.2.9.3 Numerical investigation

Additional to the experimental investigation in the frame of the SIROCO project, a comparative numerical investigation was carried out in order to assess the influence of the different clamping lengths on the slip-resistant behaviour of the connection. For this purpose, the Dassault Systemes SIMULIA Abaqus 2018 [119] software was selected.

In total, six different clamping length ratios were selected, see Table 3-4 and Figure 3-16. The numerical model was calibrated based on experimental investigation of M20 test specimens with grit blasted faying surfaces, see Table 3-2. For this reason, the models were also developed based on M20 test specimen geometry according to EN 1090-2, Annex G and the preload level of $F_{p,C}$ was selected for all numerical parametric study analyses. All models were simulated as quarter of the total specimen to take advantage of symmetry along the longitudinal and transversal axes, see Figure 3-17. Appropriate boundary conditions were selected in order to consider the symmetricity of the model.

Table 3-4: Numerical and experimental test results for GB test series – regarding the influence of different clamping lengths

Series ID	$\Sigma t/d$ [1)] [-]	Preload [kN]	$\mu_{nom,mean}$ [2)] [-]	$\mu_{ini,mean}$ [3)] [-]	$\mu_{act,mean}$ [4)] [-]
			Based on CBG/PE positions		
Experimental test - grit blasted surfaces (GB)					
GB-I	7.6		0.80/0.61	0.80/0.61	0.87/0.64
GB-II	4.2	$F_{p,C}$	0.74/0.60	0.74/0.60	0.83/0.64
GB-III	2.6		0.74/0.61	0.74/0.61	0.86/0.67
FEM analyses - calibrated base on GB-III test series					
EN1090_M20_10.5	10.5		0.78/0.57	0.77/0.58	0.85/0.64
EN1090_M20_5.5	5.5		0.77/0.59	0.76/0.58	0.85/0.64
EN1090_M20_4.5	4.5	$F_{p,C}$	0.76/0.59	0.75/0.58	0.85/0.64
EN1090_M20_3.5	3.5		0.75/0.58	0.75/0.58	0.85/0.65
EN1090_M20_2.6[5)]	2.6		0.74/0.58	0.74/0.58	0.85/0.65
EN1090_M20_2.4	2.4		0.73/0.58	0.73/0.58	0.85/0.65

[1)] clamping length ratio (Σt: clamping length, d: bolt diameter) │ [2)] $\mu_{nom,mean}$: calculated slip factors as mean values considering the nominal preload level │ [3)] $\mu_{ini,mean}$: calculated slip factors as mean values considering the initial preload when the tests start │ [4)] $\mu_{act,mean}$: calculated slip factors as mean values considering the actual preload at slip │ [5)] calibrated base on GB-III test series
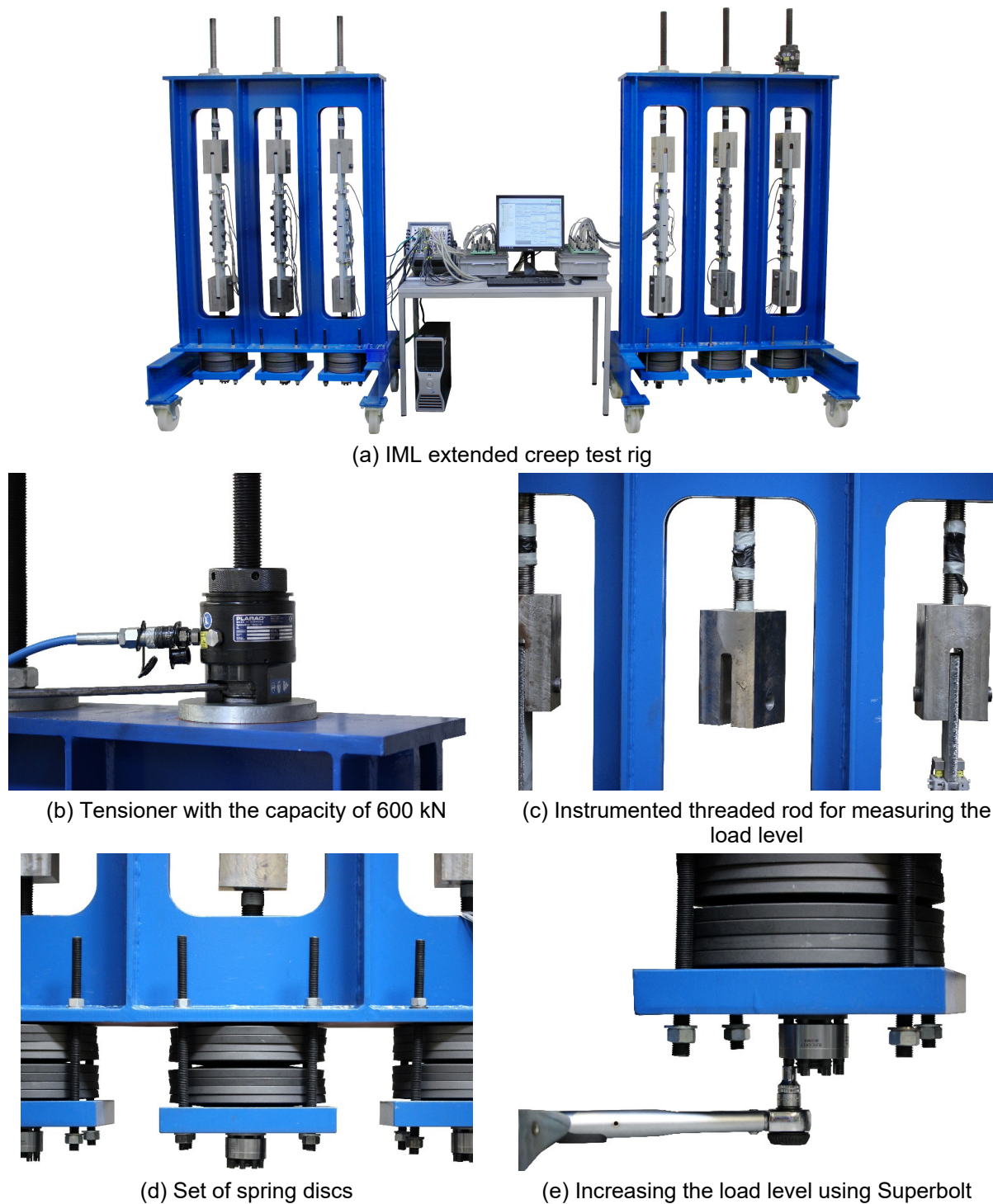
(a) $\Sigma t/d = 10.5$

(b) $\Sigma t/d = 5.5$

(c) $\Sigma t/d = 4.5$

(d) $\Sigma t/d = 3.5$

(e) $\Sigma t/d = 2.6$

(f) $\Sigma t/d = 2.4$
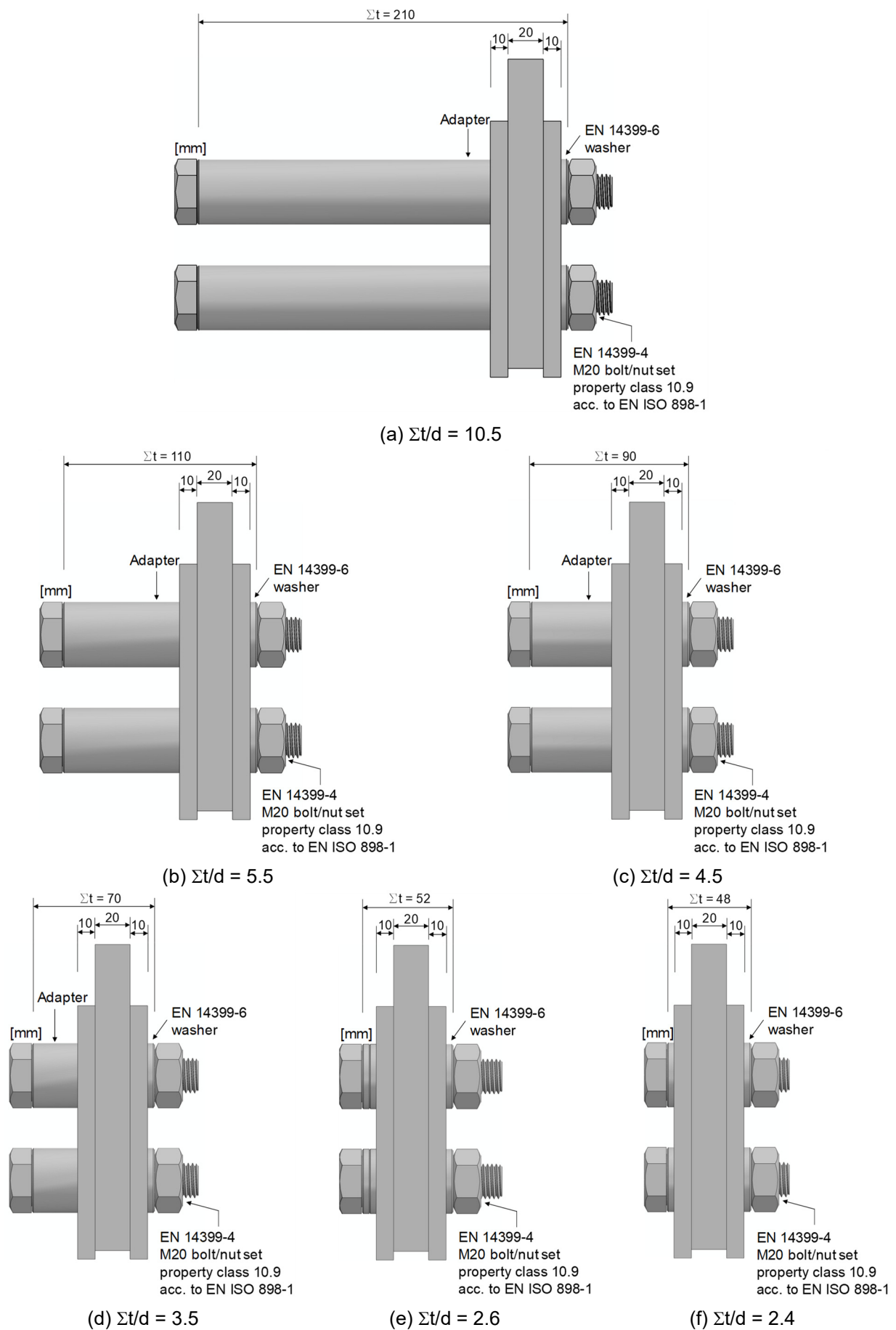
Figure 3-16: Different clamping length ratios considered in FE analyses
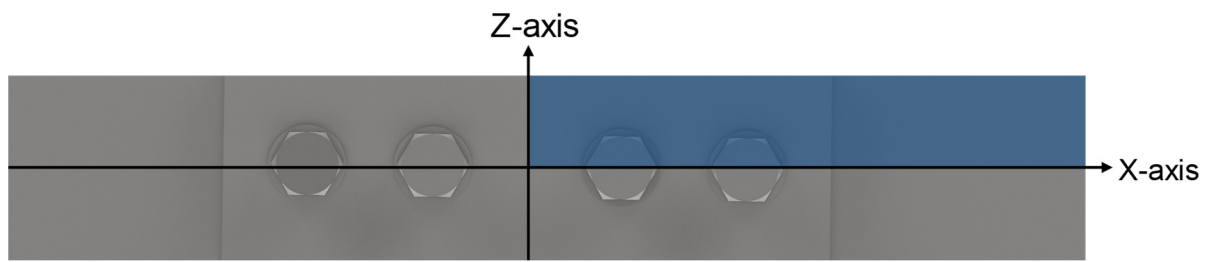
Figure 3-17: Symmetry model along the longitudinal and transversal axes

The high-strength structural bolting assemblies were modelled based on the HV system according to EN 14399 with property class 10.9. The material property of the clamped plate was defined as carbon steel S355 according to EN 10025-2. For this reason, tensile tests were performed separately on bolt and plate material in order to achieve the individual engineering stress-strain curves for each material. This relation is based on the length of the specimen and the original cross-section area. In the frame of this study, true stress-strain curves were calculated considering the results of the tensile tests which are based on the respective cross-section area and length.

A 20-node quadratic brick-type element (C3D20R) with reduced integration was selected in order to mesh all components except the threaded part of the bolts, see Figure 3-18 (a). For the threaded part of the bolts and nuts a 10-node quadratic tetrahedron-type element (C3D10) was selected, see Figure 3-18 (b).
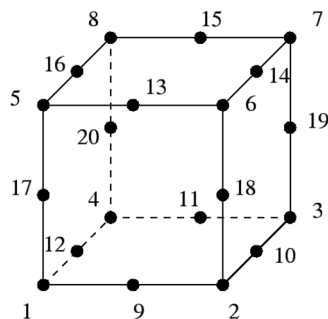
(a) 20-node brick element   (b) 10-node tetrahedral element
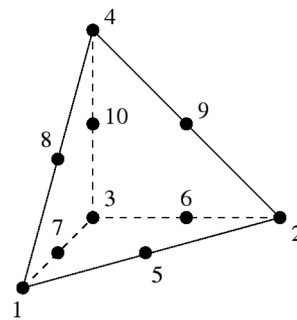
Figure 3-18: Different types of elements selected for FE analyses

The size of the mesh is an important factor to guarantee the accuracy of the results, but it also influences the time of analysis. A finer mesh may deliver more accurate results in comparison to a coarse mesh but would increase the cost of analysis. For this reason, a suitable mesh size was selected through a convergence study to deliver the required accuracy. The mesh sizes were selected in such a way that the mesh size is finer around the critical areas, see Figure 3-20.
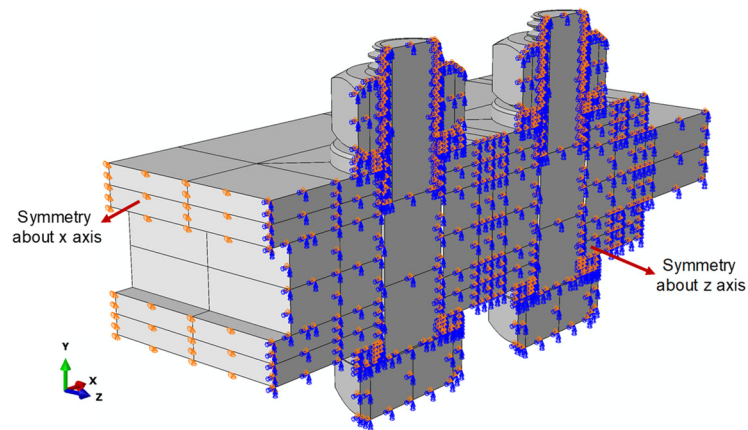
Figure 3-19: Boundary condition for FE models

a) 3D view

b) Top view
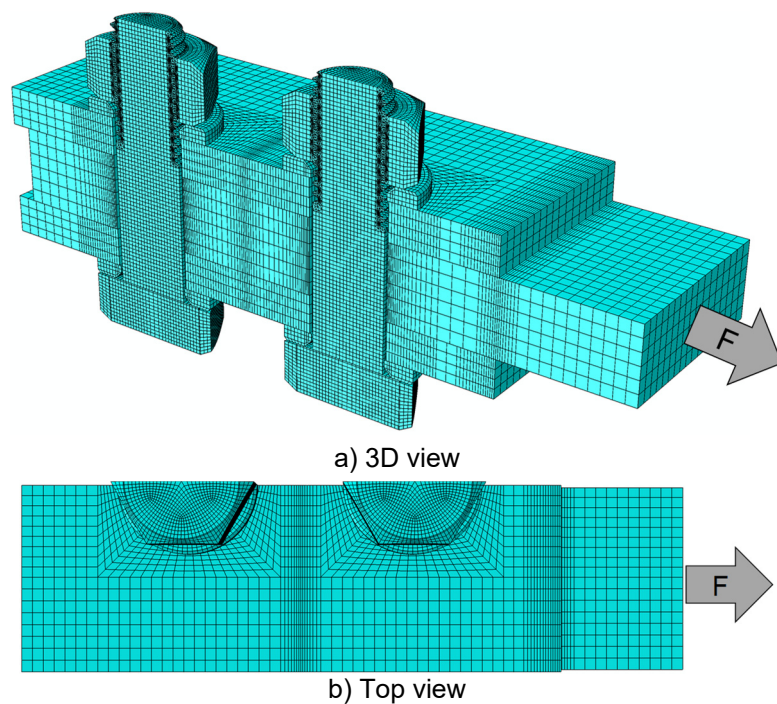
Figure 3-20: Mesh pattern for numerical investigation

A displacement-controlled loading was applied to the specimen as a uniform translational displacement at the end of the inner plate, see Figure 3-20. A displacement of 1 mm was applied to each model in order to investigate the slip-resistant behaviour of the connection.

In this study, the slip relative displacement was measured in both CBG (between points a, b and c) and PE (between points e, f and g) positions, Figure 3-21.
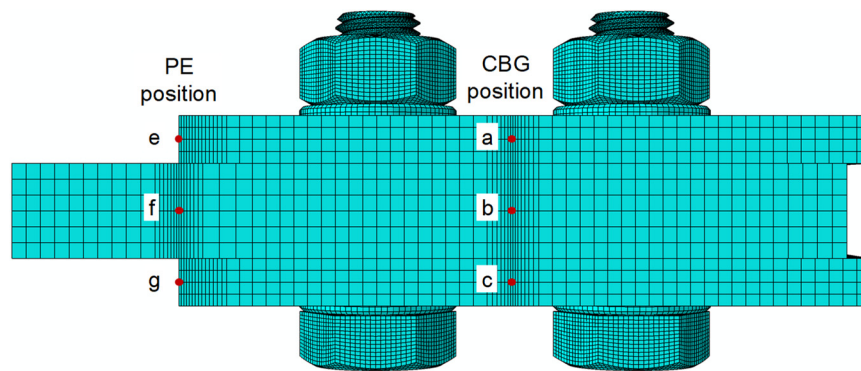
Figure 3-21: Position of measuring relative displacement at CBG and PE position in FE analysis

A penalty friction formulation was used in order to define the interaction between all contact surfaces. The friction coefficient between paired threaded parts, between the bolt head and washer and between nut and washer was set to 0.13. This value was selected based on tightening tests performed in the frame of the SIROCO project on bolting assemblies made of carbon steel. The same method was used to define interaction between the washers and cover plates, but the friction coefficient was set to 0.5 according to EN 1993-1-8 and VDI 2230 part 1 [120].

The definition of interactions between the faying surfaces is essential – beside the preload level – and the key parameter for slip-resistant behaviour of the connection. In order to calibrate the numerical model based on the experimental results, an appropriate coefficient of friction was selected in terms of interaction definition. This method was used in order to calibrate the EN1090_M20_2.6 model based on GB-III test series experimental results.

Figure 3-22 (a) shows typical load-slip displacement diagrams in order to validate the accuracy of the numerical test results. The results show agreement between the FE model and the experimental tests even for the results evaluated based on the slip measurement at CBG or PE positions.

As can be seen in Figure 3-22 (b), with preloading of the bolts, the highest concentration of stress is around the holes. This phenomenon leads to higher surface pressures around the holes in comparison with the other areas on the faying surfaces. For this reason, the deformation of the profile at the faying surfaces around the holes is more visible in the experimental test.

The static slip factors were evaluated by considering the initial preload at the beginning of the test (μ_{ini}), the nominal preload level (μ_{nom}) and the actual preload at the point of slip (μ_{act}) based on both CBG and PE positions, see Table 3-2. The results show that in general the influence of the clamping length on the slip-resistant behaviour of the connection is not significant, see Figure 3-23.

(a) Load-slip displacement diagrams

(b) Stress concentration
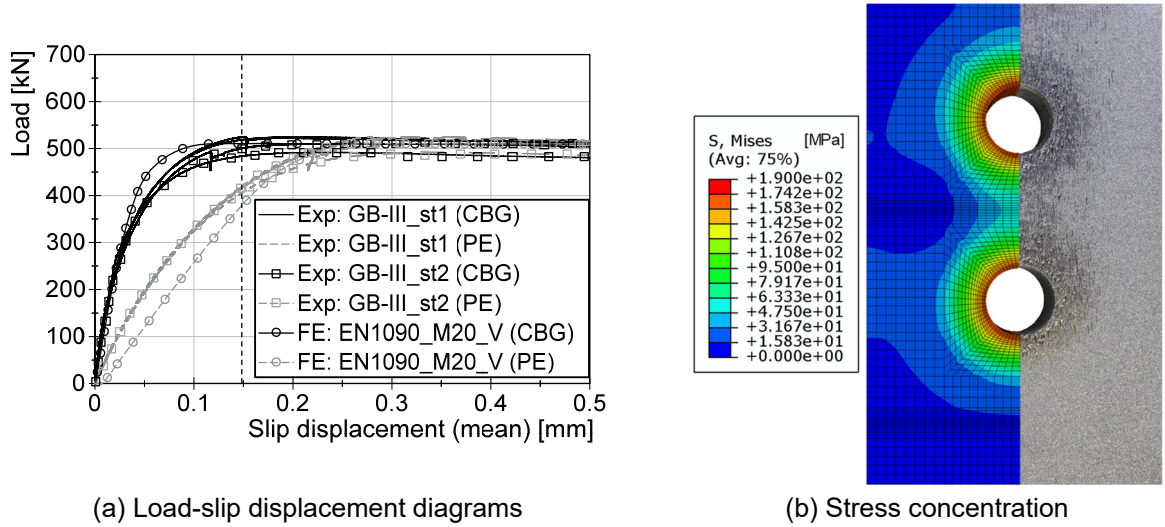
Figure 3-22: Calibration of the FE model – for grit blasted surface condition

(a) Load-slip displacement diagram based on CBG position

(b) Load-slip displacement diagram based on PE position

(c) Initial and actual slip factor based on CBG position

(d) Initial and actual slip factor based on PE position
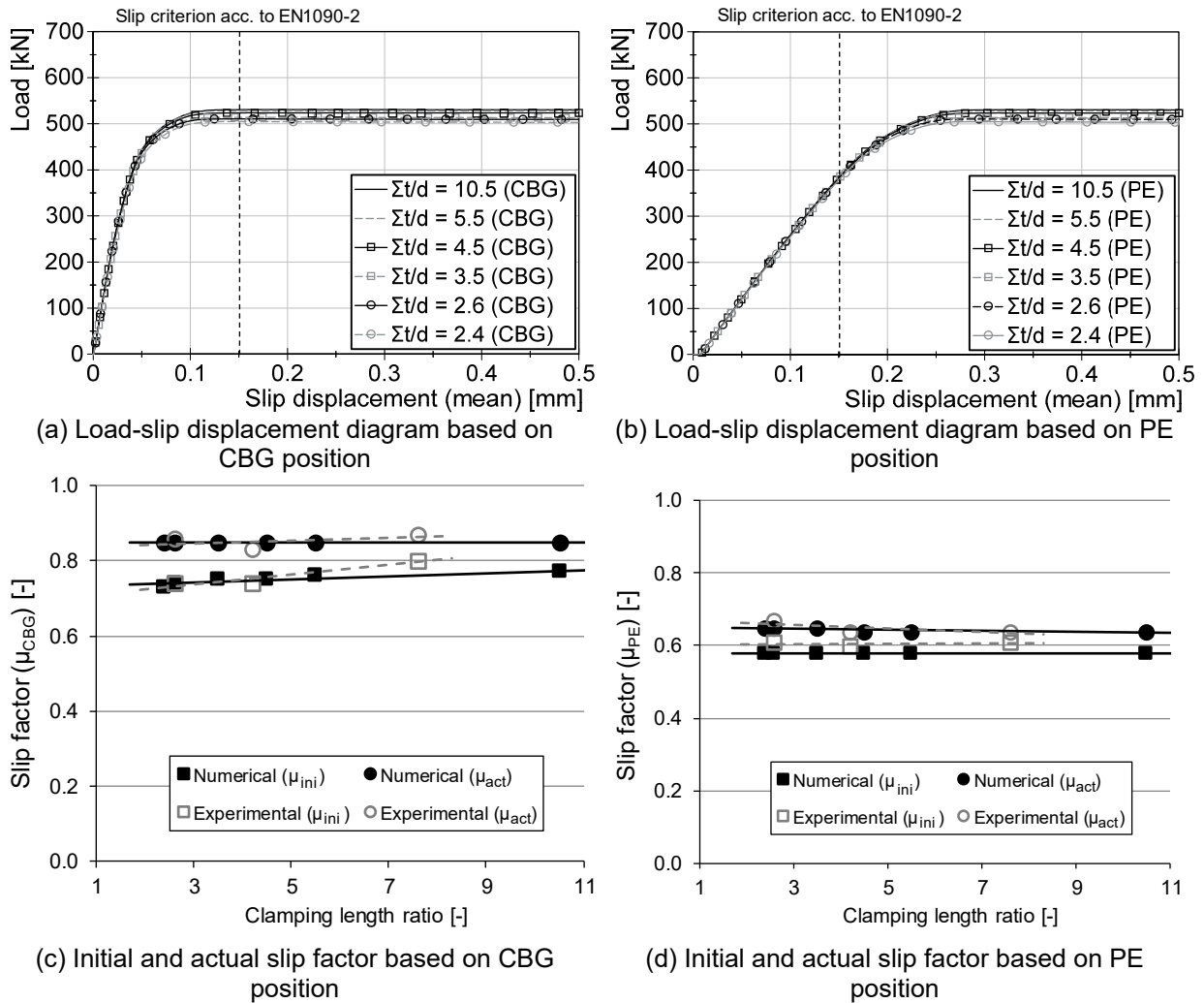
Figure 3-23: Comparison between the FE model and experimental results – influence of clamping length ratio

As can be seen in this figure, considering 0.15 mm as an evaluation criterion based on EN 1090-2 leads to very conservative results for the evaluations based on PE

position. For this reason, the numerical models reach the same slip load level at 0.15 mm at PE position for all different clamping length ratios, see Figure 3-23 (b), which leads to the same slip factors, see Figure 3-23 (d). On the other hand, the evaluation of the results based on the measured slip at CBG position shows that the slip load increases slightly if the clamping length ratio is increased, see Figure 3-23 (a). This means that slightly higher nominal/initial slip factors can be achieved by increasing the clamping length ratio, Figure 3-23 (c). This figure also shows that the actual slip factors calculated considering the actual preload level at slip are not affected by changes in the clamping length ratio.

3.2.10 Influence of different preload levels

3.2.10.1 General

The preload level in slip-resistant connections is a major parameter, which may influence the determination of the slip factor directly. In order to investigate this parameter, experimental and numerical investigations were conducted in order to provide a better insight into the influence of preload level on the slip-resistant behaviour of bolted connections.

3.2.10.2 Experimental investigation

One of the further objectives was to investigate the influence of different preload levels on the determination of the slip factor. For this purpose, several surface conditions – alkali-zinc silicate (ASI), thermal spray and metallized with zinc (Zn-SM) and a combination of alkali-zinc silicate and zinc thermal spray metallized coating (ASI–Zn-SM) with different preload levels, $F_{p,C}$, $F_{p,C}^*$ and $0.9 \cdot F_{p,C}^*$ – were investigated, which were $F_{p,C} = 172$ kN, $F_{p,C}^* = 160$ kN and $0.9 \cdot F_{p,C}^* = 144$ kN for the examined M20 bolting assemblies.

The static test results for all different surface preparations considering different preload levels are presented in Figure 3-24. The results show that the slip load increases slightly with increasing preload. However, in most cases a higher static slip factor was achieved with a lower preload level.

As shown in Chapter 3.2, the LVDTs were placed at PE position, see Figure 3-25 (a). In order to calculate the actual slip displacement at CBG position, a correlation between the measured slip displacement at CBG and PE position based on the results of the corresponding first four static tests was developed. Figure 3-25 (b) shows the PE-CBG conversion models used for all series (valid for PE LVDTs fixed to the inner plates at 12 mm distance of CBG position).

(a) ASI coating

(b) Zn-SM coating

(c) ASI – Zn-SM coating

(d) Mean initial slip factor ($\mu_{ini,mean}$)
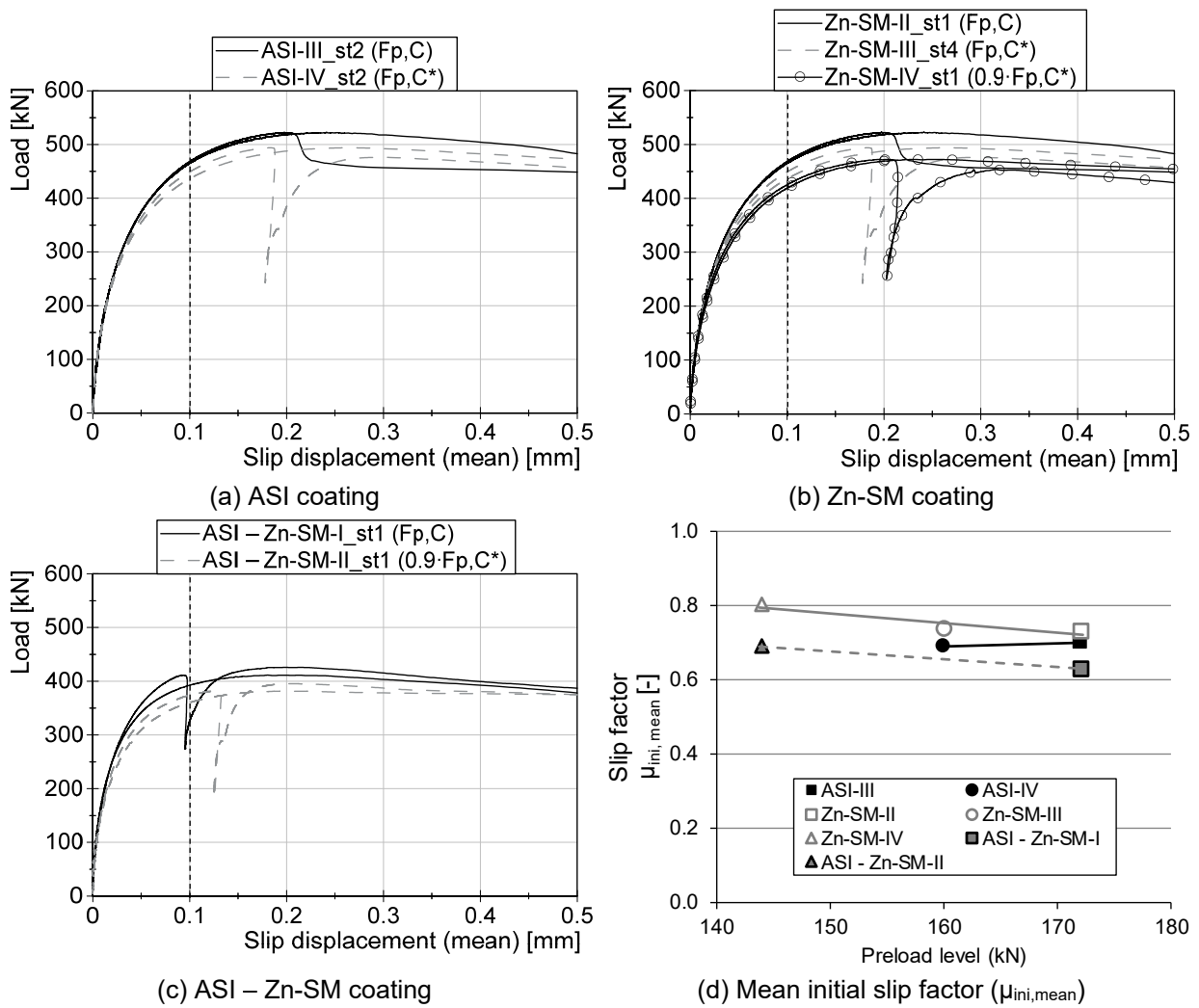
Figure 3-24: Influence of different preload levels on static slip load-slip displacement behaviour and the initial slip factor [106]

(a) Test setup
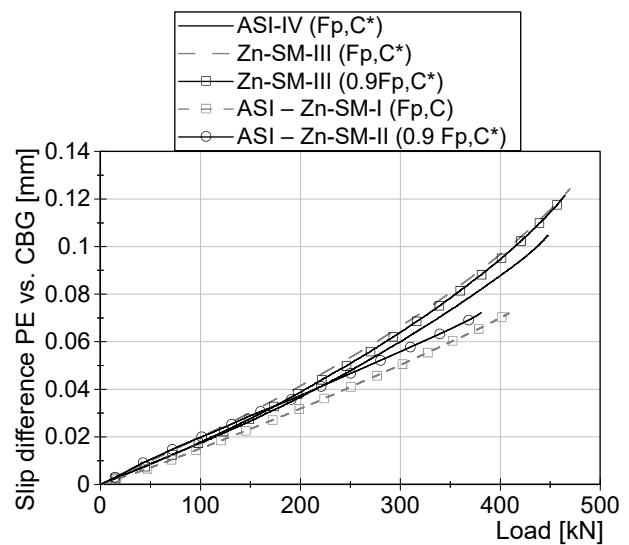
(b) Relation between load and difference between slip measured at PE and CBG position

Figure 3-25: Extended creep test setup and correlation between slip measured at PE and CBG position [106]

The results of the extended creep tests for all three different surface conditions are presented in Figure 3-26. Evaluating the slip displacement-log time curve based on the results of the creep tests is an effective way to get more information on the creep sensitivity of the coated surfaces. As can be seen in Figure 3-26 (a), the results from the creep tests for ASI coating with a preload level of $F_{p,C}*$ and a load level of $0.90 \cdot F_{Sm}$ can be considered as a passed extended creep test. However, the duration of the creep test is too short in comparison to the extended creep tests. In order to consider this load level as an appropriate load level for extended creep tests, an extended creep test with a constant load level of $0.9 \cdot F_{Sm}$ was performed. The results show that the slip is less than 0.3 mm when extrapolated to 50 years, and the test is clearly passed, see Figure 3-26 (a).

The extended creep tests for the Zn-SM test series were performed with two different preload levels of $F_{p,C}*$ and $0.9 \cdot F_{p,C}*$. The results show that the extended creep test for Zn-SM-III is passed with a preload level of $F_{p,C}*$ and $0.65 \cdot F_{Sm}$, see Figure 3-26 (b). Figure 3-26 (c) also shows that the extended creep test for Zn-SM-IV with a preload level of $0.9 \cdot F_{p,C}*$ and $0.60 \cdot F_{Sm}$ is passed.

Seven extended creep tests were performed for ASI–Zn-SM surface condition with two different preload levels of $F_{p,C}$ and $0.9 \cdot F_{p,C}*$, see Figure 3-26 (d) and (e). The extrapolated slip displacement-log time curves show that for a constant load level of $0.70 \cdot F_{Sm}$ for ASI–Zn-SM-I and for a constant load level of $0.80 \cdot F_{Sm}$ for ASI–Zn-SM-II, the slip is less than 0.3 mm when extrapolated to 50 years. Hence, they can be considered as a passed test.

For ASI-III and Zn-SM-II coating with preload level of $F_{p,C}$ the extended creep tests were carried out at FhIGP. The results show that for the ASI-III test series the extended creep tests were passed with $0.80 \cdot F_{Sm} = 375.2$ kN and for the Zn-SM-II test series with $0.60 \cdot F_{Sm} = 300.8$ kN.

All static slip factors and final slip factors of all three surface conditions with different preload levels are summarized in Figure 3-27 (a). Figure 3-27 (b) shows the influence of the preload level on the resulting final slip factors from extended creep tests. It becomes apparent that the final slip factor increases slightly with decreasing preload level, [111], [121], [122], [123].

(a) ASI coating - $F_{p,C}$* preload level

(b) Zn-SM coating - $F_{p,C}$* preload level

(c) Zn-SM coating - $0.9 \cdot F_{p,C}$* preload level

(d) ASI–Zn-SM coating - $F_{p,C}$ preload level

(e) ASI–Zn-SM coating - $0.9 \cdot F_{p,C}$* preload level
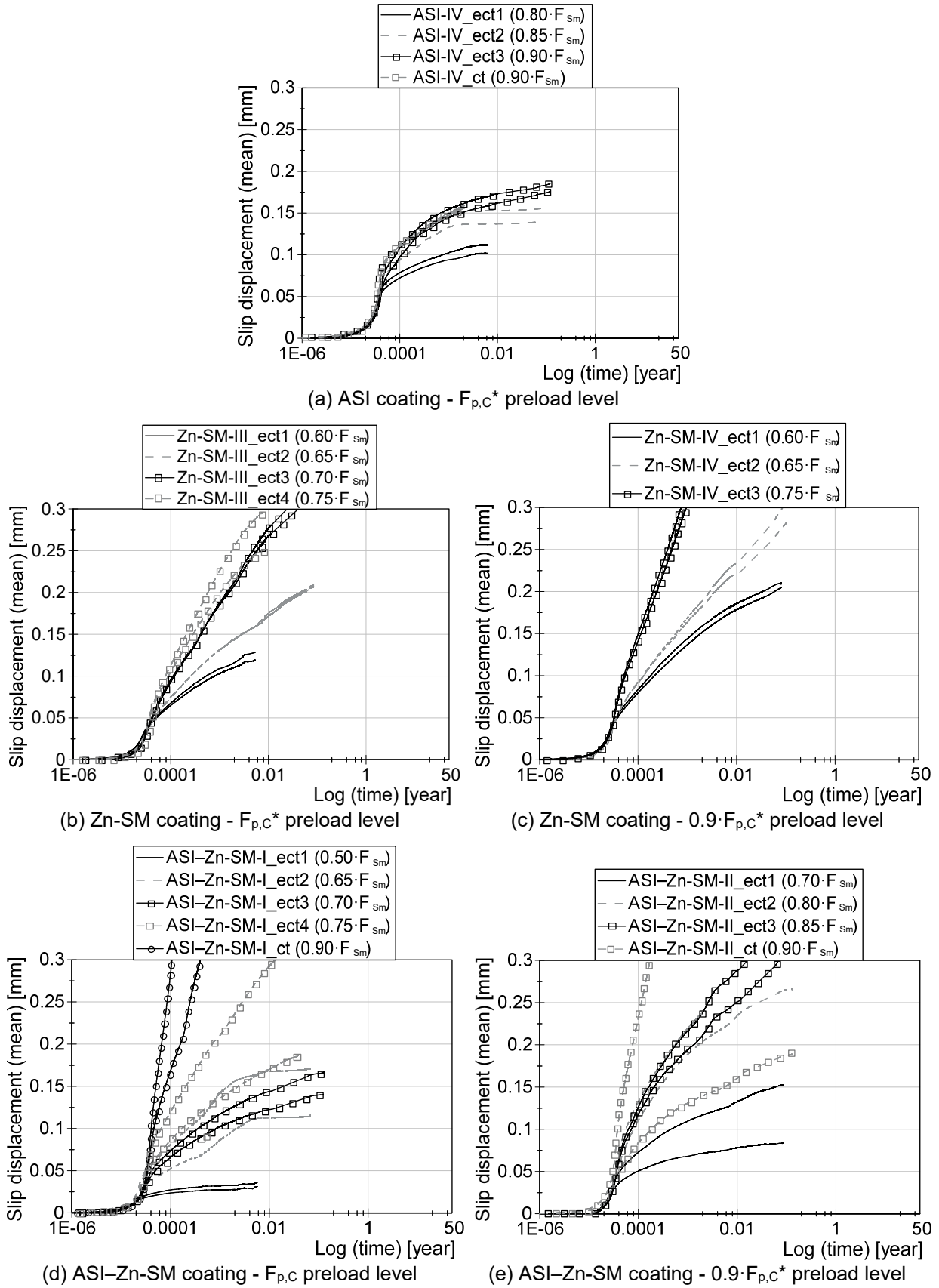
Figure 3-26: Results of the extended creep tests (each test represented by two lines which are the upper/lower section of the specimen) – influence of different preload levels [106]

(a) Mean initial slip factor ($\mu_{ini,mean}$)   (b) Final slip factor (μ_{ect})
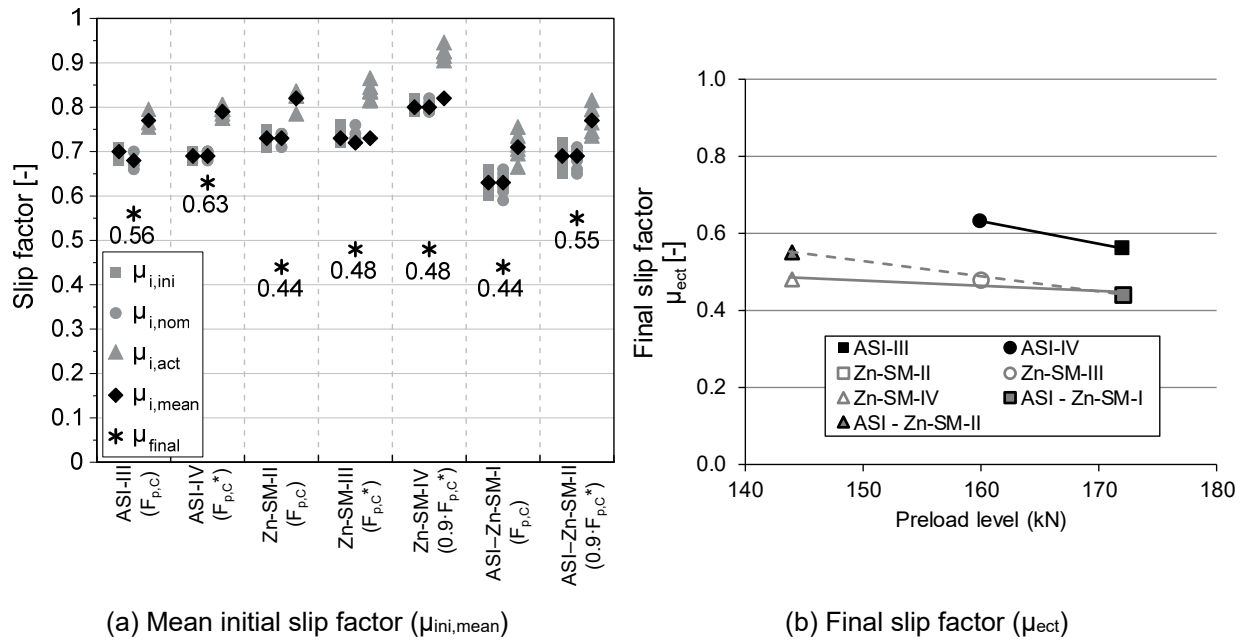
Figure 3-27: Influence of different preload levels on determination of slip factor [106]

However, the most important question that arises is: Does a lower preload level have a positive influence on the design slip resistance of a preloaded bolted connection?

This question can be answered by looking at the general equation for calculating the design slip resistance of the connection $F_{s,Rd}$ according to EN 1993-1-8.

$$F_{s,Rd} = \frac{k_s \cdot n \cdot \mu}{\gamma_{M3}} F_{p,C} \tag{3-1}$$

Where k_s is the factor for the hole detail, n is the number of the friction surfaces, γ_{M3} is the partial safety factor and $F_{p,C}$ is the required preload level which is generally equal to $0.7 \cdot f_{ub} \cdot A_s$. However, in the frame of this study, different values of the preload level were selected in order to investigate the influence of different preload levels on the slip-resistant behaviour of the connection. μ is the final slip factor after the extended creep test which shall be calculated according to Equation (3-2).

$$\mu = \frac{F_{S,Final}}{m \cdot n \cdot F_{p,C}} \tag{3-2}$$

where $F_{S,Final}$ is the adequate load level for extended creep tests in order to calculate the final slip factor and m is the number of bolts per connection. By considering Equation (3-2), Equation (3-1) can be written as:

$$F_{s,Rd} = \frac{k_s \cdot F_{S,Final}}{\gamma_{M3} \cdot m} \tag{3-3}$$

This shows that $F_{S,Final}$ is the determinative factor in order to calculate the slip resistance of the connection. Figure 3-24 shows that the static slip load increases slightly with increased preload level. However, as can be seen in Figure 3-28, it is not possible to find any relation between the final load level and the preload level. For

this reason, it is not possible to confirm the positive influence of the lower preload level on the slip resistance of the connection. The influence of preload level on slip resistance behaviour of the connection may depend on the condition of the faying surfaces.
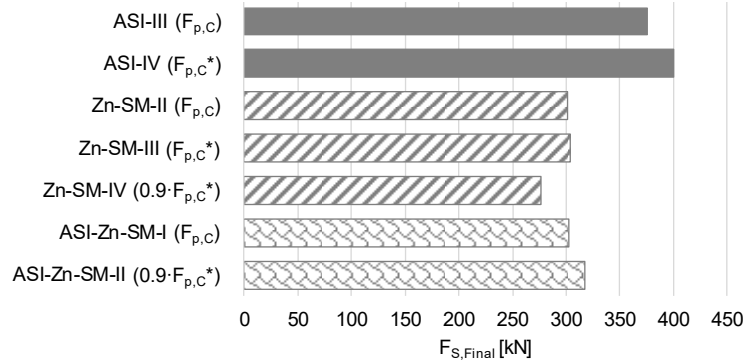
Figure 3-28: Influence of different preload levels and surface conditions on $F_{S,Final}$

EN 1090-2 prescribes that determined slip factors with specimens using bolts with property class 10.9 may also be applicable for bolts with property class 8.8. However, the other way around would not be applicable. By considering this statement, the design slip resistance of a connection including bolts with property class 8.8 and using the slip factor based on bolts with property class 10.9 can be written as Equation (3-4), since Equation (3-5) represents the relation between the preload levels for bolts with property class 8.8 and 10.9.

$$F_{s,Rd} = \frac{k_s \cdot F_{S,Final}}{\gamma_{M3} \cdot m} \cdot 0.8 \tag{3-4}$$

$$\frac{F_{p,C_{8.8}}}{F_{p,C_{10.9}}} = 0.8 \tag{3-5}$$

The comparable scenarios in this case would be the results for $F_{p,C}$ and $0.9 \cdot F_{p,C}*$, as the ratio between these two preload levels would also be about 0.8.

As can be seen in Figure 3-28, for the ASI – Zn-SM test series, if $F_{S,Final}$ from the test results using higher preload level is selected, the calculated slip-resistance for the connection would be more conservative. The only critical condition might be for the Zn-SM test series, as $F_{S,Final}$ for the Zn-SM-II test series with a preload level of $F_{p,C}$ is greater than $F_{S,Final}$ for the Zn-SM-IV test series with a preload level of $0.9 \cdot F_{p,C}*$. However, if $F_{S,Final} = 301$ kN is selected for the Zn-SM-II test series with a preload level of $F_{p,C}$ and multiplied by 0.8, this value would be less than $F_{S,Final} = 277$ for Zn-SM-IV test series with a preload level of $0.9 \cdot F_{p,C}*$. It becomes clear that the other way around would not be valid as it would lead to an overestimation in the calculated slip resistance of the connection. The results show that the EN 1090-2 statement would be valid for all tested cases in this investigation.

3.2.10.3 Numerical investigation

In order to better understand the influence of the preload level on the slip-resistant behaviour of the connection, numerical investigations were conducted with a wide range of preload levels. For this purpose, a M20 specimen geometry model with a clamping length ratio of 2.6 (as described in Chapter 3.2.9.3) was selected. All material definitions, boundary conditions and interactions are defined as described in Chapter 3.2.9.3. Five different preload levels were chosen in order to investigate the influence of different preload levels on the determination of the slip factor, see Table 3-5.

Table 3-5: Numerical slip factor test results – influence of different preload levels

Series ID	$\Sigma t/d$[4)	Preload [kN]	$\mu_{nom,mean}$[6)	$\mu_{ini,mean}$[7)	$\mu_{act,mean}$[8)
	[-]	[kN]	[-]	[-]	[-]
FEM analyses results (calibrated base on GB-III test series, see Table 3-2)					
EN1090_M20_2.6_P1		$1.2 \cdot F_{p,C}$	0.72	0.71	0.85
EN1090_M20_2.6_P2		$F_{p,C}$	0.74	0.74	0.85
EN1090_M20_2.6_P3	2.6	$F_{p,C}*$	0.75	0.75	0.85
EN1090_M20_2.6_P4		$0.9 \cdot F_{p,C}*$	0.76	0.77	0.85
EN1090_M20_2.6_P5		$0.8 \cdot F_{p,C}*$	0.78	0.78	0.85

[1) Sa: surface treatment grade | [2) Rz: surface roughness | [3) DFT: dry film thickness (coating thickness)
[4) clamping length ratio (Σt: clamping length, d: bolt diameter)

The results from the numerical analyses show that a higher preload level leads to a higher concentration of stress around the holes, which means higher surface pressures in these areas, see Figure 3-29 (a). The areas around the holes are very critical and any changes in these areas may directly influence the slip-resistant behaviour of the connection. In this case, higher surface pressures in these areas between the faying surfaces increase the load-bearing capacity of the connection, see Figure 3-29 (b).

(a) Stress distribution   (b) Load-slip displacement diagrams
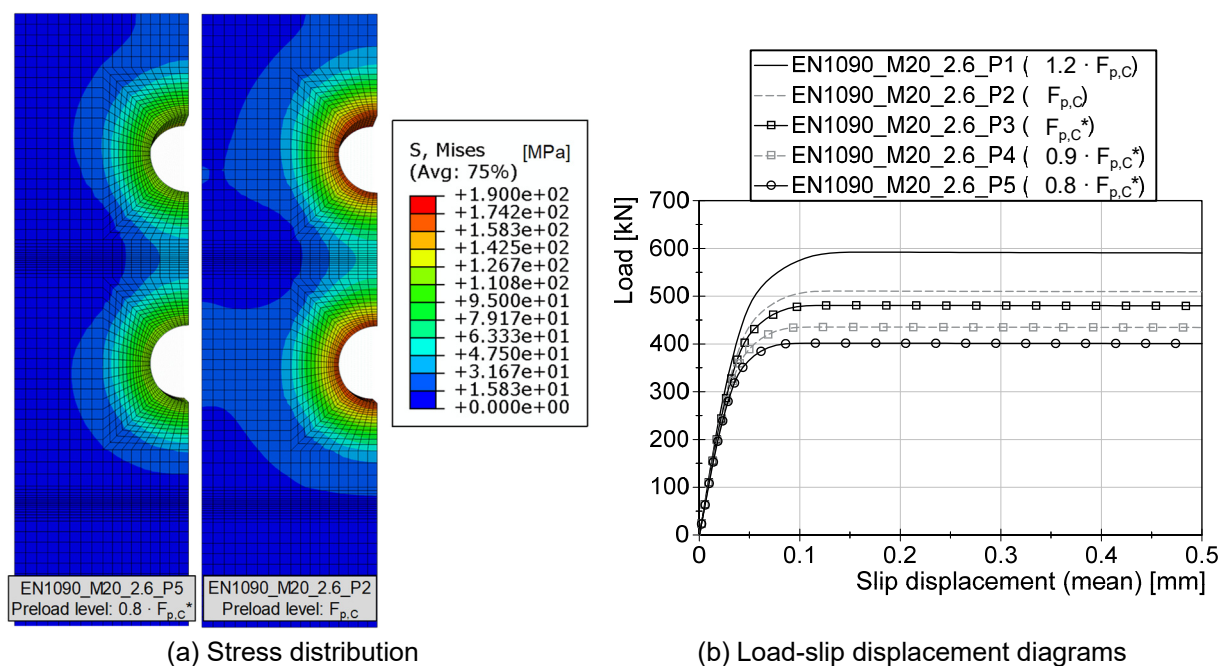
Figure 3-29: Influence of different preload levels on slip-resistant behaviour of the connection – numerical results

The results show that the slip load increases with increasing preload level. However, the nominal/initial slip factor decreases with increasing preload level, see Table 3-5 and Figure 3-30 (a). The same phenomena have also been observed in the experimental investigations.

As can be seen in Table 3-5, the actual slip factor remains constant for all investigated series with different preload level. This means that the preload at the moment of slip is much higher for a higher preload level, see Figure 3-30 (b). Increasing the slip load and decreasing the preload level at the occurrence of slip lead to the same actual slip factor.

F_{Si}: Individual slip load   LP: Loss of Preload

(a) Slip factor/slip load-preload level   (b) Slip factor/loss of preload-preload level
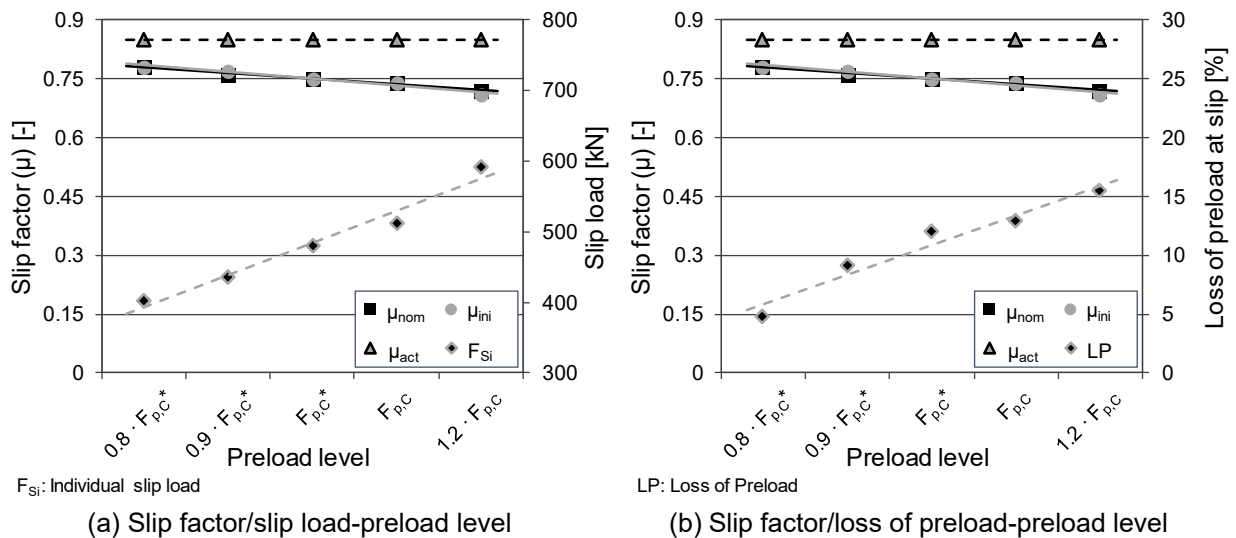
Figure 3-30: Influence of different preload levels on determination of the slip factor – numerical results

3.2.11 Influence of different surface treatments

3.2.11.1   General

As mentioned before, an essential parameter that mainly influences the load-bearing capacity of a slip-resistant connection besides the level of preloading in the bolts is the condition of the faying surfaces. A high slip factor can be achieved by blasted surfaces, but the connection might be affected by different environmental conditions, and unprotected carbon steel surfaces are susceptible to corrosive attacks which could lead to failure of components. To meet the requirements for corrosion resistance, the surfaces are usually provided with a protective coating. However, having a coating between the faying surfaces may completely change the slip resistance of the connection.

3.2.11.2   Influence of different types of coating

In the frame of this investigation, seven different surface preparations (GB-III, ASI-III, Al-SM-II, Zn-SM-II, ASI–Zn-SM-I, HDG-II and HDG-III) were selected in order to investigate the potential of achieving different slip factors by considering different surface conditions, see Table 3-1. For the GB test series, all test specimens were grit blasted to Sa 2½ according to EN ISO 8501-1 [124]. The surface roughness for all

test series was measured according to EN ISO 4287. The measured roughness Rz of the faying surfaces for GB-III test series was determined to be about 80 μm. The same preparation before the coating application was used for the ASI test series. The faying surfaces were coated with alkali-zinc silicate (ASI) coating material. In the frame of this investigation, all coating thicknesses were measured according to EN ISO 2808. The measured coating thickness was about 60 μm (DFT) for ASI-coated. This investigation was also carried out for thermal spray metallized surfaces with aluminium and zinc with coating thicknesses of 250 μm and 140 μm (DFT), respectively. Also, a combination of ASI-coated cover plates with a coating thickness of 55 μm (DFT) and Zn-SM-coated inner plates with a coating thickness of 170 μm (DFT) were tested. Finally, two different hot dip galvanized tests series with two different galvanizing processes were tested. The measured coating thicknesses were about 105 μm (DFT) for HDG-II test series and 80 μm (DFT) for HDG-III.

The results of the static, creep, and extended creep tests based on LVDTs at CBG position are summarized in Table 3-2. For all test series a full slip factor test series according to EN 1090-2 was not performed. For instance, for GB-III, ASI-III, Zn-SM-II and HDG-II only two static tests were performed instead of four static tests. Also, for some test series additional creep and extended creep tests were performed (for ASI-III, Al-SM-II and Zn-SM-II) at FhIGP [106]; its results of extended creep tests are presented in Table 3-1 and Figure 3-31 (a).

It can be seen from Figure 3-31 (a) that the highest nominal and initial slip factors were achieved for the GB test series and highest actual slip factors for the Al-SM test series, respectively. Figure 3-31 (b) shows load-slip displacement diagrams for a typical test of each type of surface preparation.

(a) Slip factor diagram   (b) Load-slip displacement diagrams
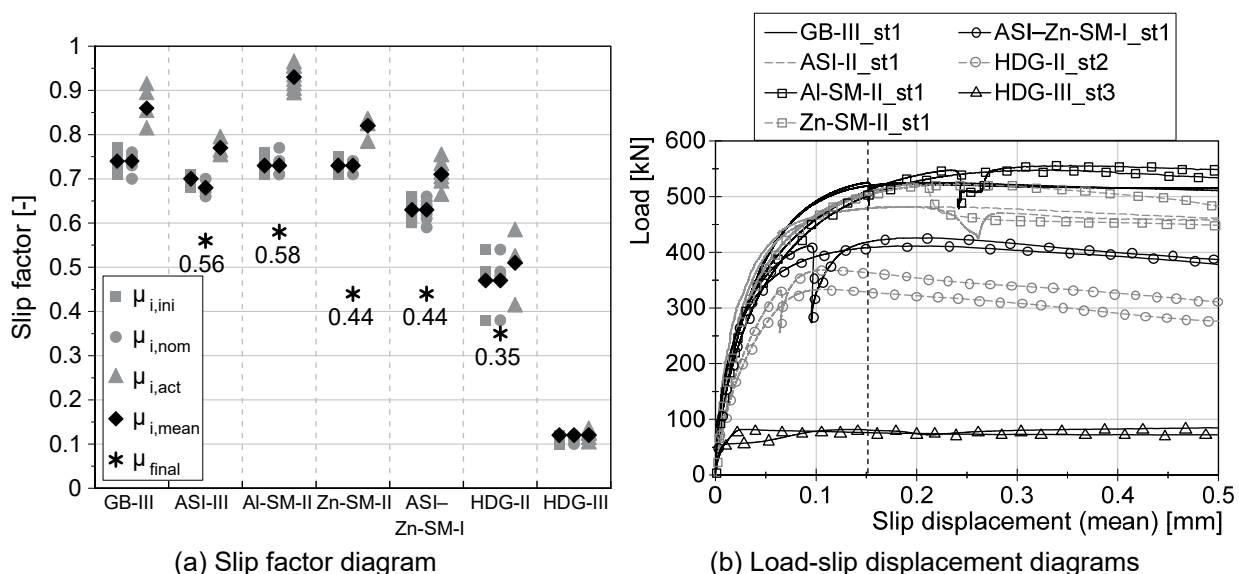
Figure 3-31: Influence of different surface treatments on the evaluation of the slip factor [106]

Approximately the same slip loads (F_{Si}) were achieved for both GB and Al-SM-surfaces. The higher actual slip factor for Al-SM may result from significantly higher losses of preload for Al-SM surfaces during the tests. The lowest slip factors were

achieved for hot dip galvanized test specimens, [116]. Both HDG-II and HDG-III are hot dip galvanized surfaces without any further surface preparations. However, they show completely different load-bearing capacities. This shows that the galvanizing process could have a very critical influence on slip-resistant behaviour of the connection. Major scattering in the reported results for hot dip galvanized surfaces can also be found in the literature, see Table 2-5. For this reason, in the frame of the SIROCO project, the influence of the surface preparation and post-treatment on the slip-resistant behaviour of HDG-coated surfaces was investigated.

3.2.11.3   Slip-resistant connections made of hot dip galvanized steel [125]

The application of hot dip galvanized steel is an efficient method of corrosion protection. Previously reported friction coefficients in hot dip galvanized plates show large variations, e.g. from 0.10 to 0.45, see Table 2-5. In practice, this results in the use of lower values in design. The thickness and structure of the zinc coating can vary depending on different factors, such as the chemical composition of the steel (some promote a stronger reaction between zinc and iron than other compositions) or the thermal mass of the steel component and other process variables. For structural sections, steel with a silicon content from 0.14 to 0.25 % (Category B steels according to EN ISO 14713-2 [126]) and, to a lesser extent, more than 0.25 % (Category D steels according to EN ISO 14713-2) is used. The influence of the steel composition may, to some extent, be controlled by the composition of the zinc melt during galvanizing. Having a softer outer zinc phase could have direct negative effects on the slip-resistant capacity of the connection. For the surfaces with a soft pure outer zinc phase, a small amount of slip load can be tolerated, even though this phase will experience a "cold welding" upon loading. However, this layer can be easily removed by abrasive sweep blast cleaning or other techniques to modify the surface in order to improve the slip resistance of the connection. Therefore, a comprehensive investigation was carried out with the aim of investigating the influence of galvanizing process and post-treatment on the slip-resistant behaviour of preloaded bolted connections with hot dip galvanized faying surfaces.

Two test series were conducted for HDG surfaces without any further surface treatment (HDG-I and HDG-II) considering different clamping lengths, see Chapter 3.2.9.

Almost all different test series were selected with the same clamping length ($\sum t = 48$ mm) in order to eliminate the effect of clamping length on the loss of preload, Figure 3-4 (b). Only for the HDG-I test series, a different clamping length was considered ($\sum t = 152$ mm) by including a long load cell in order to investigate the influence of the clamping length, see Figure 3-2 and Figure 3-4 (a).

Test series HDG-I and HDG-II were subjected to extended immersion times during galvanizing and were centrifuged after galvanizing to remove a large proportion of

the outer zinc layer prior to solidification. This is a galvanizing procedure used for small components (in this case, sample sets) and not for large components. The test samples for test series HDG-III were stripped and re-galvanized from series HDG-I and HDG-II, see Table 3-6. The galvanizing procedure for HDG-Ref test series was conducted to ensure that the outer zinc layer was present. Combined with a less reactive steel chemistry, this ensured a worst-case substrate for slip resistance prior to further modification of the surface in the other test series.

Table 3-6: Parameters of importance with regard to the interpretation of the test results [106]

Series ID	Galvanizing conditions	Steel Chemistry of relevance to reactivity during galvanizing					
		Si (%)		P (%)		Si + 2.5 P	
		10 mm plate	20 mm plate	10 mm plate	20 mm plate	10 mm plate	20 mm plate
HDG-I HDG-II	Centrifuged; Conventional galvanizing temperature; extended immersion time to ensure EN ISO 1461 coating thickness achieved.	Supplier Cert: <0.030	Supplier Cert: 0.016	Supplier Cert:<0.025	Supplier Cert: 0.020		
HDG-III	Conventional dipping procedure; Conventional galvanizing temperature; immersion time and withdrawal optimized to achieve smooth coating for slip test procedure. Sample sets were stripped and re-galvanized from series HDG-I and HDG-II.	Analysis 1: 0.0290 Analysis 2: 0.0290	0.030	Analysis 1: 0.0240 Analysis 2: 0.0260	0.0210	0.0915	0.0825
HDG-Ref	Conventional dipping procedure; Conventional galvanizing temperature; immersion time and withdrawal optimized to achieve smooth coating for slip test procedure.	Analysis 1: 0.010 Analysis 2: 0.009	Analysis 1: 0.0110 Analysis 2: 0.0110	Analysis 1: 0.018 Analysis 2: 0.019	Analysis 1: 0.0160 Analysis 2: 0.0170	0.0558	0.0523
HDG_NG-I HDG_NG-II HDG_SB-I HDG_SB-II HDG-ASI HDG-ESI		The steel chemistry of sample sets used in these test series were a mixture of those employed in series HDG-II and HDG-Ref.					
NOTES	1. Both Si and P levels in steel have an influence on the reaction between molten zinc and iron during hot dip galvanizing. EN ISO 14713-2 identifies that steels with chemistries satisfying the formula Si+2.5P ≤ 0.09% will have lower reactivity during galvanizing. Steels used for sample sets in test series HDG-II and HDG-III are at the upper boundary of this general rule and therefore exhibit higher reactivity than the sample sets used for HDG-Ref. 2. A more reactive steel used in a sample set can be expected to produce a higher proportion of Fe-Zn alloy layer within the galvanized coating structure. 3. Centrifuging of a sample set will remove a large amount of the outer zinc layer before freezing and thus increases the presence of Fe-Zn alloy at the surface.					

The faying surfaces of two test series were treated with a needle gun with 9 bar air pressure and two different angles to the coated surfaces (45° [HDG_NG-I] and 90° [HDG_NG-II]). The needle gun contained 50 needles and each needle had a diameter Ø of 2 mm. Two test series were sweep blasted with air pressure of 2.5 bar at an angle of 30° to the zinc surface but with two different particle sizes. Both series were blasted with corundum particles sized from 0.2 mm to 0.5 mm (HDG_SB-I) and 0.5 mm to 1.0 mm (HDG_SB-II). The distance between nozzle and zinc surface was

about 200 mm for both test series. Two more series were also sweep blasted using an identical blasting procedure as for series HDG_SB-I and then coated with alkali-zinc silicate (ASI) coating (HDG-ASI) and ethyl-zinc silicate (ESI) coating (HDG-ESI). All post-treatments were conducted at the Institute for Corrosion Protection (IKS) Dresden GmbH, Germany.

The roughness measurement was carried out with a stylus instrument conforming to the description in EN ISO 3274 [127] and equipped with a diamond stylus. The surface roughness was measured according to EN ISO 4287. Processing with the needle gun produced a roughness value between 30 and 40 µm.

Sweep blasting with fine grain produced a roughness of approx. 30 µm and sweep cleaning with coarser grain produced a roughness value between 50 and 60 µm. The zinc coating was measured randomly by means of magnetic induction in accordance with EN ISO 2808. The calibration was performed on a smooth steel sheet with foils of known thickness. Magnetic induction means that nonmagnetic films (e.g. zinc) are measured on steel.

The thicknesses of the coatings were measured prior to and after mechanical processing on selected test specimens. During these measurements it was detected that the thicknesses of the zinc films were partially higher after mechanical processing than before surface preparation. The phenomenon is probably caused by the fact that the roughness of the surface distorts the measured values. For this reason, the zinc film thicknesses were determined on metallographic cross sections, see Table 3-1 and Figure 3-32. The metallographic cross section of the HDG specimens before and after any post-treatment was taken at the Institute for Corrosion Protection (IKS) Dresden GmbH.

The typical zinc-phase system of steel with low silicon content is visible. In the upper area, the outer layer of pure zinc can be observed, see Figure 3-32 (a). The preparation of the surface with needle gun and sweep blasting may lead to breaks in the zinc layer, see Figure 3-32 (c) and (e). However, the blasting distance used for these tests was lower than recommended in practice to avoid such effects on the coating.

(a) HDG-Ref

(b) HDG_NG-I

(c) HDG_NG-II

(d) HDG_SB-I

(e) HDG_SB-II
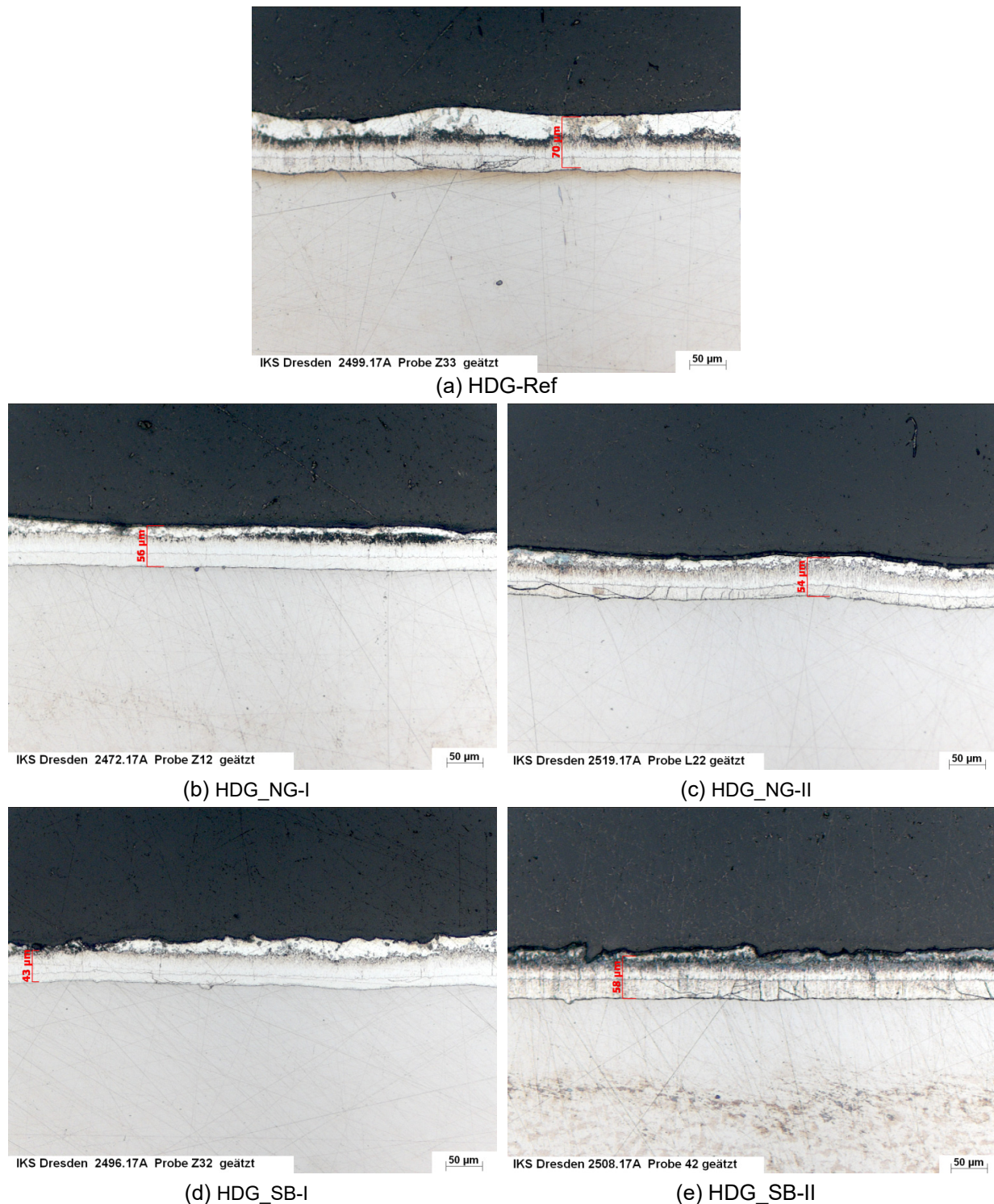
Figure 3-32: Metallographic cross section of the reference and post-treated specimen without additional coating before testing (© IKS) [106]

Figure 3-33 shows the metallographic cross sections for the galvanized test specimens with sweep blasted surfaces with ASI or ESI coating. Zinc-dust particles are visible as white particles. All test specimens were sweep blasted with white corundum, particle size 0.2 mm to 0.5 mm like test series HDG_SB-I. Afterwards, the samples were coated with additional ASI and ESI coating. The mean measured total thickness for the HDG–ASI test series was about 170 μm DFT (50 μm (HDG) + 120 μm (ASI)) and for the HDG–ESI test series about 140 μm DFT (50 μm (HDG) +

90 µm (ESI)). Generally, it can be observed that zinc-dust particles can break out during preparation of cross sections. These areas appear dark in the image.

| (a) HDG-ASI | (b) HDG-ESI |
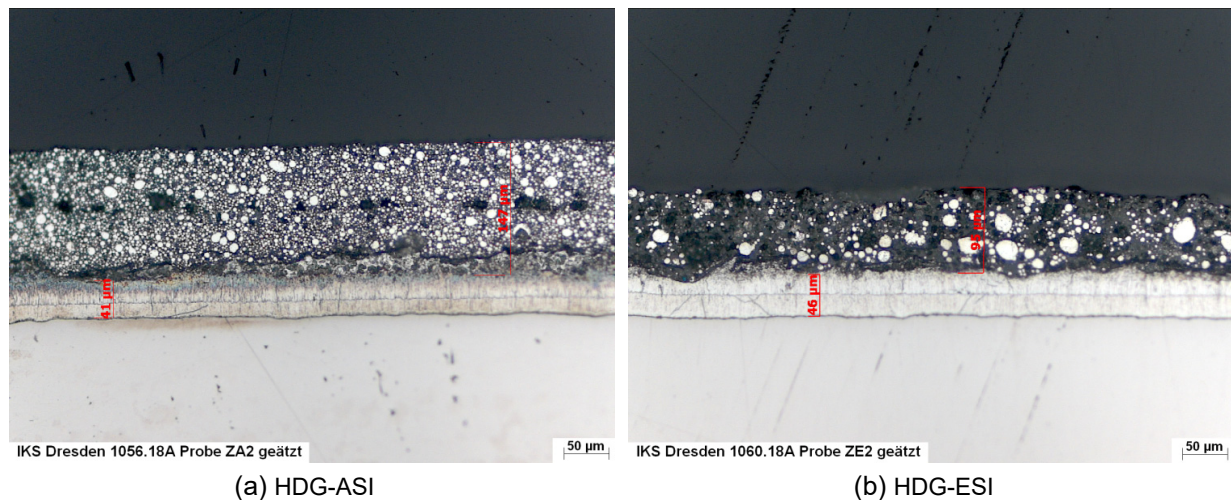
Figure 3-33: Metallographic cross section of post-treated HDG specimen with additional ASI and ESI coating before testing (© IKS) [106]

All specimens were made of carbon steel S355. However, the plate material was ordered from different batches with two different chemical compositions. In practice, non-galvanized steel is sold based on its mechanical properties. In this case, the content of reactive elements is not significant. Therefore, it is problematic to order steel with defined silicon and phosphorous content from a supplier. For the HDG-I, HDG-II and HDG-III test series, the steel was more reactive (Si 0.03 % and P 0.024 % by mass) in comparison to the other test series (Si 0.01 % and P 0.018 % by mass). The silicon and/or phosphorous content (as well as the thickness of the steel) has an influence on the morphology of the galvanized coating and its thickness. For this reason, it is notable that the plate material was delivered from different batches with two different chemical compositions of the steel. Furthermore, the galvanizing conditions were adjusted between the test series in order to optimize the sample set preparation. This included centrifuging of the sample sets used in the HDG-I and HDG-II test series. These differing steel chemistries and sample conditions are reflective of real variations in the galvanized coating but are also important for the interpretation of the results. The main influencing factors for interpretation of the results of each test series are summarized in Table 3-6.

All slip factor tests were carried out at the Institute for Metal and Lightweight Structures of the University of Duisburg-Essen (UDE), Germany, except two extended creep tests for the HDG-II test series, which were performed at the Fraunhofer Research Institution for Large Structures in Production Engineering IGP, Rostock, Germany [106].

As can be seen in Table 3-2, the influence of the clamping length is negligible for the HDG-I and HDG-II test series. In fact, having a high coefficient of variation for HDG-II

(about 13.5 %) and HDG-I (about 9 %) makes it impossible to see the influence of the clamping length on the static slip factor clearly, see Figure 3-34 (a).

Figure 3-34 (b) shows the influence of different surface treatments/preparations on the slip-load behaviour and initial slip factors for hot dip galvanized surfaces. Each test is presented by two graphs, which represent the behaviour of the upper and lower part of the connection.

As already mentioned, different post-treatments were conducted in order to improve the slip-resistant behaviour of bolted connections. Using a needle gun in different angles results in a slightly improved load-bearing capacity of the galvanized specimens, see Figure 3-34 (b).

(a) Influence of different clamping lengths
(HDG-I → Σt/d ≈ 7.6 vs. HDG-II → Σt/d ≈ 2.4)

(b) Influence of different galvanizing process and post-treatments
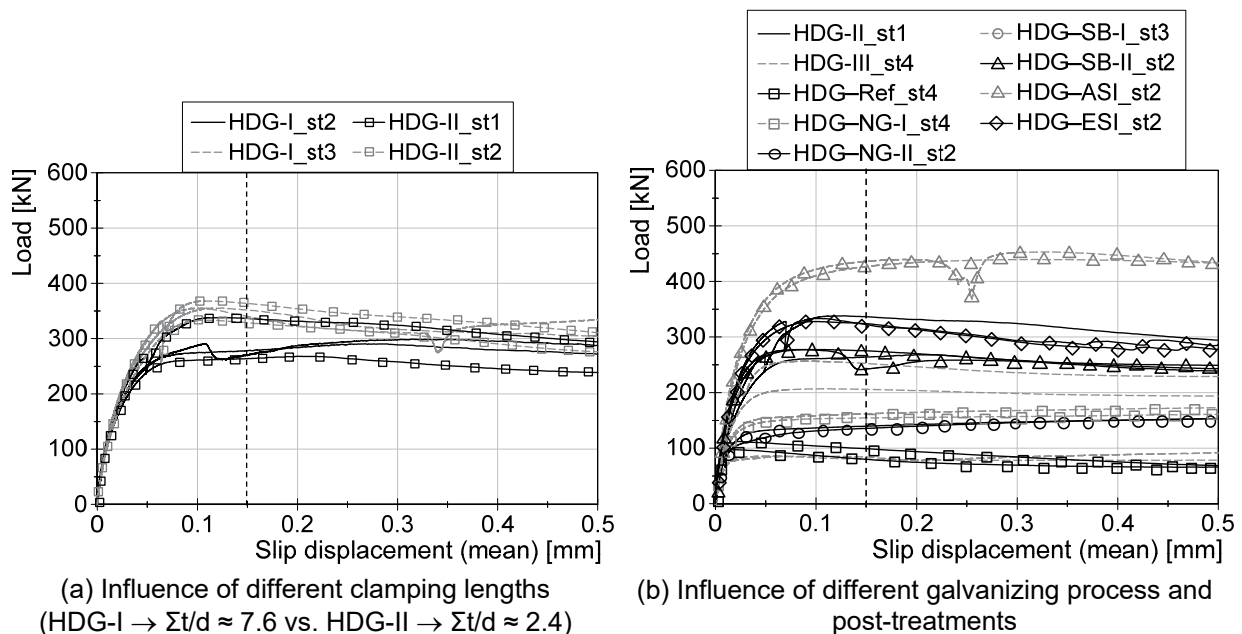
Figure 3-34: Influence of different clamping lengths, galvanizing process and post-treatments on slip-resistant behaviour of the connection [106]

The results also show that the sweep blasted surfaces achieved higher static slip factors compared to needle gun treated surfaces. Aside from that, better results can be achieved by using a bigger particle size for sweep blasting of the surfaces. By looking at the metallographic cross section after slip factor tests for these surfaces, it can be seen that higher slip load causes more damage to the zinc layer on the surfaces, see Figure 3-35. On the other hand, the surface of HDG-Ref remained quite untouched and only the soft pure zinc on the surfaces was removed, see Figure 3-35 (a). The slip factors achieved after sweep blasting showed higher coefficients of variation than for other post-treated test series. A closer examination of the test results indicates that for both test series, HDG–SB-I and HDG–SB-II, higher slip factors were achieved on sample sets of higher steel reactivity within each test series, see Table 3-6.

(a) HDG–Ref

(b) HDG–NG-I

(c) HDG–NG-II

(d) HDG–SB-I

(e) HDG–SB-II
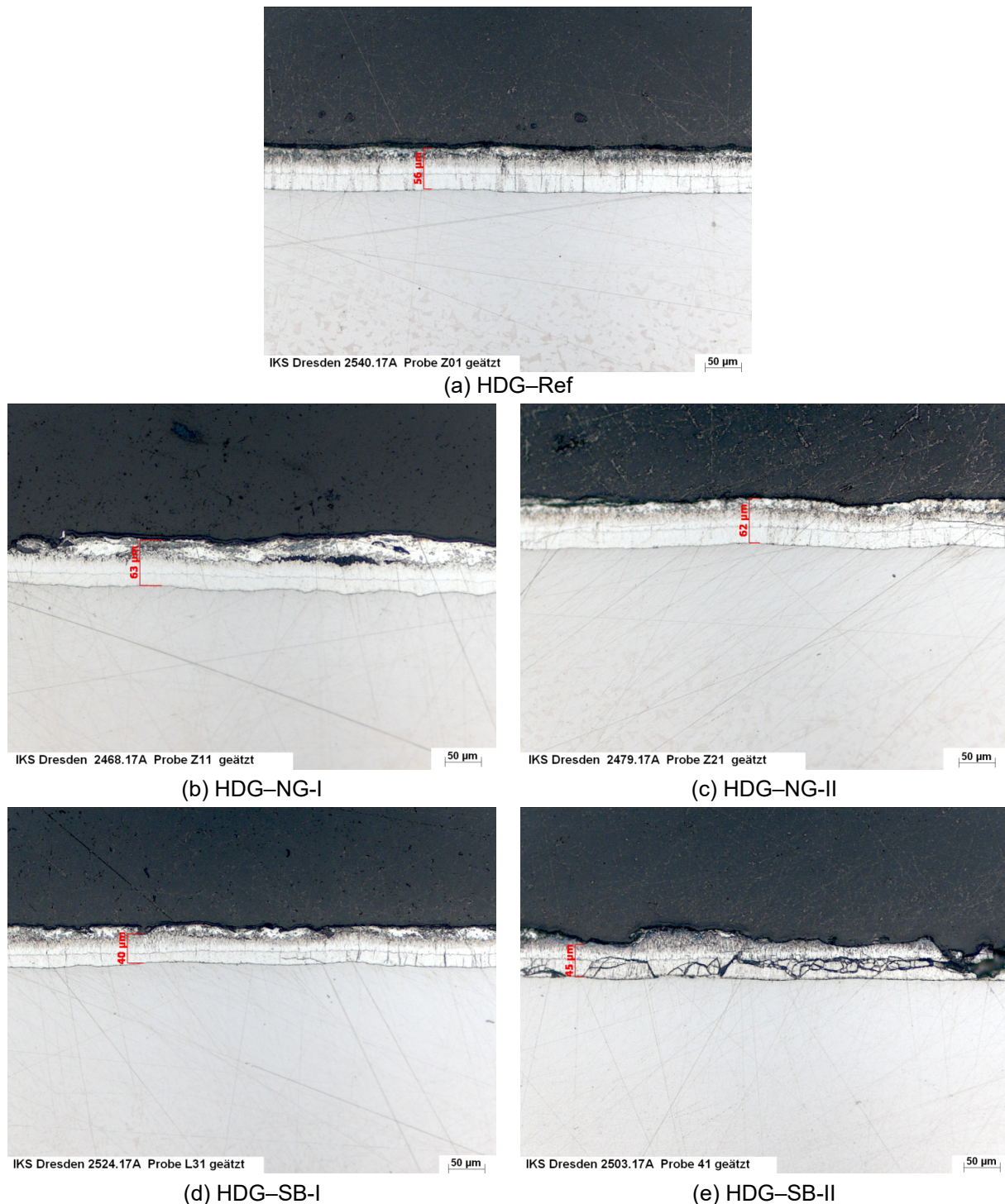
Figure 3-35: Metallographic cross section of the reference and post-treated specimen without additional coating after testing (© IKS) [106]

Assuming that (1) the sample sets with a more reactive steel have a thinner outer layer of zinc and (2) blasting conditions are constant within the test series, this indicates that increased exposure of the Fe Zn layers will yield higher slip factors. This also indicates that the average slip factors resulting from test series HDG–SB-I and HDG–SB-II can be considered conservative for moderately reactive steels encountered in practice for typical structural steels. This hypothesis is confirmed by considering that the highest determined slip factors achieved for test series HDG–

SB-II (larger blast media combined with thinner outer zinc layer) approach those measured for test series HDG-II (the same steel chemistry with the outer zinc layer largely removed during the centrifuging process).

(a) HDG–ASI   (b) HDG–ESI
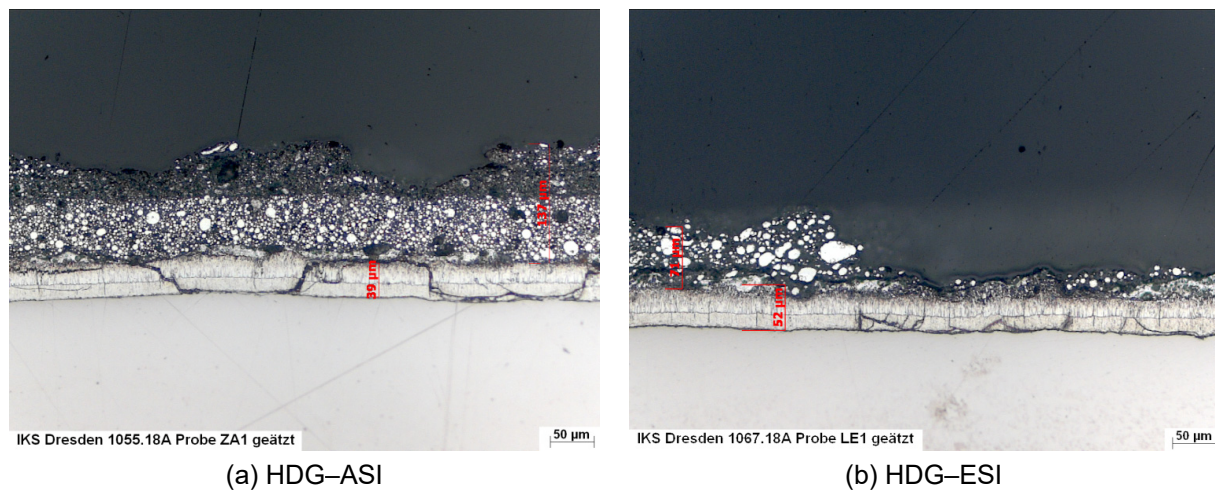
Figure 3-36: Metallographic cross section of post-treated HDG specimen with additional ASI and ESI coating after testing (© IKS) [106]

The results show that the highest static slip factors were achieved for the sweep blasted and ASI-coated (HDG–ASI) test series followed by the sweep blasted test series with ESI coating (HDG–ESI), see Figure 3-37. As can be seen in Figure 3-36, the galvanized surfaces with ASI or ESI coating show areas with large-scale detachment of the coating. Partially detached coating residues from the opposite contact area are visible. Figure 3-36 also shows many cracks in the zinc layer which might occur in the sweep blasting phase of the preparation of the surfaces.
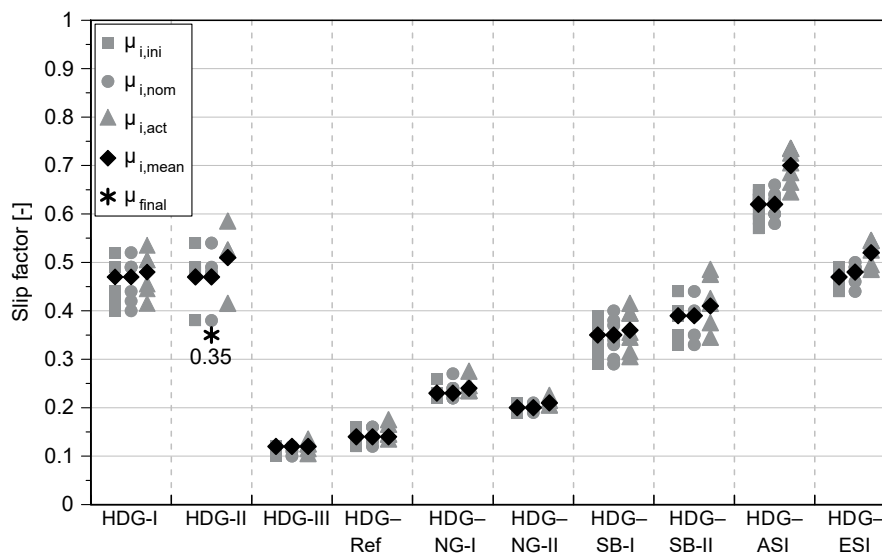
Figure 3-37: Influence of different galvanizing process and post-treatments on the evaluation of the slip factor [106]

For each post-treated test series, one creep test was carried out with 90 % of the mean slip load F_{sm} from the first four static tests. The creep tests failed for all test series for both upper and lower parts of the specimens, see Figure 3-38; thus, it was necessary to perform extended creep tests to determine the final slip factor.
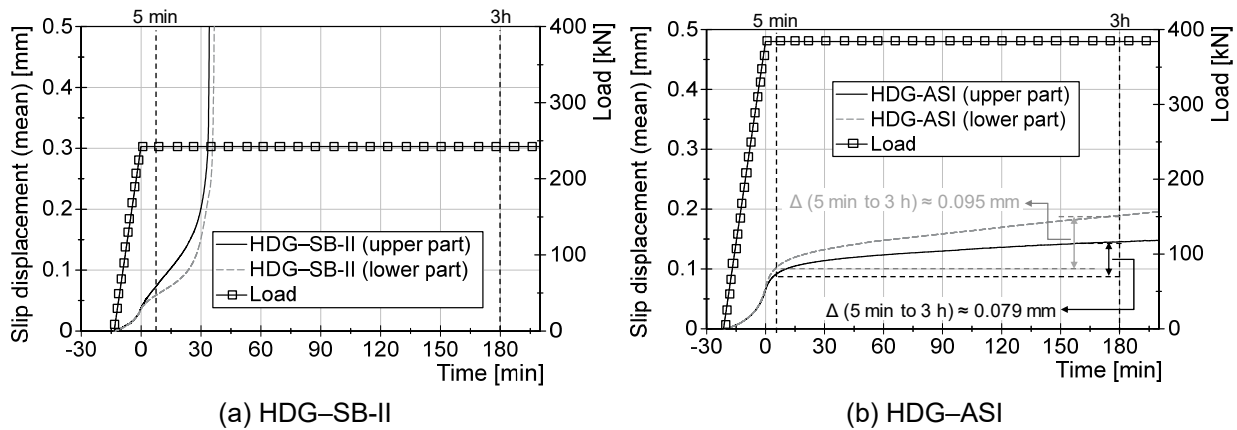
Figure 3-38: Example results of creep tests for post-treated hot dip galvanized specimens [106]

Evaluating the slip displacement-log time curve based on the results of the creep tests is a valuable way to estimate the suitable load level for performing extended creep tests for the coated surfaces. Figure 3-39 shows that 90 % of the mean slip load ($0.9 \cdot F_{Sm}$) is a high load level for performing the extended creep tests for all post-treated surfaces and the constant load level has to be reduced for further investigations.
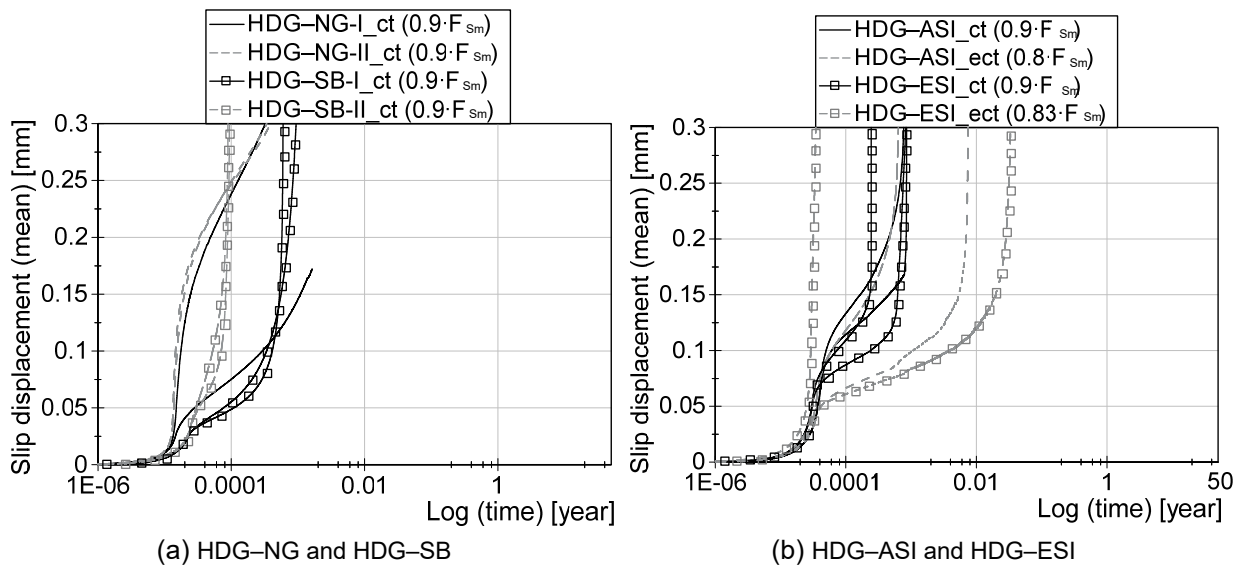
Figure 3-39: Evaluating the slip displacement-log time curves based on the results of the creep and extended creep tests for post-treated hot dip galvanized test specimens [106]

For the HDG-ASI coated surface, one extended creep test was performed with a lower constant load level of $0.8 \cdot F_{Sm}$ = 341.4 kN. As can be seen in Figure 3-39 (b), the slip suddenly increased and extrapolation was not possible. For this reason, the test cannot be considered a passed extended creep test. Furthermore, one extended creep test was conducted for HDG-ESI coated surfaces with a constant load level of $0.83 \cdot F_{Sm}$ = 272.4 kN. The results show that the extended creep test also failed for both parts of the test specimen, see Figure 3-39 (b). This means that the load level is still high and further investigations are needed to achieve the final slip factor. Hence, the achieved extended creep test results for the HDG-ASI and HDG-ESI coated surfaces do not allow a conclusion regarding the final slip factor for these test series.

At least it can be concluded that the final slip factor will be smaller than 0.5 for the HDG-ASI and 0.4 for the HDG-ESI test series respectively [128]. Further test samples were not available to perform additional extended creep tests on lower load levels. For this reason, final slip factors could not be determined for these test series.

3.3 Influence of different coating material compositions

In the literature, there are various studies in which slip factors have been determined for coated faying surfaces, see Chapter 2.3. By evaluating the literature results, however, it must be taken into account that these have not necessarily been determined under uniform boundary conditions. Besides to all mentioned parameters, the composition of the coating material itself may have influence on the slip-resistant behaviour of the preloaded bolted connections. Many types of coatings have been produced by different producers with different material compositions which may lead to different slip factors.

Six different products for ethyl-zinc silicate coating (ESI) and three different products based on epoxy primer (EP) were selected in order to investigate the influence of the coating material composition, see Table 3-7. EP-I and EP-II are pigmented with zinc phosphate and EP-III is a pigmented zinc-rich primer.

Table 3-7: Slip factor test results for ESI and EP test series [107]

Series ID	Surface preparation		Number of tests	$\mu_{nom,mean}$[4]	$\mu_{ini,mean}$[5]	$\mu_{act,mean}$[6]	V (μ_{nom})[7]
	Rz[1] [µm]	DFT[2] [µm]	st/ct/ect[3]	st/st+ct [-]	st/st+ct [-]	st/st+ct [-]	st/st+ct [%]
Ethyl-zinc silicate coating (ESI)							
ESI-I	74 ± 5	70		0.57/-	0.58/-	0.63/-	1.8/-
ESI-II	73 ± 6	59		0.43/-	0.43/-	0.45/-	3.3/-
ESI-III	75 ± 4	81	4/1/-	0.52/-	0.52/-	0.57/-	2.1/-
ESI-IV	74 ± 5	73		0.67/-	0.67/-	0.77/-	3.3/-
ESI-V	74 ± 5	69		0.56/-	0.55/-	0.61/-	3.1/-
ESI-VI	74 ± 5	55		0.54/-	0.54/-	0.59/-	3.3/-
Epoxy primer (EP)							
EP-I	74 ± 5	75		0.24/-	0.24/-	0.25/-	6.1/-
EP-II	74 ± 5	76	4/1/-	0.23/-	0.23/-	0.24/-	1.7/-
EP-III	74 ± 5	88		0.28/-	0.28/-	0.29/-	1.7/-

[1] surface roughness | [2] dry film thickness (Coating thickness) | [3] st: static test/ct: creep-/ect: extended creep test | [4] $\mu_{nom,mean}$: calculated slip factors as mean values considering the nominal preload level | [5] $\mu_{ini,mean}$: calculated slip factors as mean values considering the initial preload when the tests start | [6] $\mu_{act,mean}$: calculated slip factors as mean values considering the actual preload at slip | [7] V: coefficient of variation for μ_{nom} | [8] contain less "Volatile Organic Compounds" (VOC) or VOC Solvents than traditional coatings

The test specimens have been made of carbon steel S235JR from one batch for each plate thickness. All surfaces were blasted to Sa 3 according to EN ISO 12944-4. The nominal surface roughness Rz for ESI coated surfaces was selected to be 75 µm before the application of coating. The nominal surface roughness before the coating application was 85 µm for EP coated faying surfaces. The roughness Rz of the faying surfaces was measured before coating according to EN ISO 4287 and the values are presented in Table 3-7. The nominal coating thickness was 50 µm NDFT for both types of the coatings and the measured values are presented in Table 3-7. All slip factor tests were carried out and evaluated according to EN 1090-2, Annex G. The geometry of the test specimens was chosen to the M16-bolt-geometry according

to EN 1090-2, Annex G. The preload of the bolts was defined as $F_{p,C} = 110$ kN for M16 bolting assemblies with property class 10.9.

For each test series, four static tests and one creep test were performed. Figure 3-40 shows the selected typical load and slip displacement diagram and a comparison of all static slip factors for each test series. The results show that the initial static slip factors for ESI coated surfaces varies from 0.43 (ESI-II) to 0.67 (ESI-IV) and thus was greatly dependent on the product used.

(a) Different ESI coating material   (b) Different EP coating material

(c) Influence of different coating material composition
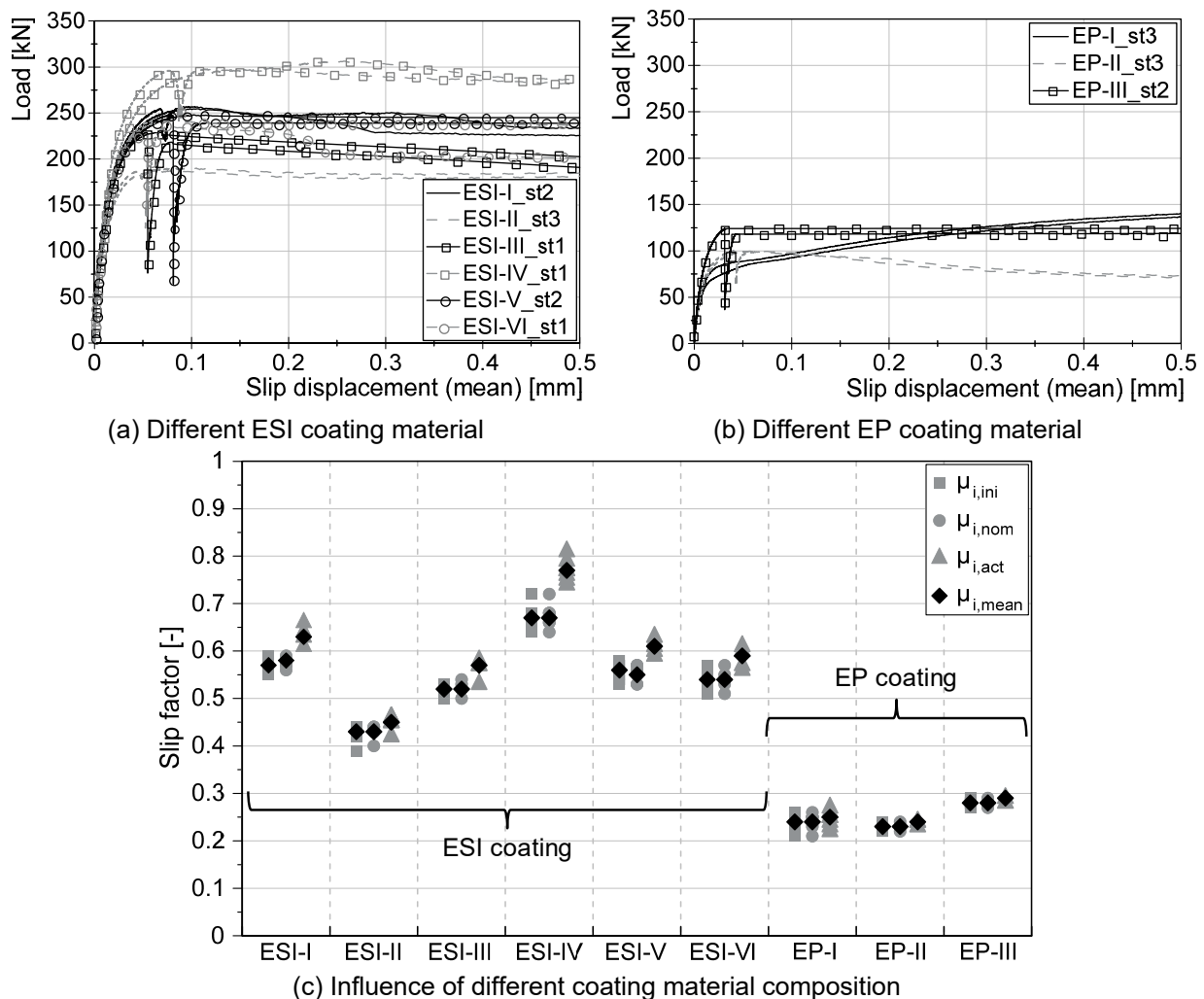
Figure 3-40: Load-slip displacement diagrams and a comparison of all static slip factors for different test series with different coating material compositions [107]

In order to better understand the composition of the coating material, the metallographic cross-section investigations were conducted at the Institute for Corrosion Protection (IKS) Dresden GmbH, see Figure 3-41. These figures show that the size and distribution of zinc dust particles are not the same for different coating compositions. For ESI-II and ESI-V test series, some of the zinc particles are > 10 µm. However, it seems for ESI-III, ESI-IV and ESI-VI that all particles are < 10 µm. By comparing these figures with the results of static slip factor tests, it can be stated that there is no correlation between distribution and the size of zinc dust particles and the static slip factor.
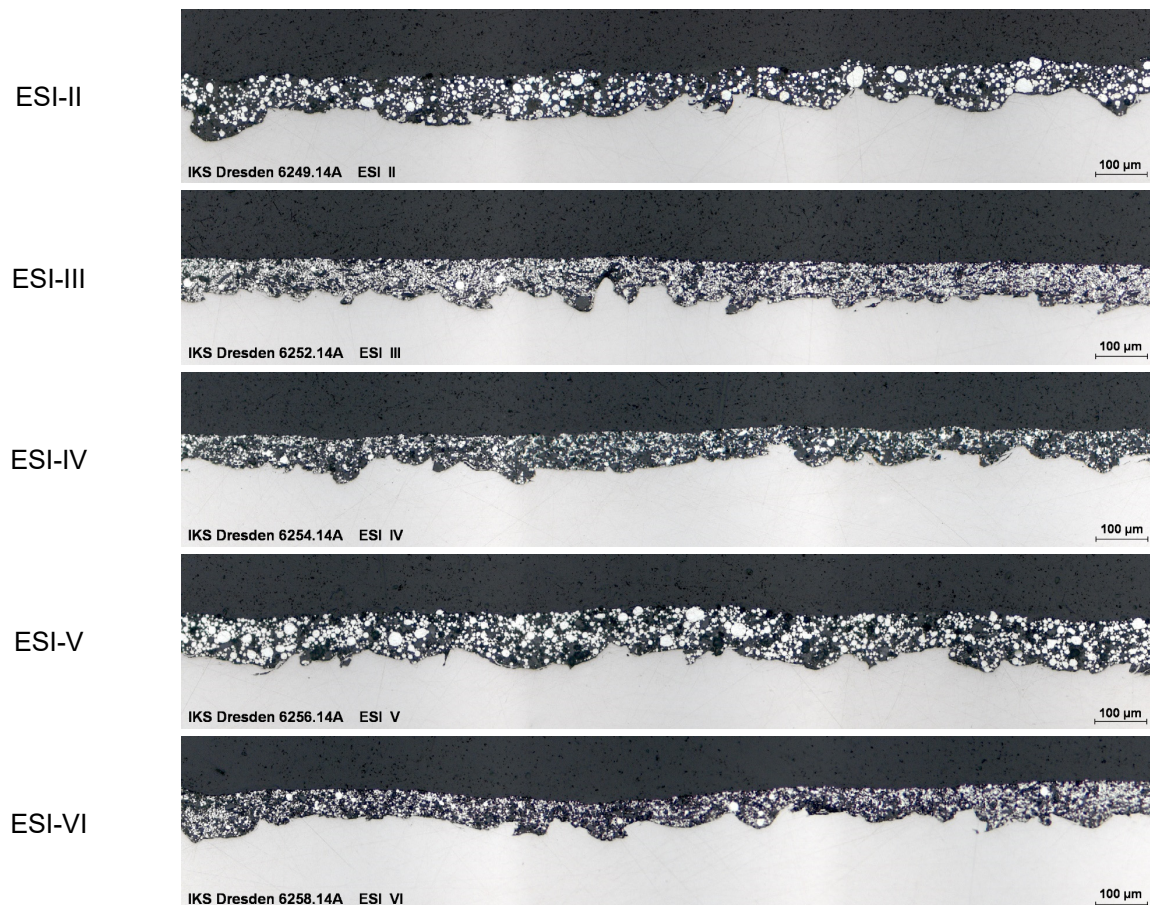
Figure 3-41: Metallographic cross section images of ESI coated faying surfaces done by IKS [107]

For comparing the results for the ESI coated surfaces with the values given in the literature, it is important to keep in mind that the creep tests failed for all investigated test series. For this reason, it is necessary to perform extended creep tests in order to be able to formulate a reliable final slip factor. It is clear that performing the extended creep tests will result in a decrease in the slip factor as the final slip factor in comparison with the static slip factor. Considering this fact still presumes that the scatter of the results for the different ESI coating compositions remains. It seems that a generalized classification for different ESI coating compositions is not recommendable. For design purposes, of course, a lower slip factor can be proposed for EN 1090-2, but it is highly recommended for coating suppliers or for individual projects to perform individual slip factor tests to take benefit from higher slip factors.

On the other hand, with consideration of testing deviations for different EP products, approximately the same static slip factors have been observed. The initial static slip factors are 0.24 for EP-I, 0.23 for EP-II and 0.29 for EP-III. That means the influence of the zinc material added to the coating in the form of zinc phosphate or zinc dust on the static slip factor is negligible [107], [129].

3.4 Influence of coating thickness and roughness of the faying surfaces before coating application

One of the further objectives was to investigate the influence of different coating thickness and roughness of the faying surfaces before coating application on the determination of the slip factor. For this purpose, several tests on ESI and EP test series were performed using the standard test specimen geometry, M16, according to EN 1090-2, Annex G, see Table 3-8.

For the ESI test series, two different surface roughness values before coating application were selected. The nominal Rz values were chosen to be 75 µm and 90 µm.

Table 3-8: Slip factor test results for PUR test series [107]

Series ID	Surface preparation			Number of tests	$\mu_{nom,mean}$[4]	$\mu_{ini,mean}$[5]	$\mu_{act,mean}$[6]	$V(\mu_{nom})$[7]
	Rz[1] [µm]		DFT[2] [µm]	st/ct/ect[3]	st/st+ct [-]	st/st+ct [-]	st/st+ct [-]	st/st+ct [%]
	Nominal value	Measured value						
Ethyl-zinc silicate coating (ESI)								
ESI-II	75	73 ± 6	59		0.43/-	0.43/-	0.45/-	3.3/-
ESI-IIa	75	78 ± 6	102		0.49/-	0.49/-	0.53/-	4.1/-
ESI-IIb	90	90 ± 6	83	4/1/-	0.52/-	0.52/-	0.57/-	2.6/-
ESI-IIc	90	85 ± 3	139		0.53/-	0.53/-	0.59/-	2.0/-
ESI-IId	90	89 ± 5	123		0.51/-	0.51/-	0.56/-	3.1/-
Epoxy primer (EP)								
EP-I	90	87 ± 5	75	4/1/-	0.24/-	0.24/-	0.25/-	6.1/-
EP-Ia	90	83 ± 7	126		0.24/-	0.24/-	0.24/-	13.7/-

[1] surface roughness [2] dry film thickness (coating thickness) [3] st: static test/ct: creep-/ect: extended creep test [4] $\mu_{nom,mean}$: calculated slip factors as mean values considering the nominal preload level [5] $\mu_{ini,mean}$: calculated slip factors as mean values considering the initial preload when the tests start [6] $\mu_{act,mean}$: calculated slip factors as mean values considering the actual preload at slip [7] V: coefficient of variation for μ_{nom}

As can be seen in Figure 3-42 (a), for ESI coated surfaces with a nominal roughness value of 75 µm, increasing the coating thicknesses from 59 µm (ESI-II) to 102 µm (ESI-IIa) improves the load-bearing capacity of the connection.

However, for ESI-IIb, ESI-IIc and ESI-IId test series with a nominal roughness value of 90 µm, the influence of increasing the coating thickness is negligible, see Figure 3-42 (b). This shows that the influence of the coating thickness on the static slip factor is no longer noticeable when the coating thickness is equal to or higher than about 80 µm.

For the surfaces coated with epoxy primer (EP-I and EP-Ia), increasing the coating thickness from to 75 µm to 126 µm did not have any influence on the load-bearing capacity of the preloaded bolted connection nor on the determination of the static slip factors, see Figure 3-42 (c) and Table 3-8.

The results also show the slightly negative influence of the lower surface roughness before the coating application for the surfaces coated with a thinner layer of ESI by comparing the results of ESI-II and ESI-IIb, see Figure 3-42 (d). However, this difference is faded for coated surfaces with thicker coated layers.
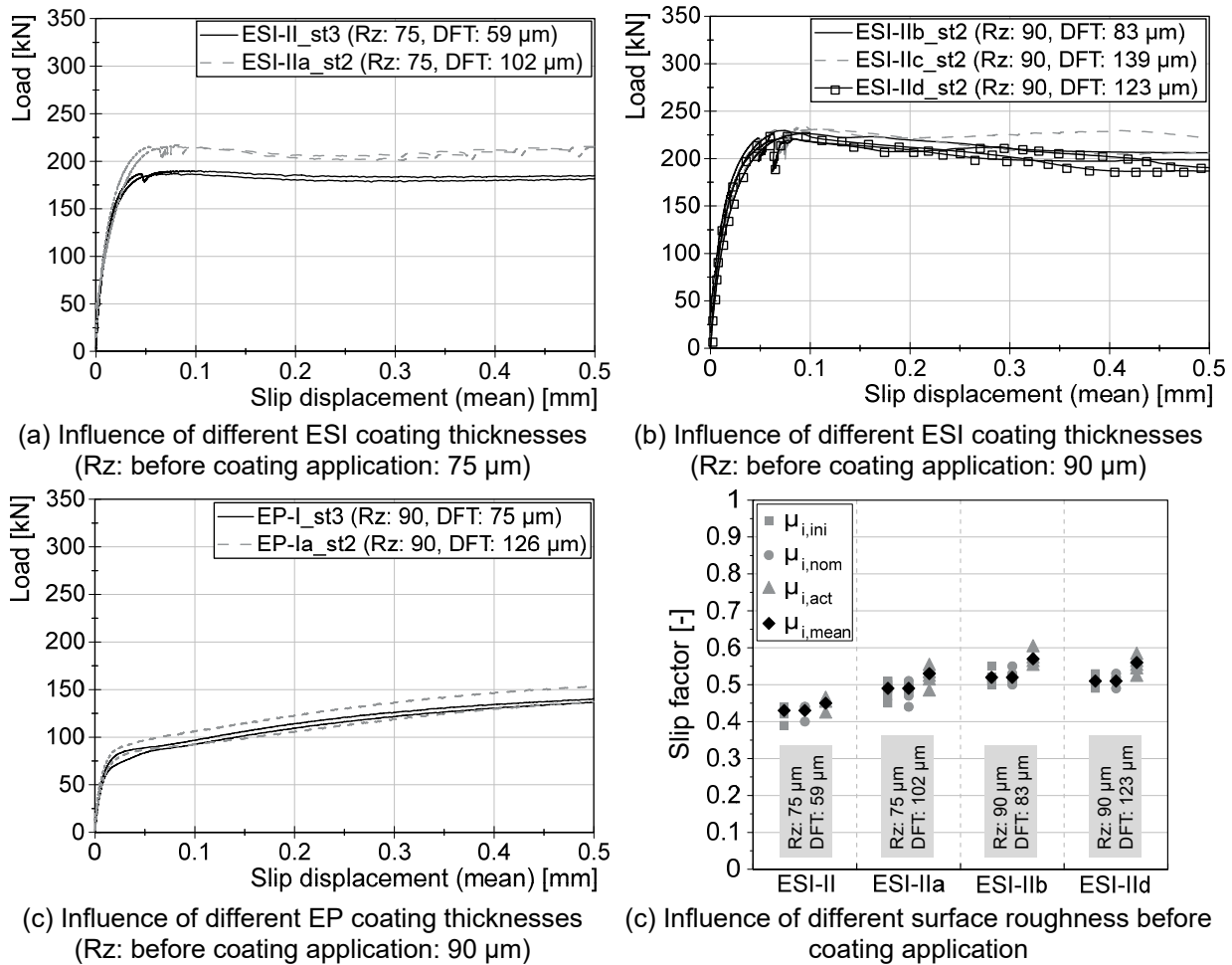
Figure 3-42: Load-slip displacement diagrams and comparison of all static slip factors for different test series - influence of coating thickness and surface roughness [107]

All the results presented in this chapter are based on static tests. All test series failed the creep tests, and performing the extended creep tests is necessary to finalize the slip factors and reach any final conclusion.

3.5 Influence of the combination of a coated inner plate with an uncoated cover plate

Within the scope of this investigation, the slip factor has been determined for slip-resistant connections with combinations of a coated inner plate with an uncoated/grit blasted cover plate. The results were compared with results of common coated faying surfaces. The selected faying surfaces were coated with a single-pack moisture-curing zinc-dust paint on polyurethane basis (PUR) with different coating thicknesses. For the PUR-I test series, both inner plate and cover plate were blasted to Sa 3 and coated with PUR coating material. The measured surface roughness and the coating thickness are presented in Table 3-9. The geometry of the test specimen was chosen to the M16 bolt geometry according to EN 1090-2, Annex G and all bolts were preloaded to $F_{p,C}$ level.

Table 3-9: Slip factor test results for combinations of a coated inner plate with an uncoated cover plate [107]

Series ID	Surface preparation		Number of tests	$\mu_{nom,mean}$[4]	$\mu_{ini,mean}$[5]	$\mu_{act,mean}$[6]	V (μ_{nom})[7]
	Rz[1] [µm]	DFT[2] [µm]	st/ct/ect[3]	st/st+ct [-]	st/st+ct [-]	st/st+ct [-]	st/st+ct [%]
Zinc-dust paint on polyurethane basis (PUR)							
PUR-I	87 ± 5	76	4/1/-	0.43/-	0.43/-	0.46/-	2.4/-
PUR-Ia		inner plates: 111 / cover plates: -		0.51/-	0.52/-	0.55/-	1.3/-

[1] surface roughness | [2] dry film thickness (coating thickness) | [3] st: static test/ct: creep-/ect: extended creep test | [4] $\mu_{nom,mean}$: calculated slip factors as mean values considering the nominal preload level | [5] $\mu_{ini,mean}$: calculated slip factors as mean values considering the initial preload when the tests start | [6] $\mu_{act,mean}$: calculated slip factors as mean values considering the actual preload at slip | [7] V: coefficient of variation for μ_{nom}

(a) PUR-I test series   (b) PUR-Ia test series   (c) Load-slip displacement diagram
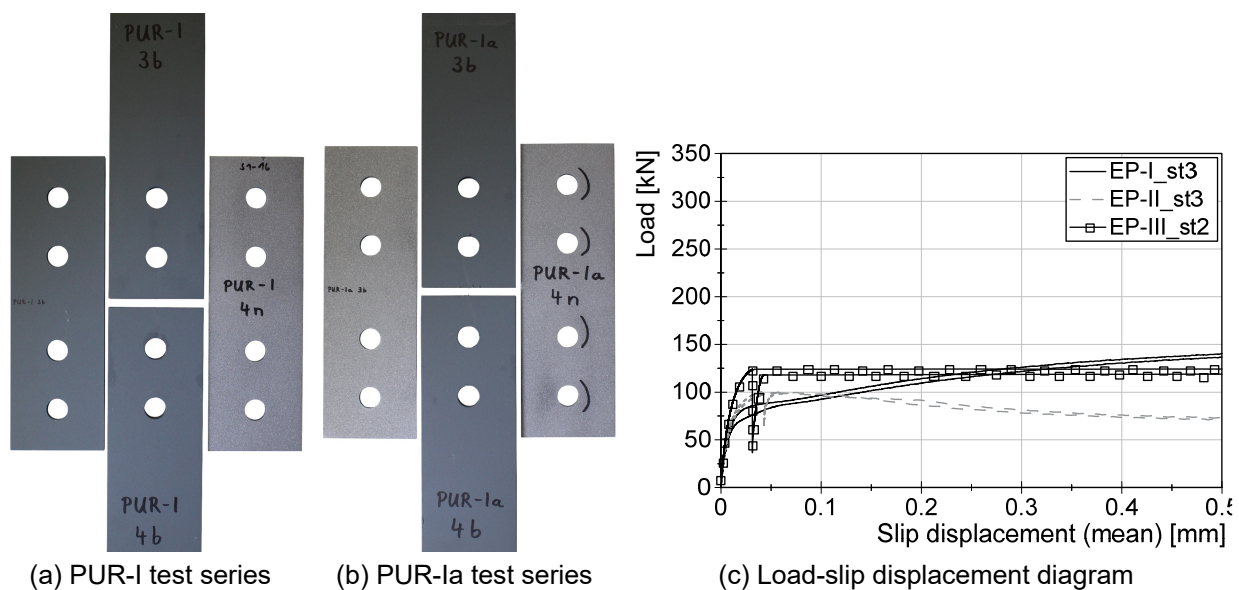
Figure 3-43: Condition of the faying surfaces and the Load-slip displacement diagram for PUR test series [107]

The results show that the initial static slip factor for the PUR-I test series with a coating thickness of 76 µm DFT is equal to 0.43. The slip-resistant behaviour of the connection has been improved for the PUR-Ia test series with a coating thickness of 111 µm DFT on the inner plates and a grit blasted contact surface on the cover plates. The initial static slip factor for the PUR-Ia test series is equal to 0.52. The results show that a combination of coated and grit blasted surfaces leads to higher static slip factor despite the fact that the sum of the coating thicknesses on the faying surfaces was greater for the PUR-I series with 304 µm DFT (4 × 76 µm) compared to the PUR-Ia series with 222 µm DFT (2 × 111 µm). The reason for this could be the better penetration of the rough surface profiles into the coated surface and better interlocking between the faying surfaces for the combined faying surface.

As the creep tests failed for both test series, the final slip factor shall be determined by performing the extended creep tests which were not covered in the scope of this study.

3.6 Conclusion

The slip-resistant behaviour of the connection might depend on different parameters, which might have a direct or indirect influence on determination of the slip factor. For this reason, special care has to be taken in interpreting and comparing slip factors from different studies.

In the frame of this study, a comprehensive investigation was conducted to take a closer look at the influence of different parameters on the slip-resistant behaviour of the connection.

The possible failure mechanisms for standard specimens according to EN 1090-2 were explained in detail, which would help to determine the critical slip load with higher accuracy. Different guidelines/standards prescribe different slip criteria for the determination of the critical slip load. As experimental results show, this criterion may have a direct influence on determination of static slip factors.

In this study, the preload level in the bolts was measured with two different methods. A comparative study regarding the accuracy of these methods was conducted. The results show that the deviations between the measured preload by instrumented bolts with strain gauges and the load cells are very small. However, using long load cells would result in lower loss of preload in the connection and therefore influence the slip-resistant behaviour of the connection. A longer clamping length ratio could lead to an overestimation in determination of the static slip factor.

The position of the slip measurement may also have an influence on the determination of the slip factor, as measuring the slip at plate edges (PE) position may lead to a lower slip factor in comparison to the slip factor based on the measurement at the centre bolt group (CBG) position.

The preload level in a slip-resistant connection is one of the main factors which influences the slip-resistant behaviour of the connection. The results of coated test specimens show that a higher nominal final slip factor might be achieved by having a lower preload level. However, a lower preload level would not always deliver a higher design slip resistance in the connection. The results show that in some cases higher preload levels would deliver higher slip resistances in connection.

According to EN 1090-2, slip factors that were determined with specimens using bolts with property class 10.9 may also be applicable for bolts with property class 8.8. The evaluation of the comparable experimental results validated this statement in all tested cases.

The condition of faying surfaces would be the most important factor in determination of the slip factor. However, beside this important parameter, other parameters like the composition of the coating material or the coating thickness could also directly influence the slip-resistant behaviour of the connection.

4 Preloaded bolted connections made of stainless steel

4.1 General

The application of stainless steel bolting assemblies in preloaded bolted connections is required for reasons of serviceability or ultimate limit state when used in particularly corrosive environments or in stainless steel structures. However, according to EN 1090-2, preloading of bolting assemblies made of stainless steel is currently not permitted in steel structures. They shall be treated as special fasteners and a procedure test would be mandatory for application of these bolting assemblies in preloaded bolted connections. Also, EN 1993-1-4 [130] requires that the acceptability in a particular application is demonstrated in experimental tests. The main reason to restrict the application of bolting assemblies made of stainless steel is the gap in knowledge on different issues. First, the viscoplastic deformation behaviour of stainless steel material may result in a higher loss of preload in preloaded bolted connections made of stainless steel in comparison with connections made of carbon steel. Second, no product standard exist for bolting assemblies made of stainless steel for preloading. Third, the tightening parameters and procedures of HR and HV bolting assemblies made of carbon steel according to EN 14399-3 [131] and -4 are not simply applicable for bolting assemblies made of stainless steel. Finally, the appearance of a galling phenomenon, as a form of cold-welding, commonly reported in preloading of the stainless steel bolting assemblies. To close these gaps in knowledge, a comprehensive investigation has been conducted in the frame of the SIROCO project.

4.2 Viscoplastic deformation behaviour

4.2.1 General

As shown in Figure 4-1, from a mechanical point of view, the deformation in the material is classified in different categories.
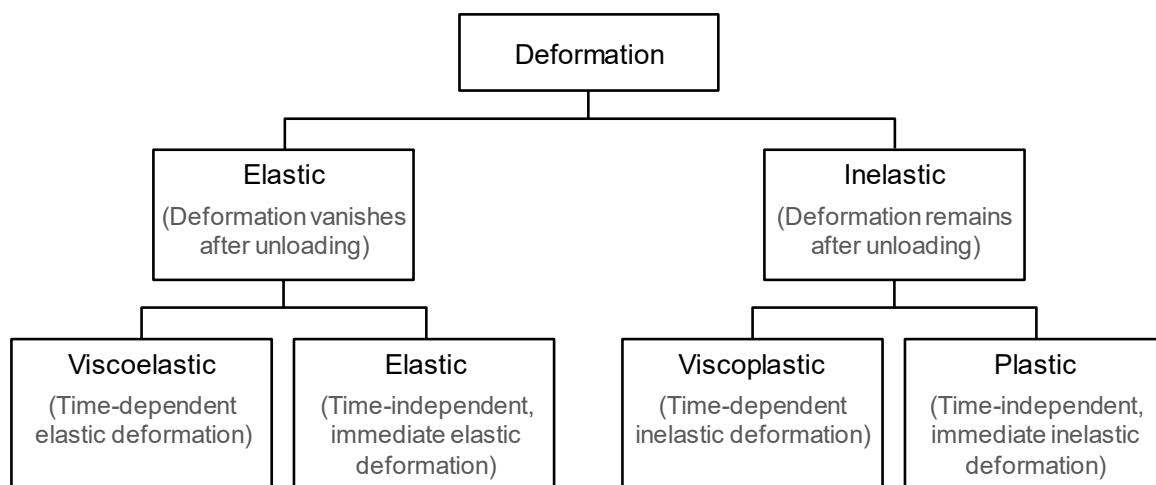
Figure 4-1: Classification of different types of deformation [132]

Stainless steel is a material that suffers from viscoplastic deformation, which is a time-dependent inelastic deformation. The creep and the stress relaxation phenomena can both be explained in terms of viscoplastic deformation.

The great concern about viscoplastic deformation of stainless steel material was one of the main obstacles in using stainless steel for structural purposes. Therefore, comprehensive investigations are needed in order to address this concern and illustrate the real influence of this phenomenon in using preloaded bolted connections made of stainless steel.

4.2.2 Creep behaviour

4.2.2.1 General

Creep deformation is a time-dependent plastic strain which occurs under a sustained applied load. The creep behaviour of a material can be described in three different stages [133], [134], as shown in Figure 4-2. In the primary creep stage, the creep rate gradually decreases with increasing strain. In the secondary creep stage, the increase of the strain proceeds and the creep rate is nearly constant. Finally, in the tertiary creep stage, the strain and creep rates increase both. This stage terminates with rupture [133], [134], [135].
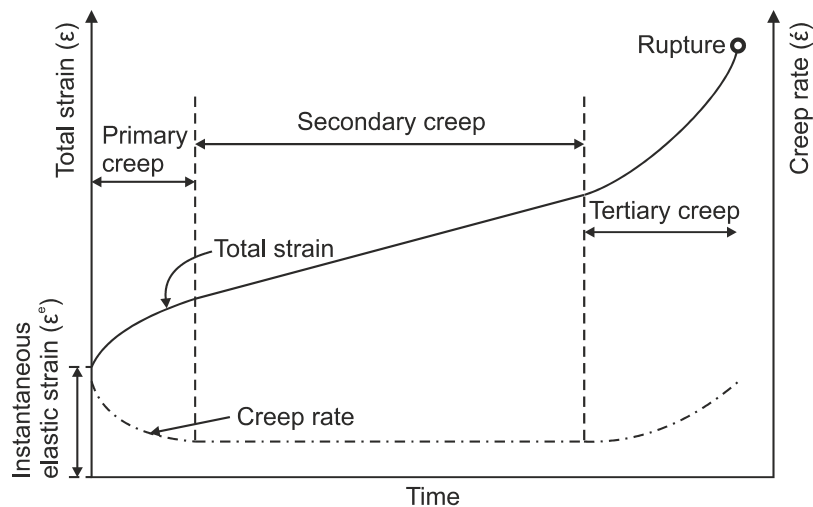
Figure 4-2: Typical creep curve showing the three stages of creep

The stress level is one of the most important factors in the creep behaviour of the material. In general, creep can occur at stresses below the yield strength of the material. Which means that if stainless steel bolting assemblies are preloaded under the yield strength of the material, creep still occurs and affects the relaxation behaviour of the preloaded bolted connection.

The temperature is another important factor on the creep behaviour of the material. The creep deformation can occur at any temperature level. In spite of that, typically the creep deformation of metals is very small if the service temperature (T) is below $0.4 \cdot T_M$, where T_M is the melting point of the metal [135]. For this reason, less attention has been paid to this issue due to the fact that many materials generally do

not experience significant time-dependent inelasticity at lower temperatures [136]. Besides this, for common structural purposes the temperature level is usually much lower than $0.4 \cdot T_M$. As already mentioned, the creep deformation is very small at the temperature below $0.4 \cdot T_M$. However, it is still of great interest to investigate the influence of viscoplastic deformation behaviour of bolted connections made of stainless steel on loss of preload in the bolted connection.

4.2.2.2 Creep behaviour of stainless steel sheets and plates

The creep behaviour of stainless steel sheets and plates was investigated at Outokumpu Avesta R&D Center and Outokumpu Tornio R&D Center and has been presented in detail in [137]. Experimental creep investigations were carried out on hot-rolled sheet 1.4404 (austenitic), hot-rolled sheet 1.4003 (ferritic), hot-rolled plate 1.4162 (lean duplex) and hot-rolled plate 1.4462 (duplex). All tests were performed at room temperature at load levels of $0.50 \cdot R_{p0.2}$ and above, simulating possible stress levels in the clamped components of preloaded bolted connections.

The results showed that the creep behaviour of stainless steel material can be described by the logarithmic creep model [137]. As expected, the amount of creep increases with increasing the load level, and the creep rate was high at the beginning of the test but drops quickly as time elapses. It was also observed that for equal loading levels a higher initial loading rate results in a higher amount of creep and, vice versa, a lower loading rate causes a lower amount of creep in the specimens.

The results also show that the amount of creep can be very small when the loading level is small, too. It could be shown that the stress in the clamped plate of a preloaded bolted connection made of stainless steel is too low to cause any significant creep deformation and therefore it does not contribute to the loss of preload in the connection. For this reason, it is expected that the main contribution to the loss of preload in this type of connection is made by stress relaxation in the bolts.

4.2.3 Stress relaxation behaviour

4.2.3.1 General

Another phenomenon which may occur in preloaded bolted connections is stress relaxation. In general, stress relaxation is a time-dependent progressive reduction of stress in a material which has been loaded and held under a constant strain [138], [139], [140], see Figure 4-3 (a). In this phenomenon, the total strain remains constant and only the elastic strain starts to be replaced with inelastic strain as time elapses [138], see Figure 4-3 (b).
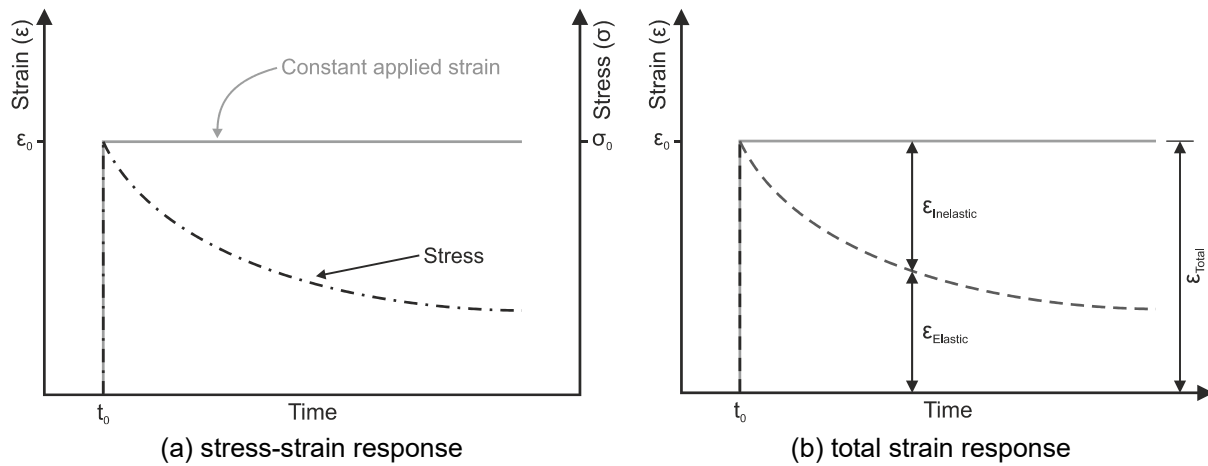
Figure 4-3: Schematic representation of stress relaxation behaviour

In preloaded bolted connections, the consequence of this transition from elastic to inelastic strain is a decrease in the stress level in the bolts. This can accelerate the loss of preload, which may influence the slip-resistant behaviour of the connection. For this reason, a comprehensive investigation of the stress relaxation behaviour of stainless steel material is needed in order to better understand the loss of preload in preloaded bolted connections made of stainless steel.

4.2.3.2 Stress relaxation behaviour of stainless steel sheets and bars

A series of investigations was carried out at Outokumpu Avesta R&D Center on the stress relaxation behaviour of stainless steel sheets and bars, which has been presented in detail in [141]. Two different steel grades for stainless steel sheets (hot-rolled sheet 1.4404 [austenitic] and hot-rolled sheet 1.4003 [ferritic]) and three different steel grades for stainless steel bars (1.4436 [austenitic], 1.4162 [lean duplex] and 1.4462 [duplex]) were selected. Three different types of potential bars (rebar, annealed bar and cold drawn) for producing the stainless steel bolts were considered for this investigation.

The stainless steel bolts can be machined, cold forged or hot forged. Usually, the machined process is preferred for small volumes of production, when the geometry is complicated, or when the bolt size is too large to be cold forged. Cold forging is usually used for high volumes of production because this process significantly increases the production rate. Cold forging can also increase the mechanical strength of austenitic and duplex stainless steel due to the cold work. For very large bolt dimensions, hot forging, which can be combined with machining as a final step of the production, is usually preferred [141].

In this investigation, cold drawn bars were selected to represent cold forged bolts and rebars and annealed bars were selected to use for machined bolts. The difference between these two types of bars is that the rebar has an as-rolled condition while the annealed bar is in a solution annealed state after rolling.

Stress relaxation tests on stainless steel sheets were carried out in such a way that the bolts were reloaded after a certain period of time in order to simulate the influence of a possible retightening of the bolts. The results showed that the amount of stress relaxation decreases after each reloading and the amount of stress relaxation increases with increasing loading rate.

The results from stress relaxation tests on stainless steel bars indicate that the stress relaxation is higher for rebars and annealed bars in comparison to cold drawn bars. The stress relaxation was similar for rebar and annealed bar test specimens made of austenitic and lean duplex. However, the duplex material showed lower stress relaxation at all stress levels. For the cold drawn bars, the stress relaxation was lower for austenitic material in comparison to duplex and lean duplex material. The highest rate of stress relaxation was at the beginning of the tests and after that the rate decreased over time. Most of the stress relaxation occurred within the first minutes of the test.

The test results show the viscoplastic behaviour of stainless steel material. This behaviour may influence the relaxation behaviour of preloaded bolted connections made of stainless steel. Some first investigations have already been presented by Shemwell and Johns in [142] for bolting assemblies made of austenitic stainless steel, property classes 70 and 80. These results already showed that there is no consistent difference in the relaxation behaviour of preloaded bolted connections made of stainless steel in comparison to carbon steel. Unfortunately, the focus of these investigations was only on austenitic stainless steel bolting assemblies. For this reason, a comprehensive investigation was needed to cover the still existing gaps on preloading and relaxation behaviour of preloaded bolted connections made of stainless steel.

4.3 Preloading of bolting assemblies made of stainless steel

Preloaded bolted connections made of stainless steel are widely requested especially when the connection is intended for a corrosive environment. Since the stainless steel material shows excellent corrosion resistance, the use of bolted connections made of stainless steel would be an efficient choice in many scenarios. According to EN 1090-2, preloading of bolting assemblies made of stainless steel is not permitted, and, due to the lack of knowledge on the viscoplastic deformation behaviour of the stainless steel material, they must be treated as special fasteners.

According to EN 1993-1-4, the application of bolting assemblies made of stainless steel in slip-resistant connections for reasons of serviceability or ultimate limit states is permitted only if all required parameters for preloading of the bolting assemblies made of stainless steel is specified in the frame of a procedure test. As EN 1090-2 does not specify any guidance on the determination of these parameters, an experienced laboratory shall perform the required tests in order to determine all necessary parameters for preloading.

The mechanical properties and chemical composition of stainless steel bolts and nuts are prescribed in EN ISO 3506-1 [143] and EN ISO 3506-2 [144], see Figure 4-4. The stainless steel bolts and nuts are classified in four main groups; austenitic (A), ferritic (F), martensitic (C) and duplex (D). The chemical composition and resulting corrosion resistance are represented by a single number (e.g. 2, 4, 6 or 8 for duplex), whereby the highest number represents the most durable material. The rate of cold working and work hardening has a great influence on the mechanical properties of bolted assemblies made of stainless steel. The property classes 80 and 100 are not comparable with the property classes 8.8 and 10.9 of carbon steel bolting assemblies according to EN ISO 898-1 and EN ISO 898-2 [145] since the yield strengths of property classes 8.8 and 10.9 are higher than the yield strengths of property classes 80 and 100. Nevertheless, comparable property classes 8.8 and 10.9 are also available for bolting assemblies made of stainless steel on the market, e.g. Bumax 88 and Bumax 109.

There is also no product standard in line with EN 14399, especially for bolting assemblies made of stainless steel that can be preloaded. For this reason, stainless steel bolting assemblies according to EN ISO 4014/4017 [146]/[147] can be considered for preloading purposes as one possibility. Bolting assemblies according to EN ISO 4014/4017 have smaller bolt heads and nuts in comparison with the HR/HV system bolting assemblies according to EN 14399-3/4. This leads to higher surface pressures which were assumed in the past to be critical and thus lead to some plastic deformations on the surfaces of the clamped components. However, from calculating the surface pressure it has become clear that the concern about the surface pressures seems to be unreasonable for the clamped plates made of stainless steel [147], [149].

| Stainless steel group | Austenitic | | | | | | | | | | | | | | Ferritic | |

Austenitic group:

Stainless steel grade	A1	A2 [a]	A3		A4 [a]	A5			A8			F1	
Property class	50	70	80	50	70	80	100	50	70	80	45	60
Usual manufacturing process [b]	Soft	Soft or cold worked	Cold worked or high strength	Soft	Soft or cold worked	Cold worked, high strength		Soft or cold worked	Cold worked, high strength		Soft	Cold worked

Martensitic group:

Stainless steel grade	C1			C3	C4	
Property class	50	70	110	80	50	70
Usual manufacturing process [b]	Soft	Hardened and tempered		Hardened and tempered	Soft	Hardened and tempered

Duplex (Austenitic-Ferritic) group:

Stainless steel grade	D2	D4	D6	D8
Property class	70	80	100	
Usual manufacturing process [b]	Soft or cold worked		Cold worked, high strength	

[a] Low carbon austenitic stainless steels with carbon content not exceeding 0.030 % may additionally be marked with an "L" after the grade. Example: A4L–80.

[b] For information only.

Figure 4-4: Designation system for stainless steel grades and property classes for bolts according to EN ISO 3506-1 [143]

In order to close this gap in knowledge about the tightening and the basic preloading behaviour of bolting assemblies made of stainless steel, a comprehensive investigation was conducted in the frame of the SIROCO project at the Institute for Metal and Lightweight Structures (IML) of the University of Duisburg-Essen (UDE). Within this chapter, a short summary of the main findings of this investigation is presented.

In total, 285 tightening tests were performed on M12, M16, M20 and M24 bolting assemblies made of austenitic and austenitic-ferritic (lean duplex, duplex and super duplex) stainless steel with EN ISO 4014/4017 bolts, EN ISO 4032 [150] nuts and EN ISO 7089 [151] washers in property classes 8.8 and 10.9. All stainless steel bolting assemblies were supplied by BUAMX AB, which produces bolting assemblies with property classes deviating from EN ISO 3506-1 and EN ISO 3506-2. However, the company applies the whole designation system of EN ISO 3506-1 for all bolting assemblies made of stainless steel but with deviating property classes.

In the absence of any suitable standard for testing of the tightening and the basic preloading behaviour of bolting assemblies made of stainless steel, all tightening tests were performed according to EN 14399-2 [152]. By performing the suitability tests for preloading according to this standard, it was possible to investigate the characteristics of/differences between carbon and stainless steel in detail. The evaluation was conducted based on EN 14399-3 for HR bolting assemblies, since the

HR-system is characterized by a longer thread and a thicker nut in comparison with the HV-system, which is more comparable with the EN ISO 4017 bolts and EN ISO 4032 nuts tested in the frame of the SIROCO project.

The results show that, in principle, if choosing a suitable material pairing (combination of different bolts, nuts and washers with different steel grades) and in particular an appropriate lubricant, preloading of all tested stainless steel bolting assemblies with property classes 8.8 and 10.9 is possible. As can be seen in Figure 4-5, the ductility of the bolting assemblies can be significantly improved by using an appropriate lubricant. This exemplary figure shows the comparison between factory provided lubricant (gleitmo 1952V) and Molykote 1000 spray for M16 Bumax LDX (lean duplex) with property class 10.9 [153].

(a) Preload - angle of rotation diagram   (b) Preload - tightening torque diagram
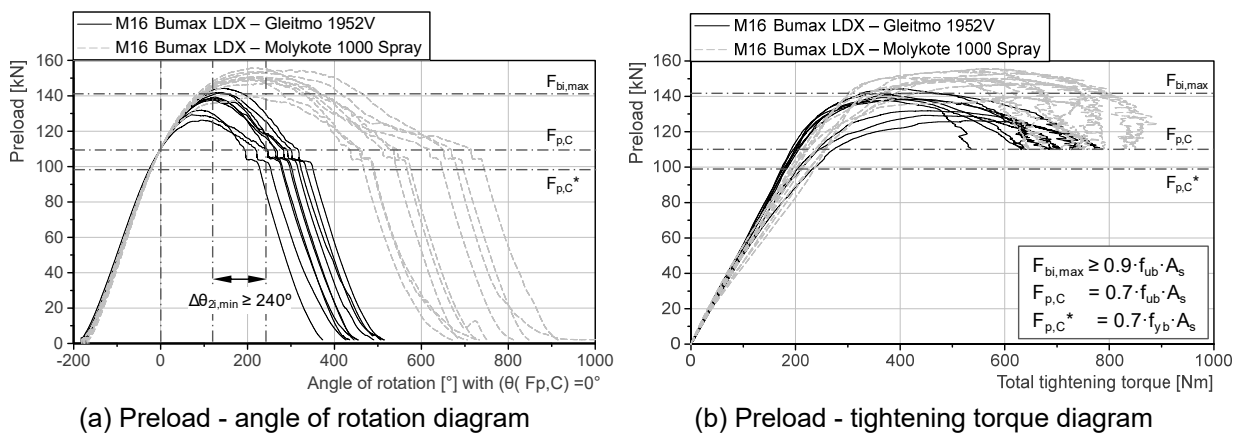
Figure 4-5: Comparison between factory-provided lubricant (gleitmo 1952V) and Molykote 1000 spray [153]

The results also show that from the practical point of view, secure tightening parameters for the modified torque method according to DASt-Richtlinie 024 [154] or for the combined method according to EN 1090-2 can be evaluated without the risk of overstressing the bolting assemblies. For more information see [155].

Furthermore, galling is a common issue in the installation of bolting assemblies made of stainless steel; it is also known as local cold welding on the interface between the washer and the nut but may also occur between the paired thread flanks. Galling causes plastic deformations on these surfaces as well as serious problems in reaching the required preload level based on the selected preloading procedure. However, the results show that galling can be avoided by using suitable lubrication and secure tightening of the stainless steel bolts limited to the elastic range. In the frame of this investigation, different types of lubricants from different producers were tested, [155], [156] [157]. DOW Corning Molykote 1000 spray/paste and Molykote D-321R spray were the most promising tested lubricants which achieved very positive results in the preloading procedure of bolting assemblies made of stainless steel, see the tightening curves presented in Figure 4-6.
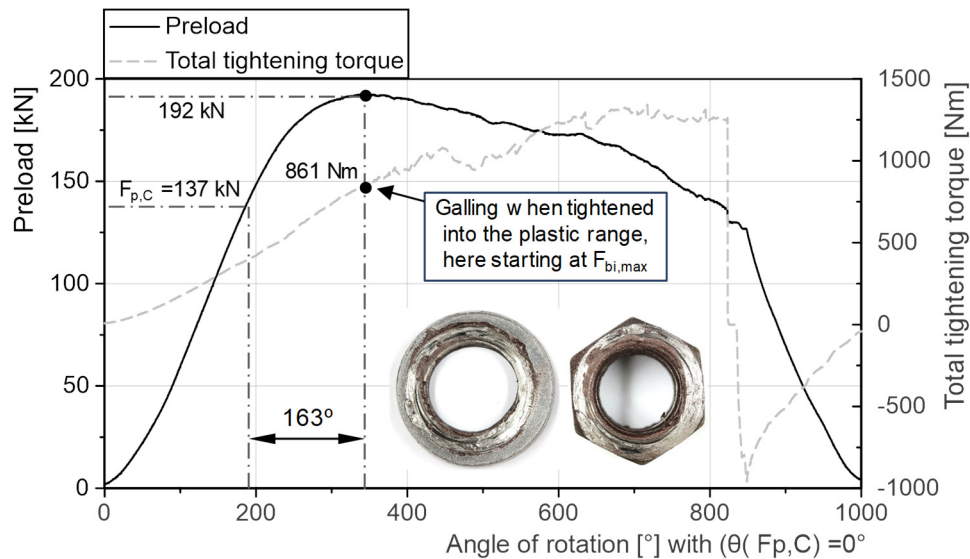
Figure 4-6: Example of major galling in the tightening curves for M20 Bumax 88 with Molykote 1000 spray [153]

In order to determine the reliable tightening parameters for each unique bolted connection, guidance for the procedure tests has been developed at the Institute for Metal and Lightweight Structures (IML) of the University of Duisburg-Essen (UDE) in the form of a "Bolt Tightening Qualification Procedure" (BTQP), see Figure 4-7. This guidance can deliver all necessary steps for the determination of secure tightening parameters, considering the tightening method. With this qualification process, it is also possible to have a secure tightening process and clear criteria for inspection purposes, see [157], [158], [159].

Definition of initial parameters for preloading

Product standard
- EN ISO 4014
- EN ISO 4017
- EN ISO 4762
- ...

Lubrication
Selection of a lubricant, which is recommended for the application

Preferred tightening method
- Torque method
- Combined method
- Yield controlled tightening
- Hydraulic tensioning
- ...

Target preload F_p
- Target level I or II
- Required preload level based on design
- Preload below or equal $F_{p,S} = 0.7\, f_{yb}\, A_s$

Mechanical properties
- Corrosion resistance
- Property class (80, 100)
- Stainless steel grade

Tensile tests for fasteners with full loadability
acc. to EN ISO 3506-1

Minimum 3 tensile tests per configuration

Mechanical properties fullfied? — no

yes

Suitability test

Minimum 20 tightening tests per configuration

Determination of

Ductility of the assemblies
$\Delta\theta_{2,i} > \Delta\theta_{2,i,min}$

Clamp length $\sum t$	$\Delta\theta_{2,i,min}$
$\sum t < 2\cdot d$	210°
$2\cdot d \leq \sum t < 6\cdot d$	240°
$6\cdot d \leq \sum t < 10\cdot d$	270°

Maximum individual bolt force
$F_{bi,max} > S_b \cdot F_p$

Property class	S_b
80	1.70
100	1.60

Friction
k-factor: $k = \dfrac{M}{d \cdot F_{p,S}}$
$0.10 \leq k_i \leq 0.23$

Evaluation of tightening tests

Suitability test passed?

Adaption of the preload level F_p

Option 1   yes   no   Option 2

Adaption of parameters
- Higher property class
- Alternative lubrication
- Different steel grade
- ...

Determination of tightening parameters

Statistical evaluation of tightening tests according to EN 1990
with 5 % and 95 % fractile values $F_{Rk,5\%}$ and $F_{Rk,95\%}$
for the determined tightening parameters

Determination of tightening parameters considering limiting criteria

Torque controlled tightening

Alternative tightening method

Combined method

Definition of limiting criteria

Limiting criteria
$F_{b,min}$	$\geq 1.03\, F_P$
$F_{Rk,5\%}$	$\geq 1.03\, F_P$
F_{bm}	$\geq 1.10\, F_P$
$F_{Rk,95\%}$	$\leq 0.95\, S_b \cdot F_P$
$F_{b,max}$	$\leq 0.95\, S_b \cdot F_P$

Limiting criteria
$F_{b,min}$	$\geq 1.03\, F_P$
$F_{Rk,5\%}$	$\geq 1.03\, F_P$
F_{bm}	$\geq 1.10\, F_P$
$F_{Rk,95\%}$	$< S_b \cdot F_P$
$F_{b,max}$	$< S_b \cdot F_P$
$\Delta\theta_c$	$< 0.5\, \Delta\theta_{2,i,min}$

Determination of tightening parameters possible?

no

yes

Inspection requirements acc. to EN 1090-2

Figure 4-7: Bolt Tightening Qualification Procedure (BTQP) [157],

4.4 Relaxation behaviour of bolted connections made of stainless steel

4.4.1 General

The viscoplastic deformation in preloaded bolted connections made of stainless steel has caused some uncertainty during the last decades. This behaviour must be considered in order to guarantee a required preload level for serviceability and ultimate limit state reasons.

For this reason, it is important to estimate the amount of the preload losses that are caused by viscoplastic deformation in the bolted connection. The clarification of the influence of this critical parameter is thus an important issue.

4.4.2 Measuring the preload in stainless steel bolting assembly

The first step in order to investigate the relaxation behaviour in bolted connections made of stainless steel is to find the most reliable method to measure the preload inside the bolt. Experience with bolted connections made of carbon steel showed that instrumenting the bolts with the strain gauges is one of the most accurate methods to measure the preload level in the bolt.

For this reason, different series of creep tests on stainless steel bolts were carried out to investigate the reliability of this method for bolting assemblies made of stainless steel. The goal of this investigation was to examine the influence of the creep deformation of the bolt material on the measured preload level.

In the frame of this investigation, two different grades of stainless steel bolts with two different property classes and three different sizes according to EN ISO 4017 were selected: M16 and M20 austenitic (1.4436) Bumax 109, M16 and M20 austenitic (1.4436) Bumax 88 and M12 super duplex (1.441) Bumax 109, see Table 4-1. The results were compared with a carbon steel HV 10.9 bolt according to EN 14399-4.

Three different types of strain gauges, BTM-6C, BTM-1C and BTMC-3 (produced by Tokyo Sokki Kenkyujo Co., Ltd.), were used to instrument all bolts. For BTM-6C and BTM-1C, the application procedure is already explained in Chapter 3.2 and Figure 3-1. For the bolts instrumented with BTMC-3, a centric hole of 2 mm diameter along the bolt shank was filled with a one-component adhesive. The strain gauge was inserted gently into the hole, see Figure 4-8.

Table 4-1: Creep test results for bolts made of carbon and stainless steel [106]

Series ID	Material	Grade	Dimension	Standard	Level of load	Duration [days]	Δ_{max}[1] [%]	ER[2] [%]
				Strain gauge type: BTM-6C				
CS	Carbon	HV 10.9	M20 x 110	EN 14399-4	$F_{p,C}$ = 172 kN	14	≈ 0	≈ 0
A-1	Austenitic (1.4436)	Bumax 109	M20 x 100	ISO 4017	$F_{p,C}$ = 172 kN	5	≈ 1.4	≈ 50
A-1R	Austenitic (1.4436)	Bumax 109	M20 x 100	ISO 4017	$F_{p,C}$ = 172 kN	14	≈ 0.6	≈ 60
A-2	Austenitic (1.4436)	Bumax 109	M20 x 100	ISO 4017	$F_{p,C}$ = 172 kN	8	≈ 4	-
SDX-1	Super duplex (1.441)	Bumax 109	M12 x 80	ISO 4017	$F_{p,C}$ = 59 kN	14	≈ 4	≈ 20
				Strain gauge type: BTM-1C				
SDX-2	Super duplex (1.441)	Bumax 109	M12 x 80	ISO 4017	$F_{p,C}$ = 59 kN	14	≈ 6	≈ 5
SDX-2R	Super duplex (1.441)	Bumax 109	M12 x 80	ISO 4017	$F_{p,C}$ = 59 kN	29	≈ 1	≈ 15
				Strain gauge type: BTMC-3				
A-3	Austenitic (1.4436)	Bumax 88	M20 x 80	ISO 4017	$F_{p,C}$ = 140 kN	4	≈ 1.6	≈ 50
A-4	Austenitic (1.4436)	Bumax 109	M16 x 100	ISO 4017	$F_{p,C}$ = 110 kN	8	≈ 4	-
A-5	Austenitic (1.4436)	Bumax 88	M16 x 80	ISO 4017	$F_{p,C}$ = 88 kN	11	≈ 6.5	≈ 7

[1] maximum difference between measured preload and constant tensile load
[2] elastic recovery of the bolt when the specimen is unloaded

(a) Strain gauge   (b) Filling adhesive into the hole   (c) Inserting the strain gauge   (d) Cutting the pipe extruded from the hole
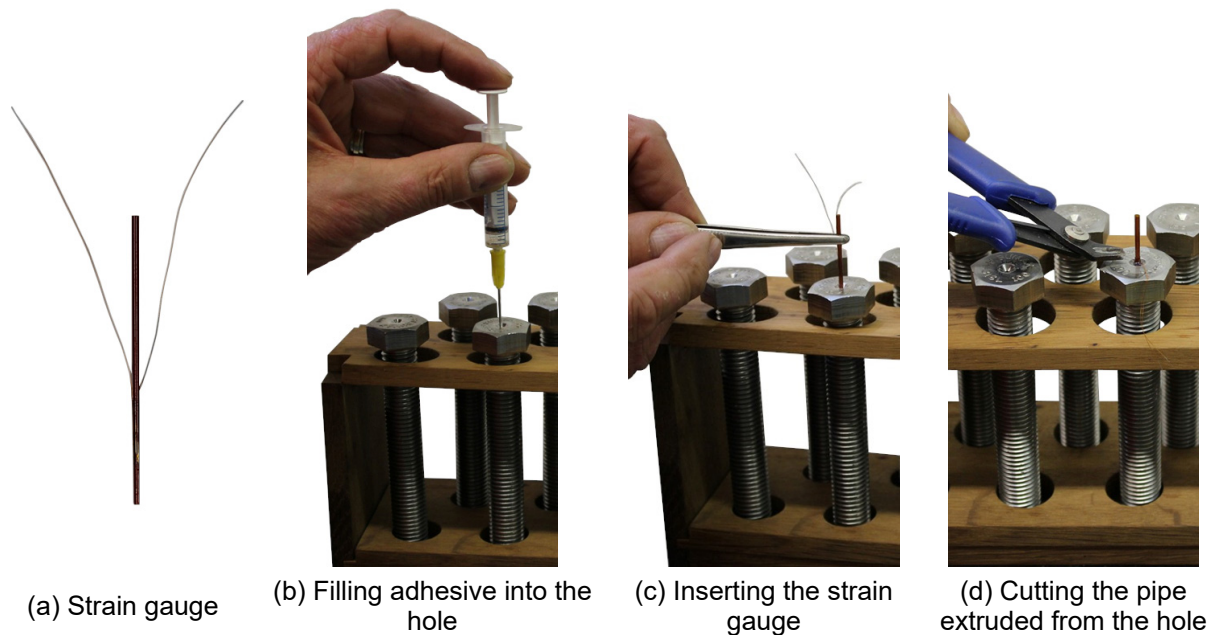
Figure 4-8: Exemplary instrumentation phases for stainless steel bolts with BTMC strain gauges

All instrumented bolts were calibrated under stepwise tensile loading and the calibration factor was evaluated for each specific bolt. The bolts with a linear load-strain behaviour were selected for the creep test. The creep tests were carried out in a universal testing machine with a maximum load capacity of ± 200 kN. The preload was measured constantly and compared to the actual existing load in the bolt (the constant tensile load from the universal testing machine). All bolts were loaded up to $F_{p,C}$. In total ten bolts were tested. One creep test was performed on a carbon steel

bolt and nine tests on stainless steel bolts, see Table 4-1. For one M20 austenitic Bumax 109 and one M12 super duplex Bumax 109 bolt, the creep tests were repeated in order to prove the reusability of the instrumented stainless steel bolts.

As can be seen in Figure 4-9, the difference between the measured preload level from strain gauges and the tensile load from the universal machine is negligible in the loading stage. However, this difference starts to grow when the load becomes constant and time elapses.
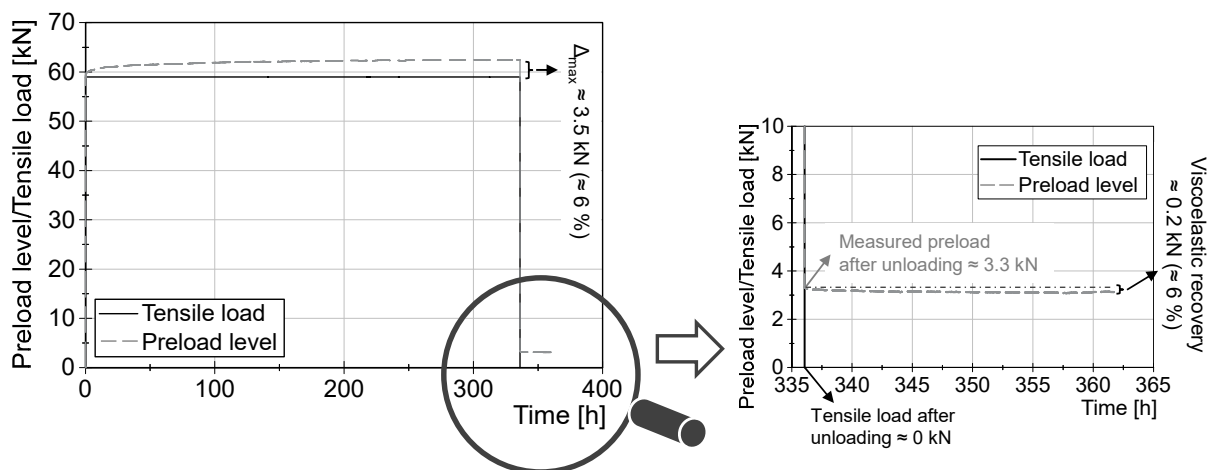
Figure 4-9: Creep test on M12 super duplex bolt (SDX-2) [106]

Table 4-1 shows that the accuracy of the instrumented stainless steel bolts with implanted strain gauges for measuring the preload inside the bolts might not be accurate enough for the long-term relaxation test.

The strain gauge which was embedded in the shank of the bolt also measures the viscoplastic creep deformation in the bolt's material, which causes different/higher values in comparison to the real preload level existing in the bolt. This phenomenon has not been observed so far in carbon steel bolts since the carbon steel material is not susceptible to creep. For this reason, instrumenting carbon steel bolts with the strain gauges is an accurate method of measuring the preload level in the bolt.

After unloading the stainless steel bolts, the preload level measured by the strain gauges did not return to zero. This phenomenon shows that the measured strain in the bolt is recorded by the strain gauges. When the bolt remains unloaded, the strain starts to recover, see Figure 4-9. The amount of this viscoelastic recovery of the bolt is presented in Table 4-1.

The creep test was repeated for two stainless steel bolts (A-1R and SDX-2R). The results show that the accuracy of the measured preload level in the bolts was improved in comparison with first creep test. The reason is that the large amount of inelastic creep occurred during the first creep test and in the second creep test only a very small amount of creep deformation could occur, see Figure 4-10.
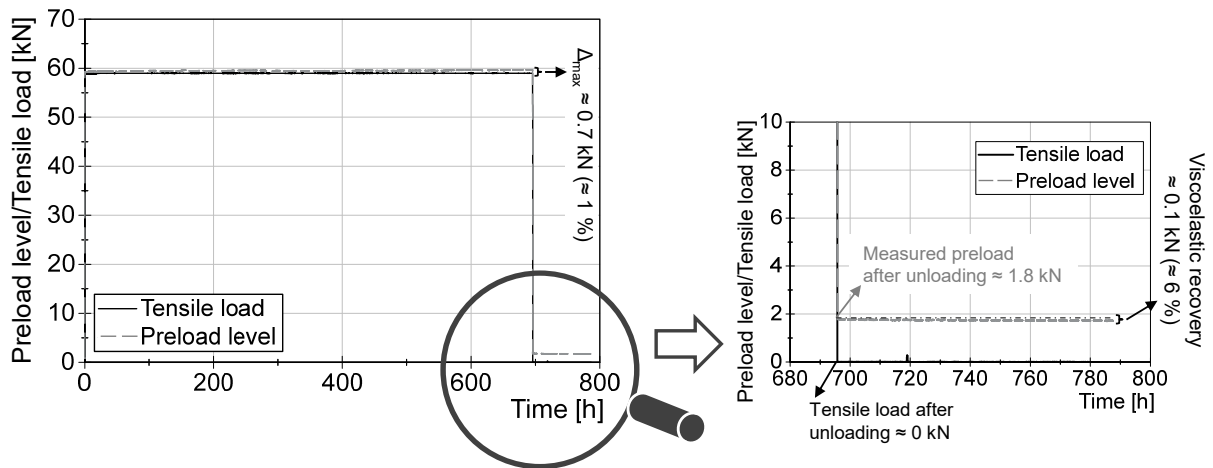
Figure 4-10: Repeated creep test on M12 super duplex bolt (SDX-2R) [106]

In order to measure the preload level in the stainless steel bolt independently from viscoplastic deformation of the material, it was decided to prepare some small/short load cells to measure the preload level. The advantage of using load cells is that the viscoplastic deformation in the bolt material could not cause any over-measuring in the existing preload level of the bolt.

For this purpose, two different sizes of load cells (for M16 and M20 bolts) were prepared, see Figure 4-11. All load cells were calibrated under stepwise tensile loading in a similar way as carried out for the instrumented bolts with strain gauges. The combination of the instrumented carbon steel bolts and the load cells was also calibrated in the tightening torque test machine in order to confirm the accuracy of the load cells, see Figure 4-12.

(a) Some production phases of load cells (LC) at the University of Duisburg-Essen

(b) Calibration phase

Figure 4-11: Preparation and calibration phases of load cells
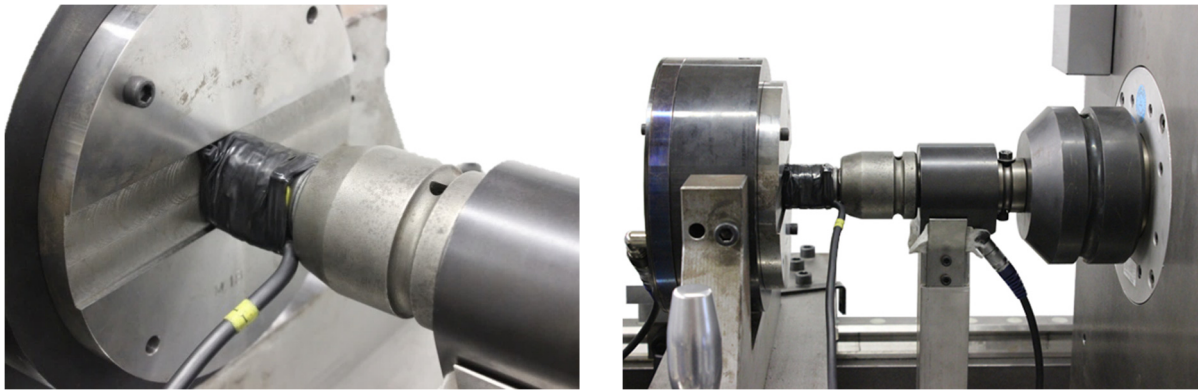
Figure 4-12: Calibration of load cells in the tightening torque testing machine

4.4.3 Loss of preload in bolted connections made of carbon and stainless steel with uncoated/untreated surfaces

To complete the investigations into the relaxation behaviour of bolted connections made of stainless steel, various sets of bolting assemblies and plates with different steel grades were tested, [153], [160], [161], [162].

To cover the wide range of available stainless steel materials, four different grades of stainless steel plate were selected: austenitic (1.4404), ferritic (1.4003), duplex (1.4462), and lean duplex (1.4162). These were combined with three different bolt sizes (M16, M20 and M24) and grades of bolting assemblies made of austenitic (1.4432), duplex (1.4462) and lean duplex (1.4162) stainless steel. The investigated stainless steel bolting assemblies include bolts according to EN ISO 4017 of grades Bumax 88 and Bumax 109, which relate to property classes 8.8 and 10.9 according to EN ISO 898-1, with nuts according to EN ISO 4032 and with washers according to EN ISO 7089. In this study, all stainless steel bolting assemblies were supplied by BUAMX AB.

Further investigations were conducted with stainless steel bolting assemblies (M16 and M20 Bumax 88 austenitic bolts) in combination with S355 carbon steel plates. Furthermore, the combination of carbon steel bolting assemblies (M16 and M20 HV 10.9 bolts according to EN 14399-4) in combination with austenitic and duplex stainless steel plates were also tested. These investigations were carried out in order to ascertain the influence of viscoplastic deformation in stainless steel bolting assemblies and plates in preloaded bolted connections separately.

More investigations were conducted on the combination of carbon steel HV bolts and S355 carbon steel plates in order to compare the preload losses in bolted connections made of stainless and carbon steel. The full test matrixes of all investigations are presented in Table 4-2, Table 4-3, Table 4-4 and Table 4-5.

Table 4-2: Loss of preload in relaxation tests of M20 stainless steel bolting assemblies [106]

Series ID	Type of specimen		No. of tests	Σt/d[1] [-]	Clamped package		F_{p,C}[2] [kN]	Loss of preload	
					Bolt	Plate		measured after days - min / mean / max [%]	after 50 years (extrapolated) min / mean / max [%]
Bumax 88 Austenitic bolts (M20x100)									
SS01	8 bolt	First row	4	3.75	Bumax 88	Austenitic	137	14 – 3.7 / 4.6 / 6.0	6.0 / 6.8 / 7.2
		Sec. row	4					14 – 4.3 / 4.6 / 4.8	7.0 / 7.1 / 7.2
	1 bolt	-	4					14 – 4.2 / 4.5 / 5.2	6.7 / 7.2 / 8.3
SS02	8 bolt	First row	4			Ferritic		14 – 4.0 / 4.4 / 4.7	6.4 / 6.7 / 7.1
		Sec. row	4					14 – 3.4 / 3.7 / 4.1	5.4 / 5.9 / 6.4
	1 bolt	-	4					14 – 3.5 / 4.1 / 4.6	5.5 / 6.4 / 7.3
SS03	8 bolt	First row	4			Duplex		14 – 3.4 / 4.0 / 4.4	5.4 / 6.2 / 7.0
		Sec. row	4					14 – 4.0 / 4.1 / 4.4	6.2 / 6.5 / 7.2
	1 bolt	-	4					14 – 3.6 / 4.1 / 4.6	5.5 / 6.3 / 7.0
SS04	8 bolt	First row	3			Lean Duplex		14 – 4.0 / 4.8 / 6.0	6.0 / 7.3 / 9.0
		Sec. row	4					14 – 4.4 / 4.6 / 5.0	6.8 / 7.0 / 7.5
	1 bolt	-	4					14 – 4.0 / 4.4 / 4.5	6.4 / 6.8 / 7.0
CS05	8 bolt	First row	4			S355		20 – 2.9 / 3.7 / 4.7	4.6 / 5.8 / 7.1
		Sec. row	2					20 – 3.0 / 3.0 / 3.0	4.6 / 4.7 / 4.7
Bumax 109 Austenitic bolts (M20x100)									
SS06	8 bolt	First row	3	3.75	Bumax 109	Austenitic	172	14 –5.0 / 5.3 / 5.6	7.8 / 8.2 / 8.6
		Sec. row	3					14 –5.6 / 5.8 / 5.9	8.6 / 8.8 / 8.9
SS07	1 bolt	-	3			Ferritic		25 –4.4 / 4.6 / 4.8	6.4 / 6.7 / 7.0
SS09	8 bolt	First row	2			Lean Duplex		20 –4.4 / 4.6 / 4.8	6.9 / 7.0 / 7.1
		Sec. row	4					20 – 4.2 / 4.8 / 5.3	6.8 / 7.5 / 8.2
CS10	8 bolt	First row	3			S355		20 – 3.9 / 4.0 / 4.0	5.8 / 5.9 / 6.0
		Sec. row	3					20 – 4.3 / 4.5 / 4.7	6.5 / 6.7 / 7.0
Bumax DX Duplex bolts (M20x100)									
SS11	8 bolt	First row	4	3.75	Bumax DX	Austenitic	172	14 – 3.5 / 4.3 / 5.2	5.5 / 6.6 / 7.9
		Sec. row	3					14 – 4.1 / 4.2 / 4.5	6.4 / 6.5 / 6.8
SS12	8 bolt	First row	4			Ferritic		20 – 3.9 / 4.7 / 5.2	5.7 / 7.2 / 8.0
		Sec. row	4					20 – 4.7 / 5.2 / 5.7	7.2 / 7.8 / 8.6
SS13	1 bolt	-	3			Duplex		20 – 4.9 / 5.1 / 5.2	7.5 / 7.8 / 8.0
SS14	1 bolt	-	3			Lean Duplex		10 – 4.3 / 4.7 / 5.0	7.3 / 7.9 / 8.4
CS15	1 bolt	-	3			S355		20 – 4.7 / 4.8 / 4.9	7.2 / 7.4 / 7.6
Bumax LDX Lean Duplex bolts (M20x100)									
SS16	8 bolt	First row	3	3.75	Bumax LDX	Austenitic	172	14 – 7.1 / 7.5 / 7.9	10.9 / 11.6 / 12.1
		Sec. row	4					14 – 6.2 / 6.7 / 6.9	9.4 / 10.1 /10.6
	1 bolt	-	4					14 – 5.2 / 6.0 / 6.7	8.2 / 9.2 / 10.2
SS17	8 bolt	First row	3			Ferritic		14 – 5.1 / 5.2 / 5.3	7.9 / 8.0 / 8.2
		Sec. row	3					14 – 5.3 / 5.4 / 5.6	8.0 / 8.2 / 8.6
	1 bolt	-	3					14 – 4.1 / 4.6 / 5.1	6.8 / 7.3 / 8.0
SS18	1 bolt	-	4			Duplex		14 – 5.2 / 5.6 / 5.9	8.3 / 8.9 / 9.5
SS19	1 bolt	-	3			Lean Duplex		14 – 5.0 / 5.4 / 5.4	7.9 / 8.2 / 8.4

[1] clamping length ratio (Σt = clamping length and d = bolt dimension) [2] preload level

Table 4-3: Loss of preload in relaxation tests of M16 stainless steel bolting assemblies [106]

Series ID	Type of specimen		No. of tests	$\Sigma t/d$[1] [-]	Clamped package Bolt	Plate	$F_{p,C}$[2] [kN]	Loss of preload measured after days - min / mean / max [%]	after 50 years (extrapolated) min / mean / max [%]
					Bumax 88 Austenitic bolts (M16x100)				
SS21	8 bolt	First row	4			Austenitic		14 – 4.7 / 5.0 / 5.5	7.3 / 7.7 / 8.5
		Sec. row	4					14 – 4.5 / 4.8 / 5.1	6.8 / 7.3 / 7.7
	1 bolt	-	4					14 – 3.9 / 4.5 / 5.0	6.1 / 6.8 / 7.8
SS22	8 bolt	First row	4			Ferritic		14 – 3.9 / 4.5 / 5.0	6.1 / 6.9 / 7.6
		Sec. row	4					14 – 3.6 / 4.5 / 5.0	5.6 / 7.0 / 7.7
	1 bolt	-	4					14 – 3.7 / 4.2 / 4.5	5.9 / 6.6 / 7.3
SS23	8 bolt	First row	4	3.7	Bumax 88	Duplex	88	14 – 4.5 / 5.2 / 5.8	6.7 / 7.8 / 8.7
		Sec. row	4					14 – 4.6 / 4.8 / 4.9	7.1 / 7.3 / 7.6
	1 bolt	-	4					14 – 3.9 / 4.8 / 5.8	6.1 / 7.3 / 8.9
SS24	8 bolt	First row	4			Lean Duplex		30 – 4.2 / 5.2 / 6.0	6.2 / 7.5 / 8.6
		Sec. row	4					30 – 4.7 / 5.1 / 5.8	6.7 / 7.4 / 8.4
	1 bolt	-	4					14 – 4.7 / 5.1 / 5.5	7.3 / 7.8 / 8.5
CS25	8 bolt	First row	1			S355		30 – 4.8	7.0
		Sec. row	4					30 – 4.1 / 4.5 / 4.7	5.8 / 6.4 / 6.7
	1 bolt	-	3					30 – 4.3 / 4.6 / 5.0	6.2 / 6.6 / 7.2
					Bumax 109 Austenitic bolts (M20x100)				
SS26	8 bolt	First row	4			Austenitic		14 – 5.6 / 5.7 / 5.9	8.6 / 8.9 / 9.2
		Sec. row	4					14 – 5.8 / 6.0 / 6.3	9.0 / 9.3 / 9.6
	1 bolt	-	3					25 – 5.1 / 5.2 / 5.3	7.3 / 7.6 / 7.8
SS27	8 bolt	First row	3			Ferritic		40 – 6.2 / 6.3 / 6.4	9.0 / 9.1 / 9.3
		Sec. row	4					40 – 6.1 / 6.3 / 6.6	8.9 / 9.0 / 9.2
	1 bolt	-	3					40 – 5.4 / 5.8 / 6.3	7.7 / 8.3 / 9.2
SS28	8 bolt	First row	4	3.7	Bumax 109	Duplex	110	55 – 4.6 / 5.0 / 5.4	6.4 / 7.1 / 7.7
		Sec. row	4					55 – 4.9 / 5.4 / 6.1	7.0 / 7.6 / 8.5
	1 bolt	-	4					55 – 5.0 / 5.3 / 5.7	7.1 / 7.7 / 8.2
SS29	8 bolt	First row	4			Lean Duplex		14 – 5.6 / 5.7 / 5.9	8.6 / 9.0 / 9.4
		Sec. row	4					14 – 5.8 / 6.0 / 6.3	9.1 / 9.3 / 9.6
	1 bolt	-	4					14 – 4.8 / 5.2 / 5.7	7.4 / 8.0 / 8.9
CS30	8 bolt	First row	4			S355		20 – 3.8 / 4.4 / 4.7	6.0 / 6.8 / 7.2
		Sec. row	4					20 – 4.6 / 4.7 / 4.8	7.1 / 7.3 / 7.5
					Bumax DX Duplex bolts (M20x100)				
SS31	8 bolt	First row	4			Austenitic		20 – 6.2 / 6.6 / 6.8	9.5 / 9.9 / 10.3
		Sec. row	4					20 – 6.9 / 7.2 / 7.4	9.4 / 10.4 / 10.9
	1 bolt	-	3					12 – 5.5 / 5.8 / 6.1	8.9 / 9.4 / 9.8
SS32	1 bolt	-	4	3.7	Bumax DX	Ferritic	110	14 – 5.4 / 5.8 / 6.6	8.3 / 9.0 / 10.3
SS33	1 bolt	-	3			Duplex		14 – 5.2 / 5.8 / 6.4	8.2 / 9.0 / 9.9
SS34	1 bolt	-	4			Lean Duplex		9 – 4.3 / 4.7 / 5.0	6.9 / 7.6 / 8.1
CS35	1 bolt	-	4			S355		14 – 4.7 / 5.0 / 5.5	7.2 / 7.7 / 8.2
					Bumax LDX Lean Duplex bolts (M16x100)				
SS36	8 bolt	First row	2			Austenitic		20 –5.2 / 6.1 / 7.0	7.9 / 9.3 / 10.7
		Sec. row	4					20 – 4.4 / 4.6 / 5.0	6.9 / 7.2 / 7.6
	1 bolt	-	3					14 – 6.1 / 6.3 / 6.4	9.3 / 9.7 / 10.0
SS37	8 bolt	First row	4			Ferritic		55 – 5.0 / 5.3 / 5.6	7.1 / 7.5 / 8.0
		Sec. row	4					55 – 5.0 / 5.3 / 5.5	7.1 / 7.5 / 7.9
	1 bolt	-	3	3.7	Bumax LDX		110	55 – 4.9 / 5.3 / 5.6	7.0 / 7.4 / 7.8
SS38	1 bolt	-	4			Duplex		14 – 4.9 / 5.5 / 6.3	7.4 / 8.2 / 9.2
SS39	8 bolt	First row	4			Lean Duplex		20 – 4.1 / 4.4 / 4.6	6.3 / 6.7 / 7.0
		Sec. row	4					20 – 5.7 / 6.1 / 6.4	8.8 / 9.3 / 9.9
	1 bolt	-	3					20 – 5.3 / 5.7 / 6.0	7.9 / 8.5 / 9.1
CS40	1 bolt	-	3			S355		55 – 5.0 / 5.6 / 6.1	7.0 / 7.9 / 8.6

[1] clamping length ratio (Σt = clamping length and d = bolt dimension) | [2] preload level

Table 4-4: Loss of preload in relaxation tests of M24 stainless steel bolting assemblies [106]

| Series ID | Type of specimen | | No. of tests | Σt/d[1] [-] | Clamped package | | $F_{p,C}$[2] [kN] | Loss of preload | after 50 years (extrapolated) min / mean / max [%] |
					Bolt	Plate		measured after days - min / mean / max [%]	
					Bumax 88 Austenitic bolts (M24x100)				
SS41	8 bolt	First row	3	3.2	Bumax 88	Austenitic	198	14 – 5.3 / 5.7 / 6.2	8.2 / 8.5 / 8.9
		Sec. row	4					14 – 5.1 / 5.6 / 6.0	8.0 / 8.7 / 9.2
SS43	8 bolt	First row	4		Bumax 88 (re-used)	Austenitic (re-used)		25 – 2.6 / 2.8 / 3.6	3.9 / 4.3 / 5.4
		Sec. row	4					25 – 2.7 / 2.8 / 3.0	4.1 / 4.2 / 4.5

[1] clamping length ratio (Σt = clamping length and d = bolt dimension) | [2] preload level

Table 4-5: Loss of preload in relaxation tests of M20 and M16 HV bolting assemblies [106]

| Series ID | Type of specimen | | No. of tests | Σt/d[1] [-] | Clamped package | | $F_{p,C}$[2] [kN] | Loss of preload | after 50 years (extrapolated) min / mean / max [%] |
					Bolt	Plate		measured after days - min / mean / max [%]	
					HV bolts M20				
SS45	8 bolt	First row	4	2.55	HV M20x75/ M20x115	Duplex	172	14 – 3.0 / 4.3 / 5.2	4.7 / 6.7 / 8.0
		Sec. row	4	4.55				14 – 2.9 / 3.5 / 4.4	4.6 / 5.5 / 6.8
CS48	8 bolt	First row	4	2.55	HV M20x75	S355		14 – 4.0 / 5.1 / 6.5	6.0 / 7.7 / 9.7
		Sec. row	-					-	-
	1 bolt	-	4					35 – 3.9 / 4.4 / 5.0	5.5 / 6.2 / 7.1
CS49	8 bolt	First row	4	4.55	HV M20×115			14 – 3.6 / 4.0 / 5.0	5.3 / 6.1 / 7.6
		Sec. row	4					14 – 2.9 / 4.3 / 5.4	4.4 / 6.4 / 8.0
	1 bolt	-	3					40 – 5.0 / 5.4 / 5.9	6.9 / 7.3 / 7.9
					HV bolts M16				
SS46	8 bolt	First row	2	2.8	HV M16x65/ M16x95	Austenitic	110	20 – 1.8 / 2.4 / 3.3	2.8 / 3.6 / 4.8
		Sec. row	4	4.7				20 – 1.3 / 1.6 / 2.0	2.0 / 2.4 / 3.0
SS47	8 bolt	First row	4	2.8		Duplex		14 – 2.6 / 2.8 / 3.0	4.0 / 4.4 / 4.6
		Sec. row	4	4.7				14 – 2.0 / 2.3 / 2.6	3.0 / 3.5 / 3.9
CS50	8 bolt	First row	4	2.8	HV M16×65	S355		14 – 3.6 / 4.4 / 5.5	5.7 / 6.7 / 8.2
		Sec. row	4					14 – 4.1 / 5.2 / 7.9	6.4 / 7.9 / 11.9
	1 bolt	-	3					40 – 6.2 / 6.5 / 6.7	9.0 / 9.4 / 9.8
CS51	8 bolt	First row	4	4.7	HV M16×95			12 – 5.2 / 5.4 / 5.7	8.2 / 8.4 / 8.8
		Sec. row	4					12 – 3.9 / 4.1 / 4.3	6.5 / 6.7 / 7.0
	1 bolt	-	2					40 – 5.0 / 5.0 / 5.1	7.0 / 7.0 / 7.1

[1] clamping length ratio (Σt = clamping length and d = bolt dimension) | [2] preload level

All stainless steel plates were tested with the "as received" 1D surface condition without any further surface treatment and all carbon steel plates in the "as received" surface condition, see Figure 4-13 (a) and (b).

In general, two different specimen configurations were developed which were used in combination with different bolt sizes: (1) one-bolt-specimen with 75 mm × 75 mm plates, and (2) eight-bolt specimen with 150 mm × 150 mm plates, see Figure 4-14. In total, forty-seven different test series were carried out. In order to investigate the influence of the clamping length a range of clamping length ratios (Σt/d) was selected, see Figure 4-15.
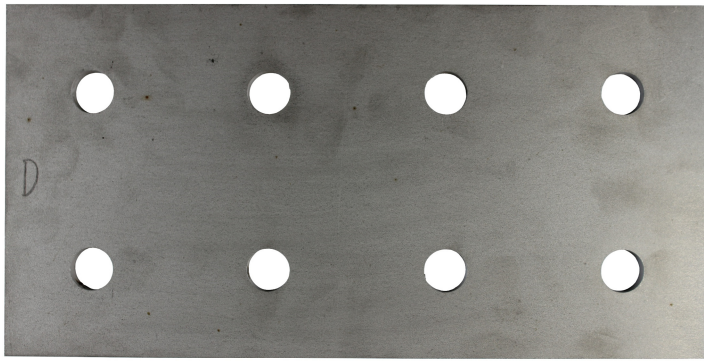
(a) Eight-bolt duplex specimen in 1D surface condition
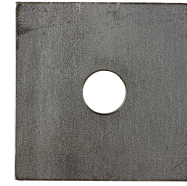
(b) One-bolt austenitic specimen in 1D surface condition

Figure 4-13: Exemplary photos of stainless steel test specimens for relaxation tests

(a) Test specimen with eight M24 bolts

(b) Test specimen with eight M20 bolts

(c) Test specimen with eight M16 bolts

(d) Test specimen with one M20 bolt

(e) Test specimen with one M16 bolt
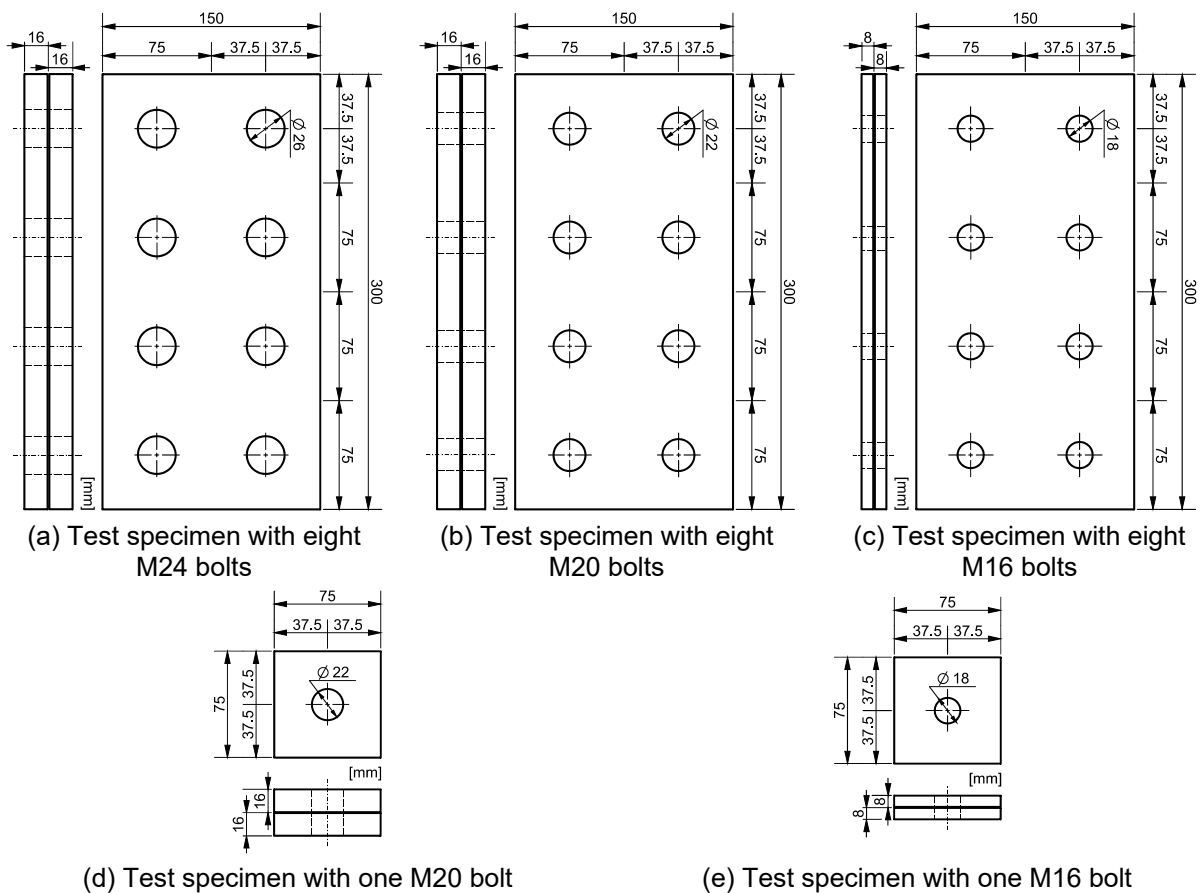
Figure 4-14: Geometry of relaxation test specimens made of carbon and stainless steel

To compare the influence of different grades of stainless steels and sizes of bolting assemblies, the same preload level ($F_{p,C}$) was considered for all relaxation tests. This means that the preload level for M16 Bumax 88 was 88 kN, for M16 Bumax 109 was 110 kN, for M20 Bumax 88 was 137 kN and for Bumax 109/HV bolts was 172 kN, respectively, which relates to $F_{p,C} = 0.7\ f_{ub}\ A_S$, (where f_{ub} is the tensile strength of the bolt and A_S is the tensile stress area of the bolt). $F_{p,C}$ is the minimum preload level according to EN 1090-2. As already discussed in Chapter 4.4.2, a suitable method to measure preloads in stainless steel bolts is to use load cells, which cannot be influenced by viscoplastic deformation in the stainless steel material. For this reason,

the preload level measured with this method represents the real existing preload level in stainless steel bolts. For this reason, special small load cells in three different sizes (M16, M20 and M24) were developed, produced and calibrated. In all tests, the preload level was measured continuously during the tests, see Figure 4-16.
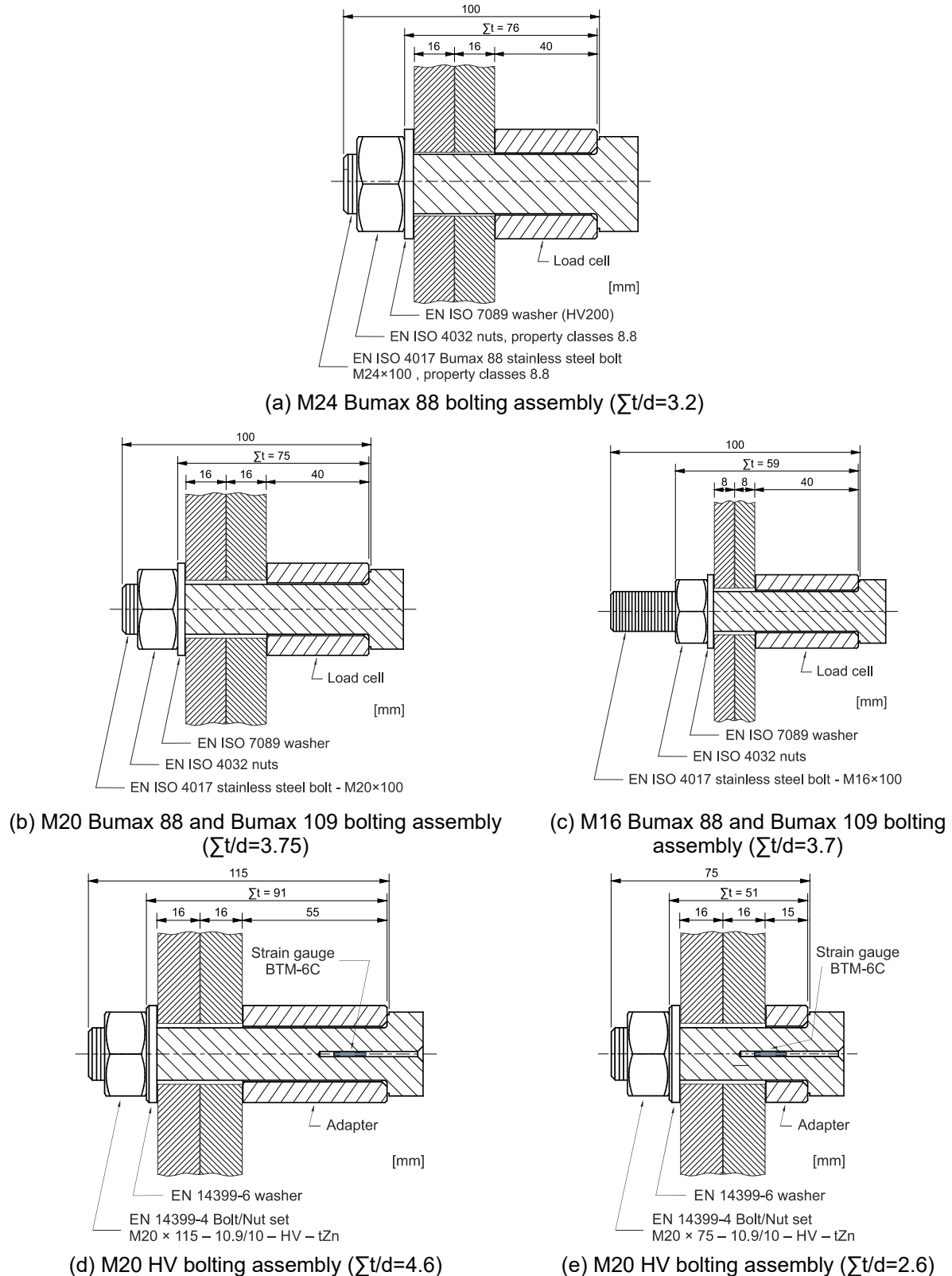
(a) M24 Bumax 88 bolting assembly (∑t/d=3.2)

(b) M20 Bumax 88 and Bumax 109 bolting assembly (∑t/d=3.75)

(c) M16 Bumax 88 and Bumax 109 bolting assembly (∑t/d=3.7)

(d) M20 HV bolting assembly (∑t/d=4.6)

(e) M20 HV bolting assembly (∑t/d=2.6)

Figure 4-15: Different clamped packages for the relaxation test specimens made of carbon and stainless steel
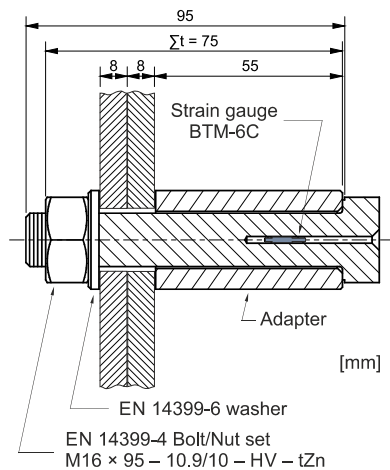
(f) M16 HV bolting assembly ($\sum t/d=4.7$)
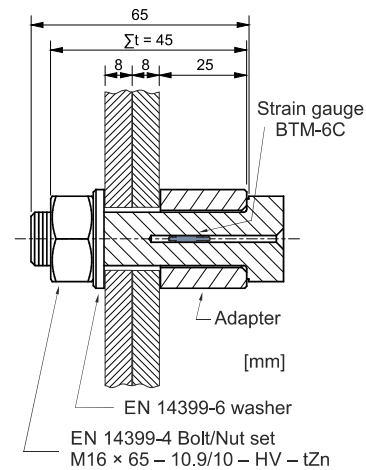
(g) M16 HV test specimen ($\sum t/d=2.8$)

Cont. Figure 4-15: Different clamped packages for the relaxation test specimens made of carbon and stainless steel

(a) Eight-bolt test specimen

(b) One-bolt test specimen

(c) Preload in the bolts continuously measured during the tests

Figure 4-16: Test setup for relaxion test on stainless steel bolted connections

Table 4-2, Table 4-3 and Table 4-4 present the test matrix and the relaxation test results including all related information for each test series for M16, M20 and M24 bolting assemblies made of stainless steel. Table 4-5 summarizes the test matrix and

the resulting preload losses for the bolted connections with M16 and M20 HV bolting assemblies.

Due to the fact that in the first seconds after tightening, the bolt experiences a considerable drop in the preload level, the definition of the starting point for the evaluation of the relaxation tests regarding the loss of preload is very important. The main amount of this instant drop can be explained by, e.g., a turning back of the nut and an elastic recovery of the bolt threads when the wrench is removed. These phenomena are not entirely related to the relaxation behaviour of the bolted connection and must not be considered in the calculation of the loss of preload. For this reason, this overshoot must be extracted. By considering the linear behaviour of the loss of preload in a logarithmic scale and removing the first seconds, it is possible to derive the accurate starting point for the evaluation of the relaxation test.

Therefore, after considering the mentioned terms, the first three seconds of the measured preload after reaching the peak of the preload level were not considered in the evaluation of the loss of preload. All presented results of the loss of preload in Table 4-2 to Table 4-5 consider the first three seconds are not taken into account.

As can be seen in Figure 4-17, the highest rate of loss of preload can always be observed instantly after tightening of the bolt. This rate decreases over time.

Figure 4-17 shows an exemplary rate of loss of preload diagrams for M16 austenitic Bumax 88 (property class 8.8) bolting assemblies with lean duplex plates (SS24 test series). The results for the first and second row of the eight-bolt test specimens and also for the one-bolt test specimens are presented separately. By having the logarithmic scale for both the rate of loss of preload and the time axis, it is possible to see a linear behaviour in the reduction of the rate of loss of preload.

The loss of preload starts immediately after tightening of the bolts and increases gradually as time elapses, see Figure 4-18. This figure also shows exemplary preload losses-log (time) diagrams of the SS24 test series. The results show that a linear loss of preload in bolted connections made of stainless steel in a logarithmic time scale can be observed. As mentioned in previous chapters, the viscoplastic deformation in stainless steel material also follows a linear behaviour in a logarithmic time scale. This linear behaviour can also be observed in the relaxation behaviour of the stainless steel connection.
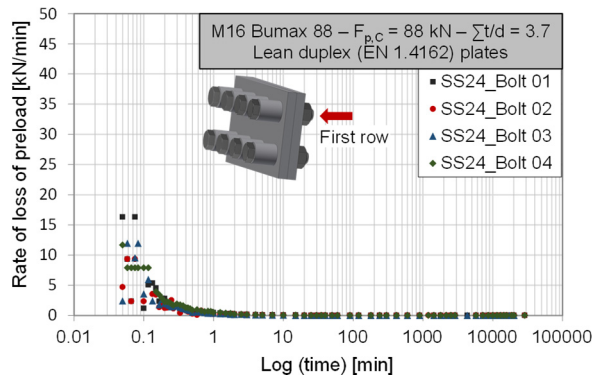
(a) Rate of loss of preload-Log (time) diagrams for eight-bolt specimens – first row
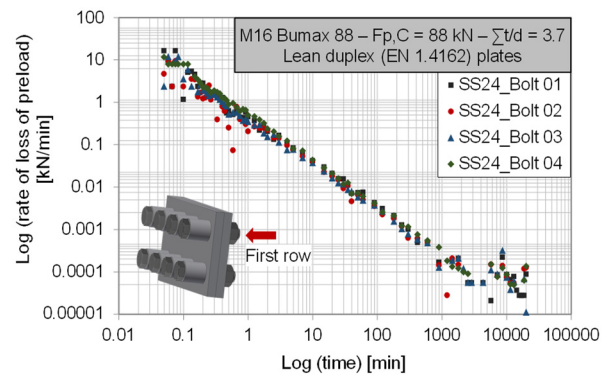
(b) Log (rate of loss of preload)-Log (time) diagrams for eight-bolt specimens – first row
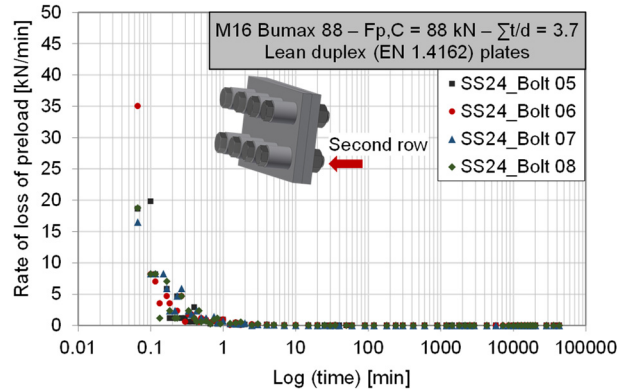
(c) Rate of loss of preload-Log (time) diagrams for eight-bolt specimens – second row
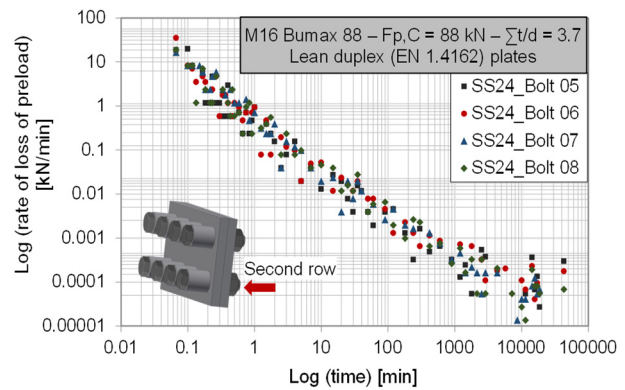
(d) Log (rate of loss of preload)-Log (time) diagrams for eight-bolt specimens – second row
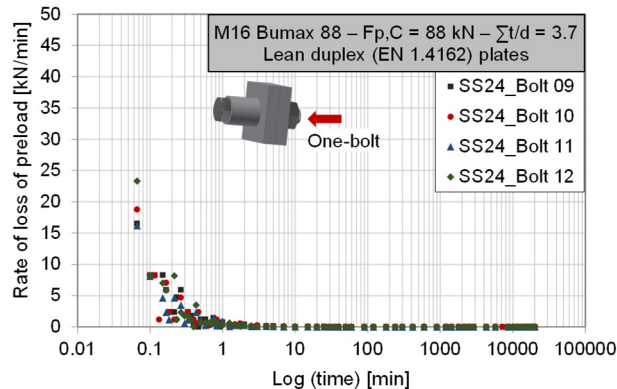
(e) Rate of loss of preload-Log (time) diagrams for one-bolt specimens
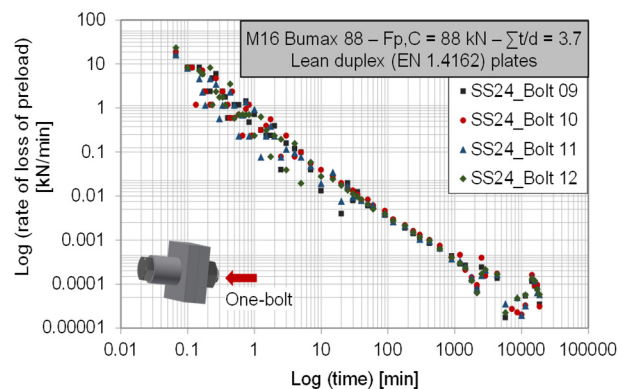
(f) Log (rate of loss of preload)-Log (time) diagrams for one-bolt specimens

Figure 4-17: Exemplary rate of loss of preload diagrams for SS24 test series (M16 Bumax 88, lean duplex plates, preload level = $F_{p,C}$) [106]

(a) Loss of preload-Log (time) diagrams for eight-bolt specimens – first row

(b) Loss of preload-Log (time) diagrams for eight-bolt specimens – second row

(c) Loss of preload-Log (time) diagrams for one-bolt specimens

(d) Loss of preload measured/extrapolated after 14 days/ 50 years
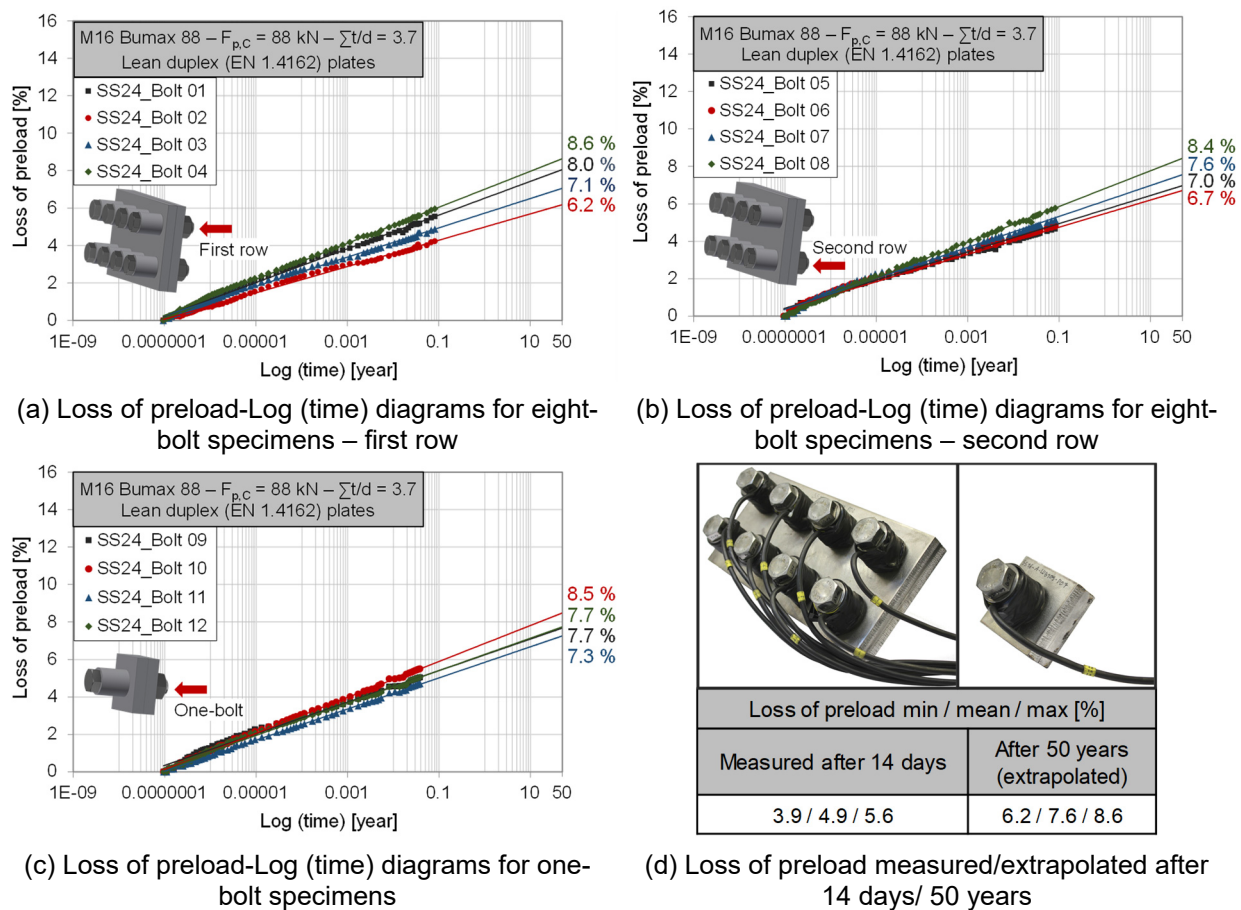
Figure 4-18: Exemplary loss of preload diagrams for SS24 test series (M16 Bumax 88, lean duplex plates, preload level = $F_{p,C}$) [106]

The results show that the highest mean loss of preload was about 10 %, which was observed for M20 lean duplex bolting assemblies in combination with austenitic plates, see Figure 4-19. It can also be seen from this figure that the percentages of loss of preload for M16, M20 and M24 stainless steel bolting assemblies are comparable for different stainless steel grades with the same clamping length ratio and preload level.

Seven test series were carried out in order to investigate the influence of the viscoplastic deformation of the plate material on the relaxation behaviour of bolted connections made of stainless steel. For this purpose, the combinations of carbon steel plates (S355) with M20 austenitic and duplex as well as M16 austenitic, duplex and lean duplex bolting assemblies were selected. As the amount of viscoplastic deformation in the carbon steel material is negligible, the main loss of preload was caused by the initial embedment effects and viscoplastic deformation of the stainless steel bolting assemblies. As Figure 4-19 shows, there is a tendency towards a slightly lower loss of preload in percent after 50 years. Nevertheless, the results are comparable (with some exceptions) between the combination of stainless steel bolting assemblies and carbon or stainless steel plates.

As mentioned before, viscoplastic deformation is an inelastic deformation, which remains after unloading. In Chapter 4.4.2, the results of the repeated creep tests on

stainless steel bolts showed that in the second creep test the stainless steel material experiences a very small amount of creep deformation, which could mean that less loss of preload occurs in preloaded bolted connections. For this reason, one series of relaxation tests was repeated on already used M24 Bumax 88 bolted assemblies in combination with used austenitic plates (SS43) in order to investigate the influence of this phenomenon on the loss of preload in bolted connections made of stainless steel. The results show about 50 % lower preload losses extrapolated after 50 years, see Table 4-4 and Figure 4-19. This phenomenon can be explained by remaining viscoplastic deformation in the stainless material after the first relaxation test, whereby only a very small amount of viscoplastic deformation appears for the second relaxation test. This explains the less loss of preload in the repeated relaxation tests.

In general, it can be concluded that the loss of preload in stainless steel bolted connections is mainly due to embedment in the clamped components and viscoplastic deformation in the bolting assemblies.

In the frame of this investigation, the influence of the clamping length ratio was also investigated. The results for both M20 and M16 bolt dimensions show that a smaller clamping length ratio leads to a higher loss of preload in the preloaded bolted connections, which is an expected phenomenon, see Figure 4-19.

The relaxation test results for untreated carbon steel bolted connections show that the loss of preload was approximately between 7 % and 8 % for different clamping length ratios (CS48, CS49, CS50 and CS51 test series), see Figure 4-19. These preload losses are comparable to those values achieved for stainless steel bolted connections. The results also show that the estimated preload losses over 50 years for different grades of stainless steel bolting assemblies in combination with stainless steel plates are approximately between 6 % and 10 %. It is clear that the viscoplastic deformation of the stainless steel material is detectable but the influence of this parameter on the relaxation behaviour of the bolted connection is insignificant. Herewith, finally, it can be concluded that the loss of preload in preloaded bolted connections made of stainless and carbon steel are comparable and concerns about the loss of preload due to viscoplastic deformation in stainless steel material seem to be unwarranted.

Figure 4-19: Comparing the loss of preload after 50 years (extrapolated) for different carbon and stainless steel test series [106]
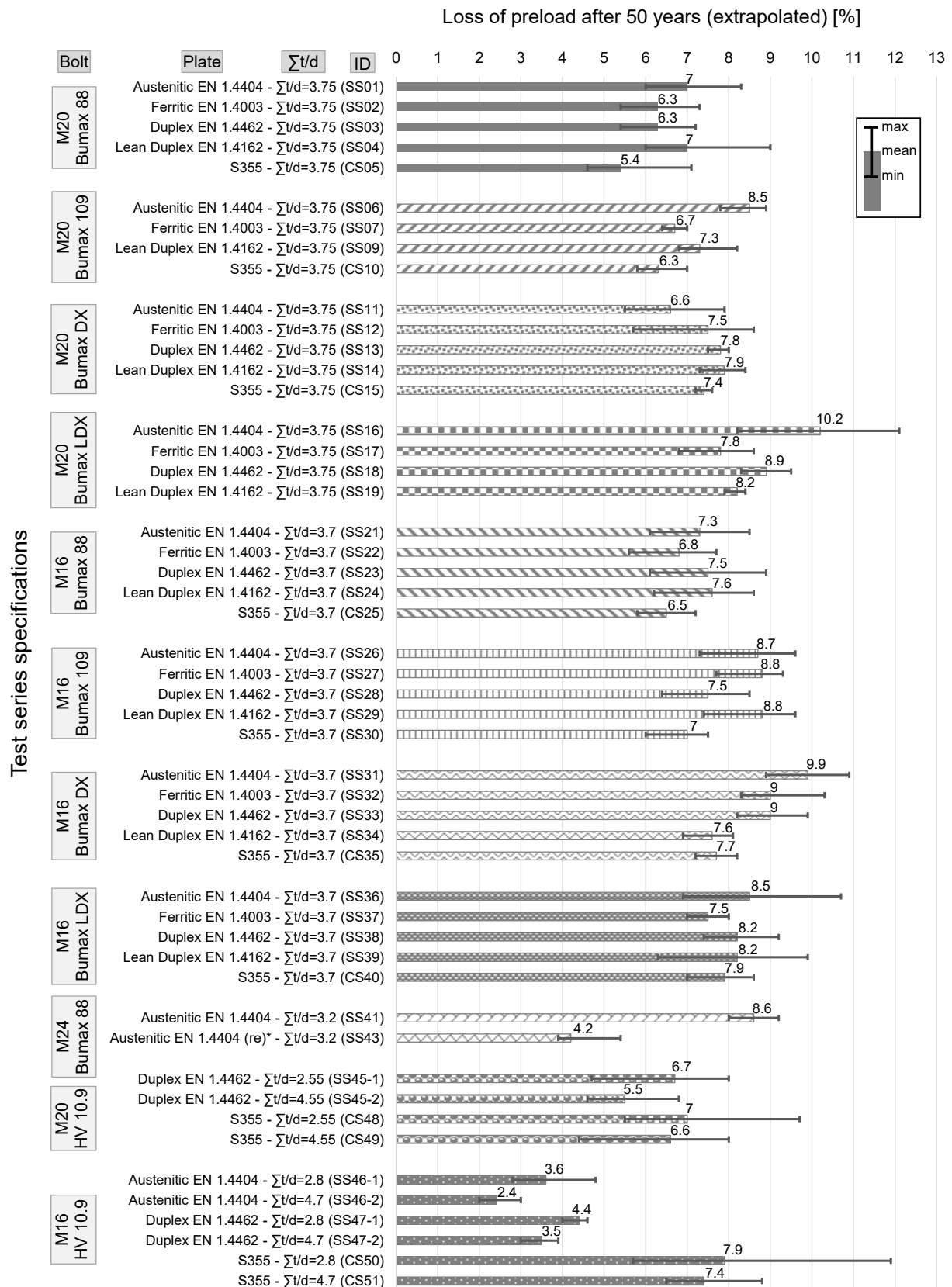
* The test was repeated with the same bolt and clamp components from SS41.

Note: The same preload level ($F_{p,C}$) was considered for all relaxation tests.

4.4.4 Loss of preload in bolted connections made of carbon steel with hot dip galvanized surfaces

Non-protected carbon steel surfaces are susceptible to corrosion. Using this type of steel without any protection in an aggressive environment is not recommended. However, using coating to protect the surfaces from corrosion in preloaded bolted connections can completely change the relaxation behaviour of the connection. Nevertheless, in most cases some protective layers are added which are very soft and in many cases more creep sensitive in comparison to the base metal. These additional layers can entirely change the calculation for estimating the loss of preload in preloaded bolted connections and usually leads to a higher loss of preload in the connection.

In order to investigate the influence of an additional coating on the relaxation behaviour of the connection, four different test series were selected in SIROCO. All surface preparations were hot dip galvanized surfaces without and with different post-treatments [128]. The first test series was hot dip galvanized (HDG) surfaces without any further treatment (HDG-Ref), the second series was hot dip galvanized surfaces with sweep blasted surfaces (HDG_SB-I) and two more series were also galvanized and sweep blasted like HDG_SB-I and coated with alkali-zinc silicate (ASI) coating (HDG-ASI) and ethyl-zinc silicate (ESI) coating (HDG-ESI), see Table 4-6. The preparation parameters of the surfaces have already been presented in Chapter 3.2.11.3.

Two different specimen configurations were developed, see Figure 4-20. All plates were made of S355 carbon steel identical to that used for the slip factor tests in Chapter 3.2.11.3. All bolts were M20 HV bolts with property class 10.9 and instrumented with implanted strain gauges to measure the level of the preload in the bolts throughout the test time, see Figure 4-21. In all test series, all bolts were preloaded to the same preload level of $F_{p,C}$, with one exception. For the HDG-ESI test series, the influence of different preload levels on the relaxation behaviour of the preloaded bolted connection was also investigated. For this reason, an additional eight-bolt specimen was tested, where all bolts in the first row were preloaded up to $F_{p,1} = 0.8 \cdot f_{ub} \cdot A_s = 197$ kN and all bolts in second row were preloaded up to $F_{p,2} = 0.5 \cdot f_{ub} \cdot A_s = 123$ kN.

Table 4-6 summarizes the resulting loss of preload for each test series. After tightening of the bolts, a considerable drop in the measured preload level in the first seconds after reaching the peak can be observed. In order to have a rational evaluation of the loss of preload, the first three seconds of the preload measurements after reaching the peak were not taken into account. After tightening of the bolts, the loss of preload starts immediately. As can be seen in Figure 4-22, with bolted connections made of stainless steel, the highest rate of loss of preload is at the beginning of the test and after that the rate decreases as time elapses.

Table 4-6: Loss of preload in for hot dip galvanized test series with or without post-treatments [106]

Series ID	Type of specimen		No. of tests	$\Sigma t/d$ [1] [-]	Surface condition		F_p [3] [kN]	Loss of preload	
					Surface treatment	DFT [2] [µm]		measured after days - min / mean / max [%]	after 50 years (extrapolated) min / mean / max [%]
HV bolts M20									
CS48	8 bolt	First row	4	2.55	-	-	-	14 – 4.0 / 5.1 / 6.5	6.0 / 7.7 / 9.7
		Sec. row	-					-	-
	1 bolt	-	4					35 – 3.9 / 4.4 / 5.0	5.5 / 6.2 / 7.1
HDG-Ref	8 bolt	First row	4		HDG [4]	70		20 – 6.9 / 7.2 / 7.4	10.5 / 11.2 / 11.7
		Sec. row	4					20 – 5.7 / 6.1 / 6.4	9.3 / 9.7 / 10.1
	1 bolt	-	2					25 – 6.3 / 6.6 / 6.9	9.8 / 10.0 / 10.2
HDG_SwB-I	8 bolt	First row	4		HDG+SwB [5]	50	$F_{p,C}$	20 – 6.8 / 7.1 / 7.4	10.3 / 10.8 / 11.3
		Sec. row	4					20 – 5.3 / 6.0 / 7.9	8.0 / 9.3 / 12.0
	1 bolt	-	3					20 – 5.2 / 6.3 / 7.2	7.9 / 9.5 / 10.8
HDG_ASI	8 bolt	First row	4	2.4	HDG+SwB+ASI [6]	170		25 – 13.2 / 14.2 / 15.3	19.6 / 21.2 / 23.0
		Sec. row	4					25 – 11.7 / 13.7 / 14.8	17.3 / 20.5 / 22.2
	1 bolt	-	3					25 – 12.7 / 13.3 / 14.4	19.1 / 20.0 / 21.5
HDG_ESI	8 bolt	First row	4		HDG+SwB+ESI [7]	140		25 – 9.1 / 9.6 / 10.0	13.8 / 14.4 / 14.9
		Sec. row	4					25 – 8.5 / 8.9 / 9.4	13.0 / 13.4 / 14.0
	1 bolt	-	2					25 – 10.2 / 10.5 / 10.8	14.9 / 15.6 / 16.2
	8 bolt	First row	4				$F_{p,1}$	55 – 9.6 / 9.9 / 10.3	13.6 / 14.2 / 14.5
		Sec. row	4				$F_{p,2}$	55 – 12.1 / 12.4 / 12.8	17.1 / 17.4 / 18.0

[1] clamping length ratio (Σt = clamping length and d = bolt dimension) | [2] total dry film thickness |
[3] preload level ($F_{p,C}$ = 0.7 f_{ub} A_s = 172 kN, $F_{p,1}$ = 0.8 f_{ub} A_s = 197 kN, $F_{p,2}$ = 0.5 f_{ub} A_s = 123 kN) |
[4] hot dip galvanized | [5] sweep blasted | [6] alkali-zinc silicate (ASI) coating | [7] ethyl-zinc silicate (ESI) coating
Note: for more information about the surface preparation see Table 3-1 and Table 3-6.
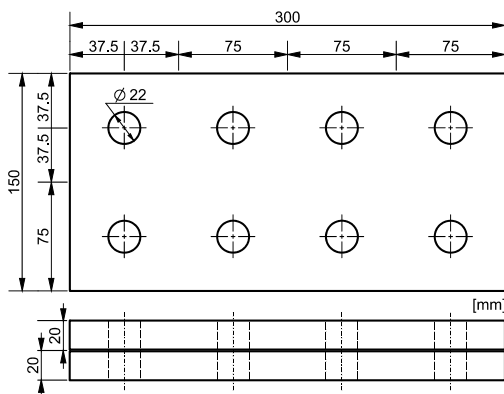
(a) Eight-bolt specimen geometry
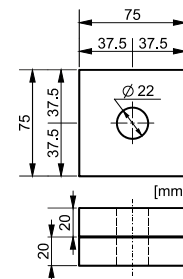
(b) One-bolt specimen geometry

(c) Eight-bolt specimen test setup

(d) One-bolt specimen test setup

Figure 4-20: Test specimen geometry and test setup for hot dip galvanized test series with or without post-treatments

(a) Clamped package including an instrumented bolt

(b) Preload measurement test setup
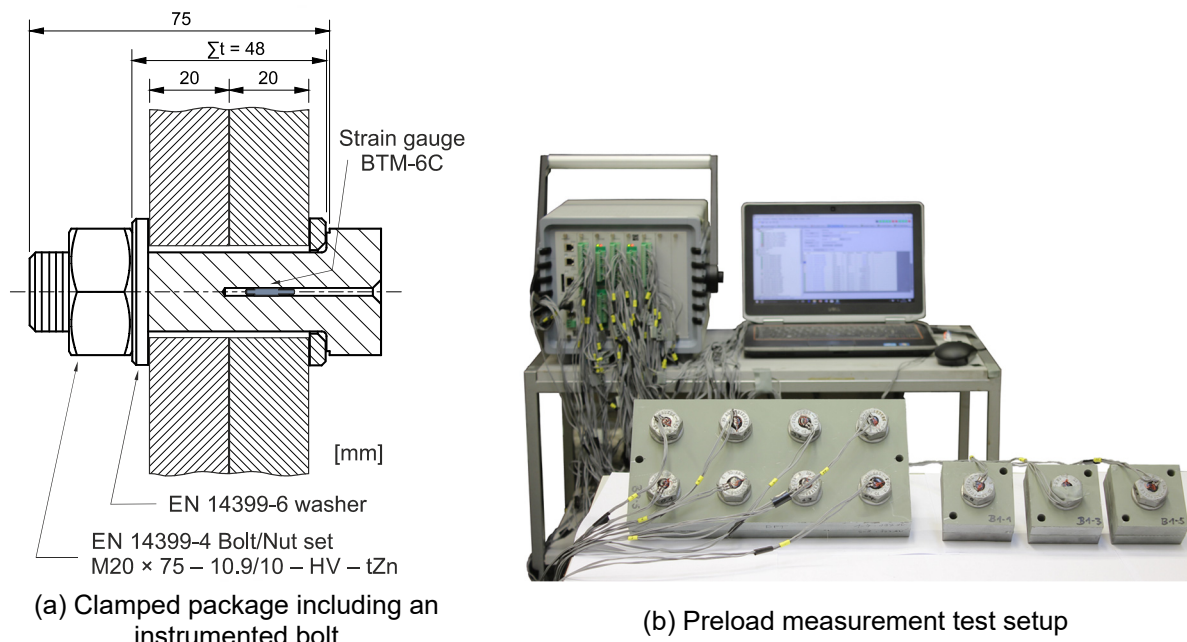
Figure 4-21: Clamped package and preload measurement test setup for hot dip galvanized test series with or without post-treatments

Figure 4-23 shows exemplary loss of preload-log (time) diagrams for the HDG_ASI test series, where the highest loss of preload (in percent) was observed for this test series, which was about 21 % after 50 years. The combination of hot dip galvanized surfaces with ESI coating shows about 14 % lower loss of preload compared to HDG_ASI surfaces with the same clamping length ratio and preload level ($F_{p,C}$), see Figure 4-24 (a).

The results also show that the lowest percentage of loss of preload was observed for HDG_SwB-I and HDG-Ref test series, which was about 10 % after 50 years, see Table 4-6 and Figure 4-24. The results of these coated surfaces were compared with the results of relaxation tests for uncoated surfaces (CS48 test series) from Chapter 4.4.3. As expected, the lowest loss of preload was observed for uncoated test series. In all test series, a linear relaxation behaviour in logarithmic time scale was observed.
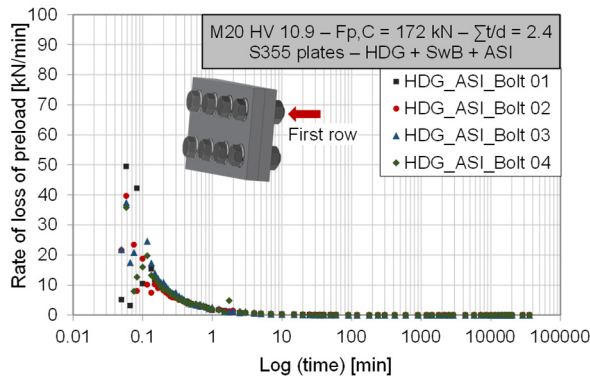
(a) Rate of loss of preload-Log (time) diagrams for eight-bolt specimens – first row
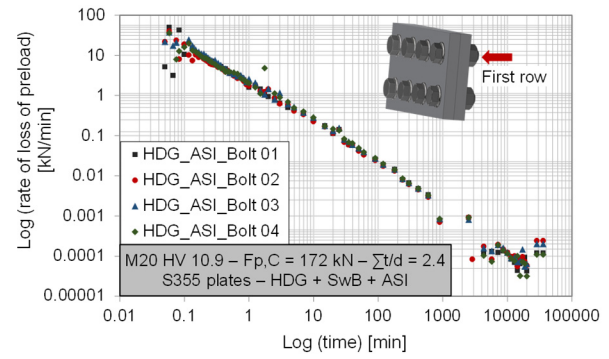
(b) Log (rate of loss of preload)-Log (time) diagrams for eight-bolt specimens – first row
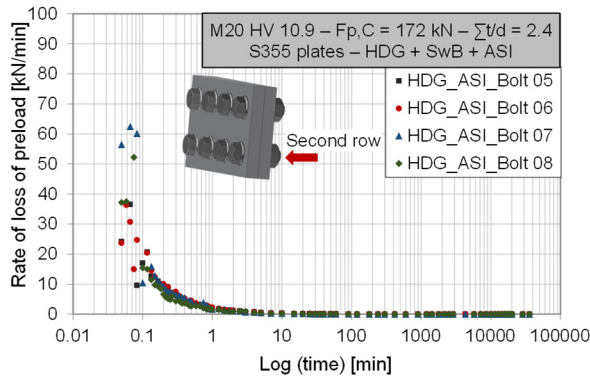
(c) Rate of loss of preload-Log (time) diagrams for eight-bolt specimens – second row
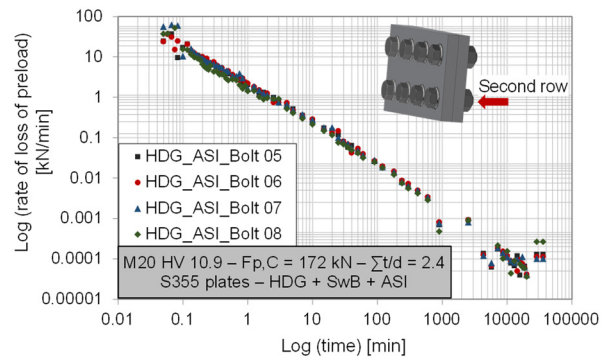
(d) Log (rate of loss of preload)-Log (time) diagrams for eight-bolt specimens – second row
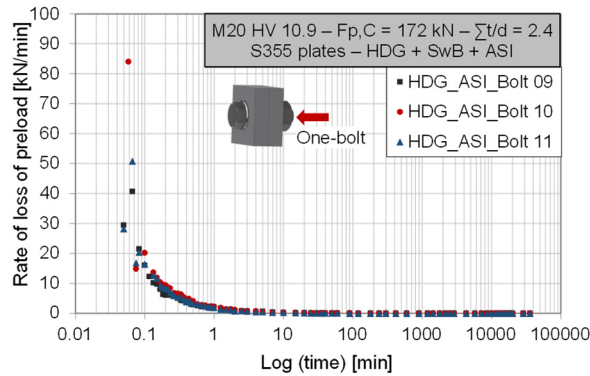
(e) Rate of loss of preload-Log (time) diagrams for one-bolt specimens
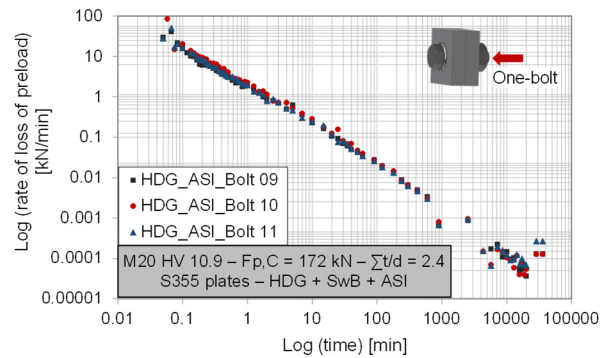
(f) Log (rate of loss of preload)-Log (time) diagrams for one-bolt specimens

Figure 4-22: Exemplary rate of loss of preload for HDG_ASI test series [106]

(a) Loss of preload-Log (time) diagrams for eight-bolt specimens – first row

(b) Loss of preload-Log (time) diagrams for eight-bolt specimens – second row

(c) Loss of preload-Log (time) diagrams for one-bolt specimens

(d) Loss of preload measured/extrapolated after 14 days/50 years
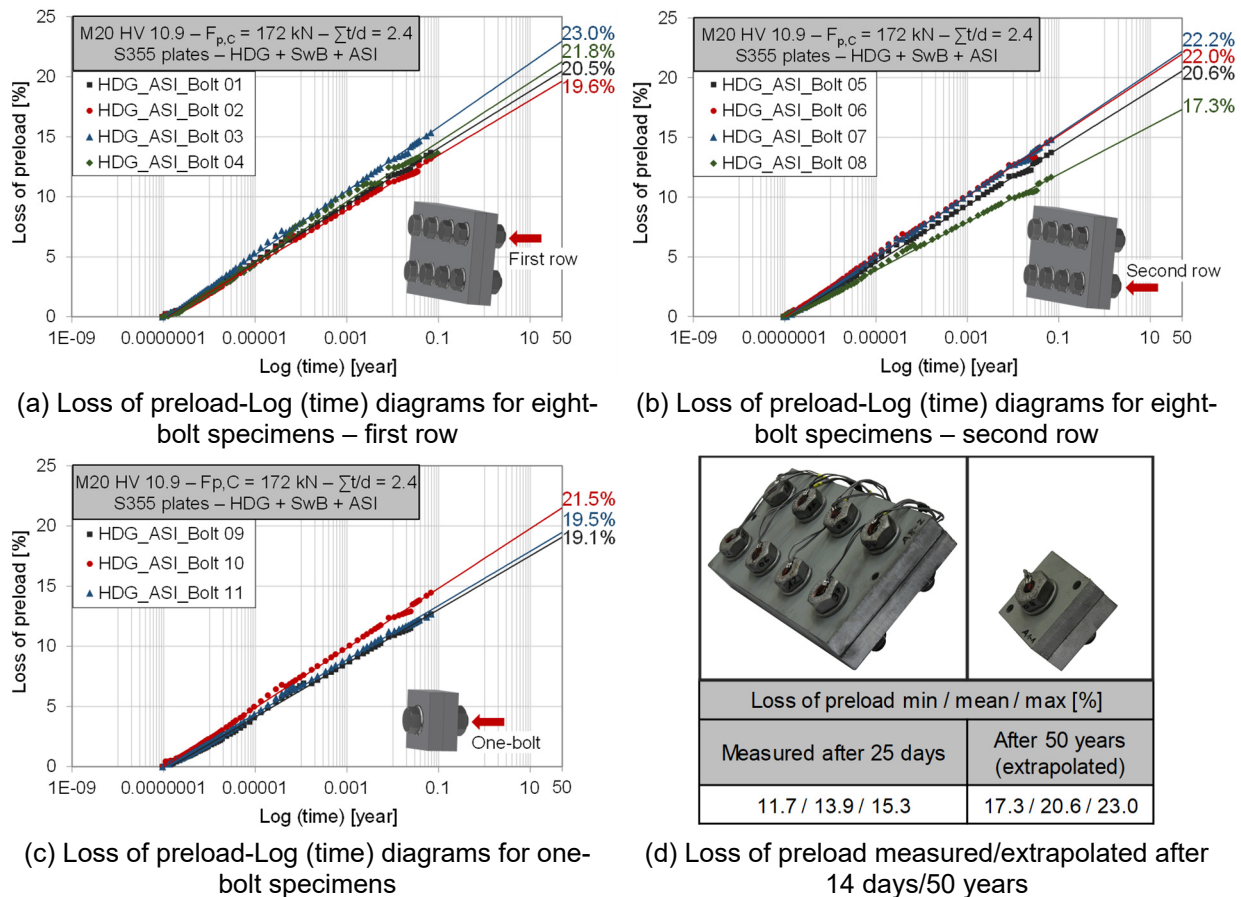
Figure 4-23: Exemplary loss of preload for HDG_ASI test series [106]

(a) Loss of preload in %

(b) Loss of preload in kN
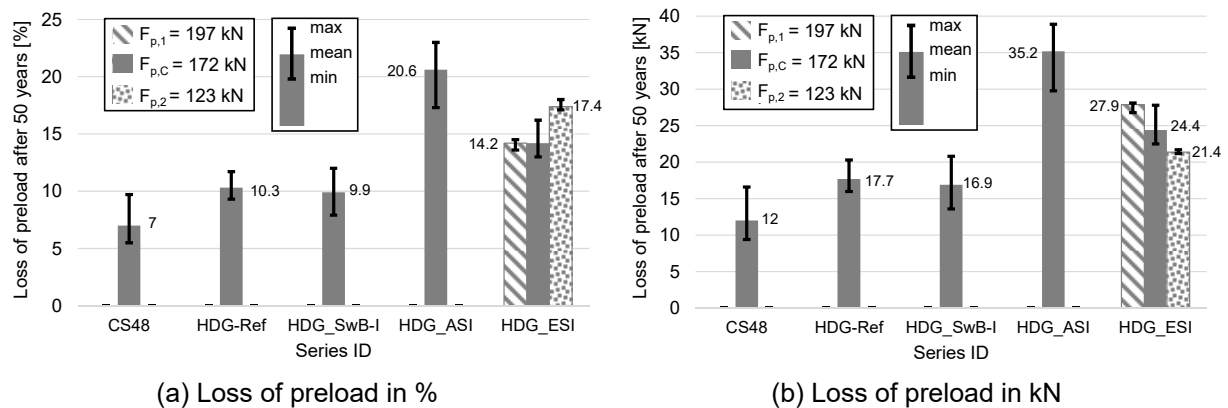
Figure 4-24: Extrapolated loss of preload at a service life of 50 years for hot dip galvanized test series with or without post-treatments [106]

In the frame of this investigation, the influence of different preload levels was also investigated. As can be seen in Table 4-6 and Figure 4-24 (a), for the HDG_ESI specimens there is a tendency towards a higher loss of preload in percent for a lower level of preload. However, by calculating the amount of loss of preload in kN, it can be seen that the amount of loss of preload in kN is higher for higher preload levels. This amount is about 28 kN, 24 kN and 21 kN for preload level $F_{p,1}$ = 197 kN, $F_{p,C}$ = 172 kN and $F_{p,2}$ = 123 kN respectively.

In coated carbon steel bolted connections, the loss of preload is mainly influenced by embedment of the clamped surfaces and viscoplastic deformation behaviour of the coating material. In comparison to stainless steel bolted connections, viscoplastic deformation in stainless steel is much smaller in comparison to the coating material. For this reason, the loss of preload can be equal between stainless steel and uncoated carbon steel connections or much higher for coated carbon steel bolted connections.

4.5 Conclusion

Unlike carbon steel, stainless steel suffers significantly more from viscoplastic deformation, a phenomenon which causes serious uncertainties in the use of stainless steel preloaded bolted connections for construction purposes.

Preloading of bolted assemblies made of stainless steel is not permitted according to EN 1090-2 unless all required parameters for preloading of stainless steel bolting assemblies are specified in the frame of a procedure test. A comprehensive experimental investigation was conducted at the Institute for Metal and Lightweight Structures of the University of Duisburg-Essen in order to close the gap in knowledge about the tightening and the basic preloading behaviour of bolting assemblies made of stainless steel. The results show very promising performance in terms of preloadability of stainless steel bolting assemblies. By choosing a suitable material pairing and appropriate lubricant, it is possible to preload stainless steel bolting assemblies with property classes 8.8 and 10.9. However, there is another concern in preloading stainless steel bolting assemblies. Since the influence of viscoplastic deformation behaviour was unknown for preloaded stainless steel bolting assemblies, it was feared that this phenomenon would dramatically increase the loss of preload in the connection. For this reason, a comprehensive experimental investigation was conducted to illustrate the contribution of stainless steel viscoplastic deformation behaviour to the loss of preload in the connection.

The experimental results show that the loss of preload in preloaded bolted connections made of stainless steel can partially be attributed to the viscoplastic deformation in stainless steel material. However, the contribution of this phenomenon in addition to the embedment of the clamped component surfaces may slightly increase the loss of preload in the connection, but the total loss of preload in the connection is still acceptable. In general, the loss of preload in preloaded bolted connections made of stainless steel is comparable to that of preloaded carbon steel bolted connections, and the high great concern about the influence of the viscoplastic deformation of stainless steel material on the loss of preload in the connection seems to be unjustified. On the other hand, carbon steel is susceptible to corrosion, and usually has a protective layer between the faying surfaces, which dramatically increases the loss of preload in the connection.

For this reason, using preloaded bolted connections made of stainless steel seems to have more advantages besides high resistance to corrosion, high material strength and ductility which might make this type of material more desirable for modern steel constructions.

5 Slip-resistant behaviour of bolted connections made of stainless steel

5.1 General

EN 1090-2 specifies the slip factors for common surface treatments. When it comes to slip-resistant connections made of stainless steel, however, neither EN 1090-2 nor other existing national or international design codes/standards specify values for possible surface treatments.

Stainless steel alloys suffer from time-dependent viscoplastic deformation behaviour at room temperature more than carbon steels. For this reason, it was always thought that higher viscoplastic deformation could lead to higher preload losses and consequently to lower slip factors in comparison with bolted connection made of carbon steel with comparable surface treatment. However, no evidence for this phenomenon can be found in the literature. In Chapter 4.4.3, the experimental results showed that the influence of viscoplastic deformation of stainless steel material on the loss of preload in preloaded bolted connections made of stainless steel is insignificant. The results also show that having a coating layer on carbon steel surfaces can increase the loss of preload significantly in comparison with uncoated bolted connections made of stainless steel, see Chapter 4.4.4.

Therefore, a comprehensive investigation is needed in order to determine slip factors of different stainless steel grades with different surface preparations. This would make it possible to observe any evidence of negative effects of time-dependant viscoplastic behaviour in stainless material on the slip-resistant behaviour of the connections [163]-[167].

5.2 Determination of slip factors for uncoated stainless steel surface finishes

In total, 19 test series with different stainless steel grades, surface treatments and preload levels were investigated, whereby 13 test series were carried out at the Institute for Metal and Lightweight Structures at the University of Duisburg-Essen and six test series were carried out at the Department of Steel and Composite Structures of the Delft University of Technology. The test matrix is presented in Table 5-1.

The two main parameters which can directly influence the slip-resistant behaviour of the connections are the condition of the faying surfaces and the level of the preload in the bolts. It is of great interest to investigate the influence of these parameters on the determination of the slip factor in slip-resistant connections made of stainless steel.

Using unprotected surfaces in stainless steel slip-resistant connections is possible because of the corrosion resistance of stainless steel alloys. For this reason, the focus of this chapter will be on uncoated faying surfaces. Four different grades of

stainless steel (austenitic (1.4404) (A), duplex (1.4462) (D), lean-duplex (1.4162) (LD) and ferritic (1.4003) (F) stainless steel) with different surface treatments were selected in combination with bolting assemblies made of austenitic stainless steel of two different bolt property classes, 8.8 (Bumax 88) and 10.9 (Bumax 109), see Table 5-1.

All bolts were preloaded up to $F_{p,C}$ preload level and the preload in the bolts was measured by small load cells which were especially produced at the Institute for Metal and Lightweight Structures (IML) of the University of Duisburg-Essen (UDE), see Figure 4-11. Using load cells artificially increases the clamping length of the connection, which consequently may have an influence on the relaxation behaviour of the connection and as a result on the determination of the slip factor. Therefore, four test series were carried out with HV bolting assemblies with property class 10.9. All bolts were instrumented with strain gauges, see Figure 3-1, in order to prevent any artificial extension in clamping length, see Table 5-1.

Table 5-1: Slip factor test results for uncoated stainless steel surface finishes

Series ID	Steel grade	Surface condition S.F.[1]	Rz[2] [µm]	$\Sigma t/d$ [3] [-]	Number of tests st/ct(sp)/ect[4]	$\mu_{nom,mean}$[5] st/st+ct [-]	$\mu_{ini,mean}$[6] st/st+ct [-]	$\mu_{act,mean}$[7] st/st+ct [-]	V (μ_{nom})[8] st/st+ct [%]	Final slip factor [-] $\mu_{5\%}$[9] / μ_{ect}[10]
M16 × 100 Bumax 88 (property class 8.8) – Preload level $F_{p,C}$ = 88 kN [106]										
A_1D_B88	1.4404	1D[11]	24		4/1/2	0.21/0.21	0.21/0.21	0.21/0.21	3.8/3.8	0.20/0.14
D_1D_B88	1.4462	1D	25		3/-/-	0.23/-	0.22/-	0.23/-	1.7/-	-/-
A_TWB_B88	1.4404	TWB[12]	22		2/-/-	0.16/-	0.16/-	0.16/-	10.7/-	-/-
A_SB_B88	1.4404	SB[13]	38	4.7	4/1/2	0.29/-	0.29/-	0.30/-	5.5/-	-/0.2
A_GB-G_B88	1.4404	GB-G[14]	45		4/1/1	0.56/0.55	0.56/0.55	0.60/59	5.7/6.0	0.49/0.51
D_GB-G_B88	1.4462	GB-G	47		4/1/1	0.60/0.60	0.60/0.60	0.63/0.62	5.5/5.0	0.54/0.54
LD_GB-G_B88	1.4162	GB-G	41		4/1/2	0.51/0.52	0.51/0.51	0.53/0.53	9.4/8.6	0.43/0.44
F_GB-G_B88	1.4003	GB-G	45		4/-/4	0.65/-	0.64/-	0.69/-	3.2/-	-/0.55
M16 × 100 Bumax 109 (property class 10.9) – Preload level $F_{p,C}$ = 110 kN										
A_1D_B109*	1.4404	1D	24	4.9	4/2/2	0.19/-	0.20/-	0.20/-	2.9/-	-/0.16
LD_1D_B109	1.4162	1D	27	4.7	2/1/-	0.25/-	0.25/-	0.25/-	2.1/-	0.22/-
A_SB_B109*	1.4404	SB	34		4/2/1	0.32/-	0.33/-	0.34/-	10.4/-	-/0.28
A_GB-G_B109*	1.4404	GB-G	41		4/2/1	0.57/-	0.58/-	0.65/-	7.0/-	-/0.48
D_GB-G_B109*	1.4462	GB-G	47	4.9	4/2/2	0.66/0.66	0.66/0.66	0.69/0.70	3.1/3.4	0.62/0.59
LD_GB-G_B109*	1.4162	GB-G	40		4/2/1	0.62/0.62	0.62/0.62	0.65/0.64	3.5/4.2	0.56/0.49
F_GB-G_B109*	1.4003	GB-G	42		4/2/2	0.68/0.68	0.68/0.68	0.74/0.75	3.3/3.0	0.64/0.59
M16 × 90 HV (property class 10.9) – Preload level $F_{p,C}$ = 110 kN										
D_1D_HV10.9	1.4462	1D	26		4/1/-	0.24/0.25	0.24/0.25	0.25/0.25	4.3/4.7	0.22/-
D_1D-B_HV10.9	1.4462	1D-B[15]	26	2.5	4/-/-	0.39/-	0.39/-	0.41/-	18.8/-	-/-
LD_1D_HV10.9	1.4162	1D	27		4/1/-	0.26/0.26	0.26/0.26	0.27/0.27	5.0/4.5	0.24/-
D_GB-A_HV10.9	1.4462	GB-A[16]	76		4/1/-	0.72/0.72	0.71/0.71	0.80/0.81	2.7/2.9	0.68/-

[1] surface finish | [2] surface roughness | [3] clamping length ratio (Σt: clamping length, d: bolt diameter) | [4] st: static test/ct: creep-/ect: extended creep test | [5] $\mu_{nom,mean}$: calculated slip factors as mean values considering the nominal preload level | [6] $\mu_{ini,mean}$: calculated slip factors as mean values considering the initial preload when the tests start | [7] $\mu_{act,mean}$: calculated slip factors as mean values considering the actual preload at slip |
[8] V: coefficient of variation for μ_{nom} | [9] $\mu_{5\%}$: slip factors as 5 % fractile calculated on the basis of the static tests and the passed creep test | [10] μ_{ect}: slip factor resulting from the passed extended creep test | [11] 1D: as delivered/rolled | [12] TWB: tensioned wire blasted | [13] SB: shot blasted with Chronital particles | [14] GB-G: grit blasted with GRITTAL particles | [15] 1D-B: as delivered/rolled (bolt holes with burr) | [16] GB-A: grit blasted with brown corundum (aluminium oxide)
Note: all test series shown in italics are carried out in the frame of the SIROCO project.
* These tests were carried out at the Department of Steel and Composite Structures of Delft University of Technology (TUD)

The clamping lengths of the bolts used during the slip factor tests were 75 mm for the Bumax 88, 78 mm for the Bumax 109, and 40 mm for test specimens with HV bolting assemblies, see Figure 5-1. The M16 test specimen geometry according to EN 1090-2, Annex G was selected for all test series, see Figure 2-1 (b) and Figure 5-2.

(a) $\Sigma t = 78$ mm   (b) $\Sigma t = 75$ mm   (c) $\Sigma t = 40$ mm
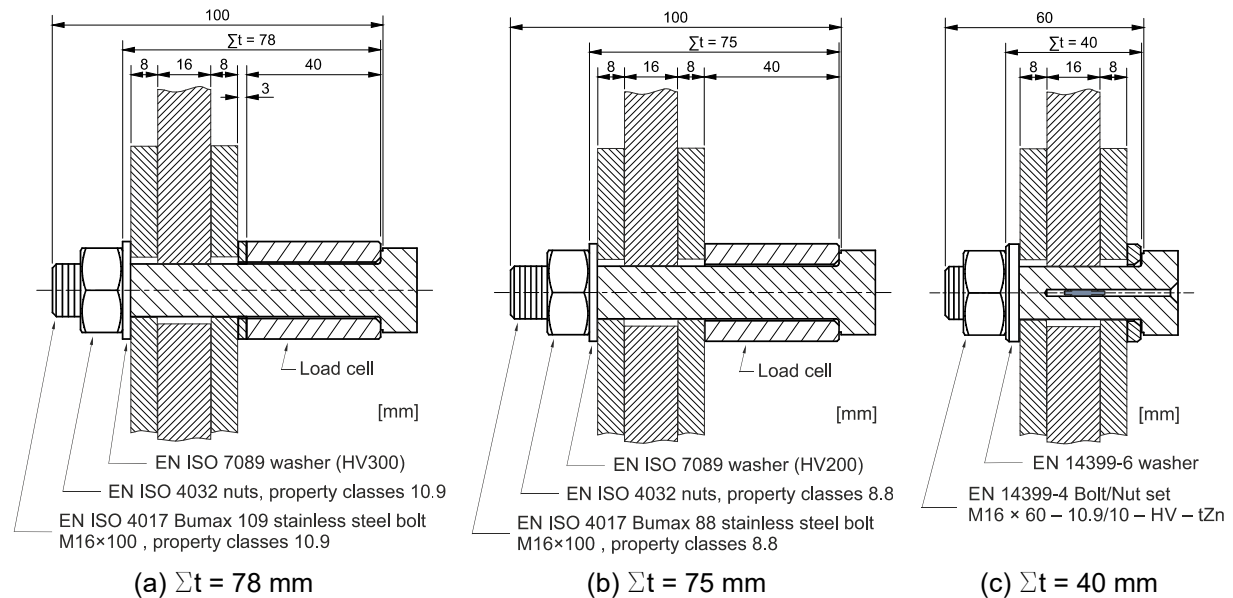
Figure 5-1: Clamping length for different stainless steel test series with uncoated faying surfaces

(a) Test series with Bumax 88   (b) Test series with HV bolts
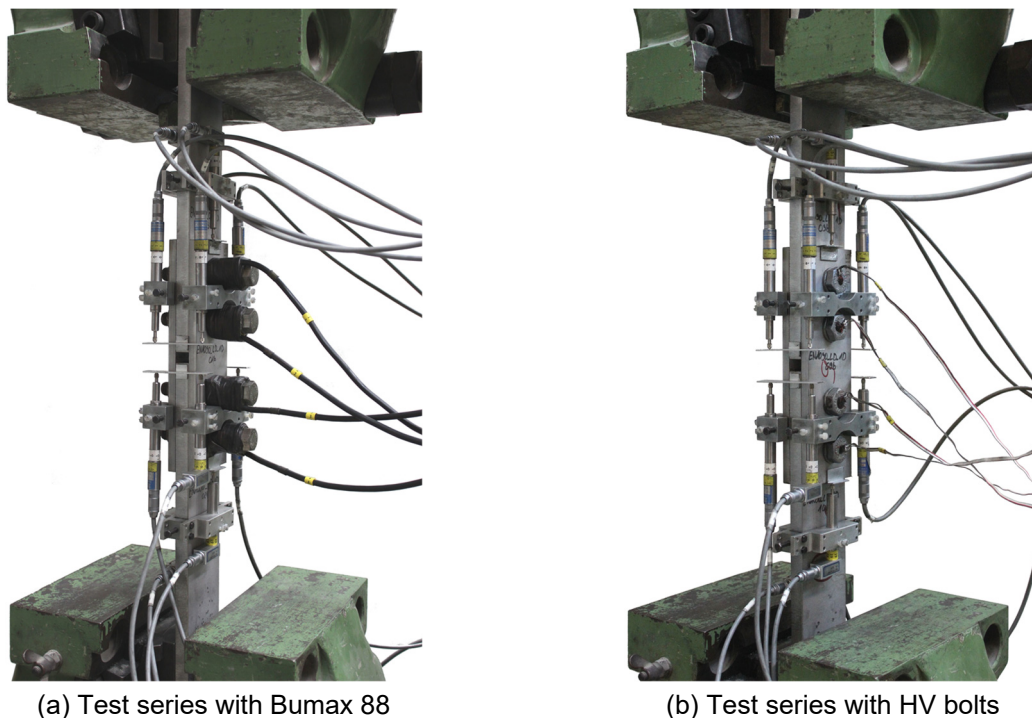
Figure 5-2: Slip factor test setup for uncoated stainless steel bolted connections

In the frame of this study, different surface preparations were investigated. As experience has shown that grit blasting results in the highest slip factor, see Chapter 3.2.11, it was decided to test the grit blasted (GB) surface condition as the main

surface condition for all different stainless steel grades. Two different grit blasting media were selected in order to investigate the influence of the roughness of the faying surfaces on the slip-resistant behaviour of the connection. GB-G is a grit blasted surface condition for the test specimens which were blasted with GRITTAL GM 30 particles with sizes between 0.14 mm and 0.50 mm. GRITTAL GM is a stainless steel grit, crushed, delta-ferrite with chromium carbides produced by Vulkan Inox GmbH. All surfaces were blasted with 5.5 bars at a blasting angle of 70° to 80°.

All test specimens for the GB-A test series were blasted with brown corundum, f20, Al_2O_3 (aluminium oxide). The particle sizes were between 0.85 mm and 1.18 mm. All surfaces were blasted with 5.5 bars at a blasting angle of 90°.

Three further surface conditions – as delivered/rolled (1D), tensioned wire blasted (TWB) and shot blasted (SB) – were also selected for the austenitic test series in order to compare the influence of different surface treatments. All SB surfaces were blasted with Chronital S-40 with sizes between 0.4 mm and 0.8 mm. Chronital is austenitic stainless steel spherical particle produced by Vulkan Inox GmbH.

As can be seen in Table 5-1, both the SB and GB-G test series delivered approximately the same surface roughness (about 40 µm). At the same time, the measured Rz value for GB-A test series is about 70 µm, which is clearly higher in comparison with other grit blasting methods. Having higher surface roughness may improve the slip-resistant behaviour of the connection. However, the topography of the surfaces is also an important factor which may have a great influence on the quality of the interlocking between the faying surfaces. For this reason, some microscopic photos were taken using the VHX 7000 digital microscope device from Keyence in order to compare the surface characteristic of the faying surfaces, see Figure 5-3. As can be seen from comparing the topography of the surface for SB and GB-G surfaces, the asperity of the GB-G faying surface is sharper than that of the SB surface, which may provide better mechanical interlocking between the faying surfaces. On the other hand, it can be seen that grit blasting with brown corundum (aluminium oxide) provides a noticeably rougher surface in comparison with the GB-G surface, which may also lead to a higher slip factor for this surface condition.

(a) Shot blasted faying surface condition (SB)

(b) Grit blasted with GRITTAL GM 30 media (GB-G)

(c) Grit blasted with brown corundum (aluminium oxide) media (GB-A)
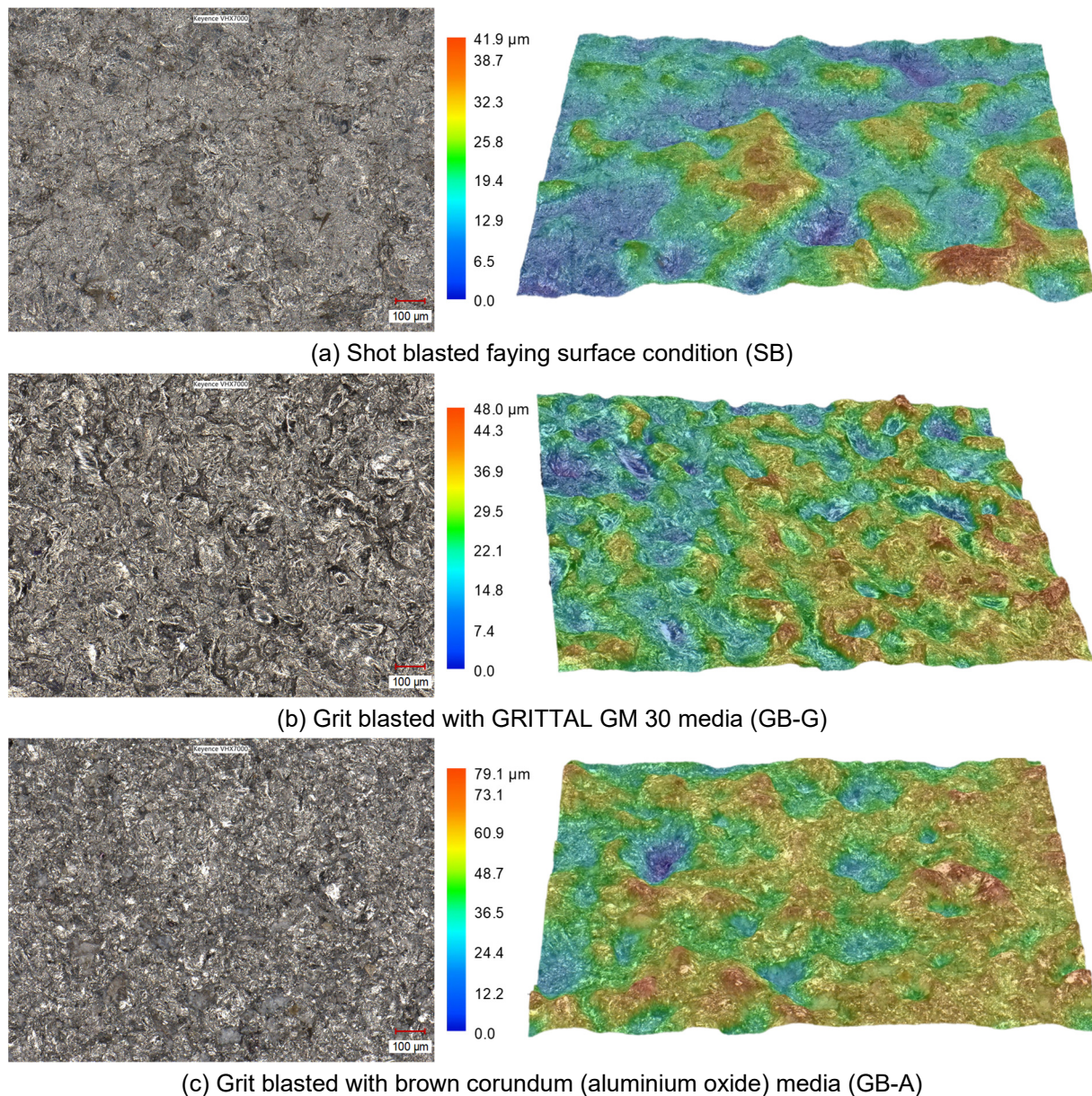
Figure 5-3: Topography of the faying surfaces before performing the tests captured by Keyence VHX7000

The results of the static and creep tests as well as the final slip factor are summarized in Table 5-1. The typical load-slip displacement diagrams for all uncoated test series with Bumax 88 are presented in Figure 5-4 (a). In this figure, each test series is illustrated with two lines which represent the upper and lower section of the test specimen. As can be seen in this figure, the highest slip load is achieved for the grit blasted ferritic grade, followed by grit blasted duplex, austenitic and lean duplex grades.

The lowest static slip loads are achieved for the tensioned wire blasted, as-rolled surface condition and the specimens with shot blasted faying surfaces, respectively.

The results show that the presence of burrs around the holes has a positive influence on slip-resistant behaviour of the connection for as-rolled surface condition (1D), see Table 5-1. However, the coefficient of variation was very high for this test series

(about 19 %), since the slip-resistant behaviour of the connection strongly depends on the random patterns of the existing burrs around the holes.

Figure 5-4 (b) shows the load-slip displacement diagrams for the test series with bolting assemblies with property class 10.9 which were carried out at the Institute for Metal and Lightweight Structures (IML) of the University of Duisburg-Essen (UDE). The diagrams of all other test series that were carried out at TUD are presented in [167]. As can be seen in Figure 5-4 (b) the highest slip load is also achieved for the grit blasted test series.

The creep tests were carried out for different test series. In most cases the creep tests were successful and the recorded slip at CBG position between 5 min and 3 hours after reaching constant load level (0.9·FSm) did not exceed 0.002 mm, see Figure 5-5.

(a) Test series with Bumax 88 bolting assemblies

(b) Test series with Bumax 109 bolting assemblies
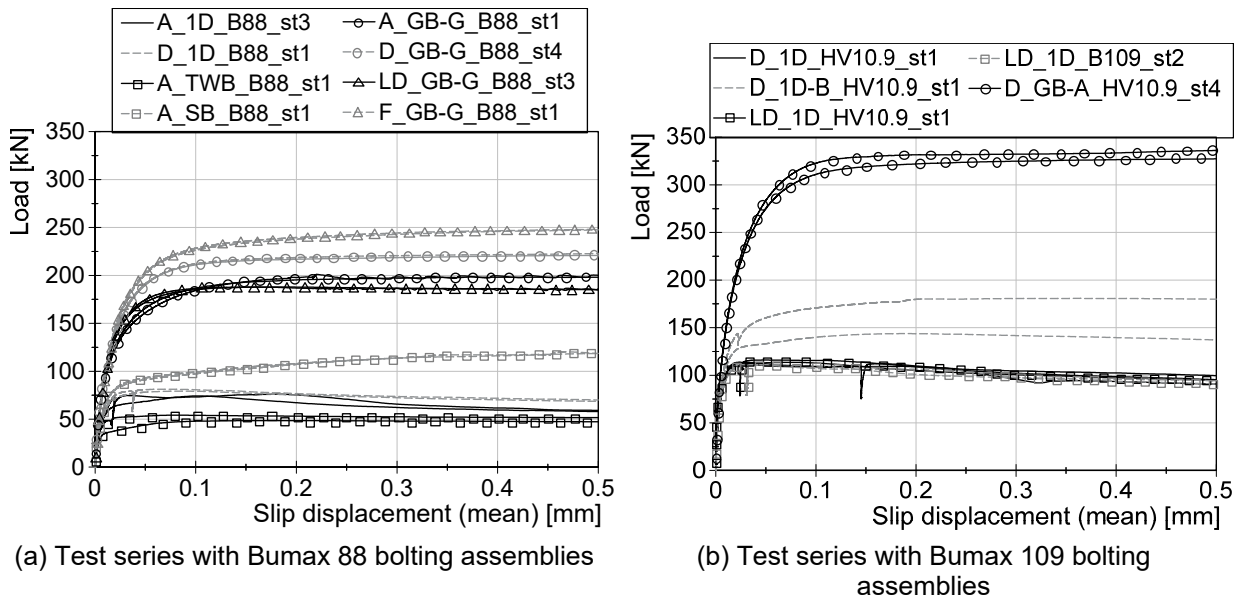
Figure 5-4: Load-slip displacement diagrams for uncoated test series made of stainless steel

(a) Austenitic plates – 1D surfaces

(b) Austenitic plates – grit blasted (with Grittal)
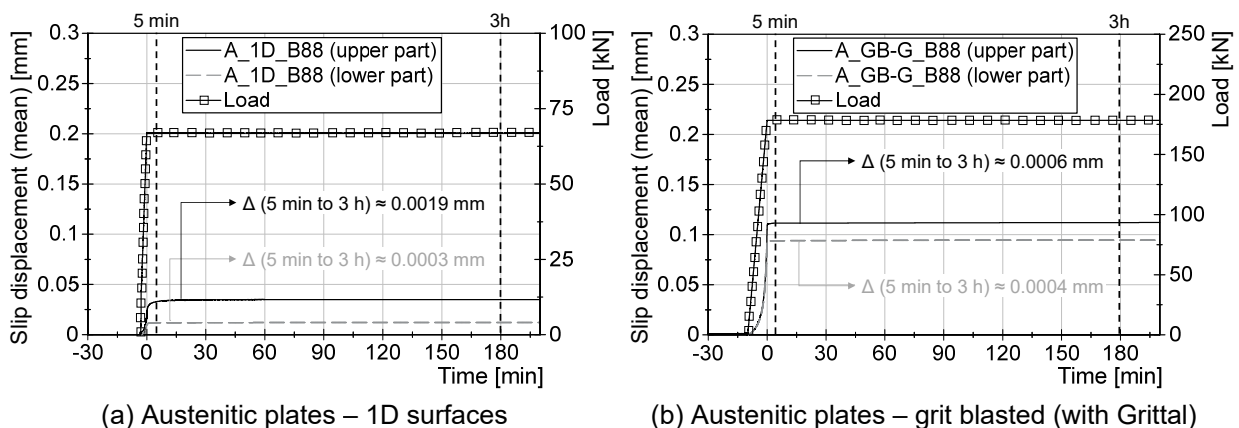
Figure 5-5: Exemplary creep test results for uncoated (1D and GB-G) test specimens made of stainless steel – bolting assemblies with property class 8.8 (Bumax 88)

Usually, the extended creep tests shall only be carried out if the specimen fails the creep test. However, in this study, for some cases the extended creep test was conducted without considering the results of the creep test. The reason for such a decision was to confirm whether the criteria for a successful creep test according to EN 1090-2 Annex G for slip-resistant connections made of carbon steel is also applicable for slip-resistant connections made of stainless steel.

All creep and extended creep tests for the test series with stainless steel bolting assemblies were conducted with a set of new/unused bolting assemblies, in order to consider the maximum effect of viscoplastic deformation in stainless steel material.

Figure 5-6 shows by way of example the results of the extended creep tests for austenitic test specimens with 1D and grit blasted (with Grittal) surface condition which were conducted with Bumax 88 bolting assemblies. In this figure, each test specimen is presented with two lines which represent the upper and lower part of the test specimen.

(a) Austenitic plates – 1D surfaces   (b) Austenitic plates – grit blasted (with Grittal)
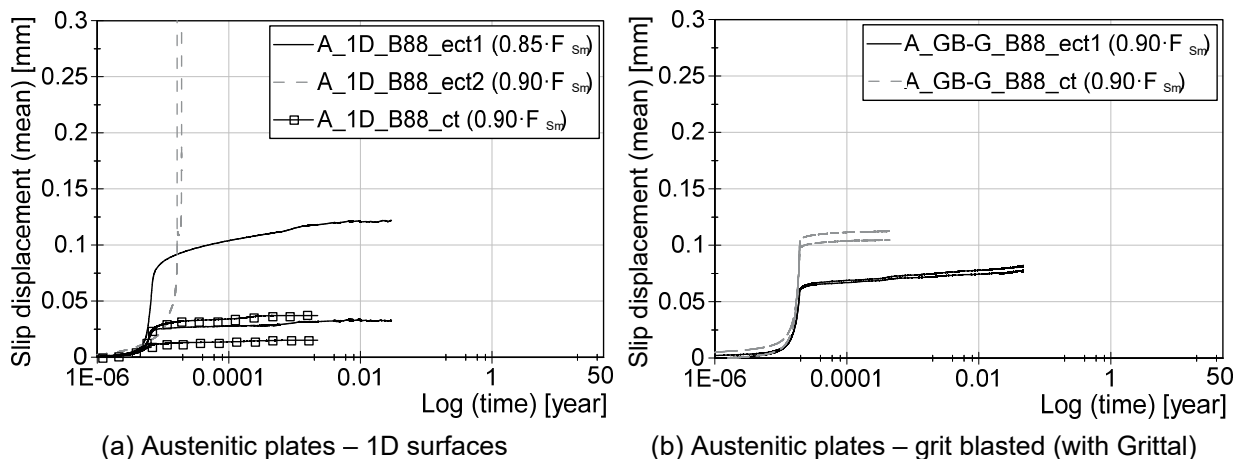
Figure 5-6: Exemplary extended creep test results for uncoated (1D and GB-G) test specimens made of stainless steel – bolting assemblies with property class 8.8 (Bumax 88)

As it can be seen in Figure 5-7 and Figure 5-8, the highest final slip factors were achieved for grit blasted surfaces. This means that the slip factor can be strongly influenced by the surface treatment of the faying surfaces. Blasting of the faying surfaces may significantly improve the slip-resistant behaviour of the connection. However, it mainly depends on the type of blasting. Blasting the surfaces with grit (abrasive blasting media with sharp edges) is much more efficient in improving the slip-resistant behaviour of the connection than shot (spherical) abrasive blasting media. A sharper asperity for grit blasted faying surfaces can provide better mechanical interlocking between the faying surfaces and improve the slip-resistant behaviour of the connection. This phenomenon can lead to higher slip loads and slip factors, even though the measured surface roughness Rz is approximately the same for both grit and shot blasted surfaces.

In the frame of this study, two different types of blasting media were selected. The results show that faying surfaces blasted with brown corundum show better slip-resistant behaviour and achieved higher slip factors, see Figure 5-8.

Improving the blasting procedure to achieve higher roughness might yield a higher slip factor. However, special care must be taken in selecting appropriate blasting media. During the blasting process, small particles of blasting media will be implanted in the surfaces. Selecting the wrong blasting media may increase galvanic corrosion susceptibility of the stainless steel connections. In this study, galvanic corrosion in a slip-resistant connection made of stainless steel was not the main focus. For this reason, brown corundum beads were selected only to improve the roughness of the faying surfaces.

Two different test series were carried out on lean duplex test specimens with 1D surface condition with two different clamping length ratios ($\Sigma t/d$ = 4.9 and 2.5), see Figure 5-1 (b) and (c). The aim was to investigate the influence of different clamping length ratios on the determination of the slip factor. The results show that using small load cells and artificially increasing the clamping length from 40 mm (LD_1D_HV10.9) to 75 mm (LD_1D_B109) has no visible influence on the determination of the static slip factors, see Table 5-1.

The results show that for all stainless steel grades, the slip factors achieved for test specimens with the lower preload level (Bumax 88) are equal or lower to those resulting for the higher preload level (Bumax 109), see Figure 5-9.
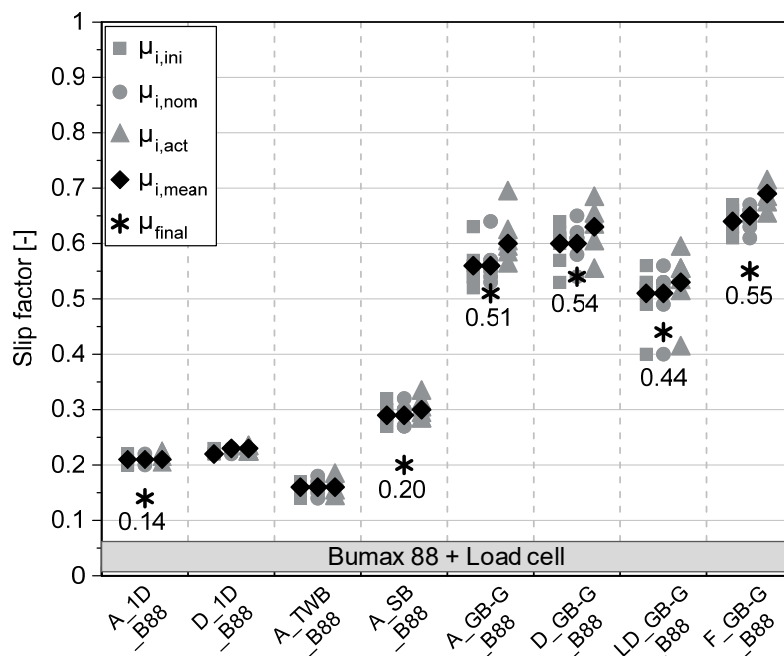
Figure 5-7: Static and final slip factors uncoated test specimens made of stainless steel considering different surface conditions and Bumax 88 bolting assemblies
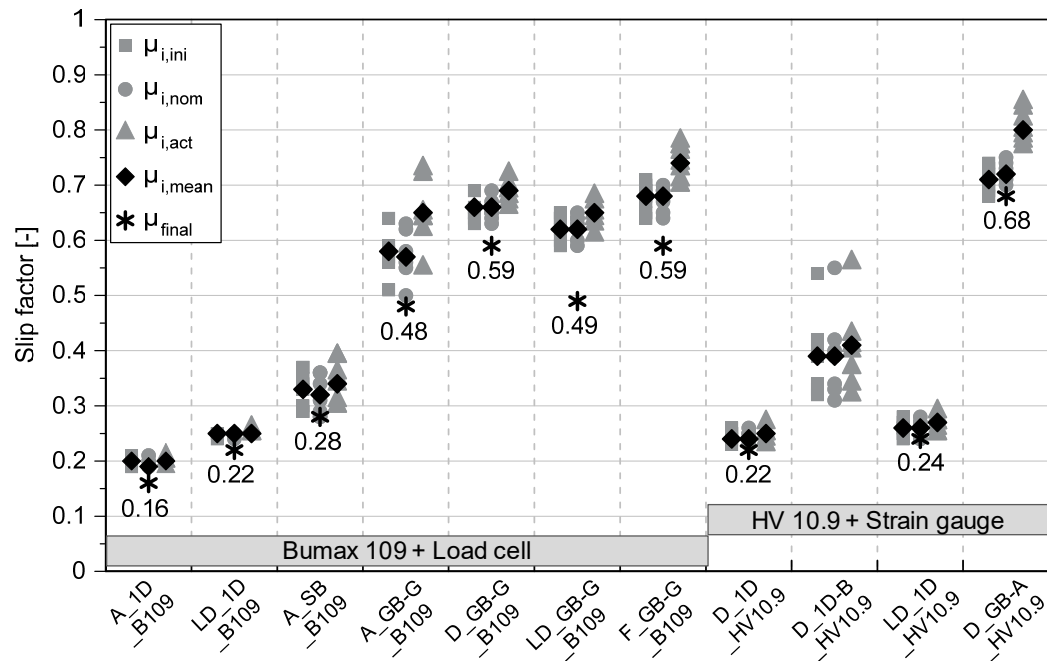
Figure 5-8: Static and final slip factors uncoated test specimens made of stainless steel considering different surface conditions and bolting assemblies with property class 10.9
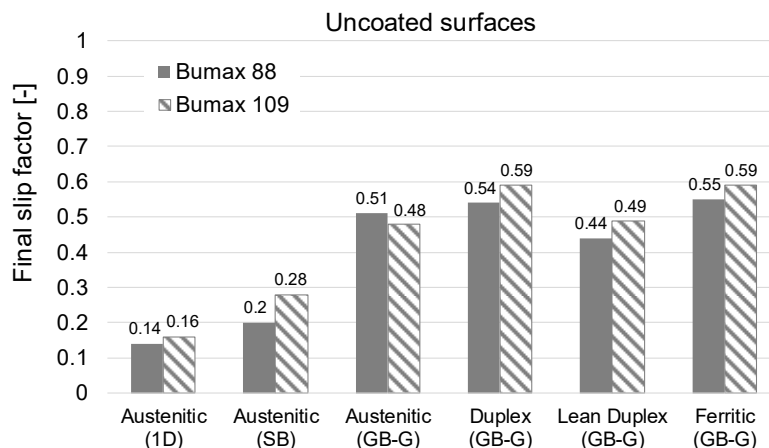
Figure 5-9: Final slip factors for Al-SM coated test specimens made of stainless steel considering different bolting assemblies (Bumax 88 and Bumax 109) [106]

A possible explanation for this phenomenon could be the appearance of cold welding between the faying surfaces as a result of the combination of the surface pressure and slipping of the surfaces. Figure 5-10 (a) illustrates the topography of the faying surface after a slip factor test for a test specimen with 1D surface condition [168]. The black arrow shows flat and uniform contact spot where sliding occurred in the form of scratches on these flat surfaces, shown by blue arrows in Figure 5-10 (a). For the shot blasted test specimens, the faying surface is much rougher after sliding and no flat contact spots could be seen, see Figure 5-10 (b). This is probably due to cold welding (red arrow), which causes deep scratches in the faying surface (magenta arrow). Figure 5-10 (c) shows that the grit blasted faying surface was even

more damaged by heavy cold welding (red arrow) and that deep scratches appeared on the surface (magenta arrow).

(a) Faying surfaces for 1D specimens	(b) Faying surfaces for shot blasted specimens	(c) Faying surfaces for grit blasted specimens
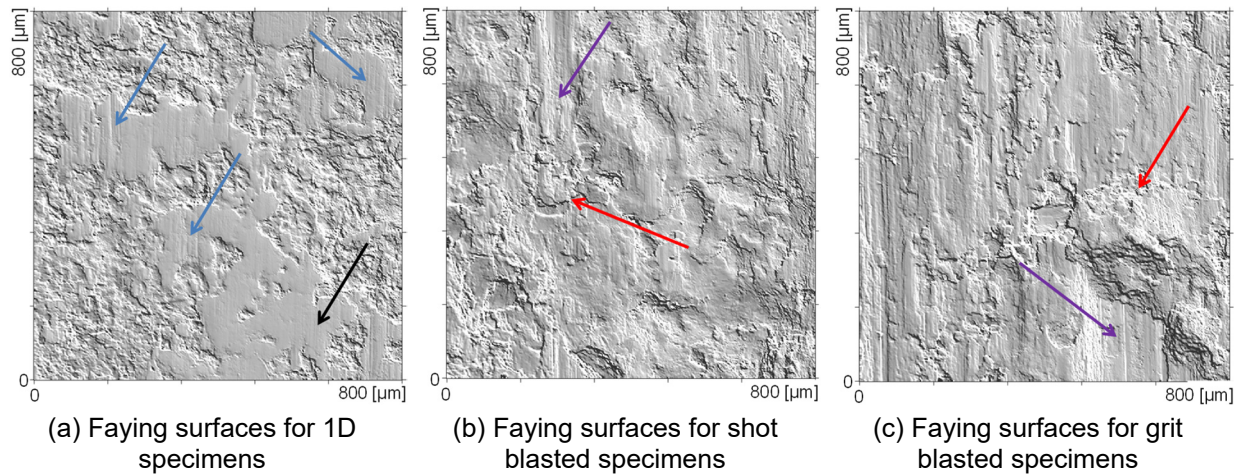
Figure 5-10: Topography of the faying surfaces after the slip factor test [168]

The cold welding spots are caused by the surface pressure and slipping of the surfaces. A higher preload level can cause higher surface pressures and consequently more cold welding spots on the faying surfaces. This phenomenon helps to achieve better slip-resistant behaviour in the connection and also leads to higher slip factors for the specimens with a higher preload level (Bumax 109).

5.3 Determination of slip factors for thermal spray metallized surface finish

Unlike carbon steel, stainless steel does not need any additional protective coating in order to protect the surfaces against corrosion. However, it might be possible to coat the stainless steel surfaces in slip-resistant connections for other reasons. It was therefore decided to conduct a comparative study in order to investigate the influence of an additional coating on the slip-resistant behaviour of the connection and its possible potential to achieve higher slip factors. For this reason, a thermal aluminium spray metallized coating (Al-SM) was selected based on the results from Chapter 3.2.11, in order to improve the slip-resistant behaviour and achieve a higher slip factor. It is important to mention that the influence of the coating application on the corrosion-resistant behaviour of the stainless steel alloy (susceptibility to galvanic corrosion) must be checked for each coating application scenario. This was not the focus of this study.

The thermal aluminium spray metallized coating was applied on all four different stainless steel grades – austenitic (1.4404) (A), duplex (1.4462) (D), lean duplex (1.4162) (LD) and ferritic (1.4003) (F) stainless steel – in combination with bolting assemblies made of austenitic stainless steel with two different bolt property classes 8.8 (Bumax 88) and 10.9 (Bumax 109), see Table 5-2. The M16 specimen geometry was selected for all test series Figure 2-1 (b).

Table 5-2: Slip factor test results for stainless steel bolted connections with thermal spray metallized surface finish [106]

Series ID	Steel grade	Surface condition		Number of tests	$\mu_{nom,mean}$[5]	$\mu_{ini,mean}$[6]	$\mu_{act,mean}$[7]	V (μ_{nom})[8]	Final slip factor [-]
		S.F.B.[1] / Rz[2] [µm]	DFT[3] [µm]	st/ct(sp)/ect[4]	st/st+ct [-]	st/st+ct [-]	st/st+ct [-]	st/st+ct [%]	$\mu_{5\%}$[9] / μ_{ect}[10]
M16 × 100 Bumax 88 (property class 8.8) – Preload level $F_{p,C}$ = 88 kN – $\Sigma t/d$=4.7									
A_Al-SM_B88	1.4404	GB-G[11]/45	100[12]	4/1/2	0.79/-	0.78/-	0.94/-	1.5/-	-/0.71
D_Al-SM_B88	1.4462	GB-G/43	116	4/1/2	0.87/-	0.85/-	0.98/-	1.6/-	-/0.79
LD_Al-SM_B88	1.4404	GB-G/51	105	4/1/2	0.81/-	0.79/-	0.89/-	4.3/-	-/0.72
F_Al-SM_B88	1.4003	GB-G/44	91	4/1/2	0.82/-	0.81/-	0.93/-	1.6/-	-/0.74
M16 × 100 Bumax 109 (property class 10.9) – Preload level $F_{p,C}$ = 110 kN – $\Sigma t/d$=4.9									
A_Al-SM_B109*	1.4404	GB-G/45	100[12]	4/2/1	0.70/-	0.70/-	0.84/-	1.3/-	-/0.63
D_Al-SM_B109*	1.4162	GB-G/43	116	4/2/1	0.82/-	0.81/-	0.90/-	3.3/-	-/0.73
LD_Al-SM_B109*	1.4404	GB-G/51	105	4/2/1	0.78/-	0.78/-	0.86/-	3.8/-	-/0.70
F_Al-SM_B109*	1.4003	GB-G/44	91	4/2/1	0.76/-	0.76/-	0.89/-	1.7/-	-/0.68

[1] surface finish │ [2] surface roughness │ [3] dry film thickness (DFT) │ [4] st: static test/ct: creep-/ect: extended creep test │ [5] $\mu_{nom,mean}$: calculated slip factors as mean values considering the nominal preload level │
[6] $\mu_{ini,mean}$: calculated slip factors as mean values considering the initial preload when the tests start │
[7] $\mu_{act,mean}$: calculated slip factors as mean values considering the actual preload at slip │ [8] V: coefficient of variation for μ_{nom} │ [9] $\mu_{5\%}$: slip factors as 5 % fractile calculated on the basis of the static tests and the passed creep test │ [10] μ_{ect}: slip factor resulting from the passed extended creep test │ [11] GB-G: grit blasted with GRITTAL particles │ [12] nominal dry film thickness (NDFT)

* these tests were carried out at the Department of Steel and Composite Structures of Delft University of Technology (TUD)

Before the coating was applied, all test specimens were grit blasted (GB-G) and the surface roughness Rz of the faying surfaces was measured according to EN ISO 4287. The measured roughness of the faying surfaces was between 43 µm and 51 µm for different stainless steel grades, see Table 5-2. The nominal coating thickness for all test series was 100 µm NDFT (NDFT: nominal dry film thickness). Due to the non-magnetic properties of the austenitic stainless steel alloy, the coating thickness for the austenitic series (A_Al-SM) could not be measured. The coating thicknesses for the other steel grades were measured according to EN ISO 2808. The measured coating thickness was about 116 µm DFT for the duplex series (D_Al-SM), 105 µm DFT for the lean duplex series (LD_Al-SM) and 91 µm DFT for the ferritic series (F_Al-SM). The first four test series were assembled with austenitic bolts M16 A4-88, austenitic nuts M16 A4-88, and washers 17-88, HV 200, A4 (all Bumax 88). For the other four test series, austenitic bolts M16 A4-109, austenitic nuts M16 A4-109 and washers 17-109, HV 300, A4 (all Bumax 109) were used. All bolts comply with EN ISO 4017, nuts with EN ISO 4032 and washers with EN ISO 7089. All bolts were lubricated with Molykote® 1000 lubricant and tightened to the specified preload level $F_{p,C}$. Small load cells were used to measure the preload in the bolts continuously, see Figure 5-11 (a).

Eight different test series with two different preload levels were selected with approximately the same clamping lengths in order to eliminate the possible effect of the clamping length on the loss of preload. The Al-SM test series with Bumax 109 bolting assemblies and preload level of 110 kN ($F_{p,C}$) and clamping length of 78 mm (Figure 5-1 (a)) were carried out at the Department of Steel and Composite Structures of Delft University of Technology (TUD). All test series with Bumax 88

bolting assemblies and preload level of 88 kN ($F_{p,C}$) and clamping length of 75 mm (Figure 5-1 (b)) were carried out at the Institute for Metal and Lightweight Structures (IML) of the University of Duisburg-Essen (UDE).

The results show that for the Al-SM test series the load-bearing capacity of the connection was noticeably improved in comparison with uncoated test series (1D, TWB, SB and GB-G), see Figure 5-11 (b) and Figure 5-4 (a).
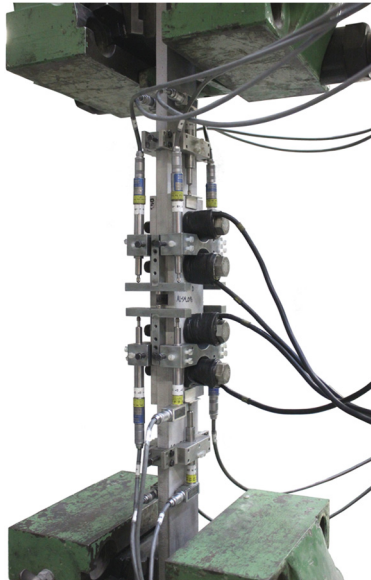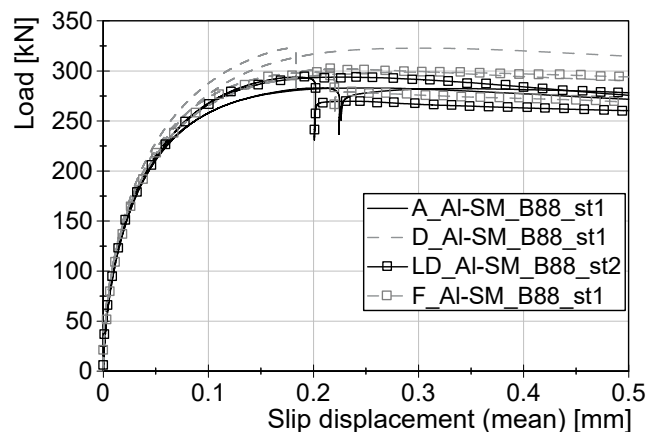
| (a) Test setup | (b) Test series with Bumax 88 bolting assemblies [106] |

Figure 5-11: Test setup and typical load-slip displacement diagrams for Al-SM test specimens made of stainless steel

The creep tests were carried out for all Al-SM test series. The results show that all stainless steel grades with AL-SM coating behave slightly creep sensitive according to the creep test criteria of EN 1090-2, Annex G.

Figure 5-12 shows exemplary the creep test results for Al-SM coated duplex and ferritic test specimens with Bumax 88 bolting assemblies. The difference between the relative displacements at the end of 5 min and 3 hours after reaching the constant load exceeded slightly the limit of 0.002 mm for both upper and lower parts of the specimen. For this reason, the creep tests were considered as failed and performing extended creep tests was necessary.

All extended creep tests were performed with new/unused sets of stainless steel bolting assemblies. Figure 5-13 shows as an example the results of the extended creep tests for the Al-SM coated duplex and ferritic test series with Bumax bolting assemblies.
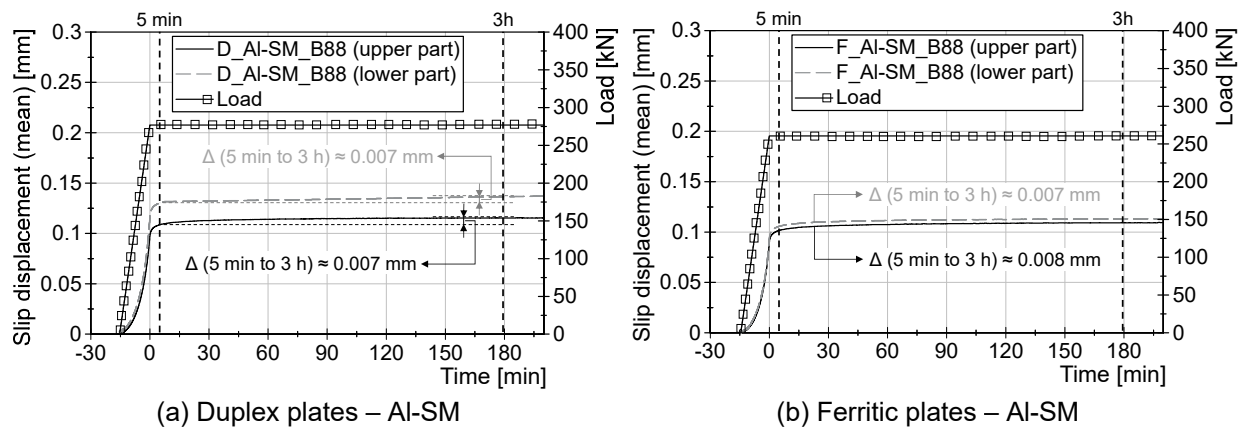
Figure 5-12: Exemplary creep test results for Al-SM coated test specimens made of stainless steel with Bumax 88 bolting assemblies [106]
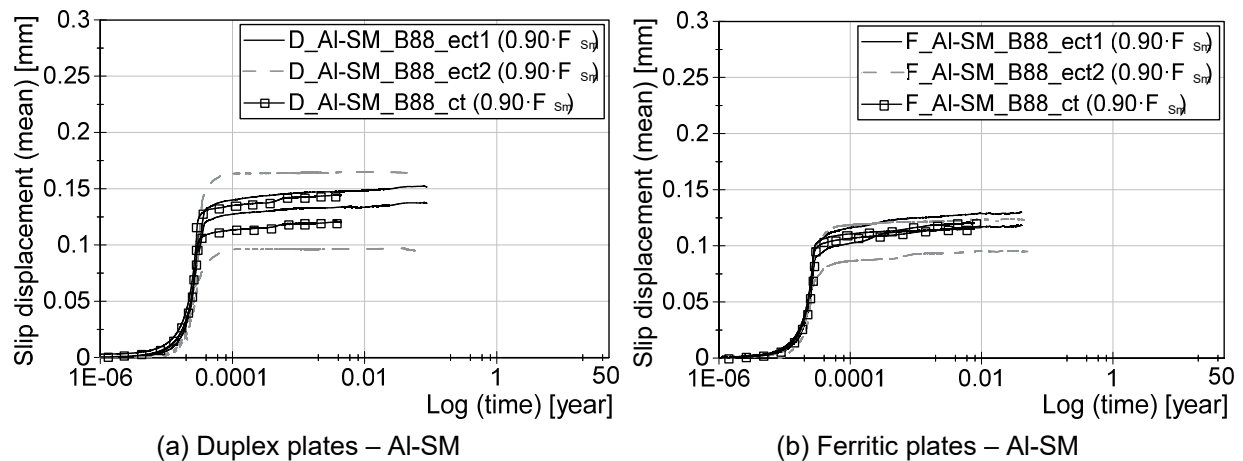
Figure 5-13: Exemplary extended creep test results for Al-SM coated test specimens made of stainless steel with Bumax 88 bolting assemblies [106]

By evaluating the slip displacement-log time curve based on the results of the creep tests for the Al-SM test series (on $0.9 \cdot F_{Sm}$ load level), it become clear that this load level could be suitable for performing a successful extended creep test. The duration of the creep test is quite short in comparison with an extended creep test. For this reason, the extended creep tests were performed to confirm this load level for the determination of the final slip factor. As can be seen in Figure 5-13, the extended creep tests were successful for both test series at a load level of $0.9 \cdot F_{Sm}$. The extrapolated displacement-log time curve shows less than 0.3 mm slip when the curve is extrapolated to 50 years. All static and final slip factors for all different test series are presented in Figure 5-14. As can be seen, the influence of different stainless grades on the slip-resistant behaviour of the Al-SM-coated connections is negligible.
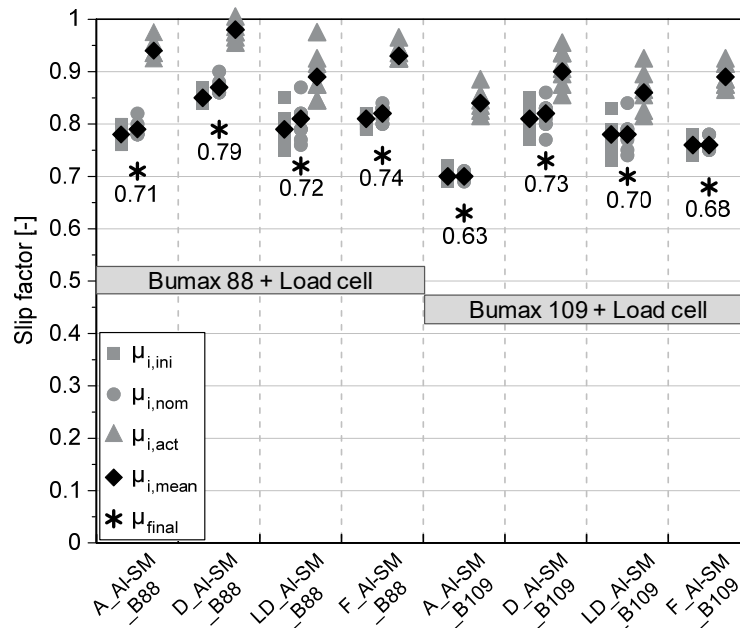
Figure 5-14: Static and final slip factors considering different stainless steel grades with Al-SM coated faying surfaces for both bolt property classes [106]

The results show that for all stainless steel grades with Al-SM-coated faying surfaces, higher slip factors were achieved with a lower preload level (Bumax 88), see Figure 5-15.

A possible explanation may be that, unlike the uncoated surfaces, cold welding could not happen between the faying surfaces because the contact surfaces are covered with aluminium and there was no direct contact between the stainless steel surfaces. For this reason, similar to the phenomenon known for coated specimens made of carbon steel, increasing the preload level decreases the slip factor slightly, see Figure 5-15 and Chapter 3.2.10.
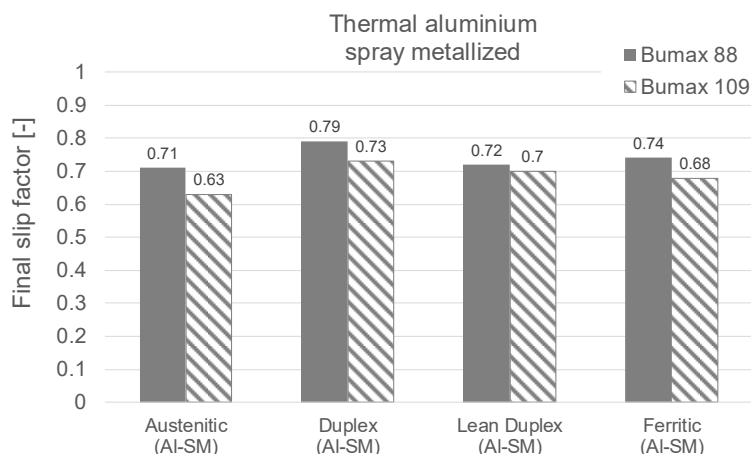
Figure 5-15: Final slip factors for Al-SM coated test specimens made of stainless steel considering different bolting assemblies (Bumax 88 and Bumax 109) [106]

5.4 Alternative preparation method in order to achieve higher slip factors

Experience shows that untreated/as-received faying surface condition in slip-resistant connections does not deliver high slip factors and preparation of the faying surfaces always takes a noticeable amount of money and time. Having an alternative method in order to achieve a higher slip factor for untreated/as-received faying surface condition would be desirable.

In the frame of this study, an alternative method has been developed in order to save cost and time for the preparation of the faying surfaces and, besides this, achieving a higher slip factor. For this investigation, the M16 test specimen geometry was selected according to EN 1090-2, Annex G, see Figure 2-1 (b). All tests were conducted with two different stainless steel grades: austenitic (1.4404) and duplex (1.4462) in combination with Bumax 109 stainless steel bolting assemblies. One test series was also conducted with Bumax 88 in order to investigate the influence of preload level in combination with this alternative surface preparation of the slip-resistant behaviour of the connection. All stainless steel plates were in "as-received" 1D surface condition without any further surface treatment.

In order to improve the slip-resistant behaviour of the connection, two simple elements were considered to be added on the faying surfaces of the bolted connection: epoxy resin and stainless steel small particles. The epoxy resin was chosen as the two-component epoxy resin DELO-DUOPOX® AD897 by Delo Industrie Klebstoffe GmbH & Co. KGaA, see Figure 5-16. The two important parameters for choosing this epoxy resin were the high tensile strength in comparison with other products of this company and the possibility of curing at room temperature offered by this type of resin. According to the data sheet, the tensile strength of this resin is 42 MPa according to EN ISO 527 [169]. The curing time until initial tensile strength (1- 2 MPa) is about six hours, and it takes about 24 hours until the final tensile strength is reached.

In the frame of this study, three different resin application patterns were selected: a very thin layer of resin on the faying surfaces (tR), see Figure 5-17 (a); a very thick layer of resin on the faying surfaces (thR), see Figure 5-17 (b); and a very thick layer of resin around the holes on the faying surfaces (thhR), see Figure 5-17 (c).

In this investigation, GRITTAL GH stainless steel (martensitic with chromium carbides) grit was used as particles between the faying surfaces, with different sizes, see Figure 5-18.

Figure 5-16: Two-component epoxy resin DELO-DUOPOX® AD897 and mixing and dispensing gun

(a) Very thin resin layer (tR)   (b) Very thick resin layer (thR)   (c) Very thick resin layer around the holes (thhR)
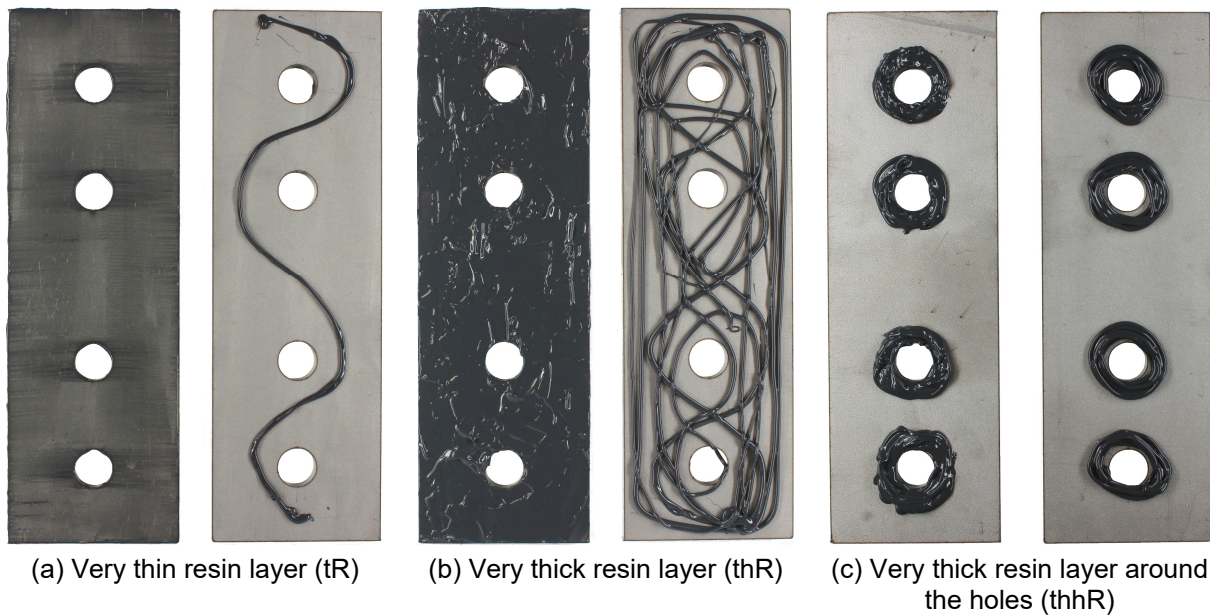
Figure 5-17: Different resin application patterns

(a) GH-10	(b) GH-20	(c) GH-30	(d) GH-40	(e) GH-60
0.05 – 0.20 mm	0.09 – 0.32 mm	0.14 – 0.50 mm	0.40 – 0.80 mm	0.70 – 1.25 mm

Figure 5-18: Different GRITTAL GH particle sizes

Different combinations of resin application patterns and different sizes of particles were selected in order to study the influence of this treatment on the slip-resistant behaviour of the connections, see Table 5-3. The main idea was to develop a very simple preparation method which could be carried out without any special skills. The particles cannot be applied on the faying surfaces without any resin on the surfaces. For this reason, the existence of the resin is necessary. The resin allows the particles to stick to the surfaces and not drop off during the assembly process. It was decided

to fill a salt shaker with the particles and use it to add them to the resin surfaces. For the application of the particles, three different patterns were selected. For different test series, the resin surface was covered partially or fully with the particles in order to see the influence of the amount of applied particles on determination of the slip factor. Figure 5-19 shows different combinations of resin and particles for different test series.

Table 5-3: Slip factor test results for alternative preparation method on stainless steel faying surfaces

Series ID	Surface preparation			Number of tests	$\mu_{nom,mean}$[2]	$\mu_{ini,mean}$[3]	$\mu_{act,mean}$[4]	V (μ_{nom})[5]	Final slip factor [-]
	Resin Appl.	Particle		st/ct(sp)/ect[1]	st/st+ct [-]	st/st+ct [-]	st/st+ct [-]	st/st+ct [%]	$\mu_{5\%}$[6] / μ_{ect}[7]
		Size	Appl.						
Austenitic (1.4404)									
A_tR	t[8]	-	-	4/1/-	0.61/-	0.60/-	0.63/-	1.8/-	-/-
A_tR+fP10	t	P10	f[9]	4/1/-	0.57/-	0.57/-	0.60/-	2.0/-	-/-
A_tR+fP20	t	P20	f	1/-/-	0.49/-	0.50/-	0.53/-	0.0/-	-/-
A_tR+pP40	t	P40	p[10]	1/-/-	0.57/-	0.57/-	0.61/-	2.1/-	-/-
A_tR+fP40	t	P40	f	1/-/-	0.36/-	0.36/-	0.41/-	0.1/-	-/-
A_thR	th[11]	-	-	1/-/-	0.62/-	0.63/-	0.65/-	0.0/-	-/-
A_thR+fP10	th	P10	f	4/1/-	0.77/-	0.77/-	0.83/-	2.9/-	-/-
A_thR+fP20	th	P20	f	1/-/-	0.74/-	0.73/-	0.79/-	0.0/-	-/-
A_thR+fP40	th	P40	f	1/-/-	0.77/-	0.77/-	0.85/-	0.0/-	-/-
A_thR+pP60	th	P60	p	1/-/-	0.64/-	0.63/-	0.68/-	3.4/-	-/-
Duplex (1.4462)									
D_tR	t	-	-	4/1/-	0.65/-	0.64/-	0.66/-	6.5/-	-/-
D_tR+fP10	t	P10	f	4/1/-	0.51/-	0.49/-	0.51/-	4.2/-	-/-
D_thR+fP10	th	P10	f	4/1/-	0.87/-	0.87/-	0.89/-	7.2/-	-/-
D_thR+fP102030	th	P10, P20 and P30	f	1/-/-	0.76/-	0.75/-	0.80/-	5.2/-	-/-
D_thhR	thh[12]	-	-	4/1/2	0.70/-	0.69/-	0.70/-	2.9/-	-/0.45
D_thhR+fP10	thh	P10	f	4/1/3	0.86/-	0.85/-	0.87/-	1.7/-	-/0.65
D_thhR+fmP10	thh	P10	fm[13]	1/-/-	0.88/-	0.88/-	0.88/-	0.0/-	-/-
D_thhR+fP10_B88	thh	P10	f	4/1/3	1.04/-	1.03/-	1.05/-	1.5/-	-/0.73

[1] st: static test/ct: creep-/ect: extended creep test | [2] $\mu_{nom,mean}$: calculated slip factors as mean values considering the nominal preload level | [3] $\mu_{ini,mean}$: calculated slip factors as mean values considering the initial preload when the tests start | [4] $\mu_{act,mean}$: calculated slip factors as mean values considering the actual preload at slip |
[5] V: coefficient of variation for μ_{nom} | [6] $\mu_{5\%}$: slip factors as 5 % fractile calculated on the basis of the static tests and the passed creep test | [7] μ_{ect}: slip factor resulting from the passed extended creep test | [8] thin layer | [9] fully covered | [10] partially covered | [11] thick layer | [12] thick layer around the hole | [13] mixed with resin before application

For one test series the resin and particles were mixed before application. The mix was applied by syringe to the faying surfaces around the holes, see Figure 5-20.

Having a thick layer of resin between the faying surfaces will cause some difficulties in the assembling process. Pressing the plates together will cause the resin or resin and particles to run through the bolt holes, and when the bolts are inserted in the holes the resin will cover the threads of the bolt. This phenomenon may decisively affect the preloading procedure of the bolts. In order to keep the threads of the bolts clean, a simple solution was found. The threads of the bolts were covered with aluminium foil like a cap, as shown in Figure 5-21. After the bolts were inserted in the holes, the aluminium caps were removed and the bolts were tightened. This simple technique helped to keep the bolt threads completely clean and ready for tightening.

The preload level of $F_{p,C}$ was selected for all test series and the preload level in the bolts was measured continually in all tests using small load cells with a length of 40 mm, see Figure 4-11.
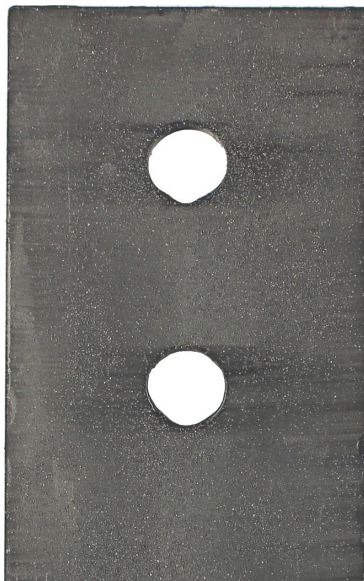
(a) Surface was covered with thin layer of resin and partially covered with particles (tR+pP)	(b) Surface was covered with thick layer of resin and partially covered with particles (thR+pP)	(c) Surface around the hole was covered with thick layer of resin and partially covered with particles (thhR+pP)
(d) Surface was covered with thin layer of resin and fully covered with particles (tR+fP)	(e) Surface was covered with thick layer of resin and fully covered with particles (thR+fP)	(c) Surface around the hole was covered with thick layer of resin and fully covered with particles (thhR+pP)
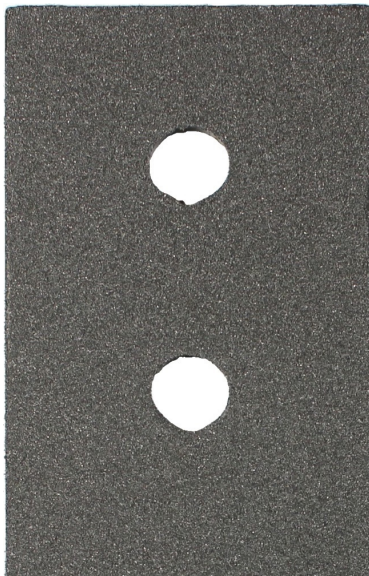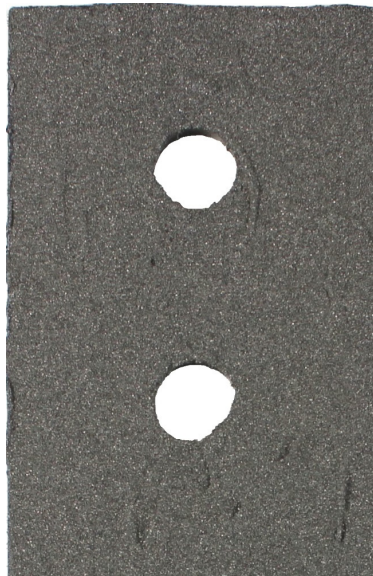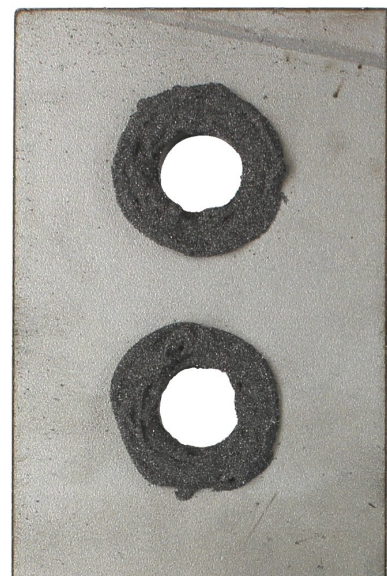
Figure 5-19: Different combinations of resin and particles

| (a) 100 grams GH-10 particles | (b) 100 grams resin | (c) Application process |
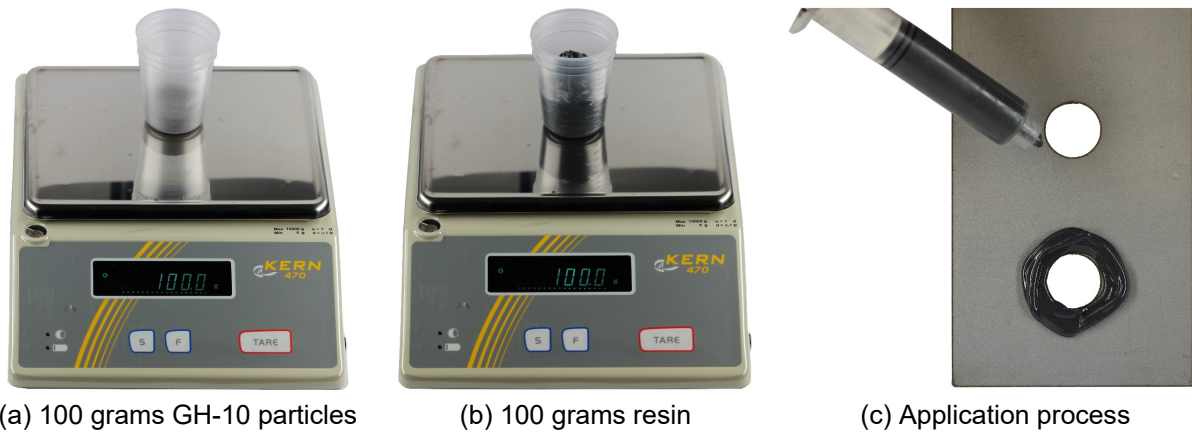
Figure 5-20: Mixing resin and particles before application on faying surfaces

Figure 5-21: Using aluminium cap to protect the thread of the bolts

As the curing time until the final tensile strength of the resin is about 24 hours, after assembling the test specimens and preloading the bolts, each test specimen rested for at least one day to let the resin harden and reach its final tensile strength. During this time, the loss of preload started as soon as the bolts were tightened. The relaxation behaviour of the preloaded bolted connection made of stainless steel was already investigated in Chapter 4.4. However, having an additional layer of resin and particles between the faying surfaces may decisively change the relaxation behaviour of the connection. For this reason, it is important to be able to estimate the long-term loss of preload of the connection.

One random test specimen for each test series was selected in order to investigate the relaxation behaviour of the connection. The loss of preload was calculated for all four bolts in the connection in the last 24 hours and was extrapolated to 50 years. All results are presented in Table 5-4.

Table 5-4: Loss of preload for bolted connections with faying surfaces prepared with resin and particles

Series ID	Surface preparation			No. of tests	Clamped package			Loss of preload	
	Resin Appl.	Particle			Bolt	Plate	$F_{p,C}$ [kN]	measured after one day - min / mean / max [%]	after 50 years (extrapolated) min / mean / max [%]
		Size	Appl.						
Austenitic (1.4404)									
A_tR	t[1]	-	-					4.1 / 4.6 / 5.0	8.5 / 9.4 / 10.2
A_tR+fP10	t	P10	f[2]					4.0 / 4.9 / 5.6	7.5 / 9.0 / 10.0
A_tR+fP20	t	P20	f					4.8 / 5.2 / 5.8	9.1 / 9.9 / 11.0
A_tR+pP40	t	P40	p[3]					5.0 / 6.0 / 7.2	9.7 / 10.7 / 12.1
A_tR+fP40	t	P40	f	4 bolts	Bumax 109	Austenitic (1.4404)	110	4.8 / 5.9 / 7.1	8.5 / 10.0 / 11.0
A_thR	th[4]	-	-					4.5 / 5.0 / 5.4	8.2 / 8.7 / 9.0
A_thR+fP10	th	P10	f					4.5 / 4.8 / 5.0	8.3 / 8.6 / 9.0
A_thR+fP20	th	P20	f					4.5 / 4.9 / 5.2	8.4 / 8.8 / 9.2
A_thR+fP40	th	P40	f					5.5 / 6.5 / 7.6	10.1 / 11.3 / 12.4
A_thR+pP60	th	P60	p					6.1 / 6.4 / 6.7	10.4 / 10.7 / 11.2
Duplex (1.4462)									
D_tR	t	-	-					4.1 / 4.2 / 4.3	8.1 / 8.3 / 8.6
D_tR+fP10	t	P10	f					4.1 / 4.3 / 4.5	8.2 / 8.8 / 9.4
D_thR+fP10	th	P10	f	4 bolts	Bumax 109	Duplex (1.4462)	110	3.7 / 4.4 / 4.8	6.9 / 7.5 / 8.3
D_thR+fP102030	th	P10, P20 and P30	f					4.4 / 4.7 / 5.1	7.9 / 8.3 / 8.7
D_thhR	thh[1]	-	-					5.3 / 5.5 / 5.6	10.2 / 10.4 / 10.6
D_thhR+fP10	thh	P10	f					3.8 / 4.2 / 4.4	7.7 / 8.4 / 9.3
D_thhR+fP10_B88	thh	P10	f		Bumax 88		88	4.9 / 5.2 / 5.8	8.3 / 8.5 / 9.1

[1] thin layer | [2] fully covered | [3] partially covered | [4] thick layer | [5] thick layer around the hole

The loss of preload instantly starts after tightening of the bolts and gradually increases as time elapses. As expected, the rate of loss of preload decreases over time, see Figure 5-22 (a) and (b). This figure illustrates the rate of loss of preload for D_thhR+fP10 test series (with Bumax 109 bolting assemblies) and D_thhR+fP10_B88 test series (with Bumax 88 bolting assemblies). In both test series, the bolts were tightened to a preload level of $F_{p,C}$, which is 110 kN for Bumax 109 and 88 kN for Bumax 88. By having the logarithmic scale for both the rate of loss of preload and the time axis, a linear behaviour can be recognized in the reduction of the rate of loss of preload. This phenomenon was also observed in Chapters 4.4.3 and 4.4.4 for preloaded bolted connections made of carbon and stainless steel.

Figure 5-23 shows the exemplary loss of preload-log (time) diagrams for the same two test series. As can be seen, a perfect linear behaviour can be observed after the first hours, which helps to achieve an accurate estimation for the loss of preload after 50 years. The highest rate of viscoplastic deformation in the stainless steel material (plates, bolting assemblies and particles) appears at the beginning of the test. However, this phenomenon cannot change the general long-term linear behaviour of this diagram. Having an additional resin layer between the faying surfaces also can not affect this phenomenon, since preloading of the bolts will press out the extra added soft resin between the faying surfaces. A very thin layer of resin will remain between the faying surfaces, which more or less only fills the gaps between the faying surfaces and the topography of the faying surfaces. This thin layer of resin

would not play any role in transferring the vertical surface pressure between the faying surfaces.

The results also show that the estimated loss of preload after 50 years for all different test series is approximately between 8 % and 11 %, see Table 5-4, Figure 5-23 and Figure 5-24. These results are comparable with the results of uncoated/ untreated preloaded bolted connections made of carbon and stainless steel presented in Chapter 4.4.3.

(a) Rate of loss of preload-Log (time) diagrams for D_thhR+fP10 test series

(b) Rate of loss of preload – Log (time) diagrams for D_thhR+fP10_B88 test series

(c) Log (rate of loss of preload) – Log (time) diagrams for D_thhR+fP10 test series

(d) Log (rate of loss of preload) – Log (time) diagrams for D_thhR+fP10_B88 test series
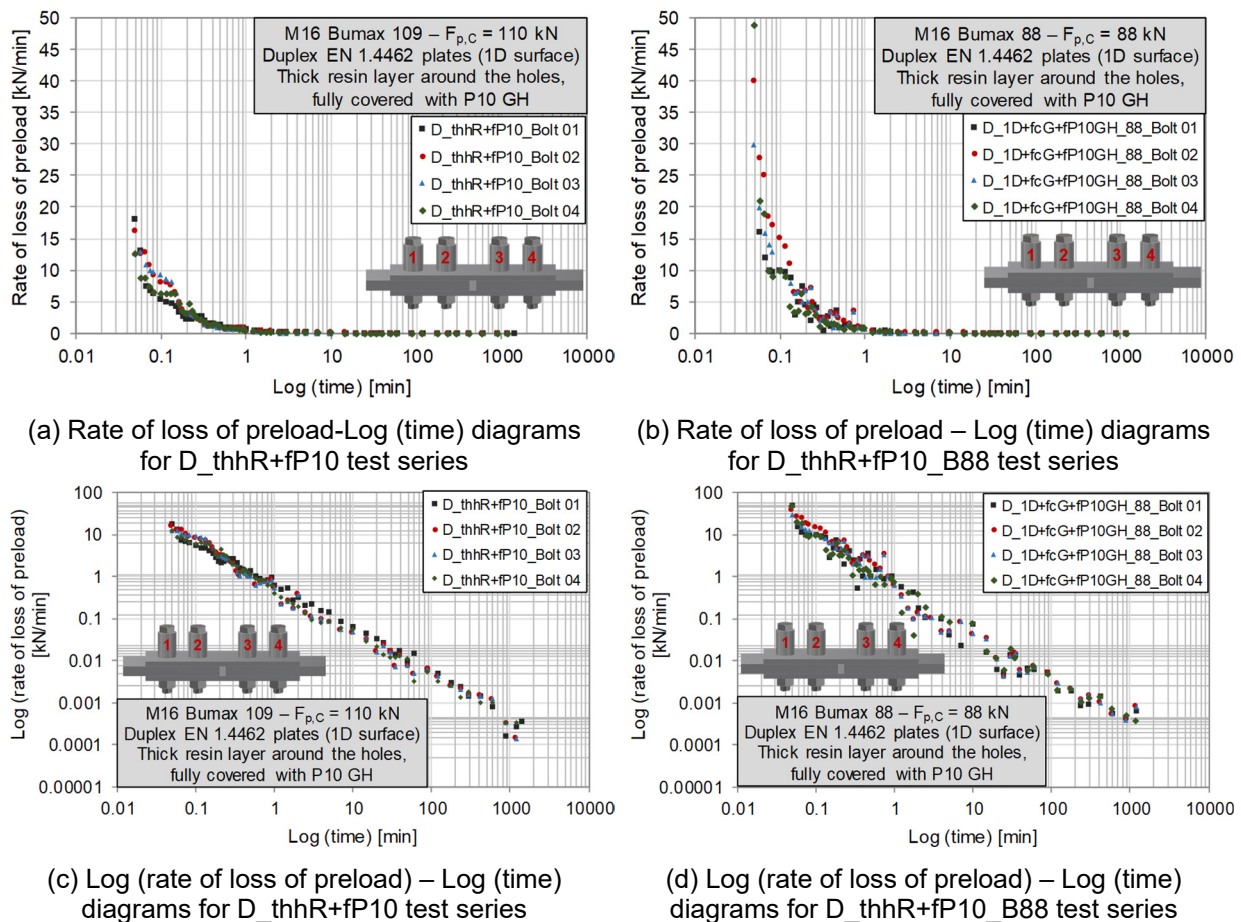
Figure 5-22: Exemplary rate of loss of preload for D_thhR+fP10 and D_thhR+fP10_B88 test series

(a) Loss of preload-Log (time) diagrams for D_thhR+fP10 test series

(b) Loss of preload-Log (time) diagrams for D_thhR+fP10_B88 test series
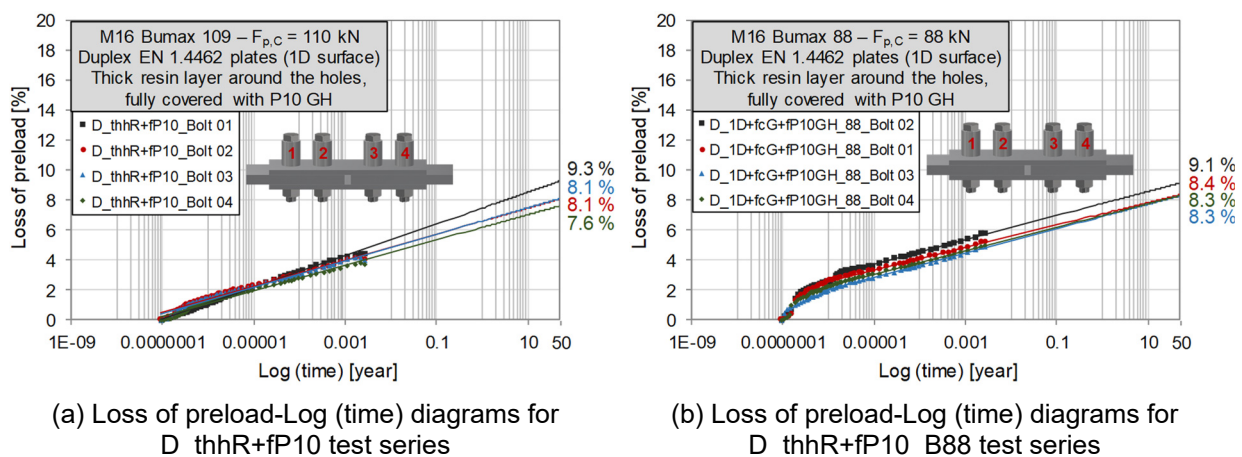
Figure 5-23: Exemplary loss of preload diagram for D_thhR+fP10 and D_thhR+fP10_B88 test series
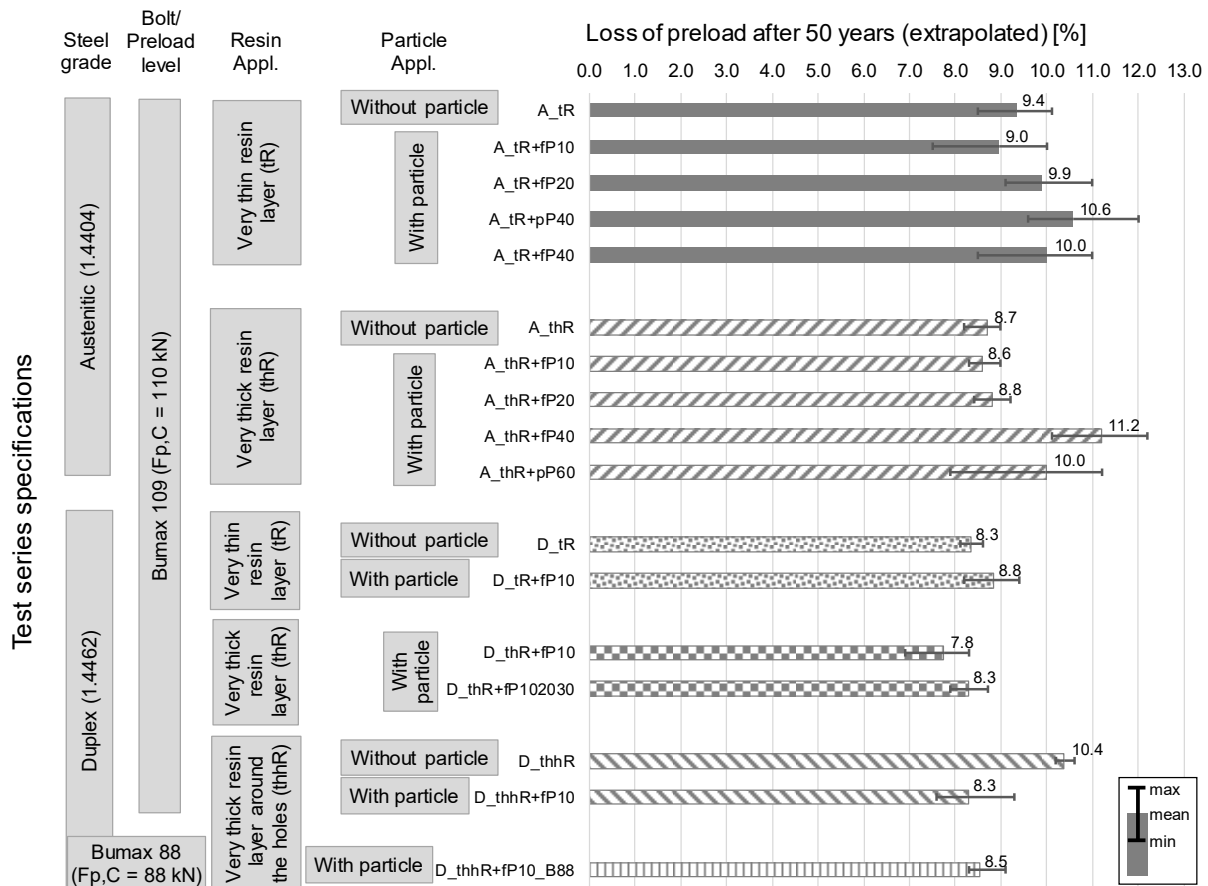
Figure 5-24: Comparing the loss of preload after 50 years (extrapolated) for different combinations of resin and particles

The static slip factor test results and the final slip factors based on a passed extended creep test are presented in Table 5-3. All presented results are based on the slip measured in the centre bolt group (CBG) position, see Figure 5-25 (a). As can be seen in Table 5-3 and Figure 5-17, two different resin application patterns were chosen for the austenitic test series. Figure 5-25 (b) shows the load-slip displacement diagrams for austenitic test specimens with a very thin resin layer (tR) between faying surfaces. For this test series, the results show that the slip load value is higher when there is no particle between the faying surfaces and the slip load decreases with increasing particle size. However, with a very thick resin layer (thR) between the faying surfaces and adding the particles on the resin surfaces, the slip-resistant behaviour was improved, see Figure 5-25 (c). Adding the P60 particles on very thick resin layers between the faying surfaces (A_thR+pP60) delivers lower results in comparison with smaller particles, see Table 5-3.

For the duplex test series, three different patterns were selected for application of the resin between the faying surfaces, see Table 5-3 and Figure 5-17. The negative influence of the combination of the very thin layer of resin (tR) and particles between the faying surfaces on the slip-resistant behaviour of the connection was also observed for duplex test specimens, see Figure 5-25 (d).

(a) Test setup

(b) Austenitic (1.4404) + very thin resin layer (tR)

(c) Austenitic (1.4404) + very thick resin layer (thR)

(d) Duplex (1.4462) + very thin resin layer (tR)

(e) Duplex (1.4462) + very thick resin layer (thR)

(f) Duplex (1.4462) + very thick resin layer around the holes (thhR)
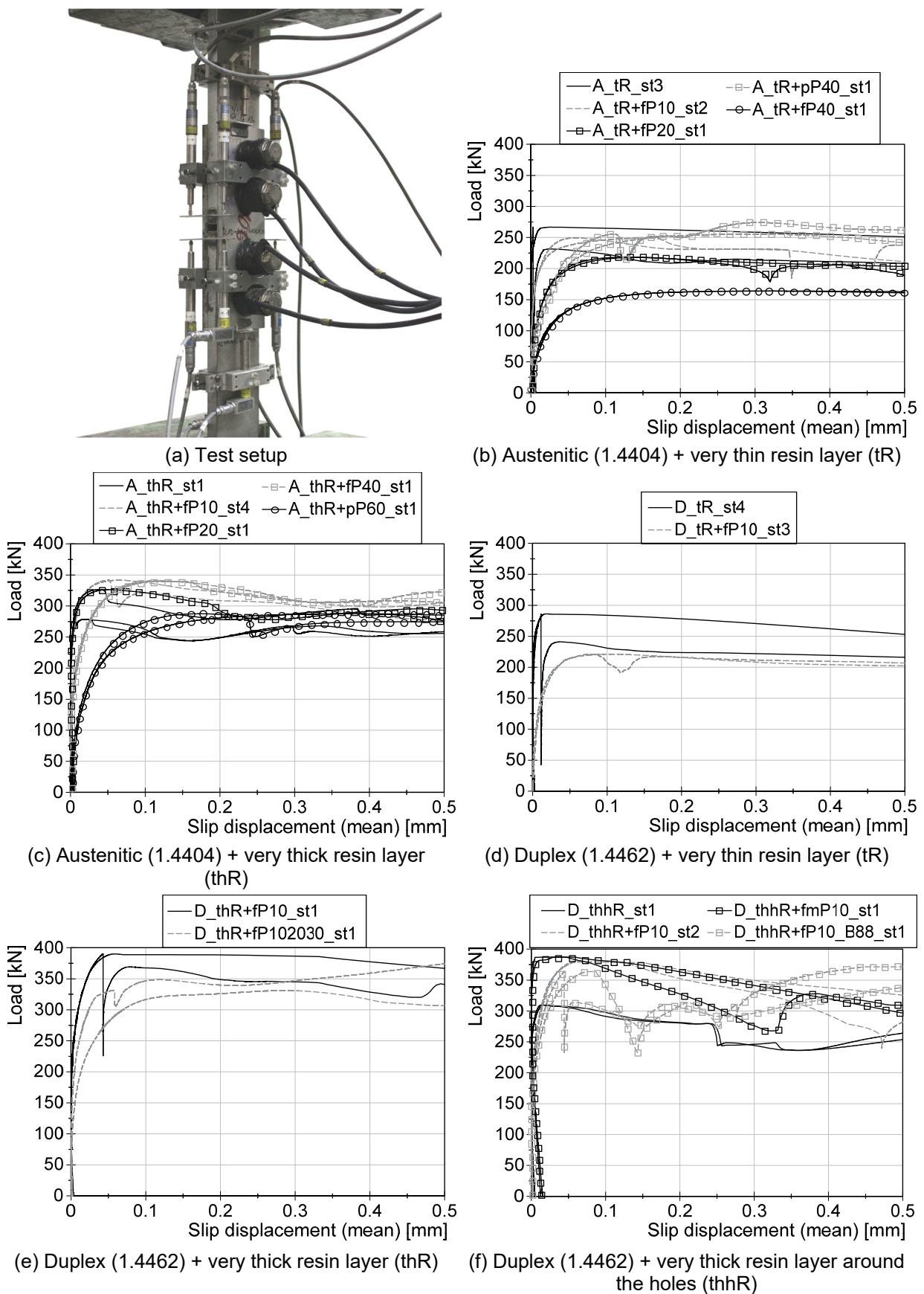
Figure 5-25: Test setup and load-slip displacement diagrams for different stainless steel grades with combination of resin and particles

Two test series were conducted on duplex test specimens with a very thick layer of resin between the faying surfaces (thR); one test series was with P10 particles and the other with a combination of three different particle sizes: P10, P20 and P30. Equal weights of particles were mixed together and added to the resin surfaces. The results show that a lower slip load was achieved by mixing P10 particles with larger particle sizes, see Figure 5-25 (e). A very thick resin layer around the holes on the faying surfaces (thhR) was the last resin application pattern which was selected for duplex test specimens, see Table 5-3 and Figure 5-17 (c). The results show that a higher slip load was achieved by adding the P10 particles to this pattern, see Figure 5-25 (f).

All static and final slip factors considering a different mixture of resin and particles for austenitic and duplex test specimens are summarized in Figure 5-26. In this figure, the results were compared with the final slip factor results from Chapter 5.2 for the austenitic and duplex test series with 1D faying surfaces.

In order to explain these phenomena, closer attention is needed to the condition of the faying surfaces after preloading of the bolts. Figure 5-27 shows the schematic condition of the faying surfaces for different surface conditions. As can be seen in Figure 5-27 (a) for the faying surfaces with a very thin resin layer, the plate surfaces lie on each other perfectly during the preloading process. In this situation, pressing the plates against each other causes additional resin between the faying surfaces to move into the hole clearance and out of the connection. However, the amount of resin in the hole clearance was minimal and did not have any additional influence on the slip-resistant behaviour of the connection. Having resin between the faying surfaces improved the slip-resistant behaviour of the connection in comparison with the results of the specimens with as-received (1D) faying surfaces. As can be seen, the determined mean initial static slip factor increased from 0.19 for the A_1D_B109 test series, see Table 5-1, to 0.61 for the A_tR test series, see Table 5-3.

As a result of adding the particles on a very thin resin layer (tR) between the faying surfaces, the slip mechanism changes. As can be seen in Figure 5-27 (b), having the particles between the faying surfaces causes a gap and prevents full contact between the faying surfaces. This gap would be increased by increasing the particle size. The reduced contact area between the faying surfaces has a negative influence on the slip-resistant behaviour of the connection.
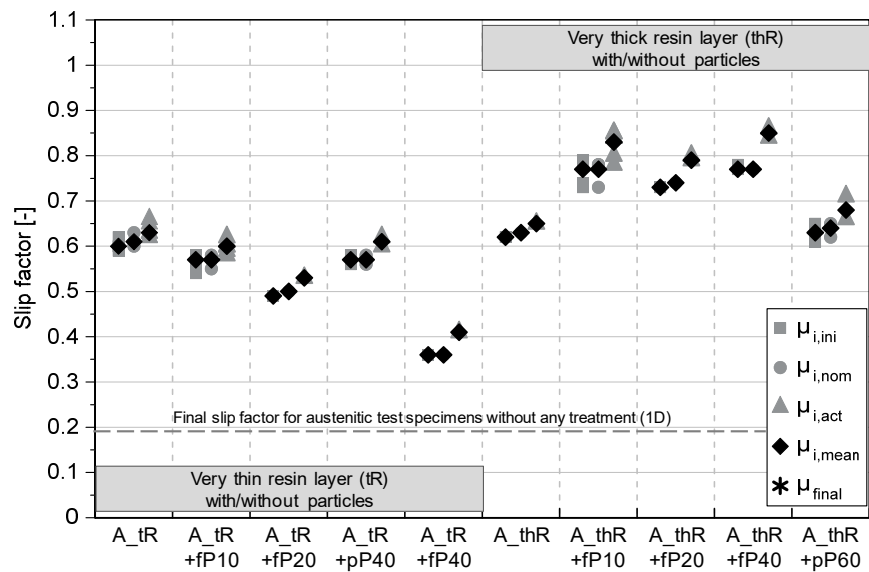
(a) Austenitic test specimens
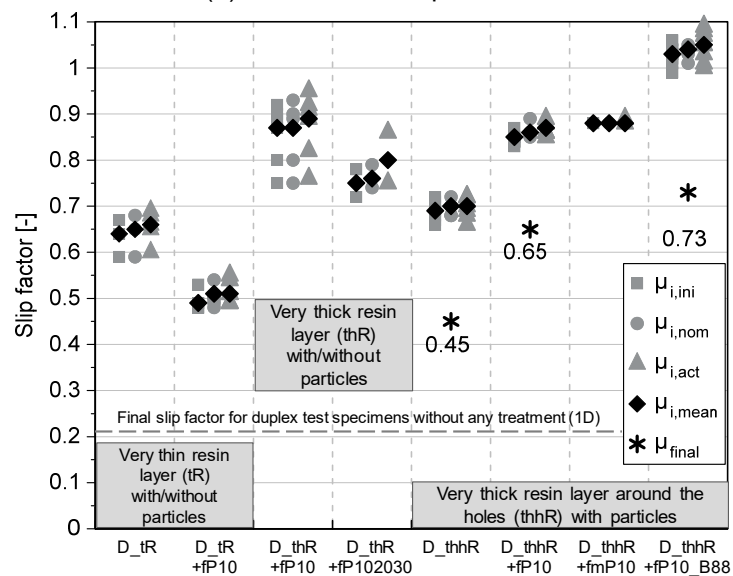
(b) Duplex test specimens

Figure 5-26: Static and final slip factors for different mixtures of resin and particles between the faying surfaces for different types of stainless steel test specimens

During the loading process, the plates slip on the deformed particles. By increasing the particle size, the gap between the faying surfaces would be larger and sliding of the plates on these particles would be easier. This phenomenon causes a lower slip factor for larger particle sizes. For very thin resin layers (tR) covered partially with particles, see Figure 5-19 (a), it is still possible for the faying surfaces to come closer to each other with preloading of the bolts.

During the preloading process, the surface pressure should transferred by a lower number of particles between the faying surfaces. Due to higher surface pressure between the particles and faying surfaces, the particles start to deform and penetrate the faying surfaces. As can be seen in Table 5-3, the mean initial slip factor for surfaces covered with a thin layer of resin and partially covered with particles

(A_tR+pP40) is 0.57, and for surfaces covered with a thin layer of resin and fully covered with particles (A_tR+fP40) is 0.36, see Table 5-3.

In order to fill the gap between the particles and the faying surfaces it was decided to add more resin between the faying surfaces. However, this solution had a very important effect on the slip mechanism of the connection other than filling the gap between the particles and the faying surfaces. As can be seen in Figure 5-27 (c), during the preloading process, the mix of resin and particles flows into the hole clearance and completely fills it. Filling the hole clearance with this mixture will limit the slip in the connection additionally to the slip-resistant properties of the faying surfaces. Slip can still occur if the load reaches the compressive strength of the mixture in the hole clearance.

The static slip factor test results show that for the austenitic test series the mean initial slip factor increased from 0.57 for test specimens with a very thin resin layer on the faying surfaces and fully covered with P10 particles (A_tR+fP10) to 0.77 for test specimens with a very thick resin layer on the faying surfaces and fully covered with P10 particles (A_thR+fP10).

For the duplex test series, the combination of P10 particles and a very thin resin layer delivered a mean initial slip factor of 0.51 and 0.87 with a very thick resin layer. For the combination of thick resin layer around the holes and P10 particles, the mean initial slip factor was 0.86. As can be seen, having a very thick resin layer on the whole faying surfaces has no special advantage in comparison with adding the resin layer only around the holes on the faying surfaces.

Adding only a thick resin layer on the faying surfaces will help to fill the hole clearance as can be seen in Figure 5-27 (d). However, the results show a negative influence if the particles are removed, see Table 5-3. The mean initial slip factor decreases from 0.86 to 0.70.

As with concrete, the resin assumes the role of the cement paste and the particles are the aggregates in this mixture. Adding particles to the resin increases the compressive strength of the mixture.

(a) Very thin resin layer (tR)

(b) Very thin resin layer (tR) + particles

(c) Very thick resin layer on whole faying surface or around the hole (thR or thhR) + particles

(d) Very thick resin layer on whole faying surface or around the hole (thR or thhR) without particles
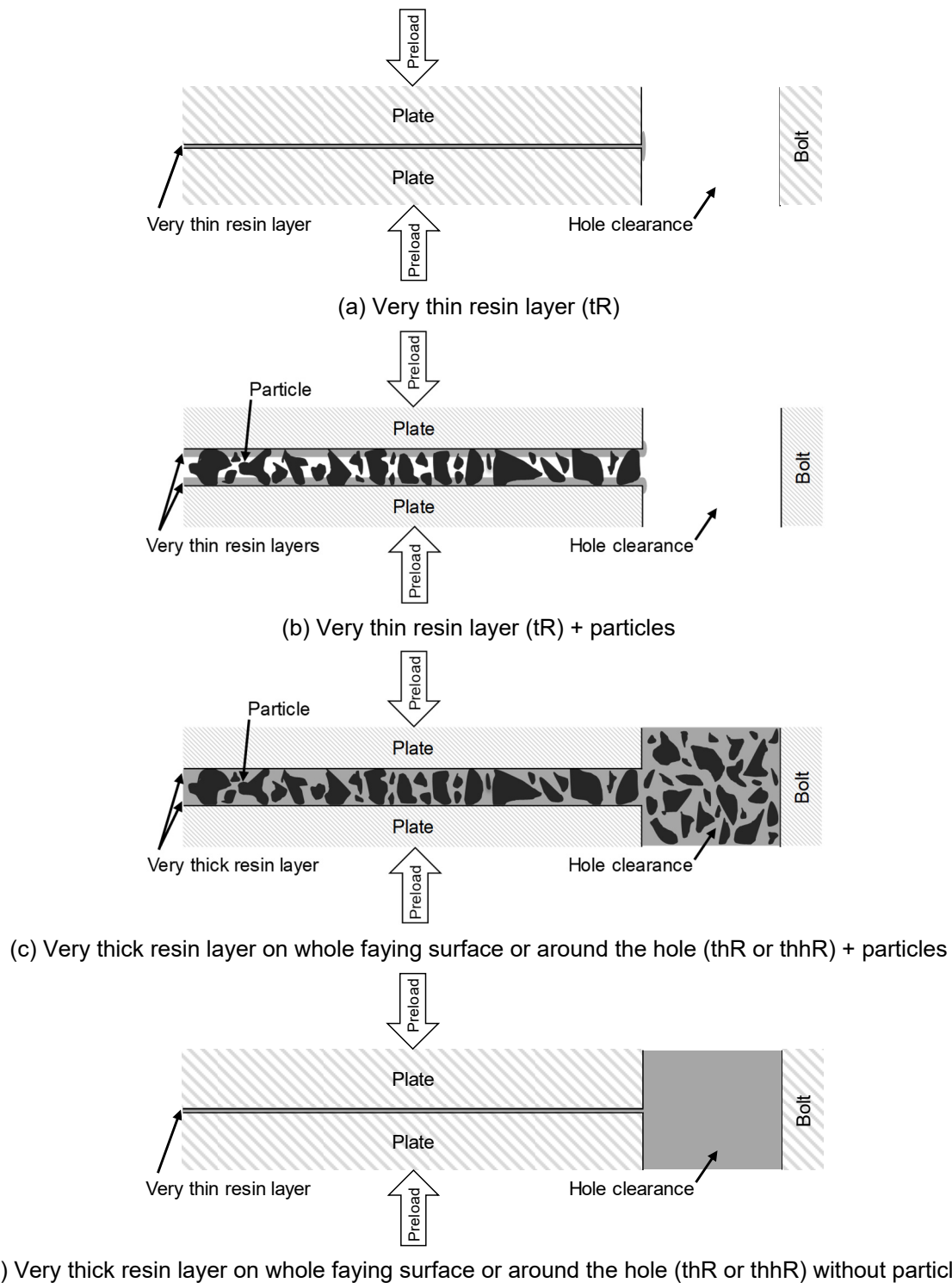
Figure 5-27: Schematic condition of the faying surfaces and hole clearance after bolt preloading

Figure 5-26 (a) shows that the slip factors for the test specimens with a very thick layer of resin and partially covered with P60 particles are lower in comparison with surfaces fully covered with P10, P20 and P40. The reason might be the lack of particles in the mixture in the hole clearance. However, the slip factors were approximately the same with fully covered surfaces with different particle sizes.

The results show that filled hole clearances with resin and particles have a great influence on the slip-resistant behaviour of the connection. For this reason, it is very

important to be sure that the hole clearance is fully filled with the mixture. After disassembling the test specimens with a very thick resin layer between the faying surfaces, a mixture core was seen around the bolt thread which completely filled the hole clearance, see Figure 5-28. As the results show, the thick layer of resin around the hole delivers the same results as faying surfaces entirely covered with a thick resin layer. During the preloading process, the extra resin between the faying surfaces flows out from the sides of the specimens. For this reason, adding more resin than required would not have any positive effect.

In order to see the distribution of the resin through the faying surfaces and inside the hole clearance, a M16 test specimen made of plexiglass was prepared, see Figure 5-29 (a). A very thick layer of resin was added around the holes on the faying surfaces. As soon as the plates are laid on each other the resin starts to distribute between the faying surfaces and flows into the holes, see Figure 5-29 (b). As Figure 5-29 (c) shows, when the bolts are hand-tightened, all hole clearances were completely filled with the resin. Hence, in order to take advantage of the filled hole clearance, it is not necessary to have a high preload level. As can be seen in Figure 5-26, higher slip factors were achieved for the D_thhR+fP10_B88 test series with lower preload level in comparison with the D_thhR+fP10 test series with higher preload level. This phenomenon was already observed in Chapters 3.2.10 and 5.3. As with coated test specimens, the higher preload level leads to higher mean slip load and slightly lower slip factor. This means that the influence of filled hole clearances is the same for both specimens with different preload levels.

(a) Very thick resin layer on whole faying surface (thR) + particles

(b) Very thin resin layer (tR) + particles
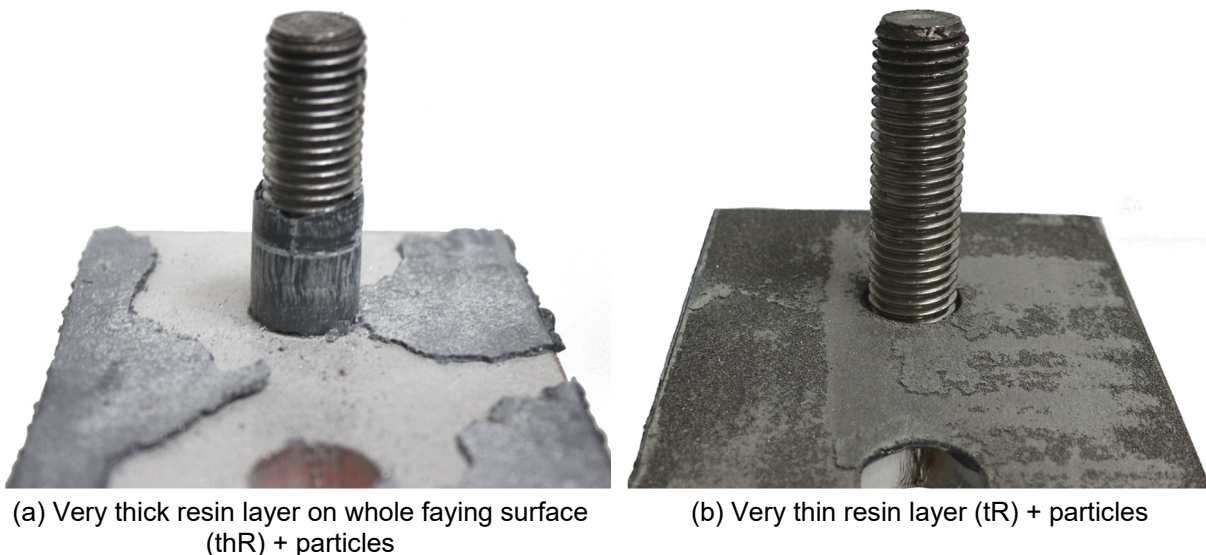
Figure 5-28: Condition of the hole clearance after dissembling of the test specimen

(a) No resin between the faying surfaces

(b) Distribution of the resin between the faying surfaces

(c) Condition of the hole clearances after hand-tightening of the bolts

Figure 5-29: Condition of the hole clearance without and with resin between the faying surfaces

The creep tests were performed only for some test series. All creep tests failed for all investigated test series for both upper and lower parts of the specimens. Figure 5-30 shows as an example the creep test results for the D_tR and D_thhR+fP10 test series. In all creep tests, the upper and lower part of the specimens slipped through in the first minutes after reaching the constant load. This emphasizes the creep sensitivity of the test specimens and thus it is necessary to perform extended creep tests to determine the final slip factor.

(a) D_tR test series

(b) D_thhR+fP10 test series
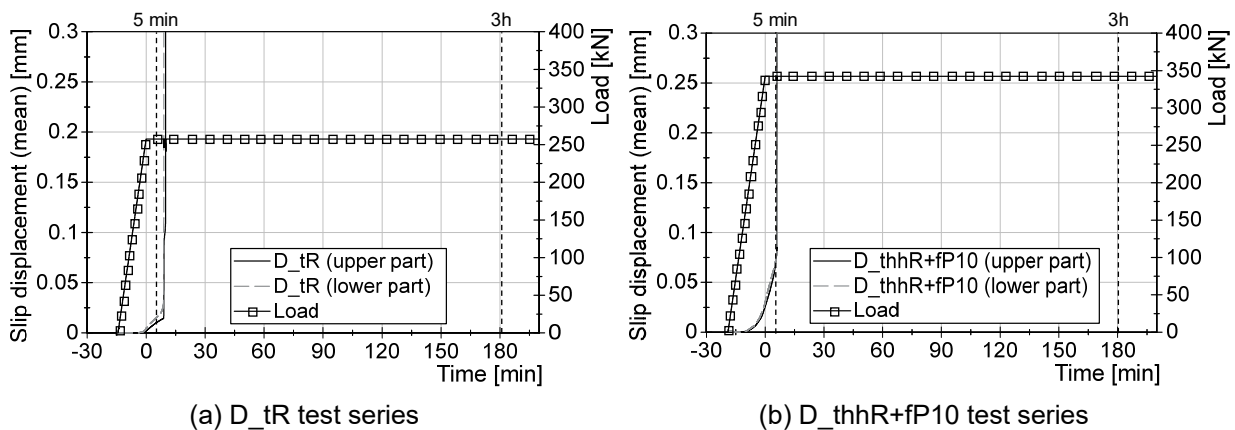
Figure 5-30: Exemplary results of creep tests for two test series made of duplex steel with combination of resin and particles on the faying surfaces

For the D_thhR test series, evaluating the slip displacement-log time curve based on the results of the creep tests shows the creep sensitivity of the test specimens. For this reason, the first extended creep test was performed with a load level of $0.65 \cdot F_{Sm}$ = 199.2 kN. Figure 5-31 (a) shows that that the test specimen passed the extended creep test at this load level. For this reason, the load level was increased to $0.70 \cdot F_{Sm}$ = 214.5 kN in order to achieve a higher slip factor. By evaluating the slip displacement - log time diagram for this load level, it became apparent that the slip was more than 0.3 mm when extrapolated to 50 years and the test could not be considered as a passed extended creep test. For this reason, the final slip factor must be calculated with $0.65 \cdot F_{Sm}$, which is equal to 0.45.

For the D_thhR+fP10 test series, three extended creep tests were performed. Considering the creep sensitivity of this method of surface preparation, it was decided to perform the first extended creep test with a load level of $0.70 \cdot F_{Sm}$ = 266.2 kN. As can be seen in Figure 5-31 (b), the slip is less than 0.3 mm when extrapolated to 50 years and the test was clearly passed. For the second extended creep test, the load level was increased to $0.75 \cdot F_{Sm}$ = 285.2 kN. The results show that the test is also passed at this level. For this reason, the load level was increased again to check the possibility of achieving a higher slip factor. However, the results show that the test failed with a load level of $0.80 \cdot F_{Sm}$ = 304.2 kN. This means that the final slip factor is equal to 0.65 based on $0.75 \cdot F_{Sm}$.

As mentioned before, the influence of the preload level on the slip-resistant behaviour of the connection was already investigated in Chapters 3.2.10, 5.2 and 5.3. In these investigations, all tests were performed with Bumax 109 bolting assemblies with a preload level of $F_{p,C}$ = 110 kN. Only one test series was conducted with Bumax 88 bolting assemblies with the preload level of $F_{p,C}$ = 88 kN.

In order to finalize the slip factor for this test series (D_thhR+fP10_B88), three extended creep tests were carried out. As can be seen in Figure 5-31 (c), the extended creep tests failed for both $0.75 \cdot F_{Sm}$ = 273.5 kN and $0.80 \cdot F_{Sm}$ = 291.7 kN load levels. For this reason, the load level was reduced to $0.70 \cdot F_{Sm}$ = 255.2 kN for the next extended creep test. The result shows that the slip was less than 0.3 mm when extrapolated to 50 years and the test could be considered as a passed test, see Figure 5-31 (c). The final slip factor based on this load level is equal to 0.73. As with coated carbon and stainless steel test specimens, the final slip factor was higher for test series with a lower preload level.

However, a closer look at the adequate load level for the extended creep tests ($F_{S,Final}$) makes it clear that higher $F_{S,Final}$ can be reached with a higher preload level. By considering Equation (3-3), it would be possible to confirm the positive influence of the higher preload level on the slip resistance of the connection.

(a) D_thhR test series

(b) D_thhR+fP10 test series

(c) D_thhR+fP10_B88 test series
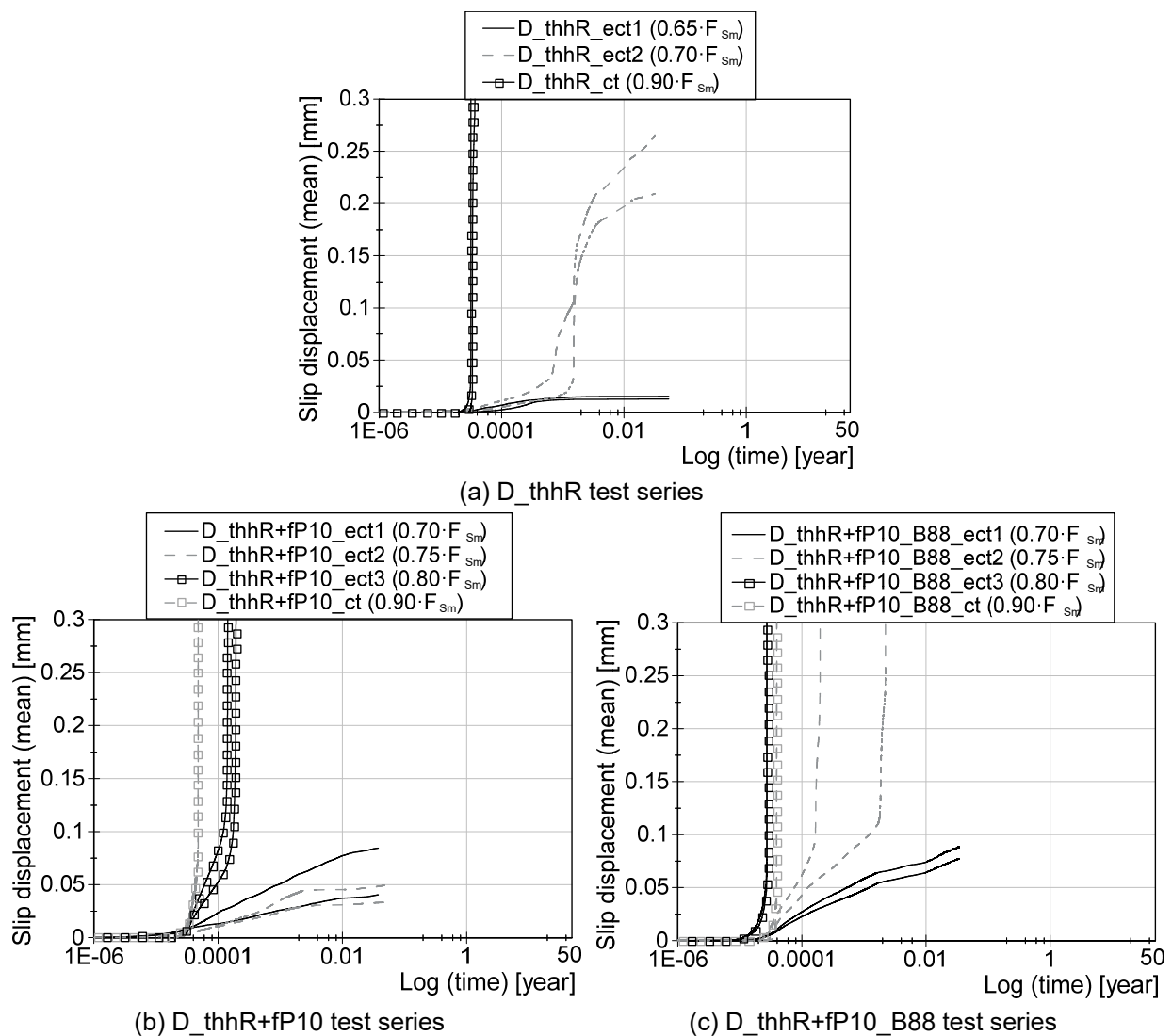
Figure 5-31: Evaluating the slip displacement-log time curves based on the results of the creep and extended creep tests for three test series made of duplex steel with a combination of resin and particles on the faying surfaces

This alternative preparation method was developed based on the experimental investigation of stainless steel bolted connections, but with some small modification it can also be used for carbon steel bolted connections. As the results show, adding a thick layer of resin around the holes, fully covered with GRITTAL GH-10 particles, would be a very convenient way to improve the slip-resistant behaviour of the connection significantly.

5.5 Conclusion

In general, the slip-resistant behaviour of bolted connections is mainly influenced by two main parameters: the condition of the faying surfaces and the preload level in the bolts. Different guidelines/standards specify the slip factor only for slip-resistant connections made of carbon steel with some specific surface conditions. However, none of them recommend any slip factor for slip-resistant connections made of stainless steel. As is known, stainless steel alloys suffer more from time-dependent viscoplastic deformation than carbon steel. This could lead to higher preload losses

or some additional microstructural deformations between the faying surfaces over a long period of time which could consequently result in lower slip factors than already achieved for carbon steel connections with comparable surface treatment.

For this reason, a comprehensive investigation was conducted on slip-resistant connections made of different grades of stainless steel with different surface treatments and preload levels. The results show a very promising slip-resistant behaviour for these connections. The condition of the faying surfaces still plays a determinative role in the slip-resistant behaviour of the connections. The results also show the importance of the topography of the faying surfaces. Having the same roughness value for the faying surfaces would not result in the same slip factors for these surfaces. For instance, grit blasted faying surfaces with sharp asperity would provide better mechanical interlock on the surfaces which consequently leads to a higher slip factor in comparison with shot blasted faying surfaces.

Blasting of the stainless steel plates is a challenging procedure. During the blasting procedure, small particles might be implanted in the surfaces. Selecting an inappropriate blasting media would increase the galvanic corrosion susceptibility of the stainless steel material. For this reason, choosing a suitable blasting media is very important. Even with a suitable blasting media, it might still not be possible to reach a desirable roughness value by the blasting process since, in general, the hardness of stainless steel is higher compared to carbon steel. For this reason, selecting a suitable coating might make it possible to improve the slip-resistant behaviour of the connection. A suitable coating for stainless steel is also very important in order to prevent any galvanic corrosion. However, this phenomenon was not the focus of this study. In the frame of this study, the thermal aluminium spray metallized surface finish was selected in order to improve the slip-resistant behaviour of the connection. The results show that the slip-resistant behaviour has noticeably improved for different stainless steel grades with thermal aluminium spray metallized surface finish.

Additional surface preparation for the faying surfaces always costs money and time. An innovative method to reduce these two important factors would therefore always be appreciated. Another aim of this study was to develop a method for improving the slip-resistant behaviour of the connection without additional preparation of the faying surfaces. For this purpose, two simple elements were selected to be added to the faying surfaces: resin and particles. To prevent any galvanic corrosion in the connection, stainless steel particles were selected. Different patterns for application of these two elements were tested. The results show a significant improvement compared to test series with as-received/1D surface condition. The best method for the application of the resin and particles between the faying surfaces can be described as follows: Adding enough resin on the faying surfaces, specifically around the holes, and covering the surface of the resin with particles would give the mixture

a chance to flow into and completely fill the hole clearance in a similar way to injection bolts according to EN 1090-2. After the curing time for the resin, the slip in the connection will only happen with compression of the hard mixture of resin and particles in the hole clearance whereby the slip-resistant behaviour of the connection will be increased considerably. It is also possible to mix the resin and particles before application and the results will be approximately the same. Only covering the surface of the resin with particles provides enough particles in the mixture to sufficiently increase the compressive strength of the mixture.

The loss of preload was considered in the determination of the final slip factors, as the extended creep tests were performed in those specific cases. However, the long-term losses of preload could be the biggest concern. For this reason, the relaxation behaviour of the connections was investigated in the first 24 hours, which is also the curing time for the resin, and it was extrapolated to 50 years in order to estimate the loss of preload during the service life of the structure. The results show that the estimated loss of preload after 50 years for all these test series with additional resin and particles between the faying surfaces is comparable with the results of uncoated/untreated preloaded bolted connections made of carbon and stainless steel.

6 Comparative investigation into the determination of slip factors according to different standards

6.1 General

Several standards specify slip factors for often-used surface conditions for carbon steel structures. For deviating conditions, slip factors can be determined experimentally according to the specified test procedures. However, not only the test procedure but also the test specimen geometry, clamping length, preload level, etc. vary between different standards/guidelines. Generally, the slip-resistant behaviour of bolted connections mainly depends on the condition of the faying surfaces and on the preload level in the bolts. These two parameters control the slip-resistant behaviour of the connections in a direct way. However, these two factors are not the only key parameters in the determination of the slip factor.

As many steel constructors operate internationally, it is of great interest to examine the comparability of these tests. In the frame of this investigation, the main focus is on the test procedure according to EN 1090-2, Annex G and RCSC, Appendix A [170]. Besides this comparison, an experimental investigation in the frame of the Euronorm project has also been carried out in order to compare the test procedure according to EN 1090 2, Annex G, and TL/TP-KOR-Stahlbauten, Annex E, Sheet 85 [107].

6.2 EN 1090-2 vs. RCSC (2014)

6.2.1 General

Before starting any numerical or experimental investigations, it was examined whether these two test procedures are theoretically comparable. To answer this question, a closer look was taken at the essential parameters of both test procedures. An experimental investigation was carried out by Maiorana et al. [171] in order to compare the determination of the slip factor according to both EN 1090-2 and RCSC. However the slip displacement in that study was measured at PE position. The results in Chapter 3.2.8 show that measuring the slip displacement at plate edges (PE position) may lead to a very conservative result for some surface conditions like grit blasted surfaces which can handle higher slip loads. For this reason, performing a comprehensive investigation to compare these two standards is still desired.

6.2.2 Theoretical comparison

The geometry of the test specimens, the type of bolts, the preload level, the clamping length ratio ($\sum t/d$) and the way of evaluating the slip factor are all important parameters in the experimental determination of the slip factor.

Each standard prescribes a test specimen geometry for determination of the slip factor. RCSC Appendix A prescribes a one-bolt (7/8 in. ≈ M22) test specimen, see Figure 2-11. EN 1090-2, Annex G meanwhile specifies a four-bolt M16 or M20 test specimen, see Figure 2-1. However, by considering the related bolt dimensions and the thickness of each clamped component, it can be seen that all test specimens according to both standards deliver the same clamping length ratio, see Table 6-1. As both standards prescribe a comparable preload level ($0.7 \cdot f_{ub} \cdot A_s$) for the determination of the slip factor, the relaxation behaviour in both tests would be comparable.

Table 6-1: Comparison of the key parameters between EN 1090-2 and RCSC (2014)

Parameters	EN 1090-2		RCSC 2014
Geometry			
Bolt dimension	M 16	M 20	7/8 in. (≈ M 22)
Type of test specimen	Four-bolt	Four-bolt	One-bolt
Clamping length ratio ($\sum t/d$)	2.5	2.4	2.5
Preload level			
Preload level	$F_{p,C}$	$F_{p,C}$	T_t
Test specification			
Type of static test	Tension	Tension	Compression/Tension
Type of creep/extended creep test	Tension	Tension	Tension
Slip factor (μ)	$\mu_i = \dfrac{\text{slip load}}{4 \cdot \text{preload level}}$		$k_s = \dfrac{\text{slip load}}{2 \cdot \text{clamping force}}$
Number of static tests	4		5
Number of creep tests	1		- [*)]
Number of extended creep tests	3		3
Slip criterion for static test	0.15 mm		0.02 in. (≈ 0.51 mm)
Slip criterion for creep test	0.002 mm		-
Slip criterion for extended creep test	Displacement during the design life ≤ 0.3 mm		First step: 0.005 in (≈ 0.127 mm)
			Second step: 0.015 in. (≈ 0.38 mm)

$F_{p,C} = T_t = 0.7 \cdot f_{ub} \cdot A_s$ (where: f_{ub} = tensile strength of the bolt and A_s = tensile stress area of the bolt) | $\sum t$: clamping length| d: bolt diameter

[*)] Note: the creep test mentioned in RCSC is more comparable with the extended creep test in EN 1090-2; for this reason, in the frame of this study the same naming according to EN 1090-2 has been selected for both test procedures.

The static tests according to EN 1090-2 must be carried out in tension. However, according to RCSC, it is possible to perform static tests in compression or in tension as long as the contact surface area per bolt remains the same. According to RCSC, during the short-term static tests (comparable with the static tests according to EN 1090-2) the preload level shall be maintained at a constant level, which might lead to a higher static slip factor. This means that the influence of the loss of preload will be considered in the determination of the final slip factor.

For the determination of the final slip factor, both standards specify a tension-type test for creep and extended creep tests. According to EN 1090-2, one creep test has to be performed with a constant load duration of at least three hours. When the creep test is successfully passed, the characteristic value of the slip factor μ shall be calculated as the 5 % fractile value with a confidence level of 75 %. Otherwise, at least three extended creep tests must be performed. All three tests must be evaluated using an extrapolated slip displacement-log time curve. The test will be considered a passed test when the slip does not exceed 0.3 mm after extrapolation

to 50 years or the service life of the structure. In that case, the final slip factor shall be calculated based on the corresponding load level. The creep test according to RCSC is more comparable with the extended creep test according to EN 1090-2, as the duration of the test shall be at least 1000 hours. Three creep tests (extended creep test) must be performed with three tension-type specimens linked together with loose bolts as a single chain in order to have the same load level in all specimens. The test shall be done in two steps. In the first step, the specimens are loaded to a specific load level, calculated according to the Equation (2-12). The specimen should be loaded with the specified load level for at least 1000 hours. The difference between the slip after 0.5 hours and 1000 hours after application of the constant load does not exceed 0.005 in. (0.127 mm). If this is the case, the first step of the creep test can be considered as passed and the specimen shall be loaded in tension to the final load level ($R_{s,final}$) according to Equation (2-13). According to RCSC, the average relative slip displacement at the moment of reaching that load level shall be less than 0.015 in. (0.38 mm) for all three extended creep tests. Otherwise, the coating will be considered to have failed to meet that slip factor. As can be seen, unlike EN 1090-2, the load will not be kept constant at the final load level. In addition, the extended creep test evaluation criterion according to EN 1090-2 is smaller than in RCSC. The parameters may result in lower or equal slip factors compared to RCSC.

On the other hand, based on RCSC test procedure, the slip factor shall not be greater than 0.5; EN 1090-2 does not have such a limitation. This could lead to a very conservative result for the surface conditions with very high slip-resistant capacities. This limitation was not considered in this investigation, since the aim of the study was to investigate the comparability of the test procedures.

6.2.3 Numerical investigation

In the frame of this investigation, comparative numerical investigations have been carried out into the determination of slip factors for slip-resistant connections between EN 1090-2, Annex G, and RCSC, Appendix A. For this reason, four different numerical models were developed based on standard test specimen geometries from both standards, see Table 6-2. Both test specimens according to EN 1090-2 were modelled as a quarter of an entire model as described in Chapter 3.2.9.3, see Figure 3-17. However, the test specimens according to RCSC were modelled as a half part of an entire model since the geometry was symmetrical only along the longitudinal axis, see Figure 6-1 (a). The M22 bolt was modelled according to ASME B18.2.6M [172] and the bolt grade was defined based on ASTM F3125 [173] with grade of A490. The washers and nuts were also modelled according to ASTM F436M [174] and ASTM A563M [175] respectively, see Figure 6-1 (b). As already explained in Chapter 3.2.9.3 for both M20 and M16 test models, the HV bolting assemblies according to EN 14399 with property class 10.9 were selected, see Figure 6-1 (c) and (d).

Table 6-2: Numerical test results according EN 1090 2 vs. RCSC (2014)

Series ID	$\Sigma t/d$ [1] [-]	Type of test	$\mu_{nom,mean}$[2] [-]	$\mu_{ini,mean}$[3] [-]	$\mu_{act,mean}$[4] [-]
FEM analyses results (calibrated based on GB-III test series, see Table 3-2)					
EN1090_M16	2.5		0.72	0.73	0.84
EN1090_M20	2.4	Tension	0.73	0.73	0.85
RCSC_M22_T	2.5		0.76	0.75	0.84
RCSC_M22_C		Compression	0.84	0.82	0.89

[1] clamping length ratio (Σt: clamping length, d: bolt diameter) [2] $\mu_{nom,mean}$: calculated slip factors as mean values considering the nominal preload level [3] $\mu_{ini,mean}$: calculated slip factors as mean values considering the initial preload when the tests start [4] $\mu_{act,mean}$: calculated slip factors as mean values considering the actual preload at slip
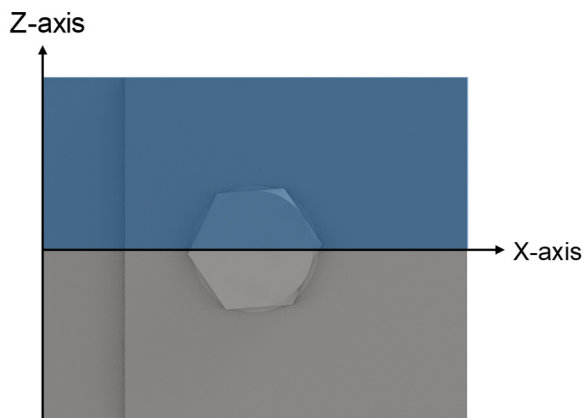
(a) Symmetry of the one bolt test specimen model
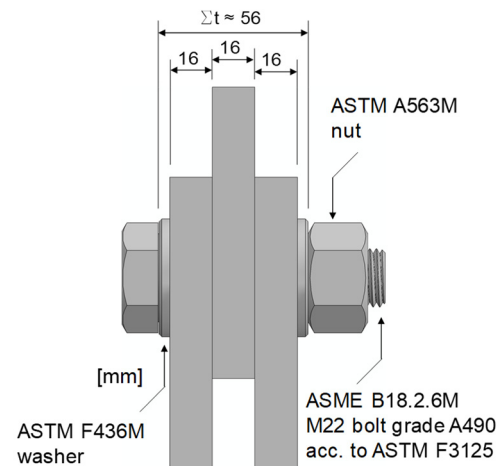
(b) M22 test specimen model acc. to RCSC
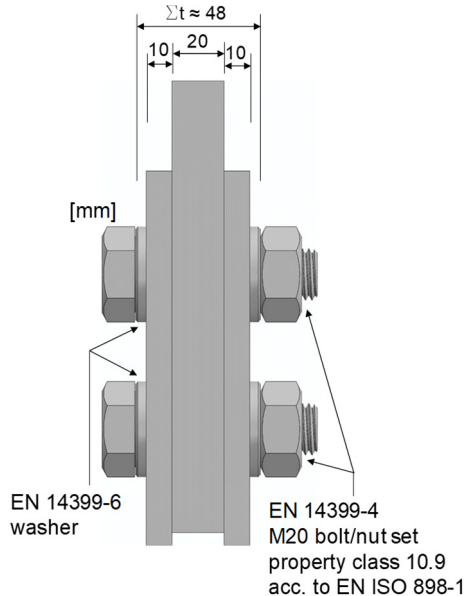
(c) M20 test specimen model acc. to EN 1090-2
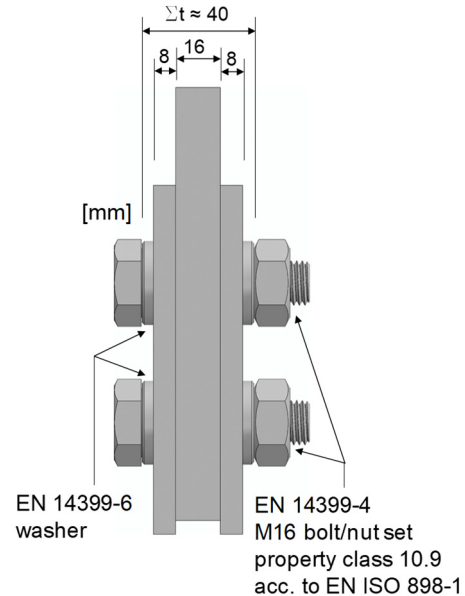
(d) M16 test specimen model acc. to EN 1090-2

Figure 6-1: Symmetry of one-bolt test specimens and developed model acc. to both standards

The preload level in all models was selected as $F_{p,C} = T_t = 0.7 \cdot f_{ub} \cdot A_S$ (where f_{ub} is the tensile strength of the bolt and A_S is the tensile stress area of the bolt) which was equal to 221 kN for M22 bolts according to AISC 360-16, 172 kN for M20 HV bolts and 110 kN for M16 HV bolts according to EN 1090-2.

This comparative study includes four different series as described in Table 6-2. Both models were analyzed in tension according to EN 1090-2. According to RCSC, as long as the contact surface area per bolt remains the same, the tests may also be performed in tension.

By this statement, the main parameter which may affect the slip-resistant behaviour of the connection is the contact surface area and performing the test in tension or compression by itself would not influence this behaviour. For this reason, two series of numerical analyses were conducted on two models with the same contact surface area per bolt, one in tension and the other in compression.

It is important to keep in mind that the final slip factor would not be determined based on static tests only. The creep test to finalize the results shall be conducted in tension according to RCSC. However, knowing the capacity of the test specimens in tension or compression will help to select a reasonable slip factor and consequently find the decisive load level for performing the creep tests.

(a) Load-slip displacement diagram   (b) Static slip factors
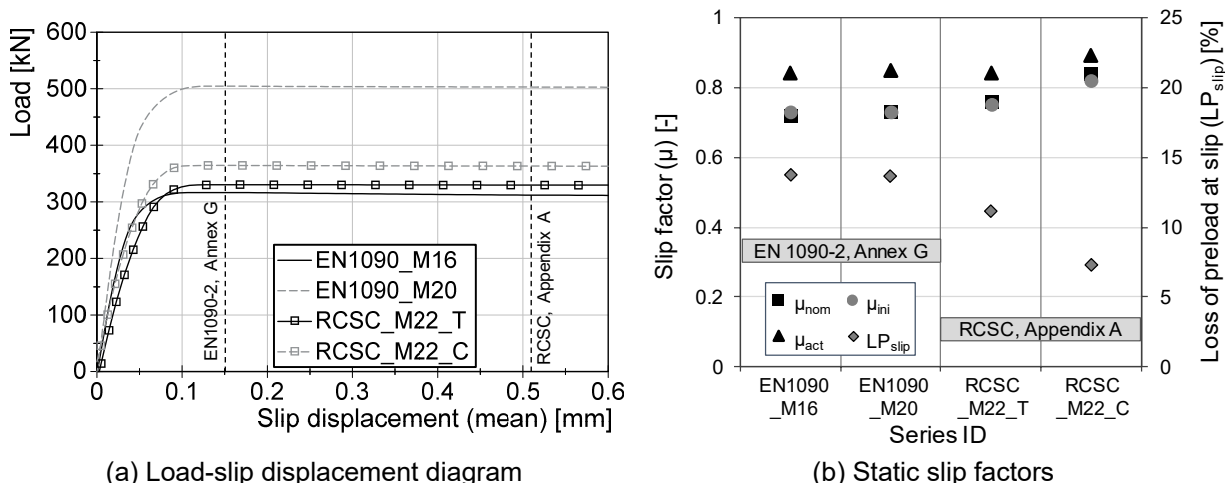
Figure 6-2: Comparison of the numerical results based on EN 1090-2 and RCSC models

The conducted numerical analyses were comparable with the static slip factor tests, since the factor of time (the long-term creep behaviour of the models) was not considered in this investigation.

In both standards different slip criteria are prescribed in order to evaluate the critical slip load which may lead to different static slip factors. However, the load-slip displacement diagram shows that the maximum slip load in these analyses occurred always before 0.15 mm and the load level remains constant or decreases slightly with increasing slip in the connection. This means that whichever slip criterion is selected, it would lead to the same results for the slip load, see Figure 6-2 (a).

The slip factors were calculated as nominal, initial and actual slip factor (explained in Chapter 3.2) and are summarized in Table 6-2 and Figure 6-2 (b). The results show that, as expected, both standard test specimens according to EN 1090-2 deliver the same slip factors. Meanwhile, the numerical analyses on RCSC test specimen geometry clearly show two different results.

Performing the analyses in compression lead to noticeably higher slip factors. However, performing analyses in tension leads to more or less comparable results with EN 1090-2 and delivers slightly higher nominal/initial slip factors. The reason for such results might lie in the geometry of the specimens, as the preload levels, the condition of the faying surfaces and the clamping length ratio are identical for both models.

In the standard test geometry according to EN 1090-2, the thickness of the cover plates is half of the bolt size, which is equal to 8 mm for M16 test specimens and 10 mm for M20 test specimens. On the other hand, the thickness of the cover plates is equal to 16 mm for the M22 test specimens according to RCSC.

Having higher cover plate thickness ratio leads to a larger active surface area between the faying surfaces, which could lead to a higher slip factor. However, in this case, increasing the active surface area was not significant in comparison to the size of the bolts. For this reason, slightly higher nominal/initial slip factors were observed for the RCSC model in tension in comparison with EN 1090-2. Having larger active surface areas between the faying surfaces leads to lower surface pressures in these areas and lower losses of preload at slip moment. For this reason, the calculated actual slip factor was approximately equal for both the EN 1090-2 model and the RCSC model in tension, see Figure 6-2 (b).

As can be seen in this figure, the highest slip factor was achieved by RCSC models analyzed in compression. The only difference between the RCSC models was the method of testing, so the most important question is: Why do the tests performed in compression lead to higher slip factors?

This question can be answered by taking a closer look at the analyzed models. Figure 6-3 shows the deformation in the Y-axis of the RCSC models in tension and compression.

As can be seen, in the model under tension load, the edges of the cover plates lift up slightly, perpendicular to the direction of the load. However, performing the analysis in compression does not show any uplifting of the cover plates. This phenomenon could cause a smaller active contact area between the faying surfaces and consequently lead to a lower slip load.

(a) Under tension   (b) Under compression
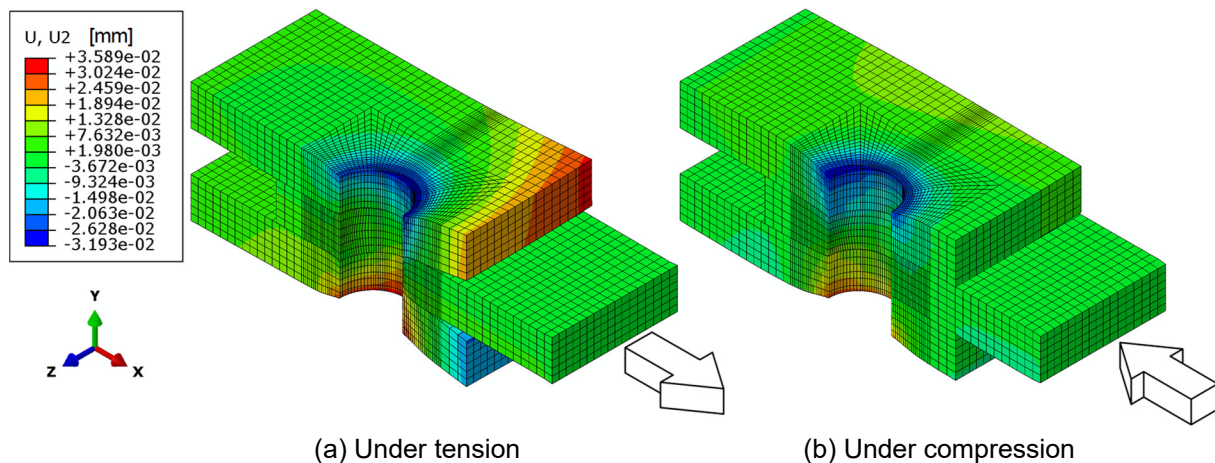
Figure 6-3: Deformed shape of the RCSC model under tension and compression with scale factor of 100

Many other parameters can still cause differences between the determined slip factors based on RCSC and EN 1090-2. For instance, having a coating as an additional layer between the faying surfaces, testing speed or considering different slip criteria may amplify/minify the effects of these parameters. Besides all these parameters, investigating the long-term behaviour of the connection is a very critical step, as the final slip factor shall be finalized based on creep/extended creep tests according to both standards. For this reason, performing an experimental investigation is mandatory in order to confirm the achieved results according to the numerical study as well as to investigate the long-term slip-resistant behaviour of the connection and to finalize the comparison of these two standards.

6.2.4 Experimental investigations on slip-resistant connections made of carbon steel

A comprehensive experimental investigation was conducted into the determination of slip factors according to several standards. This study focuses on European standard EN 1090-2, Annex G, and North American specifications RCSC, Appendix A. Both test procedures are explained in Chapters 2.4.2.2 and 2.4.9. According to RCSC, the test specimens shall be fabricated from a steel with minimum yield strength of between 36 ksi (248 Mpa) and 50 ksi (345 Mpa). According to EN 1090-2, carbon steel material shall meet the specifications according to EN 10025-2 and EN 10025-6. In order to cover the requirements of both standards, all test specimens were made of S355, which is comparable with steel with the minimum required yield strength according to RCSC.

The RCSC Specification and AISC 360-16 specify that the bolting assemblies with property classes of A325 or A490 shall be used in slip-resistant connections. ASTM F3125 covers chemical, physical and mechanical requirements of both property classes. By looking at the mechanical properties of these classes it can be seen that A325 and A490 are comparable with bolt property classes of 8.8 and 10.9 according to EN 1993-1-8, see Table 6-3. Besides this, both standards prescribe the same preload level for tightening of the high-strength bolts, which is equal to 0.70

times the tensile strength of the bolts. Table 6-4 presents the nominal preload level for different bolt sizes which are presented in both European and North American test procedures for the determination of the slip factor.

Table 6-3: Required mechanical property for specimens machined from bolts

	EN 1993-1-8		ASTM F3125	
Property class	8.8	10.9	A325	A490
Tensile strength - f_{ub} (MPa)	800	1000	830	1040
Yield strength - f_{yb} (MPa)	640	900	660	940

Table 6-4: Minimum preload level in kN

	EN 1090-2		AISC 360-16 / RCSC	
Bolt size	8.8	10.9	A325	A490
M16 (5/8 in.)	88	110	91	114
M20 (3/4 in.)	137	172	142	179
M22 (7/8 in.)	170	212	176	221

As the geometries of the test specimens (M16 or M20) which are specified in Annex G of EN 1090-2 have negligible influence on the determination of the slip factor, it was decided to choose the M16 specimen geometry for this comparative investigation, see Figure 2-1 (b). RCSC meanwhile prescribes only one test specimen geometry for 7/8 in. (M22) bolting assemblies, which was already presented in Figure 2-11. In the frame of this study, the bolts with property class 10.9 were chosen because they are comparable with A490 bolts according to ASTM F3125. RCSC also specifies the A490 bolts for performing the creep tests in the frame of the determination of the slip factor, since the loss of preload for these bolts is larger than that for A325 bolts.

In order to determine the slip factor according to RCSC, Appendix A, some small modifications were made to the way of performing the tests, whereby none of these modifications should have a decisive influence on the determination of the final slip factor. As mentioned in Chapter 2.4.9, the preload shall be applied through a 7/8 in. diameter threaded rod. The preload level shall be maintained constant during the static test with an accuracy of 0.5 kips (≈ 2 kN). However, due to the metric system, M22 bolting assemblies were selected instead of a 7/8 in. diameter threaded rod, since they are geometrically comparable, see EN 14399-4 and ASME B18.2.6M. From an engineering point of view there might not be any difference between using bolting assemblies or threaded rods since both target about the same specific preload level. As the geometry of the bolting assembly and the treaded rod/washer/nut set was the same, it was expected that both deliver the same amount of surface pressure between the faying surfaces. In the frame of this study, there was no attempt to keep the preload level constant during the static test. On the other hand, in the RCSC test setup, a tensioner shall increase the preload level during the static test, since the loss of preload occurs as the load level increases and the slip starts to happen in the test specimen. This reduction in preload level during the static slip factor test might lead to a lower slip load. Regardless of how to perform the static tests and the accuracy of measuring the preload or the constancy of the preload level

during the tests, the final slip factor shall be determined from the creep tests. In the creep test there is no need to keep the preload level constant and the loss of preload influences the load-bearing capacity of the connection. The results of the static tests could give an idea of how to select the right load level for subsequent creep tests. For this reason, it was decided not to keep the preload level constant during the static tests in order to have more realistic results and a better chance to choose an appropriate load level for the creep tests.

RCSC also prescribes that the preload of at least 49 kips (218 kN) shall be applied with an accuracy of ± 1 %, which means that A490 bolting assemblies with a minimum preload level of 218 kN should be used. For this reason, in the frame of this investigation, M22 10.9 HV bolting assemblies were selected in order to meet the RCSC requirements, see Figure 6-4.

(a) According to EN 1090-2, Annex G   (b) According to RCSC, Appendix A
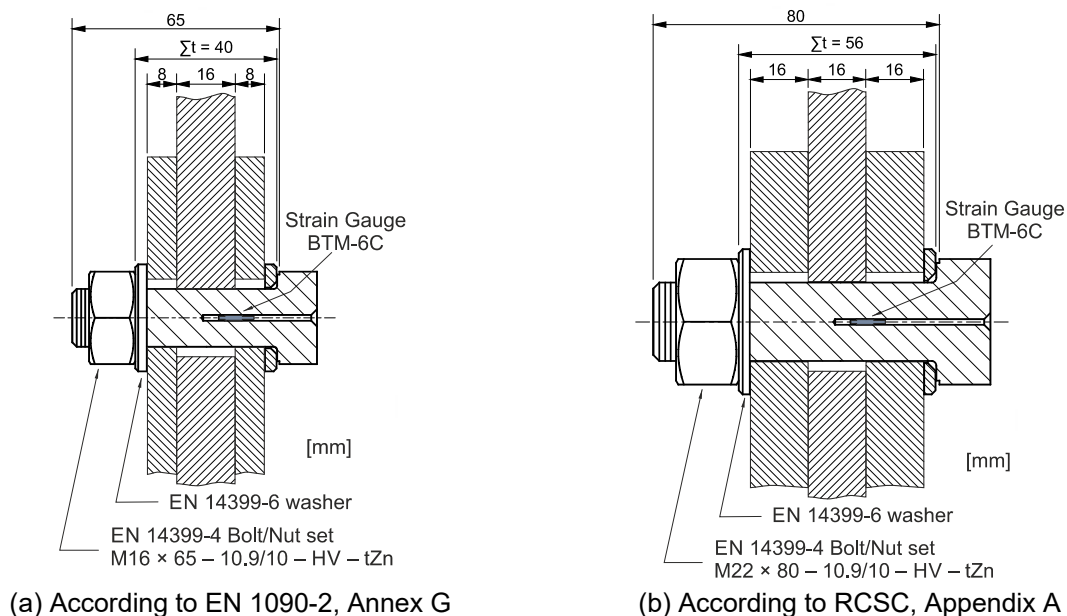
Figure 6-4: Clamped package according to EN 1090-2, Annex G, and RCSC, Appendix A

In the frame of this investigation, two different surface treatments were chosen for each standard test specimen geometry in order to investigate the influence of different test procedures on the determination of the slip factor, see Table 6-5.

All test specimens were blasted with brown corundum, f20, Al_2O_3 (aluminium oxide). The particle sizes were between 0.85 mm and 1.18 mm. All surfaces were blasted with 5 bars at a blasting angle of 90° in order to reach the highest roughness for the faying surfaces. The surface roughness was measured according to EN ISO 4287. For each test series, the mean roughness value (Rz) of the specimen's faying surfaces is presented in Table 6-5. Half of the test specimens according to each standard were coated with alkali-zinc silicate (ASI-Zn) coating. The coating thickness was measured according to EN ISO 2808. The mean dry film thickness (DFT) for each test series is presented in Table 6-5.

Table 6-5: Slip factor test results according to EN 1090 2 and RCSC (2014) for GB and ASI test specimens

Series ID	$Rz^{2)}$ [μm]	$DFT^{3)}$ [μm]	Loading method	Number of tests st/ct/ect[5]	$\mu_{nom,mean}$[6] st/st+ct [-]	$\mu_{ini,mean}$[7] st/st+ct [-]	$\mu_{act,mean}$[8] st/st+ct [-]	V (μ_{nom})[9] st/st+ct [%]	Final slip factor [-] $\mu_{5\%}$[10] / μ_{ect}[11]
				According to EN 1090-2, Annex G					
				Grit blasted surfaces (GB)					
EN1090_CS_GB-A	74	-	Disp. control	4/1/-	0.73/0.73	0.70/0.71	0.82/0.80	1.8/1.9	0.70/-
				Alkali-zinc silicate coating (ASI)					
EN1090_CS_ASI	75	104	Disp. control	4/1/3	0.69/-	0.69/-	0.82/-	2.1/-	-/0.62
				According to RCSC					
				Grit blasted surfaces (blasted with aluminium oxide) (GB-A)					
RCSC_CS_GB-A_I	70	-	Load control	5/-/3	0.80/-	0.82/-	0.90/-	6.7/-	-/0.72
				Alkali-zinc silicate coating (ASI)					
RCSC_CS_ASI_I	78	115	Load control	5/-/3	0.84/-	0.86/-	0.95/-	3.4/-	-/0.71
RCSC_CS_ASI_d			Disp. control	1/-/-	0.85/-	0.87/-	0.93/-	-/-	-/-

[1] Sa: surface treatment grade [2] Rz: surface roughness [3] DFT: dry film thickness (coating thickness)
[4] clamping length ratio (Σt: clamping length, d: bolt diameter)

EN 1090-2 does not specify any specific test speed for performing the static tests. It only states that the duration of a static test should be about 10 to 15 min. Based on the experience from previous chapters, it was decided to perform all static tests according to EN 1090-2 at normal speed of 0.01 mm/s (0.6 mm/min). Meanwhile, RCSC specifies that the loading rate shall not exceed 25 kips/minute (≈ 111 kN/min) nor 0.003 inch/minute (≈ 0.076 mm/min) until the slip load is reached. In order to have a comparable test result between both test procedures, it was decided to select the load speed so as to have approximately the same test duration for both test procedures. For this reason, the incremental tensile load was applied using load-controlled loading at normal speed of 400 N/s (24 kN/min). One test was also performed by applying displacement-controlled loading at normal speed of 0.001 mm/s (0.06 mm/min) in order to compare the slip-resistant behaviour of the connection under both load application methods, see Table 6-5.

In order to perform the static tests according to RCSC, Appendix A, a special testing adapter was developed as shown in Figure 6-5. With this adapter it was possible to mount the long LVDTs to the specimen.

RCSC prescribes that the relative slip displacement shall be measured on both sides of the specimen. For this reason, two LVDTs were mounted on both sides, see Figure 6-5 and Figure 6-6. Measuring the slip displacement in this way will help to eliminate the influence of any eccentricity on the slip-resistant behaviour of the connection.

(a) 3D test setup for static tests

(b) Experimental test setup for static tests
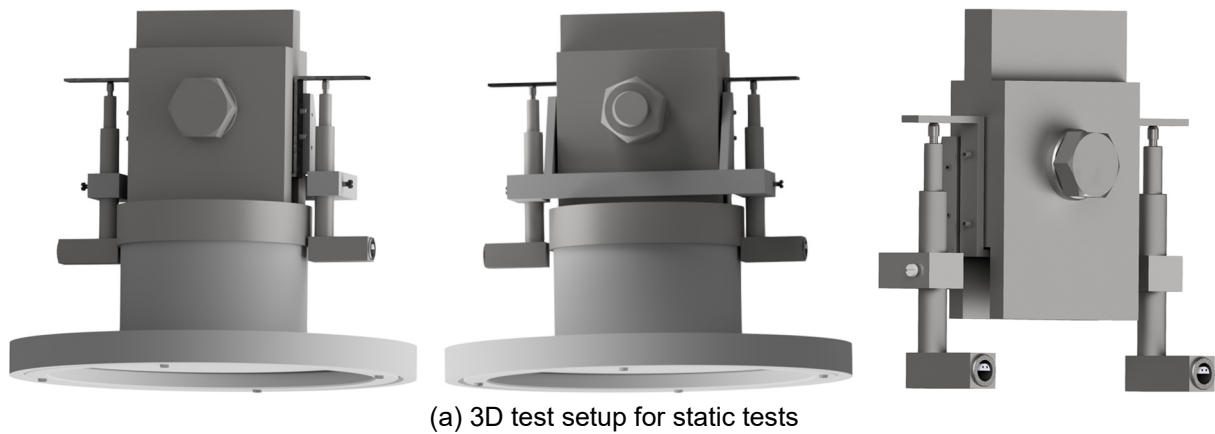
Figure 6-5: Testing adapter in order to perform the static tests according to RCSC, Appendix A

The creep tests according to RCSC were also carried out with three tension-type specimens as a single chain. Each test specimen was equipped with two LVDTs in order to measure the relative slip displacement accurately, see Figure 6-6.

The detailed information for performing the slip factor tests according to EN 1090-2, Annex G was already provided in Chapter 2.4.2. In all tests, the preload level was measured continuously by instrumented bolts with strain gauges, see Figure 3-1 and Figure 6-4. In the first step, four static tests were performed for each test series according to EN 1090-2, all results of which are presented in Table 6-5. For both the EN1090_CS_GB-A and EN1090_CS_ASI test series, four static tests according to EN 1090-2, Annex G were performed, the results of which are presented in Table 6-5. For both RCSC_CS_GB-A_I and RCSC_CS_ASI_I test series, five static tests were conducted. The load-slip displacement diagrams for a typical test from each test series are presented in Figure 6-7. As these diagrams show, the static test according to RCSC leads to higher slip factors in comparison to the EN 1090-2 test procedure for exactly the same surface preparation. This provides an interesting perspective for further consideration.
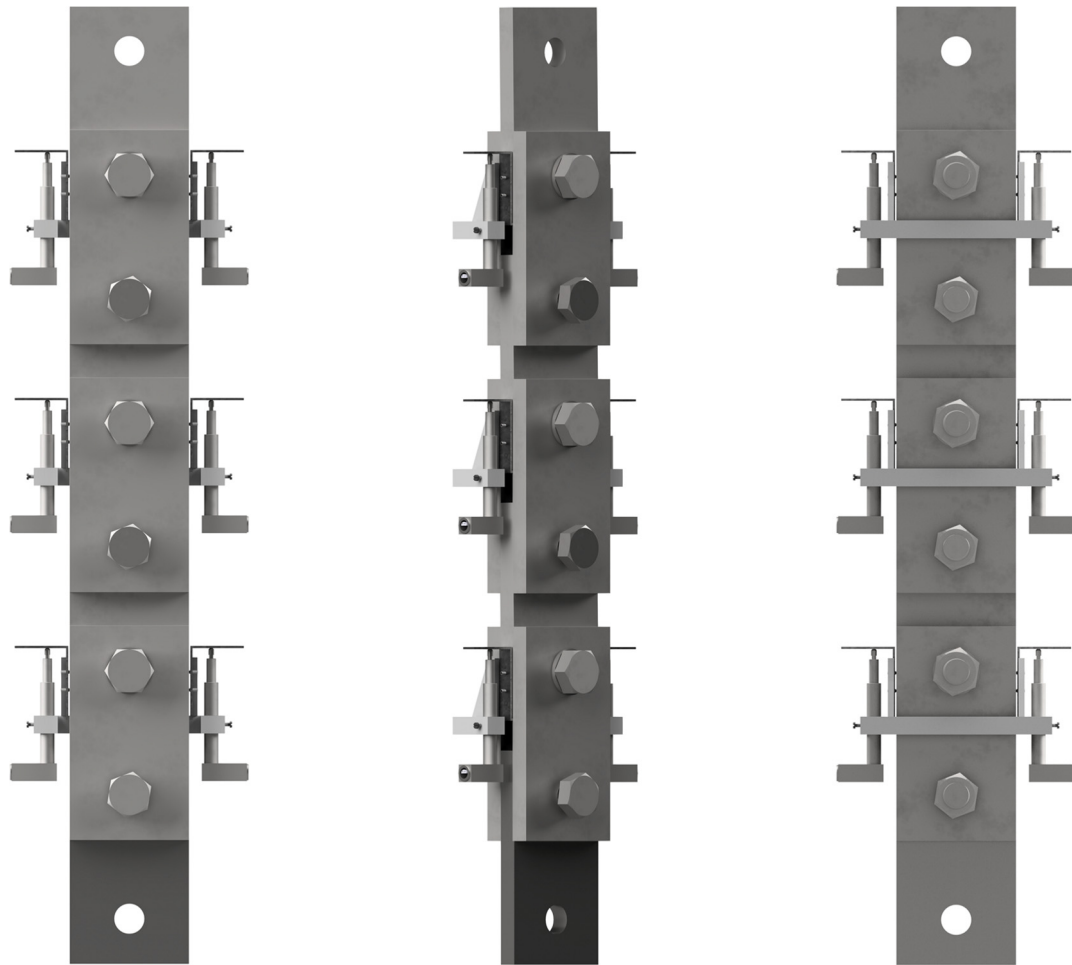
(a) 3D test setup for creep tests

(b) Experimental test setup for creep test

Figure 6-6: Position of LVDTs for creep test according to RCSC, Appendix A

Each test procedure represents a different slip criterion for the evaluation of the static slip factor. As can be seen in Figure 6-7 (a), having the same slip criterion at 0.15 mm leads to almost the same slip load for the test specimens with grit blasted faying surfaces. However, the RCSC test specimens show higher load-bearing capacity for a slip displacement higher than 0.15 mm. Besides this, the test specimen with ASI coating according to RCSC shows better slip-resistant behaviour nearly from the beginning of the test in comparison with the EN 1090-2 test specimen, see Figure 6-7 (b). This means that, besides the criterion for the evaluation of the slip factor, there are some other parameters that might have a direct influence on the slip-resistant behaviour of bolted connections.

The way of performing the static test is also an important parameter which can cause a decisive difference in the static slip factor, see Chapter 6.2.3.

(a) Grit blasted faying surfaces   (b) ASI coated faying surfaces
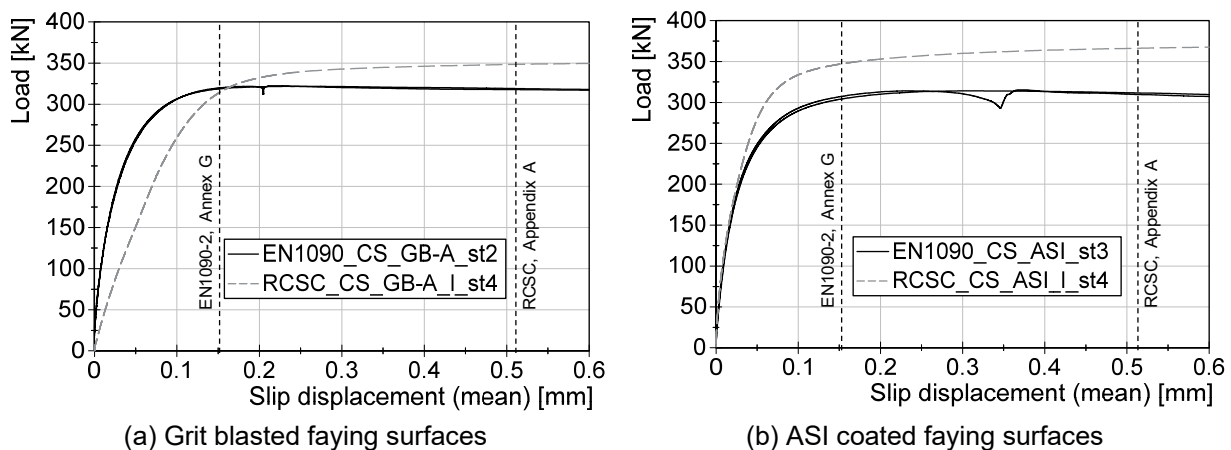
Figure 6-7: Load-slip displacement diagrams for grit blasted and ASI coated surface preparations according to EN 1090-2 and RCSC

The numerical investigations already confirmed that performing the tests in compression yields higher slip factors compared to the tests in tension. This phenomenon can also be observed in experimental results for the same surface preparation. The geometry of the specimens may also have an influence on the slip-resistant behaviour of the connection. According to EN 1090-2, the thickness of the cover plate is half of the diameter of the bolt; this is 8 mm for M16 test specimens and 10 mm for M20 test specimens. However, this value is slightly higher according to RCSC, at 16 mm for M22 test specimens. Having thicker cover plates leads to a larger active contact area between the faying surfaces, which might lead to higher slip loads with these test specimens. The numerical investigations have shown that the influence of having thicker cover plates in comparison with the bolt size will lead to slightly higher slip factors. However, the influence of this phenomenon is negligible compared to the influence of the way of performing the test in tension or compression.

RCSC, Appendix A specifies whether the static tests shall be performed load-controlled or displacement-controlled. However, EN 1090-2, Annex G does not specify any detail for the type of loading application. In order to investigate the

influence of the type of loading application on the slip-resistant behaviour of the connections, one additional static test according to RCSC on ASI coated specimens was performed. As mentioned before, the displacement-controlled test was performed at a speed of 0.06 mm/min. The load-controlled test, on the other hand, was performed at a speed of 400 N/S (24 kN/min), which is acceptable according to RCSC, Appendix A. Despite the small differences in the slip-resistant behaviour, the results show that both tests lead to the same slip load, see Figure 6-8 (a). Figure 6-8 (b) shows that the loading speed was much slower for displacement-controlled tests, where it took about 35 min to reach the slip load. However, for load-controlled tests the slip load was already reached in 15 min. The results show that for ASI-coated faying surfaces the test speed has no influence on the slip-resistant behaviour of the connection. This phenomenon was also confirmed for the results of the SIROCO project, see Chapter 3.2.5.

(a) Load-slip displacement diagram   (b) Load-slip displacement diagram
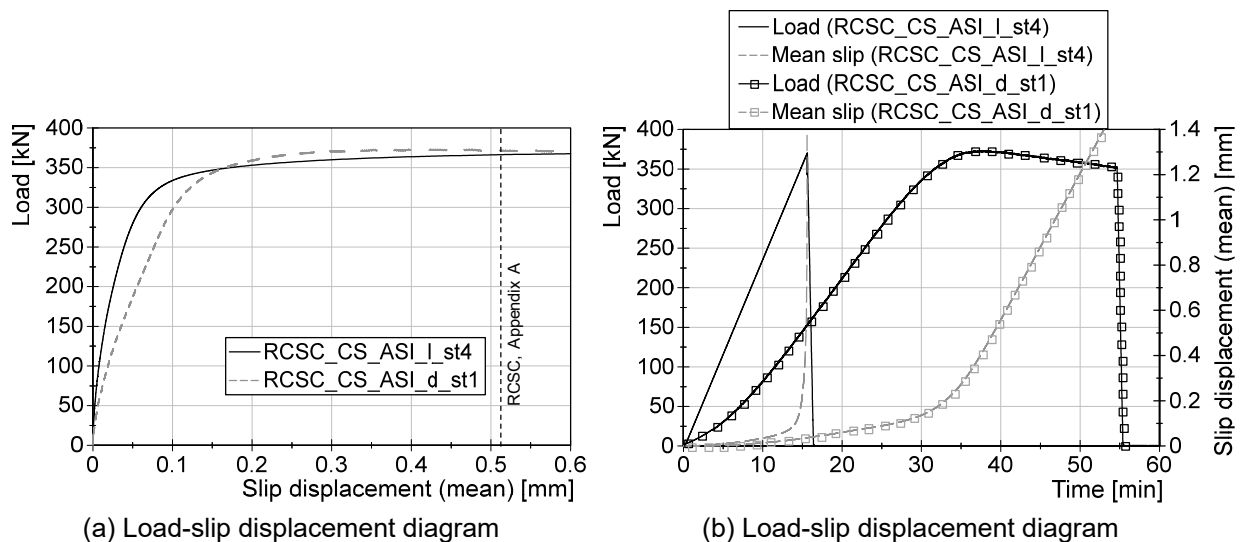
Figure 6-8: Influence of the type of loading application for ASI coated surfaces

In the second step for the determination of the slip factor according to EN 1090-2, Annex G, a creep test was conducted with 90 % of the mean slip load (F_{Sm}) of the first four static tests. The results show that the creep test was passed for grit blasted test specimens (EN1090_CS_GB-A test series), see Figure 6-9 (a). As can be seen in this figure, the differences between the recorded slip displacements at five minutes and at three hours after reaching the constant load level do not exceed 0.002 mm. For this reason, a static test was carried out in order to determine the last two slip loads. The results show that the coefficient of variation obtained from five tests does not exceed 8 %, see Table 6-5. That means the final slip factor shall be calculated as the 5 % fractile value with a confidence level of 75 %, which is equal to 0.70.

The creep test was also performed according to EN 1090-2, Annex G for ASI coated test specimens. As can be seen in Figure 6-9 (b), the creep test failed as the differences between the recorded slip displacements exceeded 0.002 mm and it was necessary to perform an extended creep test in order to finalize the slip factor.

(a) GB-A (grit blasted) test specimen   (b) ASI coated test specimen
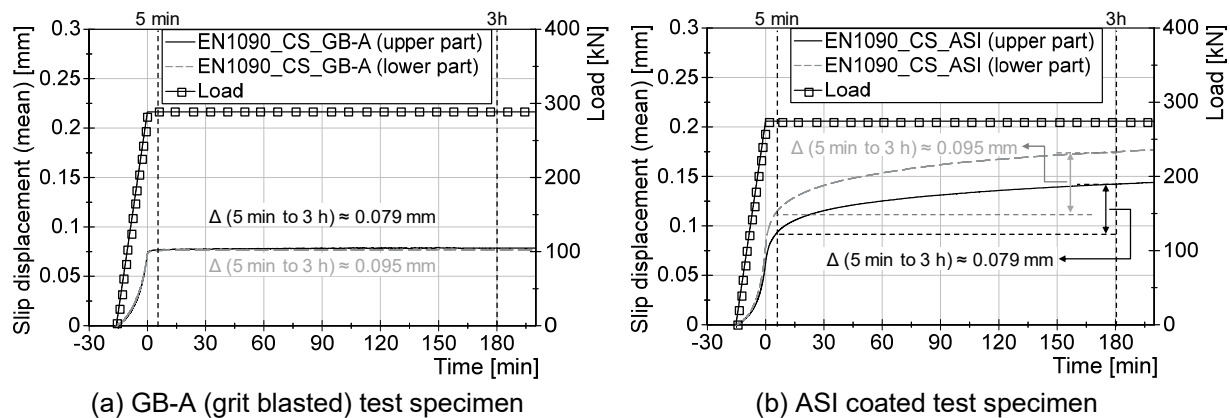
Figure 6-9: Creep test results for grit blasted and ASI coated surfaces according to EN 1090-2, Annex G

Evaluating the slip displacement-log time curve based on the results of the creep test shows that the load level for the creep test ($0.9 \cdot F_{Sm}$) might be suitable for performing the extended creep test. For this reason, two extended creep tests with the same load level were carried out. The results show that the mean relative slip displacements for both parts of the test specimens were less than 0.3 mm when extrapolated to 50 years and the tests can be considered as passed, see Figure 6-10.

(a) Test setup   (b) ASI-Zn-coated test specimen
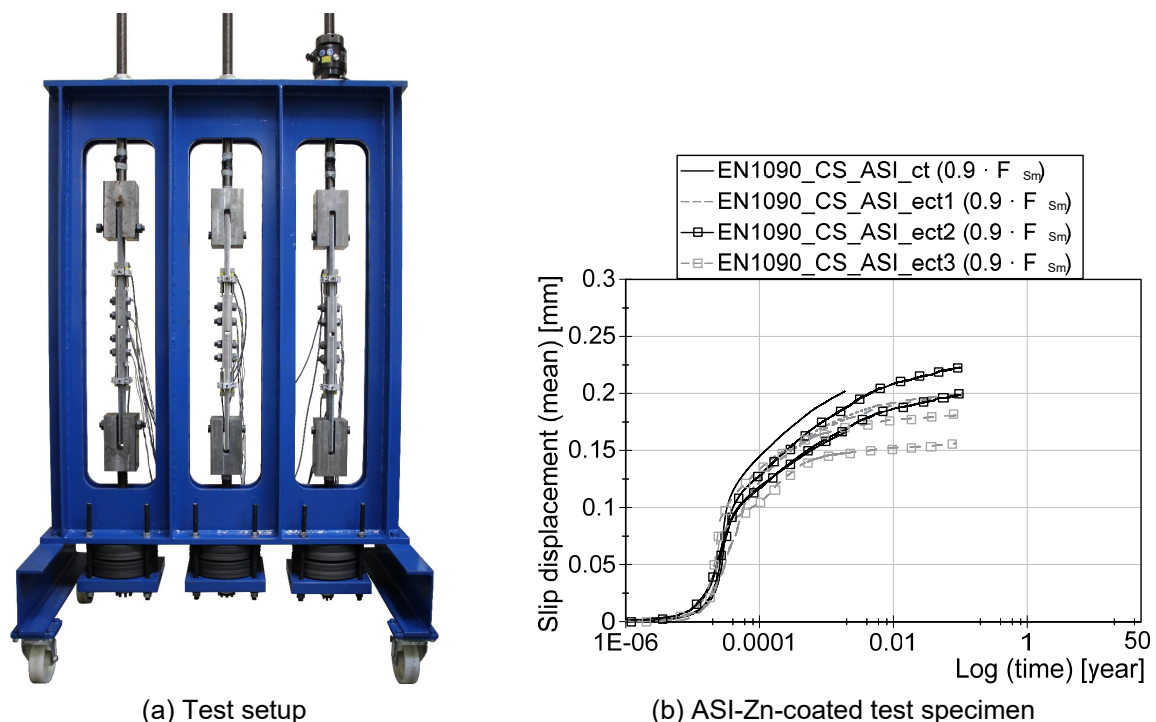
Figure 6-10: Extended creep test setup and results for ASI coated test specimen according to EN 1090-2, Annex G

According to RCSC, Appendix A, in the second step the creep test (which is comparable with the extended creep test according to EN 1090-2) shall be performed with three tension-type specimens linked together as a single chain, see Figure 2-12. The creep test shall be performed in two loading steps. The load levels for the creep test shall be determined based on the particular slip factor category (which should

not be greater than 0.5) under consideration of Equation (2-12) and Equation (2-13). However, choosing 0.5 as the maximum slip factor for the considered surface preparations leads to very conservative results which are not comparable with the results according to EN 1090-2.

The aim of this investigation was to evaluate the comparability of the determined slip factors according to these test procedures. For this reason, the particular slip factor for the determination of the load level for the creep test was selected in a way that shows the real capacity of the surface preparation. For this reason, for grit blasted surface treatment the particular slip factor based on 90 % of the mean slip load of the first five static tests was determined to be 0.72. For ASI-coated test series the particular slip factor based on 85 % of the mean slip load was selected as 0.71. The reason for this decision was based on the results of the static tests. As can be seen in Table 6-5, performing the static test in compression according to RCSC leads to higher static slip factors in comparison with EN 1090-2 for both surface preparations. However, this increase in the static slip factors is much higher for the ASI-coated test series. For this reason, it was expected that using 90 % of the mean slip load from the first five static tests would be too high for performing the creep test in tension according to RCSC.

Based on the selected slip factor and Equation (2-12), an adequate load level was calculated for the first step of the creep tests. As can be seen in Table 6-6, the differences between the slip displacements at 30 min and 1000 hours after reaching the constant load do not exceed 0.005 in. (0.127 mm) for all creep tests for both surface treatments. For this reason, in the second step the specimens were loaded again in tension to a load level based on Equation (2-13). As can be seen in Table 6-6, the slip displacements for all test specimens did not exceed 0.015 in. (0.381 mm). Consequently, the selected slip factors are considered to be the final values for both test series.

Table 6-6: Creep test results for carbon steel test specimens with different surface treatments according to RCSC Appendix A

Series ID	Test number	First step load level [1]	Slip (mean) Δ (0.5 h to 1000 h) [2]	Second step load level [3]	Slip (mean) at the second step load level	Final slip factor [-] (μ_{ct})
Grit blasted test specimens (GB-A)						
RCSC_CS_GB-A_I	ct1	210.5	0.0010	315.7 [4]	0.12	0.72
	ct2		0.0012		0.15	
	ct3		0.0001		0.13	
Alkali-zinc silicate coated test specimens (ASI)						
RCSC_CS_ASI_I	ct1	206.5	0.017	309.7 [5]	0.20	0.71
	ct2		0.012		0.09	
	ct3		0.022		0.10	

[1] based on Equation (2-12) | [2] difference between the slip displacement at 30 min and 1000 hours after reaching the constant load | [3] based on Equation (2-13) | [4] $\approx 0.9 \cdot F_{Sm}$ of first five static tests | [5] $\approx 0.85 \cdot F_{Sm}$ of first five static tests

Figure 6-11 (a) shows a very low creep sensitivity for grit blasted test specimens in the first step. However, in the second step after reaching the second load level and keeping the load constant at that load level, two of three test specimens slip through.

This means that if the tests are evaluated according to EN 1090-2 and loaded directly to the final load level, there is a very high chance that the test specimens will slip through, Figure 6-11 (b).

Figure 6-12 (a) shows the creep test results for ASI-coated test series. Like creep tests for grit blasted test series, the ASI-coated test specimens show very low creep sensitivity in the first step. After reaching the second load level, one of the test specimens slips through. This shows that the load level of $0.85 \cdot F_{Sm}$ might still not be suitable for performing the test according to EN 1090-2, see Figure 6-12 (b). However, the selected load levels seemed to be suitable load levels for performing the creep test according to RCSC, see Table 6-6. This result can be explained by the way of determining the mean slip load based on the static tests, since according to RCSC all static tests were performed in compression, which consequently led to higher mean slip loads in comparison to EN 1090-2. On the other hand, unlike EN 1090-2, according to RCSC the load level in the creep tests was not kept constant at the final load level. Here, only the average slip displacements that occur at this load level shall be less than 0.015 in. (0.38 mm) for all three test specimens. This criterion is already higher than the criterion of 0.3 mm for the extended creep tests according to EN 1090-2. All these factors lead to higher slip factors according to RCSC for the same surface preparation. That means the delivered results according to EN 1090-2 are more conservative in comparison with RCSC. For the ASI-coated test series it is still possible to perform the creep tests with a higher load level to achieve higher slip factors. However, no more tests were conducted, since it was not expected to achieve any noticeable improvement in the determination of the slip factor.

Figure 6-13 summarizes all the test results according to both standards. As can be seen in this figure, testing according to RCSC clearly leads to higher static slip factors for both surface treatments. The results also show that the achieved final slip factor according to RCSC is higher in comparison with EN 1090-2 for the same surface treatment. This difference is smaller for uncoated (grit blasted) surfaces, since the grit blasted surfaces are not at all creep-sensitive. According to the EN 1090-2 test procedure, the final slip factor was calculated based on a passed creep test as the 5 % fractile value from 10 test results. There was no need to perform any extended creep tests with reduced load level. For this reason, the difference between the final slip based on both standards for grit blasted surfaces is negligible.

(a) Slip displacement/load-time curve

(b) Slip displacement-log time curve
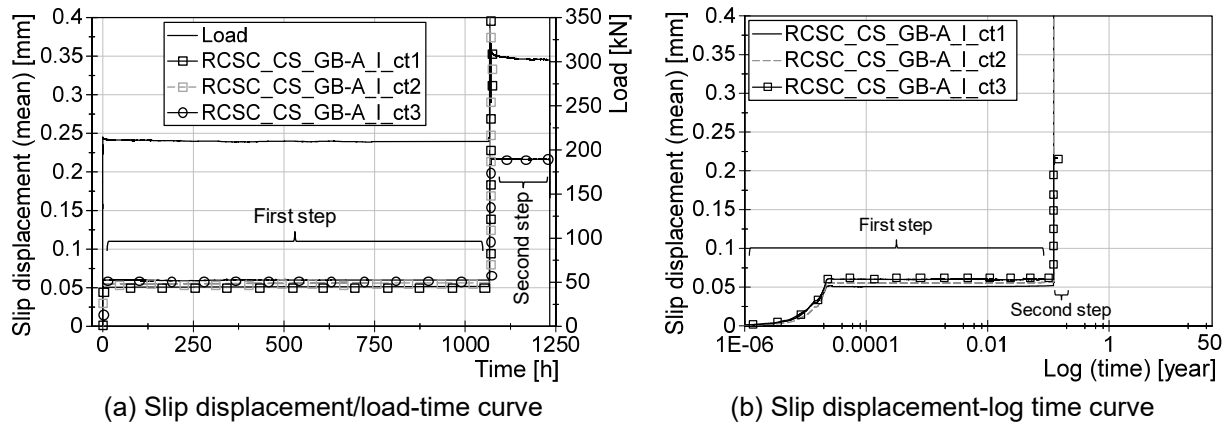
Figure 6-11: Creep test results for GB-A coated test specimen according to RCSC Appendix A

(a) Slip displacement/load-time curve

(b) Slip displacement-log time curve
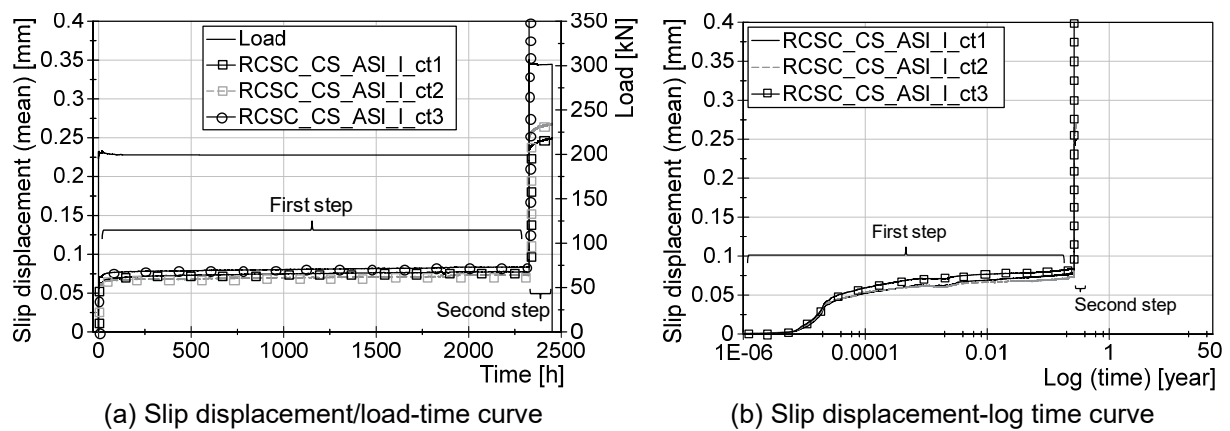
Figure 6-12: Creep test results for ASI coated test specimen according to RCSC Appendix A

(a) Test chain setup according to RCSC, Appendix A

(b) Static and final slip factors according to two different test procedures
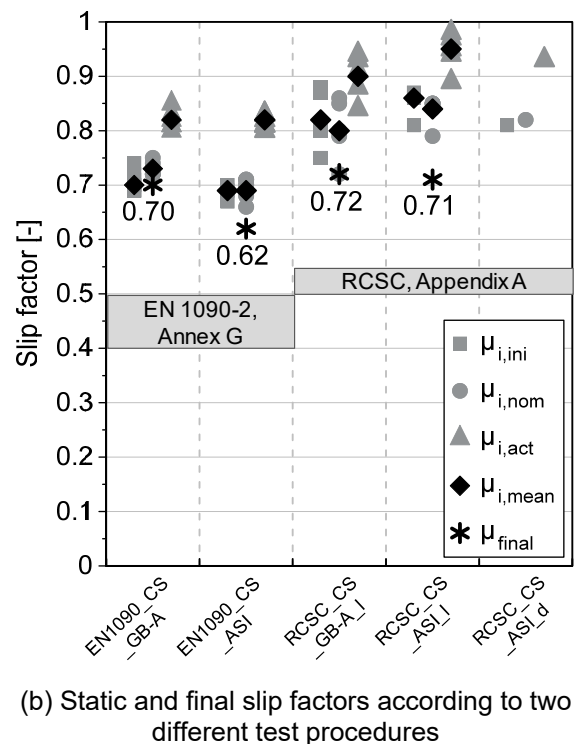
Figure 6-13: Creep test setup according to RCSC Appendix A, and static and final slip factors according to EN 1090-2 and RCSC test procedures for carbon steel connections

6.2.5 Experimental investigation on slip-resistant connections made of stainless steel

Like for EN 1090-2, the slip factors presented in RCSC are valid only for slip-resistant connections made of carbon steel. For this reason, slip factors for slip-resistant connections made of stainless steel have to be determined experimentally for each surface condition. Therefore, an individual experimental investigation was required to fill the gap in knowledge regarding their significance and to improve the test procedure for implementation in RCSC. Within the scope of this study, an investigation into the determination of slip factors according RCSC Appendix A were carried out on three different stainless steel grades (austenitic (1.4404) (A), duplex (1.4462) (D), lean duplex (1.4162) (LD)) considering two different faying surface conditions (as delivered/rolled (1D) and grit blasted (GB-A)). In total, seven different test series were conducted. Three different test series were performed on 1D surface condition. One additional static test was also performed on a lean duplex test specimen with 1D surface condition without removing the burrs around the holes (1D-B). Finally, three test series were performed with the grit blasted faying surfaces. The results are compared with the results of tests according to EN 1090-2 with comparable surface conditions, see Table 6-7.

Table 6-7: Slip factor test results according to EN 1090-2 and RCSC (2014) for stainless steel bolted connections

Series ID	Rz[1] [µm]	Loading method	Number of tests st/ct/ect[2]	$\mu_{nom,mean}$[3] st/st+ct [-]	$\mu_{ini,mean}$[4] st/st+ct [-]	$\mu_{act,mean}$[5] st/st+ct [-]	V (μ_{nom})[6] st/st+ct [%]	Final slip factor [-] $\mu_{5\%}$[7] / μ_{ect}[8]
According to EN 1090-2, Annex G								
As rolled (1D)								
A_1D_B109*	24	Disp. control	4/2/2	0.19/-	0.20/-	0.20/-	2.9/-	-/0.16
D_1D_HV10.9	26	Disp. control	4/1/-	0.24/0.25	0.24/0.25	0.25/0.25	4.3/4.7	0.22/-
LD_1D_B109	27	Disp. control	2/1/-	0.25/-	0.25/-	0.25/-	2.1/-	0.22/-
LD_1D_HV10.9		Disp. control	4/1/-	0.26/0.26	0.26/0.26	0.27/0.27	5.0/4.5	0.24/-
Grit blasted surfaces (GB-A)								
D_GB-A_HV10.9	76	Disp. control	4/1/-	0.72/0.72	0.71/0.71	0.80/0.81	2.7/2.9	0.68/-
According to RCSC								
As rolled (1D)								
RCSC_A_1D	25	Load control	5/-/3	0.26/-	0.26/-	0.27/-	5.9/-	-/0.23
RCSC_D_1D	27	Load control	5/-/3	0.24/-	0.24/-	0.24/-	4.9/-	-/0.22
RCSC_LD_1D	23	Load control	5/-/3	0.26/-	0.25/-	0.26/-	4.2/-	-/0.23
RCSC_LD_1D-B		Load control	1/-/-	0.34/-	0.34/-	0.34/-	-/-	-/-
Grit blasted surfaces (GB-A)								
RCSC_A_GB-A	75	Load control	5/-/3	0.79/-	0.80/-	0.87/-	1.4/-	-/0.71
RCSC_D_GB-A	78	Load control	5/-/3	0.82/-	0.83/-	0.88/-	3.1/-	-/0.74
RCSC_LD_GB-A	73	Load control	5/-/3	0.78/-	0.79/-	0.84/-	5.3/-	-/0.70

[1] Rz: surface roughness | [2] st: static test/ct: creep-/ect: extended creep test | [3] $\mu_{nom,mean}$: calculated slip factors as mean values considering the nominal preload level | [4] $\mu_{ini,mean}$: calculated slip factors as mean values considering the initial preload when the tests start | [5] $\mu_{act,mean}$: calculated slip factors as mean values considering the actual preload at slip | [6] V: coefficient of variation for μ_{nom} | [7] $\mu_{5\%}$: slip factors as 5 % fractile calculated on the basis of the static tests and the passed creep test | [8] μ_{ect}: slip factor resulting from the passed extended creep test

Note: The creep test according to RCSC is more comparable with the extended creep test according to EN 1090-2. For this reason, μ_{ect} for RCSC means the results of the creep test.

All GB-A test series were blasted with brown corundum (aluminium oxide) with the same specification as described in Chapter 5.2. For this reason, these test series

were compared with the results of the duplex test series with the same blasting specification. The test specimens that were blasted with brown corundum showed a noticeably better slip-resistant behaviour in comparison with test specimens blasted with GRITTAL GM. Slip factor tests were performed using predefined standard specimens according to RCSC Appendix A as shown in Figure 2-11. Since the 7/8 in. A490 high-strength bolting assemblies were not available, similar HV M22 bolting assemblies with property class 10.9 were selected, see 6.2.4. The combination of bolted assemblies made of carbon steel and stainless steel plates might lead to galvanic corrosion in the connection. However, the corrosion resistance of the connection was not within the main scope of this investigation. Furthermore, the results in Chapter 5.2 show that using bolting assemblies made of carbon steel in slip-resistant connections made of stainless steel has no influence on the slip-resistant behaviour of the connection. The preload in the bolts was measured continually during the test by strain gauges implanted inside the bolt shank, see Figure 3-1.

In the first step the static tests were performed for all test series according to RCSC Appendix A by applying load-controlled loading at normal speed of 400 N/s (24 kN/min). Figure 6-14 shows typical load-slip displacement diagrams for two different investigated surface conditions according to different testing procedures. As can be seen in Figure 6-14 (a), approximately the same slip loads were achieved for the test specimens with 1D faying surfaces and different steel grades. The results also show that the influence of performing the tests under compression according to RCSC, is quite negligible for 1D surface condition compared to performed tests in tension according to EN 1090-2. As can be seen in Figure 6-14 (a) and also presented in Chapter 5.2, the presence of burrs around the holes improved the slip-resistant behaviour of the connection. However, the tendency towards higher slip load becomes more visible for grit blasted surfaces, see Figure 6-14 (b). A closer look at this diagram also shows that considering different slip criteria can lead to different slip factors. Considering the 0.15 mm slip criterion leads to approximately the same slip load for all tests. However, considering 0.51 mm results in higher slip load for RCSC test series. On the other hand, for 1D faying surfaces, it seems that considering different slip criteria has no influence on the determination of the slip load, see Figure 6-14 (a). In the second step, the creep tests according to RCSC were performed on six test series. The slip factors were selected based on 90 % of the mean slip load from the first five static tests. The load levels for the first and second step of the test were then calculated based on Equation (2-12) and Equation (2-13) respectively, see Table 6-8. Figure 6-15 illustrates the creep test results for all three different stainless steel grades with 1D surface condition. As can be seen in this figure, all test series show very low creep sensitivity in both steps of the tests. Only one austenitic test specimen was slipped through a few moments after reaching the second load level.
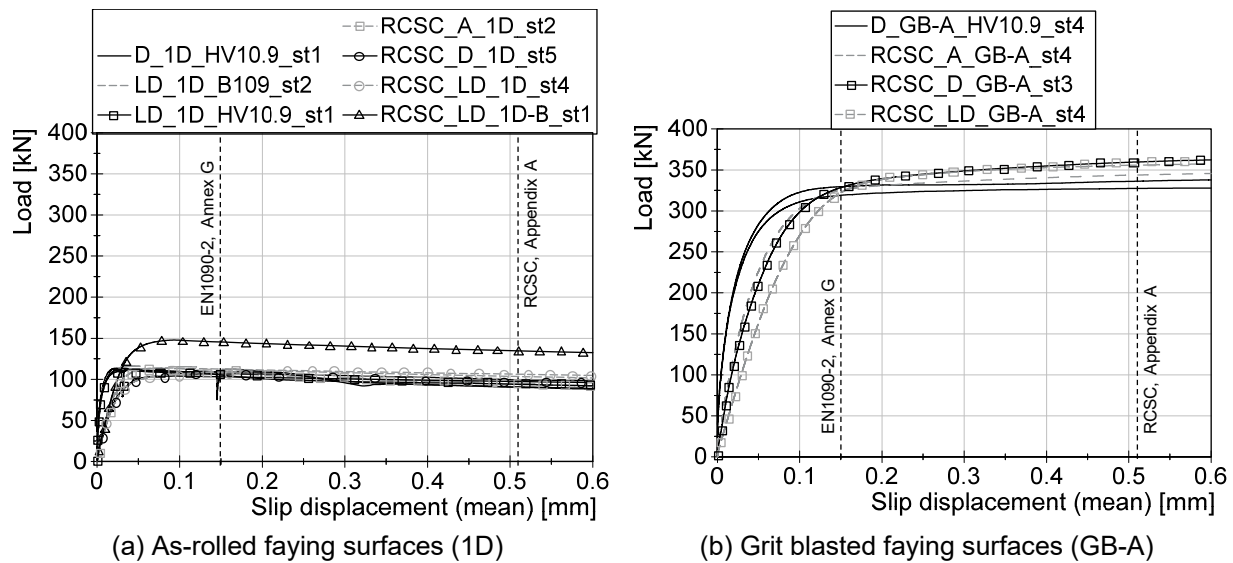
Figure 6-14: Influence of different testing procedures (EN1090-2 and RCSC) on slip-resistant behaviour of the stainless steel bolted connection

However, the mean slip displacements occurring in the specimens did not exceed the limit of 0.38 mm according to RCSC and all tests can be considered passed creep tests, see Table 6-8. This means that the selected slip factors are suitable to represent the level of slip resistance for each test series. The results also show that if the second load level is reached directly at the beginning of the tests, most of the test specimens have a very good chance to pass also if the results are evaluated according to EN 1090-2. Performing the tests both in tension and compression for 1D surfaces leads to approximately the same slip loads.

Table 6-8: Creep test results for stainless steel test specimens with different surface treatments according to RCSC Appendix A

Series ID	Test number	First step load level [1]	Slip (mean) Δ (0.5 h to 1000 h) [2]	Second step load level [3]	Slip (mean) at the second step load level	Final slip factor [-] (μ_{ct})
As rolled faying surfaces (1D)
RCSC_A_1D	ct1		0.004		0.06	
	ct2	67.9	0.006	101.9 [4]	0.04	0.23
	ct3		0.001		0.04	
RCSC_D_1D	ct1		0.004		0.06	
	ct2	62.5	0.005	93.8 [4]	0.06	0.22
	ct3		0.005		0.07	
RCSC_LD_1D	ct1		0.003		0.06	
	ct2	66.5	0.001	99.8 [4]	0.04	0.23
	ct3		0.002		0.05	
Grit blasted faying surfaces (GB-A)
RCSC_A_GB-A	ct1		0.001		0.13	
	ct2	206.5	0.001	309.8 [4]	0.12	0.71
	ct3		0.002		0.12	
RCSC_D_GB-A	ct1		0.001		0.21	
	ct2	215.8	0.002	323.6 [4]	0.18	0.74
	ct3		0.002		0.19	
RCSC_LD_GB-A	ct1		0.003		0.11	
	ct2	202.8	0.001	304.1 [4]	0.15	0.70
	ct3		0.002		0.22	

[1] based on Equation (2-12) | [2] difference between the slip displacement at 30 min and 1000 hours after reaching the constant load | [3] based on Equation (2-13) | [4] ≈ 0.9·F_{Sm} of first five static tests

(a) Slip displacement-time diagram (austenitic-1D)

(b) Slip displacement-log (time) diagram (austenitic-1D)

(c) Slip displacement-time diagram (duplex-1D)

(d) Slip displacement-log (time) diagram (duplex-1D)

(e) Slip displacement-time diagram (lean duplex-1D)

(f) Slip displacement-log (time) diagram (lean duplex-1D)

Figure 6-15: Creep test results according to RCSC for different stainless steel grades with as-received surface condition

The load level based on compression tests was not high enough to cause any major slip in the connection with 1D surface condition. The creep tests were also performed for grit blasted surfaces. All test results are presented in Table 6-8. As for the test series with 1D surface condition, the selected slip factors for each test series were also calculated based on 90 % of the mean slip load from the first five static tests. The results show that the selected slip factors can be considered as the final slip factors as all tests fulfil the creep test criteria according to RCSC, see Table 6-8.

However, Figure 6-16 shows that performing the creep tests with a load level of $0.90 \cdot F_{Sm}$ according to EN 1090-2 will probably fail if the test specimens are directly

loaded to this load level at the beginning of the test, since the mean slip load was calculated based on static tests performed in compression and creep tests performed in tension.

(a) Slip displacement-time diagram (austenitic-GB)

(b) Slip displacement-log (time) diagram (austenitic-GB)

(c) Slip displacement-time diagram (duplex-GB)

(d) Slip displacement-log (time) diagram (duplex-GB)

(e) Slip displacement-time diagram (lean duplex-GB)

(f) Slip displacement-log (time) diagram (lean duplex-GB)
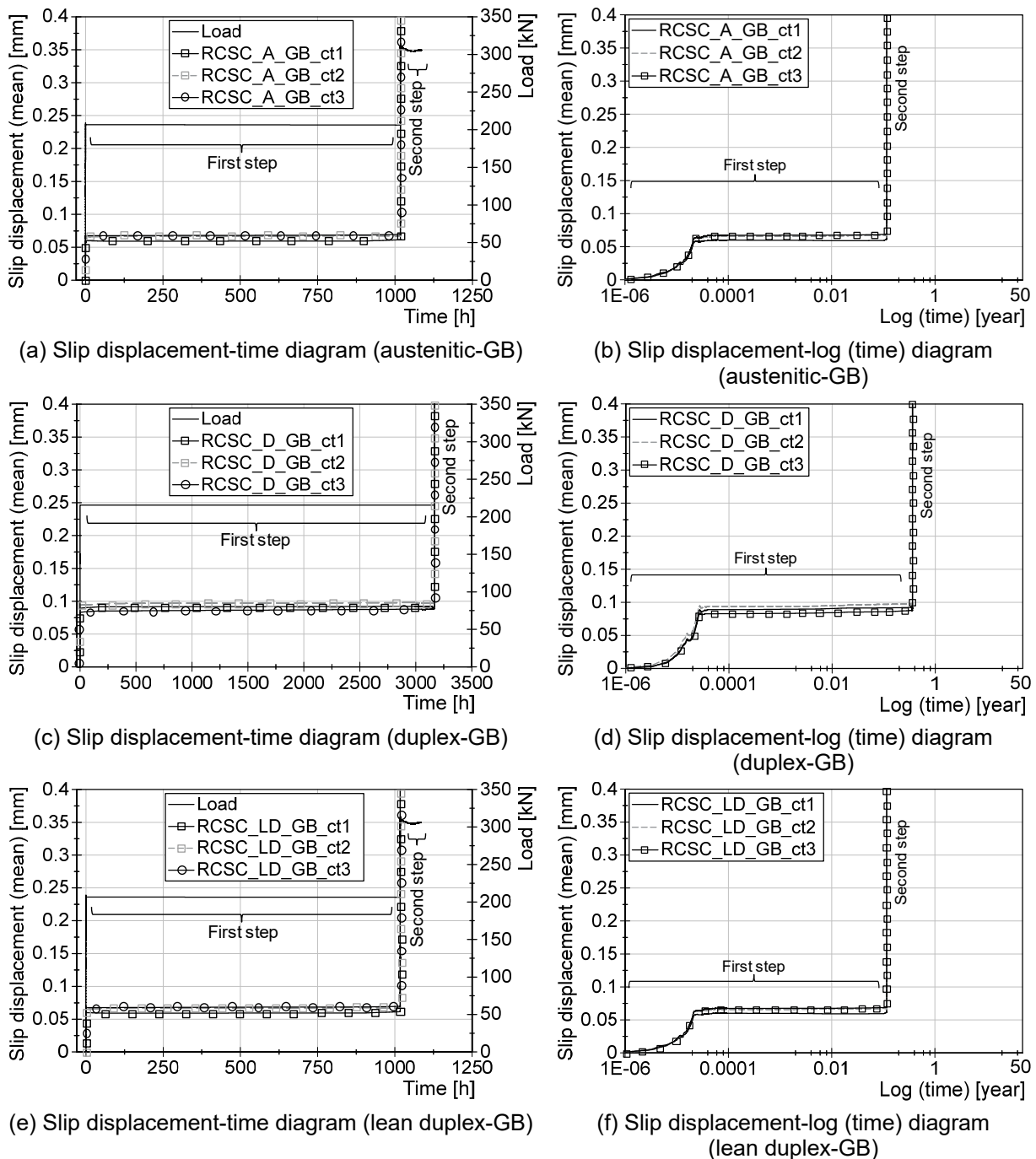
Figure 6-16: Creep test results according to RCSC for different stainless steel grades with grit blasted surface condition

All static and final slip factors are presented in Figure 6-17. As can be seen, the highest slip factors were achieved for test specimens with grit blasted faying surfaces. Test specimens with 1D surface conditions delivered more or less the same slip factors at about 0.2, which shows that the influence of performing the tests according different standards seems to be negligible for this surface condition. However, the only noticeable difference between the test series with 1D surface

condition occurs for achieved slip factors for the austenitic test series according to EN 1090-2 and RCSC. Only the A_1D_B109 test series was from a different batch. Products from different batches having different surface properties is a possible explanation for such a difference between the determined slip factors.

For grit blasted test series, there is a tendency towards a slightly higher slip factor for tests performed according to the RCSC Appendix A test procedure. The reason for such a difference is based on the way of performing and evaluating the creep tests.

For more creep-sensitive surface conditions, it is expected that there will be larger differences in determining slip factors according to these test procedures.
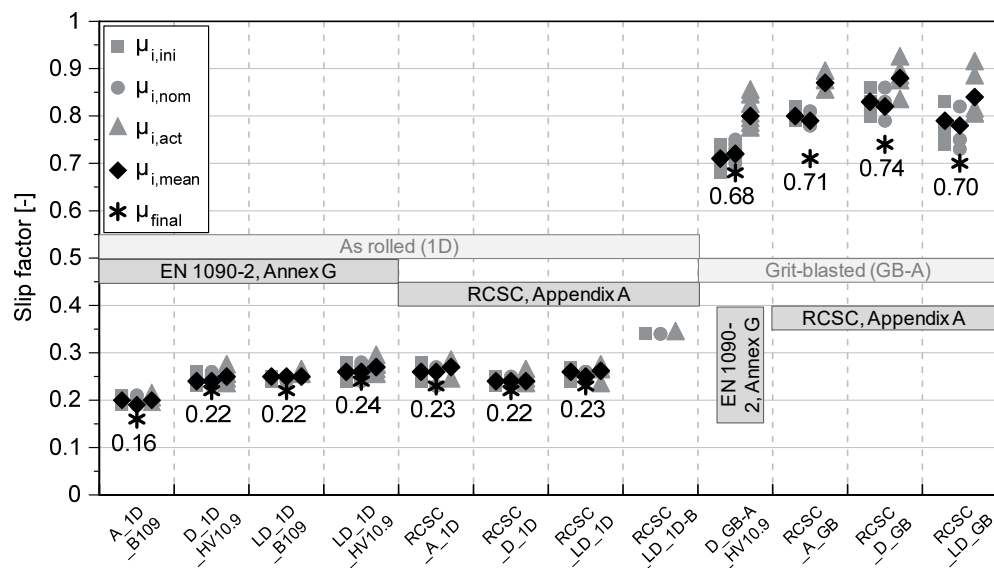
Figure 6-17: Comparison between the static and final slip factors according to EN 1090-2 and RCSC test procedures for slip-resistant connections made of stainless steel

6.3 EN 1090-2 vs. TL/TP-KOR-Stahlbauten

The determination of slip factors is specified according to EN 1090-2, Annex G, which was previously covered in TL/TP-KOR-Stahlbauten, Annex E, Sheet 85. The test procedures according to these two standards are already explained in Chapters 2.4.2.2 and 2.4.5. The new revision of TL/TP-KOR-Stahlbauten no longer includes the test procedure according to Annex E, Sheet 85. In the new revision of TL/TP-KOR-Stahlbauten, the determination of the slip factor shall be done according to EN 1090-2, Annex G.

An analytical comparison between both test procedures was conducted and summarized in Table 6-9. The old test procedure according to TL/TP-KOR-Stahlbauten prescribes a M16 test specimen geometry for the determination of the slip factor, see Figure 2-6. For this reason, a M16 test specimen geometry was selected, see Figure 2-1 (b). As can be seen, both standards represent the specimens with different inner and cover plate thicknesses, which leads to different clamping length and critical surface areas between the faying

surfaces, see Figure 6-18. Having larger critical surface areas might lead to a higher slip-resistance in the connection. Besides the geometry differences, each standard prescribes different preload levels for conducting the slip factor tests, see Table 6-9. Also, according to TL/TP-KOR-Stahlbauten there is no obligation to measure the preload level before or during the test.

However, besides all these differences, the main difference is the test procedure itself. According to TL/TP-KOR-Stahlbauten, the final slip factor shall be determined based only on a static test without considering the long-term behaviour of the connection which may lead to an overestimation of the determined slip factor.

Table 6-9: Comparison of the key parameters between EN 1090-2 and TL/TP-KOR-Stahlbauten, Annex E, Sheet 85

Parameters	EN 1090-2, Annex G	TL/TP-KOR-Stahlbauten, Annex E, Sheet 85
Geometry		
Bolt dimension	M 16	M16
Test specimen geometry	Figure 2-1 (b)	Figure 2-6
Clamping length ratio ($\sum t/d$)	2.5	3.3
Active surface area ratio (A/d)	8.8	12.9
Preload level		
Preload level	$F_{p,C}$	$F_{p,C}{}^*$
Preload measurement	Direct (± 5 %)	-
Test specification		
Type of static test	Tension	Tension
Type of creep/extended creep test		-
Slip factor (μ)	$\mu_i = \dfrac{\text{slip load}}{4 \cdot F_{p,C}}$	$\mu = \dfrac{Fg}{4 \cdot F_{p,C}{}^*}$
Number of static tests	4	5
Number of creep tests	1	-
Number of extended creep tests	3, if creep test failed	-
Evaluation	As 5 % fractile if the creep test evaluated as passed test. $\mu = \mu_{5\%} = \mu_{mean}$ (n = 10) – 2.05 S Otherwise calculation of μ with load level of the passed extended creep tests.	μ = min. μ (n = 10) ≥ 0,5

$F_{p,C} = T_t = 0.7 \cdot f_{ub} \cdot A_s$, $F_{p,C}{}^* = 0.7 \cdot f_{yb} \cdot A_s$ (where: f_{ub} = tensile strength of the bolt, f_{yb}: nominal yield strength of the bolt and A_s = tensile stress area of the bolt) | $\sum t$: clamping length (in cm) | d: bolt diameter (in cm) | A: contact surface area per bolt (in cm²)
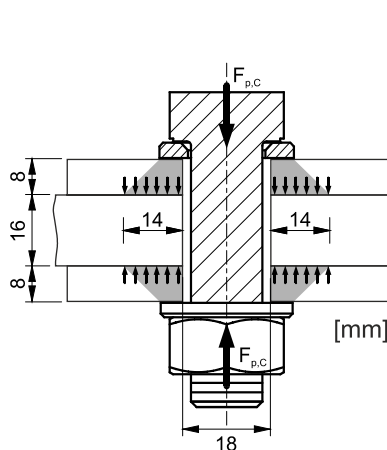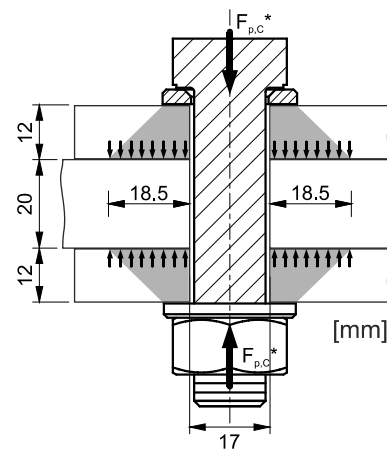
(a) EN 1090-2, Annex G   (b) TL/TP-KOR-Stahlbauten, Annex E, Sheet 85

Figure 6-18: Critical surface area between the faying surfaces for M16 test specimen geometry

In order to confirm the analytical investigations, two test series made of steel S235JR were planned on ASI-Zn-coated specimens with a coating thickness of about 76 µm (DFT), see Table 6-10. The dry film thickness (DFT) of the coated test specimens was measured according to EN ISO 2808.

All specimens were degreased using organic solvent and blast cleaned until they achieved preparation grade Sa 3 according to EN ISO 8501-1 and roughness "medium (G)" according to EN ISO 8503-1 [176]. The roughness Rz of the steel surface varied from 70 to 80 µm. The surface roughness was measured according to EN ISO 4287.

Table 6-10: Slip factor test results according to EN 1090-2 and TL/TP-KOR-Stahlbauten

Series ID	Surface condition		Preload level	Number of tests	$\mu_{nom,mean}$[5]	$\mu_{ini,mean}$[6]	$\mu_{act,mean}$[7]	V (μ_{nom})[8]	Final slip factor [-]
	S.P.G.[1] / Rz[2] [µm]	DFT[3] [µm]		st/ct(sp)/ect[4]	st/st+ct [-]	st/st+ct [-]	st/st+ct [-]	st/st+ct [%]	μ_{min}[9] / μ_{ect}[10]
According to EN 1090-2, Annex G – M16 test specimen									
ASI-E	Sa 3 / 75	73 ± 8	$F_{p,C}$ = 110 kN	4/1/-	0.70/-	0.69/-	0.80/-	2.8/-	-/-
According to TL/TP-KOR-Stahlbauten, Annex E, Sheet 85 – M16 test specimen									
ASI-T	Sa 3 / 75	78 ± 8	$F_{p,C}$* = 100 kN	5/-/-	0.81/-	0.81/-	0.89/-	3.7/-	0.75[9]

[1] surface preparation grade according to EN ISO 8501-1 | [2] surface roughness | [3] dry film thickness (coating thickness) | [4] st: static test/ct: creep-/ect: extended creep test | [5] $\mu_{nom,mean}$: calculated slip factors as mean values considering the nominal preload level | [6] $\mu_{ini,mean}$: calculated slip factors as mean values considering the initial preload when the tests start | [7] $\mu_{act,mean}$: calculated slip factors as mean values considering the actual preload at slip | [8] V: coefficient of variation for μ_{nom} | [9] $\mu_{5\%}$: slip factors as 5 % fractile calculated on the basis of the static tests and the passed creep test | [10] μ_{ect}: slip factor resulting from the passed extended creep test

The same incremental tensile load at normal speed of 0.01 mm/s (0.6 mm/min) was selected for both test procedures in order to eliminate any influence from the test speed on the slip-resistant behaviour of the connections. For the ASI-T test series, five static tests according to TL/TP-KOR-Stahlbauten were carried out. Four static and one creep tests were also performed according to EN 1090-2 Annex G.

Figure 6-19 (a) shows the load-slip displacement diagrams for both test series. As can be seen, despite a lower preload level, the TL/TP-KOR test specimens reached higher slip loads. However, as mentioned also in Chapters 3.2.10 and 5.3, for the test specimens with coated faying surfaces, lower preloads lead to lower slip loads.

The reason for such a difference is the geometry of the specimens. TL/TP-KOR-Stahlbauten specifies the test specimens with thicker cover plates and smaller hole clearances. As can be seen in Figure 6-18, these specifications for the test specimen geometry lead to larger critical surface area and better bonding between the faying surfaces. The condition of the faying surfaces after static tests also shows a larger area of deformed coating around the holes for TL/TP-KOR-Stahlbauten test specimens. The coating on the faying surfaces deforms when slip occurs in the specimen. This means that the loads will be transferred by larger active surface areas between the faying surfaces and consequently the load-bearing capacity of the connection will be improved, see Figure 6-19 (b) and (c).

(a) Load-slip displacement diagrams

(b) After test according to EN 1090-2

(c) After test according to TL/TP-KOR
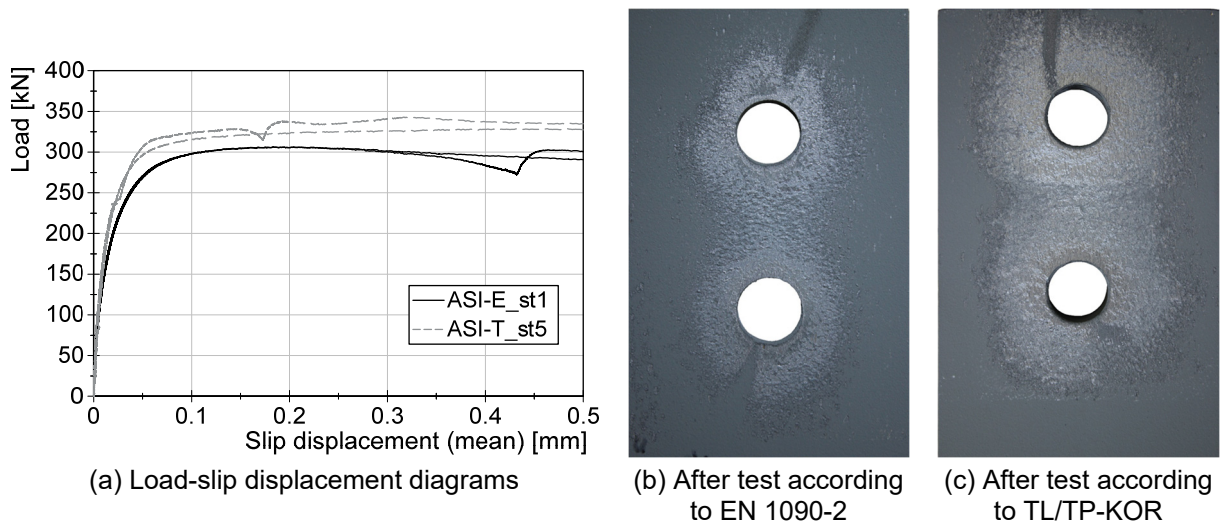
Figure 6-19: Comparison of load-slip displacement diagrams and the critical surface area for ASI coated test specimens according to EN 1090-2 and TL/TP KOR

All static test results are presented in Figure 6-20 (a). Based on the test procedure according to TL/TP-KOR-Stahlbauten, the final nominal slip factor can be determined as a minimum value of all static tests to 0.75. Based on this test procedure, the long-term creep sensitivity of coated faying surfaces does not affect the determination of the slip factor. On the other hand, a creep test was carried out in order to evaluate the creep sensitivity of the connection according to EN 1090-2, see Figure 6-20 (a). As can be seen in this figure, the creep test failed in the first minutes after reaching the constant load, which means that performing an extended creep test is necessary to finalize the determination of the slip factor. Unfortunately, in the frame of these investigations, no extended creep test has been carried out. The results from the creep tests therefore do not allow a conclusion regarding the final slip factor for this test series. It can, however, at least be concluded that the final slip factor for ASI will be smaller than 0.63, as 90 % of the mean slip load ($0.9 \cdot F_{Sm}$ = 275 kN) is a relatively high load level for performing the extended creep test, see Figure 6-20 (a).

(a) Creep test according to EN 1090-2

(b) Slip factor test results based on different standards
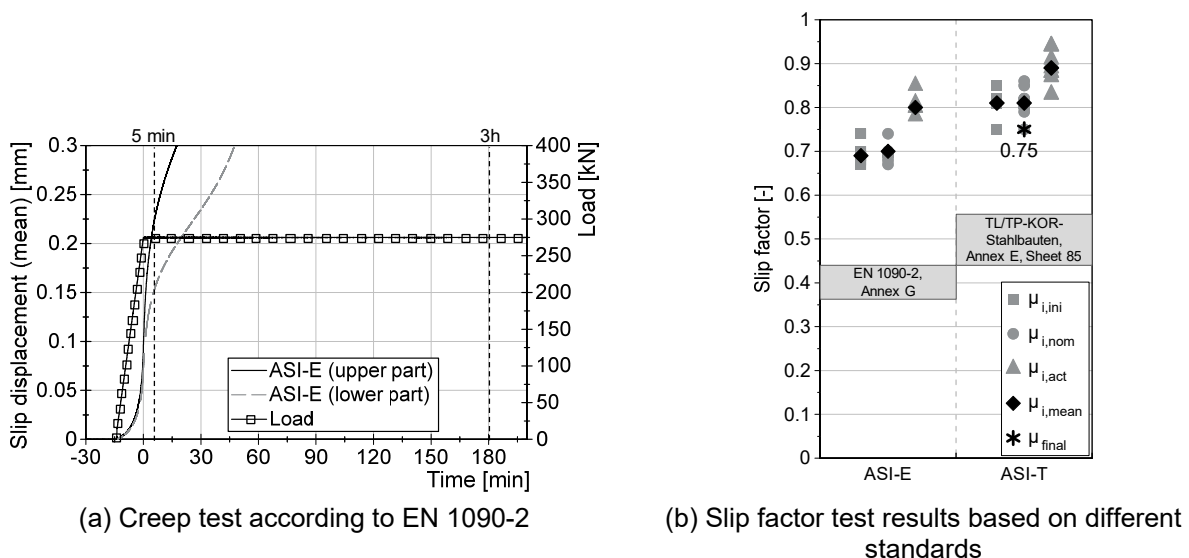
Figure 6-20: Influence of different test procedures (EN 1090 2 vs. TL/TP-KOR-Stahlbauten) on determination of slip factor (static and creep test results)

All results of the static tests are summarized in Figure 6-20 (b). As can be seen in this figure, the static test results according to EN 1090-2 are more conservative in comparison with TL/TP-KOR-Stahlbauten. Performing the creep/extended creep tests in order to consider the long-term creep behaviour of the connection in the determination of the slip factor would make this difference more noticeable.

6.4 Conclusion

Evidence has been provided that the different test procedures have potential to influence the determination of the slip factor. The level of influence is directly related not only to the test procedure itself but also to the condition of the faying surfaces. In some cases, the difference could be more dramatic for creep-sensitive surface conditions, for instance, or very small (maybe negligible) for non-creep-sensitive surface conditions. Having a coating on the faying surfaces in most cases would increase the creep sensitivity of the connection. For this reason, the long-term creep behaviour of the connection shall be investigated by performing creep/extended creep tests.

The old version of TL/TP-KOR-Stahlbauten does not specify performance of any kind of long-term creep tests for the determination of slip factor. According to this test procedure, the final slip factor shall be determined based on the static test results only. The results show that the difference in the final slip factor results could be noticeable. Having a more creep-sensitive surface preparation would increase this difference significantly.

Another important factor that might influence the determination of the slip factor is the geometry of the test specimens. The influence of the clamping length ratio was already investigated in Chapter 3.2.9. However, having different specimen geometries may lead to different active surface areas around the holes, between the faying surfaces. Having a larger active area improves the slip-resistant behaviour of the connection.

The new revision of TL/TP-KOR-Stahlbauten does not specify any new test procedures for the determination of slip factors. The old test procedure according to this standard was discontinued and the test procedure according to EN 1090-2, Annex G shall be applied in order to determine the slip factor for any specific surface condition.

Another scenario which might influence the determination of the slip factor is the predefined testing method and the evaluation criterion according to each standard. The main focus in this area was on EN 1090-2, Annex G and RCSC, Appendix A. Performing static tests in tension or compression and considering different slip criteria for the evaluation of the slip load might lead to different static slip factors according to the standard used. However, in both standards the creep/extended creep tests shall be performed in tension in order to finalize the slip factor. Hence,

performing the static tests in tension or compression would not have any influence on the determination of the final slip factors.

Regarding the way of performing the creep tests and the evaluation criteria according to RCSC in comparison with EN 1090-2, the determination of the slip factor according to EN 1090-2 might lead to more conservative results especially for coated faying surfaces. This phenomenon might be negligible when the faying surfaces are not creep-sensitive and/or slip takes place at the lower load level.

It is important to keep in mind that according to RCSC the value of the slip factor shall not be greater than 0.5, for design purposes. This means that the creep tests will be performed considering this limitation which might not represent the real capacity of the connection for some surface conditions.

7 Simplified test procedure on the basis of the RCSC

7.1 General

The test procedure according to EN 1090-2, Annex G specifies two possible test specimen geometries with four bolts for the determination of the slip factor, see Figure 2-1. In comparison with RCSC, Appendix A, the preparation of the test specimens is more cost-intensive and requires a greater workload since the size of the specimens is much smaller according to RCSC, see Figure 2-11 and Figure 2-12.

The objective of this study is to develop an alternative and optimized test procedure based on a simplified test specimen geometry on the basis of RCSC Appendix A, without influencing the test results in comparison with EN 1090-2, Annex G. This would reduce the required material, the preparation cost, the workload for preparation/testing and, finally, the required equipment for performing the tests.

7.2 Numerical investigation

In the frame of this study, two different simplified test specimen geometries based on EN 1090-2 and RCSC were developed. Both M20 and M16 test specimens are presented in Figure 7-1. For simplification, the contact surface area per bolt was kept approximately constant for both test specimens in comparison with related test specimens according to EN 1090-2. Like for the test procedure according to EN 1090-2, the same parameters will be considered in these tests. As the same plate thickness and bolting assembly were selected for each test specimen geometry, the simplified geometry also delivers the same clamping length ratio in comparison with EN 1090-2, see Figure 7-2. The test specimens can also be modified in order to perform the tests in tension as long as the contact surface area per bolt remains constant.

All bolts shall be preloaded to $F_{p,C}$ with the same accuracy that is mentioned in EN 1090-2. The static tests shall be performed in tension or compression at normal speed, with a duration of each test of about 10 min to 15 min. Both test specimen geometries consist of only one bolt and have two interfaces, which leads to two slip planes in a failure mechanism, see Figure 7-1. In order to avoid any influence of eccentricity on the measured slip in the connection, the relative displacement shall be measured on both sides of the test specimen.

(a) For M20 bolting assemblies   (b) For M16 bolting assemblies
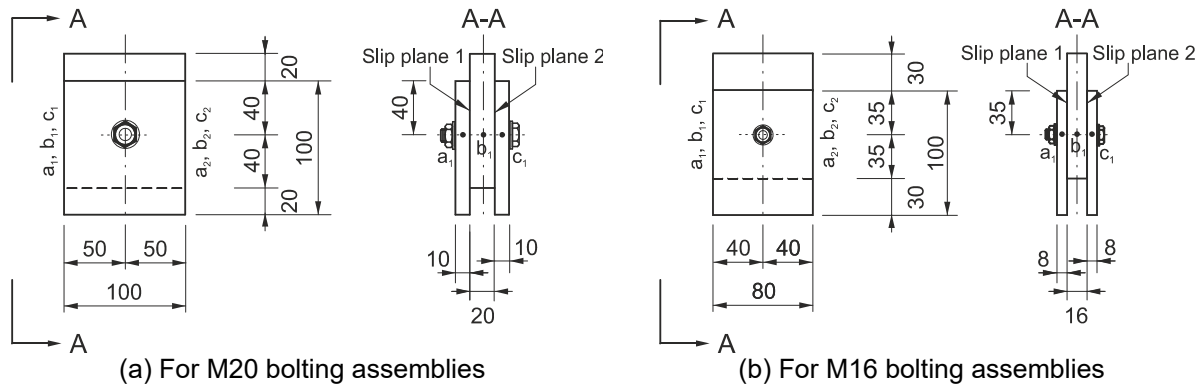
Figure 7-1: Simplified test specimen geometry based on EN 1090-2, Annex G and RCSC, Appendix A

(a) For M20 bolting assemblies   (b) For M16 bolting assemblies
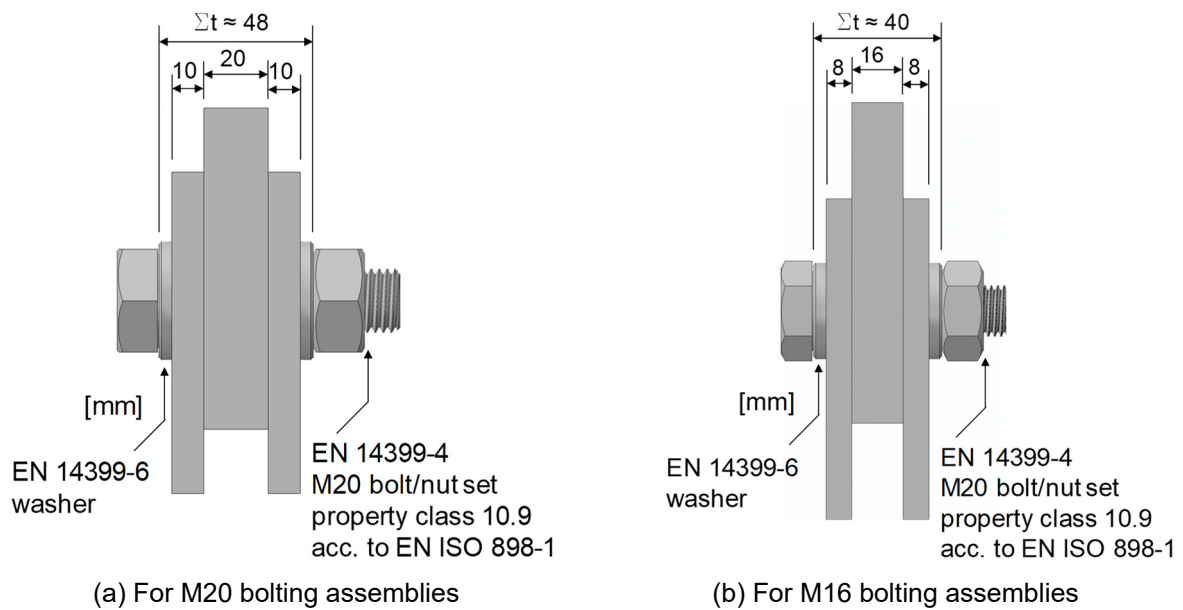
Figure 7-2: Clamping length for simplified test specimen geometries

Performing the static test is the first step for the determination of the slip factor. In order to investigate the comparability of the results of these simplified geometries with the standard geometries according to EN 1090-2, Annex G a numerical investigation was conducted. All specific parameters for developing this model were defined as described in Chapter 3.2.9.3. The results based on calibrated models according to GB-III were selected, see Table 4-3.

In the frame of this study, numerical simulations were conducted in order to compare the results of the static tests according to EN 1090-2 and the simplified test specimen geometry in both tension and compression, see Table 7-1 and Figure 7-3. The relative displacements shall be measured between specific points of the inner (b) and the cover plate (a and c), as shown in Figure 7-4 (a).

Table 7-1: Numerical slip factor test results according to EN 1090-2 and simplified test specimen geometry

Series ID	$\Sigma t/d$ [1)] [-]	Type of test	$\mu_{nom,mean}$[6)] [-]	$\mu_{ini,mean}$[7)] [-]	$\mu_{act,mean}$[8)] [-]
FEM analyses results (calibrated based on GB-III test series, see Table 3-2)					
EN1090_M16	2.5	Tension	0.72	0.73	0.84
EN1090_M20	2.4		0.73	0.73	0.85
Simp_EN1090_M16_T	2.5		0.73	0.74	0.85
Simp_EN1090_M20_T	2.4		0.74	0.74	0.85
Simp_EN1090_M16_C	2.5	Compression	0.80	0.80	0.86
Simp_EN1090_M20_C	2.4		0.82	0.81	0.87

[1)] clamping length ratio (Σt: clamping length, d: bolt diameter) │ [5)] $\mu_{nom,mean}$: calculated slip factors as mean values considering the nominal preload level │ [6)] $\mu_{ini,mean}$: calculated slip factors as mean values considering the initial preload when the tests start │ [7)] $\mu_{act,mean}$: calculated slip factors as mean values considering the actual preload at slip

(a) Under tension   (b) Under compression
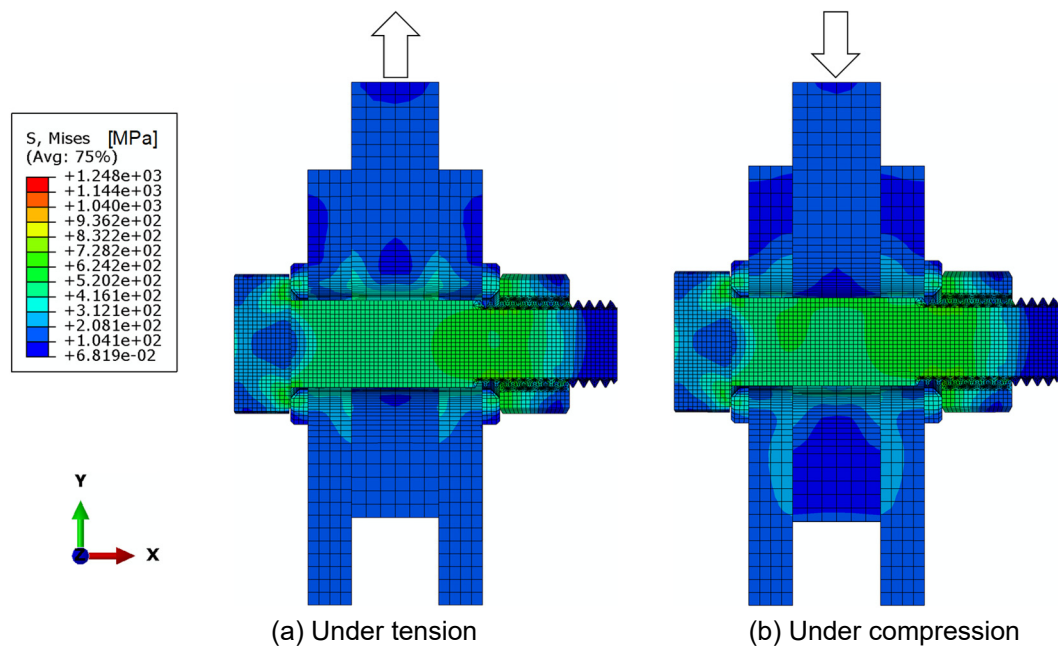
Figure 7-3: Stress distribution for M20 test specimen at reaching point of slip load

(a) Position of measuring relative displacement   (b) Load-slip displacement diagram
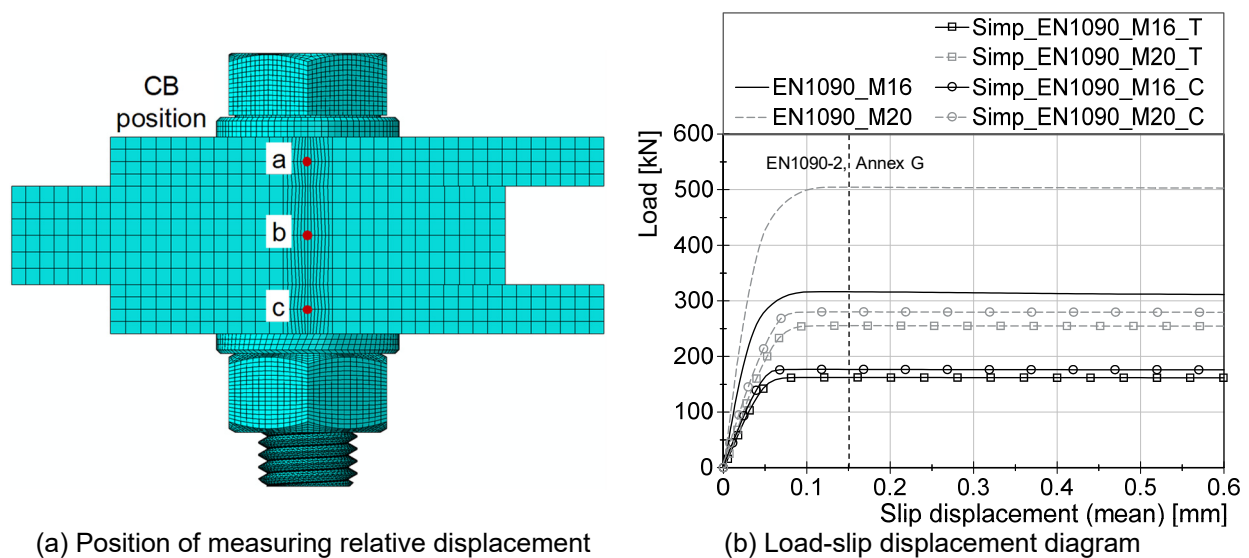
Figure 7-4: Position for measuring relative displacement and load-slip displacement diagram for all different test specimen geometries under different types of loading

The load-slip displacement diagrams for all test series are presented in Figure 7-4 (b). As can be seen in this diagram, the critical slip load occurred before the slip criterion of 0.15 mm in all cases. By evaluating the slip load and considering the relevant preload level, the static slip factors were calculated as nominal, initial and actual slip factors, which are presented in Table 7-1 and Figure 7-5.
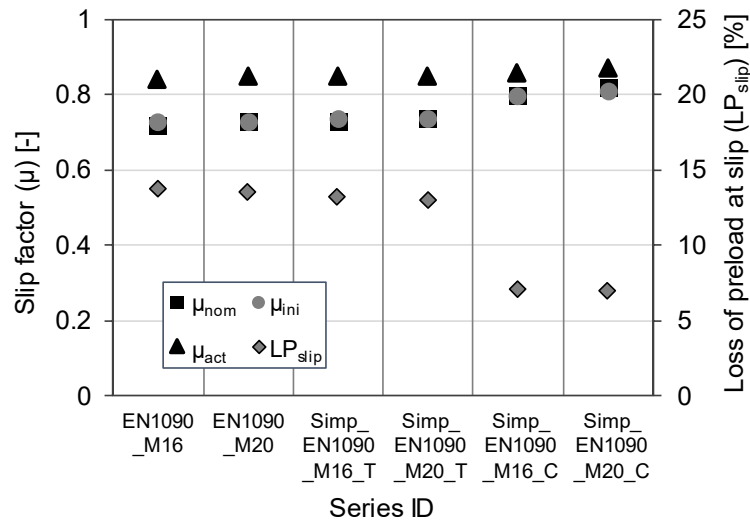
Figure 7-5: Numerical comparison of static slip factor based on EN 1090-2 and simplified test specimen geometries

As can be seen in Figure 7-5, performing the tests in tension with a test specimen geometry according to EN 1090-2 or using the simplified one leads to the same static slip factors. As can be seen, the loss of preload at slip is also approximately between 13 % and 14 %, which leads to nearly the same actual slip factors. On the other hand, as the results in Chapters 6.2.3 and 6.2.4 also show, performing the static tests in compression may lead to higher static slip factors compared with loading the test specimens in tension. However, the calculated actual slip factors for both M16 and M20 test specimens show approximately the same values, as the loss of preload in the test specimens loaded in compression is much lower. The loss of preload for these models was only about 7 %. Unlike test specimens under tension, not only would the bolted connection not suffer from a transverse contraction of the clamped plates, but the opposite phenomenon, whereby the loss of preload decreases in the connection, would also occur.

As explained in Chapter 6.2.3, uplifting of the cover plates was also observed in this investigation for the models under tension loading, see Figure 7-6. This phenomenon reduces the contact area on the faying surfaces, which might be one of the main reasons for achieving lower slip factors in comparison with test models under compression.

| (a) Under tension | (b) Under compression |
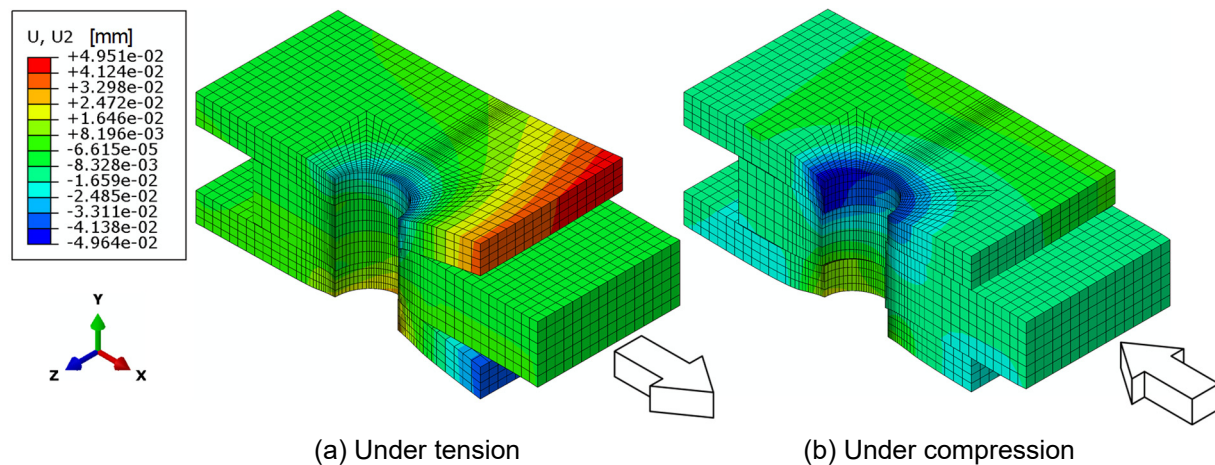
Figure 7-6: Deformed shape of the M16 simplified static model with scale factor of 100

As the results show, performing the tests in compression leads to higher slip factors. However, there are still some parameters which may influence the determination of the slip factor. For instance, if the critical slip load for compression test series occurs somewhere beyond 0.15 mm, evaluating the results at this criterion may lead to approximately the same static test results.

Considering all the results in this study, it was decided to perform all static tests in the following experimental investigation in compression on simplified test series, since the final slip factor must be calculated based on the results of creep tests and extended creep tests which shall both be performed in tension. For this reason, regardless of the selected type of testing for static tests, the final slip factor will be the same.

7.3 Experimental investigation

In the frame of this study, an experimental investigation was conducted in order to confirm the result of the numerical study and to investigate the long-term slip-resistant behaviour of the simplified geometry. The influence of this simplification on the determination of the slip factor was investigated on grit blasted (GB-A) and alkali-zinc silicate (ASI) coated test specimens. The results were compared with the results in Chapter 6.2.3 on GB-A and ASI based on EN 1090-2, Annex G. For this reason, all specimens in this study were made of S355. The simplified test specimens were made based on both M16 and M20 standard test specimen geometry according to EN 1090-2, Annex G, see Figure 7-1. All test specimens were blasted based on the same blasting procedure as explained in Chapter 5.2 for GB-A test specimens. The surface roughness was measured according to EN ISO 4287 and the results are summarized in Table 7-2. For each M16 and M20 test specimen, the geometries were coated with alkali-zinc silicate (ASI-Zn) coating. The coating thickness was measured according to EN ISO 2808. The mean dry film thickness (DFT) for each test series is presented in Table 7-2.

The preload level of $F_{p,C}$ was selected for all test series. In the frame of this study, the slip factor tests were performed in three steps as described in Figure 2-2. The main difference was that the static tests were performed under compression at 0.002 mm/s. For each simplified test series, one test was also performed by applying load-controlled loading at normal speed of 200 N/s in order to check the comparability of the loading capacity of the connection under both load application methods.

The same evaluation criteria as in EN 1090-2, Annex G were used for the interpretation of the results. The extended creep tests were performed with three tension-type specimens linked together with loose bolts as a single chain, similar to the creep test setup according to RCSC, Appendix A, see Figure 7-7.

Table 7-2: Experimental slip factor test results according to EN 1090-2 and simplified test procedure

Series ID	Rz[1] [μm]	DFT[2] [μm]	Loading method	Number of tests st/ct/ect[3]	$\mu_{nom,mean}$[4] st/st+ct [-]	$\mu_{ini,mean}$[5] st/st+ct [-]	$\mu_{act,mean}$[6] st/st+ct [-]	V (μ_{nom})[7] st/st+ct [%]	Final slip factor [-] $\mu_{5\%}$[8] / μ_{ect}[9]
According to EN 1090-2, Annex G									
Grit blasted surfaces (blasted with aluminium oxide) (GB-A)									
EN1090_CS_GB-A	74	-	Disp. control	4/1/-	0.73/0.73	0.70/0.71	0.82/0.80	1.8/1.9	0.70/-
Alkali-zinc silicate coating (ASI)									
EN1090_CS_ASI	75	104	Disp. control	4/1/2	0.69/-	0.69/-	0.82/-	2.1/-	-/0.62
According to simplified test setup									
Grit blasted surfaces (blasted with aluminium oxide) (GB-A)									
S_M16_EN1090_GB-A_d	70	-	Disp. control	5/2*/3	0.81/-	0.80/-	0.85/-	4.2/-	0.70/0.69
S_M20_EN1090_GB-A_d				5/1/3	0.80/-	0.81/-	0.87/-	2.9/-	-/0.68
S_M16_EN1090_GB-A_l			Load control	1/-/-	0.77/-	0.76/-	0.81/-	-/-	-/-
S_M20_EN1090_GB-A_l				1/-/-	0.82/-	0.81/-	0.93/-	-/-	-/-
Alkali-zinc silicate coating (ASI)									
S_M16_EN1090_ASI_d	72	83	Disp. control	5/1/3	0.69/-	0.68/-	0.77/-	2.2/-	-/0.59
S_M20_EN1090_ASI_d				5/1/3	0.70/-	0.70/-	0.74/-	3.9/-	-/0.60
S_M16_EN1090_ASI_l			Load control	1/-/-	0.69/-	0.67/-	0.74/-	-/-	-/-
S_M20_EN1090_ASI_l				1/-/-	0.71/-	0.71/-	0.76/-	-/-	-/-

[1] surface roughness [2] dry film thickness (coating thickness) [3] st: static test/ct: creep-/ect: extended creep test [4] $\mu_{nom,mean}$: calculated slip factors as mean values considering the nominal preload level [5] $\mu_{ini,mean}$: calculated slip factors as mean values considering the initial preload when the tests start [6] $\mu_{act,mean}$: calculated slip factors as mean values considering the actual preload at slip [7] V: coefficient of variation for μ_{nom} [8] $\mu_{5\%}$: slip factors as 5 % fractile calculated on the basis of the static tests and the passed creep test [9] μ_{ect}: slip factor resulting from the passed extended creep test

* The first creep test failed at load $0.90 \cdot F_{Sm}$ level and the second creep test was passed at $0.85 \cdot F_{Sm}$

(a) 3D model   (b) Experimental test setup
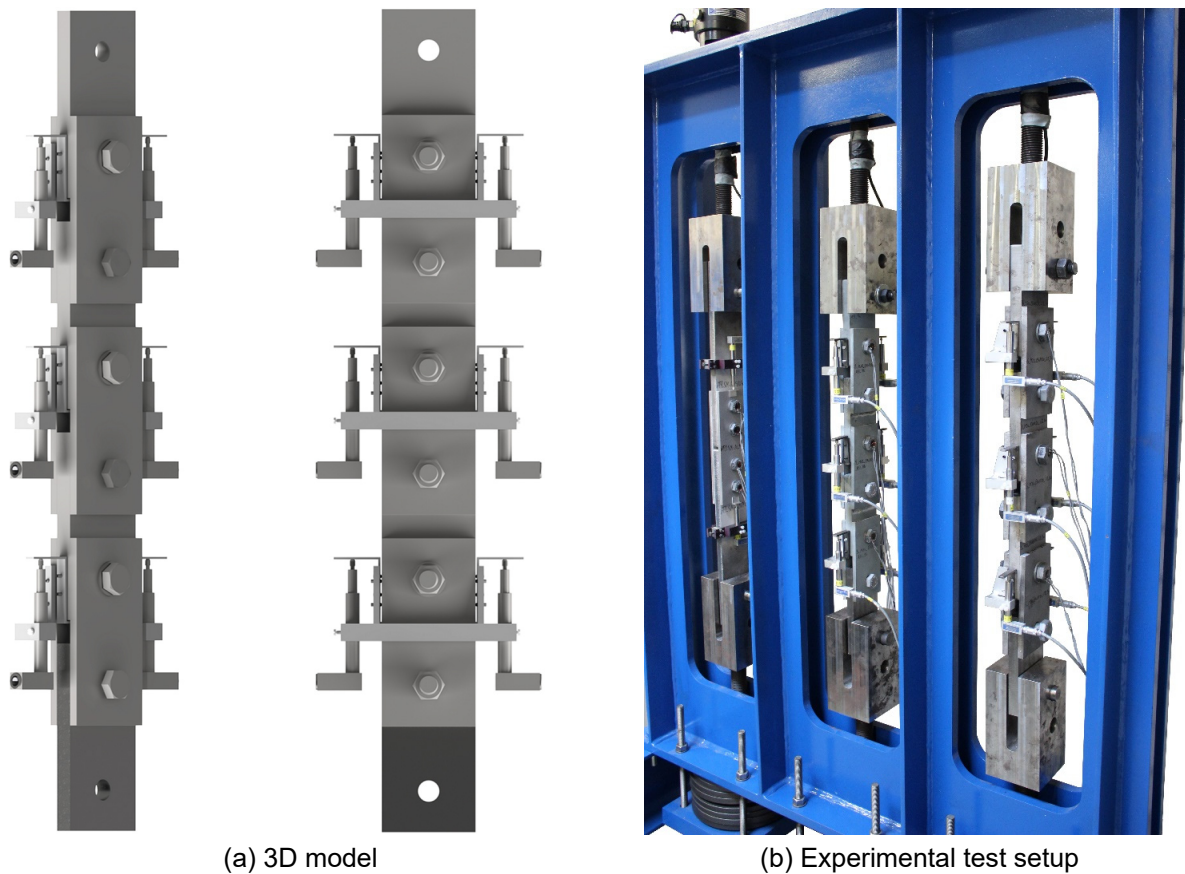
Figure 7-7: Test setup for performing the extended creep test for simplified test specimen geometry

As it became clear from the investigations described in previous chapters, performing static tests in compression might lead to higher slip loads and consequently to higher static slip factors. Performing static tests in tension might be more desirable in order to estimate the correct load level for performing the creep/extended creep test, but it would not have any influence on the determination of the final slip factor. The final slip factor will be determined based on passed creep or extended creep tests, whereby both shall be carried out in tension in all scenarios. For this reason, in the first step, it was decided to perform all static tests in compression, see Figure 7-8, since a smaller amount of material was needed for performing the test in compression. Besides this, performing the tests in compression was easier and less time consuming.

(a) 3D model   (b) Experimental test setup
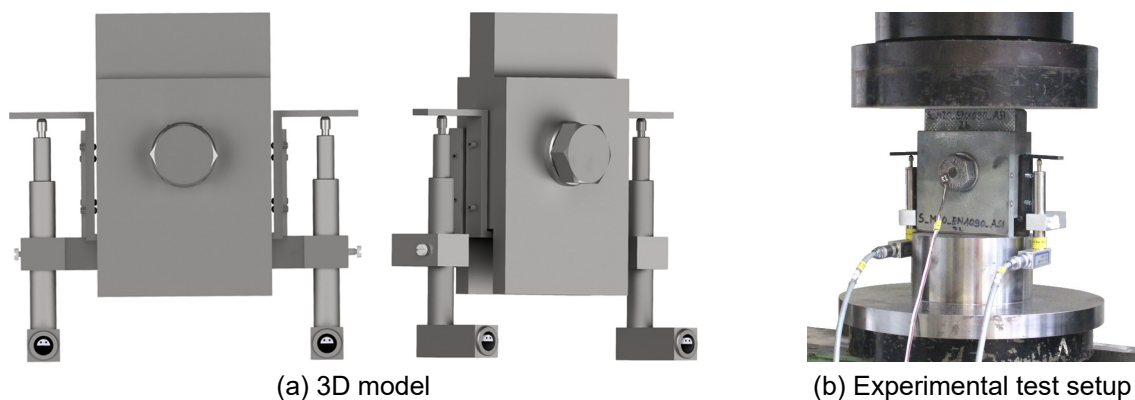
Figure 7-8: Test setup for performing the static test for simplified test specimen geometry

Figure 7-9 shows the load-slip displacement diagrams for standard and simplified test specimen geometry for GB-A and ASI test series. This figure shows that the slip criterion according to EN 1090-2 approximately represents the maximum capacity of the connection. However, only in some cases (especially for the simplified test specimens) the slip load appears somewhere above this slip criterion. It was not possible to directly compare the critical slip load of each test series as there were two different specimen sizes (M16 and M20). As can be seen, the M16 test specimen according to EN 1090-2 reaches about two times higher load level compared to the M16 simplified test specimen geometry, as each side of the standard test specimen geometry according to EN 1090-2 was assembled with two bolts.

(a) Grit blasted test series   (b) Alkali-zinc silicate coated test series
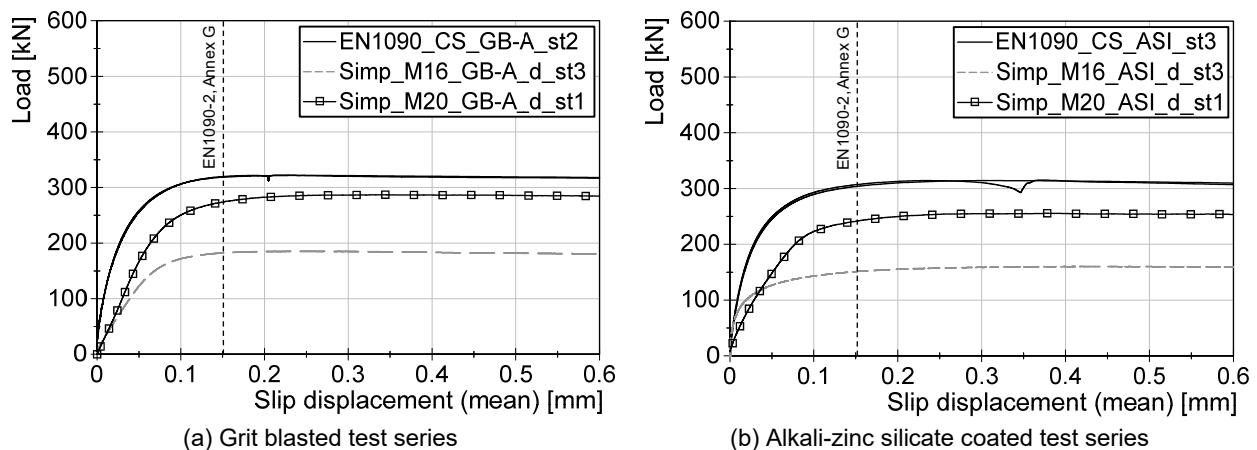
Figure 7-9: Load-slip displacement diagrams for both different test specimen geometries for GB-A and ASI test specimens

All different static slip factors (μ_{nom}, μ_{ini} and μ_{act}) were calculated and are summarized in Table 7-2. The results show that performing static tests under load-control or displacement-control modes leads to approximately the same slip loads, see Figure 7-10. The results also show that both M16 and M20 simplified test specimen geometries lead to approximately the same slip loads and consequently the same slip factors, see Table 7-2. All static tests of the simplified test series were carried out in compression.

As was expected for the GB-A test series, performing the test in compression leads to higher slip factors in comparison to the tension-type standard test specimens according to EN 1090-2. However, for the ASI-coated test series the static slip factors were comparable in both tension and compression. The reason might be the preparation of the simplified test specimens. As can be seen in Table 7-2, all test series were blasted to the same level of surface roughness (about Rz = 70-75 μm). However, the coating thickness for ASI-test series according to EN 1090-2 is about 20 μm thicker in comparison to simplified test series.

The results in Chapter 3.4 show that higher coating thicknesses may lead to higher slip factors. In this case, it seems that performing the test in compression and having a thinner coating thickness have neutralized each other's influence.

The creep tests for each test series were carried out with 90 % of the mean slip load from the first four static tests. For performing the creep tests, no correction in the load level was considered, as the difference between the results under tension and compression was not constant and depended heavily on the surface condition, see Chapters 6.2.4 and 6.2.5.

As can be seen in Figure 7-11 (a) and (b), the creep tests failed in all cases and thus it was necessary to perform extended creep tests to determine the final slip factor.

The creep tests were typically failed for coated surfaces. Experience also shows that grit blasted surfaces are not creep-sensitive and there is a high probability that they pass the creep test. However, for the simplified test specimens also failed the creep tests. The results presented in previous chapters also show that performing the static tests in compression instead of tension leads to higher slip loads.

Performing the creep test in tension and calculating a higher load level by considering the results of static tests in compression could lead to failure in the creep test. For this reason, an additional creep test with a slightly lower load level $(0.85 \cdot F_{Sm})$ was carried out for the M16 simplified test specimens with grit blasted faying surfaces.

The results show that the creep test was passed for this load level, see Figure 7-11 (c), and the final slip factor could be calculated as the 5 % fractile value, which is equal to 0.72. In Figure 7-11, the slip displacements in the connection are presented with only one line, as the simplified specimens are used in these tests, see Figure 7-11 (d).

(a) Grit blasted test series

(b) Alkali-zinc silicate coated test series
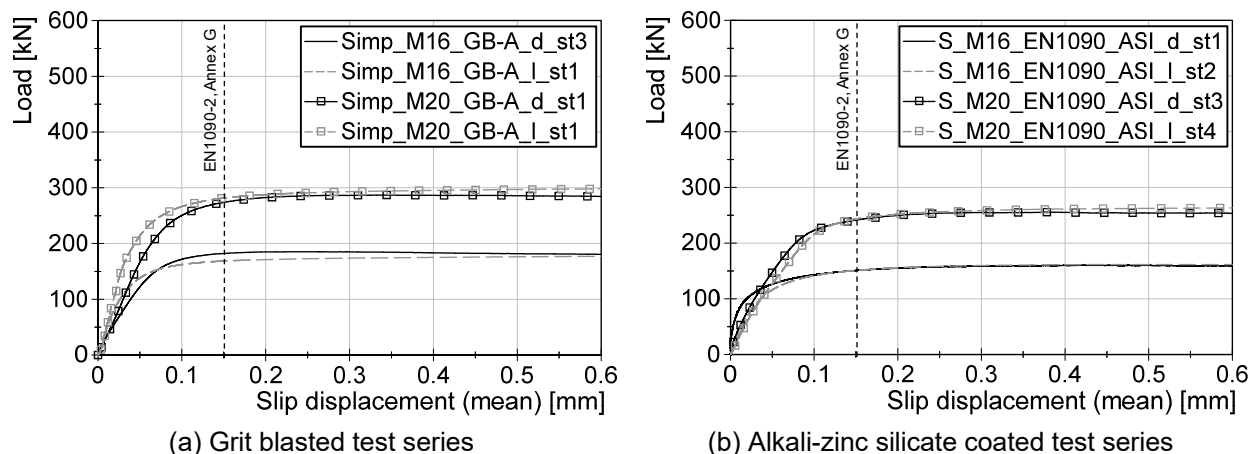
Figure 7-10: Load-slip displacement diagrams for GB-A and ASI test specimens in load-control or displacement-control modes
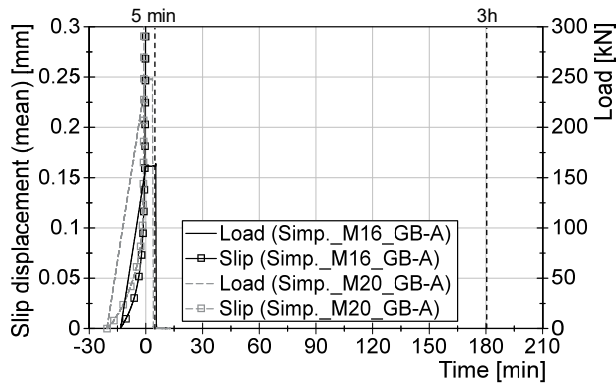
(a) GB-A test specimen loaded with 0.9 · F$_{Sm}$
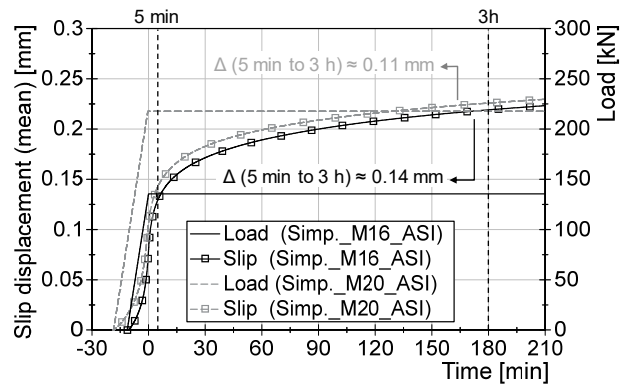
(b) ASI test specimen loaded with 0.9 · F$_{Sm}$
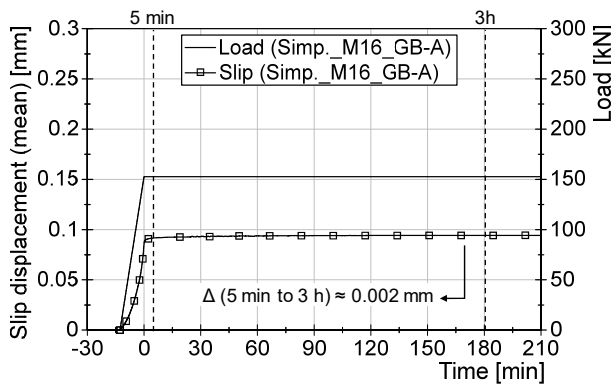
(c) GB-A test specimen loaded with 0.85 · F$_{Sm}$
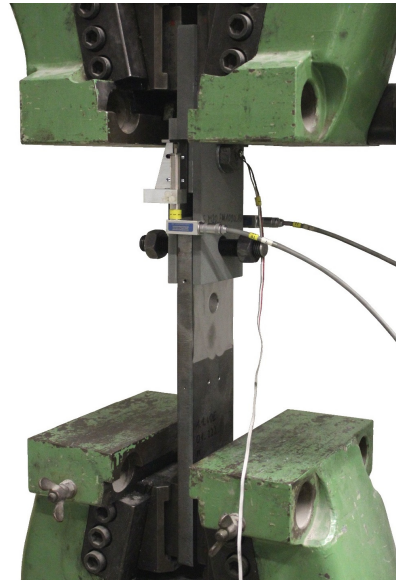
(d) Creep test setup

Figure 7-11: Creep test results for simplified GB-A and ASI test series

The extended creep tests were performed for all test series, since the creep tests failed at a load level of 0.9·F$_{Sm}$. In order to select a suitable load level for the extended creep test, all creep tests were also evaluated by slip displacement-log time curves. The results show that for the simplified M16 and M20 test specimens with grit blasted surface conditions will clearly fail the extended creep tests at 0.9·F$_{Sm}$, see Figure 7-12 (a) and (b). On the other hand, the results of the second creep test show that the load level of 0.85·F$_{Sm}$ seems to be suitable for performing the extended creep tests. The duration of the creep test was quite short in comparison with the extended creep test. For this reason, the extended creep tests were performed with three tension-type specimens as a single chain to confirm this load level, see Figure 7-7. The results show that the mean relative slip displacement is less than 0.3 mm when extrapolated to 50 years for both M16 and M20 test specimens with grit blasted surface condition at load level equal to 0.85·F$_{Sm}$. The final slip factor could be calculated as 0.69 for M16 and 0.68 for M20 simplified test specimen geometries.

Evaluating the slip displacement-log time curves based on the results of the creep tests for simplified M16 and M20 test specimens shows that these curves could not

be considered passed extended creep tests, see Figure 7-12 (c) and (d). For this reason, the extended creep tests were performed at a load level of 0.85·F_{Sm}. The results show that at this load level the slip displacement is less than 0.3 mm when extrapolated to 50 years for both test specimen geometries (M16 and M20) and the tests can be considered as passed extended creep tests. The final slip factor can be calculated as 0.59 for M16 and 0.60 for M20 simplified test specimens.

(a) Simplified M16 grit blasted test specimens

(b) Simplified M20 grit blasted test specimens

(c) Simplified M16 ASI-coated test specimens

(d) Simplified M20 ASI-coated test specimens
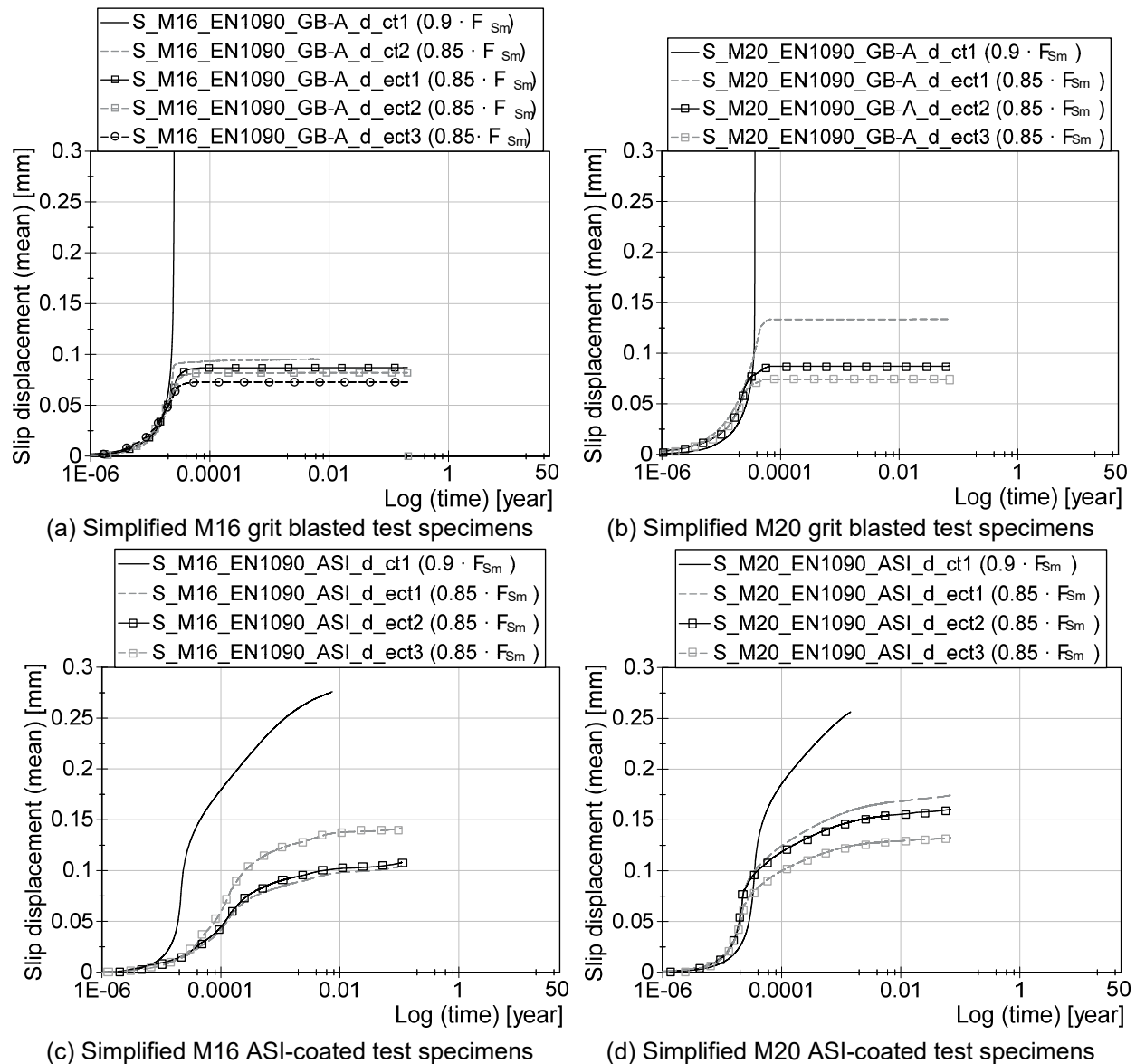
Figure 7-12: Extended creep test for simplified GB-A and ASI test series

Considering all the results achieved with the simplified test specimens and comparing them with results of EN 1090-2, it becomes clear that both standards and the method with the simplified test specimens deliver equal slip factors, see Figure 7-13. The results show that the final slip factor is about 0.70 for grit blasted test specimens and about 0.60 for those with ASI coating.
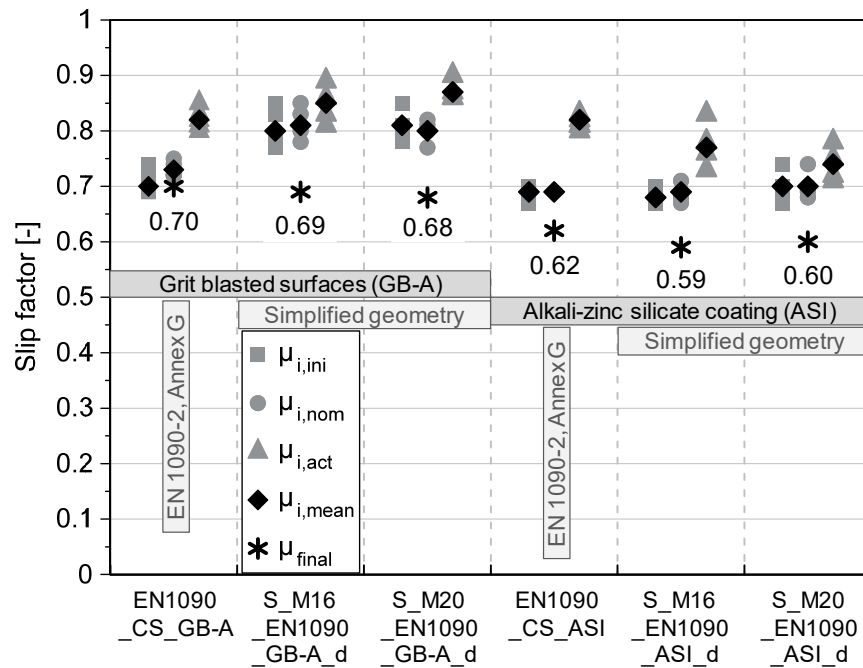
Figure 7-13: Comparison between the static and final slip factors according to EN 1090-2 and simplified test procedures

7.4 Conclusion

The main objective of this investigation was to develop a simplified test specimen geometry for the experimental determination of slip factors in order to reduce the material and equipment, preparation cost and workload required for the determination of slip factors. For this reason, numerical and experimental investigations were carried out in order to verify the comparability of the results between the simplified test specimen geometry and standard test specimens according to EN 1090-2, Annex G. In the frame of this study, two simplified test specimens were developed in such a way that the contact surface area per bolt remains approximately the same in comparison with the original test specimens.

The numerical investigations verified the comparability of the static test results for both simplified and standard test specimens. The results show that loading both types of specimens in tension delivers equal slip factors. However, loading the simplified specimens in compression leads to slightly higher slip factors.

Based on the test procedure, the final slip factor shall be determined based on creep and/or extended creep tests, whereby both shall be performed in tension. Performing the static tests in compression would therefore not have any effect on the determination of the final slip factor. For this reason, both types of testing would be allowed according to the simplified test procedure as long as the contact surface area per bolt remains constant.

The experimental investigations were carried out in order to compare the long-term behaviour of both simplified and standard test specimens. For this reason, two different surface preparations were selected: GB-A and ASI-coated faying surfaces.

All evaluation parameters for the simplified test series remained the same as for EN 1090-2, Annex G. There was no correction needed in the load level for creep tests, as the difference between the results under tension and compression was not constant and depended heavily on the surface conditions. For the test series where slip occurred at a very low load level, this difference might be negligible.

Both standard and simplified test series lead to very similar results, which could be confirmed for both GB-A and ASI test series. Both M16 and M20 simplified test specimen geometries also delivered the same results. There is therefore no need to perform a slip factor test with large test specimens according EN 1090-2. Using the simplified test specimens would thus achieve the same results and also save a considerable amount of time and money for the determination of the slip factor.

8 Amendments for standardization

8.1 General

A comprehensive investigation was conducted in order to improve the various aspects of the slip factor test procedure and to gain a deeper insight into the parameters that can potentially influence the determination of slip factors. Some of these results, which were part of the European research project SIROCO, have already been implemented in the latest version of EN 1090-2.

In the frame of this study, a comprehensive investigation was conducted on slip-resistant connections made of stainless steel to prove the acceptability of preloaded connections made of stainless steel. Different guidelines/standards specify slip factors only for slip-resistant connections made of carbon steel. Historically, there have been a number of major concerns about the long-term behaviour of preloaded bolted connections made of stainless steel. The reason for such concern was more or less based on the lack of knowledge about viscoplastic deformations of stainless steel alloys.

A simplified test specimen geometry was also developed based on standard test specimens according to EN 1090-2 and RCSC. The aim for having a simplified test specimen was not only to reduce the cost of specimen preparation but also to reduce the equipment and hours of labour required for performing the slip factor tests. For this reason, a simplified test procedure is proposed in Chapter 8.3.

8.2 Proposed classifications for slip-resistant connections made of stainless steel

There is currently no standard or guideline that specifies any classifications for slip-resistant connections made of stainless steel. Current suggested slip factors for different surface conditions are only valid for connections made of carbon steel. For this reason, a classification for slip-resistant connections made of stainless steel was developed based on comprehensive experimental investigations and presented in frame of this thesis, see Table 8-1 and Table 8-2. The proposed classification was supported with the experimental results according to EN 1090-2, Annex G and RCSC, Appendix A. In the near future, this classification will be implemented in the new version of EN 1993-1-4 and AISC 370.

Table 8-1: Proposed slip factors μ for preloaded stainless steel bolted connections for EN 1993-1-4

Surface condition		Class	Slip factor μ [b]
Surface finish [a]	Rz [μm]		
Surfaces blasted with grit	≥ 55	A	0.50
Surfaces blasted with grit	≥ 45	B	0.40
Surfaces blasted with shot	≥ 35	C	0.20
Surfaces as rolled	≥ 25	D	0.15
[a] Care is needed during grit and shot blasting processes to ensure there is no detrimental effect on the corrosion resistance.			
[b] The potential loss of preloading force from its initial value is considered in these slip factor values.			

The proposed classification for both standards is divided into four different classes for three different surface conditions. The faying surface may be grit blasted, shot blasted, or as rolled. No special surface preparation is needed for as-rolled surface conditions. In the new version of EN 1993-1-4, the classification and the surface condition will be presented in one table and the roughness value Rz according to EN ISO 4287 was given in order to check the quality of faying surfaces, see Table 8-1. In AISC 370, the classification and definition of the surface classes proposed in two different tables and the roughness of the surfaces are presented in both Rz according to ASTM D7127 [177] (comparable with Rz value according to EN ISO 4287) and Rt according to ASTM D4417 0, see Table 8-2 and Table 8-3.

Table 8-2: Proposed slip coefficients μ for friction surfaces for AISC 370

Class [a]	Slip coefficient μ [b]
SSA	0.15
SSB	0.20
SSC	0.40
SSD	0.50
[a] Surface classes are defined in Table 8-3. [b] The potential loss of preloading force due to time-dependent relaxation from its initial value is considered in these slip coefficient values.	

Table 8-3: Proposed definition of surface classes for slip-critical faying surfaces for AISC 370

Class	Rz [a]		Rt [b]	
	μm	μin.	μm	μin.
SSA[c]	≥ 25	1000	≥ 30	1200
SSB[d]	≥ 35	1400	≥ 50	2000
SSC[e]	≥ 45	1800	≥ 60	2400
SSD[e]	≥ 55	2200	≥ 70	2800
[a] Rz is the surface roughness according to ASTM D7127. [b] Rt is the surface roughness according to ASTM D4417. [c] Class SSA surfaces can generally be achieved on as rolled surfaces. [d] Class SSB surfaces can be achieved through use of clean stainless steel shot media. [e] Class SSC and Class SSD surfaces can be achieved through use of clean stainless steel grit media.				

The blasting procedure can be very critical for stainless steel specimens. Achieving high surface roughness can be very challenging as stainless steel provides a higher surface hardness. The quality of the blasted faying surfaces may have a direct influence on the slip-resistant behaviour of the connection. For this reason, the roughness values for the faying surfaces are specified for each class as quality control parameters for the blasting process, see Table 8-1. As can be seen in this table, a higher surface roughness may lead to higher slip factors for grit blasted surfaces.

As observed in Chapter 5.2, it is not possible to classify both grit and shot blasted faying surfaces in one class, as the topography of both faying surfaces will play a very important role in the slip-resistant behaviour of the connection and causes significant differences in the determined slip factor.

In general, blasting of the faying surfaces might affect the corrosion-resistant behaviour of the stainless steel plate, as water may remain on the surface for a longer time and cause some corrosion damage. During the blasting process, the

small particles of the blasting media may also be implanted in the stainless steel surface. If inappropriate blasting media are used, this phenomenon may increase the galvanic corrosion susceptibility of the connection. For this reason, special care is needed during the blasting process to ensure that there is no detrimental effect on the corrosion resistance of the connection.

8.3 Simplified test procedure for the determination of slip factor tests according to EN 1090-2, Annex G

8.3.1 General

A simplified testing procedure based on EN 1090-2, Annex G was developed. The necessary changes to the current version of Annex G are proposed in the following chapter. Content to be removed from Annex G is shown in red and proposed entries are shown in green.

8.3.2 Proposed version of simplified EN 1090-2, Annex G

G.1 General

The purpose of this test is to determine the slip factor for a particular surface treatment, often involving a surface coating.

The test procedure is intended to ensure that account is taken of the possibility of creep deformation of the connection.

The validity of the test results for coated surfaces is limited to cases where all significant variables are similar to those of the test specimens.

G.2 Significant variables

The following variables shall be taken as significant on the test results:

a) the composition of the coating;

b) the surface treatment and treatment of primary layers in case of multi-layer systems (see G.3);

c) the maximum thickness of the coating (see G.3);

d) the curing procedure;

e) the minimum time interval between application of the coating and application of load to the connection;

f) the property class of the bolt (see G.6);

g) number and configuration of washers;

h) grade of steel plates.

G.3 Test specimens

The test specimens shall conform to the dimensional details shown in Figure G.1.

The steel material shall conform to EN 10025-2 to EN 10025-6 and stainless steels according to EN 10088-4 or EN 10088-5.

To ensure that the two inner plates have the same thickness, they shall be produced by cutting them consecutively from the same piece of material and assembled in their original relative positions.

The plates shall have accurately cut edges that do not interfere with contact between the plate surfaces. They shall be sufficiently flat to permit the prepared surfaces to be in contact when the bolts have been preloaded in accordance with 8.1 and 8.5.

a) M20 bolts in 22 mm hole diameter   b) M16 bolts in 18 mm hole diameter
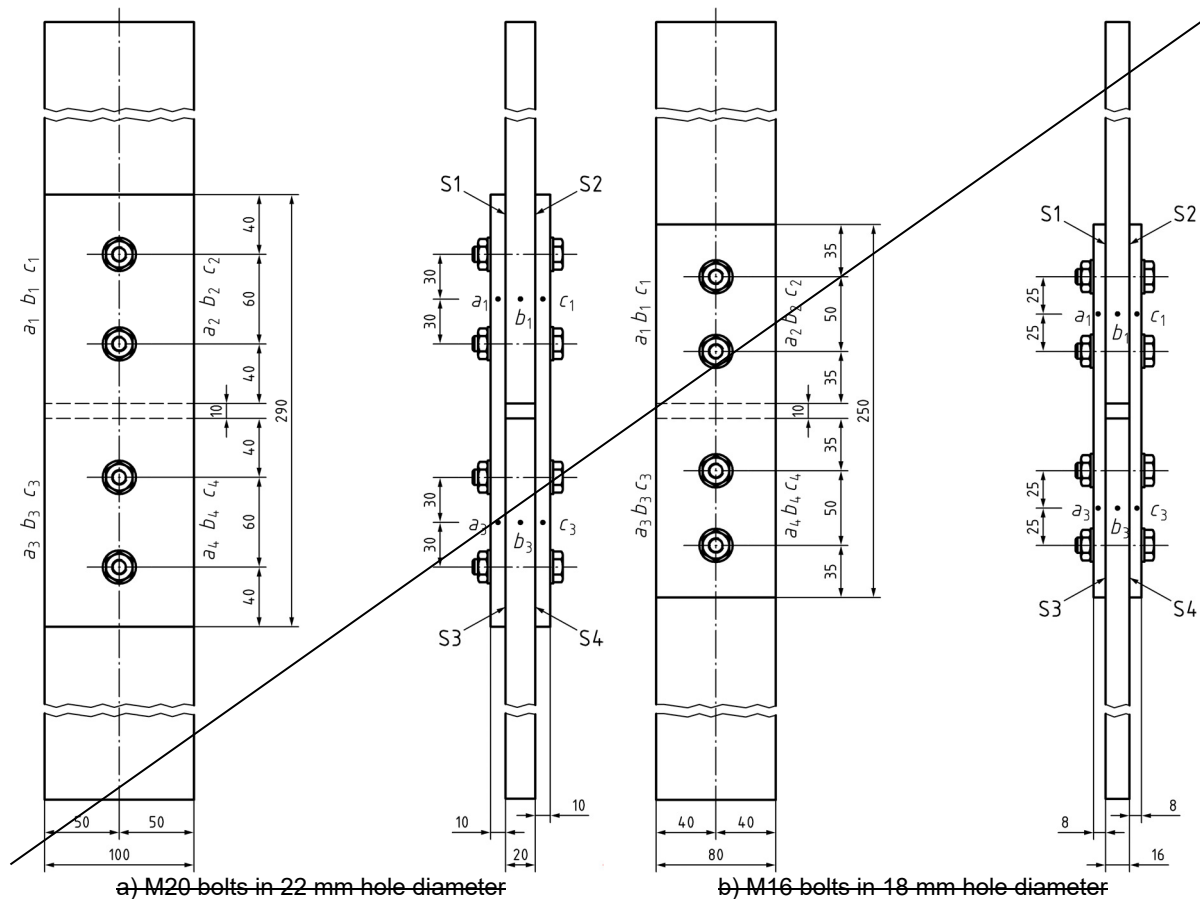
Key
S1 Slip plane 1
S2 Slip plane 2
S3 Slip plane 3
S4 Slip plane 4

Figure G.1 — Standard test specimens for slip factor test

a) M20 bolts in 22 mm hole diameter   b) M16 bolts in 18 mm hole diameter
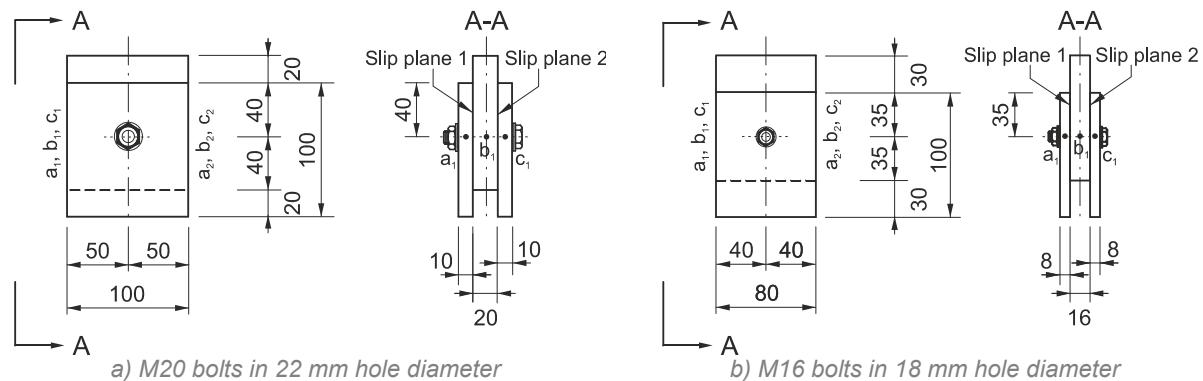
Key
  S1 Slip plane 1
  S2 Slip plane 2

Figure G.1 — *Compression type test specimens for static slip factor test*

The specified surface treatment and coating shall be applied to the contact surfaces of the test specimens in a manner consistent with the intended structural application. The mean coating thickness on the contact surface of the test specimens shall be at least 25 % thicker than the nominal thickness specified for use in the structure.

The curing procedure shall be documented, either by reference to published recommendations or by description of the actual procedure.

The specimens shall be assembled such that the bolts are bearing in the opposite direction to the applied tension.

The time interval (in hours) between coating and testing shall be recorded.

The bolts shall be tightened to within ± 5 % of the specified preload, $F_{p,C}$, for the size and property class of the bolt used.

The preload in the bolts shall be directly measured with equipment that is accurate to ± 4 %.

If it is required to estimate bolt preload losses over time, the test specimens may be left for a specified period at the end of which the preloads may be again measured.

The bolt preloads in each test specimen shall be measured just prior to testing and, if necessary, the bolts shall be retightened to the required ± 5 % accuracy.

G.4 Slip test procedure and evaluation of results

~~Initially, five test specimens shall be tested. Four tests shall be loaded at normal speed (duration of test approximately 10 min to 15 min). The fifth test specimen shall be used for the creep test.~~

Initially, in a first step, four static tests shall be tested in compression at normal speed (duration of test approximately 10 min to 15 min).

The specimens shall be tested in a ~~tension-loading~~ *universal testing* machine. The load-slip relationship shall be recorded.

The load-slip relationship can be determined from a tension-type test setup as an alternative test method, as long as the contact surface area per bolt remains the same in comparison with test specimens presented in Figure G.1, see Figure G.2.

In the second step, the fifth test specimen shall be tested in tension in a creep test.

a) M20 bolts in 22 mm hole diameter   b) M16 bolts in 18 mm hole diameter
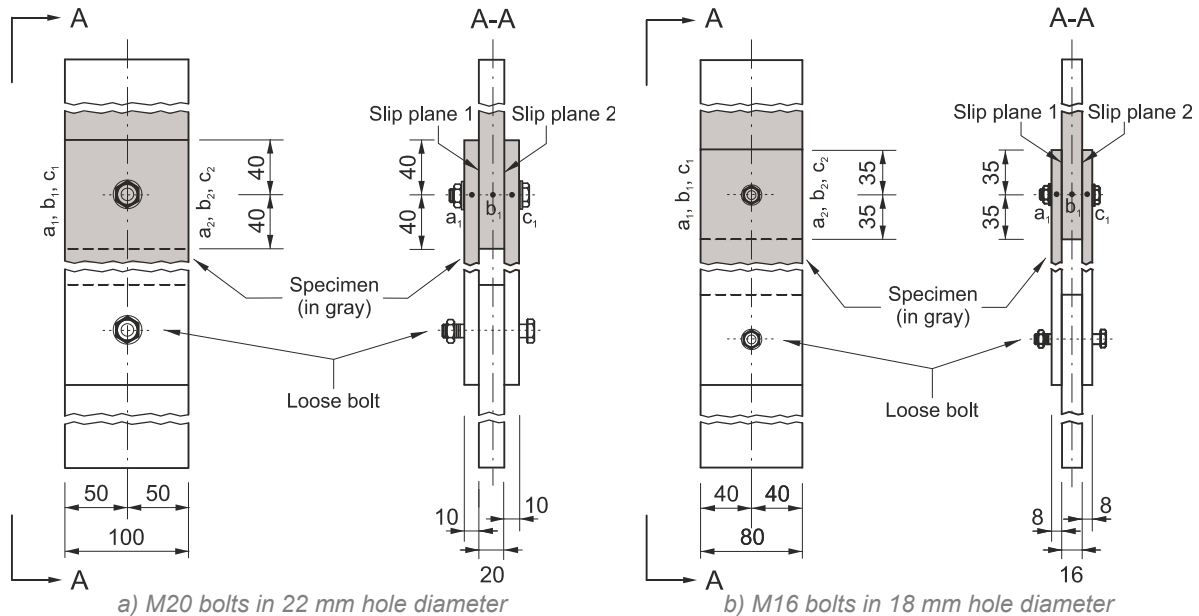
Key
 S1 Slip plane 1
 S2 Slip plane 2

Figure G.2 — *Tension-type test specimen for creep test (could also be an alternative test setup for static test)*

In a test specimen, ~~four~~ *two* slip planes exist: slip planes 1 ~~to 4~~ *and 2* according to Figure G.1.

The slip shall be taken as the relative displacement between adjacent points on an inner plate (position b, Figure G.1) and a cover plate (positions a and c, Figure G.1), in the direction of the applied load. ~~It shall be measured for each end and each side of the specimen separately resulting in eight displacement values, see Figure G.1.~~ *The slip displacement shall be measured on both sides of the specimen.*

~~Slip may occur in a failure mode of combination of slip in slip planes 1 and 2, 3 and 4 or diagonal in slip planes 1 and 4 or 2 and 3. The slip has to be evaluated according to the existing failure mode, so that finally two mean slip values are determined on the basis of eight measured displacements.~~

Slip occurs in a failure mode of combination of slip in slip planes 1 and 2. The slip must be evaluated according to this failure mode, so that finally one mean slip value shall be determined on the basis of two measured displacements.

The individual slip load for a connection, F_{Si}, is defined as the load at 0,15 mm displacement or at the peak load before 0,15 mm displacement according to the load-displacement diagram as given in Figure G.~~2~~*3*.

Key
 X slip displacement [mm]
 Y load
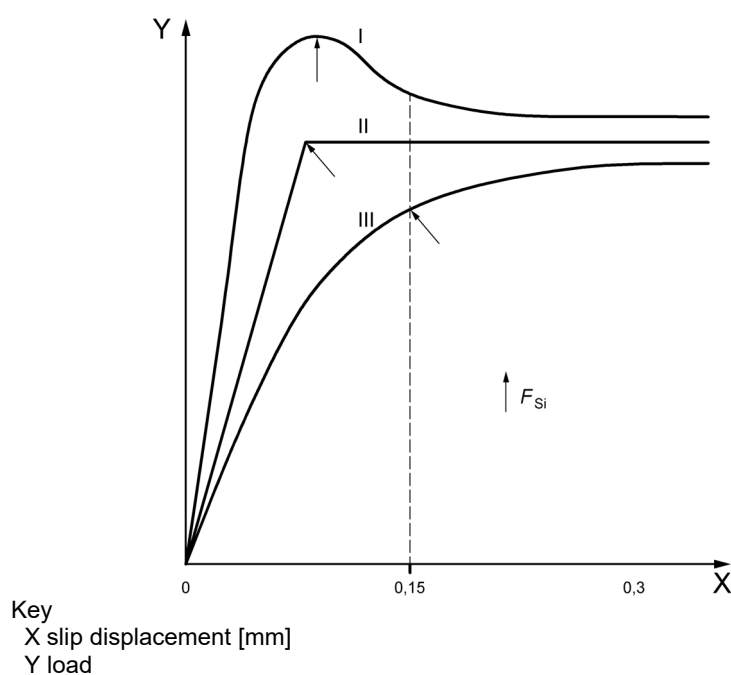
NOTE   I Slip load is the peak load before slip of 0,15 mm.
             II Slip load is load at sudden slip before 0,15 mm
             III Slip load is the load at slip of 0,15 mm.

Figure G.23 — Definition of the slip load for different load-displacement behaviour

The fifth test specimen shall be loaded with a specific load of 90 % of the mean slip load F_{Sm} from the first four specimens (i.e. the mean of eight values).

If, for the fifth specimen, the delayed slip, i.e. difference between the recorded slip at five minutes and at three hours after the application of the full load, does not exceed 0,002 mm, the slip loads for the fifth test specimen shall be determined as for the first four. If the delayed slip exceeds 0,002 mm, extended creep tests shall be carried out in accordance with G.5.

If the standard deviation s_{Fs} of the ten values (obtained from the five test specimens) for the slip load exceeds 8 % of the mean value, additional specimens shall be tested.

The total number of test specimens (including the first five) shall be determined from:

$$n > (s / 3.5)^2 \hspace{3cm} (G.1)$$

where

     n   is the number of test specimens;

     s   is the standard deviation s_{Fs} for the slip load from the first five specimens (ten values) expressed as a percentage of the mean slip load value.

G.5 Extended creep test procedure and evaluation

If it is necessary to carry out extended creep tests, following G.4 at least three test specimens (six connections) shall be tested. *Tension-type test specimens shall be*

used in these tests. The specimens can be linked as a single chain-like arrangement using loose bolting assemblies, preferably with higher property class, for instance 12.9, see Figure G.4. Assembling the specimens like a chain means that the same load will be applied to all specimens.
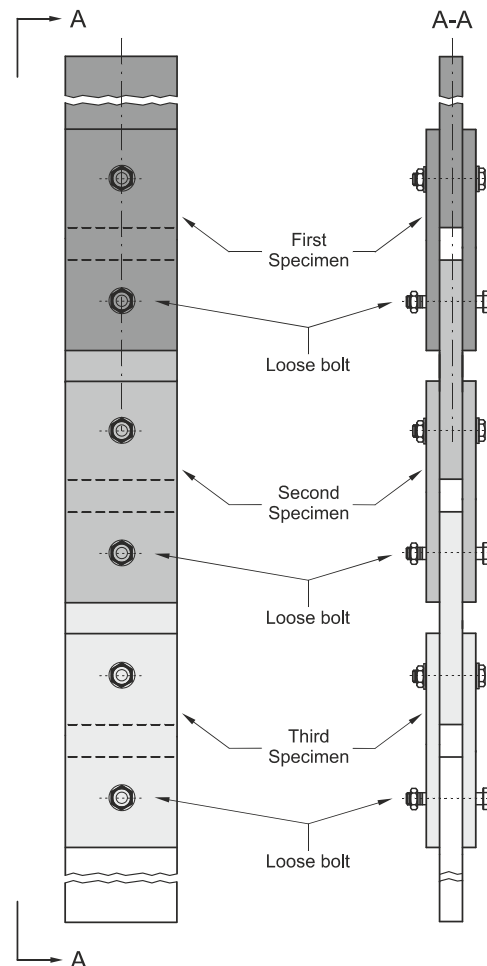
Figure G.4 *— Use of the displacement-log time curve for extended creep test*

A specific load shall be applied to the test specimen whose value shall be determined so as to account both for the result of the creep test carried out in G.4 and for the results of all preceding extended creep tests.

A load corresponding to the slip factor proposed for use in the structural application may be adopted. If the surface treatment is to belong to a specified class, a load corresponding to the slip factor for that class may be taken in accordance with Table 1̶6̶7.

A "displacement-log time" curve shall be plotted (see Figure G.3̶5) to demonstrate that the load determined using the proposed slip factor will not cause displacements greater than 0.3 mm during the design life of the structure, taken as 50 years unless otherwise specified. The "displacement-log time curve" may be extrapolated linearly as soon as the tangent can be determined with sufficient accuracy.
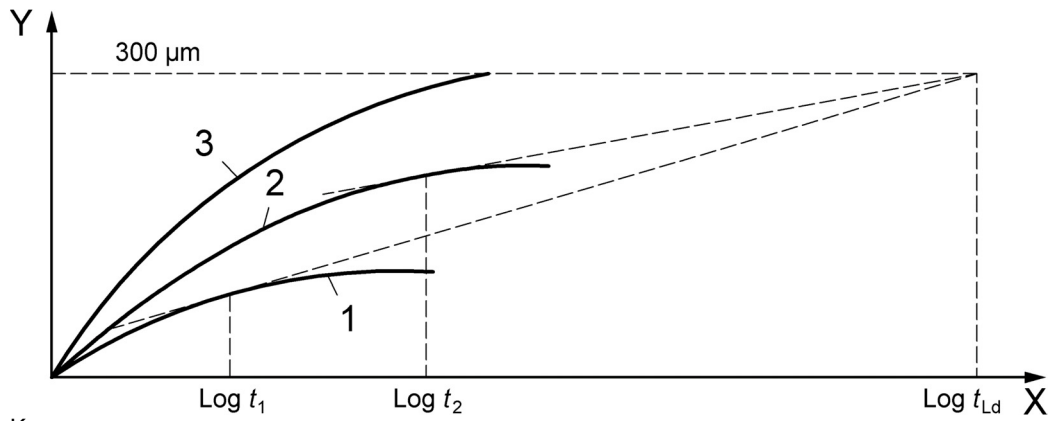
Key
  X log (time)
  Y slip displacement

NOTE t_{Ld} Design life of structure

        t_1 Minimum duration for test 1

        t_2 Minimum duration for test 2

        Curve 1   Passed extended creep test.

        Curve 2   Passed extended creep test.

        Curve 3   Extended creep test is not passed.

Figure G.3*5* — Use of the displacement-log time curve for extended creep test

G.6 Test results

Individual slip factor values are determined as follows:

$$\mu_i = \frac{F_{Si}}{4 \cdot F_{p,C}} \qquad\qquad \text{(G.2)}$$

$$\mu_i = \frac{F_{Si}}{2 \cdot F_{p,C}} \qquad\qquad (G.2)$$

The slip load mean value F_{Sm} and its standard deviation s_{FS} are determined as follows:

$$F_{Sm} = \frac{\Sigma F_{Si}}{n}, \quad s_{Fs} = \sqrt{\frac{\Sigma (F_{Si} - F_{Sm})^2}{n-1}} \qquad\qquad \text{(G.3)}$$

The slip factor mean value μ_m and its standard deviation s_μ are determined as follows:

$$\mu_m = \frac{\Sigma \mu_i}{n}, \quad s_\mu = \sqrt{\frac{\Sigma (\mu_i - \mu_m)^2}{n-1}} \qquad\qquad \text{(G.4)}$$

The characteristic value of the slip factor μ shall be taken as the 5 % fractile value with a confidence level of 75 %.

~~For ten values, n = 10, from five specimens, the characteristic value may be taken as the mean value minus 2.05 times the standard deviation.~~

For five values, n = 5, from five specimens, the characteristic value may be taken as the mean value minus 2.46 times the standard deviation.

Unless extended creep testing is required, the nominal slip factor shall be taken equal to its characteristic value.

If extended creep testing is required, the nominal slip factor may be taken as the value demonstrated to satisfy the specified creep limit, see G.5.

Slip factors determined using bolts property class 10.9 may also be used for bolts property class 8.8.

Alternatively, separate tests may be carried out for bolts property class 8.8. Slip factors determined using bolts property class 8.8 shall not be assumed valid for bolts property class 10.9.

If required, the surface treatment shall be assigned to the relevant friction surface class as follows, in accordance with the characteristic value of the slip factor μ determined in G.4 or G.5 as relevant:

$\mu \geq 0,50$ class A

$0.40 \leq \mu < 0.50$ class B

$0.30 \leq \mu < 0.40$ class C

$0.20 \leq \mu < 0.30$ class D

8.4 Proposed changes in classification according to EN 1090-2

EN 1090-2 prescribes the classification for specific surface conditions, see Table 2-6. According to this classification, the alkali-zinc silicate (ASI) coating and thermally sprayed with aluminium or zinc are classified as class B. However, the experimental results in the frame of this thesis show that all of these coatings can easily be classified as class A.

8.5 Conclusion

Current guidelines and standards do not specify any classifications for slip-resistant connections made of stainless steel. For this reason, in the frame of this study a classification was proposed for uncoated slip-resistant connections made of stainless steel based on the experimental investigations presented in Chapters 5.2 and 6.2.5.

A new revision for EN 1090-2, Annex G, was also proposed, which presents a simplified test procedure for the determination of the slip factor based on simplified test specimen geometries. These specimen geometries were developed based on the numerical and experimental investigations presented in Chapter 7.

9 Conclusions and outlook

General

Slip-resistant connections are required when slip displacement in connections must be limited to specific values either for serviceability or ultimate limit reasons.

The slip-resistant behaviour of bolted connections is essentially influenced by the preload level in the bolts and the condition of the faying surfaces. There are many other parameters which can directly or indirectly influence the slip-resistant behaviour of these connections. Unfortunately, there are no investigations on slip-resistant connections made of stainless steel. The level of viscoplastic deformation in stainless steel alloys is one of the biggest concerns for using stainless steel in preloaded bolted connections. It was feared that this phenomenon might accelerate the loss of preload in bolted connections and consequently has a negative influence on the slip-resistant behaviour of the connection. For this reason, such a study was carried out to support or disprove this theory.

The slip factor can be determined based on an experimental testing procedure. Different standards around the world prescribe different test procedures for the determination of slip factors. However, the comparability of these results is still questionable. The objective of this thesis is to close the gap in knowledge in this area. For this reason, this thesis comprises the research results from two research projects, SIROCO / Euronorm, and further investigations.

Conclusion

A comprehensive investigation was carried out in order to investigate the influence of different key parameters on the slip-resistant behaviour of preloaded bolted connections. The results show that test specimens according to EN 1090-2, Annex G, may have a different failure mechanism. With knowledge of the correct failure mechanism, it would be possible to evaluate the test results more accurately.

Different standards/guidelines prescribe different slip criteria for the evaluation of static tests, which might directly influence the determination of a static slip factor. The summarized results from SIROCO (TUD) show that the test speed can have the potential to influence the determination of the slip factor. The results show that some types of coating are more sensitive to changes in test speed. Despite this, the recommended test duration according to EN 1090-2 seems to be a suitable test duration for performing the static tests.

Furthermore, two different methods for estimating the load level for extended creep tests are presented based on the results achieved in SIROCO (FhIGP and TUD).

According to EN 1090-2, the preload level shall be measured directly with the equipment with an accuracy of ± 5 %. For this reason, two common ways of

measuring the preload level were selected which show very accurate results for both instrumented bolts with strain gauges and load cells.

Another parameter that influences the determination of the slip factor is the position of the slip measurement devices (LVDTs). Calculating the slip factor based on a slip displacement measured at plate edges (PE position) may lead to more conservative results. This is because the elongation of the plates is implicitly measured as a further slip displacement as well.

The relaxation behaviour of preloaded bolted connections can be influenced by changes in the clamping length ratio. By increasing the clamping length ratio of the connection, the loss of preload in the bolts will be decreased. Changes in the relaxation behaviour of the preloaded bolted connection will also influence the slip-resistant behaviour of the connection. The results show that a larger clamping length ratio will lead to a higher slip factor.

The preload level in the bolts is a major factor besides the surface treatment that can directly influence the determination of the slip factor. It was observed that for coated faying surfaces, the final slip factor increases slightly with decreasing preload level. However, reducing the preload level will not always have a positive influence on the design of a slip-resistant connection. EN 1090-2 prescribes that slip factors determined with specimens using bolts with property class 10.9 may also be applicable for bolts with property class 8.8. The results in this study also confirm this statement.

The condition of the faying surfaces is the most important factor in the determination of the slip factor. Grit blasted surfaces can deliver very high slip factors and having an additional coating on these surfaces may significantly influence the slip-resistant behaviour of the connection. However, having a coating to protect the carbon steel surfaces from corrosion is mandatory in many scenarios. The coating application must follow a predefined procedure in many cases in order to guarantee the quality of the coated surfaces. For some types of coatings, it is not easy to achieve a good-quality coated surface for slip-resistant connections. For instance, the preparation of hot dip galvanized surfaces can be very challenging. Many parameters influence the quality of the surfaces, which can lead to a very thick pure zinc layer on the faying surfaces. This phenomenon decreases the slip-resistant behaviour of the connection significantly. Sweeping the galvanized surfaces and coating them with an ASI or ESI coating has a positive influence on the slip-resistant behaviour of the connection.

Besides all these parameters, even the composition of the coating material or the coating thickness can play an important role in determination of the slip factor. The results show that having a thicker coating layer leads to higher static slip factor.

In the past, the lack of knowledge about the viscoplastic deformation behaviour of stainless steel caused many concerns about the use of this material in preloaded

bolted connections. The results from SIROCO confirm the viscoplastic deformations in stainless steel alloys at room temperature. The tightening test results in this project also show that using an appropriate lubricant and material pairing, it is possible to preload stainless steel bolted assemblies with property classes 8.8 and 10.9.

By confirming the preloadability of bolted assemblies made of stainless steel, a comprehensive investigation was conducted on the relaxation behaviour of preloaded bolted connections made of stainless steel. It became clear that the influence of viscoplastic deformations of the stainless steel material on the loss of preload is detectable. However, the influence of this parameter on the relaxation behaviour of bolted connections is insignificant and the results are comparable with the results of uncoated carbon steel. The loss of preload in preloaded bolted connections made of carbon steel can be much higher, as the surfaces of the carbon steel plates must be protected against corrosion. Having a coating on the surfaces may have a major influence on the relaxation behaviour of the bolted connection and may significantly increase the amount of loss of preload.

In the next step, the slip-resistant behaviour of bolted connections made of stainless steel was investigated in order to monitor the influence of viscoplastic deformation of stainless steel material on the long-term behaviour of slip-resistant connections. The investigation was conducted on both coated and uncoated surfaces with two different preload levels. Very promising slip factor results were observed for slip-resistant connections made of stainless steel. For similar surface conditions, comparable slip factor results were achieved for both stainless and carbon steel test specimens.

In general, stainless steel surfaces do not need any coating to protect them against corrosion. However, in the frame of this study the surfaces of the stainless steel specimens were coated in a thermal aluminium spray metallizing process in order to achieve higher slip factors. The results show a positive influence on the determination of the slip factors. It must be kept in mind that having an inappropriate coating may cause galvanic corrosion in a bolted connection. However, this phenomenon was not the focus of this investigation. No tests have been performed to investigate the influence of the combination of thermal aluminium spray metalized coating and stainless steel on the corrosion resistance of the stainless steel material.

Like for coated carbon steel, for stainless steel test specimens with coated faying surfaces a lower preload level leads to higher slip factors. On the other hand, for uncoated test series a higher preload level probably leads to better cold welding between the faying surfaces of uncoated faying surfaces, which in turn yields higher slip factors.

An alternative surface preparation method was developed in order to achieve higher slip factors for the untreated/as-received faying surface condition in bolted connections made of stainless steel. In this method, a combination of a two-component epoxy resin and stainless steel particles was added between the faying

surfaces to improve the slip-resistant behaviour of the connection. This study indicated that a significant improvement in the determined slip factors can be achieved by using this alternative preparation method. Adding enough of the epoxy resin around the hole and adding the particles on the surfaces of the resin will create a mixture that can flow into the hole clearances during the tightening of the bolts. After the curing time, a hard mixture of epoxy resin and particles will prevent the movement of the bolts in the hole clearance. This phenomenon helped to reach higher slip load levels in the connections.

Furthermore, different comparative investigations into the determination of slip factors according to different standards were carried out. The comparability of the determined slip factors according to EN 1090-2, Annex G, and the old TL/TP-KOR-Stahlbauten test procedure was investigated. Unlike EN 1090-2, the old version of TL/TP-KOR-Stahlbauten did not specify any kind of long-term creep tests for the determination of the slip factor. Besides this, the differences in the geometry of the test specimens and the preload level lead to an overestimation in determining the slip factor according to TL/TP-KOR-Stahlbauten. Not considering the long-term creep behaviour of the connection in the determination of the slip factor can become more critical for creep-sensitive types of coated surfaces. In addition to this important parameter, the way these tests are carried out or the evaluation criterion for these tests may also directly influence the determination of the slip factor. Both EN 1090-2 and RCSC prescribe performing the long-term creep test for the determination of the final slip factor. However, conducting and evaluating these tests on the basis of the evaluation criteria according to EN 1090-2 leads to more conservative results.

Finally, a simplified test procedure was developed on the basis of EN 1090-2, Annex G, considering the test specimen geometry format according to RCSC.

The objective of this study was to develop a simplified test specimen geometry without influencing the test results in comparison with EN 1090-2, Annex G. This simplification reduces not only the required material, the preparation costs and the workload for preparation but also the required equipment for performing the tests. The numerical and experimental investigation both confirm the comparability of the results between the simplified and standard test procedure according to EN 1090-2.

Outlook

The presented study targeted different aspects of slip-resistant connections. The influence of the most critical parameters on the slip-resistant behaviour of the connections was investigated. The main parameters for designing these connections are the preload level in the bolts and the slip factor. The influence of fatigue loads on the slip factor and on the preload are not considered in this standardized test procedure.

Furthermore, in the frame of the SIROCO project, the tightening behaviour of bolted assemblies made of stainless steel was investigated. The experimental investigations also show that the loss of preload in preloaded bolted connections made of stainless steel or carbon steel is comparable. Slip-resistant connections made of stainless steel show high slip factors that are comparable with slip factors for slip-resistant connections made of carbon steel. All these promising results for bolting assemblies made of stainless steel were achieved using EN ISO 4014/4017 bolts. These bolts are not designed for preloading, but SIROCO showed that in principle preloading of bolting assemblies made of stainless steel is possible. Up to now, no product standard exists for preloaded bolting assemblies made of stainless steel. In future, a study is needed to develop stainless steel bolting assemblies suitable for preloading comparable to those carbon steel bolting assemblies within the standard series of EN 14399, e.g. EN 14399-3 and EN 14399-4 for HR and HV bolting assemblies.

In the frame of this thesis, different surface conditions with different preload levels for bolted connections made of stainless steel were tested. The classification for slip-resistant connections made of stainless steel has been proposed and will be implemented in European and American standards. Another factor that still has an influence on slip-resistant behaviour of the connection is the factor for the hole detail, k_s. At this stage it was proposed to consider the same values for k_s for stainless steel as for carbon steel. However, in the future a comprehensive study shall be performed to verify this proposal or define a more accurate value for slip-resistant connections made of stainless steel with oversize or slotted holes.

The experimental investigations on slip-resistant connections made of stainless steel emphasizes the importance of the profile shape of the faying surfaces (topography of the faying surfaces) on the slip-resistant behaviour of the connection. A significant difference was observed between the slip factors determined for shot and grit blasted surfaces. However, according to EN 1090-2, both surface conditions are classified as class A. An experimental investigation should be carried out on shot and grit blasted carbon steel test specimens in order to ascertain the influence of the topography of the faying surfaces on the slip-resistant behaviour of bolted connections made of carbon steel. The outcome of such an investigation may possibly update the EN 1090-2 slip factor classification table in the next revision.

An alternative surface preparation method was developed to achieve higher slip factors along with reducing the cost of preparation of the faying surfaces. A future investigation will be needed in order to investigate the influence of different types of particles or epoxy resins on the determination of the slip factor.

Finally, the comparability of the slip factor results based on EN 1090-2 Annex G and RCSC Appendix A was studied. A simplified test procedure was developed based on these two standards to save time and costs as well as equipment for the determination of slip factors. Further investigation might be of interest on bolted

connections made of stainless steel with different surface conditions in order to check the comparability of the results between the simplified and standard test procedure according to EN 1090-2.

Bibliography

[1]   DIN EN 1993-1-8: 2010-11, Eurocode 3: Design of steel structures - Part 1-8: Design of joints; German version EN 1993-1-8:2005 + AC:2009.

[2]   Lin, W., Yoda, T., Bridge engineering, classifications, design loading and analysis methods, Butterworth-Heinemann, 2017, pp. 111-136

[3]   Zur Verwendung hochfester Schrauben, Stahlbau 22, Heft 9, September 1953.

[4]   Klöppel, K., Die erste Eisenbahnbrücke der Deutschen Bundesbahn mit vorgespannten, hochfesten Schrauben als Verbindungsmittel, Stahlbau 23, Heft 10, Oktober 1954.

[5]   Sossenheimer, H., Zur Anwendung von hochfesten Schrauben, Stahlbau 24, Heft 1, Januar 1955.

[6]   Hochfeste Schrauben in der amerikanischen Stahlbaupraxis, Kurze Technische Berichte, Der Bauingenieur 30, Heft 12, 1955.

[7]   Neuer amerikanische Versuche mit hochfesten Schrauben, Kurze Technische Berichte, Der Bauingenieur 30, Heft 8, 1955.

[8]   Steinhardt, O., Möhler, K., Valtinat, G.: Versuche zur Anwendung vorgespannter Schrauben im Stahlbau. I. Teil. Köln: Stahlbau-Verlags-GmbH 1954.

[9]   Steinhardt, O., Möhler, K., Valtinat, G.: Versuche zur Anwendung vorgespannter Schrauben im Stahlbau. II. Teil. Köln: Stahlbau-Verlags-GmbH 1959.

[10]   Steinhardt, O., Möhler, K., Valtinat, G.: Versuche zur Anwendung vorgespannter Schrauben im Stahlbau. III. Teil. Köln: Stahlbau-Verlags-GmbH 1962.

[11]   Steinhardt, O., Möhler, K., Valtinat, G.: Versuche zur Anwendung vorgespannter Schrauben im Stahlbau. IV. Teil. Köln: Stahlbau-Verlags-GmbH 1969.

[12]   Roth, H., Berechnung geschraubter Rahmenecken, Stahlbau 25, Heft 11, November 1956.

[13]   Dörnen, A., Trittler, G., Neue Wege der Verbindungstechnik im Stahlbau, Stahlbau 25, Heft 8, August 1956.

[14]   Born, E., Überlegungen zu den Abmessungen der Sechskantschrauben mit großen Schlüsselweiten für Stahlkonstruktionen nach Norm-Entwurf DIN 6914, DIN-Mitteilungen Bd. 41, Heft 1, Januar 1962.

[15]   Schmidt, H., Stranghöner, N., Ausführung geschraubter Verbindungen nach DIN EN 1090-2. In (Kuhlmann, U. Ed.): Stahlbau-Kalender 2011. Eurocode 3 - Grundnorm, Verbindungen. Ernst & Sohn GmbH & Co. KG, Berlin, 2011; p. 283-340.

[16]   DIN EN 1090-2: 2011-10, Execution of steel structures and aluminium structures - Part 2: Technical requirements for steel structures; German version EN 1090-2:2008+A1:2011.

[17]   DIN EN 1090-2:2018-9, Execution of steel structures and aluminium structures - Part 2: Technical requirements for steel structures; German version EN 1090-2:2018.

[18]   RCSC - Research Council on Structural Connections:2014, "Specification for Structural Joints Using High-Strength Bolts." Chicago, Illinois, August 1, 2014.

[19]   TL/TP-KOR-Stahlbauten, Technische Lieferbedingungen und Technische Prüfvorschriften für Beschichtungsstoffe für den Korrosionsschutz von Stahlbauten, Anhang E, Blatt 85, Verkehrsblatt-Dokument Nr. B5259, Vers. 12/02.

[20]   Chesson, E., Munse, W. H., Studies of the behavior of high-strength bolts and bolted joints, University of Illinois Bulletin, Volume 62, Number 26, October 1964.

[21]   Bickford, J. H., An introduction to the design and behaviour of bolted joints, - 3rd edition, revised and expanded", Marcel Dekker, Inc., New York, USA, 1995.

[22]   Heistermann, C., Behaviour of Pretensioned Bolts in Friction Connections, PhD-Thesis, Lulea University of Technology, 2011.

[23]   Kloos, K.-H., Wiegand, H., Thomala, W., Schraubenverbindungen - Grundlagen, Berechnung, Eigenschaften, Handhabung, 5. Auflage, Springer Verlag, Berlin, 2007.

[24]   Hasselmann, U., Valtinat, G., Geschraubte Verbindungen. In: Kuhlmann, U. (hg.): Stahlbau Kalender 2002, Ernst & Sohn, Berlin, 343–421.

[25]   Friede, R., Lange, J., Vorspannkraftverluste in HV-Schraubverbindungen, Stahlbau 85 (2016), Heft 12, S. 836-844.

[26]   Nah, H. S., Lee, H. J., Kim, K. S., Kim, J. H., Kim, W. B., Evaluating relaxation of high-strength bolts by parameters on slip faying surfaces of bolted connections, International Journal of Steel Structures, Volume 10, Issue 3, pp. 295–303, September 2010.

[27]   DeWolf, J. T., Yang, J., Mathematical Model for Relaxation in High-Strength Bolted Connections, Journal of Structural Engineering / Vol. 125 Issue 8, pp. 803 - 809, August 1999.

[28]   DeWolf, J. T., Yang, J., Relaxation in High-Strength Bolted Connections Using Galvanized Steel, Journal of Bridge Engineering / Vol. 5 Issue 2, pp. 99 - 106, May 2000.

[29]   H. S. Nah, H. J. Lee, S. M. Choi, Evaluating long-term relaxation of high strength bolts considering coating on slip faying surface, Steel and Composite Structures, Vol. 16, No. 6, pp. 703 – 718, March 31, 2014.

[30]   Sedlacek, G., Kammel, Chr., Dauerverhalten von GV-Verbindungen bei verzinkten Konstruktionen im Freileitungs-, Mast- und Kaminbau, Forschungsbericht für die Praxis P 409, Studiengesellschaft Stahlanwendung e.V., Verlag und Vertriebsgesellschaft mbH, Düsseldorf, 2001.

[31]   Sedlacek, G., Kammel, Chr., Zum Dauerverhalten von GV-Verbindungen in verzinkten Konstruktionen - Erfahrungen mit Vorspannkraftverlusten, Stahlbau 70 (2001), Heft 12, S. 917–926.

[32]   Katzung, W., Pfeiffer, H. Schneider, A., Zum Vorspannkraftabfall in planmäßig

vorgespannten Schraubenverbindungen mit beschichteten Kontaktflächen, Stahlbau, Ernst & Sohn, Vol. 65, Issue 9, pp. 307 – 311, 1996.

[33] DeWolf, J. T., Yang, J., Relaxation in high-strength bolted connections with galvanized steel, Final report, JHR 98-262, Project 96-4, University of Connecticut, Storrs, Connecticut, USA, 1998.

[34] K. Shemwell, D.R. Johns, Long-Term Performance of Stainless Steel Fasteners, Final Report, 7210-MA/819, European Commission, Technical Steel Research, 1997 Report EUR 1848 EN.

[35] VDI 2230, Part 1:2015-11, Systematic calculation of highly stressed bolted joints, Joints with one cylindrical bolt, VDI-guideline, The Association of German Engineers, November 2015.

[36] Lee, J. H., O'Connor, C., Fisher, J. W., Effect of surface coatings and exposure on slip behavior of bolted joints, Fritz Engineering Laboratory Report No. 318.5, Lehigh University, Bethlehem, Pennsylvania, June 1968.

[37] ORE-report: Probleme der Verbindungen mit hochfesten vorgespannten Schrauben in Stahlbauten (Frage D90). Bericht Nr. 8 (Schlußbericht) – Zusammenfassung des Inhalts der Berichte Nr. 1–7. Utrecht, 1973.

[38] Gruintjes, T. J. J.; Bouwman, L. P.: Slip factors of structural connections formed with high-strength friction grip bolts and with contact surfaces treated in various ways, TU Delft, Report 6-84-10, ECCS No. 37, July 1984.

[39] ECCS – European Recommendations for bolted connections in structural steelwork, No. 38, 1985.

[40] BS 5950-1:2000, Structural use of steelwork in building, Part 1: Code of practice for design - Rolled and welded sections, May 2001.

[41] IS 800:2007, Indian Standard, General Construction in Steel - Code of Practice (Third Revision), Bureau of Indian Standards, draft finalized by Structural Engineering and Structural Sections Sectional Committee, CED 7, December 2007.

[42] IS 4000:1992, Indian Standard high strength bolts in Steel Structures - code of practice, (first revision), Bureau of Indian Standards, draft finalized by Structural Engineering and Structural Sections Sectional Committee, CED 7, January 1992.

[43] Dusel, J. P., Stoker, J. R., Nordlin, E. F.: The Effects Of Coatings Applied To Contact Surfaces Of High-Strength Bolted Joints On Slip Behavior And Strength Of Joints. Final report D-4-112. Sacramento, California, USA 1977.

[44] Young, D.R., Hechtman, R. A., Slip of structural steel double-lap joints assembled with high-strength bolts, first progress report, University of Washington, Engineering Experiment Station in cooperation with the Research Council on Riveted and Bolted Structural Joints, Seattle, Washington, January, 1951.

[45] Rumpf, J.L., Further static tension tests of bolted joints, Fritz Laboratory Reports. Paper 1735, Lehigh University December 1958.

[46] Hansen, R. M., Rumpf, J. L., Further static tension tests of long bolted joints, Fritz Laboratory Report No. 271.15, Reports. Paper 1731, September 1960.

[47] JSCE:2009, Standard Specifications for Steel and Composite Structures,

Japan Society of Civil Engineers, First Edition, December, 2009.

[48]   Owens, G. W., Cheal, B. D.: Structural steelwork connections. London [u.a.]: Butter-worths 1989.

[49]   Cruz, A., Simões, R., Alves, R., Slip factor in slip resistant joints with high strength steel, Journal of Constructional Steel Research 70 (2012), pp. 280-288.

[50]   Kulak, G. L., Fisher, J. W., Struik, J. H. A. (2001). "Guide to Design Criteria for Bolted and Riveted Joints." 2nd Edition, AISC – American Institute of Steel Construction, Inc., Chicago, 2001.

[51]   Kulak, G. L., Fisher, J. W., Behavior of slip-resistant bolted joints, IABSE Periodica, volume 9 (1985), Issue S-32/85, pp. 48-62.

[52]   ISO 10721-1:1997-02, Steel structures - Part 1: Materials and design.

[53]   BS 5400-3:2000, Steel, concrete and composite bridges. Code of practice for design of steel bridges, October 2000.

[54]   Kim, T. S., Lee, H. S., Yoo, J. H., Tae, S. H., Oh, S. H., Lim, Y. C., Lee, S. B., Slip coefficient in high-strength bolt joints coated with Corrosion-Resistant Zn/Al Metal Spray Method, Materials and Manufacturing Processes, 26: pp. 14–21, 2011.

[55]   AASHTO LRFD Bridge design specifications 2012, sixth edition, Washington, D.C. :American Association of State Highway and Transportation Officials, 2012.

[56]   DIN 18800-7:2008-11, Steel structures – Part 7: Execution and constructor's qualification.

[57]   ANSI/AISC 360-16, Specification for structural steel buildings, An American National Standard, American Institute of Steel Construction, July 7, 2016.

[58]   GB 50017:2003, Code for Design of Steel Structures, National Standard of the People's Republic of China, the Ministry of Construction of the People's Republic of China and the General Administration of Quality Supervision, Inspection and Quarantine of the People's Republic of China, April 25, 2003.

[59]   CAN/CSA-S16-09:2009, Design of steel structures, Canadian Standards Association, September 2009.

[60]   AS 4100:1998, Steel Structures, Standards Australian (Standard Association of Australia), June 1998.

[61]   NZS 3404: Part 1:1997, Steel Structure Standard, Standards New Zealand, Steel Structures Committee (P3404), October 2007.

[62]   BS 5400-3:2000, Steel, concrete and composite bridges. Code of practice for design of steel bridges, October 2000.

[63]   Cheal, B., CIRIA Technical Note 98 - Design guidance notes for friction grip bolted connections, 1980.

[64]   SSPC Paint Specification No. 20, The Society for Protective Coatings, April 2002.

[65]   Tamba, Y., Yukiito, S., Kimura, S., Yamaguchi, T., Sugiura, K., Slip coefficient for high-strength bolted frictional joints with roughened steel surface and

inorganic zinc-rich painted surface, Journal of JSCE, Vol. 3, 19-32, 2015.

[66]   Lower, B. R., Determination of the slip coefficient for organic and inorganic primers in bolted connections, Michigan Department of Transportation, Research project 89 TI-1385, Research report No. R-1314.

[67]   Black, W., Moss, D. S.: High strength friction grip bolts –slip factors of protected faying surfaces. Road Research Laboratory, Bericht LR 153. Crowthorne, England, 1968.

[68]   Frank, K. H., Yura, J. A., An experimental study of bolted shear connections, Report No. FHWA/RD-81/148, U.S. Department of Transportation, December 1981.

[69]   Annan, C. D., Chiza, A., Characterization of slip resistance of high strength bolted connections with zinc-based metallized faying surfaces, Engineering Structures 56 (2013) 2187–2196.

[70]   Annan, C. D., Chiza, A., Slip resistance of metalized–galvanized faying surfaces in steel bridge construction, Journal of Constructional Steel Research 95 (2014) 211–219.

[71]   DIN EN ISO 1461:2009-10, Hot dip galvanized coatings on fabricated iron and steel articles - Specifications and test methods (ISO 1461:2009); German version EN ISO 1461:2009.

[72]   Heistermann, C., Veljkovic M., Simões, R., Rebelo, C., Simões da Silva, L. (2013) Design of slip resistant lap joints with long open slotted holes, Journal of Constructional Steel Research 82, Elsevier Ltd, lulea University of Technology, Sweden, University of Coimbra, Portugal.

[73]   Valtinat, G., Gleitfeste Vorgespannte Verbindungen mit Langlöchern bei feuerverzinkten Stahlbauteilen für Fassaden-Unterkonstruktionen, Gemeinschaftsausschuss Verzinken e.V., Forschungsvorhaben GAV-Nr. FG 25, Technische Universität Hamburg-Harburg, Deutschland, Bericht Nr. 132, 1996.

[74]   Birkemoe, P. C., Herrschaft, D. C.: Bolted galvanized bridges – engineering acceptance near. Civil Engineering (ASCE) 40 (1970), S. 42-46.

[75]   Valtinat, G., Albrecht,F. & Dangelmaier, P., Gleitfeste Verbindungen mit feuerverzinkten Stahlteilen und Reibfesten Beschichtungen oder anderen reibbeiwerterhöhenden Maßnahmen, Gemeinschaftsausschuss Verzinken e.V., Technische Universität Hamburg-Harburg, Deutschland, Forschungsbericht, Heft 3, Bericht Nr. 122., 1993.

[76]   Foreman, R. T., Rumpf, J. L., Static tension tests of compact belted joints, Fritz Engineering laboratory Report No. 271.6, sponsored financially by the Pennsylvania Department-of Highways and the Bureau of Public Roads, July 1959.

[77]   Chesson Jr., E., Munse, W. H., Studies of the behavior of high-strength bolts and bolted joints, the Engineering Experiment Station of the University at Illinois in cooperation with The Research Council on Riveted and Halted Structural Joints, The Illinois Division at Highways (Project IHR-51) Illinois Cooperative Highway Research Program, Series Na. 20, University of Illinois Bulletin 469, Volume 62, Number 26, October 1964.

[78]   Rumpf, J. L., The ultimate strength of bolted connections, Doctor of

Philosophy Dissertation, Lehigh University, 1960.

[79]   Bendigo, R. A., Fisher, J. L., Rumpf, J. L., Static tension tests of bolted lap joints, Fritz Laboratory Report No. 271.9, Reports. Paper 1741, August 1962.

[80]   Rumpf, J. L., Shear resistance of high strength bolts, Fritz Laboratory Report No. 271.3, Reports. 81, December 1958.

[81]   Bendigo, R. A., Static tension tests of long bolted joints, Master of Science Thesis, Lehigh University, 1960.

[82]   Fouad, F. H., Slip behavior of bolted friction-type joints with coated contact surfaces, Master of Science Thesis, The University of Texas at Austin, May 1978.

[83]   Poposka, M., Petreski, B., Cvetanovski, P., Popovski, D., Experimental procedure for slip factor determining at connections with preloaded bolts, Electronic Journal of the faculty of civil engineering Osijek - e-GFOS 5, 8, 2014, p. 37-43.

[84]   DIN 17100:1966-09, Steels for general structural purposes; quality specifications.

[85]   EN 10025-2:2019-10, Hot rolled products of structural steels - Part 2: Technical delivery conditions for non-alloy structural steels; German version EN 10025-2:2019.

[86]   Probleme der Verbindungen mit hochfesten vorgespannten Schrauben in Stahlbauten: ORE-Frage D 90 / Forschungs- und Versuchsamt des Internationalen Eisenbahnverbandes; 1: Reibbeiwerte unterschiedlich behandelter Reibflächen, International Union of Railways, Office of Research and Experimentation, 1966.

[87]   Probleme der Verbindungen mit hochfesten vorgespannten Schrauben in Stahlbauten: ORE-Frage D 90 / Forschungs- und Versuchsamt des Internationalen Eisenbahnverbandes; 2: Reibbeiwerte unterschiedlich geschützter Reibflächen, International Union of Railways, Office of Research and Experimentation, 1967.

[88]   Probleme der Verbindungen mit hochfesten vorgespannten Schrauben in Stahlbauten: ORE-Frage D 90 / Forschungs- und Versuchsamt des Internationalen Eisenbahnverbandes; 3: Einfluß der Witterung auf die Reibbeiwerte ungeschützter und geschützter Reibflächen, International Union of Railways, Office of Research and Experimentation, 1968.

[89]   Probleme der Verbindungen mit hochfesten vorgespannten Schrauben in Stahlbauten: ORE-Frage D 90 / Forschungs- und Versuchsamt des Internationalen Eisenbahnverbandes; 4: Zeitstandversuche, International Union of Railways, Office of Research and Experimentation, 1969.

[90]   Probleme der Verbindungen mit hochfesten vorgespannten Schrauben in Stahlbauten: ORE-Frage D 90 / Forschungs- und Versuchsamt des Internationalen Eisenbahnverbandes; 5: Dauerschwingversuche mit geschützten Reibflächen, International Union of Railways, Office of Research and Experimentation, 1970.

[91]   Probleme der Verbindungen mit hochfesten vorgespannten Schrauben in Stahlbauten: ORE-Frage D 90 / Forschungs- und Versuchsamt des Internationalen Eisenbahnverbandes; 8: Zusammenfassung des Inhalts der

Berichte Nr.1-7: Schlußbericht, International Union of Railways, Office of Research and Experimentation, 1973.

[92]   DIN 6914: 1962-08, High-strength hexagon head bolts with large widths across flats for structural steel bolting.

[93]   DIN 6915: 1962-08, Hexagon nuts with large widths across flats for high strength structural bolting.

[94]   DIN EN 14399-4:2015-4, High-strength structural bolting assemblies for preloading – Part 4: System HV – Hexagon bolt and nut assemblies; German version EN 14399-4:2015.

[95]   DIN 6916:1962-08, Round washers for high-strength structural steel bolting.

[96]   DIN EN 14399-6:2015-4, High-strength structural bolting assemblies for preloading – Part 6: Plain chamfered washers; German version EN 14399-6:2015.

[97]   BS 4604-1: 1970, Specification for the use of high strength friction grip bolts in structural steelwork metric series - part 1: general grade.

[98]   BS 4395-1:1969, Specification for High strength friction grip bolts and associated nuts and washers for structural engineering metric series - part 1: general grade..

[99]   DIN EN ISO 898-1:2013-5, Mechanical properties of fasteners made of carbon steel and alloy steel - part 1: bolts, screws and studs with specified property classes - coarse thread and fie pitch thread (ISO 898-1:2013); German version EN ISO 898-1:2013.

[100] BS 4604-2: 1970, Specification for the use of high strength friction grip bolts in structural steelwork metric series - part 2: higher grade (parallel shank).

[101] BS 4395-2:1969, Specification for High strength friction grip bolts and associated nuts and washers for structural engineering metric series - part 2: higher grade bolts and nuts and general grade washers.

[102] AS/NZS 5131:2016, Structural steelwork - Fabrication and erection, Australian/New Zealand standard, December 2016.

[103] AS 4291.1:2015, Mechanical properties of fasteners made of carbon steel and alloy steel bolts, screws and studs.

[104] Yura, J.A. and K.H. Frank, 1985, "Testing Method to Determine Slip Coefficient for Coatings Used in Bolted Joints," Engineering Journal, Vol. 22, No. 3, (3rd Qtr.), AISC, Chicago, IL.

[105] Kim, T. S., Lee, H. S., Yoo, J. H., Tae, S. H., Oh, S. H., Lim, Y. C., Lee S. B., Slip coefficient in high-strength bolt joints coated with corrosion-resistant Zn/Al metal spray method, Materials and Manufacturing Processes, 26, 2011, p. 14-21.

[106] Stranghöner, N., Afzali, N., Jungbluth, D., Abraham, C., Veljkovic, M., Bijlaard, F., Gresnigt, N., de Vries, P., Kolstein, H., Nijgh, M., Schedin, E., Pilhagen, J., Jakobsen, E., Söderman, A., Glienke, R., Ebert, A., Baddoo, N., Chen, A., Hradil, P., Talja, A., Rantala, J., Auerkari, P., Säynäjäkangas, J., Manninen, T., Rudolf, A., Berger, S., Cook, M., Taylor, M., Huckshold, M., Execution and reliability of slip resistant connections for steel structures using CS and SS, RFCS Research project SIROCO (RFSR-CT-2014-00024), Final Report, 10

July 2018.

[107] Stranghöner, N., Afzali, N., Berg, J., Mertesacker, D., Alternative Beschichtungssysteme für gleitfeste Verbindungen, the Federal Ministry of Economics and Labour (Bundesministerium für Wirtschaft und Arbeit), Germany and EuroNorm GmbH via the programme INNO-KOM-Ost (MF130085).

[108] Schiborr, M., Berg, J., Afzali, N., Stranghöner, N., Determination of the slip factor of slip-resistant connections – Effects of different interpretation of codes of practice (in German), Proceedings of the 19. DASt-Kolloquium, Hannover, Germany, October 27th – 28th, 2014, p.120-125.

[109] EN ISO 4287:2010-07, Geometrical Product Specifications (GPS) - Surface texture: Profile method - Terms, definitions and surface texture parameters (ISO 4287:1997 + Cor 1:1998 + Cor 2:2005 + Amd 1:2009).

[110] EN ISO 2808:2007, Paints and varnishes – Determination of film thickness.

[111] Stranghöner, N., Afzali, N., de Vries, P., Glienke, R., Ebert, A.: Optimization of the test procedure for slip factor tests according to EN 1090-2, Steel Construction 10 (2017), Issue 4, p. 267-281.

[112] Stranghöner, N., Jungbluth, D., Afzali, N., Ausführung (nicht) standardisierter Verschraubungen im Stahlbau, in: Stahlbau Kalender 2019, S. 225-264, Hrsg.: Kuhlmann, U., Verlag: Ernst & Sohn GmbH & Co. KG, Berlin, 2019.

[113] Bickford, J. H., Nassar S., Handbook of bolts and bolted joints, Marcel Dekker, INC., New York, 1998.

[114] Bickford, J. H., Introduction to the design and behaviour of bolted joints, - Fourth edition, Non-Gasketed joints", Taylor & Francis Group, LLC, 2008.

[115] Horváth, P., Tóth, P., Nondestructive bolt preload measurement, Athens Journal of Technology and Engineering - Volume 5, Issue 2 – Pages 91-110.

[116] Stranghöner, N., Afzali, N., Berg, J., Recommendation of applicable methods for measuring the preload in bolts, RFCS research project SIROCO (RFSR-CT-2014-00024), Deliverable report D1.1, 24 March 2016.

[117] Stranghöner, N., Afzali, N., Berg, J., Schiborr, M., Bijlaard, F., Gresnigt, N., de Vries, P., Glienke, R., Ebert, A., Influence of different testing criteria on the slip factor of slip-resistant connections, Proceedings of the 13th Nordic Steel Construction Conference, Tampere, Finland, 23-25 September, 2015.

[118] Stranghöner, N., Afzali, N., Berg, J., Gleitfeste Verbindungen im Turm- und Mastbau - Prüfung und Beschichtung, Stahlbau 84 (2015), Heft 12, S. 966-979.

[119] Abaqus (2018), ABAQUS User's Manual, Version 6.14 Documentation, Dassault Systemes Simulia Corp. Providence, RI, USA.

[120] VDI 2230 Blatt 1:2015-11, Systematic calculation of highly stressed bolted joints - Joints with one cylindrical bolt.

[121] Stranghöner, N., Afzali, N., Comparative study on the influence of bolts preloaded in the plastic range vs. bolts preloaded in the elastic range only, RFCS research project SIROCO (RFSR-CT-2014-00024), Deliverable report D2.2, 23 March 2018.

[122] Stranghöner, N., Afzali, N., Berg, J., de Vries, P., Recent Investigations into the Slip Factor of Slip-Resistant Connections, Connections VIII, Eighth International Workshop on Connections in Steel Structures, Boston, USA, 24-26 May 2016.

[123] Afzali, N., Berg, J., Stranghöner, N., Influence of Different Preload Levels and Faying Surfaces on the Slip-Resistant Behaviour of Bolted Connections, 26th International Ocean and Polar Engineering Conference, ISOPE, Rhodes, Greece, 26 June - 1 July 2016, p. 233-240.

[124] DIN EN ISO 8501-1:2007-12, Preparation of steel substrates before application of paints and related products - Visual assessment of surface cleanliness - Part 1: Rust grades and preparation grades of uncoated steel substrates and of steel substrates after overall removal of previous coatings (ISO 8501-1:2007); German version EN ISO 8501-1:2007.

[125] Stranghöner, N., Afzali, N., Slip-resistant connections made of hot-dip galvanized steel - The EU SIROCO Project, The 25th International Galvanizing Conference, Berlin, Germany, 18-20 June 2018, p. 87-100.

[126] DIN EN ISO 14713-2:2020-5, Zinc coatings - Guidelines and recommendations for the protection against corrosion of iron and steel in structures - Part 2: Hot dip galvanizing (ISO 14713-2:2019); German version EN ISO 14713-2:2020.

[127] DIN EN ISO 3274:1998-04 Geometrical Product Specifications (GPS) - Surface texture: Profile method - Nominal characteristics of contact (stylus) instruments (ISO 3274:1996); German version EN ISO 3274:1997.

[128] Stranghöner, N., Afzali, N., Cook, M., Berger, S., Influence of the surface preparation and type of coating system on the slip factor and on the corrosion protection in case of hot dip galvanized steel, RFCS research project SIROCO (RFSR-CT-2014-00024), Deliverable report D4.2, 12 March 2018.

[129] Stranghöner, N., Afzali, N., Berg, J., Schiborr, M., Rudolf, A., Berger, S., Different coating systems for the application in slip-resistant connections, Proceedings of the 13th Nordic Steel Construction Conference, Tampere, Finland, 23-25 September, 2015.

[130] DIN EN 1993-1-4:2015-10, Eurocode 3: Design of steel structures - Part 1-4: General rules - Supplementary rules for stainless steels; German version EN 1993-1-4:2006 + A1:2015.

[131] DIN EN 14399-3:2015-04, High-strength structural bolting assemblies for preloading - Part 3: System HR - Hexagon bolt and nut assemblies; German version EN 14399-3:2015.

[132] Manninen, T.; Jakobsen, E.; Pilhagen, J: Literature study on creep and stress relaxation of stainless steel at room temperature, RFCS research project SIROCO (RFSR-CT-2014-00024), Deliverable report D5.1, 30 June 2017.

[133] W. N. Findley, J. S. Lai, K. Onaran, Creep and relaxation of nonlinear viscoelastic materials with an introduction to linear viscoelasticity, 1st Edition, North-Holland Publishing Company, January 1976.

[134] Rusinko, A., Rusinko, K., Plasticity and creep of metals, Springer-Verlag Berlin Heidelberg, 2011.

[135] Betten J., Creep Mechanics, Third Edition, Springer-Verlag Berlin Heidelberg,

2008.

[136] Kassner, M.E., Smith, K., Low temperature creep plasticity, Journal of Materials Research and Technology. 3 (2014) 280–288.

[137] Manninen, T.; Pilhagen, J: Creep and stress relaxation behavior of stainless steel plates at room temperature, RFCS research project SIROCO (RFSR-CT-2014-00024), Deliverable report D5.2, 30 June 2017.

[138] Manjoine, M. J., Stress relaxation characteristics and data utilization, Proceedings of the Twenty-eighth Sagamore Army Materials Research Conference entitled Residual Stress and Stress Relaxation, July 1981, p. 519-530.

[139] Meyers, M. A., Chawla, K. K., Mechanical behavior of materials, Cambridge University Press 2009.

[140] Smith, E. H., Mechanical engineer's reference book, Twelfth edition, Reed Educational and Professional Publishing Limited 1994.

[141] Pilhagen, J: Report on creep and stress relaxation behavior of stainless steel bars and bolts, RFCS research project SIROCO (RFSR-CT-2014-00024), Deliverable report D5.3, 30 June 2017.

[142] K. Shemwell, D.R. Johns, Long-Term Performance of Stainless Steel Fasteners, Final Report, 7210-MA/819, European Commission, Technical Steel Research, 1997 Report EUR 1848 EN.

[143] DIN EN ISO 3506-1:2020-08, Mechanical properties of corrosion-resistant stainless steel fasteners - Part 1: Bolts, screws and studs with specified property classes - Coarse pitch thread and fine pitch thread (ISO 3506-1:2020); German version EN ISO 3506-1:2020.

[144] DIN EN ISO 3506-2:2020-08, Mechanical properties of corrosion-resistant stainless steel fasteners - Part 2: Nuts with specified property classes - Coarse pitch thread and fine pitch thread (ISO 3506-2:2020); German version EN ISO 3506-2:2020.

[145] DIN EN ISO 898-2:2012-8, Mechanical properties of fasteners made of carbon steel and alloy steel - Part 2: Nuts with specified property classes - Coarse thread and fine pitch thread (ISO 898-2:2012); German version EN ISO 898-2:2012.

[146] DIN EN ISO 4014:2011-6, Hexagon head bolts - Product grades A and B (ISO 4014:2011); German version EN ISO 4014:2011.

[147] DIN EN ISO 4017:2015-5, Fasteners - hexagon head screws - product grades A and B (ISO 4017:2014); German version EN ISO 4017:2014.

[148] Stranghöner, N., Jungbluth, D., Afzali, N., Lorenz, C., Einblick in das Vorspannverhalten von geschraubten Verbindungen aus nichtrostendem Stahl, Stahlbau 86 (2017), Heft 4, S. 302-314.

[149] Stranghöner, N., Jungbluth, D., Afzali, N., Preloading of stainless steel bolting assemblies, Proceedings of Eurosteel 2017 Conference, Copenhagen, Denmark, ce/papers 1 (2017), Issue 2-3, p. 342–351.

[150] DIN EN ISO 4032:2013-04, Hexagon regular nuts (style 1) - Product grades A and B (ISO 4032:2012); German version EN ISO 4032:2012.

[151]   DIN EN ISO 7089:2000-11, Plain washers - Normal series, Product grade A (ISO 7089:2000); German version EN ISO 7089:2000.

[152]   DIN EN 14399-2:2015-4, High-strength structural bolting assemblies for preloading - Part 2: Suitability for preloading; German version EN 14399-2:2015; German version EN 14399-2:2015.

[153]   Stranghöner, N., Abraham, C., Afzali, N., Jungbluth, D., Preloading behaviour and preloading levels for stainless steel bolt assemblies including relaxation with detailed specifications for recommended preloading levels, RFCS research project SIROCO (RFSR-CT-2014-00024), Deliverable report D5.4, 30 March 2018.

[154]   DASt-Richtlinie 024:2018-06, Anziehen von geschraubten Verbindungen der Abmessungen M12 bis M36, Deutscher Ausschuss für Stahlbau, Stahlbau Verlags- und Service GmbH, Düsseldorf.

[155]   Jungbluth, D., Stranghöner, N., Abraham, C., Afzali, N., Preloading of Stainless Steel Bolting Assemblies, 28th International Ocean and Polar Engineering Conference, ISOPE, Sapporo, Japan, 10-15 June 2018, Volume IV, p. 354-362.

[156]   Stranghöner, N., Jungbluth, D., Abraham, C., Söderman, A., Tightening behaviour of preloaded stainless steel bolting assemblies, Steel Construction 10 (2017), Issue 4, p. 319-332.

[157]   Stranghöner, N., Jungbluth, D., Afzali, N., Abraham, C., Vorgespannte Schraubverbindungen aus nichtrostendem Stahl, Stahlbau 89 (2020), Heft 4, S. 326-338, DOI: 10.1002/stab.202000004.

[158]   Stranghöner, N., Jungbluth, D., Abraham, C., Guidance for Preloading of Stainless Steel Bolting Assemblies using a Bolt Tightening Qualification Procedure, Proceedings of Nordic Steel 2019 Conference, Copenhagen, Denmark, ce/papers 3 (2019), Issue 3-4, p. 919–924.

[159]   Jungbluth, D., Stranghöner, N., Afzali, N., Abraham, C., Bolt Tightening Qualification Procedure (BTQP) for Preloaded Bolted Connections Made of Stainless Steel, 29th International Society of Offshore and Polar Engineers Conference, ISOPE, Honolulu, USA, 16-21 June 2019.

[160]   Afzali, N., Pilhagen, J., Manninen, T., Schedin, E., Stranghöner, N., Creep and Relaxation Behaviour of Stainless Steel Bolted Assemblies, Fifth International Experts Seminar, Stainless Steel in Structures, Organised by The Steel Construction Institute (SCI), London, UK, 18-19 September 2017.

[161]   Afzali, N., Pilhagen, J., Manninen T., Schedin, E., Stranghöner, N., Preload losses in stainless steel bolting assemblies, Steel Construction 10 (2017), Issue 4, p. 310-318.

[162]   Afzali, N., Stranghöner, N., Pilhagen, J., Manninen T., Schedin, E., Viscoplastic deformation behaviour of preloaded stainless steel connections, Journal of Constructional Steel Research 152 (2019) 225–234.

[163]   Stranghöner, N., Afzali, N., de Vries, P., Slip factors for typical stainless steel surface finishes and new types of coatings for stainless steel, RFCS research project SIROCO (RFSR-CT-2014-00024), Deliverable report D6.2, 23 March 2018.

[164]   Stranghöner, N., Afzali, N., de Vries, P., Schedin, E., Pilhagen, J., Behaviour

of Slip-resistant Stainless Steel Bolted Connections, Fifth International Experts Seminar, Stainless Steel in Structures, Organised by The Steel Construction Institute (SCI), London, UK, 18-19 September 2017.

[165] Stranghöner, N., Afzali, N., de Vries, P., Schedin, E., Pilhagen, J., Slip-resistant bolted connections of stainless steel, Steel Construction 10 (2017), Issue 4, p. 333-343.

[166] Afzali, N., Stranghöner, N., Tragverhalten von gleitfesten Verbindungen aus nichtrostendem Stahl, 21. DASt-Forschungskolloquium, Deutscher Ausschuß für Stahlbau, Kaiserslautern, 6.-7. März 2018, S. 70-75.

[167] Stranghöner, N., Afzali, N., de Vries, P., Schedin, E., Pilhagen, J., Slip factors for slip-resistant connections made of stainless steel, Journal of Constructional Steel Research 152 (2019) 235–245.

[168] Liljedahl, F., Schedin, E., Topography between contact surfaces in slip resistant bolted joint, RFCS research project SIROCO (RFSR-CT-2014-00024), Deliverable report D6.0, 02 October 2015.

[169] DIN EN ISO 527-1:2019-12, Plastics - Determination of tensile properties - Part 1: General principles (ISO 527-1:2019); German version EN ISO 527-1:2019.

[170] Afzali, N., Abraham, C., Stranghöner, N., Comparative numerical investigations into the determination of slip factors according to the EN 1090–2 and RCSC, Proceedings of Nordic Steel 2019 Conference, Copenhagen, Denmark, ce/papers 3 (2019), Issue 3-4, p. 385–390.

[171] Maiorana E., Zampireri, P., Pellegrino C., Experimental tests on slip factor in friction joints: comparison between European and American Standards, Fracture and Structural Integrity, 43, January 2018, p. 205-217.

[172] ASME B18.2.6M - 2012, Metric fasteners for use in structural applications, the American Society of Mechanical Engineers.

[173] ASTM F3125 / F3125M - 19, Standard Specification for High Strength Structural Bolts and Assemblies, Steel and Alloy Steel, Heat Treated, Inch Dimensions 120 ksi and 150 ksi Minimum Tensile Strength, and Metric Dimensions 830 MPa and 1040 MPa Minimum Tensile Strength.

[174] ASTM F436 / F436M - 19, Standard Specification for Hardened Steel Washers Inch and Metric Dimensions.

[175] ASTM A563M - 07(2013), Standard Specification for Carbon and Alloy Steel Nuts (Metric).

[176] ISO 8503-1:2012, Preparation of steel substrates before application of paints and related products - Surface roughness characteristics of blast-cleaned steel substrates - Part 1: Specifications and definitions for ISO surface profile comparators for the assessment of abrasive blast-cleaned surfaces (ISO 8503-1:2012).

[177] ASTM D7127 - 17, Standard Test Method for Measurement of Surface Roughness of Abrasive Blast Cleaned Metal Surfaces Using a Portable Stylus Instrument, 2017.

ASTM D4417 - 20, Standard Test Methods for Field Measurement of Surface Profile of Blast Cleaned Steel, 2020.

Annex A: Loss of preload in stainless steel connections
with mixture of resin and particle between the faying surfaces

(a) Rate of loss of preload - Log (time) diagram

(b) Log (rate of loss of preload) - Log (time) diagram

(c) Loss of preload - Log (time) diagram

(d) Loss of preload after one day/ 50 years
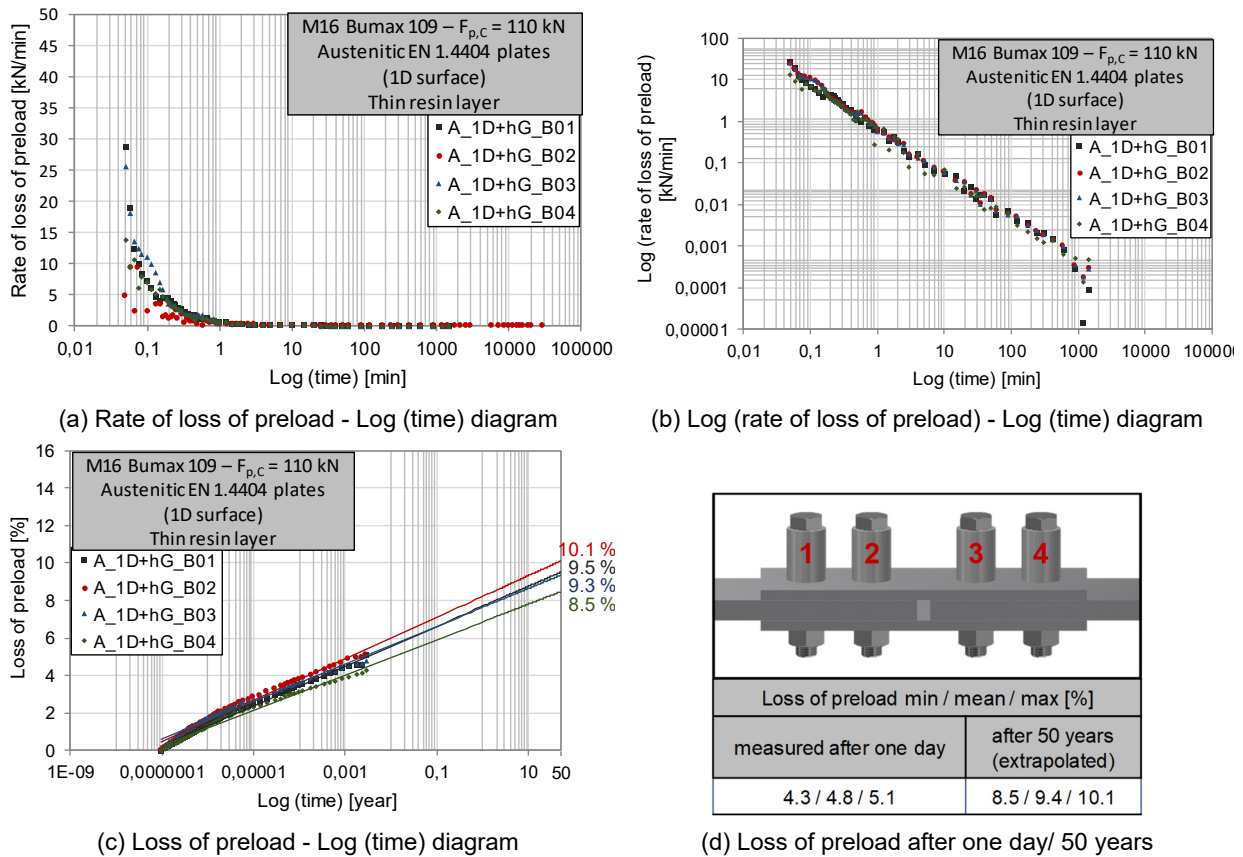
Figure A-1: Loss of preload for A_tR test specimen

(a) Rate of loss of preload - Log (time) diagram

(b) Log (rate of loss of preload) - Log (time) diagram

(c) Loss of preload - Log (time) diagram

(d) Loss of preload after one days/ 50 years
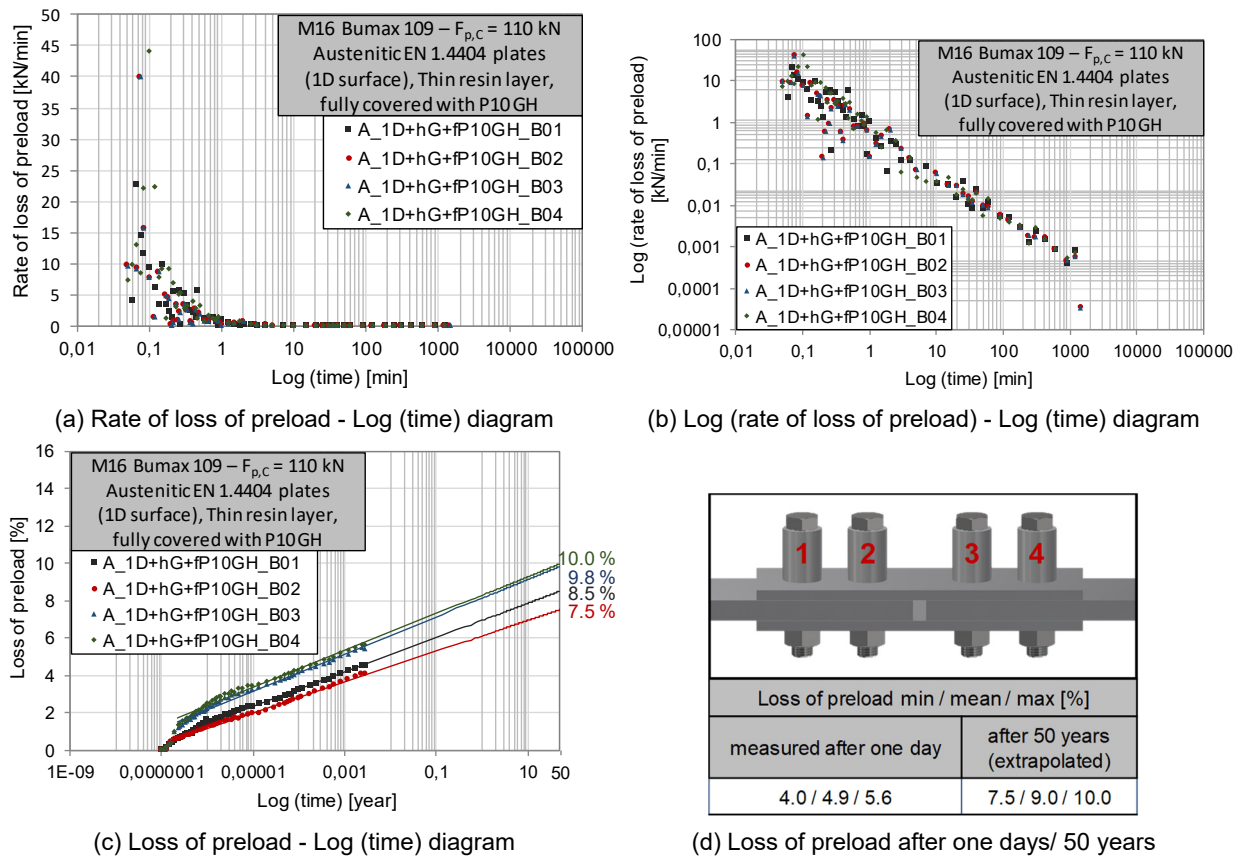
Figure A-2: Loss of preload for A_tR+fP10 test specimen

(a) Rate of loss of preload - Log (time) diagram

(b) Log (rate of loss of preload) - Log (time) diagram

(c) Loss of preload - Log (time) diagram

(d) Loss of preload after one days/ 50 years
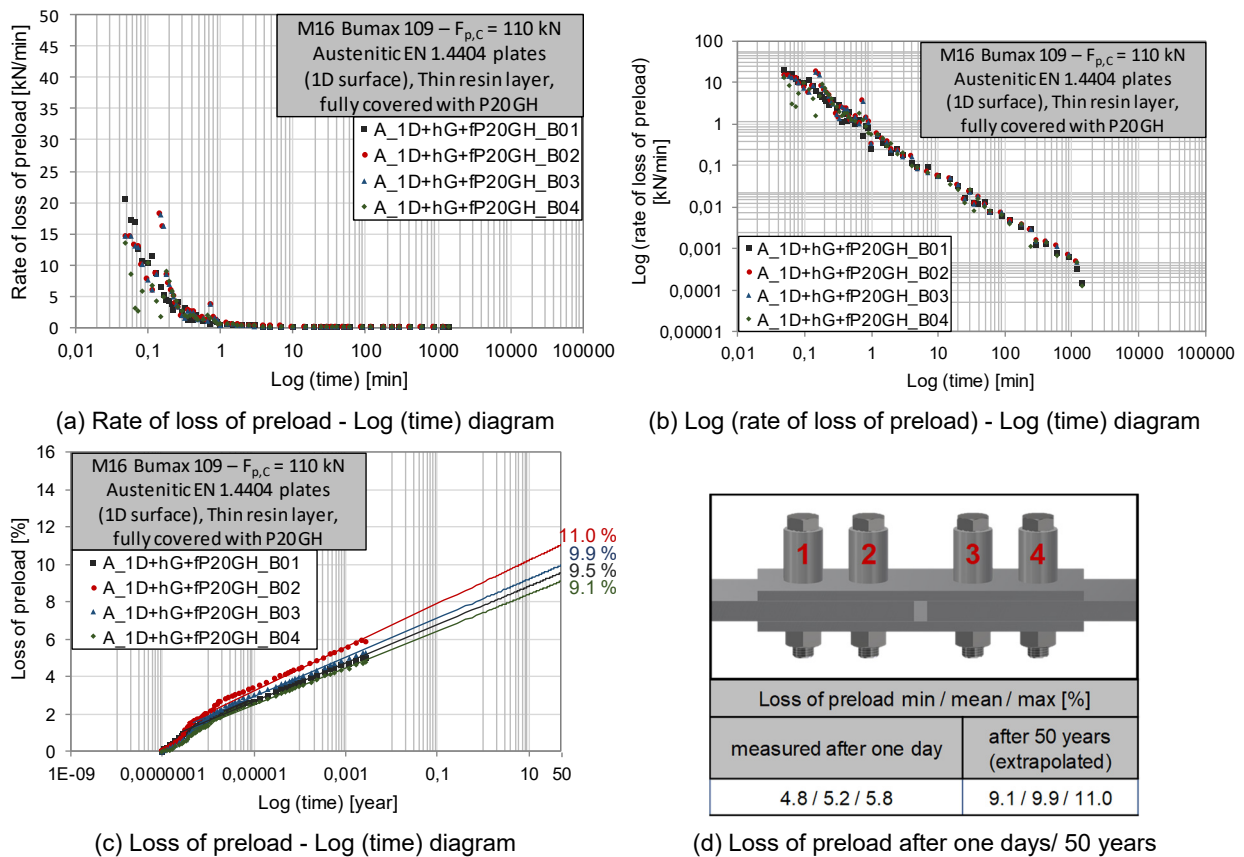
Figure A-3: Loss of preload for A_tR+fP20 test specimen

(a) Rate of loss of preload - Log (time) diagram

(b) Log (rate of loss of preload) - Log (time) diagram

(c) Loss of preload - Log (time) diagram

(d) Loss of preload after one days/ 50 years
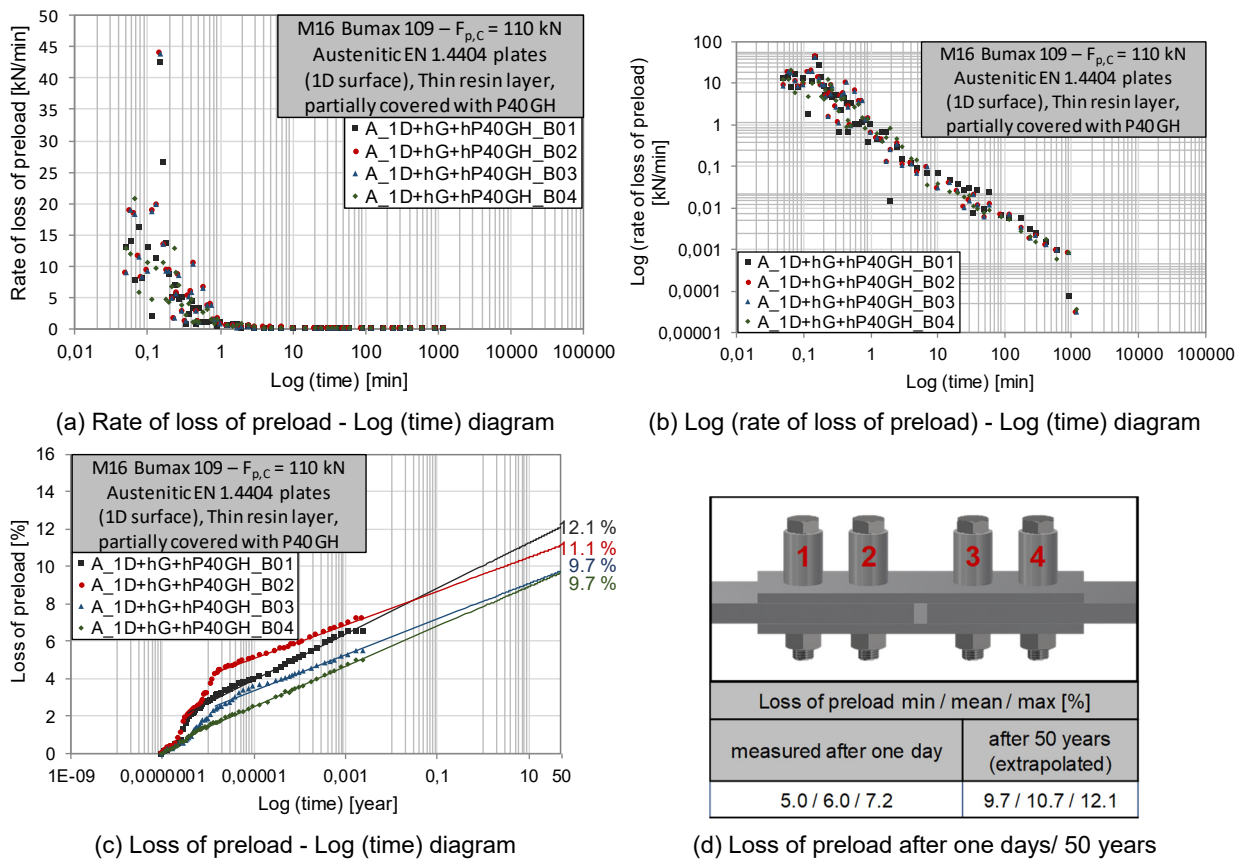
Figure A-4: Loss of preload for A_tR+pP40 test specimen

(a) Rate of loss of preload - Log (time) diagram

(b) Log (rate of loss of preload) - Log (time) diagram

(c) Loss of preload - Log (time) diagram

(d) Loss of preload after one days/ 50 years
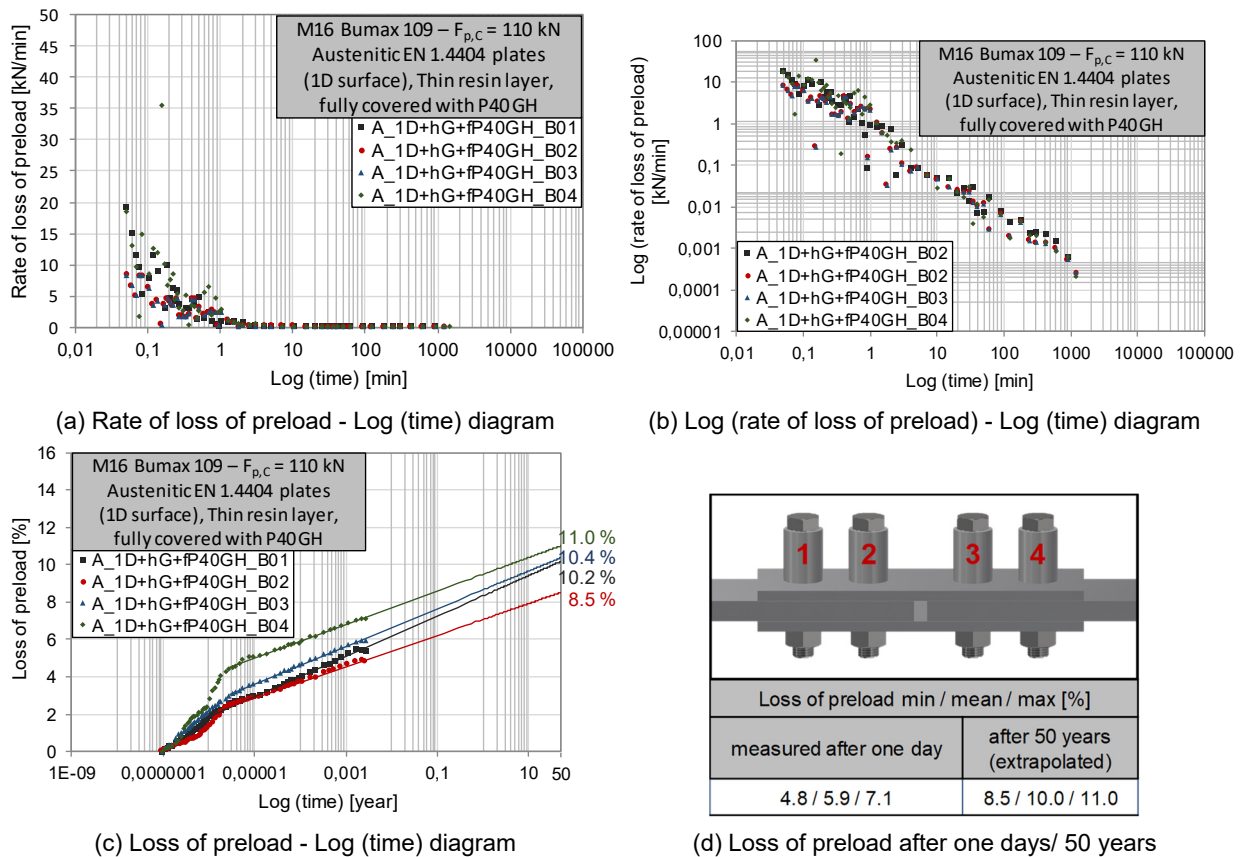
Figure A-5: Loss of preload for A_tR+fP40 test specimen

(a) Rate of loss of preload - Log (time) diagram

(b) Log (rate of loss of preload) - Log (time) diagram

(c) Loss of preload - Log (time) diagram

(d) Loss of preload after one days/ 50 years
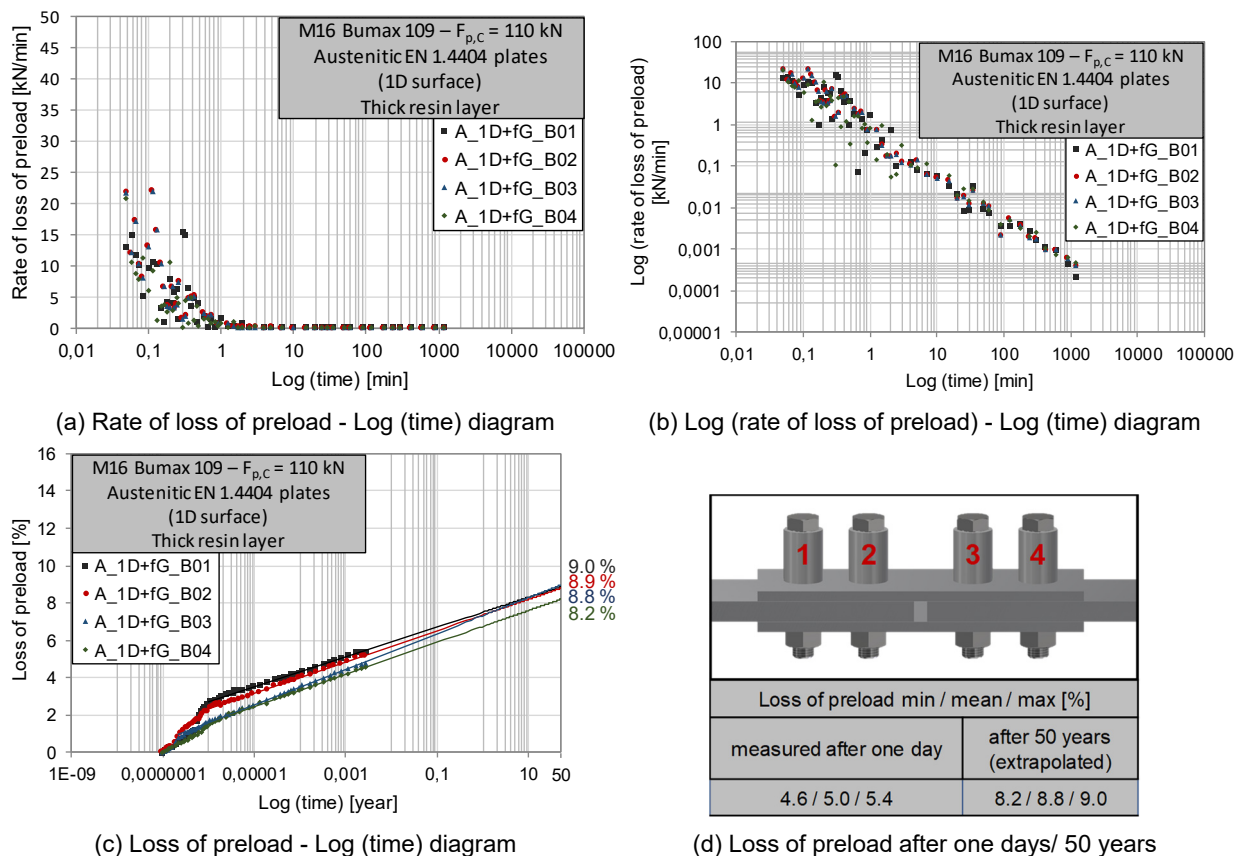
Figure A-6: Loss of preload for A_thR test specimen

(a) Rate of loss of preload - Log (time) diagram

(b) Log (rate of loss of preload) - Log (time) diagram

(c) Loss of preload - Log (time) diagram

(d) Loss of preload after one days/ 50 years
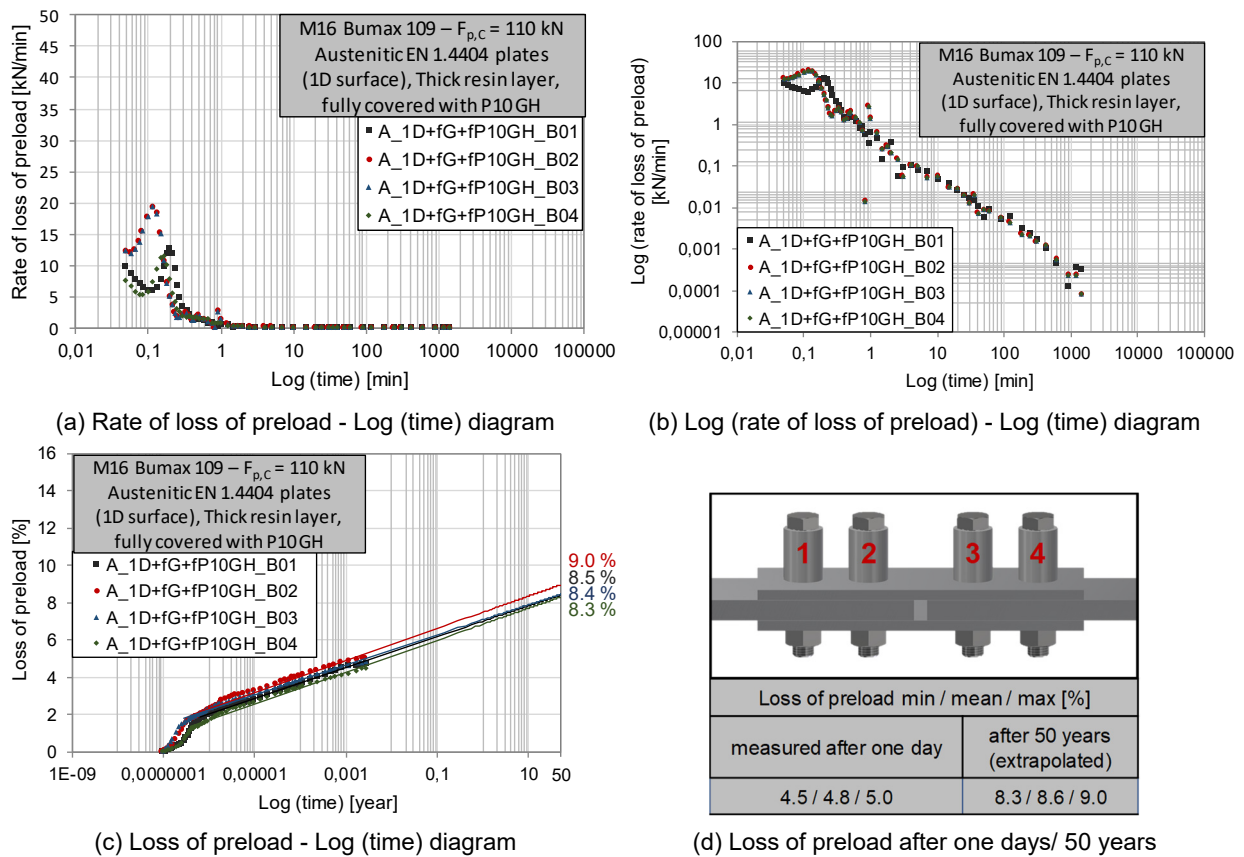
Figure A-7: Loss of preload for A_thR+fP10 test specimen

(a) Rate of loss of preload - Log (time) diagram

(b) Log (rate of loss of preload) - Log (time) diagram

(c) Loss of preload - Log (time) diagram

(d) Loss of preload after one days/ 50 years
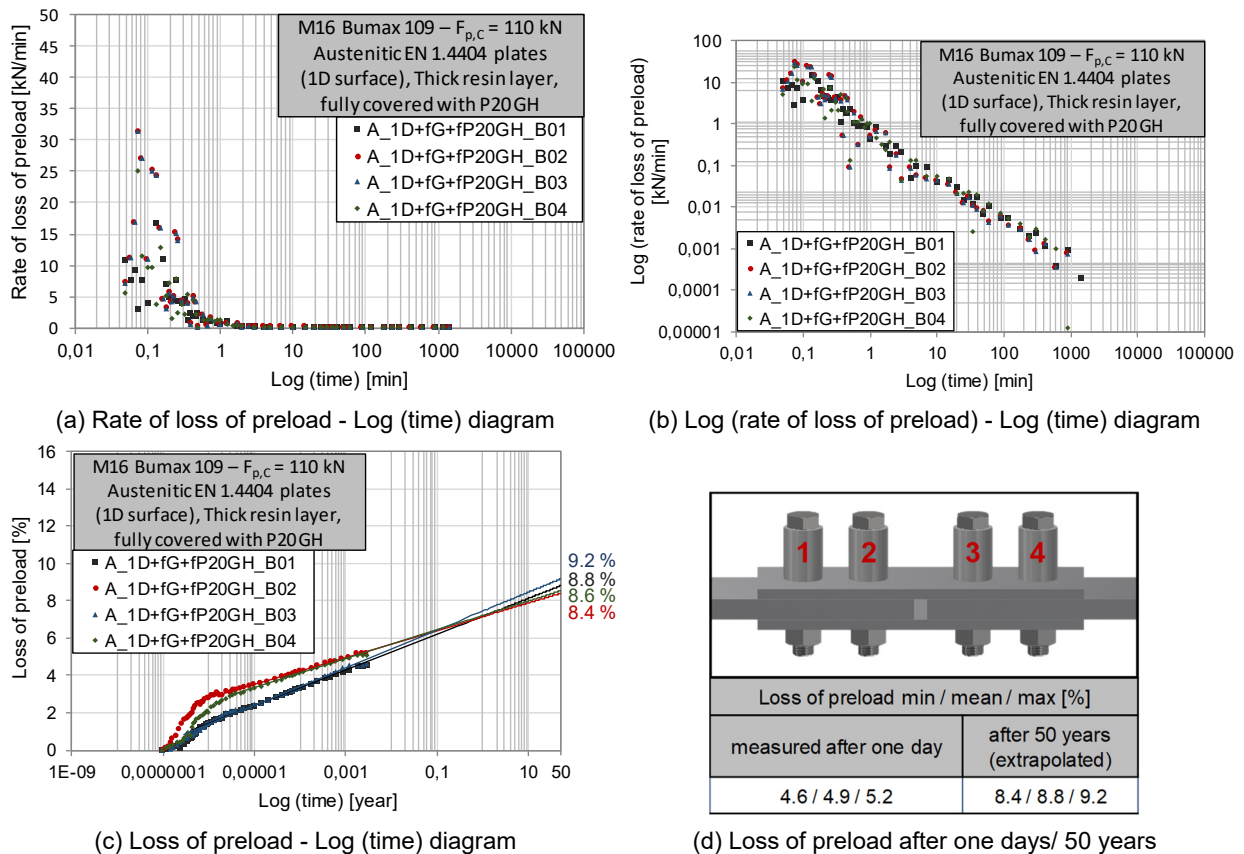
Figure A-8: Loss of preload for A_thR+fP20 test specimen

(a) Rate of loss of preload - Log (time) diagram

(b) Log (rate of loss of preload) - Log (time) diagram

(c) Loss of preload - Log (time) diagram

(d) Loss of preload after one days/ 50 years
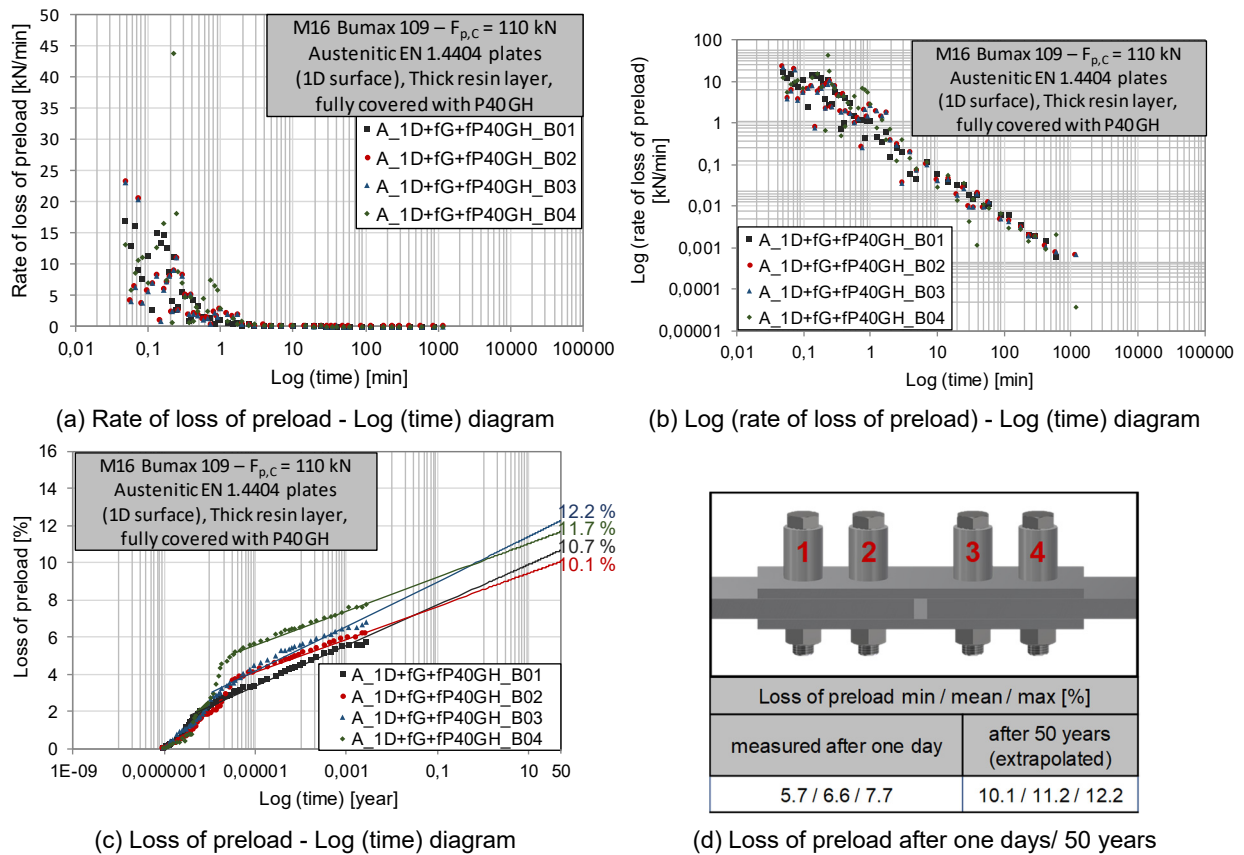
Figure A-9: Loss of preload for A_thR+fP40 test specimen

(a) Rate of loss of preload - Log (time) diagram

(b) Log (rate of loss of preload) - Log (time) diagram

(c) Loss of preload - Log (time) diagram

(d) Loss of preload after one days/ 50 years
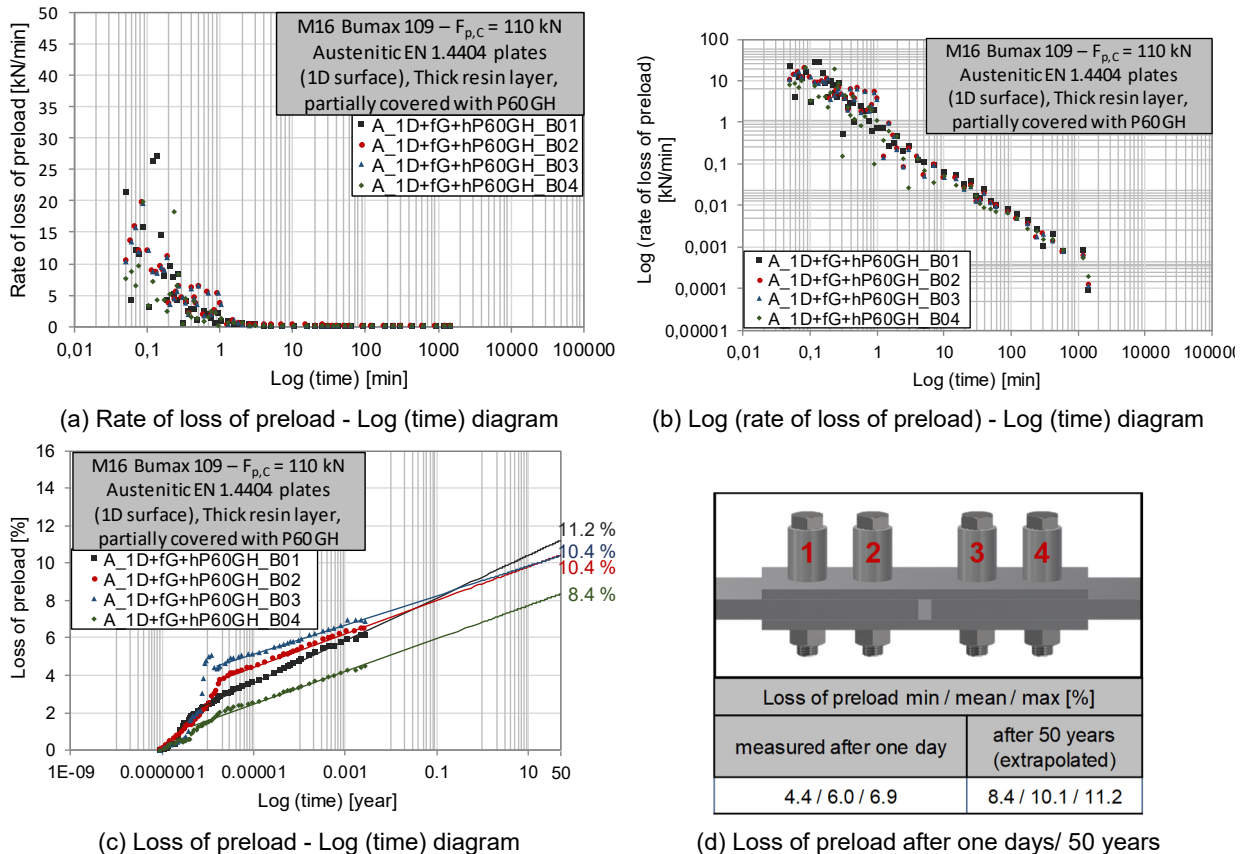
Figure A-10: Loss of preload for A_thR+pP60 test specimen

(a) Rate of loss of preload - Log (time) diagram

(b) Log (rate of loss of preload) - Log (time) diagram

(c) Loss of preload - Log (time) diagram

(d) Loss of preload after one days/ 50 years
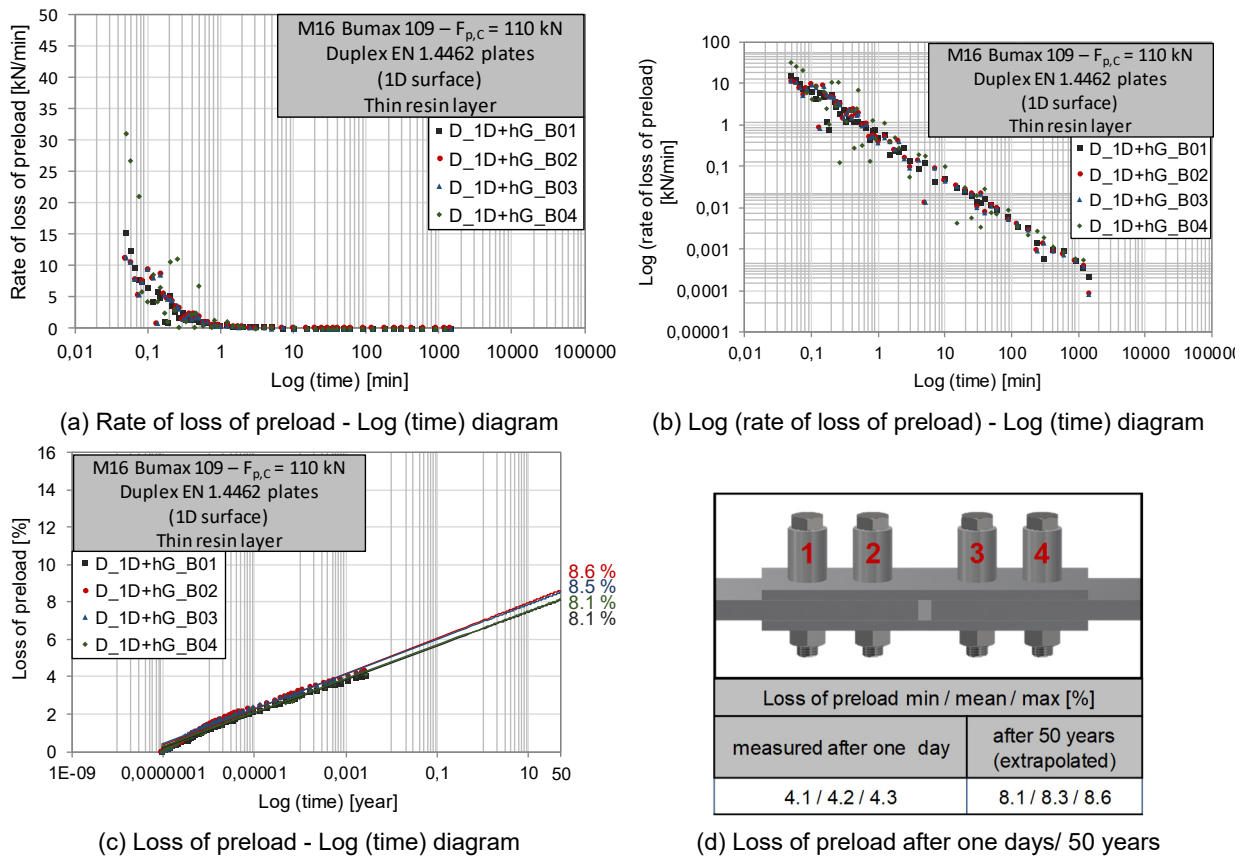
Figure A-11: Loss of preload for D_tR test specimen

(a) Rate of loss of preload - Log (time) diagram

(b) Log (rate of loss of preload) - Log (time) diagram

(c) Loss of preload - Log (time) diagram

(d) Loss of preload after one days/ 50 years
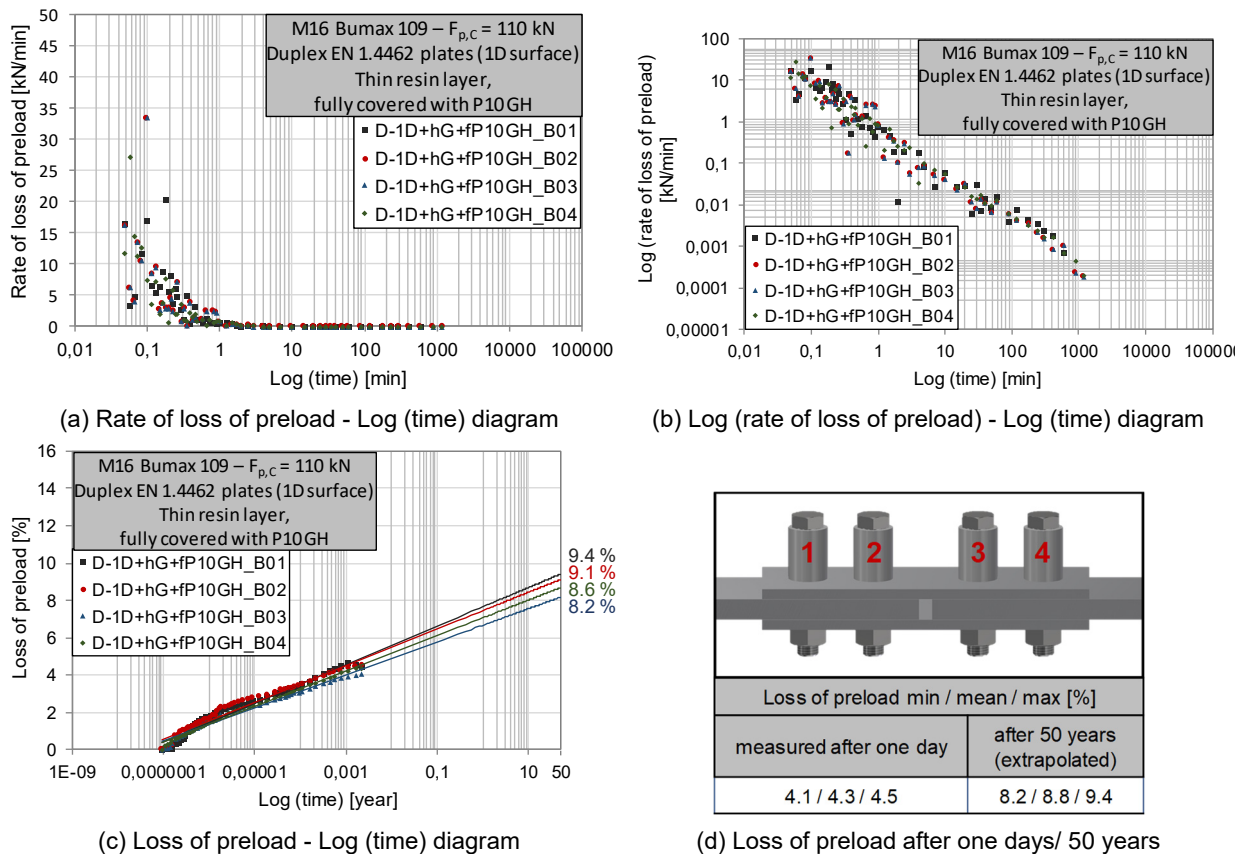
Figure A-12: Loss of preload for D_tR+fP10 test specimen

(a) Rate of loss of preload - Log (time) diagram

(b) Log (rate of loss of preload) - Log (time) diagram

(c) Loss of preload - Log (time) diagram

(d) Loss of preload after one days/ 50 years
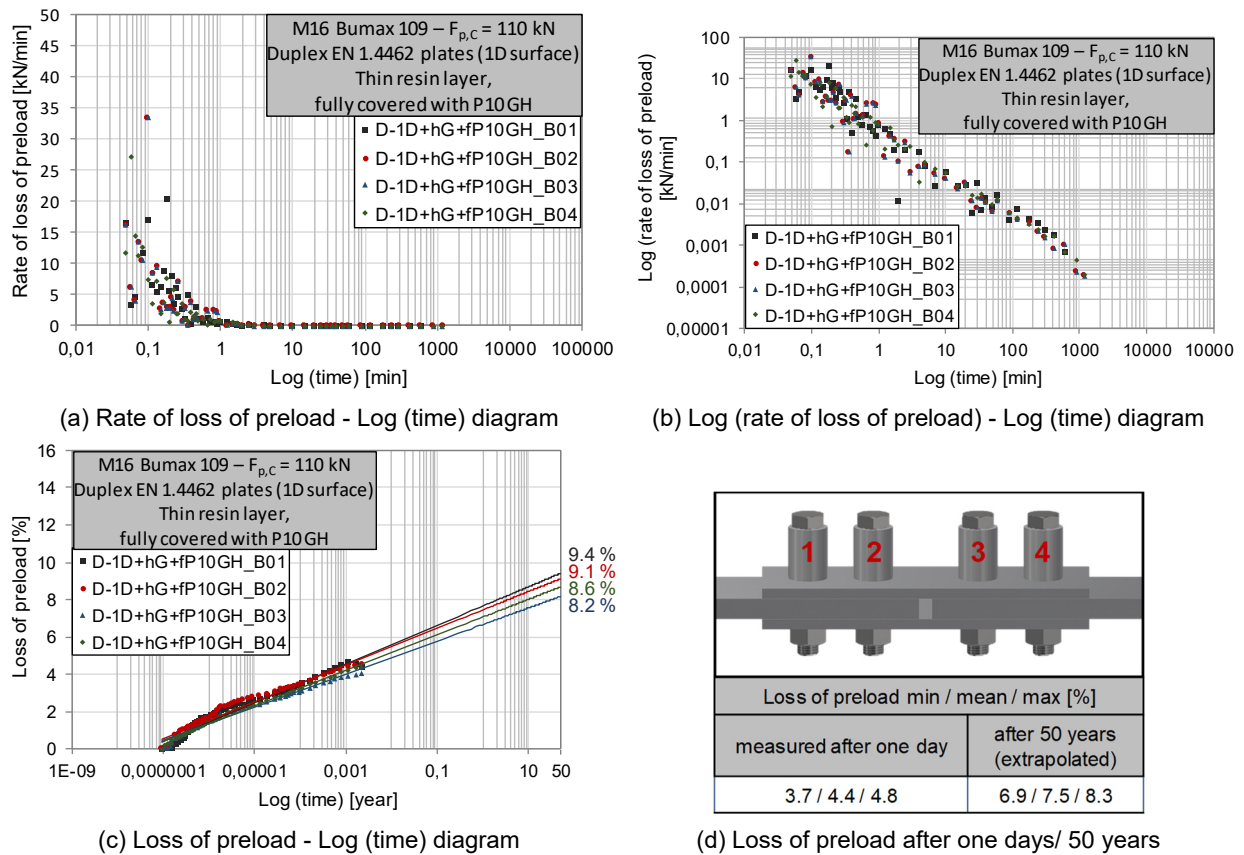
Figure A-13: Loss of preload for D_thR+fP10 test specimen

(a) Rate of loss of preload - Log (time) diagram

(b) Log (rate of loss of preload) - Log (time) diagram

(c) Loss of preload - Log (time) diagram

(d) Loss of preload after one days/ 50 years
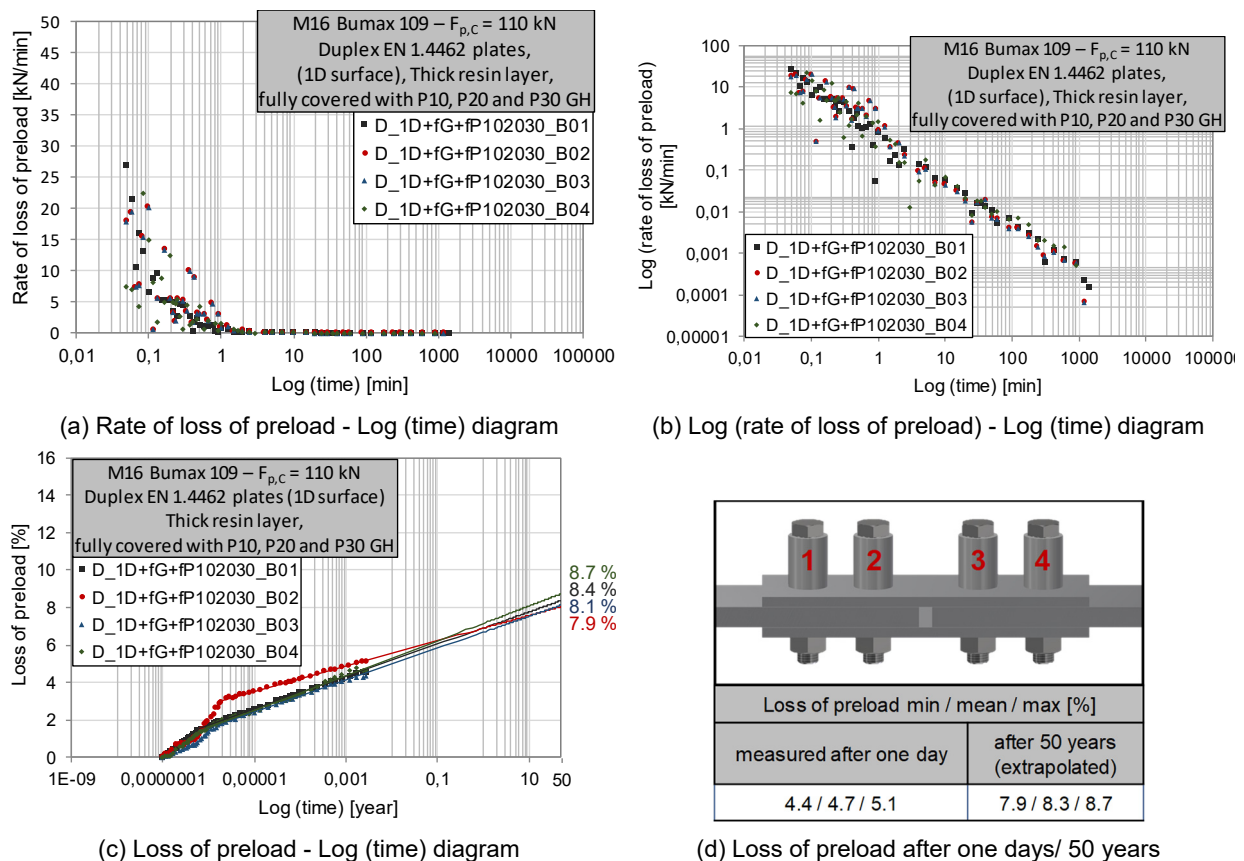
Figure A-14: Loss of preload for D_thR+fP102030 test specimen

(a) Rate of loss of preload - Log (time) diagram

(b) Log (rate of loss of preload) - Log (time) diagram

(c) Loss of preload - Log (time) diagram

(d) Loss of preload after one days/ 50 years
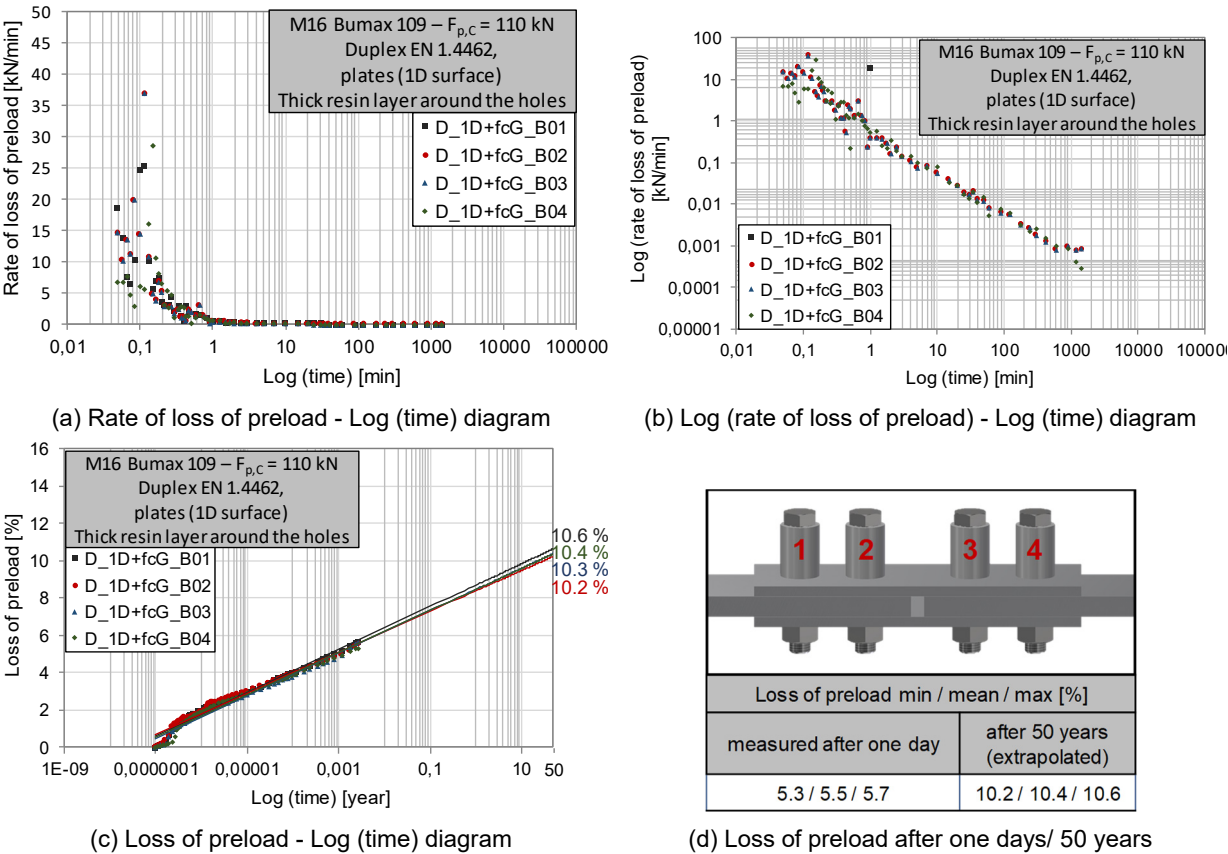
Figure A-15: Loss of preload for D_thhR test specimen

Annex B: Slip factor test evaluation tables (Stainless steel)

test results according to EN 1090-2 and RCSC 2014 for 1D and GB test specimens
made of Stainless steel

Table B-1: Slip factor test results according to EN 1090-2 for D_1D-B_HV10.9 test series

Technical characteristics of the test

Steel grade	Duplex Stainless Steel (1.4462)
Coating	–
Surface treatment	1D surface finish - Hot rolled (as received) - Bolt holes with burr
Mean coating thickness	–
Surface roughness (before coating)	26 µm
Specimen size	Standard specimens M16 (EN 14399-4, Figure G.1 b)
Bolt class, bolt type	10.9 (Set EN 14399-4 – HV – M16 x 90 – 10.9/10 – tZn)
Nominal preload level	110 kN = $F_{p,C}$
Preload measuring method	Implanted SG, measured continuously, clamping length $\Sigma t = 40$ mm
Test speed	0.01 mm/s

Static test

Specimens mark	plate ID's	Slip (average at CBG) u_i [mm]	Slip load F_{Si} [kN]	Preload at start of test (initial preload) Outer bolt $F_{bi,o,ini}$ [kN]	Mean value mean $F_{bi,ini}$ [kN]	Inner bolt $F_{bi,i,ini}$ [kN]	Slip factor based on initial preload $\mu_{i,ini}$ [-]	based on nominal preload $\mu_i = \mu_{i,nom}$ [-] ($F_{p,C}$ = 110)	based on preload at slip $\mu_{i,act}$ [-]	Preload at slip Outer bolt $F_{bi,o,act}$ [kN]	Mean value mean $F_{bi,act}$ [kN]	Inner bolt $F_{bi,i,act}$ [kN]	Test duration t [min]	Comment (Eq. according to EN 1090-2)
D_1D-B_HV10.9_01-02	1	0.150	143.0	109.2	109.0	108.8	0.33	0.33	0.34	104.0	103.8	103.6	8.8	
	2	0.150	175.5	111.2	110.1	109.1	0.40	0.40	0.41	109.4	105.8	102.2	14.2	
D_1D-B_HV10.9_03-04	3	0.150	173.3	110.6	110.6	110.6	0.39	0.39	0.41	105.4	104.6	103.9	13.3	
	4	0.150	149.3	110.3	111.0	111.8	0.34	0.34	0.37	97.7	102.0	106.3	8.8	
D_1D-B_HV10.9_05-06	5	0.150	138.4	110.1	109.7	109.2	0.32	0.31	0.32	107.4	106.9	106.3	8.6	
	6	0.150	169.7	108.6	109.0	109.4	0.39	0.39	0.40	105.9	105.9	106.0	13.5	
D_1D-B_HV10.9_07-08	7	0.150	185.7	111.4	111.3	111.2	0.42	0.42	0.43	107.4	107.3	107.1	17.6	
	8	0.150	240.0	110.7	111.1	111.5	0.54	0.55	0.56	107.5	107.6	107.7	11.7	

Statistics (4 specimens, 8 test results)

			F_{Si}				$\mu_{i,ini}$	$\mu_i = \mu_{i,nom}$	$\mu_{i,act}$					
$n = 8$	Number of tests													
max	Maximum		240.0				0.54	0.55	0.56					
min	Minimum		138.4				0.32	0.31	0.32					
mean	Mean value F_{sm} | μ_m		171.9				0.39	0.39	0.41					
R	Spread		101.6				0.22	0.23	0.23					$R = max - min$
s	Standard deviation s_{Frs}		32.3				0.071	0.073	0.072					
V	Coefficient of variation		18.8%				18.3%	18.8%	17.6%					$V = s / mean$
0,9 F_{sm}			154.7											Load level for the creep test

Comments: Eq. (2), Eq. (4); $R = max - min$; Eq. (3), Eq. (5); $V = s / mean$; Load level for the creep test

Table B-2: Slip factor test results according to EN 1090-2 for D_1D_HV10.9 test series

Technical characteristics of the test

- Steel grade: Duplex Stainless Steel (1.4462)
- Coating: –
- Surface treatment: 1D surface finish - Hot rolled (as received) - Bolt holes without burr
- Mean coating thickness: –
- Surface roughness (before coating): 26 µm
- Specimen size: Standard specimens M16 (EN 1090-2, Figure G.1 b)
- Bolt class, bolt type: 10.9 (Set EN 14399-4 – HV – M16 x 90 – 10.9/10 – iZn)
- Nominal preload level: 110 kN = $F_{p,C}$
- Preload measuring method: Implanted SG, measured continuously, clamping length $\Sigma t = 40$ mm
- Test speed: 0.01 mm/s

Static test

Specimens mark / Statistics	plate ID's	Slip load F_{si} [kN]	Slip (average at CBG) u_i [mm]	Slip factor based on initial preload $\mu_{i,ini}$ [-]	Slip factor based on nominal preload $F_{p,C}=110$ kN $\mu_i = \mu_{i,nom}$ [-]	Slip factor based on preload at slip $\mu_{i,act}$ [-]	Preload at start of test (initial preload) Outer bolt $F_{bi,o,ini}$ [kN]	Mean value mean $F_{bi,ini}$ [kN]	Inner bolt $F_{bi,i,ini}$ [kN]	Preload at slip Outer bolt $F_{bi,o,act}$ [kN]	Mean value mean $F_{bi,act}$ [kN]	Inner bolt $F_{bi,i,act}$ [kN]	Test duration t [min]	Comment (Eq. according to EN 1090-2)
D_1D_HV10.9_09-10	9	102.1	0.030	0.23	0.23	0.23	110.2	110.5	110.8	108.6	108.8	109.0	7.6	
	10	102.1	0.042	0.23	0.23	0.23	111.2	110.7	110.2	109.4	108.7	108.1	7.6	
D_1D_HV10.9_11-12	11	115.8	0.150	0.26	0.26	0.27	111.3	110.9	110.5	109.7	108.8	107.9	11.8	
	12	110.5	0.034	0.25	0.25	0.25	110.5	110.5	110.4	108.9	108.7	108.6	7.3	
D_1D_HV10.9_13-14	13	106.5	0.046	0.24	0.24	0.24	110.4	110.8	111.2	108.8	109.0	109.2	18.1	
	14	105.2	0.056	0.24	0.24	0.24	111.1	111.4	111.7	109.5	109.7	109.8	13.8	
D_1D_HV10.9_15-16	15	109.6	0.150	0.25	0.25	0.25	110.9	110.5	110.0	108.7	108.0	107.3	12.9	
	16	109.2	0.150	0.25	0.25	0.25	111.0	110.7	110.4	109.3	108.7	108.2	8.6	
Statistics (4 specimens, 8 test results) n = 8	max Maximum	115.8		0.26	0.26	0.27								
	min Minimum	102.1		0.23	0.23	0.23								
	mean Mean value F_{sm} | μ_m	**107.6**		**0.24**	**0.24**	**0.25**								
	R Spread	13.7		0.03	0.03	0.03								Eq. (2), Eq. (4); R = max – min
	s Standard deviation s_{Fs}	4.6		0.010	0.011	0.011								Eq. (3), Eq. (5)
	V Coefficient of variation	4.3%		4.3%	4.3%	4.4%								V = s / mean
	0.9 F_{sm}	**96.8**												Load level for the creep test

Creep test

Specimens mark / Statistics	plate ID's	Slip load F_{si} [kN]	Slip (average at CBG) u_i [mm]	Slip factor $\mu_{i,ini}$ [-]	Slip factor $\mu_i = \mu_{i,nom}$ [-]	Slip factor $\mu_{i,act}$ [-]	$F_{bi,o,ini}$ [kN]	mean $F_{bi,ini}$ [kN]	$F_{bi,i,ini}$ [kN]	$F_{bi,o,act}$ [kN]	mean $F_{bi,act}$ [kN]	$F_{bi,i,act}$ [kN]	t [min]	Comment
D_1D_HV10.9_17-18	17	115.1	0.027 Δ (5 min to 3 h): 0.0020	0.26	0.26	0.26	113.1	112.7	112.3	109.4	109.6	109.9	199.5	**Creep test passed** Slip during the creep test ≤0,002 mm (5 min to 3 h)
	18	115.0	0.150 Δ (5 min to 3 h): 0.0016	0.26	0.26	0.26	112.1	112.5	113.0	110.2	109.6	109.0	199.5	
Statistics (5 specimens, 10 test results) n = 10	max Maximum	115.8		0.26	0.26	0.27								
	min Minimum	102.1		0.23	0.23	0.23								
	mean Mean value F_{sm} | μ_m	109.1		0.25	0.25	0.25								
	R Spread	13.7		0.03	0.03	0.03								Eq. (2), Eq. (4); R = max – min
	s Standard deviation s_{Fs}	5.2		0.011	0.012	0.012								Eq. (3), Eq. (5)
	V Coefficient of variation	**4.7%**		**4.3%**	**4.7%**	**4.6%**								V = s / mean ≤ 8%
	0.9 F_{sm}	**98.2**												
μ_k Characteristic value of the slip factor				0.22	0.22	0.23								Eq. (6)

Comments:
- Creep test passed
- Extended creep test is not required

Test results

Table B-3: Slip factor test results according to EN 1090-2 for LD_1D_HV10.9 test series

Technical characteristics of the test

Steel grade	Lean-Duplex Stainless Steel (1.4162)
Coating	–
Surface treatment	1D surface finish - Hot rolled (as received) - Bolt holes without burr
Mean coating thickness	–
Surface roughness (before coating)	27 µm
Specimen size	Standard specimens M16 (EN 1090-2, Figure G.1 b)
Bolt class, bolt type	10.9 (Set EN 14399-4 – HV – M16 x 90 – 10.9/10 – tZn)
Nominal preload level	110 kN = $F_{p,C}$
Preload measuring method	implanted SG, measured continuously, clamping length Σt = 40 mm
Test speed	0.01 mm/s

Static test

Specimens mark	plate ID's	Slip (average at CBG) u_i [mm]	Slip load F_{si} [kN]	Preload at start of test (initial preload) Outer bolt $F_{bi,o,ini}$ [kN]	Mean value mean $F_{bi,ini}$ [kN]	Inner bolt $F_{bi,i,ini}$ [kN]	Slip factor based on initial preload $\mu_{i,ini}$ [-]	based on nominal preload $F_{p,C}$ [kN] 110 $\mu_i = \mu_{i,nom}$ [-]	based on preload at slip $\mu_{i,act}$ [-]	Preload at slip Outer bolt $F_{bi,o,act}$ [kN]	Mean value mean $F_{bi,act}$ [kN]	Inner bolt $F_{bi,i,act}$ [kN]	Test duration t [min]	Comment (Eq. according to EN 1090-2)
LD_1D_HV10.9_05-06	5	0.050	116.1	112.4	112.1	111.8	0.26	0.26	0.27	109.7	109.0	108.3	13.1	
	6	0.077	113.5	111.7	111.5	111.3	0.24	0.26	0.26	108.8	108.4	108.0	8.1	
LD_1D_HV10.9_07-08	7	0.064	107.8	109.6	109.6	109.7	0.25	0.24	0.25	107.3	107.2	107.1	8.4	
	8	0.044	125.2	109.5	109.8	110.1	0.28	0.28	0.29	107.2	106.8	106.5	14.1	
LD_1D_HV10.9_09-10	9	0.057	115.5	111.3	110.8	110.3	0.26	0.26	0.27	107.9	107.4	106.9	8.7	
	10	0.076	116.6	111.1	110.2	109.4	0.26	0.27	0.28	105.5	105.4	105.2	3.8	
LD_1D_HV10.9_11-12	11	0.065	106.9	109.6	109.5	109.4	0.24	0.24	0.25	106.6	106.2	105.8	8.7	
	12	0.041	117.1	110.5	110.2	109.9	0.27	0.27	0.27	107.8	106.9	106.0	13.9	
Statistics (4 specimens, 8 test results)	$n = 8$ Number of tests													
	max Maximum		125.2				0.28	0.28	0.29					
	min Minimum		106.9				0.24	0.24	0.25					
	mean Mean value F_{sm} | μ_m		**114.8**				**0.26**	**0.26**	**0.27**					Eq. (2), Eq. (4)
	R Spread		18.3				0.04	0.04	0.04					R = max – min
	s Standard deviation s_{Fs}		5.8				0.013	0.013	0.014					Eq. (3), Eq. (5)
	V Coefficient of variation		5.0%				5.0%	5.0%	5.1%					V = s / mean
	0.9 F_{sm}		**103.4**											Load level for the creep test

Creep test

Specimens mark	plate ID's	Slip (average at CBG) u_i [mm]	Slip load F_{si} [kN]	Outer bolt $F_{bi,o,ini}$ [kN]	Mean value mean $F_{bi,ini}$ [kN]	Inner bolt $F_{bi,i,ini}$ [kN]	$\mu_{i,ini}$ [-]	$\mu_i = \mu_{i,nom}$ [-]	$\mu_{i,act}$ [-]	Outer bolt $F_{bi,o,act}$ [kN]	Mean value mean $F_{bi,act}$ [kN]	Inner bolt $F_{bi,i,act}$ [kN]	t [min]	Comment
LD_1D_HV10.9_13-14	13 Δ (5 min to 3 h): **0.0017**	0.033	116.6	111.4	111.0	110.6	0.26	0.26	0.27	107.5	106.7	105.9	213.0	**Creep test passed** Slip during the creep test ≤ 0,002 mm (5 min to 3 h)
	14 Δ (5 min to 3 h): **0.0017**	0.052	116.6	111.4	111.3	111.2	0.26	0.26	0.27	109.1	107.8	106.4	213.0	
Statistics (5 specimens, 10 test results)	$n = 10$ Number of tests													
	max Maximum		125.2				0.28	0.28	0.29					
	min Minimum		106.9				0.24	0.24	0.25					
	mean Mean value F_{sm} | μ_m		115.2				0.26	0.26	0.27					Eq. (2), Eq. (4)
	R Spread		18.3				0.04	0.04	0.04					R = max – min
	s Standard deviation s_{Fs}		5.1				0.011	0.012	0.012					Eq. (3), Eq. (5)
	V Coefficient of variation		**4.5%**				**4.4%**	**4.5%**	**4.5%**					V = s / mean ≤ 8%
	0.9 F_{sm}		103.7											
μ_k Characteristic value of the slip factor							0.24	0.24	0.24					Eq. (6)

Comments

- Creep test passed
- Extended creep test is not required

Test results

Table B-4: Slip factor test results according to EN 1090-2 for LD_1D_B109 test series

Technical characteristics of the test

Steel grade	Lean-Duplex Stainless Steel (1.4162)
Coating	–
Surface treatment	1D surface finish - Hot rolled (as received) - Bolt holes without burr
Mean coating thickness	–
Surface roughness (before coating)	27 µm
Specimen size	Standard specimens M16 (EN 1090-2, Figure G.1 b)
Bolt class, bolt type	Bolt: BUMAX 109 (EN ISO 4017 – M16 x 100) - Nut: BUMAX 109 (EN ISO 4032) - Washer: HV 300 (EN ISO 7089)
Nominal preload level	110 kN = $F_{p,C}$
Preload measuring method	Load cell (h = 40 mm), measured continuously, clamping length Σt = 75 mm
Test speed	0.01 mm/s

Static test

Specimens mark	plate ID's	Slip (average at CBG) u_i [mm]	Slip load F_{si} [kN]	Preload at start of test (initial preload) Outer bolt $F_{bi,o,ini}$ [kN]	Mean value mean $F_{bi,ini}$ [kN]	Inner bolt $F_{bi,i,ini}$ [kN]	Slip factor based on initial preload $\mu_{i,ini}$ [-]	based on nominal preload $F_{p,C}$ [kN] 110 $\mu_i = \mu_{i,nom}$ [-]	based on preload at slip $\mu_{i,act}$ [-]	Preload at slip Outer bolt $F_{bi,o,act}$ [kN]	Mean value mean $F_{bi,act}$ [kN]	Inner bolt $F_{bi,i,act}$ [kN]	Test duration t [min]	Comment
														Eq. according to EN 1090-2
LD_1D_B109_01-02	1	0.046	107.5	109.6	109.7	109.7	0.25	0.24	0.25	108.1	108.0	107.9	13.0	
	2	0.046	106.7	109.9	110.0	110.0	0.24	0.24	0.25	108.5	108.3	108.1	8.1	
LD_1D_B109_03-04	3	0.051	111.1	110.4	110.0	109.7	0.25	0.25	0.26	109.0	108.3	107.7	8.3	
	4	0.023	111.1	111.1	110.8	110.5	0.25	0.25	0.25	109.6	109.1	108.6	8.3	

Statistics (4 specimens, 8 test results) $n = 8$ Number of tests

		F_{si}					$\mu_{i,ini}$	$\mu_i = \mu_{i,nom}$	$\mu_{i,act}$					Comment
max	Maximum	111.1					0.25	0.25	0.26					
min	Minimum	106.7					0.24	0.24	0.25					
mean	Mean value F_{sm} | μ_m	109.1					0.25	0.25	0.25					
R	Spread	4.4					0.01	0.01	0.01					R = max – min
s	Standard deviation s_{Fs}	2.3					0.005	0.005	0.005					Eq. (2), Eq. (4)
V	Coefficient of variation	2.1%					1.9%	2.1%	1.9%					Eq. (3), Eq. (5) / V = s / mean
0,9 F_{sm}		98.2												Load level for the creep test

Table B-5: Slip factor test results according to EN 1090-2 for D_GB-A_HV10.9 test series

Technical characteristics of the test

- Steel grade: Duplex Stainless Steel (1.4462)
- Coating: –
- Surface treatment: Grit blasted (with Brown Corundum, f20, Al2o3 (Aluminiumoxid))
- Mean coating thickness: –
- Surface roughness (before coating): 76 µm
- Specimen size: Standard specimens M16 (EN 1090-2, Figure G.1 b)
- Bolt class, bolt type: 10.9 (Set t EN 14399-4 – HV – M16 x 60 – 10.9/10 – tZn)
- Nominal preload level: 110 kN = $F_{p,C}$
- Preload measuring method: implanted SG, measured continuously, clamping length $\Sigma t = 40$ mm
- Test speed: 0.6 mm/min

Static test

Specimens mark	plate ID	Slip (average at CBG) u_i [mm]	Slip load F_{Si} [kN]	Preload at start of test (initial preload) Outer bolt $F_{bi,o,ini}$ [kN]	Mean value mean $F_{bi,ini}$ [kN]	Inner bolt $F_{bi,i,ini}$ [kN]	Slip factor based on initial preload $\mu_{i,ini}$ [-]	based on nominal preload $F_{p,C}$=110 [kN], $\mu_i = \mu_{i,nom}$ [-]	based on preload at slip $\mu_{i,act}$ [-]	Preload at slip Outer bolt $F_{bi,o,act}$ [kN]	Mean value mean $F_{bi,act}$ [kN]	Inner bolt $F_{bi,i,act}$ [kN]	Test duration t [min]	Comment
D_GB-A_HV10.9_01-02	1	0.150	318.8	114.1	113.5	112.9	0.70	0.72	0.80	101.2	100.0	98.9	14.5	Eq. according to EN 1090-2
	2	0.150	318.4	113.8	114.0	114.2	0.70	0.72	0.79	102.2	100.8	99.4	14.4	
D_GB-A_HV10.9_03-04	3	0.150	310.6	111.6	112.2	112.7	0.69	0.71	0.79	99.3	98.8	98.3	14.0	
	4	0.150	307.2	112.7	112.5	112.3	0.68	0.70	0.78	99.8	98.8	97.8	13.6	
D_GB-A_HV10.9_05-06	5	0.150	327.2	112.7	112.9	113.1	0.68	0.70	0.77	100.4	99.9	99.4	13.8	
	6	0.150	327.7	112.2	112.1	112.0	0.73	0.74	0.84	98.9	97.6	96.4	17.2	
D_GB-A_HV10.9_07-08	7	0.150	319.0	111.3	111.4	111.5	0.72	0.73	0.82	98.4	97.2	95.9	14.4	
	8	0.150	329.4	112.1	111.6	111.2	0.74	0.75	0.85	98.3	96.8	95.3	16.2	

Statistics (4 specimens, 8 test results), n = 8

		u_i	F_{Si}				$\mu_{i,ini}$	μ_i	$\mu_{i,act}$					Comment
max Maximum			329.4				0.74	0.75	0.85					Eq. (2), Eq. (4)
min Minimum			307.2				0.68	0.70	0.77					$R = max - min$
mean Mean value F_{Sm} | μ_m			317.3				0.71	0.72	0.80					Eq. (3), Eq. (5)
R Spread			22.2				0.06	0.05	0.08					$V = s / mean$
s Standard deviation s_{Fs}			8.5				0.021	0.019	0.030					
V Coefficient of variation			2.7%				3.0%	2.7%	3.7%					
$0.9\ F_{Sm}$			285.6											Load level for the creep test

Creep test

Δ (5 min to 3 h): 0,001 ; Δ (5 min to 3 h): 0,001

Specimens mark	plate ID	u_i [mm]	F_{Si} [kN]	$F_{bi,o,ini}$ [kN]	mean $F_{bi,ini}$ [kN]	$F_{bi,i,ini}$ [kN]	$\mu_{i,ini}$ [-]	$\mu_i = \mu_{i,nom}$ [-]	$\mu_{i,act}$ [-]	$F_{bi,o,act}$ [kN]	mean $F_{bi,act}$ [kN]	$F_{bi,i,act}$ [kN]	t [min]	Comment
D_GB-A_HV10.9_09-09-10	9	0.150	304.4	111.1	111.4	111.8	0.68	0.69	0.78	97.7	96.9	96.2	268.9	Creep test passed. Slip during the creep test ≤0,002 mm (5 min to 3 h)
	10	0.150	326.7	111.2	111.1	111.0	0.74	0.74	0.86	96.2	95.1	94.0	272.8	

Statistics (5 specimens, 10 test results), n = 10

		u_i	F_{Si}				$\mu_{i,ini}$	μ_i	$\mu_{i,act}$					Comment
max Maximum			329.4				0.74	0.75	0.86					Eq. (2), Eq. (4)
min Minimum			304.4				0.68	0.69	0.77					$R = max - min$
mean Mean value F_{Sm} | μ_m			316.9				0.71	0.72	0.81					Eq. (3), Eq. (5)
R Spread			25.0				0.06	0.06	0.09					$V = s / mean \leq 8\%$
s Standard deviation s_{Fs}			9.2				0.022	0.021	0.032					
V Coefficient of variation			2.9%				3.2%	2.9%	4.0%					
$0.9\ F_{Sm}$			285.3											
μ_k Characteristic value of the slip factor							0.66	0.68	0.74					Eq. (6)

Comments

Test results:
- Creep test passed
- Extended creep test is not required

Table B-6: Slip factor test results according to RCSC 2014 for RCSC_A_1D test series

Technical characteristics of the test

Steel grade	Austenitic Stainless Steel (1.4404)
Coating	–
Surface treatment	1D surface finish - Hot rolled (as received) - Bolt holes without burr
Mean coating thickness	–
Surface roughness (before coating)	25 µm
Specimen size	Standard specimens M22 (according to RCSC 2014)
Bolt class, bolt type	10.9 (Set EN 14399-4 – HV – M22 x 80 – 10.9/10 – tZn)
Nominal preload level	218 kN = $F_{p,C}$
Preload measuring method	Implanted SG, measured continuously, clamping length Σt = 56 mm
Test speed	400 N/s

Static test

Specimens mark	plate ID's	Slip (average at CB) u_i [mm]	Slip load F_{si} [kN]	Preload at beginning of the test $F_{bi,ini}$ [kN]	Slip factor based on initial preload $\mu_{i,ini}$ [-]	based on nominal preload $F_{p,C}$ [kN] 218 $\mu_i = \mu_{i,nom}$ [-]	based on preload at slip $\mu_{i,act}$ [-]	Preload at slip mean $F_{bi,act}$ [kN]	Test duration t [min]	Comment
RCSC_A_1D_01	1	0.093	101.5	212.5	0.24	0.23	0.24	210.40	4.4	Eq. according to RCSC 2014
RCSC_A_1D_02	2	0.081	114.0	214.6	0.27	0.26	0.28	205.4	6.5	
RCSC_A_1D_03	3	0.082	117.5	216.7	0.27	0.27	0.28	210.1	6.7	
RCSC_A_1D_04	4	0.128	117.4	212.5	0.28	0.27	0.28	209.8	6.7	
RCSC_A_1D_05	5	0.143	115.7	212.4	0.27	0.27	0.28	210.3	6.6	

Statistics (5 specimens, 5 test results)

$n = 5$	Number of tests							
max	Maximum	117.5		0.28	0.27	0.28		
min	Minimum	101.5		0.24	0.23	0.24		
mean	Mean value F_{sm} | μ_m	**113.2**		**0.26**	**0.26**	**0.27**		
R	Spread	15.9		0.04	0.04	0.04	Equation A3.1
s	Standard deviation s_{Fs}	6.7		0.015	0.015	0.017	$R = max - min$
V	Coefficient of variation	5.9%		5.6%	5.9%	6.1%	$V = s / mean$

Creep test

Specimens mark	plate ID's	Preload at beginning of the test $F_{bi,ini}$ [kN]	First step load level Eq. A4.1 F_{step1} [kN]	Slip (average at CB) Δ (0.5 h to 1000 h) u_{step1} [mm]	Second step load level Chap. A4.2 F_{step2} [kN]	Slip (average at CB) at the load level u_{step2} [mm]	Comment	Final slip factor Eq. A3.1 μ_{Final} [-]
RCSC_A_1D_06	6	220.0		0.004		0.06		
RCSC_A_1D_07	7	218.7	67.9	0.006	101.9	0.04		0.23
RCSC_A_1D_08	8	220.3		0.001		0.04		

Table B-7: Slip factor test results according to RCSC 2014 for RCSC_D_1D test series

Technical characteristics of the test

Steel grade	Duplex Stainless Steel (1.4462)
Coating	–
Surface treatment	1D surface finish - Hot rolled (as received) - Bolt holes without burr
Mean coating thickness	–
Surface roughness (before coating)	27 µm
Specimen size	Standard specimens M22 (according to RCSC 2014)
Bolt class, bolt type	10.9 (Set EN 14399-4 – HV – M22 x 80 – 10.9/10 – tZn)
Nominal preload level	218 kN = $F_{p,C}$
Preload measuring method	Implanted SG, measured continuously, clamping length $\Sigma t = 56$ mm
Test speed	400 N/s

Static test

Specimens mark	plate ID's	Slip (average at CB) u_i [mm]	Slip load F_{si} [kN]	Preload at beginning of the test $F_{bi,ini}$ [kN]	Slip factor — based on initial preload $\mu_{i,ini}$ [-]	based on nominal preload $F_{p,C}$ [kN] 218, $\mu_i = \mu_{i,nom}$ [-]	based on preload at slip $\mu_{i,act}$ [-]	Preload at slip mean $F_{bi,act}$ [kN]	Test duration t [min]	Comment
RCSC_D_1D_01	1	0.093	99.3	216.5	0.23	0.23	0.23	215.96	5.6	Eq. according to RCSC 2014
RCSC_D_1D_02	2	0.109	98.9	218.8	0.23	0.23	0.23	217.5	5.5	
RCSC_D_1D_03	3	0.234	110.0	215.8	0.25	0.25	0.25	216.4	7.0	
RCSC_D_1D_04	4	0.113	108.7	215.3	0.25	0.25	0.26	212.1	6.2	
RCSC_D_1D_06	6	0.096	104.0	216.4	0.24	0.24	0.24	214.2	5.9	

Statistics (5 specimens, 5 test results)

n = 5	Number of tests							
max	Maximum		110.0		0.25	0.25	0.26	
min	Minimum		98.9		0.23	0.23	0.23	
mean	Mean value F_{sm} | μ_m		104.2		0.24	0.24	0.24	
R	Spread		11.1		0.03	0.03	0.03	Equation A3.1; R = max – min
s	Standard deviation s_{Fs}		5.2		0.013	0.012	0.013	
V	Coefficient of variation		4.9%		5.4%	4.9%	5.5%	V = s / mean

Creep test

Specimens mark	plate ID's	Preload at beginning of the test $F_{bi,ini}$ [kN]	First step load level F_{step1} [kN] Eq. A4.1	Slip (average at CB) u_{step1} [mm] Δ (0.5 h to 1000 h)	Second step load level F_{step2} [kN] Chap. A4.2	Slip (average at CB) u_{step2} [mm] at the load level	Comment	Final slip factor μ_{Final} [-] Eq. A3.1
RCSC_D_1D_07	7	218.7		0.004		0.06		
RCSC_D_1D_08	8	218.8	62.5	0.005	93.8	0.06		0.22
RCSC_D_1D_09	9	224.0		0.005		0.07		

Table B-8: Slip factor test results according to RCSC 2014 for RCSC_LD_1D test series

Technical characteristics of the test

Steel grade	Lean-Duplex Stainless Steel (1.4162)
Coating	–
Surface treatment	1D surface finish - Hot rolled (as received) - Bolt holes without burr
Mean coating thickness	–
Surface roughness (before coating)	23 µm
Specimen size	Standard specimens M22 (according to RCSC 2014)
Bolt class, bolt type	10.9 (Set EN 14399-4 – HV – M22 x 80 – 10.9/10 – tZn)
Nominal preload level	218 kN = $F_{p,C}$
Preload measuring method	Implanted SG, measured continuously, clamping length $\Sigma t = 56$ mm
Test speed	400 N/s

Static test

Specimens mark	plate ID's	Slip (average at CB) u_i [mm]	Slip load F_{si} [kN]	Preload at beginning of the test $F_{bi,ini}$ [kN]	based on initial preload $\mu_{i,ini}$ [-]	based on nominal preload $F_{p,C}$ [kN] 218 $\mu_i = \mu_{i,nom}$ [-]	based on preload at slip $\mu_{i,act}$ [-]	Preload at slip mean $F_{bi,act}$ [kN]	Test duration t [min]	Comment
RCSC_LD_1D_01	1	0.297	115.1	212.5	0.27	0.26	0.27	215.20	6.5	Eq. according to RCSC 2014
RCSC_LD_1D_03	3	0.126	112.6	213.9	0.26	0.26	0.26	213.8	6.4	
RCSC_LD_1D_04	4	0.508	103.1	214.0	0.24	0.24	0.23	220.3	5.5	
RCSC_LD_1D_05	5	0.218	110.2	214.0	0.26	0.25	0.26	214.0	6.2	
RCSC_LD_1D_06	6	0.117	113.5	214.6	0.26	0.26	0.26	215.3	6.4	

Statistics (5 specimens, 5 test results) — $n = 5$ Number of tests

		F_{si}	$\mu_{i,ini}$	$\mu_{i,nom}$	$\mu_{i,act}$	Comment
max	Maximum	115.1	0.27	0.26	0.27	
min	Minimum	103.1	0.24	0.24	0.23	
mean	Mean value $F_{sm} \mid \mu_m$	**110.9**	**0.26**	**0.25**	**0.26**	
R	Spread	12.0	0.03	0.03	0.03	$R = max - min$
s	Standard deviation s_{Fs}	4.7	0.011	0.011	0.013	
V	Coefficient of variation	4.2%	4.4%	4.2%	5.2%	$V = s / mean$

Equation A3.1

Creep test

Specimens mark	plate ID's	Preload at beginning of the test $F_{bi,ini}$ [kN]	First step load level Eq. A4.1 F_{step1} [kN]	Slip (average at CB) Δ (0.5 h to 1000 h) u_{step1} [mm]	Second step load level Chap. A4.2 F_{step2} [kN]	Slip (average at CB) at the load level u_{step2} [mm]	Comment	Final slip factor Eq. A3.1 μ_{Final} [-]
RCSC_LD_1D_06	6	222.8	66.5	0.003	99.8	0.06		0.23
RCSC_LD_1D_07	7	220.5		0.001		0.04		
RCSC_LD_1D_08	8	222.7		0.002		0.05		

Table B-9: Slip factor test results according to RCSC 2014 for RCSC_LD_1D-B test series

Technical characteristics of the test

Steel grade	Lean-Duplex Stainless Steel (1.4162)
Coating	–
Surface treatment	1D surface finish - Hot rolled (as received) - Bolt holes with burr
Mean coating thickness	–
Surface roughness (before coating)	23 µm
Specimen size	Standard specimens M22 (according to RCSC 2014)
Bolt class, bolt type	10.9 (Set EN 14399-4 – HV – M22 x 80 – 10.9/10 – tZn)
Nominal preload level	218 kN = $F_{p,C}$
Preload measuring method	Implanted SG, measured continuously, clamping length $\Sigma t = 56$ mm
Test speed	400 N/s

Static test

Specimens		Slip (average at CB)	Slip load	Preload at beginning of the test	Slip factor				Preload at slip	Test duration	Comment
mark	plate ID's				based on initial preload	based on nominal preload $F_{p,C}$ [kN] **218**		based on preload at slip			Eq. according to RCSC 2014
		u_i [mm]	F_{Si} [kN]	$F_{bi,ini}$ [kN]	$\mu_{i,ini}$ [-]	$\mu_i = \mu_{i,nom}$ [-]		$\mu_{i,act}$ [-]	mean $F_{bi,act}$ [kN]	t [min]	
RCSC_LD_1D-B_02	2	0.093	147.8	217.2	0.34	0.34		0.34	215.56	8.3	

Table B-10: Slip factor test results according to RCSC 2014 for RCSC_A_GB-A test series

Technical characteristics of the test

Steel grade	Austenitic Stainless Steel (1.4404)
Coating	–
Surface treatment	Grit blasted (with Brown Corundum, f20, Al2o3 (Aluminiumoxid)) - Bolt holes without burr
Mean coating thickness	–
Surface roughness (before coating)	75 µm
Specimen size	Standard specimens M22 (according to RCSC 2014)
Bolt class, bolt type	10.9 (Set EN 14399-4 – HV – M22 x 80 – 10.9/10 – tZn)
Nominal preload level	218 kN = $F_{p,C}$
Preload measuring method	Implanted SG, measured continuously, clamping length Σt = 56 mm
Test speed	400 N/s

Static test

Specimens mark	plate ID's	Slip (average at CB) u_i [mm]	Slip load F_{si} [kN]	Preload at beginning of the test $F_{bi,ini}$ [kN]	Slip factor based on initial preload $\mu_{i,ini}$ [-]	Slip factor based on nominal preload $F_{p,C}$ [kN] 218 $\mu_i = \mu_{i,nom}$ [-]	Slip factor based on preload at slip $\mu_{i,act}$ [-]	Preload at slip mean $F_{bi,act}$ [kN]	Test duration t [min]	Comment
										Eq. according to RCSC 2014
RCSC_A_GB-A_01	1	0.508	341.6	214.0	0.80	0.78	0.87	196.94	19.1	
RCSC_A_GB-A_02	2	0.508	343.4	214.0	0.80	0.79	0.87	197.7	19.2	
RCSC_A_GB-A_03	3	0.508	339.6	212.7	0.80	0.78	0.87	195.9	19.0	
RCSC_A_GB-A_04	4	0.508	343.8	216.8	0.79	0.79	0.85	202.7	19.2	
RCSC_A_GB-A_05	5	0.508	352.5	213.7	0.82	0.81	0.89	198.1	19.7	

Statistics (5 specimens, 5 test results) — $n = 5$ Number of tests

		F_{si} [kN]	$\mu_{i,ini}$ [-]	$\mu_i = \mu_{i,nom}$ [-]	$\mu_{i,act}$ [-]	Comment
max	Maximum	352.5	0.82	0.81	0.89	
min	Minimum	339.6	0.79	0.78	0.85	
mean	Mean value F_{sm} | μ_m	344.2	0.80	0.79	0.87	
R	Spread	12.9	0.03	0.03	0.04	$R = max - min$
s	Standard deviation s_{Fs}	4.9	0.012	0.011	0.015	
V	Coefficient of variation	1.4%	1.5%	1.4%	1.7%	$V = s / mean$

Creep test

Specimens mark	plate ID's	Preload at beginning of the test $F_{bi,ini}$ [kN]	First step load level F_{step1} [kN] Eq. A4.1	Slip (average at CB) u_{step1} [mm] Δ (0.5 h to 1000 h)	Second step load level F_{step2} [kN] Chap. A4.2	Slip (average at CB) u_{step2} [mm] at the load level	Comment	Final slip factor μ_{Final} [-] Eq. A3.1
RCSC_A_GB-A_06	6	220.5	206.5	0.001	309.8	0.13		0.71
RCSC_A_GB-A_07	7	220.1		0.001		0.12		
RCSC_A_GB-A_08	8	218.4		0.002		0.12		

Table B-11: Slip factor test results according to RCSC 2014 for RCSC_D_GB-A test series

Technical characteristics of the test

Steel grade	Duplex Stainless Steel (1.4462)
Coating	–
Surface treatment	Grit blasted (with Brown Corundum, f20, Al2o3 (Aluminiumoxid)) - Bolt holes without burr
Mean coating thickness	–
Surface roughness (before coating)	78 µm
Specimen size	Standard specimens M22 (according to RCSC 2014)
Bolt class, bolt type	10.9 (Set EN 14399-4 – HV – M22 x 80 – 10.9/10 – tZn)
Nominal preload level	218 kN = $F_{p,C}$
Preload measuring method	Implanted SG, measured continuously, clamping length Σt = 56 mm
Test speed	400 N/s

Static test

Specimens mark	plate ID's	Slip (average at CB) u_i [mm]	Slip load F_{si} [kN]	Preload at beginning of the test $F_{bi,ini}$ [kN]	Slip factor based on initial preload $\mu_{i,ini}$ [-]	Slip factor based on nominal preload $F_{p,C}$ [kN] **218** $\mu_i = \mu_{i,nom}$ [-]	Slip factor based on preload at slip $\mu_{i,act}$ [-]	Preload at slip mean $F_{bi,act}$ [kN]	Test duration t [min]	Comment
RCSC_D_GB-A_01	1	0.508	375.2	218.0	0.86	0.86	0.89	210.95	20.9	Eq. according to RCSC 2014
RCSC_D_GB-A_02	2	0.508	360.0	219.5	0.82	0.83	0.92	196.0	20.1	
RCSC_D_GB-A_03	3	0.508	359.6	217.6	0.83	0.82	0.88	204.3	20.0	
RCSC_D_GB-A_04	4	0.508	359.3	216.5	0.83	0.82	0.87	207.1	20.1	
RCSC_D_GB-A_05	5	0.508	343.9	215.8	0.80	0.79	0.83	206.8	19.2	

Statistics (5 specimens, 5 test results) — $n = 5$ Number of tests

max	Maximum	375.2		0.86	0.86	0.92
min	Minimum	343.9		0.80	0.79	0.83
mean	Mean value F_{sm} | μ_m	**359.6**		**0.83**	**0.82**	**0.88**
R	Spread	31.3		0.06	0.07	0.09	Equation A3.1
s	Standard deviation s_{Fs}	11.1		0.023	0.025	0.032	R = max – min
V	Coefficient of variation	3.1%		2.8%	3.1%	3.6%	V = s / mean

Creep test

Specimens mark	plate ID's	Preload at beginning of the test $F_{bi,ini}$ [kN]	First step load level Eq. A4.1 F_{step1} [kN]	Slip (average at CB) Δ(0.5 h to 1000 h) u_{step1} [mm]	Second step load level Chap. A4.2 F_{step2} [kN]	Slip (average at CB) at the load level u_{step2} [mm]	Comment	Final slip factor Eq. A3.1 μ_{Final} [-]
RCSC_D_GB-A_06	6	218.4	215.8	0.001	323.6	0.21		0.74
RCSC_D_GB-A_07	7	220.9		0.002		0.18		
RCSC_D_GB-A_08	8	220.2		0.002		0.19		

Table B-12: Slip factor test results according to RCSC 2014 for RCSC_LD_GB-A test series

Technical characteristics of the test

Steel grade	Lean-Duplex Stainless Steel (1.4162)
Coating	–
Surface treatment	Grit blasted (with Brown Corundum, f20, Al2o3 (Aluminiumoxid)) - Bolt holes without burr
Mean coating thickness	–
Surface roughness (before coating)	73 µm
Specimen size	Standard specimens M22 (according to RCSC 2014)
Bolt class, bolt type	10.9 (Set EN 14399-4 – HV – M22 x 80 – 10.9/10 – tZn)
Nominal preload level	218 kN = $F_{p,C}$
Preload measuring method	Implanted SG, measured continuously, clamping length Σt = 56 mm
Test speed	400 N/s

Static test

Specimens mark	plate ID's	Slip (average at CB) u_i [mm]	Slip load F_{si} [kN]	Preload at beginning of the test $F_{bi,ini}$ [kN]	Slip factor based on initial preload $\mu_{i,ini}$ [-]	Slip factor based on nominal preload $F_{p,C}$ [kN] 218 $\mu_i = \mu_{i,nom}$ [-]	Slip factor based on preload at slip $\mu_{i,act}$ [-]	Preload at slip mean $F_{bi,act}$ [kN]	Test duration t [min]	Comment
RCSC_LD_GB-A_01	1	0.508	319.2	215.6	0.74	0.73	0.81	196.35	17.9	Eq. according to RCSC 2014
RCSC_LD_GB-A_02	2	0.508	328.0	214.8	0.76	0.75	0.80	204.0	18.3	
RCSC_LD_GB-A_03	3	0.508	358.3	215.4	0.83	0.82	0.91	196.0	20.0	
RCSC_LD_GB-A_04	4	0.508	355.8	214.2	0.83	0.82	0.88	202.1	19.9	
RCSC_LD_GB-A_05	5	0.508	328.4	214.4	0.77	0.75	0.80	204.8	18.3	

Statistics (5 specimens, 5 test results) n = 5   Number of tests

		F_{si}	$\mu_{i,ini}$	$\mu_i = \mu_{i,nom}$	$\mu_{i,act}$	Comment
max	Maximum	358.3	0.83	0.82	0.91	
min	Minimum	319.2	0.74	0.73	0.80	
mean	Mean value $F_{sm} \mid \mu_m$	337.9	0.79	0.78	0.84	
R	Spread	39.2	0.09	0.09	0.11	$R = max - min$
s	Standard deviation s_{Fs}	17.9	0.042	0.041	0.051	
V	Coefficient of variation	5.3%	5.3%	5.3%	6.1%	$V = s / mean$

Creep test

Specimens mark	plate ID's	Preload at beginning of the test $F_{bi,ini}$ [kN]	First step load level Eq. A4.1 F_{step1} [kN]	Slip (average at CB) Δ (0.5 h to 1000 h) u_{step1} [mm]	Second step load level Chap. A4.2 F_{step2} [kN]	Slip (average at CB) at the load level u_{step2} [mm]	Comment	Final slip factor Eq. A3.1 μ_{Final} [-]
RCSC_LD_GB-A_06	6	217.3		0.003		0.11		
RCSC_LD_GB-A_07	7	222.5	202.8	0.001	304.1	0.15		0.70
RCSC_LD_GB-A_08	8	221.7		0.002		0.22		

Annex C: Slip factor test evaluation tables (Resin/particles)
test results according to EN 1090-2 for slip-resistant connections
made of *Stainless steel* with mixture of resin and particles

Table C-1: Slip factor test results according to EN 1090-2 for A_tR test series

Technical characteristics of the test

Steel grade	Austenitic Stainless Steel (1.4404) (hot rolled)
Coating	–
Surface treatment	Resin (DELO-DUOPOX® AD897: Multi-purpose 2c epoxy resin)
Resin application status	Very thin resin layer on the faying surfaces
Particle application status	–
Mean coating thickness	–
Surface roughness (before coating)	23 µm
Duration of curing	at least 24 hours
Specimen size	Standard specimens M16 (EN 1090-2, Figure G.1 b)
Bolt class, bolt type	Bolt: BUMAX109 (EN ISO 4017 – M16 x 100) - Nut: BUMAX 109 (EN ISO 4032) - Washer: HV 300 (EN ISO 7089)
Nominal preload level	110 kN = $F_{p,C}$
Preload measuring method	Load cell (h = 40 mm), measured continuously, clamping length Σt = 75 mm
Test speed	0.6 mm/min

Static test

Specimens mark	plate IDs	Slip (average at CBG) u_i [mm]	Slip load F_{Si} [kN]	Preload at start of test (initial preload) Outer bolt $F_{bi,o,ini}$ [kN]	Mean value mean $F_{bi,ini}$ [kN]	Inner bolt $F_{bi,i,ini}$ [kN]	Slip factor based on initial preload $\mu_{i,ini}$ [-]	based on nominal preload $F_{p,C}$ [kN] = 110; $\mu_i = \mu_{i,nom}$ [-]	based on preload at slip $\mu_{i,act}$ [-]	Preload at slip Outer bolt $F_{bi,o,act}$ [kN]	Mean value mean $F_{bi,act}$ [kN]	Inner bolt $F_{bi,i,act}$ [kN]	Test duration t [min]	Comment Eq. according to EN 1090-2
A_tR_01-02	1	0.031	266.2	111.6	111.7	111.7	0.60	0.61	0.62	106.8	106.6	106.5	13.2	
	2	0.017	266.2	110.3	110.5	110.8	0.60	0.61	0.63	105.6	105.3	105.1	13.2	
A_tR_03-04	3	0.026	262.5	109.8	110.5	111.1	0.59	0.60	0.62	104.7	105.4	106.0	13.3	
	4	0.019	262.5	109.8	110.3	110.9	0.59	0.60	0.63	104.7	104.8	105.0	13.3	
A_tR_05-06	5	0.020	266.7	110.7	110.8	111.0	0.60	0.61	0.63	105.1	105.2	105.3	13.1	
	6	0.001	266.7	110.4	111.0	111.6	0.60	0.61	0.63	105.7	106.2	106.8	13.1	
A_tR_07-08	7	0.010	275.1	111.1	110.8	110.5	0.62	0.63	0.66	105.2	104.5	103.8	16.0	
	8	0.002	275.1	110.7	111.0	111.4	0.62	0.63	0.65	105.6	105.3	105.0	16.0	

Statistics (4 specimens, 8 test results) — n = 8 Number of tests

		F_{Si} [kN]			$\mu_{i,ini}$	$\mu_i = \mu_{i,nom}$	$\mu_{i,act}$				Comment
max	Maximum	275.1			0.62	0.63	0.66				Eq. (2), Eq. (4)
min	Minimum	262.5			0.59	0.60	0.62				R = max − min
mean	Mean value F_{Sm}	μ_m	267.6		0.60	0.61	0.63				Eq. (3), Eq. (5)
R	Spread	12.6			0.03	0.03	0.04				V = s / mean
s	Standard deviation s_{Fs}	4.9			0.011	0.011	0.014				Load level for the creep test
V	Coefficient of variation	1.8%			1.8%	1.8%	2.1%				
0.9 F_{Sm}		240.9									

Creep test

mark	plate IDs	Slip			Preload Outer bolt $F_{bi,o,ini}$	mean $F_{bi,ini}$	Inner bolt $F_{bi,i,ini}$	$\mu_{i,ini}$	$\mu_{i,nom}$	$\mu_{i,act}$	Outer bolt $F_{bi,o,act}$	mean $F_{bi,act}$	Inner bolt $F_{bi,i,act}$	t [min]	Comment
A_tR_09-10	9	Δ (5 min to 3 h): 4.333	0.146	–	109.7	110.7	111.6	–	–	–	103.6	104.2	104.8	31.4	**Creep test failed** Slip during the creep test > 0,002 mm (5 min to 3 h)
	10	Δ (5 min to 3 h): 4.004	0.151	–	110.5	109.3	108.2	–	–	–	105.5	102.9	100.3	21.3	

Comments

Test results
● Creep test failed
● Extended creep test is required

Table C-2: Slip factor test results according to EN 1090-2 for A_tR+fP10 test series

Technical characteristics of the test

Property	Value
Steel grade	Austenitic Stainless Steel (1.4404)
Coating	–
Surface treatment	Resin (DELO-DUOPOX® AD897: Multi-purpose 2c epoxy resin) + GRITTAL GH-10 (stainless steel grit, crushed, martensitic with chromium carbides)-(Grain sizes (GH-10): 0.05 – 0.20 mm)
Resin application status	Very thin resin layer on the faying surfaces
Particle application status	Surfaces fully covered with particles
Mean coating thickness	–
Surface roughness (before coating)	23 µm
Duration of curing	at least 24 hours
Specimen size	Standard specimens M16 (EN 1090-2, Figure G.1 b)
Bolt class, bolt type	Bolt: BUMAX 109 (EN ISO 4017 – M16 x 100) - Nut: BUMAX 109 (EN ISO 4032) - Washer: HV 300 (EN ISO 7089)
Nominal preload level	110 kN = $F_{p,C}$
Preload measuring method	Load cell (h = 40 mm), measured continuously, clamping length Σt = 75 mm
Test speed	0.6 mm/min

Static test

Specimens mark	plate ID's	Slip (average at CBG) u_i [mm]	Slip load F_{si} [kN]	Preload at start of test (initial preload) — Outer bolt $F_{bi,o,ini}$ [kN]	mean $F_{bi,ini}$ [kN]	$F_{bi,ini}$ [kN]	Slip factor — based on initial preload $\mu_{i,ini}$ [-]	based on nominal preload $F_{p,C}$ 110 $\mu_i = \mu_{i,nom}$ [-]	based on preload at slip $\mu_{i,act}$ [-]	Preload at slip — Outer bolt $F_{bi,o,act}$ [kN]	mean $F_{bi,act}$ [kN]	Inner bolt $F_{bi,i,act}$ [kN]	Test duration t [min]	Comment
A_tR+fP10_01-02	1	0.033	252.3	110.0	109.5	109.0	0.58	0.57	0.60	105.1	104.3	103.5	13.5	Eq. according to EN 1090-2
	2	0.084	252.3	109.8	110.2	110.7	0.57	0.57	0.61	104.2	103.7	103.1	13.5	
A_tR+fP10_03-04	3	0.150	249.4	110.4	110.4	110.3	0.56	0.57	0.61	104.2	102.5	100.7	13.3	
	4	0.062	249.4	110.4	110.6	110.9	0.56	0.57	0.60	105.8	104.7	103.5	13.4	
A_tR+fP10_05-06	5	0.044	255.4	111.5	110.9	110.2	0.58	0.58	0.62	105.5	103.3	101.1	13.2	
	6	0.115	255.4	109.7	110.5	111.3	0.58	0.58	0.62	103.0	103.3	103.7	13.2	
A_tR+fP10_07-08	7	0.098	242.8	111.5	111.5	111.4	0.54	0.55	0.59	105.0	103.5	102.0	13.2	
	8	0.067	242.8	110.8	111.0	111.3	0.55	0.55	0.58	105.5	104.2	102.9	13.2	

Statistics (4 specimens, 8 test results), n = 8

Statistic	F_{si} [kN]	$\mu_{i,ini}$ [-]	$\mu_i = \mu_{i,nom}$ [-]	$\mu_{i,act}$ [-]	Comment
max Maximum	255.4	0.58	0.58	0.62	
min Minimum	242.8	0.54	0.55	0.58	
mean Mean value $F_{sm} \mid \mu_m$	**250.0**	**0.57**	**0.57**	**0.60**	
R Spread	12.5	0.03	0.03	0.04	$R = max - min$
s Standard deviation s_{Fs}	4.9	0.013	0.011	0.013	Eq. (3), Eq. (5)
V Coefficient of variation	2.0%	2.3%	2.0%	2.2%	$V = s$ / *mean*
0.9 F_{sm}	**225.0**				Load level for the creep test

Comment: Eq. (2), Eq. (4)

Creep test

Specimens mark	plate ID's	Slip u_i [mm]	F_{si} [kN]	Preload at start — Outer bolt $F_{bi,o,ini}$ [kN]	mean $F_{bi,ini}$ [kN]	$F_{bi,ini}$ [kN]	$\mu_{i,ini}$ [-]	$\mu_i = \mu_{i,nom}$ [-]	$\mu_{i,act}$ [-]	Preload at slip — Outer bolt $F_{bi,o,act}$ [kN]	mean $F_{bi,act}$ [kN]	Inner bolt $F_{bi,i,act}$ [kN]	t [min]	Comment
A_tR+fP10_09-10	9	Δ (5 min to 3 h): ≈ **0.06** / 0.150	–	110.9	110.3	109.7	–	–	–	102.3	101.9	101.5	984.8	**Creep test failed** Slip during the creep test > 0.002 mm (5 min to 3 h)
	10	Δ (5 min to 3 h): ≈ **0.07** / 0.179	–	110.6	110.7	110.8	–	–	–	102.6	101.1	99.5	969.7	

Comments
- Creep test failed

Test results
- Extended creep test is required

Table C-3: Slip factor test results according to EN 1090-2 for A_tR+fP20 test series

Technical characteristics of the test

Steel grade	Austenitic Stainless Steel (1.4404)
Coating	–
Surface treatment	Resin (DELO-DUOPOX® AD897: Multi-purpose 2c epoxy resin) + GRITTAL GH-20 (stainless steel grit, crushed, martensitic with chromium carbides) - (Grain sizes (GH-20): 0.09 – 0.32 mm)
Resin application status	Very thin resin layer on the faying surfaces
Particle application status	Surfaces fully covered with particles
Mean coating thickness	–
Surface roughness (before coating)	23 µm
Duration of curing	at least 24 hours
Specimen size	Standard specimens M16 (EN 1090-2, Figure G.1 b)
Bolt class, bolt type	Bolt: BUMAX 109 (EN ISO 4017 – M16 x 100) - Nut: BUMAX 109 (EN ISO 4032) - Washer: HV 300 (EN ISO 7089)
Nominal preload level	110 kN = $F_{p,c}$
Preload measuring method	Load cell (h = 40 mm), measured continuously, clamping length Σt = 75 mm
Test speed	0.6 mm/min

Static test

Specimens mark — plate ID's	Slip (average at CBG) u_i [mm]	Slip load F_{si} [kN]	Preload at start of test (initial preload) — Outer bolt $F_{bi,o,ini}$ [kN]	Mean value mean $F_{bi,ini}$ [kN]	Inner bolt $F_{bi,i,ini}$ [kN]	Slip factor based on initial preload $\mu_{i,ini}$ [-]	based on nominal preload $F_{p,c}$ [kN] 110 / $\mu = \mu_{i,nom}$ [-]	based on preload at slip $\mu_{i,act}$ [-]	Preload at slip — Outer bolt $F_{bi,o,act}$ [kN]	Mean value mean $F_{bi,act}$ [kN]	Inner bolt $F_{bi,i,act}$ [kN]	Test duration t [min]	Comment — Eq. according to EN 1090-2
A_tR+fP20_01-02 1	0.142	218.2	111.5	111.1	110.7	0.49	0.50	0.53	103.7	102.7	101.8	11.5	
2	0.123	218.2	109.9	110.4	110.9	0.49	0.50	0.53	103.2	103.0	102.8	11.5	
Statistics (4 specimens, 8 test results) $n = 2$ Number of tests													
max Maximum		218.2				0.49	0.50	0.53					Eq. (2), Eq. (4)
min Minimum		218.2				0.49	0.50	0.53					$R = max - min$
$mean$ Mean value F_{sm} | μ_m		**218.2**				**0.49**	**0.50**	**0.53**					
R Spread		0.0				0.00	0.00	0.00					Eq. (3), Eq. (5)
s Standard deviation s_{Fs}		0.0				0.002	0.000	0.001					$V = s / mean$
V Coefficient of variation		0.0%				0.5%	0.0%	0.2%					

Table C-4: Slip factor test results according to EN 1090-2 for A_tR+pP40 test series

Technical characteristics of the test

Steel grade	Austenitic Stainless Steel (1.4404)
Coating	–
Surface treatment	Resin (DELO-DUOPOX® AD897: Multi-purpose 2c epoxy resin) + GRITTAL GH-40 (stainless steel grit, crushed, martensitic with chromium carbides)-(Grain sizes (GH-40): 0.40 – 0.80 mm)
Resin application status	Very thin resin layer on the faying surfaces
Particle application status	Surfaces partially covered with particles
Mean coating thickness	–
Surface roughness (before coating)	23 µm
Duration of curing	at least 24 hours
Specimen size	Standard specimens M16 (EN 1090-2, Figure G.1 b)
Bolt class, bolt type	Bolt: BUMAX 109 (EN ISO 4017 – M16 x 100) - Nut: BUMAX 109 (EN ISO 4032) - Washer: HV 300 (EN ISO 7089)
Nominal preload level	110 kN = $F_{p,C}$
Preload measuring method	Load cell (h = 40 mm), measured continuously, clamping length Σt = 75 mm
Test speed	0.6 mm/min

Static test

Specimens mark	plate ID's	Slip (average at CBG) u_i [mm]	Slip load F_{si} [kN]	Preload at start of test (initial preload)			Slip factor			Preload at slip			Test duration	Comment
				Outer bolt $F_{bi,o,ini}$ [kN]	Mean value mean $F_{bi,ini}$ [kN]	Inner bolt $F_{bi,i,ini}$ [kN]	based on initial preload $\mu_{i,ini}$ [-]	based on nominal preload $F_{p,C}$ [kN] 110 $\mu_i = \mu_{i,nom}$ [-]	based on preload at slip $\mu_{i,act}$ [-]	Outer bolt $F_{bi,o,act}$ [kN]	Mean value mean $F_{bi,act}$ [kN]	Inner bolt $F_{bi,i,act}$ [kN]	t [min]	Eq. according to EN 1090-2
A_tR+pP40_01-02	1	0.111	255.6	111.6	110.5	109.4	0.58	0.58	0.62	106.1	103.5	101.0	16.8	Eq. (2), Eq. (4)
	2	0.150	248.0	113.3	111.4	109.6	0.56	0.56	0.60	106.8	103.2	99.6	17.4	
Statistics (4 specimens, 8 test results)	n = 2	Number of tests												
	max	Maximum	255.6				0.58	0.58	0.62					
	min	Minimum	248.0				0.56	0.56	0.60					
	mean	Mean value F_{sm} | μ_m	251.8				0.57	0.57	0.61					
	R	Spread	7.5				0.02	0.02	0.02					R = max – min
	s	Standard deviation s_{Fs}	5.3				0.015	0.012	0.012					Eq. (3), Eq. (5)
	V	Coefficient of variation	2.1%				2.7%	2.1%	1.9%					V = s / mean

Table C-5: Slip factor test results according to EN 1090-2 for A_tR+fP40 test series

Technical characteristics of the test

Steel grade	Austenitic Stainless Steel (1.4404)
Coating	–
Surface treatment	Resin (DELO-DUOPOX® AD897: Multi-purpose 2c epoxy resin) + GRITTAL GH-40 (stainless steel steel grit, crushed, martensitic with chromium carbides) - (Grain sizes (GH-40): 0.40 – 0.80 mm)
Resin application status	Very thin resin layer on the faying surfaces
Particle application status	Surfaces fully covered with particles
Mean coating thickness	–
Surface roughness (before coating)	23 µm
Duration of curing	at least 24 hours
Specimen size	Standard specimens M16 (EN 1090-2, Figure G.1 b)
Bolt class, bolt type	Bolt: BUMAX 109 (EN ISO 4017 – M16 x 100) - Nut: BUMAX 109 (EN ISO 4032) - Washer: HV 300 (EN ISO 7089)
Nominal preload level	110 kN = $F_{p,C}$
Preload measuring method	Load cell (h = 40 mm), measured continuously, clamping length Σt = 75 mm
Test speed	0.6 mm/min

Static test

Specimens		Slip (average at CBG)	Slip load	Preload at start of test (initial preload)			Slip factor			Preload at slip			Test duration	Comment
mark	plate ID's			Outer bolt	Mean value	Inner bolt	based on initial preload	based on nominal preload $F_{p,C}$ [kN] **110**	based on preload at slip	Outer bolt	Mean value	Inner bolt		Eq. according to EN 1090-2
		u_i [mm]	F_{Si} [kN]	$F_{bi,o,ini}$ [kN]	mean $F_{bi,ini}$ [kN]	$F_{bi,i,ini}$ [kN]	$\mu_{i,ini}$ [-]	$\mu_i = \mu_{i,nom}$ [-]	$\mu_{i,act}$ [-]	$F_{bi,o,act}$ [kN]	mean $F_{bi,act}$ [kN]	$F_{bi,i,act}$ [kN]	t [min]	
A_tR+fP40_01-02 1	1	0.150	159.4	111.1	109.9	108.6	0.36	0.36	0.41	98.9	97.3	95.7	13.0	
	2	0.150	159.5	109.8	110.4	111.0	0.36	0.36	0.41	97.2	96.9	96.6	13.0	

Statistics (4 specimens, 8 test results)

			F_{Si}				$\mu_{i,ini}$	$\mu_i = \mu_{i,nom}$	$\mu_{i,act}$					
n = 2	Number of tests													
max	Maximum		159.5				0.36	0.36	0.41					Eq. (2), Eq. (4)
min	Minimum		159.4				0.36	0.36	0.41					R = max – min
mean	Mean value $F_{Sm} \mid \mu_m$		**159.5**				**0.36**	**0.36**	**0.41**					Eq. (3), Eq. (5)
R	Spread		0.1				0.00	0.00	0.00					V = s / mean
s	Standard deviation s_{Fs}		0.1				0.001	0.000	0.001					
V	Coefficient of variation		0.1%				0.3%	0.1%	0.3%					

Table C-6: Slip factor test results according to EN 1090-2 for A_thR test series

Technical characteristics of the test

Characteristic	Value
Steel grade	Austenitic Stainless Steel
Coating	–
Surface treatment	Resin (DELO-DUOPOX® AD897: Multi-purpose 2c epoxy resin)
Resin application status	Very thick resin layer on the faying surfaces
Particle application status	–
Mean coating thickness	–
Surface roughness (before coating)	23 µm
Duration of curing	at least 24 hours
Specimen size	Standard specimens M16 (EN 1090-2, Figure G.1 b)
Bolt class, bolt type	Bolt: BUMAX109 (EN ISO 4017 – M16 x 100) - Nut: BUMAX 109 (EN ISO 4032) - Washer: HV 300 (EN ISO 7089)
Nominal preload level	110 kN = $F_{p,C}$
Preload measuring method	Load cell (h = 40 mm), measured continuously, clamping length Σt = 75 mm
Test speed	0.6 mm/min

Data table

Specimens mark	plate ID's	Slip (average at CBG) u_i [mm]	Slip load F_{si} [kN]	Preload at start of test (initial preload) Outer bolt $F_{bi,o,ini}$ [kN]	Inner bolt $F_{bi,i,ini}$ [kN]	Mean value mean $F_{bi,ini}$ [kN]	Slip factor based on initial preload $\mu_{i,ini}$ [-]	based on nominal preload $F_{p,C}$ [kN] 110 $\mu_i = \mu_{i,nom}$ [-]	based on preload at slip $\mu_{i,act}$ [-]	Preload at slip Outer bolt $F_{bi,o,act}$ [kN]	Mean value mean $F_{bi,act}$ [kN]	Inner bolt $F_{bi,i,act}$ [kN]	Test duration t [min]	Comment Eq. according to EN 1090-2
A_thR_01-02	1	0.015	278.9	112.5	111.2	111.8	0.62	0.63	0.65	107.5	107.9	108.4	13.9	
	2	0.013	278.9	111.6	112.8	112.2	0.62	0.63	0.65	107.6	107.8	108.0	13.9	

Static test — Statistics (4 specimens, 8 test results)

		F_{si} [kN]					$\mu_{i,ini}$ [-]	$\mu_i = \mu_{i,nom}$ [-]	$\mu_{i,act}$ [-]					Comment
n = 2	Number of tests													
max	Maximum	278.9					0.62	0.63	0.65					Eq. (2), Eq. (4)
min	Minimum	278.9					0.62	0.63	0.65					R = max – min
mean	Mean value F_{sm} | μ_m	**278.9**					**0.62**	**0.63**	**0.65**					Eq. (3), Eq. (5)
R	Spread	0.0					0.00	0.00	0.00					V = s / mean
s	Standard deviation s_{Fs}	0.0					0.001	0.000	0.001					
V	Coefficient of variation	0.0%					0.2%	0.0%	0.1%					

Table C-7: Slip factor test results according to EN 1090-2 for A_thR+fP10 test series

Technical characteristics of the test

Steel grade	Austenitic Stainless Steel (1.4404)
Coating	–
Surface treatment	Resin (DELO-DUOPOX® AD897: Multi-purpose 2c epoxy resin) + GRITTAL GH-10 (stainless steel grit, crushed, martensitic with chromium carbides) - (Grain sizes (GH-10): 0.05 – 0.20 mm)
Resin application status	Very thick resin layer on faying surfaces
Particle application status	Surfaces fully covered with particles
Mean coating thickness	–
Surface roughness (before coating)	23 µm
Duration of curing	at least 24 hours
Specimen size	Standard specimens M16 (EN 1090-2, Figure G.1 b)
Bolt class, bolt type	Bolt: BUMAX109 (EN ISO 4017 – M16 x 100) - Nut: BUMAX 109 (EN ISO 4032) - Washer: HV 300 (EN ISO 7089)
Nominal preload level	110 kN = $F_{p,C}$
Preload measuring method	Load cell (h = 40 mm), measured continuously, clamping length Σt = 75 mm
Test speed	0.6 mm/min

Static test

Specimens mark	plate ID's	Slip (average at CBG) u_i [mm]	Slip load F_{si} [kN]	Preload at start of test (initial preload) — Outer bolt $F_{bi,o,ini}$ [kN]	Mean value mean $F_{bi,ini}$ [kN]	Inner bolt $F_{bi,i,ini}$ [kN]	Slip factor — based on initial preload $\mu_{i,ini}$ [-]	based on nominal preload $F_{p,C}$=110 [kN] $\mu_i=\mu_{i,nom}$ [-]	based on preload at slip $\mu_{i,act}$ [-]	Preload at slip — Outer bolt $F_{bi,o,act}$ [kN]	Mean value mean $F_{bi,act}$ [kN]	Inner bolt $F_{bi,i,act}$ [kN]	Test duration t [min]	Comment (Eq. according to EN 1090-2)
A_thR+fP10_01-02	1	0.040	344.5	109.0	109.3	109.6	0.79	0.78	0.85	101.8	101.9	102.0	18.4	
	2	0.070	344.5	110.4	110.6	110.7	0.78	0.78	0.84	102.5	102.8	103.0	18.4	
A_thR+fP10_03-04	3	0.077	321.4	108.7	109.7	110.7	0.73	0.73	0.78	102.4	103.2	104.0	16.5	
	4	0.069	322.1	108.9	108.8	108.6	0.74	0.73	0.80	102.8	101.0	99.2	17.2	
A_thR+fP10_05-06	5	0.049	343.1	108.2	108.5	108.8	0.79	0.78	0.85	100.4	101.0	101.6	18.5	
	6	0.075	343.1	108.0	108.8	109.5	0.79	0.78	0.85	100.6	101.3	102.0	18.5	
A_thR+fP10_07-08	7	0.064	341.7	110.5	109.1	107.7	0.78	0.78	0.84	104.1	101.5	98.9	18.0	
	8	0.048	341.7	108.3	109.6	110.8	0.78	0.78	0.84	100.1	101.4	102.7	18.0	

Statistics (4 specimens, 8 test results), n = 8

		F_{si} [kN]	$\mu_{i,ini}$ [-]	$\mu_i=\mu_{i,nom}$ [-]	$\mu_{i,act}$ [-]	Comment
Maximum	*max*	344.5	0.79	0.78	0.85	
Minimum	*min*	321.4	0.73	0.73	0.78	
Mean value $F_{sm} \mid \mu_m$	*mean*	337.8	0.77	0.77	0.83	
Spread	*R*	23.1	0.06	0.05	0.07	Eq. (2), Eq. (4); R = max – min
Standard deviation s_{Fs}	*s*	9.9	0.023	0.023	0.027	Eq. (3), Eq. (5); V = s / mean
Coefficient of variation	*V*	2.9%	3.0%	2.9%	3.2%	
0.9 F_{sm}		304.0				Load level for the creep test

Creep test

Specimens mark	plate ID's	Slip (average at CBG) u_i [mm]	Slip load F_{si} [kN]	Outer bolt $F_{bi,o,ini}$ [kN]	Mean value mean $F_{bi,ini}$ [kN]	Inner bolt $F_{bi,i,ini}$ [kN]	$\mu_{i,ini}$ [-]	$\mu_i=\mu_{i,nom}$ [-]	$\mu_{i,act}$ [-]	Outer bolt $F_{bi,o,act}$ [kN]	Mean value mean $F_{bi,act}$ [kN]	Inner bolt $F_{bi,i,act}$ [kN]	Test duration t [min]	Comment
A_thR+fP10_09-10	9	Δ (5 min to 3 h): 0.913 / 0.151	–	109.3	108.4	107.5	–	–	–	104.2	102.6	101.1	25.7	Creep test failed; Slip during the creep test > 0.002 mm (5 min to 3 h)
	10	Δ (5 min to 3 h): 0.999 / 0.149	–	109.4	109.4	109.4	–	–	–	103.7	101.7	99.7	24.4	

Comments
- Creep test failed
- Extended creep test is required

Test results

Table C-8: Slip factor test results according to EN 1090-2 for A_thR+fP20 test series

Technical characteristics of the test

Steel grade	Austenitic Stainless Steel (1.4404)
Coating	–
Surface treatment	Resin (DELO-DUOPOX® AD897: Multi-purpose 2c epoxy resin) + GRITTAL GH-20 (stainless steel grit, crushed, martensitic with chromium carbides) - (Grain sizes (GH-20): 0.09 – 0.32 mm)
Resin application status	Very thick resin layer on the faying surfaces
Particle application status	Surfaces fully covered with particles
Mean coating thickness	–
Surface roughness (before coating)	23 µm
Duration of curing	at least 24 hours
Specimen size	Standard specimens M16 (EN 1090-2, Figure G.1 b)
Bolt class, bolt type	Bolt: BUMAX 109 (EN ISO 4017 – M16 x 100) - Nut: BUMAX 109 (EN ISO 4032) - Washer: HV 300 (EN ISO 7089)
Nominal preload level	110 kN = $F_{p,c}$
Preload measuring method	Load cell (h = 40 mm), measured continuously, clamping length Σt = 75 mm
Test speed	0.6 mm/min

Static test

Specimens mark	plate ID's	Slip (average at CBG) u_i [mm]	Slip load F_{Si} [kN]	Preload at start of test (initial preload) Outer bolt $F_{bi,o,ini}$ [kN]	Mean value mean $F_{bi,ini}$ [kN]	Inner bolt $F_{bi,i,ini}$ [kN]	Slip factor based on initial preload $\mu_{i,ini}$ [-]	based on nominal preload $F_{p,C}$ [kN] 110 $\mu_i = \mu_{i,nom}$ [-]	based on preload at slip $\mu_{i,act}$ [-]	Preload at slip Outer bolt $F_{bi,o,act}$ [kN]	Mean value mean $F_{bi,act}$ [kN]	Inner bolt $F_{bi,i,act}$ [kN]	Test duration t [min]	Comment Eq. according to EN 1090-2
A_1D+fG+fP20GH_01-02	1	0.033	326.4	111.5	112.2	112.9	0.73	0.74	0.80	101.9	102.5	103.2	16.8	
	2	0.046	326.4	111.2	112.4	113.7	0.73	0.74	0.79	101.0	103.6	106.3	16.8	

Statistics (4 specimens, 8 test results)

		Slip load F_{Si} [kN]	$\mu_{i,ini}$ [-]	$\mu_i = \mu_{i,nom}$ [-]	$\mu_{i,act}$ [-]	Comment
	n = 2 Number of tests					
max	Maximum	326.4	0.73	0.74	0.80	Eq. (2), Eq. (4)
min	Minimum	326.4	0.73	0.74	0.79	
mean	Mean value F_{Sm} | μ_m	326.4	0.73	0.74	0.79	
R	Spread	0.0	0.00	0.00	0.01	R = max – min
s	Standard deviation s_{Fs}	0.0	0.001	0.000	0.006	Eq. (3), Eq. (5)
V	Coefficient of variation	0.0%	0.1%	0.0%	0.7%	V = s / mean

Table C-9: Slip factor test results according to EN 1090-2 for A_thR+fP40 test series

Technical characteristics of the test

Characteristic	Value
Steel grade	Austenitic Stainless Steel (1.4404)
Coating	–
Surface treatment	Resin (DELO-DUOPOX® AD897: Multi-purpose 2c epoxy resin) + GRITTAL GH-40 (stainless steel grit, crushed, martensitic with chromium carbides) - (Grain sizes (GH-40): 0.40 – 0.80 mm
Resin application status	Very thick resin layer on the faying surfaces
Particle application status	Surfaces fully covered with particles
Mean coating thickness	–
Surface roughness (before coating)	23 µm
Duration of curing	at least 24 hours
Specimen size	Standard specimens M16 (EN 1090-2, Figure G.1 b)
Bolt class, bolt type	Bolt: BUMAX109 (EN ISO 4017 – M16 x 100) - Nut: BUMAX 109 (EN ISO 4032) - Washer: HV 300 (EN ISO 7089)
Nominal preload level	110 kN = $F_{p,C}$
Preload measuring method	Load cell (h = 40 mm), measured continuously, clamping length Σt = 75 mm
Test speed	0.6 mm/min

Static test

Specimens mark	plate ID's	Slip (average at CBG) u_i [mm]	Slip load F_{si} [kN]	Preload at start of test (initial preload) — Outer bolt $F_{bi,o,ini}$ [kN]	Mean value mean $F_{bi,ini}$ [kN]	Inner bolt $F_{bi,i,ini}$ [kN]	Slip factor based on initial preload $\mu_{i,ini}$ [-]	based on nominal preload $F_{p,C}$ [kN] 110, $\mu_i = \mu_{i,nom}$ [-]	based on preload at slip $\mu_{i,act}$ [-]	Preload at slip — Outer bolt $F_{bi,o,act}$ [kN]	Mean value mean $F_{bi,act}$ [kN]	Inner bolt $F_{bi,i,act}$ [kN]	Test duration t [min]	Comment — Eq. according to EN 1090-2
A_thR+fP40_01-02	1	0.120	340.1	111.8	111.0	110.2	0.77	0.77	0.84	102.7	100.9	99.1	17.6	
	2	0.109	340.1	108.8	109.6	110.3	0.78	0.77	0.86	100.4	99.1	97.8	17.6	

Statistics (4 specimens, 8 test results), n = 2

		Slip load F_{si} [kN]	$\mu_{i,ini}$ [-]	$\mu_i = \mu_{i,nom}$ [-]	$\mu_{i,act}$ [-]	Comment
max	Maximum	340.1	0.78	0.77	0.86	
min	Minimum	340.1	0.77	0.77	0.84	Eq. (2), Eq. (4)
mean	Mean value F_{sm} | μ_m	340.1	0.77	0.77	0.85	
R	Spread	0.0	0.01	0.00	0.02	R = max – min
s	Standard deviation s_{Fs}	0.0	0.007	0.000	0.011	Eq. (3), Eq. (5)
V	Coefficient of variation	0.0%	0.9%	0.0%	1.3%	V = s / mean

Table C-10: Slip factor test results according to EN 1090-2 for A_thR+pP60 test series

Technical characteristics of the test

Steel grade	Austenitic Stainless Steel (1.4404)
Coating	–
Surface treatment	Resin (DELO-DUOPOX® AD897: Multi-purpose 2c epoxy resin) + GRITTAL GH-60 (stainless steel grit, crushed, martensitic with chromium carbides) - (Grain sizes (GH-60): 0.70 – 1.25 mm)
Resin application status	Very thick resin layer on faying surfaces
Particle application status	Surfaces partially covered with particles
Mean coating thickness	–
Surface roughness (before coating)	23 µm
Duration of curing	at least 24 hours
Specimen size	Standard specimens M16 (EN 1090-2, Figure G.1 b)
Bolt class, bolt type	Bolt: BUMAX 109 (EN ISO 4017 – M16 x 100) - Nut: BUMAX 109 (EN ISO 4032) - Washer: HV 300 (EN ISO 7089)
Nominal preload level	110 kN = $F_{p,C}$
Preload measuring method	Load cell (h = 40 mm), measured continuously, clamping length Σt = 75 mm
Test speed	0.6 mm/min

Static test

Specimens mark	plate IDs	Slip (average at CBG) u_i [mm]	Slip load F_{si} [kN]	Preload at start of test (initial preload) Outer bolt $F_{bi,o,ini}$ [kN]	Mean value mean $F_{bi,ini}$ [kN]	Inner bolt $F_{bi,i,ini}$ [kN]	Slip factor based on initial preload $\mu_{i,ini}$ [-]	based on nominal preload $F_{p,C}$ [kN] 110 $\mu_i = \mu_{i,nom}$ [-]	based on preload at slip $\mu_{i,act}$ [-]	Preload at slip Outer bolt $F_{bi,o,act}$ [kN]	Mean value mean $F_{bi,act}$ [kN]	Inner bolt $F_{bi,i,act}$ [kN]	Test duration t [min]	Comment Eq. according to EN 1090-2
A_thR+pP60_01-02	1	0.150	273.2	112.2	111.3	110.5	0.61	0.62	0.66	105.4	103.8	102.1	13.6	
	2	0.150	286.6	110.4	110.5	110.6	0.65	0.65	0.71	103.9	101.4	98.9	14.7	
Statistics (4 specimens, 8 test results)	n = 2	Number of tests												
	max	Maximum	286.6				0.65	0.65	0.71					
	min	Minimum	273.2				0.61	0.62	0.66					
	mean	Mean value F_{sm} | μ_m	279.9				0.63	0.64	0.68					Eq. (2), Eq. (4)
	R	Spread	13.4				0.04	0.03	0.05					R = max – min
	s	Standard deviation s_{Fs}	9.5				0.025	0.022	0.034					Eq. (3), Eq. (5)
	V	Coefficient of variation	3.4%				3.9%	3.4%	5.0%					V = s / mean

Table C-11: Slip factor test results according to EN 1090-2 for D_tR test series

Technical characteristics of the test

Steel grade	Duplex Stainless Steel (1.4462)
Coating	–
Surface treatment	Resin (DELO-DUOPOX® AD897: Multi-purpose 2c epoxy resin)
Resin application status	Very thin glue layer on the faying surfaces
Particle application status	–
Mean coating thickness	26 µm
Surface roughness (before coating)	–
Duration of curing	at least 24 hours
Specimen size	Standard specimens M16 (EN 1090-2, Figure G.1 b)
Bolt class, bolt type	Bolt: BUMAX 109 (EN ISO 4017 – M16 x 100) - Nut: BUMAX 109 (EN ISO 4032) - Washer: HV 300 (EN ISO 7089)
Nominal preload level	110 kN = $F_{p,c}$
Preload measuring method	Load cell (h = 40 mm), measured continuously, clamping length Σt = 75 mm
Test speed	0.6 mm/min

Static test

Specimens mark	plate ID's	Slip (average at CBG) u_i [mm]	Slip load F_{Si} [kN]	Preload at start of test (initial preload) — Outer bolt $F_{bi,o,ini}$ [kN]	mean $F_{bi,ini}$ [kN]	Inner bolt $F_{bi,i,ini}$ [kN]	Slip factor based on initial preload $\mu_{i,ini}$ [-]	based on nominal preload $F_{p,C}$ 110 [kN] $\mu_i = \mu_{i,nom}$ [-]	based on preload at slip $\mu_{i,act}$ [-]	Preload at slip — Outer bolt $F_{bi,o,act}$ [kN]	mean $F_{bi,act}$ [kN]	Inner bolt $F_{bi,i,act}$ [kN]	Test duration t [min]	Comment — Eq. according to EN 1090-2
D_tR_01-02	1	0.046	257.4	110.0	109.8	109.7	0.59	0.59	0.60	108.7	107.9	107.2	14.0	
	2	0.020	257.4	110.0	109.8	109.6	0.59	0.59	0.60	108.2	107.6	107.0	14.0	
D_tR_03-04	3	0.011	298.9	111.5	112.0	112.6	0.67	0.68	0.68	109.6	109.6	109.5	15.1	
	4	0.023	298.9	110.8	110.9	111.0	0.67	0.68	0.69	108.8	108.5	108.2	15.1	
D_tR_05-06	5	0.015	301.2	112.8	112.2	111.7	0.67	0.68	0.69	110.7	109.3	108.0	14.3	
	6	0.001	301.2	111.6	112.2	112.8	0.67	0.68	0.69	109.5	109.6	109.8	14.3	
D_tR_07-08	7	0.016	286.1	111.8	112.1	112.5	0.64	0.65	0.66	109.6	109.1	108.6	14.4	
	8	0.011	286.1	112.2	111.7	111.1	0.64	0.65	0.65	110.3	109.5	108.7	14.4	

Statistics (4 specimens, 8 test results), n = 8

		F_{Si} [kN]	$\mu_{i,ini}$	$\mu_i = \mu_{i,nom}$	$\mu_{i,act}$	Comment
max	Maximum	301.2	0.67	0.68	0.69	
min	Minimum	257.4	0.59	0.59	0.60	
mean	Mean value F_{sm} | μ_m	**285.9**	**0.64**	**0.65**	**0.66**	
R	Spread	43.8	0.09	0.10	0.09	R = max – min
s	Standard deviation s_{Fs}	18.6	0.037	0.042	0.039	Eq. (2), Eq. (4)
V	Coefficient of variation	6.5%	5.8%	6.5%	6.0%	V = s / mean
0,9 F_{sm}		257.3				Load level for the creep test

Additional comment notes: Eq. (3), Eq. (5)

Creep test

Specimens mark	plate ID's	Slip	u_i [mm]	Preload (initial) Outer bolt [kN]	mean [kN]	Inner bolt [kN]	Slip factor $\mu_{i,ini}$	$\mu_{i,nom}$	$\mu_{i,act}$	Preload at slip Outer bolt [kN]	mean [kN]	Inner bolt [kN]	Test duration t [min]	Comment
D_tR_09-10	9	Δ (5 min to 3 h): **4.449**	0.154	111.7	111.7	111.8	–	–	–	109.9	108.8	107.8	24.2	**Creep test failed** — Slip during the creep test
	10	Δ (5 min to 3 h): **4.314**	0.148	112.2	111.8	111.5	–	–	–	110.1	108.6	107.1	23.3	> 0.002 mm (5 min to 3 h)

Comments / Test results

- Creep test failed
- Extended creep test is required

Table C-12: Slip factor test results according to EN 1090-2 for D_tR+fP10 test series

Technical characteristics of the test

- Steel grade: Duplex Stainless Steel (1.4462)
- Coating: –
- Surface treatment: Resin (DELO-DUOPOX® AD897: Multi-purpose 2c epoxy resin) + GRITTAL GH-10 (stainless steel grit, crushed, martensitic with chromium carbides) - (Grain sizes (GH-10): 0.05 – 0.20 mm)
- Resin application status: Very thin resin layer
- Particle application status: Faying surfaces fully covered with particles
- Mean coating thickness: –
- Surface roughness (before coating): 26 µm
- Duration of curing: at least 24 hours
- Specimen size: Standard specimens M16 (EN 1090-2, Figure G.1 b)
- Bolt class, bolt type: Bolt: BUMAX 109 (EN ISO 4017 – M16 x 100) - Nut: BUMAX109 (EN ISO 4032) - Washer: HV 300 (EN ISO 7089)
- Nominal preload level: 110 kN = $F_{p,C}$
- Preload measuring method: Load cell (h = 40 mm), measured continuously, clamping length Σt = 75 mm
- Test speed: 0.6 mm/min

Static test

Specimens mark	plate ID's	Slip (average at CBG) u_i [mm]	Slip load F_{si} [kN]	Preload at start of test (initial preload) Outer bolt $F_{bi,o,ini}$ [kN]	Mean value mean $F_{bi,ini}$ [kN]	Inner bolt $F_{bi,i,ini}$ [kN]	Slip factor based on initial preload $\mu_{i,ini}$ [–]	based on nominal preload $F_{p,C}$ [kN] 110, $\mu_i = \mu_{i,nom}$ [–]	based on preload at slip $\mu_{i,act}$ [–]	Preload at slip Outer bolt $F_{bi,o,act}$ [kN]	Mean value mean $F_{bi,act}$ [kN]	Inner bolt $F_{bi,i,act}$ [kN]	Test duration t [min]	Comment (Eq. according to EN 1090-2)
D_tR+fP10_01-02	1	0.119	218.1	111.7	111.1	110.5	0.49	0.50	0.51	107.5	106.5	105.6	11.7	
	2	0.047	218.1	116.1	114.1	112.1	0.48	0.50	0.49	109.2	110.8	112.4	11.7	
D_tR+fP10_03-04	3	0.039	236.7	112.1	112.4	112.7	0.53	0.54	0.54	109.6	109.6	109.6	11.7	
	4	0.097	236.7	112.2	112.5	112.8	0.53	0.54	0.55	108.8	108.5	108.1	11.7	
D_tR+fP10_05-06	5	0.101	221.1	112.6	112.8	113.1	0.49	0.50	0.51	108.7	109.0	109.3	11.7	
	6	0.077	221.1	112.4	112.9	113.5	0.49	0.50	0.51	109.7	109.0	108.2	11.7	
D_tR+fP10_07-08	7	0.052	213.8	112.3	111.9	111.5	0.48	0.49	0.49	109.2	108.2	107.3	15.8	
	8	0.095	213.0	110.9	112.0	113.1	0.48	0.48	0.49	107.0	108.0	109.0	11.2	

Statistics (4 specimens, 8 test results), $n = 8$

	Number of tests	F_{si} [kN]					$\mu_{i,ini}$ [–]	$\mu_i = \mu_{i,nom}$ [–]	$\mu_{i,act}$ [–]					Comment
max	Maximum	236.7					0.53	0.54	0.55					R = max – min
min	Minimum	213.0					0.48	0.48	0.49					
mean	Mean value F_{sm} | μ_m	222.3					0.49	0.51	0.51					Eq. (2), Eq. (4)
R	Spread	23.7					0.05	0.05	0.05					
s	Standard deviation s_{Fs}	9.3					0.021	0.021	0.021					Eq. (3), Eq. (5)
V	Coefficient of variation	4.2%					4.2%	4.2%	4.1%					V = s / mean
0,9 F_{sm}		200.1												Load level for the creep test

Creep test

Specimens mark	plate ID's	Slip (average at CBG) u_i [mm]	Slip load F_{si} [kN]	$F_{bi,o,ini}$ [kN]	mean $F_{bi,ini}$ [kN]	$F_{bi,i,ini}$ [kN]	$\mu_{i,ini}$	$\mu_{i,nom}$	$\mu_{i,act}$	$F_{bi,o,act}$ [kN]	mean $F_{bi,act}$ [kN]	$F_{bi,i,act}$ [kN]	t [min]	Comment
D_tR+fP10_09-10	9	Δ (5 min to 3 h): 0.048 / 0.085	–	111.6	112.2	112.9	–	–	–	107.4	106.9	106.5	1089.6	**Creep test failed** Slip during the creep test > 0.002 mm (5 min to 3 h)
	10	Δ (5 min to 3 h): 2.277 / 0.150	–	112.4	112.7	113.1	–	–	–	107.7	107.8	107.9	34.4	

Comments

- Creep test failed
- Extended creep test is required

Test results: Creep test failed / Slip during the creep test > 0.002 mm (5 min to 3 h)

Table C-13: Slip factor test results according to EN 1090-2 for D_thR+fP10 test series

Technical characteristics of the test

- Steel grade: Duplex Stainless Steel (1.4462)
- Coating: –
- Surface treatment: Resin (DELO-DUOPOX® AD897: Multi-purpose 2c epoxy resin) + GRITTAL GH-10 (stainless steel grit, crushed, martensitic with chromium carbides) - (Grain sizes (GH-10): 0.05 – 0.20 mm
- Resin application status: Very thick resin layer
- Particle application status: Surfaces fully covered with particles
- Mean coating thickness: –
- Surface roughness (before coating): 26 μm
- Duration of curing: at least 24 hours
- Specimen size: Standard specimens M16 (EN 1090-2, Figure G.1 b)
- Bolt class, bolt type: Bolt: BUMAX 109 (EN ISO 4017 – M16 x 100) - Nut: BUMAX 109 (EN ISO 4032) - Washer: HV 300 (EN ISO 7089)
- Nominal preload level: 110 kN = $F_{p,C}$
- Preload measuring method: Load cell (h = 40 mm), measured continuously, clamping length Σt = 75 mm
- Test speed: 0.6 mm/min

Static test

Specimens mark	plate IDs	Slip (average at CBG) u_i [mm]	Slip load F_{Si} [kN]	Preload at start of test (initial preload) Outer bolt $F_{bi,o,ini}$ [kN]	Mean value mean $F_{bi,ini}$ [kN]	Inner bolt $F_{bi,i,ini}$ [kN]	Slip factor based on initial preload $\mu_{i,ini}$ [-]	based on nominal preload $F_{p,C}$ [kN] 110 $\mu_i = \mu_{i,nom}$ [-]	based on preload at slip $\mu_{i,act}$ [-]	Preload at slip Outer bolt $F_{bi,o,act}$ [kN]	Mean value mean $F_{bi,act}$ [kN]	Inner bolt $F_{bi,i,act}$ [kN]	Test duration t [min]	Comment
D_thR+fP10_01-02	1	0.056	389.9	112.0	111.7	111.4	0.87	0.89	0.90	109.3	108.1	106.9	17.3	
	2	0.039	389.9	111.9	112.0	112.2	0.87	0.89	0.89	109.4	109.1	108.8	17.3	
D_thR+fP10_03-04	3	0.060	395.8	111.1	111.5	112.0	0.89	0.90	0.91	108.4	108.3	108.2	17.0	
	4	0.045	395.8	111.3	110.1	108.9	0.90	0.90	0.92	108.9	107.2	105.5	17.0	
D_thR+fP10_05-06	5	0.057	407.4	109.4	110.4	111.3	0.92	0.93	0.95	107.1	106.7	106.3	16.5	
	6	0.065	407.4	110.5	110.1	109.7	0.92	0.93	0.95	108.2	107.3	106.5	16.5	
D_thR+fP10_07-08	7	0.048	351.6	111.0	110.5	110.0	0.80	0.80	0.82	108.8	107.1	105.5	18.4	
	8	0.078	330.3	110.4	110.4	110.3	0.75	0.75	0.76	108.4	108.1	107.8	15.1	

Statistics (4 specimens, 8 test results), n = 8

	Number of tests	F_{Si}					$\mu_{i,ini}$	$\mu_i = \mu_{i,nom}$	$\mu_{i,act}$					Comment
max	Maximum	407.4					0.92	0.93	0.95					$R = max - min$
min	Minimum	330.3					0.75	0.75	0.76					
mean	Mean value F_{Sm} | μ_m	383.5					0.87	0.87	0.89					
R	Spread	77.0					0.18	0.18	0.19					Eq. (2), Eq. (4)
s	Standard deviation s_{Fs}	27.7					0.062	0.063	0.066					Eq. (3), Eq. (5)
V	Coefficient of variation	7.2%					7.2%	7.2%	7.4%					$V = s / mean$
	0.9 F_{Sm}	345.2												

Creep test

Specimens mark		Δ (5 min to 3 h)		$F_{bi,o,ini}$	mean $F_{bi,ini}$	$F_{bi,i,ini}$				$F_{bi,o,act}$	mean $F_{bi,act}$	$F_{bi,i,act}$	t [min]	Comment
D_thR+fP10_09-10	9	0.979	0.150	109.7	110.1	110.6	–	–	–	108.1	108.5	108.8	27.9	**Creep test failed** Slip during the creep test > 0.002 mm (5 min to 3 h)
	10	1.152	0.150	110.8	110.0	109.2	–	–	–	107.9	105.3	102.8	29.3	Load level for the creep test

Comments / Test results

- Creep test failed
- Extended creep test is required

Table C-14: Slip factor test results according to EN 1090-2 for D_thR+fP102030 test series

Technical characteristics of the test

Steel grade	Duplex Stainless Steel (1.4462)
Coating	–
Surface treatment	Resin (DELO-DUOPOX® AD897: Multi-purpose 2c epoxy resin) + GRITTAL GH-10+20+30 (stainless steel grit, crushed, martensitic with chromium carbides) - (Grain sizes (GH-10+20+30): 0.05 – 0.50 mm)
Resin application status	Very thin Resin layer
Particle application status	Surfaces partially covered with particles
Mean coating thickness	–
Surface roughness (before coating)	26 µm
Duration of curing	at least 24 hours
Specimen size	Standard specimens M16 (EN 1090-2, Figure G.1 b)
Bolt class, bolt type	Bolt: BUMAX109 (EN ISO 4017 – M16 x 100) - Nut: BUMAX 109 (EN ISO 4032) - Washer: HV 300 (EN ISO 7089)
Nominal preload level	110 kN = $F_{p,C}$
Preload measuring method	Load cell (h = 40 mm), measured continuously, clamping length $\Sigma t = 75$ mm
Test speed	0.6 mm/min

Static test

Specimens mark	plate IDs	Slip (average at CBG) u_l [mm]	Slip load F_{sl} [kN]	Preload at start of test (initial preload) Outer bolt $F_{bi,o,ini}$ [kN]	Mean value mean $F_{bi,ini}$ [kN]	Inner bolt $F_{bi,i,ini}$ [kN]	Slip factor based on initial preload $\mu_{i,ini}$ [-]	based on nominal preload $F_{p,C}$ [kN] 110 $\mu_i = \mu_{i,nom}$ [-]	based on preload at slip $\mu_{i,act}$ [-]	Preload at slip Outer bolt $F_{bi,o,act}$ [kN]	Mean value mean $F_{bi,act}$ [kN]	Inner bolt $F_{bi,i,act}$ [kN]	Test duration t [min]	Comment Eq. according to EN 1090-2
D_thR+fP102030_01-02	1	0.116	348.6	112.4	111.8	111.2	0.78	0.79	0.86	102.6	101.9	101.2	17.1	
	2	0.150	323.7	111.6	112.3	113.1	0.72	0.74	0.75	108.9	108.2	107.5	14.8	

Statistics (4 specimens, 8 test results) n = 2

		Slip load F_{sl} [kN]	$\mu_{i,ini}$ [-]	$\mu_i = \mu_{i,nom}$ [-]	$\mu_{i,act}$ [-]	Comment
max	Maximum	348.6	0.78	0.79	0.86	Eq. (2), Eq. (4)
min	Minimum	323.7	0.72	0.74	0.75	R = max – min
mean	Mean value F_{sm} | μ_m	336.1	0.75	0.76	0.80	Eq. (3), Eq. (5)
R	Spread	24.9	0.06	0.06	0.11	V = s / mean
s	Standard deviation s_{Fs}	17.6	0.042	0.040	0.076	
V	Coefficient of variation	5.2%	5.6%	5.2%	9.4%	

Table C-15: Slip factor test results according to EN 1090-2 for D_thhR test series

Technical characteristics of the test

Steel grade	Duplex Stainless Steel (1.4462)
Coating	–
Surface treatment	Resin (DELO-DUOPOX® AD897: Multi-purpose 2c epoxy resin)
Resin application status	Very thick resin layer around the holes
Particle application status	–
Mean coating thickness	–
Surface roughness (before coating)	26 µm
Duration of curing	at least 24 hours
Specimen size	Standard specimens M16 (EN 1090-2, Figure G.1 b)
Bolt class, bolt type	Bolt: BUMAX 109 (EN ISO 4017 – M16 x 100) - Nut: BUMAX 109 (EN ISO 4032) - Washer: HV 300 (EN ISO 7089)
Nominal preload level	110 kN = $F_{p,C}$
Preload measuring method	Load cell (h = 40 mm), measured continuously, clamping length Σt = 75 mm
Test speed	0.6 mm/min

Static test

Specimens mark	plate ID's	Slip (average at CBG) u_i [mm]	Slip load F_{Si} [kN]	Preload at start of test (initial preload) Outer bolt $F_{bi,o,ini}$ [kN]	Mean value mean $F_{bi,ini}$ [kN]	Inner bolt $F_{bi,i,ini}$ [kN]	Slip factor based on initial preload $\mu_{i,ini}$ [-]	based on nominal preload $F_{p,C}$ [kN] 110 $\mu_i = \mu_{i,nom}$ [-]	based on preload at slip $\mu_{i,act}$ [-]	Preload at slip Outer bolt $F_{bi,o,act}$ [kN]	Mean value mean $F_{bi,act}$ [kN]	Inner bolt $F_{bi,i,act}$ [kN]	Test duration t [min]	Comment Eq. according to EN 1090-2
D_thhR_01-02	1	0.009	309.7	110.7	110.6	110.6	0.70	0.70	0.71	109.3	109.2	109.2	14.6	
	2	0.011	309.7	109.7	109.7	109.6	0.71	0.70	0.72	108.3	108.2	108.1	14.6	
D_thhR_03-04	3	0.008	297.2	114.3	112.8	111.4	0.66	0.68	0.66	112.7	112.0	111.2	14.1	
	4	0.008	297.2	110.3	111.2	112.1	0.67	0.68	0.68	108.7	108.7	108.7	14.1	
D_thhR_09-10	9	0.020	318.4	111.4	111.2	111.0	0.72	0.72	0.72	109.5	109.9	110.2	14.6	
	10	0.006	318.4	109.5	111.2	113.0	0.72	0.72	0.72	108.2	110.2	112.2	14.6	
D_thhR_11-12	11	0.001	300.3	111.4	110.9	110.4	0.68	0.68	0.69	109.3	108.7	108.1	14.4	
	12	0.023	300.3	110.1	109.6	109.0	0.69	0.68	0.70	108.0	107.7	107.5	14.4	

Statistics (4 specimens, 8 test results)   n = 8

Statistic	F_{Si} [kN]	$\mu_{i,ini}$ [-]	$\mu_i = \mu_{i,nom}$ [-]	$\mu_{i,act}$ [-]	Comment
max Maximum	318.4	0.72	0.72	0.72	Eq. (2), Eq. (4)
min Minimum	297.2	0.66	0.68	0.66	R = max – min
mean Mean value F_{Sm} | μ_m	306.4	0.69	0.70	0.70	Eq. (3), Eq. (5)
R Spread	21.2	0.06	0.05	0.06	
s Standard deviation s_{Fs}	8.9	0.022	0.020	0.021	V = s / mean
V Coefficient of variation	2.9%	3.2%	2.9%	3.0%	
0.9 F_{Sm}	275.8				Load level for the creep test

Creep test

Specimens mark	plate ID's	Slip (average at CBG) u_i [mm]	Slip load F_{Si} [kN]	Preload at start of test Outer bolt [kN]	Mean value [kN]	Inner bolt [kN]	Slip factor based on initial preload	based on nominal preload	based on preload at slip	Preload at slip Outer bolt [kN]	Mean value [kN]	Inner bolt [kN]	Test duration t [min]	Comment
D_thhR_13-14	13	Δ (5 min to 3 h): - 0.150	–	107.4	111.1	114.8	–	–	–	106.7	110.7	114.8	17.6	Creep test failed; Slip during the creep test > 0.002 mm (5 min to 3 h)
	14	Δ (5 min to 3 h): - 0.149	–	111.6	111.0	110.4	–	–	–	108.4	111.6	114.8	16.6	

Comments
- Creep test failed
- Extended creep test is required

Extended creep test results
- First extended creep test: 0.70·F_{Sm} = 214.5 kN ⟹ test is failed
- Second extended creep test: 0.65·F_{Sm} = 199.2 kN ⟹ test is passed ⟹ μ_{final} = 0.45

Table C-16: Slip factor test results according to EN 1090-2 for D_thhR+fP10 test series

Technical characteristics of the test

- Steel grade: Duplex Stainless Steel (1.4462)
- Coating: –
- Surface treatment: Resin (DELO-DUOPOX® AD897: Multi-purpose 2c epoxy resin) + GRITTAL GH-10 (stainless steel grit, crushed, martensitic with chromium carbides) - (Grain sizes (GH-10): 0.05 – 0.20 mm)
- Resin application status: Very thick resin layer around the holes
- Particle application status: Resin surfaces fully covered with particles
- Mean coating thickness: –
- Surface roughness (before coating): 26 µm
- Duration of curing: at least 24 hours
- Specimen size: Standard specimens M16 (EN 1090-2, Figure G.1 b)
- Bolt class, bolt type: Bolt: BUMAX 109 (EN ISO 4017 – M16 x 100) - Nut: BUMAX 109 (EN ISO 4032) - Washer: HV 300 (EN ISO 7089)
- Nominal preload level: 110 kN = $F_{p,C}$
- Preload measuring method: Load cell (h = 40 mm), measured continuously, clamping length Σt = 75 mm
- Test speed: 0.6 mm/min

Static test

Specimens mark	plate ID's	Slip (average at CBG) u_i [mm]	Slip load F_{si} [kN]	Preload at start of test (initial preload) Outer bolt $F_{bl,o,ini}$ [kN]	mean $F_{bo,ini}$ [kN]	Inner bolt $F_{bi,ini}$ [kN]	Slip factor based on initial preload $\mu_{i,ini}$ [-]	based on nominal preload $F_{p,C}$ [kN] 110 $\mu_i = \mu_{i,nom}$ [-]	based on preload at slip $\mu_{i,act}$ [-]	Preload at slip Outer bolt $F_{bi,o,act}$ [kN]	Mean value mean $F_{bl,act}$ [kN]	Inner bolt $F_{bi,act}$ [kN]	Test duration t [min]	Comment (Eq. according to EN 1090-2)
D_thhR+fP10_01-02	1	0.099	378.1	114.5	112.7	110.9	0.84	0.86	0.86	111.4	109.9	108.3	17.3	
	2	0.048	378.1	111.7	113.2	114.8	0.83	0.86	0.85	109.6	110.8	112.0	17.3	
D_thhR+fP10_03-04	3	0.055	379.5	112.3	112.2	112.1	0.85	0.86	0.86	110.3	110.7	111.1	16.7	
	4	0.062	379.5	113.7	113.2	112.6	0.84	0.86	0.86	111.9	110.8	109.8	16.7	
D_thhR+fP10_05-06	5	0.036	373.6	109.2	109.4	109.6	0.85	0.85	0.88	107.3	106.3	105.3	16.6	
	6	0.068	373.6	112.1	111.7	111.3	0.84	0.85	0.86	110.2	108.6	106.9	16.6	
D_thhR+fP10_07-08	7	0.048	389.7	113.9	112.5	111.0	0.87	0.89	0.89	111.6	109.0	106.3	17.4	
	8	0.043	389.7	111.8	111.7	111.6	0.87	0.89	0.89	110.0	109.8	109.6	17.4	

Statistics (4 specimens, 8 test results), $n = 8$

		Slip load F_{si} [kN]	$\mu_{i,ini}$ [-]	$\mu_i = \mu_{i,nom}$ [-]	$\mu_{i,act}$ [-]	Comment
max	Maximum	389.7	0.87	0.89	0.89	
min	Minimum	373.6	0.83	0.85	0.85	
mean	Mean value F_{Sm} / μ_m	**380.2**	0.85	**0.86**	**0.87**	
R	Spread	16.1	0.04	0.04	0.04	$R = max - min$
s	Standard deviation s_{Fs}	6.3	0.014	0.014	0.016	Eq. (3), Eq. (5)
V	Coefficient of variation	1.7%	1.7%	1.7%	1.8%	$V = s / mean$
$0.9 \cdot F_{Sm}$		342.2				Load level for the creep test

Eq. (2), Eq. (4)

Creep test

Specimens mark	plate ID's	Slip (average at CBG) Δ (5 min to 3 h) [mm]	Slip load F_{si} [kN]	Preload at start Outer bolt $F_{bl,o,ini}$ [kN]	mean $F_{bo,ini}$ [kN]	Inner bolt $F_{bi,ini}$ [kN]	$\mu_{i,ini}$	$\mu_{i,nom}$	$\mu_{i,act}$	Preload at slip Outer bolt [kN]	Mean value [kN]	Inner bolt [kN]	t [min]	Comment
D_thhR+fP10_09-10	9	1.285 / 0.150	–	113.1	111.8	110.6	–	–	–	110.9	109.7	108.5	25.0	Creep test failed. Slip during the creep test > 0.002 mm (5 min to 3 h)
	10	1.171 / 0.149	–	111.4	111.3	111.2	–	–	–	110.0	109.7	109.4	25.1	

Comments:
- Creep test failed
- Extended creep test is required

Extended creep test results
- First extended creep test: 0.80·F_{Sm} = 304.2 kN ⇒ test is failed
- Second extended creep test: 0.75·F_{Sm} = 285.2 kN ⇒ test is passed ⇒ μ_{final} = 0.65
- Third extended creep test: 0.70·F_{Sm} = 266.1 kN ⇒ test is passed

Table C-17: Slip factor test results according to EN 1090-2 for D_thhR+fmP10 test series

Technical characteristics of the test

Steel grade	Duplex Stainless Steel (1.4462)
Coating	–
Surface treatment	Resin (DELO-DUOPOX® AD897: Multi-purpose 2c epoxy resin) + GRITTAL GH-10 (stainless steel grit, crushed, martensitic with chromium carbides) - (Grain sizes (GH-10): 0.05 – 0.20 mm)
Resin application status	Very thick resin layer (mixed with particle - mix ratio: 1) 100gr resin+100gr particles
Particle application status	Mixed with resin
Mean coating thickness	–
Surface roughness (before coating)	26 µm
Duration of curing	at least 24 hours
Specimen size	Standard specimens M16 (EN 1090-2, Figure G.1 b)
Bolt class, bolt type	Bolt: BUMAX109 (EN ISO 4017 – M16 x 100) - Nut: BUMAX 109 (EN ISO 4032) - Washer: HV 300 (EN ISO 7089)
Nominal preload level	110 kN = $F_{p,C}$
Preload measuring method	Load cell (h = 40 mm), measured continuously, clamping length Σt = 75 mm
Test speed	0.6 mm/min

Static test

Specimens mark	plate ID's	Slip (average at CBG) u_i [mm]	Slip load F_{si} [kN]	Preload at start of test (initial preload) — Outer bolt $F_{bi,o,ini}$ [kN]	Inner bolt $F_{bi,i,ini}$ [kN]	Mean value mean $F_{bi,ini}$ [kN]	Slip factor based on initial preload $\mu_{i,ini}$ [-]	based on nominal preload $F_{p,C}$ [kN] 110, $\mu_i = \mu_{i,nom}$ [-]	based on preload at slip $\mu_{i,act}$ [-]	Preload at slip — Outer bolt $F_{bi,o,act}$ [kN]	Inner bolt $F_{bi,i,act}$ [kN]	Mean value mean $F_{bi,act}$ [kN]	Test duration t [min]	Comment (Eq. according to EN 1090-2)
D_thhR+fmP10_01-02	1	0.030	387.4	108.6	111.3	109.9	0.88	0.88	0.89	107.4	111.4	109.4	16.5	
	2	0.038	387.4	109.0	111.9	110.4	0.88	0.88	0.88	108.1	110.8	109.5	16.5	

Statistics (4 specimens, 8 test results)		F_{si} [kN]		$\mu_{i,ini}$ [-]	$\mu_i = \mu_{i,nom}$ [-]	$\mu_{i,act}$ [-]	Comment
$n = 2$	Number of tests						
max	Maximum	387.4		0.88	0.88	0.89	Eq. (2), Eq. (4)
min	Minimum	387.4		0.88	0.88	0.88	R = max – min
mean	Mean value F_{sm} | μ_m	387.4		0.88	0.88	0.88	Eq. (3), Eq. (5)
R	Spread	0.0		0.00	0.00	0.00	V = s / mean
s	Standard deviation s_{Fs}	0.0		0.003	0.000	0.000	
V	Coefficient of variation	0.0%		0.3%	0.0%	0.1%	

Table C-18: Slip factor test results according to EN 1090-2 for D_thhR+fP10_B88 test series

Technical characteristics of the test

Steel grade	Duplex Stainless Steel (1.4462)
Coating	–
Surface treatment	Resin (DELO-DUOPOX® AD897: Multi-purpose 2c epoxy resin) + GRITTAL GH-10 (stainless steel grit, crushed, martensitic with chromium carbides) - (Grain sizes (GH-10): 0.05 – 0.20 mm)
Resin application status	Very thick resin layer around the holes
Particle application status	Resin surfaces fully covered with particles
Mean coating thickness	–
Surface roughness (before coating)	26 µm
Duration of curing	at least 24 hours
Specimen size	Standard specimens M16 (EN 1090-2, Figure G.1 b)
Bolt class, bolt type	Bolt: BUMAX88 (EN ISO 4017 – M16 x 100) - Nut: BUMAX88 (EN ISO 4032) - Washer: HV 200 (EN ISO 7089)
Nominal preload level	88 kN = $F_{p,C}$
Preload measuring method	Load cell (h = 40 mm), measured continuously, clamping length Σt = 75 mm
Test speed	0.6 mm/min

Static test

Specimens mark	plate ID's	Slip (average at CBG) u_i [mm]	Slip load F_{si} [kN]	Preload at start of test (initial preload) Outer bolt $F_{bi,o,ini}$ [kN]	mean $F_{bi,ini}$ [kN]	$F_{bi,i,ini}$ [kN]	Slip factor based on initial preload $\mu_{i,ini}$ [-]	based on nominal preload $F_{p,C}$=88 $\mu_i=\mu_{i,nom}$ [-]	based on preload at slip $\mu_{i,act}$ [-]	Preload at slip Outer bolt $F_{bi,o,act}$ [kN]	mean $F_{bi,act}$ [kN]	Inner bolt $F_{bi,i,act}$ [kN]	Test duration t [min]	Comment
D_1D+fcG+fP10GH_88_01-02	1	0.085	364.0	86.4	87.3	88.3	1.04	1.03	1.08	83.5	84.4	85.4	19.6	Eq. according to EN 1090-2
	2	0.010	364.0	87.9	88.3	88.7	1.03	1.03	1.00	86.6	90.7	94.8	19.6	
D_1D+fcG+fP10GH_88_03-04	3	0.039	368.6	88.3	88.5	88.7	1.04	1.05	1.07	86.0	86.0	85.9	16.7	
	4	0.059	368.6	90.8	90.0	89.2	1.02	1.05	1.05	89.3	88.2	87.1	16.7	
D_1D+fcG+fP10GH_88_05-06	5	0.047	369.7	86.7	86.9	87.1	1.06	1.05	1.09	85.2	84.9	84.5	16.6	
	6	0.067	369.7	89.1	90.0	90.9	1.03	1.05	1.05	87.3	87.8	88.2	16.6	
D_1D+fcG+fP10GH_88_07-08	7	0.026	356.3	88.6	88.4	88.1	1.01	1.01	1.03	86.8	86.7	86.6	15.8	
	8	0.056	356.3	89.8	89.6	89.4	0.99	1.01	1.01	88.6	88.0	87.5	15.8	

Statistics (4 specimens, 8 test results) — n = 8

		F_{si} [kN]	$\mu_{i,ini}$	$\mu_i=\mu_{i,nom}$	$\mu_{i,act}$	Comment
Number of tests	n = 8					
Maximum	max	369.7	1.06	1.05	1.09	
Minimum	min	356.3	0.99	1.01	1.00	
Mean value F_{Sm} | μ_m	mean	364.6	1.03	1.04	1.05	
Spread	R	13.4	0.07	0.04	0.09	R = max – min
Standard deviation s_{Fs}	s	5.6	0.021	0.016	0.031	Eq. (3), Eq. (5)
Coefficient of variation	V	1.5%	2.1%	1.5%	3.0%	V = s / mean
0.9 F_{Sm}		**328.2**				

Eq. (2), Eq. (4)
R = max – min

Creep test

Specimens mark	plate ID's	Slip u_i [mm]	Slip load F_{si} [kN]	Preload at start Outer bolt $F_{bi,o,ini}$	mean $F_{bi,ini}$	$F_{bi,i,ini}$	Preload at slip Outer bolt $F_{bi,o,act}$	mean $F_{bi,act}$	Inner bolt $F_{bi,i,act}$	t [min]	Comment
D_1D+fcG+fP10GH_88_13-14	13	Δ (5 min to 3 h): - / 0.150	–	87.8	88.0	88.2	85.2	84.6	84.0	20.7	Load level for the creep test
	14	Δ (5 min to 3 h): - / 0.150	–	89.1	88.3	87.4	87.7	86.1	84.5	20.6	**Creep test failed** Slip during the creep test > 0.002 mm (5 min to 3 h)

Comments
- Creep test failed
- Extended creep test is required

Extended creep test results
- First extended creep test: 0.80·F_{Sm} = 291.7 kN ⇒ test is failed
- Second extended creep test: 0.75·F_{Sm} = 273.45 kN ⇒ test is failed
- Third extended creep test: 0.70·F_{Sm} = 255.22 kN ⇒ test is passed ⇒ μ_{final} = 0.73

Annex D: Slip factor test evaluation tables (Carbon steel)

test results according to EN 1090-2, Simplified EN1090-2 and RCSC for ASI and GB
test specimens made of carbon steel

Table D-1: Slip factor test results according to EN 1090-2 for EN1090_CS_ASI test series

Technical characteristics of the test

Steel grade	Structural Steel EN 10025-2 – S355
Coating	Alkali-zinc silicate (ASI), Inorganic Zinc Silicate (Interzinc® 697)
Surface treatment	Grit blasted (with Brown Corundum, f20, Al_2O_3 (Aluminiumoxid))
Mean coating thickness	104 µm
Surface roughness (before coating)	75 µm
Specimen size	Standard specimens M16 (EN 1090-2, Figure G.1 b)
Bolt class, bolt type	10.9 (Set EN 14399-4 – HV – M16 x 90 – 10.9/10 – tZn)
Nominal preload level	110 kN = $F_{p,C}$
Preload measuring method	implanted SG, measured continuously, clamping length $\Sigma t = 40$ mm
Test speed	0.01 mm/s

Static test

Specimens mark	plate IDs	Slip (average at CBG) u_i [mm]	Slip load F_{Si} [kN]	Preload at start of test (initial preload) Outer bolt $F_{bi,o,ini}$ [kN]	Inner bolt $F_{bi,i,ini}$ [kN]	Mean value mean $F_{bi,ini}$ [kN]	Slip factor based on initial preload $\mu_{i,ini}$ [-]	based on nominal preload $F_{p,C}$=110 $\mu_i=\mu_{i,nom}$ [-]	based on preload at slip $\mu_{i,act}$ [-]	Preload at slip Outer bolt $F_{bi,o,act}$ [kN]	Mean value mean $F_{bi,act}$ [kN]	Inner bolt $F_{bi,i,act}$ [kN]	Test duration t [min]	Comment Eq. according to EN 1090-2
EN 1090_CS_ASI_01-02	1	0.146	312.5	111.2	112.4	111.8	0.70	0.71	0.83	95.2	94.1	93.1	14.6	
	2	0.150	305.7	112.7	110.2	111.4	0.69	0.69	0.81	95.7	93.8	92.0	14.0	
EN 1090_CS_ASI_03-04	3	0.150	307.7	109.3	111.7	110.5	0.70	0.70	0.83	92.5	92.3	92.1	13.7	
	4	0.150	311.0	111.5	109.7	110.6	0.70	0.71	0.83	96.2	93.1	90.1	13.8	
EN 1090_CS_ASI_05-06	5	0.150	303.8	114.6	112.7	113.7	0.67	0.69	0.80	96.7	94.5	92.3	13.8	
	6	0.150	307.0	113.8	113.7	113.8	0.67	0.70	0.81	95.7	94.4	93.2	14.0	
EN 1090_CS_ASI_07-08	7	0.150	300.4	109.8	108.2	109.0	0.69	0.68	0.82	94.0	91.4	88.9	13.9	
	8	0.150	291.9	110.1	108.4	109.2	0.67	0.66	0.81	92.8	90.4	88.0	13.3	

Statistics (4 specimens, 8 test results) — n = 8 Number of tests

	F_{Si} [kN]			$\mu_{i,ini}$ [-]	$\mu_i=\mu_{i,nom}$ [-]	$\mu_{i,act}$ [-]				Comment
max Maximum	312.5			0.70	0.71	0.83				
min Minimum	291.9			0.67	0.66	0.80				
mean Mean value $F_{Sm}\mid\mu_m$	**305.0**			**0.69**	**0.69**	**0.82**				Eq. (2), Eq. (4)
R Spread	20.7			0.04	0.05	0.03				R = max − min
s Standard deviation s_{Fs}	6.5			0.014	0.015	0.012				Eq. (3), Eq. (5)
V Coefficient of variation	2.1%			2.0%	2.1%	1.5%				V = s / mean
0.9 F_{Sm}	274.5									Load level for the creep test

Creep test

Specimens mark	plate IDs	Δ (5 min to 3 h)	Slip load F_{Si} [kN]	$F_{bi,o,ini}$ [kN]	$F_{bi,i,ini}$ [kN]	mean $F_{bi,ini}$ [kN]	$\mu_{i,ini}$ [-]	$\mu_i=\mu_{i,nom}$ [-]	$\mu_{i,act}$ [-]	$F_{bi,o,act}$ [kN]	mean $F_{bi,act}$ [kN]	$F_{bi,i,act}$ [kN]	t [min]	Comment
EN 1090_CS_ASI_11-12	11	Δ (5 min to 3 h): **0,079**	–	113.2	110.3	111.7	–	–	–	92.3	88.9	85.6	310.1	**Creep test failed** Slip during the creep test > 0,002 mm (5 min to 3 h)
	12	Δ (5 min to 3 h): **0,095**	–	111.4	109.8	110.6	–	–	–	91.2	88.5	85.9	64.9	

Statistics (5 specimens, 10 test results) — n = 10 Number of tests

	F_{Si} [kN]			$\mu_{i,ini}$ [-]	$\mu_i=\mu_{i,nom}$ [-]	$\mu_{i,act}$ [-]				Comment
max Maximum	312.5			0.70	0.71	0.83				
min Minimum	291.9			0.67	0.66	0.80				
mean Mean value $F_{Sm}\mid\mu_m$	305.0			0.69	0.69	0.82				Eq. (2), Eq. (4)
R Spread	20.7			0.04	0.05	0.03				R = max − min
s Standard deviation s_{Fs}	6.5			0.014	0.015	0.012				Eq. (3), Eq. (5)
V Coefficient of variation	**2.1%**			**2.0%**	**2.1%**	**1.5%**				V = s / mean ≤ 8%
0.9 F_{Sm}	274.5									
μ_k Characteristic value of the slip factor	274.5			0.66	0.66	0.80				Eq. (6)

Comments
- Creep test failed
- Extended creep test is required

Extended creep test results
- First extended creep test: $0.90 \cdot F_{Sm} = 274.5$ kN $\Rightarrow$ test is passed $\Rightarrow \mu_{final} = 0.62$
- Second extended creep test: $0.90 \cdot F_{Sm} = 274.5$ kN $\Rightarrow$ test is passed $\Rightarrow \mu_{final} = 0.62$
- Third extended creep test: $0.90 \cdot F_{Sm} = 274.5$ kN $\Rightarrow$ test is passed $\Rightarrow \mu_{final} = 0.62$

Table D-2: Slip factor test results according to simplified EN 1090-2 for S_M16_EN1090_ASI_d test series

Technical characteristics of the test

Steel grade	Structural Steel EN 10025-2 – S355
Coating	Alkali-zinc silicate (ASI), Inorganic Zinc Silicate (Interzinc® 697)
Surface treatment	Grit blasted (with Brown Corundum, ≠20, Al_2O_3 (Aluminiumoxid))
Mean coating thickness	104 µm
Surface roughness (before coating)	75 µm
Specimen size	Modified specimens M16 (based on EN 1090-2:2018 and RCSC 2014)
Bolt class, bolt type	10.9 (Set EN 14399-4 – HV – M16 x 90 – 10.9/10 – tZn)
Nominal preload level	110 kN = $F_{p,C}$
Preload measuring method	Implanted SG, measured continuously, clamping length Σt = 40 mm
Test speed	0.002 mm/s

Static test

Specimens mark	plate ID's	Slip (average at CB) u_i [mm]	Slip load F_{si} [kN]	Preload at beginning of the test $F_{bi,ini}$ [kN]	Slip factor based on initial preload $\mu_{i,ini}$ [-]	Slip factor based on nominal preload $F_{p,C}$ [kN] 110, $\mu_i = \mu_{i,nom}$ [-]	Slip factor based on preload at slip $\mu_{i,act}$ [-]	Preload at slip mean $F_{bi,act}$ [kN]	Test duration t [min]	Comment Eq. according to EN 1090-2
S_M16_EN1090_ASI_d_05	5	0.150	148.0	111.1	0.67	0.67	0.73	101.8	5.0	
S_M16_EN1090_ASI_d_04	4	0.150	150.7	111.9	0.67	0.68	0.78	96.2	10.9	
S_M16_EN1090_ASI_d_03	3	0.150	151.0	111.5	0.68	0.69	0.76	99.5	7.4	
S_M16_EN1090_ASI_d_02	2	0.150	156.1	111.9	0.70	0.71	0.83	94.0	15.6	

Statistics (4 specimens, 4 test results), n = 8

max Maximum	156.1	0.70	0.71	0.83
min Minimum	148.0	0.67	0.67	0.73
mean Mean value F_{sm} | μ_m	151.5	0.68	0.69	0.77
R Spread	8.1	0.03	0.04	0.10
s Standard deviation s_{Fs}	3.4	0.014	0.015	0.044
V Coefficient of variation	2.2%	2.0%	2.2%	5.6%
0.9 F_{sm}	136.3			

Statistics comment: Eq. (2), Eq. (4); R = max – min; Eq. (3), Eq. (5); V = s / mean; Load level for the creep test

Creep test

Specimens mark	plate ID's	Δ (5 min to 3 h): 0,14	Slip (average at CB) u_i [mm]	Slip load F_{si} [kN]	Preload at beginning of the test $F_{bi,ini}$ [kN]	$\mu_{i,ini}$	$\mu_i = \mu_{i,nom}$	$\mu_{i,act}$	Preload at slip mean $F_{bi,act}$ [kN]	Test duration t [min]	Comment
S_M16_EN1090_ASI_d_06	6		0.150	–	108.7	–	–	–	92.0	13.7	**Creep test failed** Slip during the creep test > 0,002 mm (5 min to 3 h)

Statistics (5 specimens, 5 test results), n = 10

max Maximum	156.1	0.70	0.71	0.83
min Minimum	148.0	0.67	0.67	0.73
mean Mean value F_{sm} | μ_m	151.5	0.68	0.69	0.77
R Spread	8.1	0.03	0.04	0.10
s Standard deviation s_{Fs}	3.4	0.014	0.015	0.044
V Coefficient of variation	2.2%	2.0%	2.2%	5.6%
0.9 F_{sm}	136.3			

Creep statistics comment: Eq. (2), Eq. (4); R = max – min; Eq. (3), Eq. (5); V = s / mean ≤ 8%

Characteristic value of the slip factor μ_k: – 0.65 / 0.66 / 0.69 — Eq. (6)

Comments / Test results
- Creep test failed
- Three extended creep tests as a chain: 0.85·F_{Sm} = 128.8 kN ⟹ test is passed ⟹ μ_{final} = 0.59

Table D-3: Slip factor test results according to simplified EN 1090-2 for S_M16_EN1090_ASI_I test series

Technical characteristics of the test

Steel grade	Structural Steel EN 10025-2 – S355
Coating	Alkali-zinc silicate (ASI), Inorganic Zinc Silicate (Interzinc® 697)
Surface treatment	Grit blasted (with Brown Corundum, f20, Al_2O_3 (Aluminiumoxid))
Mean coating thickness	104 µm
Surface roughness (before coating)	75 µm
Specimen size	Modified specimens M16 (based on EN 1090-2:2018 and RCSC 2014)
Bolt class, bolt type	10.9 (Set EN 14399-4 – HV – M16 x 90 – 10.9/10 – tZn)
Nominal preload level	110 kN = $F_{p,C}$
Preload measuring method	Implanted SG, measured continuously, clamping length $\Sigma t = 40$ mm
Test speed	200 N/s

Static test

Specimens mark	plate ID's	Slip (average at CB) u_i [mm]	Slip load F_{si} [kN]	Preload at beginning of the test $F_{bi,ini}$ [kN]	Slip factor based on initial preload $\mu_{i,ini}$ [-]	based on nominal preload $F_{p,C}$ [kN] 110 $\mu_i = \mu_{i,nom}$ [-]	based on preload at slip $\mu_{i,act}$ [-]	Preload at slip mean $F_{bi,act}$ [kN]	Test duration t [min]	Comment Eq. according to EN 1090-2
S_M16_EN1090_ASI_I_01	1	0.150	151.0	112.2	0.67	0.69	0.74	102.1	12.6	

Table D-4: Slip factor test results according to simplified EN 1090-2 for S_M20_EN1090_ASI_d test series

Technical characteristics of the test

Steel grade	Structural Steel EN 10025-2 – S355
Coating	Alkali-zinc silicate (ASI), Inorganic Zinc Silicate (Interzinc® 697)
Surface treatment	Grit blasted (with Brown Corundum, f20, Al₂O₃ (Aluminiumoxid))
Mean coating thickness	104 µm
Surface roughness (before coating)	75 µm
Specimen size	Modified specimens M20 (based on EN 1090-2:2018 and RCSC 2014)
Bolt class, bolt type	10.9 (Set EN 14399-4 – HV – M20 x 75 – 10.9/10 – tZn)
Nominal preload level	172 kN = $F_{p,C}$
Preload measuring method	Implanted SG, measured continuously, clamping length Σt = 48 mm
Test speed	0.002 mm/s

Static test

Specimens mark	plate ID's	Slip (average at CB) u_i [mm]	Slip load F_{si} [kN]	Preload at beginning of the test $F_{bi,ini}$ [kN]	Slip factor based on initial preload $\mu_{i,ini}$ [-]	Slip factor based on nominal preload $F_{p,C}$ [kN] 172 $\mu_i = \mu_{i,nom}$ [-]	Slip factor based on preload at slip $\mu_{i,act}$ [-]	Preload at slip mean $F_{bi,act}$ [kN]	Test duration t [min]	Comment (Eq. according to EN 1090-2)
S_M20_EN1090_ASI_d_01	1	0.150	241.3	176.2	0.68	0.70	0.71	170.9	15.7	
S_M20_EN1090_ASI_d_02	2	0.150	232.4	172.3	0.67	0.68	0.72	161.1	15.4	
S_M20_EN1090_ASI_d_03	3	0.150	238.4	170.8	0.70	0.69	0.75	159.3	15.5	
S_M20_EN1090_ASI_d_04	4	0.150	254.5	171.2	0.74	0.74	0.78	163.4	15.3	

Statistics (4 specimens, 4 test results) — $n = 8$

		F_{si}	$\mu_{i,ini}$	$\mu_{i,nom}$	$\mu_{i,act}$	Comment
max	Maximum	254.5	0.74	0.74	0.78	Eq. (2), Eq. (4)
min	Minimum	232.4	0.67	0.68	0.71	R = max – min
mean	Mean value F_{sm} | μ_m	**241.6**	**0.70**	**0.70**	**0.74**	Eq. (3), Eq. (5)
R	Spread	22.1	0.07	0.06	0.07	V = s / mean
s	Standard deviation s_{Fs}	9.3	0.030	0.027	0.032	
V	Coefficient of variation	3.9%	4.3%	3.9%	4.3%	Load level for the creep test
0.9 F_{sm}		217.5				

Creep test

Δ (5 min to 3 h): **0,11**

Specimens mark	plate ID's	u_i [mm]	F_{si} [kN]	$F_{bi,ini}$ [kN]	$\mu_{i,ini}$ [-]	$\mu_{i,nom}$ [-]	$\mu_{i,act}$ [-]	mean $F_{bi,act}$ [kN]	t [min]	Comment
S_M20_EN1090_ASI_d_06	6	0.150	–	171.7	–	–	–	143.6	23.8	Creep test failed — Slip during the creep test > 0,002 mm (5 min to 3 h)

Statistics (5 specimens, 5 test results) — $n = 10$

		F_{si}	$\mu_{i,ini}$	$\mu_{i,nom}$	$\mu_{i,act}$	Comment
max	Maximum	254.5	0.74	0.74	0.78	Eq. (2), Eq. (4)
min	Minimum	232.4	0.67	0.68	0.71	R = max – min
mean	Mean value F_{sm} | μ_m	241.6	0.70	0.70	0.74	Eq. (3), Eq. (5)
R	Spread	22.1	0.07	0.06	0.07	V = s / mean ≤ 8%
s	Standard deviation s_{Fs}	9.3	0.030	0.027	0.032	
V	Coefficient of variation	**3.9%**	**4.3%**	**3.9%**	**4.3%**	
0.9 F_{sm}		217.5				

Characteristic value of the slip factor μ_k: 0.64 | 0.65 | 0.67 — Eq. (6)

Comments
- Creep test failed
- Three extended creep tests as a chain: $0.85 \cdot F_{sm}$ = 128.8 kN $\Rightarrow$ test is passed $\Rightarrow \mu_{final}$ = 0.60

Test results

Table D-5: Slip factor test results according to simplified EN 1090-2 for S_M20_EN1090_ASI_I test series

Technical characteristics of the test

Steel grade	Structural Steel EN 10025-2 – S355J2 +N (hot rolled)
Coating	Alkali-zinc silicate (ASI), Inorganic Zinc Silicate (Interzinc® 697)
Surface treatment	Grit blasted (with Brown Corundum, f20, Al_2O_3 (Aluminiumoxid))
Mean coating thickness	104 µm
Surface roughness (before coating)	75 µm
Specimen size	Modified specimens M20 (based on EN 1090-2:2018 and RCSC 2014)
Bolt class, bolt type	10.9 (Set EN 14399-4 – HV – M20 x 75 – 10.9/10 – tZn)
Nominal preload level	172 kN = $F_{p,C}$
Preload measuring method	Implanted SG, measured continuously, clamping length $\Sigma t = 48$ mm
Test speed	200 N/s

Static test

Specimens mark	plate ID's	Slip (average at CB) u_i [mm]	Slip load F_{si} [kN]	Preload at beginning of the test $F_{bi,ini}$ [kN]	Slip factor based on initial preload $\mu_{i,ini}$ [-]	Slip factor based on nominal preload $F_{p,C}$ [kN] 172 $\mu_i = \mu_{i,nom}$ [-]	Slip factor based on preload at slip $\mu_{i,act}$ [-]	Preload at slip mean $F_{bi,act}$ [kN]	Test duration t [min]	Comment
S_M20_EN1090_ASI_I_05	5	0.150	243.5	171.8	0.71	0.71	0.76	159.7	20.3	Eq. according to EN 1090-2

Table D-6: Slip factor test results according to EN 1090-2 for EN1090_CS_GB-A test series

Technical characteristics of the test

Steel grade	Structural Steel EN 10025-2 – S355
Coating	–
Surface treatment	Grit blasted (with Brown Corundum, f20, Al_2O_3 (Aluminiumoxid))
Mean coating thickness	–
Surface roughness (before coating)	74 µm
Specimen size	Standard specimens M16 (EN 1090-2, Figure G.1 b)
Bolt class, bolt type	10.9 (Set EN 14399-4 – HV – M16 x 60 – 10.9/10 – tZn)
Nominal preload level	110 kN = $F_{p,C}$
Preload measuring method	implanted SG, measured continuously, clamping length $\Sigma t = 40$ mm
Test speed	0.01 mm/s

Static test (4 specimens, 8 test results)

Specimens mark	plate ID's	Slip (average at CBG) u_i [mm]	Slip load F_{Si} [kN]	Preload at start of test (initial preload) Outer bolt $F_{bi,o,ini}$ [kN]	mean value mean $F_{bi,ini}$ [kN]	Inner bolt $F_{bi,i,ini}$ [kN]	Slip factor based on initial preload $\mu_{i,ini}$ [-]	based on nominal preload $F_{p,C}$ [kN] 110 $\mu_i = \mu_{i,nom}$ [-]	based on preload at slip $\mu_{i,act}$ [-]	Preload at slip Outer bolt $F_{bi,o,act}$ [kN]	mean value mean $F_{bi,act}$ [kN]	Inner bolt $F_{bi,i,act}$ [kN]	Test duration t [min]	Comment
EN 1090_CS_GB_01-02	1	0.150	331.4	114.5	114.3	114.1	0.72	0.75	0.85	99.2	97.0	94.8	17.8	Eq_t according to EN 1090-2
	2	0.150	317.0	116.3	114.9	113.4	0.69	0.72	0.81	101.5	97.5	93.4	14.0	
EN 1090_CS_GB_05-06	5	0.150	319.7	115.4	114.2	112.9	0.70	0.73	0.83	99.2	96.6	94.0	14.3	
	6	0.150	318.6	112.6	112.9	113.3	0.71	0.72	0.83	96.9	95.7	94.6	14.2	
EN 1090_CS_GB_07-08	7	0.150	315.6	113.9	113.7	113.5	0.69	0.72	0.81	98.7	97.2	95.6	14.6	
	8	0.150	327.4	107.8	110.5	113.2	0.74	0.74	0.83	101.9	98.2	94.4	18.1	
EN 1090_CS_GB_11-12	11	0.150	317.7	115.1	114.0	112.9	0.70	0.72	0.82	99.2	96.8	94.4	14.2	
	12	0.150	316.1	115.2	115.0	114.7	0.69	0.72	0.80	100.1	98.4	96.8	14.1	

Statistics (n = 8)

			F_{Si}				$\mu_{i,ini}$	$\mu_i = \mu_{i,nom}$	$\mu_{i,act}$					Comment
max	Maximum		331.4				0.74	0.75	0.85					
min	Minimum		315.6				0.69	0.72	0.80					
mean	Mean value F_{Sm} | μ_m		320.4				0.70	0.73	0.82					
R	Spread		15.8				0.05	0.04	0.05					Eq. (2), Eq. (4)
s	Standard deviation s_{Fs}		5.8				0.019	0.013	0.016					R = max – min
V	Coefficient of variation		1.8%				2.6%	1.8%	1.9%					Eq. (3), Eq. (5)
0.9 F_{Sm}			288.4											V = s / mean
														Load level for the creep test

Creep test (5 specimens, 10 test results)

Specimens mark	plate ID's	Slip Δ (5 min to 3 h)	u_i [mm]	F_{Si} [kN]	$F_{bi,o,ini}$ [kN]	mean $F_{bi,ini}$ [kN]	$F_{bi,i,ini}$ [kN]	$\mu_{i,ini}$ [-]	$\mu_{i,nom}$ [-]	$\mu_{i,act}$ [-]	$F_{bi,o,act}$ [kN]	mean $F_{bi,act}$ [kN]	$F_{bi,i,act}$ [kN]	t [min]	Comment
EN 1090_CS_GB_09-10	9	0,0018	0.150	325.5	114.2	113.4	112.6	0.72	0.74	0.72	114.2	113.4	112.6	858.7	**Creep test passed** Slip during the creep test < 0,002 mm (5 min to 3 h)
	10	0,0009	0.150	331.2	113.6	114.2	114.8	0.73	0.75	0.73	113.6	114.2	114.8	859.1	

Statistics (n = 10)

			F_{Si}				$\mu_{i,ini}$	$\mu_{i,nom}$	$\mu_{i,act}$					Comment
max	Maximum		331.4				0.74	0.75	0.85					
min	Minimum		315.6				0.69	0.72	0.80					
mean	Mean value F_{Sm} | μ_m		322.0				0.71	0.73	0.80					
R	Spread		15.8				0.05	0.04	0.14					Eq. (2), Eq. (4)
s	Standard deviation s_{Fs}		6.3				0.018	0.014	0.046					R = max – min
V	Coefficient of variation		1.9%				2.5%	1.9%	5.7%					Eq. (3), Eq. (5)
0.9 F_{Sm}			289.8											V = s / mean ≤ 8%
μ_k	Characteristic value of the slip factor						0.67	0.70	0.71					Eq. (6)

Comments
- Creep test passed
- Extended creep test is not required

Test results

Table D-7: Slip factor test results according to simplified EN 1090-2 for S_M16_EN1090_GB-A_d test series

Technical characteristics of the test

Steel grade	Structural Steel EN 10025-2 – S355
Coating	–
Surface treatment	Grit blasted (with Brown Corundum, f20, Al_2O_3 (Aluminiumoxid))
Mean coating thickness	–
Surface roughness (before coating)	74 µm
Specimen size	Modified specimens M16 (based on EN 1090-2:2018 and RCSC 2014)
Bolt class, bolt type	10.9 (Set EN 14399-4 – HV – M16 x 60 – 10.9/10 – tZn)
Nominal preload level	110 kN = $F_{p,C}$
Preload measuring method	Implanted SG, measured continuously, clamping length Σt = 40 mm
Test speed	0.002 mm/s

Section	Specimens mark / plate ID's	Slip (average at CB) u_i [mm]	Slip load F_{Si} [kN]	Preload at beginning of the test $F_{bi,ini}$ [kN]	Slip factor based on initial preload $\mu_{i,ini}$ [-]	Slip factor based on nominal preload $F_{p,C}$ [kN] 110 $\mu_i = \mu_{i,nom}$ [-]	Slip factor based on preload at slip $\mu_{i,act}$ [-]	Preload at slip mean $F_{bi,act}$ [kN]	Test duration t [min]	Comment (Eq. according to EN 1090-2)
Static test	S_M16_EN1090_GB-A_d_01 — 1	0.150	175.6	112.8	0.78	0.80	0.83	105.4	10.1	
	S_M16_EN1090_GB-A_d_02 — 2	0.150	170.6	111.3	0.77	0.78	0.81	105.2	10.3	
	S_M16_EN1090_GB-A_d_03 — 3	0.150	182.3	109.9	0.83	0.83	0.89	102.5	14.7	
	S_M16_EN1090_GB-A_d_04 — 4	0.150	188.0	111.1	0.85	0.85	0.86	108.9	10.9	
Statistics (4 specimens, 4 test results) $n = 8$	Number of tests									
	max Maximum		188.0		0.85	0.85	0.89			
	min Minimum		170.6		0.77	0.78	0.81			
	mean Mean value F_{Sm} | μ_m		179.2		0.80	0.81	0.85			Eq. (2), Eq. (4)
	R Spread		17.4		0.08	0.08	0.08			R = max – min
	s Standard deviation s_{Fs}		7.6		0.039	0.035	0.034			Eq. (3), Eq. (5)
	V Coefficient of variation		4.2%		4.8%	4.2%	4.0%			V = s / mean
	0.9 F_{Sm}		161.2							Load level for the creep test
Creep test	S_M16_EN1090_GB-A_d_07 — 7	Δ (5 min to 3 h): – 0.150	–	113.1	–	–	–	100.6	12.8	**Creep test failed** Slip during the creep test > 0.002 mm (5 min to 3 h)
Statistics (5 specimens, 5 test results) $n = 10$	Number of tests									
	max Maximum		188.0		0.85	0.85	0.89			
	min Minimum		170.6		0.77	0.78	0.81			
	mean Mean value F_{Sm} | μ_m		179.2		0.60	0.81	0.85			Eq. (2), Eq. (4)
	R Spread		17.4		0.08	0.08	0.08			R = max – min
	s Standard deviation s_{Fs}		7.6		0.039	0.035	0.034			Eq. (3), Eq. (5)
	V Coefficient of variation		4.2%		4.8%	4.2%	4.0%			V = s / mean ≤ 8%
	0.9 F_{Sm}		161.2							
Additional Creep test	S_M16_EN1090_GB-A_d_06 — 6	Δ (5 min to 3 h): 0.002 0.150	164.8	112.0	0.74	0.75	0.86	96.2	3678.8	**Creep test passed** Slip during the creep test ≤ 0.002 mm (5 min to 3 h)
Statistics (5 specimens, 5 test results) $n = 10$	Number of tests									
	max Maximum		188.0		0.85	0.85	0.89			
	min Minimum		164.8		0.74	0.75	0.81			
	mean Mean value F_{Sm} | μ_m		176.3		0.79	0.80	0.85			Eq. (2), Eq. (4)
	R Spread		23.2		0.11	0.11	0.08			R = max – min
	s Standard deviation s_{Fs}		84.7		0.045	0.042	0.030			Eq. (3), Eq. (5)
	V Coefficient of variation		5.2%		5.7%	5.2%	3.5%			V = s / mean ≤ 8%
	0.85 F_{Sm}		152.3							
	μ_k Characteristic value of the slip factor				0.68	0.70	0.78			Eq. (6)

Comments
- The specimen was loaded with 85% of the mean slip load from the first four static tests (0.85 F_{Sm} = 152.3 kN)
- Additional creep test with 0.85·F_{Sm} passed

Test results
- Creep test with 0.9·F_{Sm} failed
- Three extended creep tests as a chain: 0.85·F_{Sm} = 152.3 kN ⇒ test is passed ⇒ μ_{final} = 0.69

Table D-8: Slip factor test results according to simplified EN 1090-2 for S_M16_EN1090_GB-A_I test series

Technical characteristics of the test

Steel grade	Structural Steel EN 10025-2 – S355
Coating	–
Surface treatment	Grit blasted (with Brown Corundum, f20, Al_2O_3 (Aluminiumoxid))
Mean coating thickness	–
Surface roughness (before coating)	74 µm
Specimen size	Modified specimens M16 (based on EN 1090-2:2018 and RCSC 2014)
Bolt class, bolt type	10.9 (Set EN 14399-4 – HV – M16 x 60 – 10.9/10 – tZn)
Nominal preload level	110 kN = $F_{p,C}$
Preload measuring method	Implanted SG, measured continuously, clamping length $\Sigma t = 40$ mm
Test speed	200 N/s

Static test

Specimens mark	plate ID's	Slip (average at CB) u_i [mm]	Slip load F_{si} [kN]	Preload at beginning of the test $F_{bi,ini}$ [kN]	Slip factor based on initial preload $\mu_{i,ini}$ [–]	Slip factor based on nominal preload $F_{p,C}$ [kN] 110, $\mu_i = \mu_{i,nom}$ [–]	Slip factor based on preload at slip $\mu_{i,act}$ [–]	Preload at slip mean $F_{bi,act}$ [kN]	Test duration t [min]	Comment Eq. according to EN 1090-2
S_M16_EN1090_GB-A_I_05	5	0.150	168.7	111.0	0.76	0.77	0.81	104.4	14.0	

Table D-9: Slip factor test results according to simplified EN 1090-2 for S_M20_EN1090_GB-A_d test series

Technical characteristics of the test

Steel grade	Structural Steel EN 10025-2 – S355
Coating	–
Surface treatment	Grit blasted (with Brown Corundum, f20, Al$_2$O$_3$ (Aluminiumoxid))
Mean coating thickness	–
Surface roughness (before coating)	75 µm
Specimen size	Modified specimens M20 (based on EN 1090-2:2018 and RCSC 2014)
Bolt class, bolt type	10.9 (Set EN 14399-4 – HV – M20 x 75 – 10.9/10 – tZn)
Nominal preload level	172 kN = F$_{p,C}$
Preload measuring method	Implanted SG, measured continuously, clamping length Σt = 48 mm
Test speed	0.002 mm/s

Static test

Specimens mark	plate ID's	Slip (average at CB) u_i [mm]	Slip load F_{Si} [kN]	Preload at beginning of the test $F_{bi,ini}$ [kN]	Slip factor based on initial preload $\mu_{i,ini}$ [-]	Slip factor based on nominal preload $F_{p,C}$ [kN] 172 $\mu_i = \mu_{i,nom}$ [-]	Slip factor based on preload at slip $\mu_{i,act}$ [-]	Preload at slip mean $F_{bi,act}$ [kN]	Test duration t [min]	Comment (Eq. according to EN 1090-2)
S_M20_EN1090_GB-A_d_01	1	0.150	273.8	170.7	0.80	0.80	0.86	159.0	13.7	
S_M20_EN1090_GB-A_d_02	2	0.150	283.7	167.0	0.85	0.82	0.87	163.0	12.2	
S_M20_EN1090_GB-A_d_03	3	0.150	278.0	171.5	0.81	0.81	0.90	153.9	15.1	
S_M20_EN1090_GB-A_d_04	4	0.150	264.9	170.7	0.78	0.77	0.86	153.2	14.3	

Statistics (4 specimens, 4 test results) — n = 8 Number of tests

	F_{Si}	$\mu_{i,ini}$	$\mu_{i,nom}$	$\mu_{i,act}$	Comment
max Maximum	283.7	0.85	0.82	0.90	Eq. (2), Eq. (4)
min Minimum	264.9	0.78	0.77	0.86	
mean Mean value F_{Sm} | μ_m	**275.1**	**0.81**	**0.80**	**0.87**	
R Spread	18.8	0.07	0.05	0.04	R = max – min
s Standard deviation s_{Fs}	7.9	0.030	0.023	0.019	Eq. (3), Eq. (5)
V Coefficient of variation	2.9%	3.7%	2.9%	2.2%	V = s / mean
0.9 F_{Sm}	247.6				Load level for the creep test

Creep test

Specimens mark	plate ID's	Slip u_i [mm]	Slip load F_{Si} [kN]	Preload at beginning $F_{bi,ini}$ [kN]	$\mu_{i,ini}$ [-]	$\mu_i = \mu_{i,nom}$ [-]	$\mu_{i,act}$ [-]	Preload at slip mean $F_{bi,act}$ [kN]	Test duration t [min]	Comment
S_M20_EN1090_GB-A_d_06	6	0.150	–	169.4	–	–	–	151.5	19.3	**Creep test failed** Slip during the creep test > 0.002 mm (5 min to 3 h)

Δ (5 min to 3 h): –

Statistics (5 specimens, 5 test results) — n = 10 Number of tests

	F_{Si}	$\mu_{i,ini}$	$\mu_{i,nom}$	$\mu_{i,act}$	Comment
max Maximum	283.7	0.85	0.82	0.90	Eq. (2), Eq. (4)
min Minimum	264.9	0.78	0.77	0.86	
mean Mean value F_{Sm} | μ_m	**275.1**	**0.81**	**0.80**	**0.87**	
R Spread	18.8	0.07	0.05	0.04	R = max – min
s Standard deviation s_{Fs}	7.9	0.030	0.023	0.019	Eq. (3), Eq. (5)
V Coefficient of variation	**2.9%**	**3.7%**	**2.9%**	**2.2%**	V = s / mean ≤ 8%
0.9 F_{Sm}	247.6				

μ_k Characteristic value of the slip factor		0.75	0.75	0.83	Eq. (6)

Comments / Test results:
- Creep test failed
- Three extended creep tests as a chain: 0.85·F$_{Sm}$ = 233.8 kN ⟹ test is passed ⟹ μ_{final} = 0.68

Table D-10: Slip factor test results according to simplified EN 1090-2 for S_M20_EN1090_GB-A_I test series

Technical characteristics of the test

Steel grade	Structural Steel EN 10025-2 – S355
Coating	–
Surface treatment	Grit blasted (with Brown Corundum, f20, Al_2O_3 (Aluminiumoxid))
Mean coating thickness	–
Surface roughness (before coating)	75 µm
Specimen size	Modified specimens M20 (based on EN 1090-2:2018 and RCSC 2014)
Bolt class, bolt type	10.9 (Set EN 14399-4 – HV – M20 x 75 – 10.9/10 – tZn)
Nominal preload level	172 kN = $F_{p,C}$
Preload measuring method	Implanted SG, measured continuously, clamping length Σt = 48 mm
Test speed	200 N/s

Static test

Specimens mark	plate ID's	Slip (average at CB) u_i [mm]	Slip load F_{si} [kN]	Preload at beginning of the test $F_{bi,ini}$ [kN]	Slip factor based on initial preload $\mu_{i,ini}$ [-]	Slip factor based on nominal preload $F_{p,C}$ [kN] 172, $\mu_i = \mu_{i,nom}$ [-]	Slip factor based on preload at slip $\mu_{i,act}$ [-]	Preload at slip mean $F_{bi,act}$ [kN]	Test duration t [min]	Comment Eq. according to EN 1090-2
S_M20_EN1090_GB-A_I_05	5	0.150	281.7	173.1	0.81	0.82	0.93	151.5	23.5	

Table D-11: Slip factor test results according to RCSC 2014 for RCSC_CS_ASI_I test series

Technical characteristics of the test

Steel grade	Structural Steel EN 10025-2 – S355
Coating	Alkali-zinc silicate (ASI), Inorganic Zinc Silicate (Interzinc® 697)
Surface treatment	Grit blasted (with Brown Corundum, f20, Al$_2$O$_3$ (Aluminiumoxid))
Mean coating thickness	115 µm
Surface roughness (before coating)	78 µm
Specimen size	Standard specimens M22 (according to RCSC 2014)
Bolt class, bolt type	10.9 (Set EN 14399-4 – HV – M22 x 80 – 10.9/10 – tZn)
Nominal preload level	218 kN = F$_{p,C}$
Preload measuring method	Implanted SG, measured continuously, clamping length Σt = 56 mm
Test speed	400 N/s

Static test

Specimens mark	plate ID's	Slip (average at CB) u_i [mm]	Slip load F_{Si} [kN]	Preload at beginning of the test $F_{bi,ini}$ [kN]	Slip factor based on initial preload $\mu_{i,ini}$ [-]	Slip factor based on nominal preload $F_{p,C}$ [kN] 218, $\mu_i = \mu_{i,nom}$ [-]	Slip factor based on preload at slip $\mu_{i,act}$ [-]	Preload at slip mean $F_{bi,act}$ [kN]	Test duration t [min]	Comment
RCSC_CS_ASI_I_02	2	0.508	371.8	212.9	0.87	0.85	0.94	198.06	20.9	Eq. according to RCSC 2014
RCSC_CS_ASI_I_03	3	0.508	342.8	211.2	0.81	0.79	0.89	193.1	19.2	
RCSC_CS_ASI_I_04	4	0.508	370.4	212.2	0.87	0.85	0.98	188.1	15.6	
RCSC_CS_ASI_I_05	5	0.508	366.2	211.8	0.86	0.84	0.97	188.1	15.5	
RCSC_CS_ASI_I_06	6	0.508	370.6	211.9	0.87	0.85	0.95	195.6	15.6	

Statistics (5 specimens, 5 test results)

n = 5	Number of tests						
max	Maximum	371.8		0.87	0.85	0.98	
min	Minimum	342.8		0.81	0.79	0.89	
mean	Mean value F_{Sm} | μ_m	364.4		0.86	0.84	0.95	
R	Spread	28.9		0.06	0.07	0.10	R = max – min
s	Standard deviation s_{Fs}	12.2		0.027	0.028	0.038	
V	Coefficient of variation	3.4%		3.1%	3.4%	4.0%	V = s / mean

Creep test

Specimens mark	plate ID's	Preload at beginning of the test $F_{bi,ini}$ [kN]	First step load level F_{step1} [kN] Eq. A4.1	Slip (average at CB) Δ (0.5 h to 1000 h) u_{step1} [mm]	Second step load level F_{step2} [kN] Chap. A4.2	Slip (average at CB) at the load level u_{step2} [mm]	Comment	Final slip factor μ_{Final} [-] Eq. A3.1
RCSC_CS_ASI_I_09	9	219.8	206.5	0.023	309.7	0.20		0.71
RCSC_CS_ASI_I_10	10	216.9		0.017		0.09		
RCSC_CS_ASI_I_11	11	218.7		0.022		0.10		

Table D-12: Slip factor test results according to RCSC 2014 for RCSC_CS_ASI_d test series

Technical characteristics of the test

Steel grade	Structural Steel EN 10025-2 – S355
Coating	Alkali-zinc silicate (ASI), Inorganic Zinc Silicate (Interzinc® 697)
Surface treatment	Grit blasted (with Brown Corundum, f20, Al_2O_3 (Aluminiumoxid))
Mean coating thickness	115 µm
Surface roughness (before coating)	78 µm
Specimen size	Standard specimens M22 (according to RCSC 2009)
Bolt class, bolt type	10.9 (Set EN 14399-4 – HV – M22 x 80 – 10.9/10 – tZn)
Nominal preload level	218 kN = $F_{p,C}$
Preload measuring method	Implanted SG, measured continuously, clamping length $\Sigma t = 56$ mm
Test speed	0.001 mm/s

Static test

Specimens mark	plate ID's	Slip (average at CB) u_i [mm]	Slip load F_{Si} [kN]	Preload at beginning of the test $F_{bi,ini}$ [kN]	Slip factor based on initial preload $\mu_{i,ini}$ [–]	Slip factor based on nominal preload $F_{p,C}$ [kN]	$\mu_i = \mu_{i,nom}$ [–]	Slip factor based on preload at slip $\mu_{i,act}$ [–]	Preload at slip mean $F_{bi,act}$ [kN]	Test duration t [min]	Comment Eq. according to RCSC 2014
RCSC_CS_ASI_d_01	1	0.429	372.5	213.3	0.87	218	0.85	0.93	199.22	37.9	Eq. A3.1

Table D-13: Slip factor test results according to RCSC 2014 for RCSC_CS_GB-A_I test series

Technical characteristics of the test

Steel grade	Structural Steel EN 10025-2 – S355
Coating	–
Surface treatment	Grit blasted (with Brown Corundum, f20, Al$_2$O$_3$ (Aluminiumoxid))
Mean coating thickness	–
Surface roughness (before coating)	70 µm
Specimen size	Standard specimens M22 (according to RCSC 2009)
Bolt class, bolt type	10.9 (Set EN 14399-4 – HV – M22 x 80 – 10.9/10 – tZn)
Nominal preload level	218 kN = $F_{p,C}$
Preload measuring method	Implanted SG, measured continuously, clamping length Σt = 56 mm
Test speed	400 N/s

Static test

Specimens mark	plate IDs	Slip (average at CB) u_i [mm]	Slip load F_{si} [kN]	Preload at beginning of the test $F_{bi,ini}$ [kN]	Slip factor based on initial preload $\mu_{i,ini}$ [-]	Slip factor based on nominal preload $F_{p,C}$ [kN] 218 $\mu_i = \mu_{i,nom}$ [-]	Slip factor based on preload at slip $\mu_{i,act}$ [-]	Preload at slip mean $F_{bi,act}$ [kN]	Test duration t [min]	Comment Eq. according to RCSC 2014
RCSC_CS_GB-A_I_01	1	0.508	369.5	212.7	0.87	0.85	0.94	197.29	15.5	
RCSC_CS_GB-A_I_02	2	0.508	315.8	211.8	0.75	0.72	0.84	188.9	13.3	
RCSC_CS_GB-A_I_03	3	0.508	345.3	215.6	0.80	0.79	0.88	195.2	14.6	
RCSC_CS_GB-A_I_04	4	0.508	348.4	215.3	0.81	0.80	0.91	191.7	14.7	
RCSC_CS_GB-A_I_05	5	0.508	375.1	213.9	0.88	0.86	0.93	202.2	15.8	

Statistics (5 specimens, 5 test results)

$n = 5$	Number of tests						
max	Maximum	375.1		0.88	0.86	0.94	
min	Minimum	315.8		0.75	0.72	0.84	
mean	Mean value F_{sm} / μ_m	350.8		0.82	0.80	0.90	
R	Spread	59.2		0.13	0.14	0.10	R = max – min
s	Standard deviation s_{Fs}	23.4		0.054	0.054	0.040	
V	Coefficient of variation	6.7%		6.6%	6.7%	4.5%	V = s / mean

Eq. A3.1

Creep test

Specimens mark	plate IDs	Preload at beginning of the test $F_{bi,ini}$ [kN]	First step load level F_{step1} [kN] Eq. A4.1	Slip (average at CB) Δ (0.5 h to 1000 h) u_{step1} [mm]	Second step load level F_{step2} [kN] Chap. A4.2	Slip (average at CB) at the load level u_{step2} [mm]	Final slip factor μ_{Final} [-] Eq. A3.1	Comment
RCSC_CS_GB-A_I_09	9	219.1	210.5	0.0010	315.7	0.118	0.72	
RCSC_CS_GB-A_I_10	10	219.7		0.0012		0.154		
RCSC_CS_GB-A_I_11	11	217.5		0.0001		0.132		